Department of Medicine

Custer of Neurosciences

Faculty of sciences

University of Fribourg (Switzerland)

Motor system lesions in non-human primates: evidences for large scale plasticity and the challenge of treatments

THESIS

presented to the Faculty of Science of the University of Fribourg (Switzerland)

in consideration for the award of the academic grade of *Doctor rerum naturalium*

by

Julie Savidan

from

France

Thesis No: XXXX

2015

Accepted by the Faculty of Science of the University of Fribourg (Switzerland) upon the recommendation of …….. and …….. (thesis co-examiners)

Fribourg, …….. (date of the oral examination)

Thesis supervisor(s) Dean

…… ……..

(name) (name of the Dean at the time of the oral examination)

Table of content

Abbreviation lists

AIP	Anterior intraparietal area
APB	Abductor pollicis brevis
BDNF	Brain Derived Neurotrophic Factor
c	Caudal
CIMT	Constraint-Induced Movement Therapy
CM	Corticomotoneuronal
CMA	Cingulate motor areas
CNS	Central nervous system
CS(T)	Corticospinal (tract)
d	Dorsal
DCN	Brainstem dorsal column nuclei
EEG	Electroencephalography
EMG	Electromyography
F	Frontal
GABA	Acid gamma-aminobutyrique
ICMS	Intracortical microstimulation
IOM	Intraoperative monitoring
LTP	Long-term potentiation
LTD	Long-term depression
MCI	Motor cortex injury
MEG	Magnetoencephalography
MEP	Motor Evoked Potential
MRI	Magnetic resonance imaging
M1	Primary motor cortex
MIP	Medial intraparietal area
NMDA	N-methyl-D-aspartate
PMRF	Pontomedullary reticular formation
PM	Premotor cortex
PT	Pyramidal tract
PV	Parietal ventral
r	Rostral
SI	Primary somatosensory cortex

SII	Secondary somatosensory cortex
SCI	Spinal cord injuries
SMA	Supplementary motor
StTA	Stimulus triggered averaging
SpTA	Spike triggered averaging
TBI	Traumatic brain injuries
TES	Transcranial electrical stimulation
TMS	Transcranial magnetic stimulation
Trk	Tropomyosin-related kinase
v	Ventral
VIP	Ventral intraparietal area

Abstract

Improving the functional recovery following motor system lesion affecting the control of voluntary movements represents an important challenge. Voluntary movement such as manual dexterity (e.g. precision grip) requires strong and sophisticated cooperation among the neural networks including motor and parietal cortical areas, brainstem structures and spinal cord. My work investigates effects and outcomes following primary motor cortex lesion restricted to the hand area (MCI) or spinal cord hemisection at C7/C8 (SCI) to elaborate strategy aiming to restore the lost function.

My work first addresses the intrinsic capacity of these networks to be subjected to plastic changes in response to motor system lesion, examining the possible extent to which such plastic changes can occur. I explore whether different components of these motor networks underlying such plastic changes are involved in the functional recovery. My work finally addresses the beneficial effects of a therapy strategy using a blocker of the inhibitory membrane protein of the myelin sheath Nogo-A. As such promoted functional recovery remains however limited, my work assesses the possibility to further promote beneficial effects investigating an original therapy strategy using a combined treatment of the later treatment with the neurotrophin, BDNF.

My work provides behavioral, electrophysiological and anatomical data suggesting that plastic changes occurs over long distances following motor system lesion, either at the cortical or at spinal cord level. Afterward, adapting analysis criteria, my work highlights the possibility to reveal distinct roles for the different regions of the network involved in the motor control for the functional recovery of the precision grip, planning and execution,. The different results suggest the occurrence of plastic changes and a possible role for the perilesional cortex, the contralesional intact M1, the subcortical structures and brainstem somatosensorial dorsal column nuclei. Finally, I observe the beneficial effects promoting functional recovery of the anti-Nogo-A antibody treatment in case of MCI. However, the therapy using combined treatment resulted in deleterious rather than in beneficial effects. To conclude, my study evidences the necessity to address the motor system lesion effects and functional recovery with new perspectives to define optimal therapy which could lead to better restore the lost functions.

Résumé

Promouvoir la récupération fonctionnelle suite à une lésion du système moteur affectant le control des mouvements volontaires représente un défi important. Le control moteur des mouvements volontaires, telle que la dextérité manuelle (par ex. pince de précision), sollicite une coopération poussée et complexe au sein des circuits neuronaux comprenant les aires corticales motrices et pariétales, les structures du tronc cérébral et la moelle épinière. Mon travail s'intéresse aux effets et implications des lésions du système moteur situés à la fois dans le cas d'une lésion de M1 focalisée sur la région de la main ou dans le cas d'une hémisection de la moelle épinière au niveau C7/C8.

Dans mon travail je m'intéresse préalablement à la capacité intrinsèque de ces circuits à être soumis à des changements plastiques consécutivement à une lésion du système moteur et cela en examinant l'étendue possible de ces changements. En relation avec cette plasticité, j'explore la possibilité pour les différentes composantes de ces circuits impliqués dans le control moteur d'être impliqués dans la récupération fonctionnelle. Un autre aspect de mon travail aborde le potentiel bénéfique d'un traitement bloquant une protéine de la myéline inhibitrice, Nogo-A. La récupération fonctionnelle restant toutefois limité, mon travail s'intéresse à la possibilité d'améliorer encore celle-ci en utilisant une stratégie thérapeutique consistant à utiliser une combinaison de traitement, associant le précédant traitement avec la neurotrophin BDNF.

Mon travail apporte des informations comportementales, électrophysiologiques et anatomiques suggérant que de la plasticité survient à longue distance suite à une lésion du système moteur, et que celle-ci se trouve localisée au niveau cortical ou au niveau spinal. Je suggère également la possibilité de révéler des rôles différentiés des structures de ces circuits impliqués dans le système moteur dans la récupération fonctionnelle de la planification et l'exécution du mouvement de pince de précision en adaptant les critères d'analyse. Finalement les différents résultats montrent des effets bénéfiques du traitement avec l'anticorps anti-Nogo-A sur la récupération fonctionnelle suite à une lésion de M1 focalisée sur la région de la main. Cependant, la thérapie basée sur l'utilisation du traitement combiné génère plutôt des effets délétères. Mon travail met en avant la nécessité d'aborder l'étude des effets des lésions du système moteur et de la récupération fonctionnelle qui s'ensuit sous de nouvelles perspectives pour définir une thérapie permettant une restauration optimale des fonctions perdues.

1. General introduction

Loss of the motor functions consequently to spinal cord injury or stroke has been extensively studied since decades. Their large incidence and their severe impact on the quality of life and autonomy of the patients make their studies of high interest to understand the mechanisms involved and to elaborate strategies improving functional recovery. In a first attempt, the present work aimed to give further understanding about the post-lesion mechanisms following cortical and spinal cord injuries and, in a second attempt, to evaluate the possibility to improve the post-lesion outcomes.

First, I will introduce the general notions addressed in the present work. An extensive part of the literature in neurosciences covers the fine manual dexterity to understand and explore the motor system. The fine manual dexterity has emerged during the course of the species evolution, resulting in a prerogative of the primates (humans and monkeys). Planning, execution and control of such voluntary movements involve many different regions of the central nervous system. Briefly, fine manual dexterity, as an example of sophisticated motor control, directly involves neurons of the cortical motor areas, sending direct projections to the spinal cord, via the so-called corticospinal (CS) tract, addressing the spinal motoneurons which, in turn, control skeletal muscles' activity. Along the species evolution, the fine manual dexterity has emerged in close relationship with the development of the corticospinal pathways (*e.g.* Courtine et al., 2007). The exquisite precision of manual dexterity requires high level of control for the correct execution, at cortical level but also involving subcortical loops, as well as somatosensory pathways sending information to brainstem, subcortical and cortical structures in order to

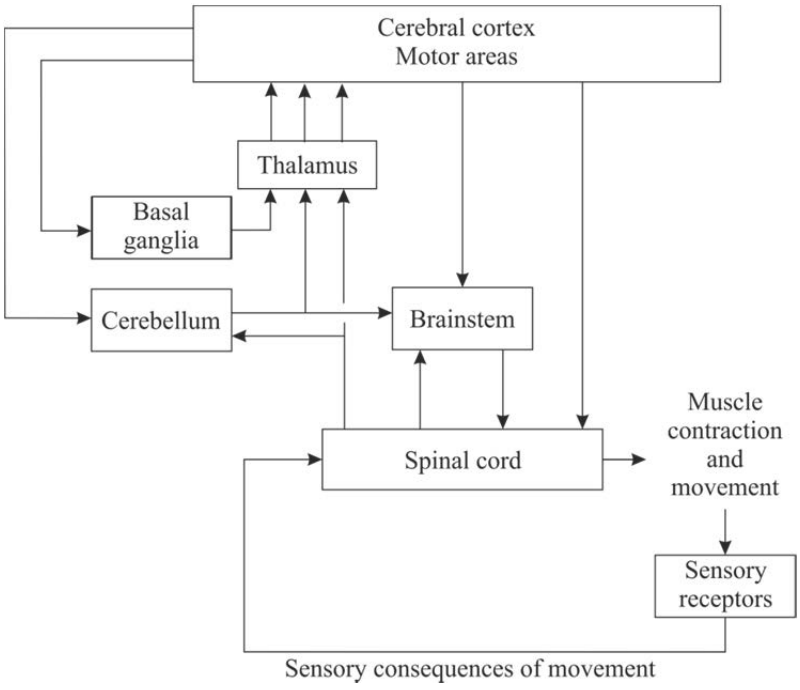

Figure 1: Schematic representation of the simplified pathways and structures involved in the motor control for voluntary movement execution.

correct errors and adjust the desired movements (Fig. 1).

Consequences of central nervous system (CNS) injury on the motor function depend on the location and size of the injury, thus affecting different attributes of voluntary movements. A certain degree of functional recovery is observed following motor system injury (in most cases incomplete), which implies some ability of the motor system to supply the lost functions to a limited extent. To date, no complete restorative therapies have been proposed to regenerate the damaged motor system. The different therapies developed aimed at promoting the limited functional recovery following motor system injuries, for instance by challenging the spared structures via behavioral and/or molecular therapies (Thuret et al., 2006; Oujamaa et al., 2009).

The present work focus on the fine manual dexterity in the macaque monkey model subjected to spinal cord or cortical injury. Previous to the general basis descriptions, I will describe some basis of current techniques used to study the CNS injuries affecting the motor control, in relation to the present work. To this aim, I will firstly introduce the anatomical bases involved in the planning, execution and control of the voluntary movement, specifically for the precision grip. Afterward, the plasticity will be discuss as a primordial property of the central nervous system largely involved in the motor control of voluntary movement. The spinal cord or cortical lesion addressed in the present work will be then described, to finally discuss about some therapeutic possibilities promoting improved outcomes, mainly to those addressed in the present work.

1.1. Introduction of the current techniques for CNS investigations

Development of adequate experimental approaches has permitted to make progress on the understanding and knowledge of anatomy and functional mechanisms supporting the planning and execution of voluntary movements.

Histological staining currently used to document anatomy and functions of the brain have been introduced by the end of the XIXth century. This was initiated with the development of the silver nitrate staining by Golgi and used later by Ramón y Cajal to describe neurons for the first time. The later development of the immunohistochemistry has started with the first interest in antigen-antibody reaction in 1930 by Reiner, then, followed by

the first report of the use of fluorescent compounds in 1942 by Conns and colleagues (Coons, 1971). Since, the development of a large variety of antigen-antibody reactions have been developed, permanently enlarged in direct correlation with the development of the microscopy tools, to microscopically visualize a wide range of tissue, cells, proteins, genes and others. Nowadays a wide range of techniques are used to label and visualize brain structures at the cellular, molecular and neural network levels.

The increasing interest in the precise distribution of neural pathways within the central nervous system led to the development of new methods to visualize the origin, trajectory and target of these pathways. To achieve this goal, the degenerative method was primarily extensively used to observe the presence of *boutons terminaux*, stained using histological methods, along the course of the nerves consecutively to their lesion (Hoff, 1932). Since the first work of Lasek and colleagues (1967), refined methods of neuroanatomical tracing are currently used, based on the axonal property to transport molecules. These neuroanatomical tracing methods are used to demonstrate the axonal origins, trajectories and terminations by injections of specific molecules, the neuroanatomical tracers, captured and then transported along axons in the retrograde and/or anterograde direction from the uptake site (cell body or axon terminals). In contrast to the old degenerative methods, these neuroanatomical tracing methods advantageously allow to visualize a specific tract as a whole, without damaging it, in order to establish the actual route followed by various axonal populations.

Lesions have substantially contributed to the understanding and knowledge of the anatomy and functional mechanisms of the central nervous system. Consecutive effects indirectly revealed the function sustained by the lesioned part with the limitation that the spontaneous CNS post-lesion plasticity may interfere with the interpretation of such lesional observations.

The goal to explore electrophysiological properties and routes of neural tracts involved the necessity to develop method allowing *in vivo* investigations of the central nervous system.

The first evidence of the electrical excitability of the motor cortex has been provided by Fritsch and Hitzig in 1870 (Fritsch and Hitzig, 2009). In their study, they elicited movements in the contralateral body side in response to the electrical stimulation of the frontal cortex in the dog, principally in the rostral most part adjacent to the central sulcus. The first stimulation of the brain in intact human subjects was conducted by Merton and Morton in 1980. Their findings gave rise to the development of the currently used transcranial electrical

stimulation (TES) method to document anatomical and electrophysiological characteristics and changes of the motor tracts, both in clinic and research. However, diffusion of the electrical current over the tissue makes this technology particularly painful for the subject. The further development of the transcranial magnetic stimulation (TMS) method has allowed to document excitability, connectivity and plasticity of the motor cortex in a non-invasive approach in intact and awake human subjects. Since the first report using efficiently the TMS (Barker et al., 1985), numerous studies have promoted this method in clinic and research (for reviews see Kobayashi and Pascual-Leone, 2003; Ferreri and Rossini, 2013). To refine the precision of the cortical stimulation, invasive electrophysiological experimental methods, introduced by Asanuma and Sakata (1966), have been developed to directly stimulate the brain structures in animal models: the intracortical microstimulation (ICMS) (*e.g.* Sessle and Wiesendanger, 1982; Eisner-Janowicz et al., 2008; Liu and Rouiller, 1999; Wyss et al., 2013), the stimulus triggered averaging (StTA) (*e.g.* Park et al., 2001, 2004, Davidson and Buford, 2004, 2006; Davidson et al., 2007) or spike triggered averaging (SpTA) (*e.g.* Fetz et al., 1976; Cheney and Fetz, 1985; Lemon et al., 1986; Baker et al., 1997; Widener et al., 1997).

The recent development of non-invasive methods of neurological monitoring, mainly devoted to the medical field, has allowed to access anatomical and functional information on the brain *in vivo*. To mention only the main imagery methods, anatomy of the brain has been apprehended with magnetic resonance imaging (MRI) and scanner techniques whereas the monitoring of neuronal activity was achieved by recording electrical or magnetic changes, using electroencephalography (EEG) and/or magnetoencephalography (MEG). Alternatively, neural activity was derived from regional metabolic changes (*e.g.* blood flow) resulting from neuronal activity, recorded with functional magnetic resonance imaging (fMRI) or positron emission tomography (PET) (for review see Crosson et al., 2010).

1.2. Anatomical bases of the central nervous system for planning and execution of voluntary movements

Numerous structures of the central nervous system contribute to the correct planning and execution of voluntary movements (Fig. 1). The motor control of voluntary movement is coordinated by the motor system in close collaboration with the somatosensory system. As a generalization (Fig. 1), information for voluntary movements is generated at the cortical level,

predominantly in the motor cortex, in specific neurons projecting to the spinal cord via the pyramidal tract (PT). Regardless of the origin of its component fibers, the PT is so called due to its course longitudinally in the pyramid of the medulla oblongata. On one hand, these projections terminate (directly or indirectly) onto the spinal motoneurons, located in the ventral horn of the spinal cord, thus forming the corticospinal tract (CST). On the other hand, these corticofugal projections terminate also at bulbar level, so-called the corticobulbar tract which in turn connects to the spinal cord via bulbospinal pathways. These two types of descending projections contribute to the control of voluntary muscles activity. Among these descending projections, some have the particularity to directly connect to the motoneurons (Fetz and Cheney, 1980), thus forming the direct corticomotoneuronal (CM) projection system. These direct CM projections are considered to be a primate specialization allowing the fine motor control, underlying the fractionated and independent finger movements (Bortoff and Strick 1993). The set of projections originating from the brainstem structures and connecting to the spinal cord motoneurons are generally considered as modulatory systems contributing to voluntary movements, in addition to a crucial role played for the control of posture and balance.

Three hierarchical levels of control for voluntary movement are organized in parallel, each involving somatosensory pathways to inform on the body position and the ongoing execution of movements, integrating all these inputs to adjust and modulate the movements. The lower level of motor control takes place in the spinal cord without intervention of upper structures. Considered as reflexes, this automatic and stereotyped motor control is carried out by intrinsic spinal cord neuronal circuits. The second hierarchical level of motor control is achieved at brainstem level, in order to modulate and adjust intrinsic spinal cord neuronal circuits. The third hierarchical level of motor control is located at cortical level. The cortical control of voluntary movements occurs both at time points preceding the movement execution itself to plan complex movement sequences and in real time to coordinate and adjust movements while they are executed. Two main additional subcortical structures take part indirectly to the motor control through connections with the previously mentioned levels of motor control. Comparisons between the executed and the planned motor movement as well as between information from somatosensory and motor regions takes place in the cerebellum. These comparisons lead to improve movement accuracy through connections to the brainstem and thalamus, thus giving access to cortical areas involved in the motor control. As parallel subcortical loops, the basal ganglia are highly connected with cortical areas involved in the

motor planning. The basal ganglia are considered as participating to the movement initiation and facilitation/suppression. These two subcortical structures will not be discussed any further in the present thesis focusing on cortical areas involved in the control of voluntary movement, together with related ascending and descending tracts connecting the cerebral cortex with the brainstem and/or the spinal cord.

1.2.1. The motor system

1.2.1.1. Motor cortex

Motor cortical areas

The motor cortex has been firstly identified by Fritsch and Hitzig (2009) in the rostral most part of the frontal cortex. The motor cortex was initially described as a typical six-layered cortical organization, later described as agranular due to the absence of the granular layer IV (for review see Brodmann, 2007; Fig. 2).

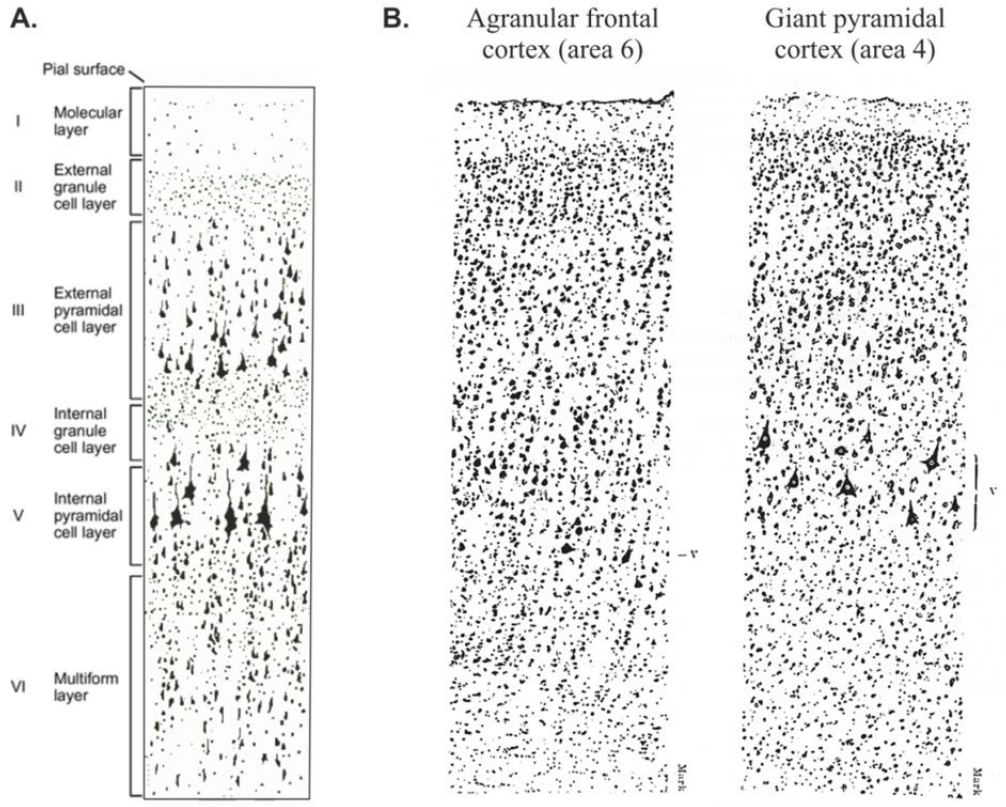

Figure 2: Nissl staining photographs illustrations of the layered organization of motor cortex. (A) The general layered organization illustrating the different six layers (I to VI) of the cortex from the pial surface to the white matter in depth (Modified from Kandel et al., 2000). (B) Differences of cytoarchitecture between the agranular cortex respectively of the area 4 and 6. The giant pyramidal neurons of the layer V has the typical characteristic of the area 4 giving rise to the corticospinal tract (Brodmann, 2007).

The early cortical cartography reported by Brodmann (2007) distinguished two cytoarchitecturally distinct areas within the precentral region of the agranular frontal cortex: (*i*) the area 4 in the territory immediately rostral to the central sulcus containing giant pyramidal cells in layer V, referred to as Betz cells; (*ii*) the area 6 extending rostrally to the area 4, without the giant pyramidal (Betz) cells (Fig. 2 and 3). The transition from area 4 to area 6 is progressive, with a gradual decrease of Betz cells' size and density. The concept of a distinct premotor cortex (PM), corresponding to the area 6 of Brodmann, separated from the precentral primary motor cortex (M1), is based on electrophysiological and cytoarchitectonic evidences (Weinrich and Wise, 1982). However, the premotor cortex areas were firstly described as a pure agranular cortex where Betz cells were absent, later study has revealed the presence of fairly large pyramidal cell in the layer V (Weinrich and Wise, 1982). These large pyramidal cells in the layer V remain generally smaller and less dense than in the area 4. The presence of corticospinal (CS) cells, the support of fine and precise voluntary movements, has been reported in most cortical areas involved in motor control. However, the initial cytoarchitectonic description of the motor cortex as agranular cortex tends to be revised. The absence/presence of a layer IV in the motor cortex gave rise to a recent debate (García-Cabezas and Barbas, 2014; Barbas and García-Cabezas, 2015). Recent evidences have exhibited the presence of the granular layer IV mainly in the motor cortex. The description of such layer IV invaded by the pyramidal neurons of the neighboring layer III and V differed from the classical description.

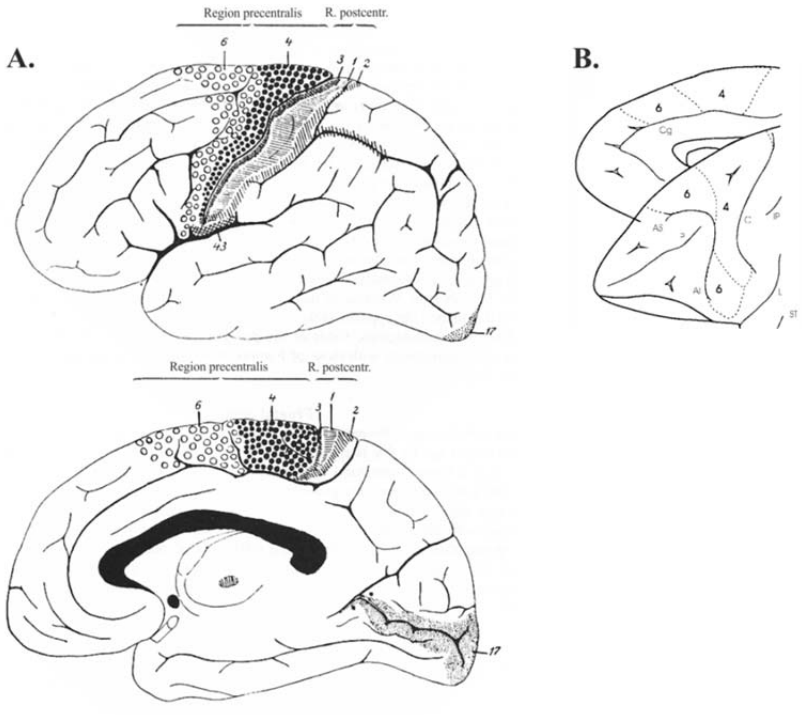

Figure 3: Brodmann (2007) subdivisions of the motor cortex in human (A) and monkey (B) based on cytoarchitectonic differences. 1, 2, 3, 4 and 6, areas 1, 2, 3, 4 and 6; AI, inferior arcuate sulcus; AS, arcuate sulcus; Cg, cingulate sulcus; C, central sulcus; IP, intraparietal sulcus; L, lateral fissure; P, principle sulcus; ST, superior temporal sulcus.

The motor cortex in the large sense has long been known to be organized into different areas (for review see: Hepp-Reymond, 1988; Fig. 4). Anatomical and electrophysiological data led to characterize the motor cortex as an assembly of several motor areas located at different regions of the frontal cortex and organized as networks of highly interconnected cortical areas. The modern concept of motor cortex emerging from these data takes into consideration at least 6 premotor areas (*e.g.* Rizzolatti et al., 1998; Dum and Strick, 2002; Fig. 4). This subdivision of Brodmann area 6 comprises: (*i*) the ventral and the dorsal premotor areas (PMv and PMd) extending on the lateral surface of the hemisphere rostral to M1; (*ii*) the supplementary motor area (SMA) and cingulate motor areas (CMA), the rostral, dorsal and ventral areas (CMAr, CMAd and CMAv) also considered as the Brodmann's area 23 and 24, all extending along the medial wall of the two hemispheres. The existence of corticospinal projections originating from these different non-primary motor areas gives them the potential to rather take part to direct motor control of voluntary movement (Dum and Strick, 1991), although some of their effects are suggested to be relayed via M1 (*e.g.* Schmidlin et al., 2008). Some authors consider further subdivisions differentiating the rostral (PMv-r/F5, PMd-r/F7 and pre-SMA/F6) from the caudal (PMv-c/F4, PMd-c/F2, and SMA-proper/F3) parts of PMv, PMd and SMA (for reviews see Matelli 1985, 1991; Matsuzaka et al., 1992; Rizzolatti et al., 1998; Wu et al., 2000; Fig. 4). PMd-r and pre-SMA have been further differentiated anatomically, in a study using retrograde labelling, by the lack of corticospinal projections,

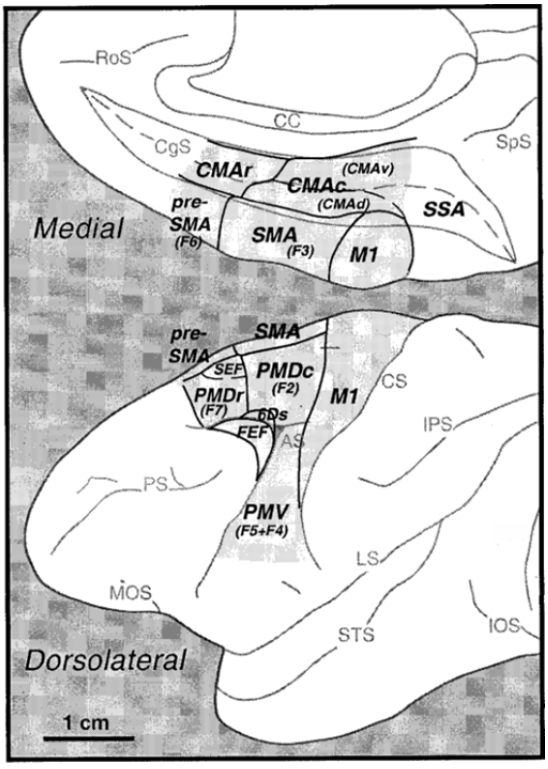

Figure 4: Medial and dorsolateral views of the motor cortex subdivisions based on different features and leading to different nomenclature in monkey: (*i*) the modern functional map: M1, primary motor cortex; CMA, cingulate motor cortex; FEF, frontal eye field; PMD, dorsal premotor cortex; PMV, ventral premotor cortex; Pre-SMA, pre-supplementary motor cortex; SMA, supplementary motor cortex; SEF, supplementary eye field; SSA, supplementary sensory; (*ii*) the histochemical and cytoarchitectonic map: F, frontal, 1 to 7 (Matelli et al., 1985, 1991). (Modified from Wu et al., 2000). AS, arcuate sulcus; CC, corpus callosum; CgS, cingulate sulcus; CS, central sulcus; IOS, inferior occipital sulcus, IPS, intraparietal sulcus; LS, lateral sulcus; MOS, medial orbital sulcus; PS, principle sulcus; RoS, rostral sulcus; SpS, splenial sulcus; STS, superior temporal sulcus; r, rostral; c, caudal.

their descending projections terminating mainly in the brainstem (Keizer and Kuypers, 1989).

Somatotopic organization

Extensive early electrophysiological studies have described a detailed and precise mapping of the different body parts over M1 (Fig. 5), culminating with the famous homunculus for human (Penfield and Rasmussen, 1950) and the simiusculus for the non-human primate (Woolsey et al., 1950). This early representation of the somatotopic organization segregated point-to-point the control of the different body parts mediolaterally from the lower limb to the upper limb and the face parts, down to different segments of the fingers in the limb representations. Since then, evidences amend this segregated and sequential body parts representation on the medio-lateral axis of M1, arguing instead for a tendency towards a certain degree of overlaps of smaller body part inside larger body parts representations. A certain degree of overlaps and multiple representations of fingers, hand, elbow and shoulder territories has been demonstrated with extensive anatomical (Rathelot and Strick, 2009), electrophysiological (for review see Schieber, 2001) and imagery (Rao et al., 1995; Lotze et al., 2000) assessments of the somatic representation (Fig. 6). The concept of a mosaic representation of multiple body parts has emerged (*e.g.* Schieber, 2001). More precisely, a systematic mapping of the arm representation of M1, using the StTA technique, has revealed a representation with a central core zone evoking movement of distal muscles surrounded by horshoe-shaped zone evoking movement of proximal muscles, the two separated by a large zone evoking intermingled movement of both distal and proximal muscles (Park et al., 2001). Furthermore, ICMS studies have frequently exhibited the possibility to regularly evoked movements in other different body parts applying supra-threshold stimulations, remaining however movements of adjacent body parts of those evoked by the lower-threshold stimulation (Nudo 1992).

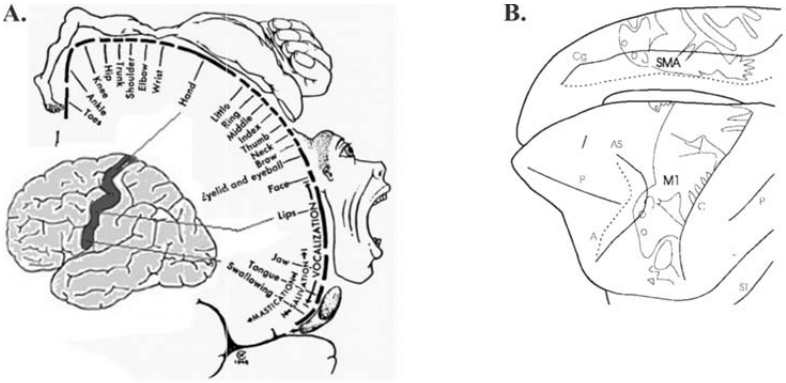

Figure 5: Representation of the somatotopic body map organization of the precentral motor cortex: the motor homunculus for human (modified from Penfield and Rasmussen, 1950) and the simiusculus for the non-human primate (Woolsey et al., 1950).

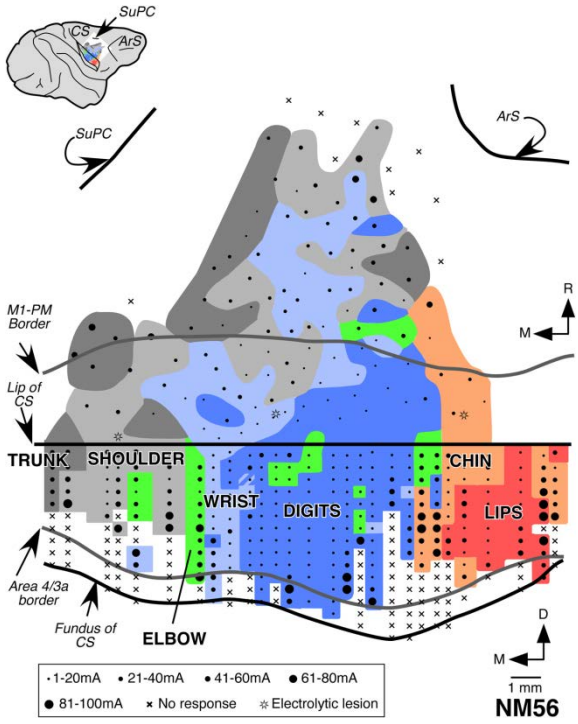

Figure 6: Example of somatotopic body parts representation in the primary motor cortex (M1) for the upper body parts in a macaque monkey. Cortical mapping are delineated by movement evoked at low-threshold stimulation following ICMS at these different cortical sites (reproduced from Kambi et al., 2011). ArS; arcuate sulcus; CS, central sulcus; PM, premotor; SuPC, superior precentral dimple; D, dorsal; M, medial; R, rostral.

Considering the arm representation within M1, higher degrees of cortical motor organization has been emphasized. Two distal representations spatially separated have been described within the M1 arm area in a retrograde tracing study of the CST from lower cervical spinal cord segment controlling the upper limb (He et al., 1993). Within M1, a rostral region on the crest of the precentral gyrus distinguished from a caudal region extending into the anterior bank of the central sulcus has emerged, in a study assessing the repartition of the CM cells innervating the lower cervical spinal cord within M1 (Rathelot and Strick, 2009). The localization of the CST in two peaks located in these two distinct regions of M1 does not totally agree with the restrained location of the CM cells in the anterior bank of the central sulcus. Consequently, the rostral region has been designated as an "old" M1, lacking CM cells and containing CST axons connecting indirectly the spinal cord through the intrinsic neuronal circuit of spinal interneurons, and the caudal region has been designated as an "new" M1, containing the CM cells (Rathelot and Strick, 2009).

Extensive studies have reported, into further detail, that different aspects of higher order movements are themselves represented at the single-neuron level. Using a reversed approach recording the neuronal activity in the primary motor cortex during a motor task execution, the representation of muscles and movements have been depicted at the single-neuron level in M1 (Kakei et al., 1999). Neurons in M1 have been reported to code for the force (Evarts, 1968), direction of movements (Georgopoulos et al., 1982), trajectory of movements (Hocherman and Wise, 1990), movement distance and target position (Fu et al., 1995), as for a non-exhaustive listing. Taking these data into consideration, some attempts have been made to segregate spatial representation of various movement parameters

(Graziano, 2006; Z'Graggen et al., 2009; Zartl et al., 2014), however, no clear somatotopic movement parameters segregation has been widely accepted.

Considering the motor cortex as a whole, a certain degree of somatotopic organization has been identified in the non-primary motor areas as well, although not as extensive as in M1. Early, the existence of 4 somatotopic organizations have been suggested to correspond to the PMv, PMd, SMA and CMA, revealed by the neuroanatomical tracing of the direct corticocortical connections with the M1 forelimb, face and leg representations (Muakkassa and Strick, 1979). To date, complementary anatomical and electrophysiological studies led to establish the extent of the somatotopic representations in the different motor areas (for summary review see Rizzolatti and Luppino, 2001). Based on the corticospinal projections traced from the dedicated spinal cord segments, topographic differentiation of arm and leg representations have been reported in the PMd, PMv, SMA, CMAd, CMAv, CMAr, in addition to the established M1 somatotopy (He et al., 1993, 1995). ICMS investigations in PMv exhibited that stimulations elicit movements in the forelimb, precisely in the proximal and distal forelimb mainly wrist and digit, and orofacial movements (Gentilucci et al., 1988; Preuss et al., 1996). Similar investigations in PMd exhibited that stimulations in the rostral part elicit movements in the face, the neck and the eyes whereas stimulations in the caudal part elicit movements in the hindlimb and the forelimb, precisely in the proximal and distal forelimb mainly the shoulder and the elbow (Gentilucci et al., 1988; Preuss et al., 1996). Concerning the SMA, ICMS investigations have revealed a rostrocaudal somatotopic representation progressing from orofacial, forelimb and hindlimb movements (Mitz and Wise, 1987, Kurata, 1991). Finally, the connectional data resulting from the examination of the cingulate projections distribution over the equivalent somatotopic primary and non-primary areas have revealed an antero-posterior somatotopic organization progressing from the face, to the forelimb and the hindlimb (Morecraft and Hoesen, 1992).

Corticocortical connectivity of the motor cortex

High degrees of corticocortical connectivity exist between the various motor areas revealing their arrangement in the form of a network. This characteristic has been used as a criterion to define the different motor cortical areas as part of the motor cortex for the control of voluntary movement and their somatotopic organizations. The corticocortical connectivity can be considered at the intrahemispheric level and at the interhemispheric (callosal) level.

Intrahemispheric corticocortical interconnections

Giving early evidences for four different "premotor" areas (CMA, SMA, PMv and PMd), anatomical tracing study exhibited the somatotopic intrahemispheric projections onto the face, arm and leg M1 territories. Evidences exist also for reciprocal connection of M1 with the somatosensory cortex (Künzle, 1978; Matsumura and Kubota, 1979; Muakkassa and Strick, 1979). The extent of the somatosensory corticocortical projections in the context of the motor control will be further described [in the following paragraph addressing the *Corticocortical connectivity of the somatosensory cortex*].

Many studies have raised the question of the motor areas corticocortical connectivity. These reports led to the definition of networks of interconnected motor, parietal and somatosensory areas. Well described by Stepniewska and colleagues (1993), these M1 corticocortical interconnections interestingly appeared to differ considering the caudal or the rostral parts of M1, in part due to the difference of somatosensory connections. The corticocortical connectivity was specifically addressed for the digit representation common to all the non-primary motor cortical areas and primary motor cortex. These studies revealed a high density of reciprocal connections between M1, PMv and PMd, representing a dense interconnected network, and additional though less dense connections (Leichnetz, 1986; Tokuno and Tanji, 1993; Dum and Strick, 2005; Dancause et al., 2006) (Fig. 7). In more detail, the strongest projections to the digit representation of M1 have been shown to arise from the PMv and PMd areas, SMA representing the third source of inputs to M1. All cingulate motor areas have been shown to project to the M1 digit representation. However, CMAd quantitatively represents the main cingulate origin, giving rise to stronger projections than the other two CMA areas. PMv and PMd have been shown to receive their strongest inputs from M1, the second source of inputs being from SMA and the third one from the second premotor area, respectively from PMd for PMv and from PMv for PMd. As for M1, all the cingulate areas have been shown to project to the digit representation of PMv, but only CMAd has been shown to give strong inputs to PMd. Within M1, the origins

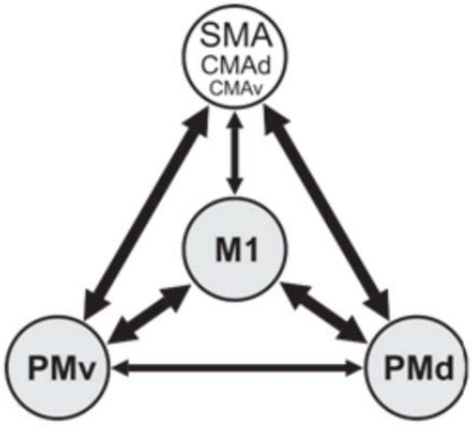

Figure 7: Schematic representation of the network connectivity between the motor cortical areas on the lateral surface (field in grey) and on the medial wall (field in white) for the motor control of the voluntary hand movement. The different widths of the arrow indicate the strength of connectivity (Modified from Dum and Strick, 2005) Abbreviation as in figure 4.

of the somatotopically organized connections to PMv and PMd are restricted to specific regions devoted to each body territory as well as to region intermingling projections to these two areas. Within each premotor area, the origin of the projections to M1 overlaps the regions projecting to the other premotor areas. In these three motor areas (M1, PMd and PMv), corticocortical projections have been shown to originate from neurons located mainly in both deep and superficial layers (Layer III and V). In contrast, the projections arising from CMA have been shown to originate mainly from deep layers (Layer V).

Considering further subdivisions of some non-primary motor areas, the pre-SMA (F6) and the PMd-r (F7) do not exhibit connections with any of the M1, PMd and PMv digit representations (Luppino et al., 1993; Dum and Strick, 2005). Not addressed for the digit representation because deprived of it, these two specific areas appeared to be mainly connected to the non-primary motor areas. The SMA-proper (F3) receives strong inputs from M1, PMd, PMv and CMA. The pre-SMA sub-region, projecting mainly to PMv-r (F5) area, receives strong projections from PMv-r and from the cingulate area 24c, as well as weak inputs from PMd and other cingulate areas (Luppino et al., 1993). The PMd-r region has been shown to mainly receive inputs from non-motor areas such as the frontal eye field, the dorsolateral prefrontal cortex and from the cingulate area 24 (Luppino et al., 2003).

Further corticocortical projections have been revealed with cortical areas which do not belong to the motor cortex but take part to motor control. Anatomical studies have demonstrated the presence of somatosensory inputs to the motor cortex and the presence of motor inputs to the somatosensory cortex (Künzle, 1978; Asanuma, 1981; Leichnetz, 1986). The extent of these reciprocal projections with the somatosensory cortex has been correlated for long time with the correct execution of movement. Of particular interest, forming specific circuit for the motor control, the premotor areas receive inputs from the posterior parietal cortex, with specifically strong inputs to PMv (F4 and F5) from the ventral intraparietal area (VIP) and the anterior intraparietal area (AIP) and to PMd from the VIP and medial intraparietal area (MIP) (Luppino et al., 1999; Tanné-Gariépy et al., 2002).

Interhemispheric corticocortical interconnections

Early anatomical studies have described the interhemispheric connections through the corpus callosum. They have identified different main sources of interhemispheric connections, homologous or not, over the frontal cortex (SMA, CMA and inferior frontal premotor part) as well as with non-primary somatosensory areas (Künzle, 1978; Leichnetz,

1986). However, only sparse and unevenly distributed callosal connections have been described over M1, mainly on the crest region of M1. Retrograde tracing studies have demonstrated regions of sparse or absent callosal projections in the distal forelimb representation of M1 areas. Differently, regions of strong and dense callosal projections in the proximal body part representations of M1 areas have been demonstrated, such as the trunk and proximal forelimb (Jenny, 1979; Künzle, 1978; Leichnetz, 1986; Gould et al., 1986; Rouiller et al., 1994). The interhemispheric connections to M1 hand area have been described to originate mainly from the premotor cortex, the homotopic interhemispheric connections originating from CMA and SMA appeared sparse, nearly inexistent (Rouiller et al., 1994). The M1 hand area has been described to send limited callosal projections, restrained to the ventral zone of PMv and PMd (Boussaoud et al., 2005).

Detailed anatomical studies, focused on the distal forelimb representations, assessed the interhemispheric connectivity of the different subdivisions of the motor cortex. The distal forelimb area of SMA have been shown to send dense homotopic projections to the distal forelimb area of the contralateral SMA, homotopic projections to CMA and heterotopic projections to the premotor cortex (Rouiller et al., 1994; Dancause et al., 2007). Origins of the callosal inputs to SMA have been shown to differ for the pre-SMA and the SMA-proper subdivisions, based on a retrograde tracing study (Liu et al., 2002). The neuronal origins of the callosal inputs to the pre-SMA subdivision have been predominantly observed in the rostral part of the SMA, CMA, PMv and PMd. In contrast, the neuronal origins of the callosal inputs to the SMA-proper have been found predominantly in the caudal part of the SMA, PMv and PMd and described to be homogenously distributed in the CMA regions. Concerning the premotor cortex, PMv-r and PMd-r have been shown to receive callosal projections from homotopic different areas, mainly restrained to their dorsal part. These regions, especially PMd-r, have been described to receive dense callosal projections from the prefrontal cortex and their homotopic counterpart, but not from M1. The PMv-c and PMd-c have been described to receive strong input from their respective rostral PMv-r and PMd-r counterparts and weak callosal projections from M1, as already mentioned (Marconi et al., 2003; Boussaoud et al., 2005).

Role of the different cortical motor areas

As a result of the described presence of CST projections originating from the different motor areas, each of the SMA, PMd, PMv and CMA sub-regions, and also obviously M1, are able to generate movements (Keizer and Kuypers, 1989). However, studies assessing the

electrical excitability of these motor areas have revealed differences among their electrical properties to elicit movements. M1 elicits movement at weaker electrical stimulations than all other motor areas, requiring stronger stimulations increasing from SMA, CMAv-CMAd, CMAr, PMv to PMd (Cheney et al., 2000). Although able to generate movement, the different motor areas appeared to be involved with certain specificity in different aspects of the motor control of voluntary movements. Primary motor cortex (M1)

M1 is commonly assumed to be the predominant generator of the final cortical motor outputs command (Evarts, 1968; Fetz and Cheney, 1980; Lemon et al., 1986), playing a primordial role in individualized fingers movements (Porter and Lemon, 1993; Schieber and Poliakov, 1998; Brochier et al., 1999; Fogassi et al., 2001). More specifically, M1 activity has mostly an excitatory action on the muscles of the contralateral body side (*e.g.* Maier et al., 2002). This activity has been shown to be coded at the neuronal level for a wide range of movement parameters (Fetz, 1992), including the force, direction, speed/acceleration, muscles activity and position of the hand or the joint rotation, multijoint posture, movement distance, target position and others (*e.g.* Evarts, 1968; Georgopoulos et al., 1982; Caminiti et al., 1990, 1991; Ashe and Georgopoulos, 1994; Fu et al., 1995; Schieber and Poliakov, 1998; Kakaei et al., 1999; Sergio et al., 2005; Hamel-Pâquet et al., 2006). Evidences emerged in favor of a dichotomy between the caudal and the rostral parts of M1 (Friel et al., 2005; Sergio et al., 2005). The caudal part of M1 has been described to participate to the temporal pattern of force production, the dynamics of motor output and the accuracy of the movement. The rostral part of M1 rather participates to the overall direction and kinematics of hand motion and in the processing or integration of the cutaneous information with motor commands.

M1 exhibits neuronal activity mainly before and during the movement execution of the contralateral arm. However, activity related to the ipsilateral arm has also been reported, revealing an obvious role of M1 in bilateral/bimanual control of movement, as well as ipsilaterally during unilateral movement (Salmelin et al., 1995; Kermadi et al., 1998, 2000; Ehrsson et al., 2000; Cisek et al., 2003). M1 bilateral activation in case of unilateral movement has been reported for complex finger movements (Shibasaki et al., 1993; Salmelin et al., 1995; Chen et al., 1997; Ehrsson et al., 2000).

Supplementary motor area (SMA)

Early suggested to be mainly active before the movement (Brinkman, 1979), SMA (for review see Nachev et al., 2008) was described to play a major role in initiation of self-paced

movement sequences (Kermadi et al., 1997) and in the preparatory/initiation of more complex movement (Rouiller et al., 1997). Moreover, SMA exhibits a movement-related activity presenting a correlated bilateral increase of activity linked to the increase of task complexity, equivalently excitatory or inhibitory (Maier et al., 2002; Nachev et al., 2008). Such findings support the importance of this motor area in the planning and the execution of complex sequential movements (Shibasaki et al., 1993). Evidences for two distinct sub-regions of SMA are correlated non-only with differences in connectivity (see the above section on *Corticocortical connectivity of the motor cortex*), but furthermore with different functionalities (Matsuzaka, 1992; for reviews see Picard and Strick, 1996; Rizzolatti et al., 1998; Luppino and Rizzolatti, 2000; Rizzolatti and Luppino, 2001). The SMA-proper area (F3) has been mainly involved in the movement execution, showing activity changes time-locked with the movement onset. The pre-SMA area (F6) has been mainly associated to the selection and the preparation of movement, exhibiting activity changes during periods preceding the movement. Generally, pre-SMA is involved in the organization of sequential movements and the learning of novel sequences during the initial phase of correct performance. Active well in advance before the movement initiation, F6 is implicated in the transformation of the potential motor actions generated by the area PMv-r (F5) in actual movement to allow and active timely and useful movement onset. The SMA-proper is suggested to play an important role in the postural control, particularly for the postural adjustments preceding voluntary movements. In relationship, SMA-proper is mainly active in association with active movement as for M1, but contrariwise to M1, the proximal and distal limb movement representations are anatomically overlapped and electrical stimulations commonly induce multiple joints movements.

Dorsal premotor cortex (PMd)

PMd, although showing activation during and after arm movements, exhibits strong activation during the period of instructed-delay. This correlates to a role of PMd in the specification of the reaching movements at the movement planning level, independently of the body side subsequently involved (Crammond and Kalaska, 2000; Cisek et al., 2003). During period preceding the movement, PMd has been described to select but also to direct the movement based on external sensory information (visual, spatial or auditory), participating thus to the visual guidance of arm movement trajectory, independently for both arms (Crammond and Kalaska, 2000; Chouinard et al., 2006; Cisek and Kalaska, 2005; Coallier et al., 2015). These roles appear to be anatomically dissociated among the PMd subdivisions

(Chouinard et al., 2006; Cisek and Kalaska, 2005). The rostral part of PMd (F7) is involved in the selection of motor actions based on the somatosensory cues. The caudal part of PMd (F2) is involved in the execution influencing the generation of movement through M1 connectivity.

Ventral premotor cortex (PMv)

PMv is mainly implicated in the planning/preparation of movements and contributes to the voluntary movement execution. However, PMv is also implicated in observatory function linked to motor actions realization. The PMv-r (F5) sub-region is involved in the selection of various hand grip movement preshaping successively in series with the AIP area, anatomically connected. PMv has been described to play an important role: (*i*) contralaterally in the preshaping of the hand grip, differently to the AIP involved bilaterally; (*ii*) in the visual guidance of hand movement; (*iii*) in monitoring the inaccuracy of the hand conformation with the real time movements (Gallese et al., 1994; Sakata et al., 1994; Castiello, 2005; Olivier et al., 2007). Nevertheless, the fact that PMv-r is contralaterally involved in preshaping functions has been disputed, suggesting rather a bilateral implication of PMv-r area as shown by its role in case of large inactivation (Fogassi et al., 2001). For the preshaping, PMv ensures the transformation of the visual properties into motor actions, coding rather for a specific action as a function of the general goal than for single movement. This facilitates association of the visual properties of objects with the appropriate movement, neurons responding selectively to size, shape and orientation of objects (for reviews see Luppino and Rizzolatti, 2000; Rizzolatti and Luppino, 2001; Chouinard et al., 2006). The further selection of correct actions from the prefrontal and cingulate cortex reaches PMv-r through the pre-SMA area. The presence of potential motor action coding for arm movement directed to specific space locations has been described in the PMv-c sub-region (Gentilluci et al., 1988). PMv-c, which forms a circuit with the anatomically connected VIP area, has been described to code for the peripersonal space and the transformation of object location into accurate movement (Luppino and Rizzolatti, 2000).

The direct contribution of PMv to the voluntary movement execution has been described for the dexterous control of force during precision grip and for the finger configuration during object manipulation with tactile exploration (Schmidlin et al., 2008; for reviews see Luppino and Rizzolatti, 2000; Rizzolatti and Luppino, 2001; Chouinard et al., 2006). While stimulation of PMv can directly evoke motor response, evidence suggests that this activity occurred through the connection of PMv-r with M1.

The implication of PMv in observation function linking to motor actions realization is related to the presence of mirror neurons. Observation of motor actions realization results in the activation of these mirror neurons. These neurons thus respond to movement performed by another individual, the same as when this movement was performed by the individual himself, but not the goal of the actions itself or for mimed action (for reviews see Rizzolatti and Luppino, 2001; Chouinard et al., 2006).

Cingulate motor areas (CMA)

The cingulate motor areas are implicated: (*i*) in the motor initiation and motor control of simple and complex movements; (*ii*) during the sensory triggered and self-paced movement; (*iii*) during bimanual coordination of hand movement (Devinsky et al., 1995; for review see Paus, 2001). The different subdivisions have been described to participate to different aspects of voluntary movements (Shima and Tanji, 1998; Picard and Strick, 1996; for reviews see Cheney et al., 2000; Paus, 2001): (*i*) CMAr is mainly activated before self-paced movements and is also critically involved in process of reward-based selection of specific movements; (*ii*) CMAv is mainly related to sensory stimuli; (*iii*) CMAd is preferentially activated when monkeys perform a sequence of arm movement from memory.

1.2.1.2. Descending motor pathways

The descending motor pathways are by definition nerve fiber pathways originating from superior structures in the brain and brainstem which project down the spinal cord to control movements of the body below the head. Ten properties have been listed to characterize a descending pathway (for review see Lemon, 2008), including: neuroanatomical properties (origin cells location, trajectory and terminating pattern and the number and size of the compound fibers), the molecular identity, the neuropharmacological characteristic (neurotransmitters and neuromodulators at the terminal fields) and electrical properties (timing, pattern and type of activity). Different pathways are considered by this definition, distinguishing the descending pathways originating from the cortical areas and those originating from the brainstem (Kuypers, 1964, 1981). Early suggested by Lawrence and Kuypers (1968a and b), two motor descending systems coexist: the lateral system comprising the pyramidal corticospinal and rubrospinal tracts and the medial system with the vestibulospinal, tectospinal and reticulospinal tracts (Fig. 8). This distinction is mainly based on their descending course locations in the spinal cord.

Spinal cord organization

To further describe the descending tract, the spinal cord anatomy has to first be overviewed. Considered for a long time as the effector of the superior structures, the spinal cord is now considered as a part of the CNS inserted in the vertebrae column. The spinal cord contains axonal projection pathways (ascending and descending fiber tracts) in the white matter and intrinsic neuronal circuits in the gray matter, able of autonomous and stereotyped movements (Fig. 8).

The spinal cord presents a general organization both on a rostro-caudal and on an horizontal axis. The rostro-caudal organization present a segmentation of the spinal cord in different levels devoted to the different body parts with four main regions: the cervical segment for the forelimb, the thoracic segment for the trunk, the lumbar segment for the lower limb and the sacral segment for the urogenital body parts. The horizontal organization of the spinal cord consists in the peripheral location of the axonal pathways composing the white matter and the central location of the neuronal cell bodies composing the gray matter, arranged in a butterfly-form structure (Fig. 8). This general organization is well preserved across all the four segmental levels, including the most relevant cervical level for this thesis. According to Rexed (1954), in spite of some variability across the four different segments of the spinal cord, the gray matter exhibits a general organization in 10 cytoarchitectonically different regions. This laminar organization comprises the laminae I to IX along the postero-anterior axis with the Xth region surrounding the central canal. The dorsal laminae relates to sensory connections whereas the ventral laminae relates to motor connections, all separated by intermediate zones were interneurons are located. The lamina IX in the ventral horn

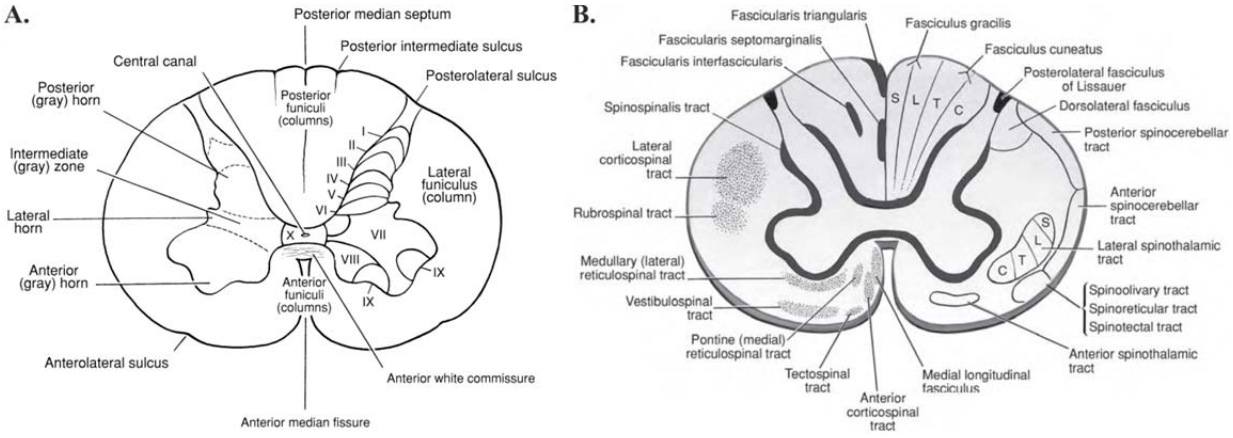

Figure 8: Schematic representations of the spinal cord organization on a transversal view at the cervical level. (**A.**) Illustration showing the gray matter organization with the different regions and the 10 laminae (I to X). (**B.**) Illustration showing the white matter organization with the different somatosensory (surrounded areas) and motor (dotted areas) pathways. (modified from Noback et al., 2005).

contains the motoneuronal cells. The organization of the white matter is more variable across the different caudo-rostral segments of the spinal cord containing the projections for the concerned and the lower body parts. Thus, the lumbar level contains the projections of the sacral and lumbar level whereas the cervical level contains the projections of the sacral, lumbar, thoracic and cervical levels.

Respectively to the segmental organization of the spinal cord, the spinal motor nerves innervating the striated muscles of the upper limb originate from the anatomical enlargement of the cervical segment. The motoneuronal cells are arranged in longitudinal columns of motoneurons extending along further vertebras, forming pools of motoneurons innervating a muscle (Fig 9). These motoneuronal pools display a specific spatial organization on the horizontal plane, forming aggregates innervating progressively from the proximal to the distal forelimb muscles along the medio-lateral axis of the ventral border of the gray matter, the extensors at the ventral most part and the flexors just dorsally (Fig 9; Kuypers, 1981; Jenny and Inukai, 1983).

At such spinal cord level, pre-motoneuronal connections have been described to form the propriospinal tract (for review see Pierrot-deseilligny, 2002; Alstermark et al., 2007). Internal to the spinal cord, the propriospinal tract originates from neurons at the C3-C4 level and projects directly or not on the motoneurons controlling upper limb at the cervical level C6-Th1. This propriospinal tract receives strong inputs from the descending motor tracts providing excitatory or inhibitory control. This tract has been thus involved in the mediation of the motor control of the voluntary movement.

As a part of the CNS, the spinal cord is potent for integration, modification and generation of information. Highly connected to supraspinal structures, the spinal cord presents however the ability to produce rhythmic movements without supraspinal control, such as for locomotion, as firstly experimentally demonstrated in decerebrate cats preserving the stretch reflex (Sherrington, 1910). The intrinsic neuronal networks of the spinal cord, referred as central pattern generators, are able to generate rhythmic movements, albeit subjected to the supraspinal control (for reviews see MacKay-Lyons, 2002; Edgerton et al., 2004). Furthermore, a study has indicated that the spinal cord is capable of specific motor tasks learning. In this study, cats subjected to complete spinal cord transection was capable to learn locomotion after step training and patient, although not capable of learning locomotion,

presented the capability to appropriately coordinated EMG activity during assisted locomotion (Hodgson, et al., 1994).

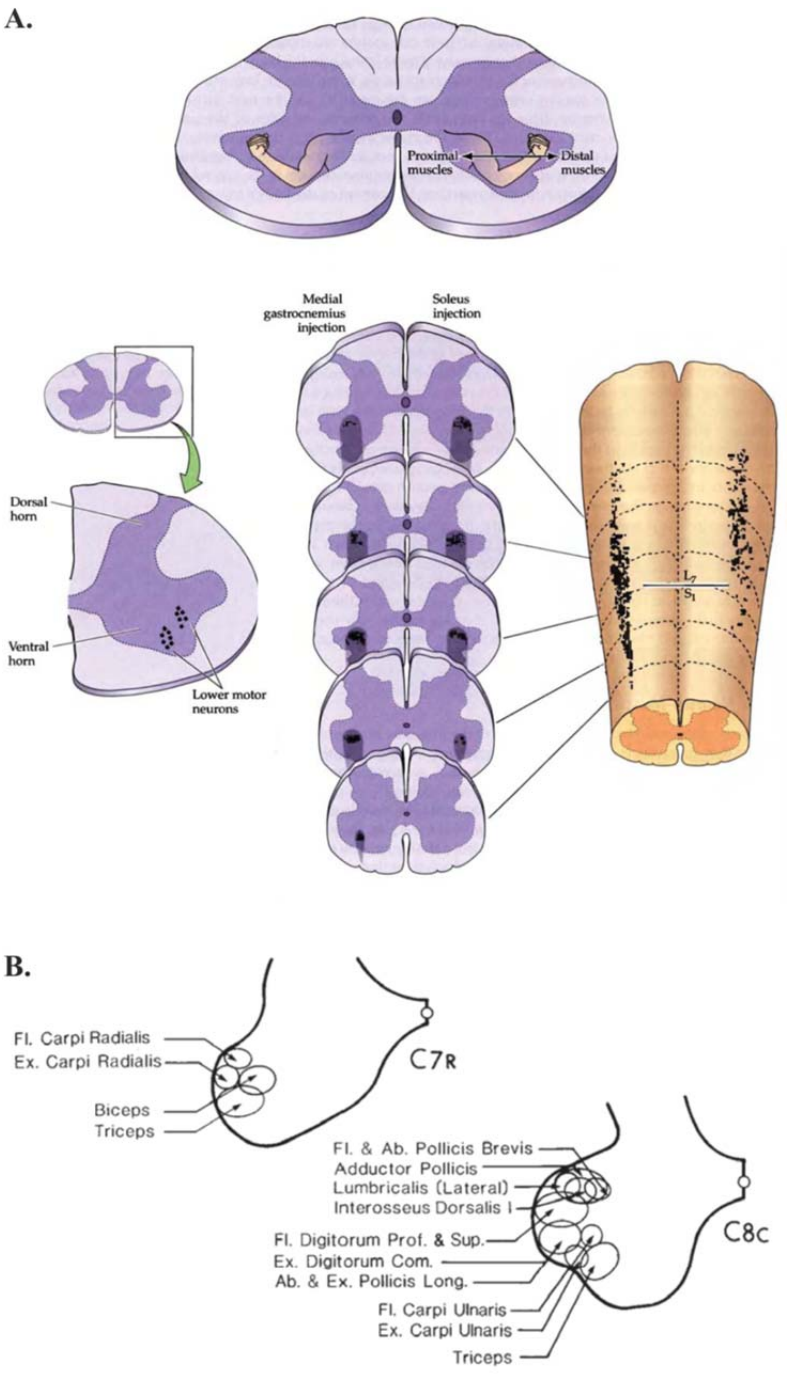

Figure 9: Somatotopic organization of the spinal cord. (**A.**) An illustration of the spinal cord on a transversal view showing the motoneurons arrangement for the forearm control among the ventral horn of the gray matter. The lower set of spinal cord illustrations represent an example of the motor neuron column arrangement extending along the caudo-rostral axis (modified from Noback et al., 2005). (**B.**) More detailed representation of somatotopic organization of several forelimb muscles motoneuronal pools on transversal views of the ventral horn of the spinal cord gray matter at C7 and C8 levels (modified from Jenny and Inukai, 1983). Ab., abductor; Ex, extensor; Fl., flexor.

Descending cortical pathways

The descending cortical pathways originate from pyramidal neurons, not only from giant Betz cells but also from other pyramidal neurons of smaller somata size in the cortical layer V. Termed pyramidal tract (PT), these pathways gather the corticospinal tract (CST) and

the corticobulbar tract, thus termed owing to their terminations, respectively in the spinal cord and in brainstem cell groups (Fig. 10).

Corticospinal tract (CST)

The CST represents a central substrate for the motor control and for the initiation of voluntary movement (for review see: Evarts, 1966; Lawrence and Kuypers, 1968a, 1968b; Kuypers, 1981; Porter and Lemon, 1993; Schieber, 2007). Since early, anatomical and electrophysiological findings have evidenced direct terminations of a subgroup of CS fibers onto spinal cord motoneurons (Bernhard and Bohm, 1954; Liu and Chambers, 1964; Lawrence et al., 1985). These fibers referred to as direct corticomotoneuronal (CM) projection system have been more recently characterized as the anatomical support for manual dexterity (Bortoff and Strick, 1993). Currently, plentiful evidences have confirmed the number of CM fibers and their contribution to the motor control of fractionated and refined dexterous movements (Lawrence and Hopkins, 1976), CM fibers foremost terminating at cervical level for the forelimb muscles. It was also demonstrated that the majority of these CM cells presents facilitatory effects on multiple distal forelimb muscles, the inhibitory effects being produced through disynaptic connections via interneurons (Fetz and Cheney, 1979; Porter and Lemon, 1993; de Noordhout et al., 1999; McKiernan et al., 1998). The CM system of connections, representing a prerogative of primates, interestingly appears to emerge along the species evolution, increasing the motor control ability of hand muscles in link to the development of the manual dexterity, in particular the precision grip between finger-thumb tips, culminating for human subjects (Courtine et al., 2007).

The corticospinal pathway contains the largest axonal diameter fibers with the largest myelin sheaths, making them the fastest fibers of the primate nervous system with conduction velocities reaching 70 ms^{-1} or so (Bernhard and Bohm, 1954; Shapovalov et al., 1971; Burke et al., 1990). Though, certain variability is observed among the CST, which contains a substantial amount of fibers of small axonal diameter and even few unmyelinated fibers. Different axonal diameters have been described to compose the CST and while containing the largest (10-20 µm) and fastest axons, the majority of the fibers have been described as small-diameter axons (1-4 µm) (Rothwell, 1987; Firmin et al., 2013). The general trajectory of the CST is well established (Schieber, 2007; Fig. 10). Originating from several motor cortical areas, the CST goes down through the internal capsule to reach the brainstem ventrally in the pyramids. At the pyramidal level of the brainstem, the majority of the fibers cross the midline to travel on the contralateral side of the spinal cord and connect directly or indirectly to

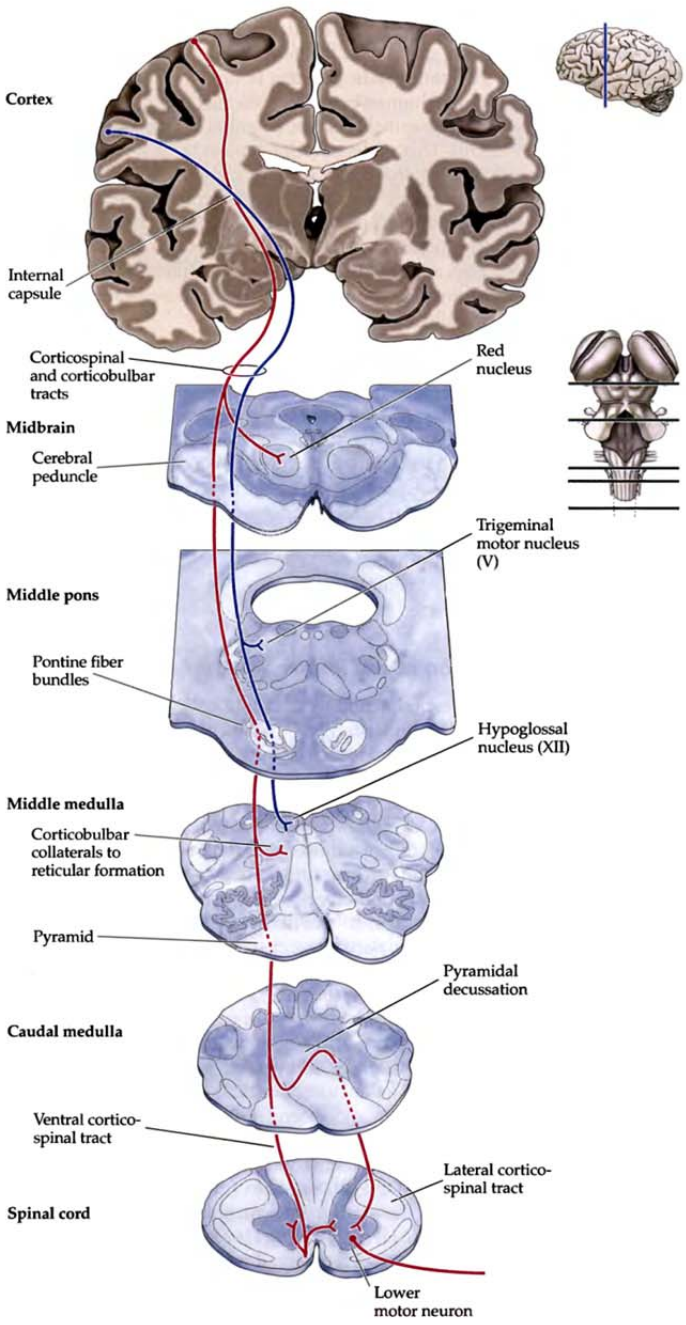

Figure 10: Descending motor tracts, the corticospinal and corticobulbar tracts from neurons at the cortical level descending to the brainstem and the spinal cord. The descending corticospinal tract is represented for its main dorsolateral component, decussated at the pyramidal level, and ventral component at the spinal cord level. The cortical level in the motor cortex is illustrated on the upper right brain picture. The different subcortical levels of illustration of the descending motor tract are represented on the right picture of the brainstem. (modified from Purves et al., 2001)

motoneurons. Thus decussating, the dorsolateral CST controls muscles of the opposite body side. The CST originates not only from M1 but also from different motor areas as well as non-motor areas. The CST originating from M1 is no longer considered as the main component of the PT. Non-primary motor areas as well as non-motor areas represent together an even larger source than M1 representing no more than 40% of the total number of CST axons (Dum and Strick, 1991; Galea and Darian-Smith, 1994). In a decreasing order of contribution, CS fibers are known to originate from the premotor areas (PMd and PMv), the SMA, the CMA, the primary somatosensory cortex (SI: areas 1, 2, 3a and 3b) and the secondary somatosensory areas (SII), area 5 and the insular cortex (Keizer, 1989; Dum and Strick, 1991, 1996; He et al., 1993, 1995; Galea and Darian-Smith, 1994; Rouiller et al., 1996; Widener et al., 1997; Maier et al., 2002). As an exception, two subdivisions of the premotor cortex and the SMA, namely PMd-r and pre-SMA, do not project to the spinal cord (Keizer and Kuypers, 1989). Leaving the different topographically separated areas, CST axons devoted to the forelimb tend to cluster

progressively from the internal capsule to be gathered at the level of the pyramids. From the pyramidal level, the course of the CST axons down to the spinal cord in the dorso-lateral funiculus presents a topographical medio-lateral arrangement of the fibers devoted to the upper limb progressively to the sacral fibers, without respect regarding the different areas of origin (Morecraft et al., 2002, 2007). At the brainstem pyramids level, the bulk of the CST decussates to descend into the dorsolateral funiculus in the spinal cord (87.9%) and a low proportion of CST axons decussate in the ventral pathway (0.3%). The remaining CST axons (11%) descends along the ipsilateral pathways, in the dorsolateral funiculus (10.1%) and in the ventral funiculus (1%) (Lacroix et al., 2004; Rosenzweig et al., 2010). At the cervical level, ipsilateral facilitatory projections to the spinal cord mainly originate from M1 and supplementary motor (SMA) (Dum and Strick., 1996; Montgomery et al., 2013). Taking separately, some differences appear in the degree of decussation of each motor areas, with the higher amount of decussation of the CST originating from the CMA, almost exclusively decussated, as compared to those from SMA and M1 (Dum and Strick., 1996). At the spinal cord level, different patterns of CST terminations can be observed depending of the areas of origin (He et al., 1995): the motor areas M1, SMA, PMd, CMAd project proportionally more on the cervical and the lumbar enlargements; CMAv preferentially projects to the lumbar enlargement; the bulk of the CMAr projections terminates at the upper cervical enlargement; the PMv does not project lower than the upper part of the cervical enlargement. Interestingly few CS fibers originating from M1 project individually to different levels of the spinal cord and, but rarely, even to both the cervical and the lumbar enlargements (He et al., 1993). A rostro-caudal gradient of CST termination fields on the motoneuronal zone of the Rexed laminae IX has been demonstrated at the cervical enlargement for both SMA and M1 CST indicating their preferential intrinsic hand muscles innervation (Maier et al., 2002; Morecraft et al., 2013). At the cervical level and both for the ipsilateral and contralateral projections, CS fibers arising from both M1 and SMA mainly terminate in the intermediate zone and also present a substantial pool of terminations in the motoneurons area of the spinal cord, Rexed laminae IX (Dum and Strick., 1996; Rouiller et al., 1996; Maier et al., 2002; Morecraft et al., 2013). The M1 projections represent the densest and the widespread distribution of CS fibers in the ventral horn area.

Corticobulbar tract

The cortical motor areas strongly project onto brainstem structures from where the descending brainstem pathways originate. Detailed in the following part (*Descending*

brainstem pathways), the different primary and secondary motor areas diversely contribute to the descending motor pathways mediated by brainstem structures.

Additionally to the corticobulbar projections involved in the descending motor pathways, the cortical motor areas broadly project onto cell groups of the somatosensory system in the brainstem, as the described corticocuneate and the corticogracilis projections participating to the motor control involving the dorsal column nuclei, the brainstem relays of the ascending somatosensory pathway (further detailed in the following part **1.2.2. The somatosensory system**).

Descending brainstem pathways

At the junction of the brain and the spinal cord, the brainstem is at the same time the passageway of numerous descending and ascending pathways controlling information flow and responsible of regulation of basic body functions. As the rostral continuity of the spinal cord, the lower brainstem displays similar axonal and neuronal cells arrangement than the one described for the spinal cord, while the upper part of the brainstem displays neuronal cells aggregates intermingled with axonal pathways migrating progressively on the horizontal plane to their location into the spinal cord along the rostro-caudal axis of the brainstem.

To focus on the motor aspects, the brainstem contains neuronal cells aggregates with axonal projections to the spinal cord controlling motor functions. Observed on a transverse view of the spinal cord, four separate tracts participating to the voluntary movement control originate from four brainstem nuclei: the tectospinal, the vestibulospinal, the rubrospinal and the reticulospinal tracts (Fig. 11). The description of fast conducting fibers among the rubro-, reticulo- and vestibulospinal tracts, is in agreement with their contribution to motor control, the rubrospinal tract conducting at up to 90 ms^{-1} while the reticulo and vestibulospinal tracts up to 80 – 150 ms^{-1} (Shapovalov et al., 1971, 1972; Rothwell, 1987).

Tectospinal tract

Originating from the superior colliculus in the mesencephalic upper most part of the brainstem, the tectospinal tract projects contralaterally down to the cervical level of the spinal cord (Fig. 11). Connecting motoneurons of neck muscles, the tectospinal tract plays a primordial role in the coordination of the eyes movements with the head movements (Wilson and Peterson, 1981).

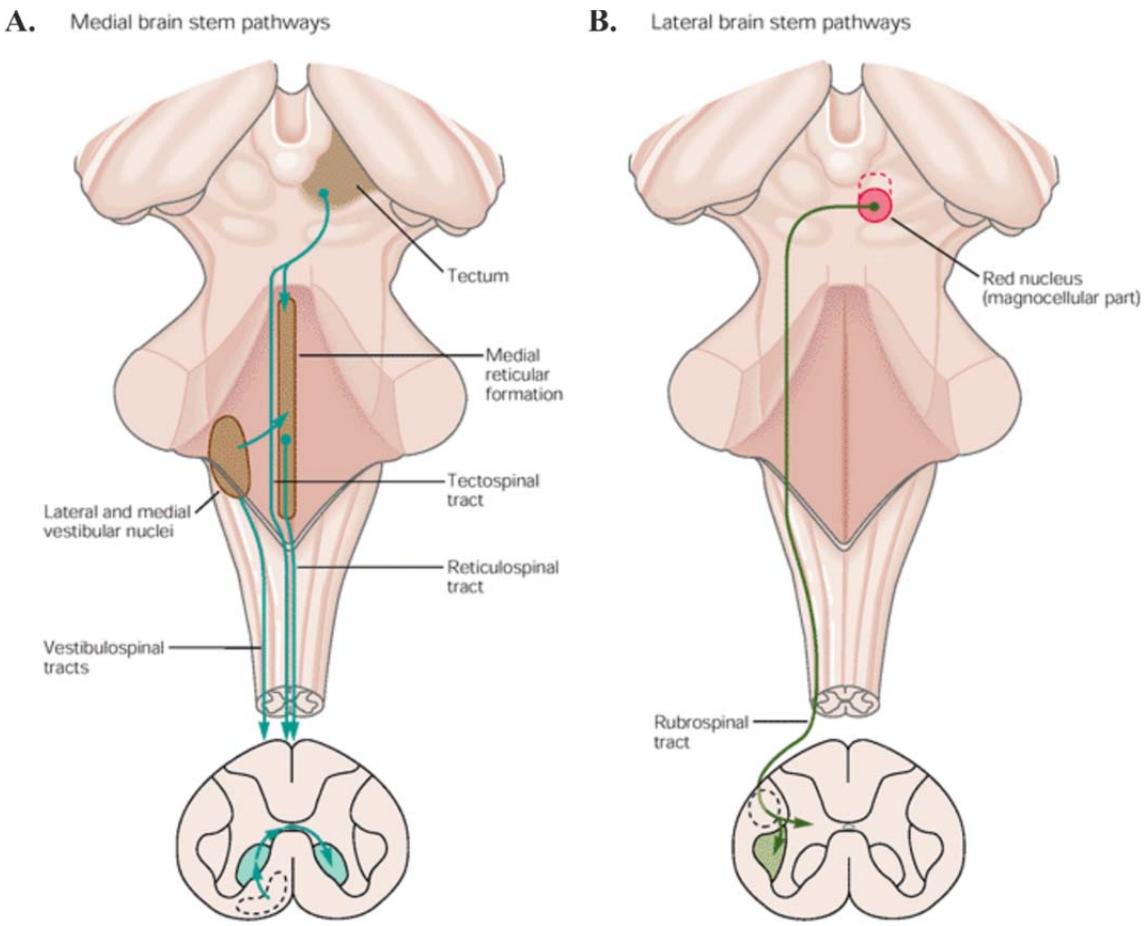

Figure 11: Illustration of the descending bulbospinal tracts, from neurons at the brainstem level descending to the spinal cord. (**A.**) Origins, courses and terminations of the vestibulospinal, tectospinal and reticulospinal tracts in the medial descending system. (**B.**) Origins, courses and terminations of the rubrospinal tracts in the lateral descending system (reproduced from Kandel et al., 2000).

Vestibulospinal tract

Originating from the vestibular nuclei in the bulbar portion of the brainstem, two vestibulospinal tracts go down to the spinal cord (Fig. 11). The mainly ipsilateral lateral vestibulospinal tract and the bilateral medial vestibulospinal tract, display monosynaptic projections on motoneurons controlling neck, back, forelimb and hindlimb muscles for reflex adjustment of the head and posture (Wilson and Peterson, 1981). A certain degree of somatotopic organization was found within the lateral vestibular nucleus which projects through the lateral vestibulospinal tract respecting segregation for forelimb and hindlimb. Differently, the medial vestibular nucleus projecting through the medial vestibulospinal tract does not project beyond the thoracic level of the spinal cord (Kneisley et al., 1978). The vestibular reflexes are subjected to cortical control through vestibulocortical inputs to the parietal cortex, the somatosensory area 3a, motor and premotor areas and corticovestibular

projections from the somatosensory areas 3a and 2, the parietal cortex and the cingulate cortex (for review see Fukushima, 1997).

Rubrospinal tract

In the mesencephalic part of the brainstem, the red nucleus (RN) projects to the spinal cord, forming the rubrospinal tract (for review see Kuypers, 1981; Fig. 11). The rubrospinal tract descends through the spinal cord ventrally to the corticospinal tract, thus, as a part of the dorsolateral motor system. The rubrospinal tract originating from the magnocellular part of the RN (RNm) decussates to reach the contralateral spinal cord, terminating principally in the intermediate zone of the gray matter of the spinal cord, sends also projections to contralateral brainstem structures. The parvocellular part of the RN (RNp) connects the ipsilateral thalamus and olivary nuclei. In link with the evolution of the manual dexterity in parallel with the CST development culminating in primates including humans as compared to rodent, the rubroolivary and the rubrothalamic tracts became predominant in contrast to the rubrospinal tract described as becoming vestigial in human. However, as a result of direct rubrospinal projections to motoneurons (Holstege, 1987; Holstege et al., 1988; Cheney, 1980; Küchler et al., 2002), the role played by the rubrospinal tract on the motor control has been extensively studied. The rubrospinal tract is involved in the facilitation of the spinal reflexes, both excitatory and inhibitory. In contradiction to earlier studies (Massion, 1967), the rubromotoneuronal cells clearly appear to control preferentially distal muscles with strong excitatory effects on extensor and inhibitory effects on flexor muscles in monkeys (Mewes and Cheney, 1991; Cheney et al., 1991; Belhaj-Saïf et al., 1998; Küchler et al., 2002). Anatomical corticorubral connections support the cortical control of the RN from different areas, differentially to the RNm and the RNp part. RNm receives inputs from areas 4 and 6 whereas RNp receives strong ipsilateral cortical input from area 4, SMA, cingulate and parietal areas and small contralateral projections from areas 4 and cingulate (Kuypers and Lawrence, 1967; Burman et al., 2000). Interestingly, the corticorubral projections from M1 display a certain degree of somatotopic organization, segregating the projections from the hand/arm to those from the leg representations of M1 in separated locations in the RNm.

Reticulospinal tract

The reticular formation is organized as a set of interconnected nuclei sparsely distributed among the brainstem (Fig. 11). Generally, three columns of reticular nuclei are considered, related to the median, medial and lateral columns corresponding respectively to the raphe, magnocellular and parvocellular nuclei. These three columns of reticular nuclei

commonly give rise to an ascending tract and a descending tract. Briefly, the ascending reticulospinal tract, considered as the activating reticular system, play a key role in the somatosensory transmission of the nociceptive information through the reticulothalamic projections. The descending reticulospinal tract, involved in the motor control, originates from the medial pontomedullary reticular formation (PMRF) and the caudal raphe nuclei, descending in the spinal cord ipsilaterally in the ventromedial (pontine) funiculus and ipsilaterally and contralaterally in the ventrolateral (medullary) funiculus (Holstege and Kuypers, 1987; Keizer, 1989, for reviews see Peterson, 1979; Kuypers, 1981). Spinal projections from the raphe magnus nuclei to the dorsal horn of the spinal cord via the dorsolateral funiculus exert an inhibitory influence on pain transmission (Holstege and Kuypers, 1987). The PMRF displays a somatotopic arrangement giving rise to two funiculi (for reviews see Peterson, 1979; Kuypers, 1981). The ventromedial funiculus originates from the dorsolateral PMRF region and is preferentially involved in the control of axial and proximal postural muscles. The second ventral bilateral funiculus originates from the ventrocaudal PMRF region and is preferentially involved in the control of the distal musculature. Well-established, the reticulospinal tract plays a predominant role for the control of posture and locomotion. On another hand, the reticulospinal tract is also responsible of the coordination of gross movements of proximal muscles. Thus, the reticulospinal tract: 1) induces the facilitation of ipsilateral flexors and contralateral extensors muscles, 2) induces the suppression of the ipsilateral extensors and the contralateral flexors muscles through monosynaptic connections with forearm and arm motoneurons, 3) has an excitatory influence on the intrinsic hand motoneurons through direct motoneuronal linkage (Peterson, 1979; Davidson et al., 2004, 2006, 2007; Riddle et al., 2009). Early suggested to be predominantly sustained by the crossed lateral funiculus (Peterson, 1979), the reticulospinal tract is involved in the preparation and the performance of voluntary reaching of forelimb movements (Buford and Davidson, 2004). As the other brainstem nuclei involved in the motor control, the reticular formation receives cortical projections. These corticoreticular bilateral projections originate from M1 and premotor cortex, PMd and PMv, sensorimotor cortex, cingulate cortex and SMA (Weinrich and Wise, 1982; Keizer and Kuypers, 1989; Kably and Drew, 1998).

1.2.2. The somatosensory system

The primordial roles of the somatosensory system in the correct realization and the control of voluntary movements are no longer disputed. Furthermore, the description of CM cells (Porter, 1985) in the somatosensory cortices has extended the interest for the direct role of the somatosensory pathways in the control of voluntary movements.

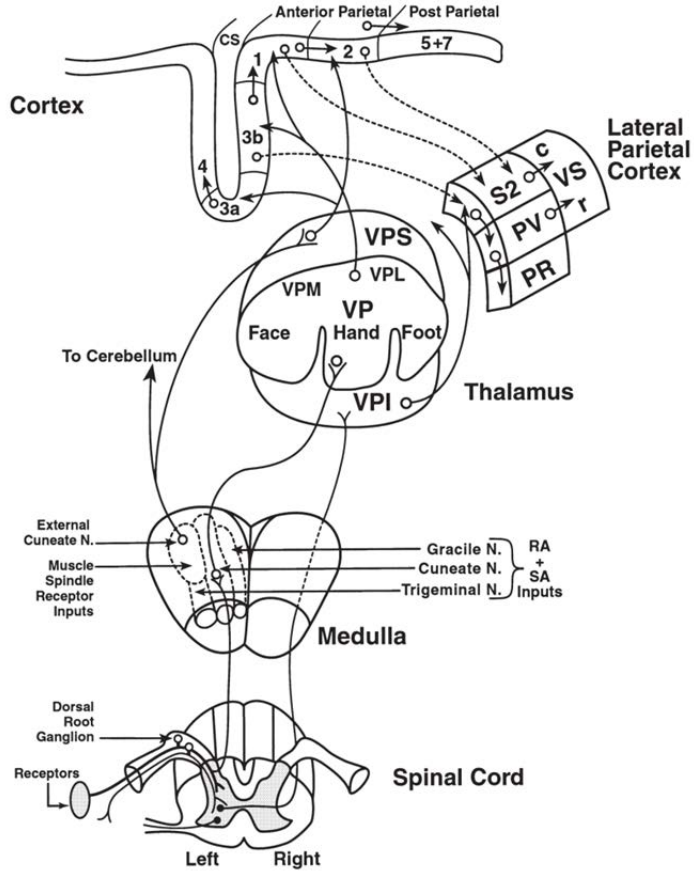

Figure 12: Illustration of the somatosensory system involved in the motor control of the voluntary movement from the peripheral receptor to the cortical regions. S2, secondary somatosensory area; PR, parietal rostral area; PV, parietal ventral; VP, ventroposterior nucleus; VPI, ventroposterior inferior subnucleus; VPL, ventroposterior lateral subnucleus; VPM, ventroposterior medial subnucleus; VPS, ventroposterior superior subnucleus; VS, ventral somatosensory area; c, caudal; n, nucleus; r, rostral (reproduced from Kaas, 2004).

The somatosensory system participates to the motor control conveying somatosensory information from peripheral receptors (the superficial cutaneous receptors of the skin and deep receptors localized in the muscles, the muscle spindle receptors, and in the articulations) to superior structures and cortical areas. Information are conveyed through the dorsal column pathways making relay at the brainstem level in the dorsal column nuclei relays (the gracile nucleus devoted to the lower limb and the cuneate nucleus devoted to the upper limb) and, then, at the subcortical level in the thalamus to finally reach the cortex (Fig. 12).

1.2.2.1. Somatosensory cortex

General organization and anatomy

Cortical areas participating to somatosensory functions have been localized in the parietal lobe. The parietal cortex is principally subdivided into the postcentral gyrus and the posterior parietal cortex containing the superior and the inferior parietal lobules (Figs. 12, 13).

Primary somatosensory cortex (SI)

The primary somatosensory cortex (SI), early described in the cartography of the cerebral cortex by Brodmann (2007), lies in the postcentral gyrus and is characterized by the distinction of four cytoarchitectonally and functionally differentiated areas, the areas 3a, 3b, 1 and 2, respectively, along a rostro-caudal axis. Common anatomical features have been described to be typical of the SI areas, defining a granular cortex which presents dense clusters of small cells in the cortical layers IV and III. Differential cytoarchitectonic features characterize and distinguish the four SI areas (Kaas, 1983; Dykes and Ruest, 1986). Interestingly, pyramidal cells in the layer V have been described in the areas 3a and 3b. These pyramidal cells present however smaller size, even smaller in 3b, and lower density than in M1.

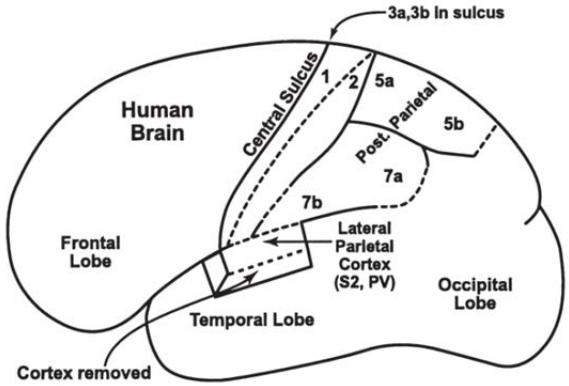

Figure 13: Illustration of the somatosensory cortical areas in the parietal lobe involved in the motor control of the voluntary movement from the peripheral receptor to the cortical regions. S2, secondary somatosensory area; PV, parietal ventral (reproduced from Kaas, 2004).

Secondary somatosensory cortex (SII)

As part of the somatosensory cortex, at least two areas have been distinguished from SI cortex lying within the parietal lobe laterally and posteriorly to the inferior part of SI, the SII caudally and the parietal ventral area (PV) rostrally (Fig. 13). Cytoarchitectonically comparable to SI, these areas present however some dissimilarity. For example, the layer IV is less distinct, less densely packed and narrower than in SI, differences more pronounced for PV than for SII (Kaas, 1983; Burton, 1986; Krubitzer et al., 1995).

Somatosensory associative areas

Considered as somatosensory associative cortices, the areas 5 and 7 are localized in the posterior parietal cortex and lye just caudally to the area 2, the area 5 lying medially to the area 7 (Fig. 13). Without going into details, several subdivisions of these areas have been distinguished, generally considering rostral and caudal parts (5a/PD, 5b/PE, 7a/PF and 7b/PG) all of which participating differently to the motor control (for reviews see Rizzolatti et al., 1998; Fogassi and Luppino, 2005). The cortex of the intraparietal sulcus is considered of main importance in the motor control, generally distinguished into the anterior intraparietal (AIP),

the ventral intraparietal (VIP) and the medial intraparietal (MIP) areas (Rizzolatti et al., 1997).

Somatotopic and functional organization

Generally described as the somatosensory homunculus paralleling the one described for M1, SI presents a somatotopic organization (Fig. 14). However, differently to M1, four separate representations of the body over SI are distinguished corresponding to each of the four SI areas, thus existing as functionally distinct subdivisions. Commonly, the somatotopic organization of the body part over SI medio-laterally represents from the lower limb, the trunk, the upper limb, digits and face body parts. This somatotopic organization presents regions proportionally distorted in favor of the highest innervated body parts. As described for M1, a certain degree of overlapping for the distal body parts representations appears rather than a point to point representation in the SI somatotopic representation. This general organization is described among each of the four SI areas in parallel, with however a tendency for the area 1 to be partially organized in mirror to the area 3b and the area 2 (Fig. 14). The four body map representations in each SI areas reflect some degree of organization

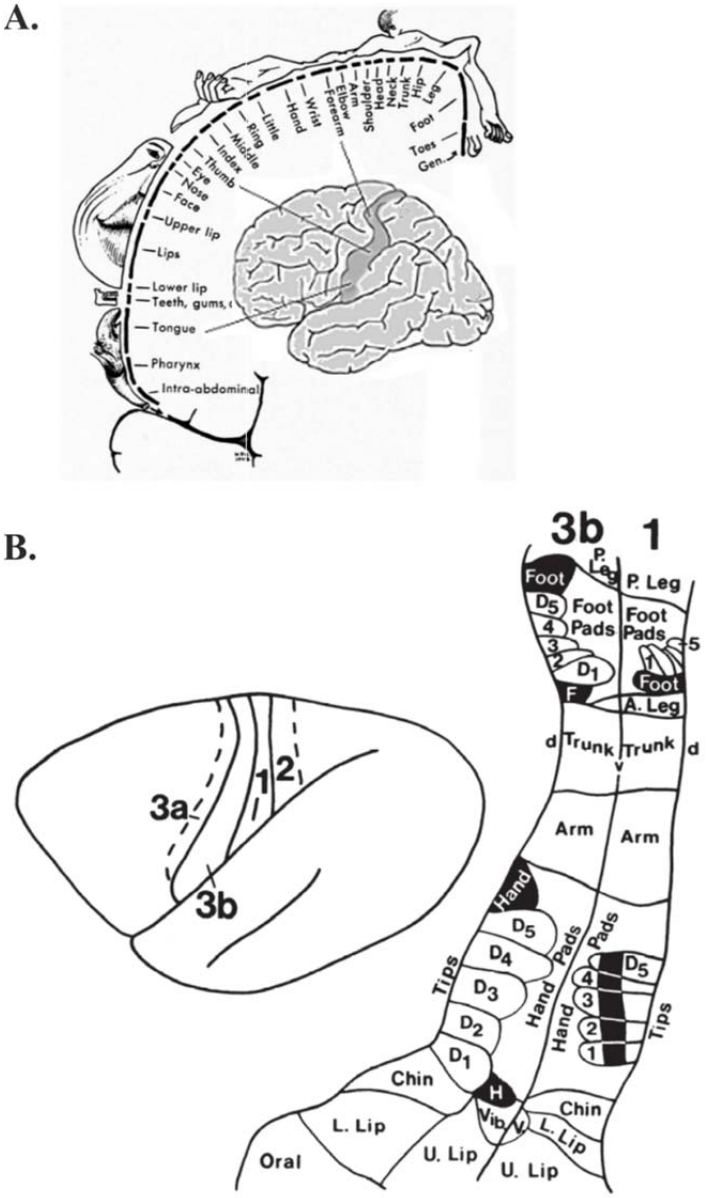

Figure 14: Illustration of the somatotopic organization of the primary somatosensory cortex. (**A.**) Representation of the somatotopic body map organization of the precentral motor cortex: the somatosensory homunculus for human (Penfield and Rasmussen, 1950). (**B.**) Illustration of the somatotopic body map organization in the areas 3b and 1 of SI in the macaque monkey (reproduced from Kaas, 1983). D, digit, Vid and V, region devoted to mystacial vibrissae; U Lip, upper lip; L Lip, lower lip; P leg, posterior leg; A leg; anterior leg; d, dorsal; v, ventral. Shaded region indicate dorsal hairy surfaces.

of the somatosensory afferents (Iwamura et al., 1983; for review see Kaas, 1983). The vast majority of area 3a afferents arise from the muscle spindle, only few neurons respond to cutaneous inputs. Concerning the areas 3b and 1, the cutaneous inputs represent the large majority of the inputs. These two areas are distinguished firstly by the presence of Pacinian receptor inputs in the area 1, not present in the area 3b, and secondly by the difference of the receptive fields, complex and larger in the area 1, contrasting with comparatively smaller and simple receptive fields in the area 3b. The area 2 afferents originate from deep receptors in both joints and muscles, although some arise from cutaneous receptors, mainly from the hand.

Evidences have suggested the presence of at least two well distinguished body maps representations located laterally and posteriorly to SI in the parietal lobe, respectively in SII and PV. These somatotopic organizations are arranged in mirror with a less fine body parts representation than in SI and they contain bilateral receptive fields (Krubitzer et al., 1995; Ruben et al., 2001; for review see Burton, 1986).

Concerning the posterior parietal lobe, although some degree of somatotopy was proposed over the areas 5 and 7, evidences support an organization in functionally distinct circuits dedicated to specific sensorimotor information or coding for specific sorts of movements, as hand-to-mouth, aggressive and defensive movements (Krubitzer et al., 1995; Luppino and Rizzolatti, 2000; Rozzi et al., 2008; Kaas et al., 2011).

Corticocortical connectivity of the somatosensory cortex

As described for the different motor cortical areas, the different somatosensory areas present high degrees of corticocortical connectivity.

Intrahemispheric corticocortical interconnections

At the intrahemispheric level, the different somatosensory areas present their own pattern of projections. Although the four areas of SI are interconnected, some preferential connections predominate. The areas 3b and 1 present dense somatotopic reciprocal interconnections. The area 1 projects densely onto area 2 which projects in turn on the areas 3a and 5. The area 3a presents strong projections onto MI in its rostral part and to area 1. All the SI areas are reciprocally connected to SII (for reviews see Asanuma, 1981; Kaas, 1983; Jones, 1986).

As already mentioned, wide corticocortical connections are described between the somatosensory areas and the motor cortex. The area 4 (MI) presents strong reciprocal

connections with the SI areas 1 and 2 and with the associative sensorimotor area 5 in the parietal cortex as well as direct projections to area 3a (for reviews see Jones, 1986; Stepniewska et al., 1993). MI projects in a somatotopic manner to SI, however the connections with area 3b remain extremely weak and sparsely distributed (Stepniewska et al., 1993). SMA receives inputs from the SI areas 3b, 1, 2 and the area 5, and separately from SII to SMA-proper and from area 7 and to pre-SMA (for reviews see Jones, 1986; Luppino et al., 1993). Concerning the premotor cortex, both PMd and PMv are connected with SII and PV and with the posterior parietal cortex, but only PMv is connected with SI areas 3a, 1 and 2, these connections remaining sparse (Stepniewska et al., 2006; Dancause et al., 2007).

Highly reciprocally interconnected, the associative somatosensory areas 5 and 7 present additional connections to those described above with the somatosensory and with the motor cortex for the participation to the motor control. The area 5 receives strong inputs from SI and appears to have reciprocal connections with MI, premotor cortex and SMA. A certain degree of segregation is reported for these projections, clustering the projections to MI in the anterior part of the area 5 and the projections to the border of MI and to the premotor cortex in its posterior part (Kalaska, 1996; for reviews see Kaas, 1983; Jones, 1986). Further subdivisions of the area 5 have been described (Kaas, 2004). The 5a part receives SI projections from area 2 and projects to the area 7, SII, MI and premotor cortex. The 5b part receives inputs in majority from the 5a part and projects to the adjoining parietal cortex and 7b, SII and PMd. The area 7 in the posterior parietal cortex receives differentiated projections, the 7a part receiving SI inputs and the 7b part receiving SII afferents. While the area 7a is connected to the frontal eye field, the area 7b projects onto PMv and sparsely to PMd (Leinonen et al., 1979; Stepniewska et al., 2006).

As already mentioned, two specific projections are of particular interest: the specific strong inputs to PMv, on the area PMv-c from the ventral intraparietal area (VIP) and on the area PMv-r from the anterior intraparietal area (AIP) and to PMd from the ventral intraparietal area (VIP) and medial intraparietal area (MIP) (Luppino et al., 1999; Tanné-Gariépy et al., 2002; Stepniewska et al., 2006).

Interhemispheric corticocortical interconnections

At the interhemispheric level, as for MI, SI projects homotopically as well as on the adjacent parts of the contralateral SI only for the proximal body parts, no callosal projections are described for the distal part of the limbs (Pandya and Vignolo, 1969; Innocenti, 1986). SI

projects in a topographic manner onto the contralateral SII and SII projects principally homotopically onto contralateral SII (Pandya and Vignolo, 1969). SII receives substantial callosal projections respecting the topographic organization from the contralateral posterior parietal areas, the rostral part of area 7 and the dorsal and medial parts of the area 5. These parietal areas present furthermore non-homotopical projections onto SI and SII (Pandya and Vignolo, 1969). SI and SII receive interhemispheric projections from MI, while SI projects onto the contralateral SI and SII, only the face part of SI sends interhemispheric projections to MI (Künzle, 1978).

Role of the somatosensory cortical areas in the motor control of the voluntary movement

The somatosensory cortex is highly involved in the motor control, not only for integration of somatosensory information for the correct planning and execution of voluntary movements. Anatomical demonstrations of somatosensory inputs in the motor cortex (Asanuma, 1981; Ghosh and Porter, 1988) and motor inputs in the somatosensory cortex (Rathelot and Strick, 2006) corroborate this collaboration. Many studies demonstrating the presence of CS neurons into the four SI areas, but also in other parietal areas, area 5 and SII, raised the question of the direct contribution of the parietal cortex in the motor control of voluntary movement (*e.g.* Sessle and Wiesendanger, 1982; Cheema et al., 1984; Galea and Darian-Smith, 1994; Kaas, 2004).

Primary somatosensory cortex (SI)

SI plays a predominant role in tactile and proprioceptive discriminations (for review see Kaas, 2004). The area 3b contains a complete representation of the cutaneous receptors of the body, almost exclusively of the contralateral side. Inactivation of this area reveals its role in the crude tactile discrimination related to the texture and shape. Thus, this area is involved in the recognition of small objects by touch, and during the grasping. The area 1 contains neurons with larger and more complex receptive fields than in area 3b. These neurons of the area 1 code for the direction of movement on the skin and are modified accordingly to which motor behavior will follow the stimulus. Inactivation of this area reveals its main role in texture discrimination. The area 2 presents a complex representation of both cutaneous and deep receptive fields, with neurons responding individually to one or the other and neurons responding to both. These receptive fields tend to be larger and more complex than those of the areas 3b and 1. Mainly responding to shape or movement directions, inputs originate

mainly from the spindle muscles receptors, suggesting the role of the area 2 in the combination of limbs and digits positions with tactile information during active touch. The area 3a, albeit some cutaneous receptive fields, is largely responsive to the deep receptors and during movements.

The fairly large amount of corticospinal projections originating from the contralateral areas 3a (2.2%), 3b/1 (9%) and 2/5 (13%) (Galea and Darian-Smith, 1994) makes the somatosensory cortex suitable to participate directly to motor control (Matyas et al., 2010). However, weak effects, principally inhibitory, are evoked following stimulations of SI in monkey (Widener and Cheney, 1997). Thus, the nature of the CST projections from SI on motoneurons is suggested to be not consistent with the notion of a robust motor control and the participation of the somatosensory cortex in motor control is suggested to be mediated by the corticocortical connectivity with the motor cortex.

Secondary somatosensory cortex (SII)

Not as extensively studied, SII contains neurons suggested to code stimulus features like roughness and to have bilateral receptive fields, similarly to PV (for review see Kaas, 2004). Giving rise to a certain amount of CST projections (3.4%) (Galea and Darian-Smith, 1994), SII has been suggested to be involved in preparation and somatosensory guidance of movements (Zarzecki, 1986).

Somatosensory associative areas

The posterior parietal cortex is involved in the integration of somatosensory inputs of different modalities, to provide a basis for perceptual process. The posterior parietal cortex is strongly involved in visual information integration and their transformation to develop subsequent movements (Rizzolatti et al., 1997). However, several studies support the role played by posterior parietal cortex in higher order aspects of motor control (Fogassi and Luppino, 2005). The different roles of the posterior parietal cortex are sustained by the different cortical areas, thus involved in the motor control of movements for different specific behaviors (Kaas et al., 2011).

The area 5 is involved in higher order somatosensory processing, participating to the response selection to visual cues and to the sensorimotor guidance (Kalaska, 1996; for review see Kaas, 2004). Among the area 5a, many neurons present bilateral receptive fields responding to somatosensory and visual stimulations, as well as to both of these stimulations. The area 5a is involved in the correct hand orientation in grasping and in providing mental

model of what the body is doing for relevant behavioral guidance. The area 5b appears to be mainly involved in somatosensory function.

The area 7 is involved in somatic function in response to passive and active somatosensory information, neurons responding to several somatosensory organs and during active arm and eye movements (Hyvarinen and Shelepin, 1979; Leinonen et al., 1979). Whereas the visual and visuomotor activities are related to the area 7a, the area 7b appears to be related to higher order processing of somatosensory information (for review see Kaas, 2004).

Areas embedded in the intraparietal sulcus exhibit an important contribution to the motor control of voluntary movements. VIP is suggested to be involved in visuomotor transformations for head, face and arm movements, and to participate in the perception of self and objects movements in the peripersonal space (Rizzolatti et al., 1997, 1998; Grefkes and Fink, 2005). Responding to visual and tactile stimulations and efficient to produce a set of movements, the VIP has been suggested to contribute to defensive behaviors triggered by stimuli on or near the head (Cooke et al., 2003). MIP, although poorly studied, appears to be involved in circuits mediating planning, execution and monitoring of reaching movements. This area participates in the coordination of hand movements and visual targets and in the detection of movement errors or position changes (Grefkes and Fink, 2005). The role of the AIP area in motor control was mentioned above, within the framework of the description of the area PMv-r (F5) role in the motor control owing to their strong anatomical connections. AIP plays an important role in the visual guidance of hand movement appropriately to the goal properties, its inactivation causing deficits in the hand preshaping (Gallese et al., 1994; Rizzolatti et al., 1997, 1998; Grefkes and Fink, 2005).

1.2.2.2. Ascending pathways

Spinal cord ascending pathways

Without going into details (for review see Kaas, 2004), ascending pathways convey somatosensory information from receptors of the skin and proprioception, namely deep receptors in muscles (muscles spindles and Golgi organs) and deep receptors in the joints (Fig. 12).

The first ascending somatosensory pathway, referred as the dorsal column pathway, comprises mainly axons of the first-order neurons of the dorsal root ganglion, as well as

higher-order axons originating from connections through the spinal cord neurons. The dorsal column pathways course ipsilaterally in the dorsal funiculus up to the brainstem relay, the dorsal column nuclei (DCN), before crossing the midline to reach the thalamus and finally the somatosensory cortex. The second somatosensory pathway, the anterolateral pathway, comprises the second-order axons of the dorsal horn neurons, crossing the midline at segmental level and ascending contralaterally to reach brainstem and thalamus relays. The dorsal column pathways are generally involved in function such as the position sense and precise touch, thus related to the motor control, whereas the anterolateral pathway is involved in the protopathic sensibility of crud touch, pain and temperature. The dorsal column pathway respects a certain somatotopic organization. The ascending fibers originating from the lower limb and forming the tractus gracilis course medially to the fibers originating from the trunk, then from those originating from the upper limb and forming the tractus cuneatus, which course laterally (Tokuno et al., 2011). A certain higher degree of somatotopic organization has been observed among the tracti, such as described for the fasciculus gracilis with further detailed segregation of the fibers originating from the tail, foot, lower and upper leg along a mediolateral axis (Qi and Kaas, 2006).

Brainstem dorsal column nuclei (DCN): relays for voluntary movements

The dorsal column pathway projections into the DCN brainstem nuclei respect a somatotopic organization of the ipsilateral body parts representations. Fibers from different body parts are segregated in different nuclei: the lower body part afferents projecting to the gracile nucleus, the upper body parts afferents to the cuneate nucleus and the oral and facial structures to the trigeminal nucleus. Among the DCN, the somatotopic organization has been shown to respect a more detailed representation of the different body parts, principally for the digits and the wrist in the cuneate nucleus and for the toes and the planta in the gracile nucleus (Culberson et al., 1989; Qi and Kaas, 2006 Strata et al., 2003; Fig. 15). Just for mention, the external cuneate nucleus is differentiated from the ventromedially situated

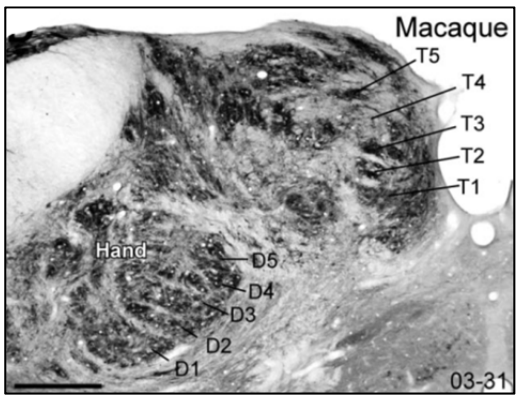

Figure 15: Photomicrograph of a transverse section of the brainstem processed for cytochrome oxidase (CO) focusing on the dorsal column nuclei in a macaque monkey. This photomicrograph reveals the somatotopic organization of the gracile nucleus with the location of the toes (T) and of the externally situated cuneate nucleus with the location of the digits (D) and the hand. Scale bar: 0.5 mm (reproduced from Qi and Kaas., 2006).

nucleus cuneatus. The external cuneate nucleus relays the proprioceptive information from the muscles spindle afferents of the forelimb, upper trunk and neck, mainly to the cerebellum, but also to the thalamus (Kaas, 2004).

The dorsal column nuclei receive descending cortical projections originating from pyramidal neurons, mainly from the somatosensory areas, but also some from motor areas (Bentivoglio and Rustioni, 1986; Kuypers and Tuerk, 1964; Cheema et al., 1985). Corticocuneate projections have been described to mostly originate from SI, principally from the areas 1 and 2, with a small amount originating from the area 3b and the smallest from the area 3a. Implicated in the present work, restricted projections originating from the motor cortex, areas 4 and 6, have also been described (Cheema et al., 1985; Bentivoglio and Rustioni, 1986). These corticocuneate projections have been shown to influence intracuneate circuits in the DCN through inhibition and disinhibition (Lue et al., 1997, 2001; Aguilar et al., 2003; Soto et al., 2004).

Thalamus relays for voluntary movements

The somatosensory information participating to the voluntary movements travels from the DCN to the contralateral somatosensory thalamus, through the medial lemniscus (for review of the literature see: Jones, 1986; Burton 1986; Kaas, 2004; Fig. 12).

Several subdivisions of the somatosensory thalamus have been identified. The most recently established and currently used nomenclature considers the ventroposterior nucleus (VP) as the main somatosensory thalamic nucleus (Fig. 12). The second-order neurons afferents from the skin and relayed by the gracile and cuneate nuclei project in the superior and dorsal regions of the contralateral VP. Among the VP, the afferents from the face are segregated in the medial subnucleus (VPM) and those from the body are segregated on the lateral subnucleus (VPL). As for the DCN, the somatosensory inputs project in the thalamic subnuclei respecting a somatotopic organization of the body parts. Furthermore, the afferents from the deep receptors mainly from the muscles spindles, relayed from the external cuneate nucleus, project separately to the ventroposterior superior nucleus (VPS). The afferents from the spinal cord terminate in the ventroposterior inferior nucleus (VPI), the pain and temperature afferents terminate distinctly in the ventromedial posterior nucleus (VMpo).

VP relay neurons project mainly to the area 3b on the layer IV and to the area 1, but to a lesser extent. These projections represent however the larger source of thalamic afferents in the area 1. VPS neuronal projections represent the main thalamic inputs to the area 3a and the

area 2, half of these VPS relay neurons projecting onto both areas. The area 2 receives additionally, but only sparse, inputs from VP in the hand representation. Projections from VPL and VPM to SII have been described, however remaining a minor component in the primate. The thalamic neurons have been described to project also to the parietal cortex, the area 5a receiving some inputs from the VP thalamic nucleus and the area 7b receiving thalamic projections from the ventral lateral and Pa thalamic nuclei. The somatosensory thalamus does not exhibit major connections with the motor cortex, described to be mainly localized in the ventral lateral thalamic nucleus, except connections of the VPL oral part with MI and SMA or VPM and VPI to PMv (Rouiller et al., 1998, 1999; Rouiller and Welker 2001; Morel et al., 2005).

1.3. The plasticity property of the CNS: primordial role in the motor control

The high degree of flexibility of adult mammal motor behaviors, such as the motor adaptability and learning, illustrates the plasticity property of the CNS. These motor adaptability and learning represent the expression of the highly dynamic architecture of the CNS, exhibiting permanently the ability to alter structure and function in response to various events. Thus, CNS fits and optimizes its functioning mechanisms and, consequently, the corresponding behaviors. Primarily observed by deprivation of normal inputs resulting of lesion, plasticity has been currently highlighted to be of great importance for the daily life motor control. The CNS plasticity property occurs permanently resulting of experience. Moreover, the CNS plasticity property is highly solicited and involved in case of pathologic events, such as in case of injury occurring all over the CNS from the time of the injury until after long-time. Understanding the plasticity property of the CNS is of primordial interest in the field of the CNS injury affecting the motor control. To understand the plasticity, the current and permanent daily life plasticity is first addressed in this paragraph. Plasticity resulting of CNS lesions is further detailed in the paragraph concerning lesions affecting the motor control (paragraph **1.4. Lesions of the motor system**).

1.3.1 Expression of the CNS plasticity

Plasticity relative to the motor control represents an extensively studied example of the CNS plasticity property. Basic mechanisms have been also well described in other cortical

areas, such as auditory and visual cortical areas (for other example see Buonomano and Merzenich, 1998). It is currently assumed that plastic changes occur at the cortical level but also all over the CNS, in the brainstem and spinal cord, two regions of interest in the present thesis. The highly dynamic architecture of the networked organization represents the substrate for modifications (for review see Sanes and Donoghue, 2000). These connections networks are subjected to modulation in link with information inputs received and are also subjected to alterations, internally from the CNS itself or from the body but also from the external environment.

1.3.1.1. Cortical plasticity

Improvement of motor performances and learning resulting from movement practices are admitted to be underlined by cortical plasticity. The cortical maps appear to represent a reflection of individual experiences. This current view is supported by observations of large changes in topographic organizations resulting *inter alia* of motor skills acquisitions, used-dependent learnings or passive manipulations. Cortical plasticity is expressed at various levels including reorganization of the body map representations, modification of networks neuronal activity of unitary or small group of neurons, modification of synaptic function and modification of the anatomical neuronal structure (for review see Nudo et al., 2001).

Motor cortex plasticity

Plastic reorganizations of the motor maps in motor cortex can be achieved by natural behaviors, motor learning skills as well as external manipulations (Nudo et al., 2001). A significant variability exists in motor topography across individuals (Nudo et al., 1992), which could results and reflects the individual behavioral experiences. The cortical body maps of M1 present significant variations in the representational topography between the two hemispheres of the same individuals. This was observed for natural behavior during which adult non-human primates presented hand preference. This thus establishes a direct relationship between interhemispheric asymmetry and behavioral asymmetry, as for the hand preference (Nudo et al., 1992). This interhemispheric asymmetry resulted in larger areas, longer boundary lengths, in larger numbers of regions and greater complexity of the hemisphere devoted to the preferred hand control.

The used-dependent learning during motor skill acquisition induces plasticity which predominantly occurs at the cortical level and results in reorganization of the representational topography. Specific behavioral tasks differentially alter movement representations, leading to

specific changes of topographic organizations in consequence to the concerned behavioral task acquisition (Fig. 16). Assessing the extensive cortical representation of a trained motor sequence over M1 using fMRI showed that it evolves through practice (for review see Karni et al., 1998). These data have allowed the distinction a fast neuroplasticity occurring from minutes to a slow neuroplasticity occurring over a much longer period. Observed using fMRI (Karni et al., 1995), the fast-learning neuroplasticity resulting from repeated practice of a motor sequence is followed firstly by an initial phase of habituation with smaller area of activation and, later, by a phase of enhancement with larger area of activation. In a second time, repeated practice resulting in a slow-learning neuroplasticity is followed by the extent of the cortical representation of the practiced sequences over M1. Thus, the reorganization consecutive to motor skill learning is suggested to occur during the later phase of skill learning and not at the early stages, as observed after 10 days of a motor skill acquisition (Kleim et al., 2004). Such extent of the cortical representation of the trained body part remains correct as far as it concerns the different movement representations among the concerned body parts and the finest subdivisions among the gross subdivisions of the cortical mapping. The boundaries of the major cortical topographic subdivisions remain rather unchanged following such used-dependent reorganization. The used-dependent reorganization of forelimb distal representation consecutively to skills acquisition results in a redistribution of the movement representation within the hand representation. Very little expansion of the

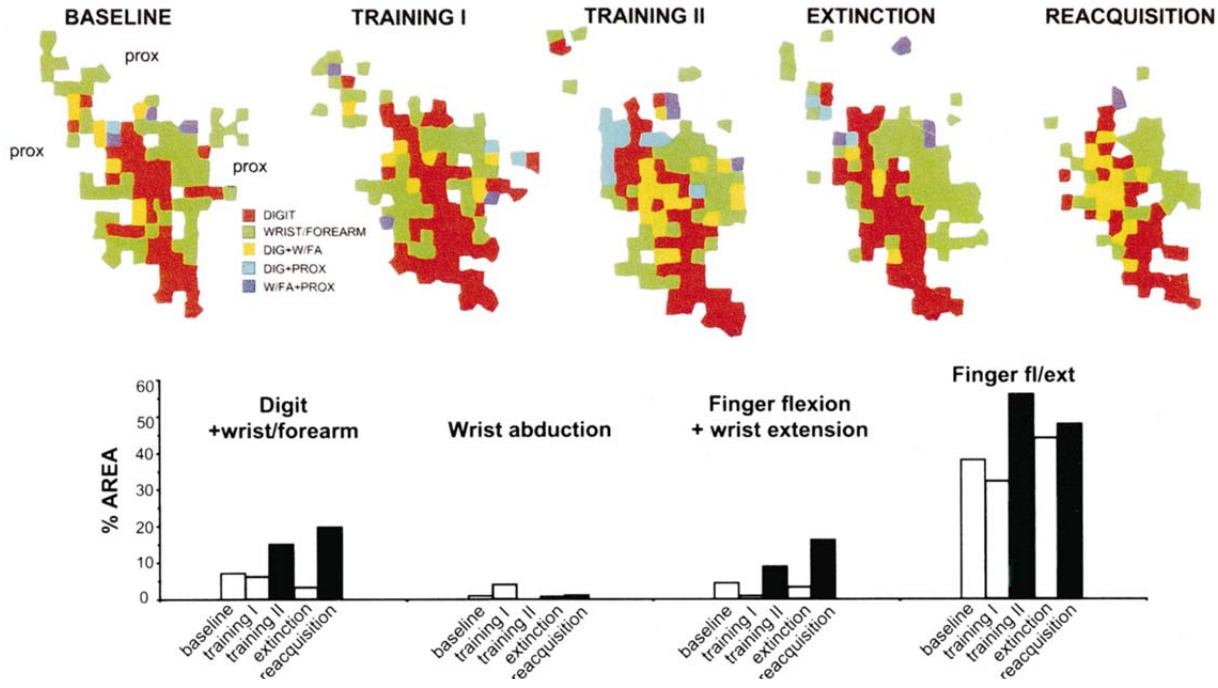

Figure 16: Illustration of the training-induced plasticity. Representations of the reorganization occurring among the cortical body map representations in M1 for specific set of movements induced by motor training and their corresponding percentages of representation. Dig, digit; W/FA, wrist forearm; PROX, proximal; fl/ext., flexion/extension (reproduced from Nudo et al., 1996).

hand representation is observed resulting from the used-dependent learning during digit skills acquisition. In this case, movement representations of the used fingers extent within the hand representation at the expense of the representation of other movements less used after the skill acquisition. These plastic changes are progressive and reversible, albeit a certain aspect of the functional cortical plasticity remains for long time once the novel motor task is learned (Nudo et al., 1996). A dichotomy has emerged tending to distinguish motor skill learning to strength training. Motor skill learning appeared to be well associated to cortical reorganization whereas strength training not (Remple et al., 2001). Interestingly, the non-use is also responsible of plasticity as a reflection of individual experiences. Reorganization of the cortical motor maps was also observed as a result of long-term limb immobilization (Liepert et al., 1995). A positive correlation was observed between a decrease of the motor cortical areas size devoted to the constrained limb and the immobilization duration. Such plasticity was described to be quickly reversible, as it was reversed by voluntary muscle contraction.

The observed reorganization of cortical motor maps can be induced and modulated artificially by external intervention. Thereby, plasticity among the motor cortex can be achieved by paired low-frequency nerve stimulation with TMS over the specific devoted cortical area (Stefan et al., 2000). This plasticity results in an improvement of electrical excitability of the concerned muscle. This plasticity was described to evolve rapidly, to be persistent but yet reversible and to be topographically specific. Such plasticity is suggested to represent the expression of the associative long-term potentiation (LTP) of cortical synapses or similar neuronal mechanisms in the human cortex. Assumed to take place at the cortical level, such plasticity leading to the modulation of muscles electrical excitability can be selectively enhanced or reduced through weak electrical current stimulations of the cortex (Nitsche and Paulus, 2000).

Somatosensory cortex plasticity

Similarly to the motor cortex, the somatosensory cortex is subjected to plastic changes of the topographical organization. In this case, plasticity can be achieved by a variety of manipulation, such as changes of the afferent somatosensory inputs (tactile and proprioceptive) or external artificial manipulation with repetitive cortical stimulation or pharmacological agent (Nudo et al., 2001).

As for the motor cortex, evidences exist also for the somatosensory cortex indicating that the cortical maps organizations depend on uses and changes to permanently conforming

to the current needs and experiences. On a more general point of view, environment is largely involved in maintenance of somatosensory representations. An environmental enrichment induces substantial plasticity of the somatosensory cortical representations, such as for the forepaw representation in somatosensory cortex of rats after exploration of such environment (Xerri et al., 1996). The opposite is also true, as it is observed a degradation of the forepaw somatosensory cortical representations with tactile environment impoverishment. In human subjects, the extensive use of daily life objects induces cortical plasticity. Reshaping of the somatosensory processing can be observed in touchscreen phone users in an EEG study assessing cortical potential response to mechanical digit touch (Gindrat et al., 2015). It has also been demonstrated that motor training resulting from extensive daily practice induces cortical plasticity. The MRI assessment of the somatosensory cortex of string players well illustrates this causality demonstrating larger cortical representations of the involved digits in these subjects as compared to non-player subjects (Elbert et al., 1995). This relationship was emphasized by the correlation of the amount of such cortical reorganization with the age at which these subjects had begun to play. As another illustration of such causality, plasticity of sensorimotor cortical organization is observed in Braille readers. Reading Braille is associated with expended sensorimotor cortical representation of the reading fingers (Pascual-Leone and Torres, 1993).

This activity-induced plasticity is experimentally reproducible. Trained on a frequency discrimination task, monkeys improve highly their ability to distinguish ever finer frequencies. This ability was correlated to a massive increase of the cortical area size and an increase of amplitude of the receptive field response related to the finger used to perform the task (for review and detailed citations see Ebner et al., 1997; Dinse and Merzenich, 2002). In another study, tactile stimulations of restricted skin surfaces induce functional cortical reorganizations resulting in enlargements of the corresponding cortical representations in the somatosensory cortex area 3b (Jenkins et al., 1990). Paradoxically, negatives consequences can result from over-activations of such plastic mechanisms. Dystonia or repetitive stress injuries are reported as consequences of repetitive tasks, performance finally declining for the concerned task.

The non-use induces also cortical plasticity as a reflection of individual experiences. A severe limb restriction is associated with a severe decrease of the corresponding somatosensory cortical representation in the overall areal extent. Such decrease of this

activity-deprived cortical area results in its invasion by contiguous skin territories (Xerri et al., 1996).

1.3.1.1. Subcortical plasticity

As generalization, change or loss of inputs activity as well as change or loss of targets activity induce plastic changes among the areas but also among all structures concerned by these connections over the CNS. As a role for motor control, the spinal cord is able to learn specific motor task. The spinal cord contributes to current skill acquisition during the motor learning course and is able to learn complex motor tasks in non-pathologic condition (for review see Hodgson, et al., 1994; Wolpaw and Tennissen, 2001; Wang et al., 2006; Wolpaw, 2007). Activity-dependent plasticity in the spinal cord can be driven by descending and peripheral inputs and is presumably responsible for maintaining spinal cord circuitry (for review see Wolpaw and Tennissen, 2001; Wolpaw, 2007). Interestingly, changes in activity resulting of plasticity induce additional plasticity in other sites, acting as compensation to restore normal reflex function. Thereby, stronger motoneuron response to an afferent underling new behavior is further likely to affect the other behaviors involving this same motoneuron afferent (for review see Wolpaw and Tennissen, 2001; Wolpaw, 2007). The activity-dependent spinal cord plasticity can be induced by extensive daily use and training as well as by ageing, observed by alteration of the size and excitability of the spinal cord reflexes (for review see Wolpaw, 2007). Plastic changes in the spinal cord circuitry are observed in association with motor training of different types, as evidenced by modifications in reflex physiology (Adkins et al., 2006). However motor skills induces plasticity primordially at the cortical level affecting the movement topographic organization, it also induces alterations in the spinal cord, at least for operant conditioned motor skills. Strength training induces alteration at the motoneuronal and synaptic level in the spinal cord.

1.3.2 Mechanisms and substrate of plasticity

1.3.2.1. Cortical plasticity

The cortical plasticity results in the reorganization of the somatotopic body map representation, modification of neuronal activity of unitary or small group of neurons, modification of synaptic function and modification of the anatomical neuronal structure (for review see Nudo et al., 2001).

The networked intracortical organization, highly subjected to plasticity, is represented by the horizontal pathways. These connections span the superficial layers II and III and the deeper layer V among M1. Behavioral evidence of motor skill acquisition occurring simultaneously with strengthening of these connections demonstrated their prominent implication in mediating such cortical plasticity (for review see Sanes and Donoghue, 2000). Plastic changes can refer to cellular ability in changing their response depending of the inputs information. This concerns the synaptic plasticity depending upon activity-induced modifications. Plastic changes arising at the cortical level can result from changes in neural activity levels (for review see Ebner et al., 1997).

Different types of plastic changes can be distinguished, making distinction between moment-to-moment alterations as short-time plasticity arising rapidly within hours and long term changes as long lasting plasticity taking place over longer periods. Considering these different periods, plasticity occurs at different levels and involves different mechanisms. The initial phase of training-induced plasticity is associated with a significant increase in immediate early gene expression and changes in neuronal ensemble activities, predictive of performances improvement (Kaczmarek and Chaudhuri, 1997; Laubach et al., 2000). Such plasticity in the initial stages might as well involve the horizontal connections including changes efficacy of existing synapses (Rioult-Pedotti et al., 1998) or increases of neuronal excitability by changes of the membrane excitability (Aou et al., 1992). Later phases of plasticity occurring after subsequent training or practice tend to be differentiated from the early phases. The principal mechanisms of cortical plasticity involve the synaptic plasticity. Changes of the strengthening of already existing synapses are recognized to underline cortical map reorganization. This mechanism implies the long-term and short-term potentiation (LTP) and depression (LTD). It is actually evidenced that the horizontal connections among the cortex, as M1, have the capacity for LTP and LTD, as expressed through the modification of the synaptic strength (Hess and Donoghue, 1994; for review see Sanes and Donoghue, 2000; Nudo et al., 2001). Such synaptic plasticity among the intracortical horizontal connections are described to occur at the cortical layer II and III and the deeper layer V (for reviews see Buonomano and Merzenich, 1998; Nudo et al., 2001). Initially proposed to represent the neural substrate of the cortical plasticity induced by motor learning (Iriki et al., 1989; Asanuma and Pavlides, 1997), LTP, as alteration of the synaptic efficacy, is currently considered as a predominant mechanism (for review see Sanes and Donoghue, 2000). LTP is considered as an associative or Hebbian synaptic mechanism. Initially, Hebbian synaptic

plasticity mechanism has been proposed to consist in an increase of synaptic strength between two neurons firing together (Hebb, 1949). The subsequent Hebbian-learning rules have thus postulated that neurons engaged by behaviorally important inputs respond in a temporally coherent manner. Such detection of temporally correlated inputs provides a mechanism sustaining the formation of topographic map arrangement and cortical cell assembly that specifically represent learned stimuli. LTP and LTD can be induced experimentally in the horizontal connections in layer II/III of the motor cortex. LTP challenged by motor learning is associated with alterations of the dendritic and synaptic morphology. Cortical plasticity resulting in modification of electrical property of cortical neurons and induced by paired stimulation was suggested to represent LTP in the cortical synapses or similar neuronal mechanisms in the human cortex (Stefan et al., 2000; for reviews see Buonomano and Merzenich, 1998; Nudo et al., 2001).

These extensive and strong horizontal pathways are supported by excitatory connections, which are mediated by glutamatergic fibers, and inhibitory connections, which are mediated by GABAergic fibers (for reviews see Ebner et al., 1997; Buonomano and Merzenich, 1998; Sanes and Donoghue, 2000). These horizontal pathways are of primordial importance to maintain integrity of the highly dynamic cortical maps. Blocking the GABAergic connections reveals this apparently masked connectivity, affecting the cortical map representations (for review see Sanes and Donoghue, 2000). Early, it was observed the existence of neurons in the somatosensory cortex which exhibited modification of their receptive field mediated by the GABA intracortical inhibition (Hicks and Dykes, 1983). Furthermore, modification of the electrical property of cortical neuron in response to stimuli was observed, influenced by GABA and glutamate drugs (Hicks and Dykes, 1983). It is postulated that the location-specific of inhibitory interneurons play an important role in practice-dependent plasticity (Teo et al. 2009; Hamada et al., 2013). The circuits involving GABAergic short-interval intracortical inhibitions are suggested to represent important controllers of rapid practice-induced plasticity. Implication of GABA and the glutamate receptors NMDA (N-methyl-D-aspartate) are of high importance in the cortical plasticity achievement (Bütefisch et al., 2000; Teo et al. 2009). The practice-dependent plasticity is at the same time abolished by NMDA antagonist and by GABAa agonist. Plasticity can be observed experimentally combining intracortical injection of GABAa agonist with stimulation (Rioult-Pedotti et al., 1998).

Additional mechanisms sustain cortical plasticity. Evidences suggest that the two phenomena, cortical motor maps reorganization and synaptogenesis, represent the consolidation of motor skill learning at the later stages of training. Such plasticity resulting in the cortical motor maps reorganization phenomenon is associated to and preceded by the synaptogenesis phenomenon (Kleim et al., 2004; Adkins et al., 2006). The synaptogenesis has been demonstrated by observing significantly more synapses per neurons among these areas which undergo physiological reorganization. Furthermore, cortical plasticity in the motor cortex, as a result of reaching motor task training, is not only associated to synaptic plasticity but also to alterations of dendrite morphology and increased spine density. Experimentally, pyramidal cells of the layer V, but also of the layer II and III, are observed with larger apical dendritic fields in trained rat animal model (Greenough et al., 1985; Withers and Greenough, 1989; for review see Nudo et al., 2001). Differentiated from the LTP, non-synaptic form of plasticity affects signal propagation in the axon, dendrite and soma. As a long-term intrinsic plasticity of neuronal excitability in the cortex, the intrinsic electrical property of cortical neuron is subjected to persistent modifications induced by neuronal or synaptic activity. The increase of synaptic intrinsic activity is initiated by glutamatergic receptor activations (Daoudal and Debanne, 2003; Debanne, 2009).

All the implicated mechanisms can be considered to be interdependently linked. Changes of the synaptic strength resulting from the activity-induced plasticity are translated into molecular cascade of events resulting from the synaptic activity (Ebner et al., 1997). Molecular events are elicited depending of the synaptic activity which induced the changes of synapses efficacy as the support of plasticity. Changes in transmitter release from the axon terminals, in glutamate receptor properties, in postsynaptic cell depolarization and in calcium activation of a cascade of intracellular events orchestrated these synaptic strength alterations (for review see Ebner et al., 1997).

Not described as a potential mechanism of plasticity, evidences have however shown that cortical plasticity can be sensitive to multiple factors, thus potentially participating to plastic changes processes. BDNF appears to be required to maintain motor maps organization and reorganization (Kleim et al., 2006; Adkins et al., 2006). Inhibition of BDNF has revealed a disruption of the motor cortex reorganization associated with an impairment of motor skill performance. Nogo-A, an inhibitory membrane protein of the myelin sheath, mainly involved in the inhibition of both axonal outgrowth and CNS regeneration, is suggested to be able to influence cortical plasticity (Zemmar et al., 2014). Blocking this protein affects the cortical

plasticity at the synaptic level in correlation with the motor learning. Such blockade results in an increase of the LTP in the cortical layer II/III whereas LTD remains unchanged, leading thus to an enlarged synaptic modification range. Nogo-A appears to be an influential molecular modulator of cortical synaptic plasticity and a cortical regulator of motor skill learning.

1.3.2.2. Subcortical plasticity

Described during reorganization and recovery of injury, the brainstem and cortex are governed by similar mechanisms of plasticity supported by GABAergic fibers (Mowery et al., 2014). In the spinal cord, it is suggested that neuronal and synaptic functions are appropriately and continually adjusted and readjusted. Short- and long-term changes are described to occur in the spinal cord, respectively resulting in differences in presynaptic inhibition and in the strengthening of the inputs to the motoneurons (Wolpaw and Tennissen, 2001). In a simple model of motor learning internal to the spinal cord, the H-reflex, the spinal cord plasticity has been observed to be conveyed by increases of: the number, size and density of GABAergic, inhibitory interneurons neurotransmitter, terminals and coverage on motoneurons (Wang et al., 2006).

1.4. Lesions of the motor system

Injuries introduced below focus on injuries of the motor system, albeit numerous injury occurring all over the CNS can affect to a various extent the motor control of the voluntary movements.

Lesions over the CNS result from traumatic injury (external cause) or pathophysiologic dysfunction such as stroke (mainly ischemic or hemorrhagic). Generally, mostly lesions of the brain or the spinal cord are considered. Motor control deficits differ depending on location and size of the injury. Clinically, several classifications have been established based on neurological and functional deficits, taking into consideration location and size of the injury. The aim of these classifications is to report injury severity and to tentatively predict prospect on the post-lesion evolution. These classifications attempt to score the lesion impact, such as the Glasgow Coma Scale or the International Standards for Neurological and Functional Classification of Spinal Cord Injury, being also indicative of the lesions site and size (*e.g.* Maynard et al., 1997; Duncan et al., 2000; Andriessen et al., 2011).

The majority of preclinical research studies investigate the most frequent CNS injuries which are the spinal cord injuries (SCI), traumatic brain injuries (TBI) and strokes. Anatomically incomplete SCI represents the most frequent type of spinal cord injury observed in humans. Animal with anatomically incomplete SCI are thus used in the majority of preclinical research studies investigating neural plasticity (McKinley et al., 2007). Anatomically incomplete SCI tends to be indicative to more favorable prognosis. The present work thus uses model of the most frequent cortical injury strokes and incomplete SCI.

1.4.1. Physiopathology of nervous system injuries

Understanding physiopathology of CNS lesions is of crucial interest to prevent consequences and promote functional recovery. Beside the trauma or the ischemia, CNS injury can result from a large variety of insults. The different types of lesions result finally in damaged tissues activating biochemical, molecular and cellular cascades leading to secondary damages.

All over the CNS, traumatic injuries generate direct tissue damages and cell death resulting from the initial mechanical impact, which corresponds to the primary injury. The initial mechanical damages initiate cascades of events resulting in secondary damages: (*i*) vascular alterations and metabolic disturbances within seconds to minutes, (*ii*) biochemical alterations (lipid peroxidation and neurotransmitter accumulation) arising within minutes to hours, (*iii*) cellular reactions (inflammation and apoptosis) within hours to weeks, (*iv*) fiber tract disturbances (demyelination, Wallerian degeneration, oligodendrocytes apoptosis and glial scar formation) within weeks to months. Interestingly, the first stage of these secondary damages following traumatic injury may be characterized as an “ischemia-like” pattern. In majority reported for the brain, stroke results in cell death consequently to energy-dependent processes failure, such as the expression of blood supply restriction or interruption (Murphy and Corbett, 2009). This results in the inability to maintain the cellular homeostasis leading to elicit cell death processes. These processes include excitotoxicity, acidotoxicity and ionic imbalance, oxidative/nitrative stress, inflammation, apoptosis and peri-infarct depolarization (Doyle et al., 2008).

Description of the time course (Fig. 17) of events following CNS injury can be done respecting the acute stage resulting from the primary impact and the secondary damages in the later stages resulting from the cascades of events initiated by the primary impact. The last stage of CNS injury consists of the chronic changes established and further modifications.

Such chronic stages refer to the outcomes of the lesion and the CNS plasticity property (see below).

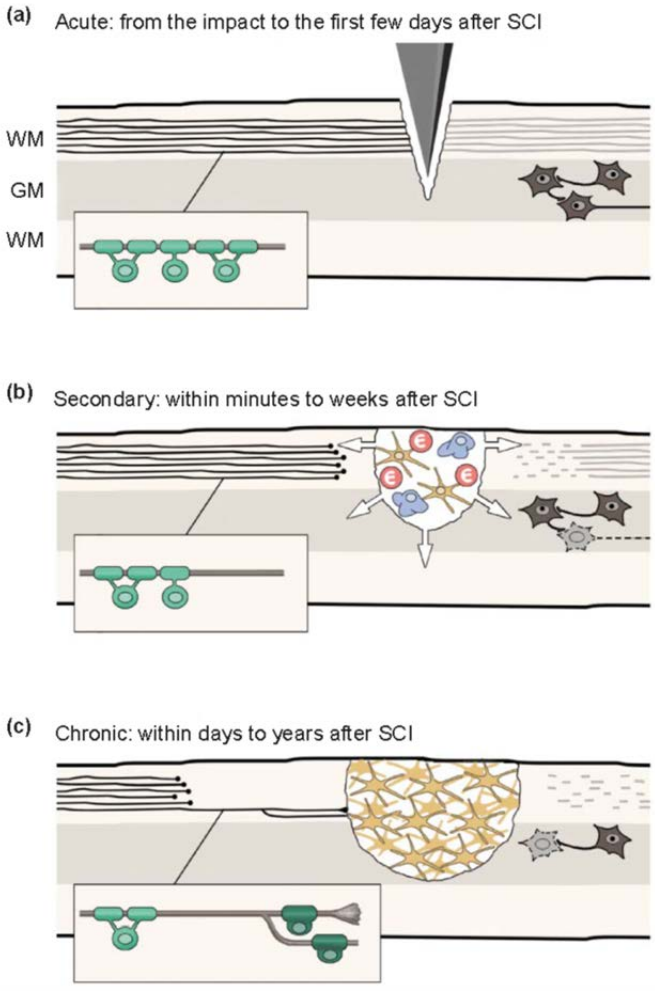

Figure 17: Schematic representation of the time course of events following traumatic injury of the spinal cord (SCI). This illustration represents oligodendrocytes (light green) degenerating partially following the lesion (a), Schwann cells (dark green) that potentially remyelinating the axons in the chronic phase, macrophages (blue) invading the lesion; neutrophils (red) invading the lesion and astrocytes (yellow) forming the glial scar in (c) and neurons (black) in the gray matter degenerating following the insult. Black lines represent axonal tracts running in the spinal cord and degenerating distal to the lesion through Wallerian degeneration in (b) and (c), and attempting to regrow in (c). GM, gray matter; WM, white matter. (reproduced from Bareyre and Schwab, 2003).

1.4.1.1. Acute stages

The acute stages following motor system injuries concern events that occurred from the moment of the impact to the first few days following CNS injury.

CNS traumatisms result in direct tissue damages and lead to disrupt the cerebral blood flow regulation and the metabolism, all creating substantial additional ischemic injury (for review concerning the following paragraphs Schwab and Bartholdi, 1996; Bareyre and Schwab, 2003; Klussmann and Martin-Villalba, 2005; Hagg and Oudega; 2006; Werner and Engelhard, 2007). This “Ischemia-like” pattern leads to an accumulation of lactic acid resulting from the anaerobic metabolism, an increase of the membrane permeability, and a consecutive edema formation. The anaerobic metabolism results finally in the failure of energy-dependent mechanisms. Edema and metabolic disturbance are a consequence of the post-traumatic effects leading to the accumulation of intracellular concentration of calcium

(Ca^{2+}) and the increase of extracellular concentration of potassium (K^{+}). This leads to a general failure of normal neural functions and the CNS shock stage lasts for days in animal to weeks in human. During this acute stage a strong upregulation of genes involved in transcription and inflammation is observed as well as a general downregulation of structural proteins and proteins involved in neurotransmission (Bareyre and Schwab, 2003)

1.4.1.2. Secondary damages

The secondary damages concern events initiated by the primary injury that occurred within minutes to weeks after (concerning the following paragraphs see Schwab and Bartholdi, 1996; Bareyre and Schwab, 2003; Klussmann and Martin-Villalba, 2005; Hagg and Oudega; 2006; Werner and Engelhard, 2007 for review). The later stages of injury comprise the increase of expression of growth factors, axonal guidance factors, extracellular matrix molecules and angiogenic factors. Such post-lesion mechanisms participate to the attempt to repair the lesioned tissue. Furthermore, the later stages of injury exhibit an upregulation of stress genes and proteases and a downregulation of cytoskeletal and synaptic mRNA. Such post-lesion mechanisms participate to the attempt for lesioned tissue to survive. In even more later stages, during the chronic stage extended from days to years following injury, apoptotic cell death continues, channel and receptor functions are impaired and scarring and demyelination accompany Wallerian degeneration. At these stages, four main mechanisms are involved, participating to deleterious effects and preventing the functional recovery: excitotoxicity and excitatory neurotransmitter-induced neurodegeneration, cell death, immunoinflammation and glial scar formation.

Excitotoxicity and excitatory neurotransmitter-induced neurodegeneration

The later stages of pathophysiological cascades are characterized by terminal membrane depolarization along with excessive release of excitatory neurotransmitters. Elevation of extracellular excitatory amino-acids, primarily the glutamate, is highly involved in mechanisms of excitotoxicity and is an important source of neurodegeneration. Glutamate, the main excitatory neurotransmitter in the CNS, is involved in the generation of brain lesions and has, thus, been assimilated to a putative neurotoxin. Excessive concentration of glutamate has been linked to: (*i*) neurotoxicity induced by the excessive mobilization of Ca^{2+} from internal stores consequently to the prolonged activation of glutamate receptor, (*ii*) the activation of specific excitotoxicity signaling pathways via the NMDA (N-methyl-D-

aspartate) glutamate receptors, (*iii*) generation of free-radical and associated cell death pathways (Arundine and Tymianski, 2004).

Cell death

The increase of Ca^{2+} and sodium (Na^{+}) influx leads to catabolic intracellular processes, activation of the peroxidase, protease and phospholipase, all resulting in the increase of free fatty acids and free radicals activating the cell death pathways.

Initiation of progressive structural changes of both biological membranes and nucleosomal DNA leads to membrane degradation of the vascular and cellular structures. This finally also results in necrotic or apoptotic cell death.

Immunoinflammation

Initiated at the acute stage, a strong inflammatory response is observed leading to the recruitment of peripherally derived immune cells (such as the neutrophils, macrophages and T-cells). Early post-lesion, insults among the CNS activate immunoinflammatory processes which play deleterious roles resulting in aggravation of the CNS damages (Hohlfeld et al., 2007; Kadhim et al., 2008). Activated in later stages post-injury, these processes dually contribute to functional recovery and repair. Molecular mediators driving the immunoinflammatory processes are pivotal in CNS injury. The activated cells produce among other molecular mediators: cytokines, chemokines, adhesion molecules and growth factors. As major mediators, cytokines are largely involved in the physiopathological processes, upregulated soon after the CNS injury. Cytokines are evidenced as the driving force of the immunoinflammatory processes, known to paradoxically exacerbate the CNS damages and to have the capacity to improve CNS damages and neurological outcomes.

Glial scar

Late stages following injury of the adult CNS are characterized by the formation of a glial scar at the lesion site (Silver and Miller, 2004). The glial scar is responsible for the observed incapacity of injured axons to regenerate beyond the lesion site taking, then, a dystrophic appearance of stalled axons. However, not only deleterious, the glial scar formation might also provide important benefices in the stabilization of the fragilized CNS tissue after injury. The glial scar components serve to repair the affected blood-brain barrier, to prevent an excessive inflammatory response and to limit cellular degeneration. In this way,

the glial scar secludes the injured site from the adjacent healthy tissue, preventing it from a cascade of uncontrollable tissue damages.

The glial scar is predominantly composed of reactive astrocytes. In the lesion site, these hypertrophic reactive astrocytes produce intermediate filaments forming a tight canvas, which represents a physical wall for the axons outgrowth. Molecules secreted in the glial scar are also responsible of axons outgrowth failure. Among several inhibitory molecules in the glial scar, reactive astrocytes are known to produce the proteglycan molecules, known for their high inhibitor potential of axons re-growth. Among the four classes of proteglycan, the chondroitin sulphate proteoglycans (CSPGs) are well known for their extreme inhibitory potential on axonal outgrowth. Largely upregulated and extracellulary secreted following CNS injury, CSPGs in excess are highly involved in the failure of axonal regeneration.

Currently not entirely established, the initiation of the glial scar mostly implicates the transformation of the growth factor β (TGFβ). Other candidates have been implicated as scar inducers such as interleukins and cytokines.

1.4.2. Outcomes of motor system injuries: behavioral effects and CNS reshaping

1.4.2.1. General behavioral outcome of motor system lesion

Lesion of the motor system induces alteration of the motor network organization at the cortical, brainstem and spinal cord level. Predictive clinical outcomes are negatively correlated with the lesion location descending along the CNS system. Functional recovery following lesion targeting upper limb has been shown to progressively decrease with the lesion location from the cortex, corona radiate to internal capsule (Shelton and Reding, 2001; Morecraft et al., 2002; Morecraft et al., 2007). This reflects the redundancy of the upper limb representation over the motor cortex projecting through the descending tract. The corticospinal tract (CST) organization respects the different cortical areas of origin progressively pooled to reach an organization respecting the somatotopic organization of the different body parts (Shelton and Reding, 2001).

The relationship between the lesion site(s) and the corresponding lost function(s) has extensively allowed to highlight and describe the different roles of structures involved in the motor control of voluntary movement. However, this relationship is not accurate as it does not take into consideration three main aspects of the CNS: 1- the effects on more or less distant

interconnected areas and structures; 2- the certain redundancy of somatotopic representations over the different motor areas sources of CST, particularly for the upper limb representation; 3- the plasticity of the CNS.

Considering the network organization, focal lesion affecting one of the cortical areas involved in the motor control will influence the entire network and will affect not only the different cortical areas but also the connected subcortical structures, at the brainstem and spinal cord levels. Thus, a lesion affecting one specific location of the network can induce effect sustained by other structures, affected through their interconnectivity with the lesioned structure. After the lesion, modification of the connectivity induces plastic processes resulting in synaptic activity modifications. This is well illustrated by the demonstration that a lesion of the motor system affects the somatosensory function as well, and reciprocally, a lesion of the somatosensory system affects the motor system. (*e.g.* Nudo et al., 2000; Xerri et al., 1998; Coq and Xerri, 1999).

The fine manual dexterity is highly sensitive and highly affected by CNS lesion targeting the motor control. Due to its complexity, the fine manual dexterity is the most affected behavior and the most challenging behavior to recover following lesion of the motor system. Functional recovery of the fine manual dexterity is rarely completely achieved and is the last behavior to recover. Early experiments pointed out the loss of the fine manual dexterity resulting from the lesion of the descending motor tracts which, albeit an observed improvement over time following the lesion, never returns back to the pre-lesion performances (Lawrence and Kuypers 1968a). Motor behavioral deficits depend upon the tract involved since the different descending tracts are located separately within the brainstem and within the spinal cord (Lawrence and Kuypers 1968b). Similar observations were performed in case of pyramidal lesion in the brainstem. Interestingly lesion of both pyramids resulted in more severe and longer deficits, but presented however a certain degree of functional recovery in spite of the section of the entire CST (Hepp-Reymond et al.,, 1974). Since, deficits in manual dexterity have been extensively studied in case of spinal cord injury (SCI) or motor cortex injury (MCI). On a general point of view, immediate paresis followed by a certain degree of spontaneous functional recovery of the lost behaviors were observed in monkeys following SCI (*e.g.* Lawrence and Kuypers 1968a, 1968b; Hepp-Reymond et al.,, 1974; Galea and Darian-smith., 1997; Schmidlin et al., 2004; Pettersson et al., 2007) and MCI (Brinkman and Kuypers, 1973; Rouiller et al., 1998; Liu and Rouiller, 1999; Murata et al., 2008; Wyss et al., 2013). In case of MCI, effects were also observed on ipsilateral/ipsilesional

hand, exhibiting a tendency of performances improvement following lesion of M1 hand area (Kaeser et al., 2010; Bashir et al., 2012). Effects of motor system lesion on the manual dexterity appeared more pronounced in case of SCI than in case of MCI (Hoogewoud et al., 2013). However, such comparison has to be taken cautiously given the restriction of the MCI to M1 hand area and the larger SCI including all the spinal cord pathways of all the areas and structures coursing along the concerned hemi-cord. This observation remains however in line with the description of increased motor deficits for lesions that occur along the CNS from the motor cortex to the pyramid (Shelton and Reding, 2001; Morecraft et al., 2002, 2007).

Taking into account a certain redundancy of somatotopic representations over different motor areas projecting in the CST, the brain presents the innate property to compensate (at least in part) cortical lesion. Such compensation implying the shift of the functional property of the lesioned area onto spared areas. This is particularly observed for the upper limb representations. Thus, the volume of the MCI greatly conditions the importance of the post-lesion effects and performances (Darling et al., 2009).

However, due to the extent of the cortical interconnections, remote effects normally depending on other distant areas can be observed following restricted cortical injury. Motor deficits of the fine manual dexterity resulting from somatosensory pathways injury have been largely highlighted (*e.g.* Xerri et al., 1998; Coq and Xerri, 1999; Darian-Smith and Ciferri, 2005; Darian-Smith, 2007; Song et al., 2008; Kaas et al., 2008; Qi et al., 2011, 2013). On the other side, descriptions of effects on the somatosensory system resulting from damage to motor cortex have been poorly reported. Mostly focused on the behavioral aspects, it has been reported the necessity for a monkey to visually inspect their hand to detect the presence of reward following M1 lesion targeting distal forelimb (Nudo et al., 2000). This later aspect on the effects on the somatosensory system resulting from motor system lesions is experimentally addressed in the chapter 4 of the present thesis.

1.4.2.2. Lesion-induced plasticity and spontaneous functional recovery

As described above, the CNS is highly subjected to plasticity in the daily life. However, the early first evidence of CNS plasticity was reported in the somatosensory cortex as a result of peripheral nerve section (Merzenich et al., 1983). Lesion of the CNS is now well known to induce plasticity. The motor behaviors deficits resulting from CNS injury exhibit improvement during the post-lesion course, as an expression of the lesion-induced plasticity.

This spontaneous functional recovery remains however limited in the adult and is generally thought not to continue past 6 months (Duncan and Lai, 2000).

The lesion-induced plasticity finally tends to compensate the lost functions to reach a certain degree of functional recovery. The general time course of the plastic changes occurring following CNS lesion has not found common agreement, and, albeit some mechanisms have been extensively described, many suggested plastic changes remain subjects of controversy. However, further plastic changes appear to present strong and common reliability. What is thought about the lesion-induced plasticity is that lesion activates and challenges the already present pathways that can rapidly sustain the lost function within the spared cortex. Thus, the lesion-induced plasticity depends on and links the networks of connections between the different structures involved in the motor control (Mohajerani et al., 2011).

The lesion-induced plasticity will be described in the following paragraph. SCI and lesion of M1 will be considered albeit lesion affecting other parts of the motor cortex and somatosensory cortex lead to behavioral impairment, plasticity and functional recovery as well.

Motor cortex plasticity

Early, Glees and Cole (1950) observed the functional recovery following an initial important deficit of thumb movements as a consequence of cortical impact of the thumb representation. It early appeared that the body part represented pre-lesion in the impacted M1 area reappeared in the intact adjacent cortex, representing other body part pre-lesion. These lesion-induced plastic changes are currently subject of controversy since later contradictory results did not show such cortical reorganization in the adjacent cortex (Nudo and Milliken, 1996). Authors attributed the lack of reemergence of the lesioned body part representation among the adjacent cortex in part to the training underwent by the tested subject of the early study from Glees and Cole (1950). The present thesis attempts to add some evidences to this debate, addressing such reorganization of the adjacent cortex in trained non-human primate following cortical injury.

Observed with fMRI, the general cortical activity following cortical injury reveals some general and global plastic changes among cortical structures (Rehme et al., 2010, 2011). In early stages following cortical injury, cortical activity and activity of the cortical connectivity appear to decrease on the ipsilesional hemisphere. A later increase of this cortical

connectivity activity has been correlated with post-lesion functional recovery and better outcome predictions. At the same time, an increase of the cortical activity in the contralesional cortex has been reported, followed by an extension of the increased cortical activity to non-primary areas, PM and SMA. Following cortical M1 injury, fMRI studies have revealed reorganization in the ipsilesional SI, becoming activated by movement of the affected contralateral hand, which was not observed for the control and unaffected hand (Jang et al., 2005).

Although there is no common agreement on the map reorganization among the perilesional cortex, this region is subjected to plastic changes. Axonal sprouting appears following cortical injury in the perilesional cortex in an activity-dependent manner by synchronous neuronal activity from the intact cortical hemisphere (Carmichael and Chesselet, 2002; for review see Nudo et al., 2006). The perilesional M1 functional connectivity increases in the late stages post-lesion, directly linked with the functional behavioral recovery (Murata et al., 2015). This supports the fMRI study showing the early decrease and the later increase of the activity of the cortical connectivity on the ipsilesional hemisphere (Rehme et al., 2011). As for the map reorganization, the post-lesion activity in the perilesional cortex linked with the post-lesion functional recovery is subject of debate as a contradictory study has observed a lack of such role for M1 (Liu and Rouiller, 1999). However, long-lasting plastic changes are observed in the perilesional cortex. The GABAergic function was observed to decrease, thus facilitating the plasticity mechanisms. This decrease has been proposed to sustain the observed propensity to LTP facilitation in the surrounding cortex (Hagemann et al., 1998; Redecker et al., 2002).

As revealed by the fMRI studies reported above, cortical activity on the ipsilesional hemisphere increases post-lesion, though following an initial decrease. The roles of different areas have been assessed in the post-lesion plasticity and functional recovery. The premotor cortex, considering SMA and PMv, undergoes plastic changes of the maps organization following M1 injury resulting in an enlargement of the body part representation lesioned in M1 (Frost et al., 2003; Eisner-Janowicz et al., 2008). Similarly to the perilesional cortex, a decrease of GABAergic function is observed with the propensity to LTP facilitation (Redecker et al., 2002). The premotor region PMv is strongly suggested to play a predominant role in the functional recovery following cortical M1 injury (Liu and Rouiller, 1999; Nudo et al., 2006; Hoogwoud et al.; 2013). As mentioned above, PMv exhibits an extension of the body part representation lesioned in M1 (Frost et al., 2003). PMv is suggested to be involved

in the early phase of the functional recovery, preceding the suggested role of perilesional intact M1 cortex in the later stages of the post-lesion functional recovery (Murata et al., 2015). However, PMv inactivation during late stages of the functional recovery following M1 injury still reinstates the initial damages and is thus also involved in the later phase of the functional recovery (Liu and Rouiller, 1999). Plastic changes occurring in PMv consequently to M1 lesion result furthermore in the apparition of novel intracortical connections from PMv to S1, only sparsely observed pre-lesion (Dancause et al., 2005). As other premotor area affected by M1 lesion mentioned above, SMA is subjected to enlargement of the corresponding body part representation lesioned in M1. This plastic change occurs during late stages of the post-lesion recovery period, preceded by the functional recovery, which does not involve SMA as support of the early functional recovery (Eisner-Janowicz et al., 2008). However, terminal axonal plasticity in the contralateral spinal cord has been shown to originate from the ipsilesional SMA CST. This was observed with the increase of the intraspinal sprouting in spinal cord region containing motoneurons (McNeal et al., 2010). Also observed to be affected by M1 lesion, PMd consecutive plasticity has been highlighted, however less involved in the functional recovery than PMv previously described. There are evidences that simple movements after cortical injury may increase the participation of ipsilateral premotor cortex (Johansen-Berg et al., 2002a). Motor outputs of the affected body part are associated with an increase of the ipsilateral PMd activity, in parallel to the extent of motor impairment. This is emphasized by the description of a significant correlation between the integrity of the tract connecting M1 with PMd and the hand motor output in well recovered patients (Schulz et al., 2015).

Plastic changes have been described in the intact contralesional hemisphere following M1 lesion (for review see Dancause et al., 2015). The plastic changes observed to occur in the contralesional intact hemisphere following M1 lesion include: (1) cortical map reorganization (Netz et al., 1997); (2) synaptogenesis in contralesional motor cortical layer V correlating the increase of motor performance of the unaffected limb (Luke et al., 2004); (3) modification of GABAergic function making the cortical network more favorable for plasticity, with the specificity to be layer dependent (Redecker et al., 2002; Lee et al., 2011). However, as for the perilesional cortex, the role of the intact contralesional cortex remains controversial. Both evidences for the non-participation of the intact contralesional hemisphere in the functional recovery (Liu and Rouiller, 1999) and for its participation (Biernaskie et al., 2005; Hoogewoud et al., 2013) have been documented. It is suggested that the lesion involves

differently the intact cortical areas depending of the lesion size. The intact contralesional hemisphere is suggested to participate to the functional recovery following cortical lesion of large size (Liu and Rouiller, 1999; Biernaskie et al., 2005; Bradnam et al., 2012; Touvykine et al., 2015). The role of the intact contralesional cortex in the functional recovery appears to depend not only on the lesion size, as mentioned above, but also of the motor task complexity used to assess the functional recovery, involved in the control of more complex task (Shibasaki et al., 1993; Salmelin et al., 1995; Chen et al., 1997), as experimentally addresses in the chapter 2 of the present thesis. Unilateral M1 lesion leads to the denervation of the transcallosal projections to the contralateral cortex resulting in the disinhibition of the intact hemisphere. This disinhibition and the resulting hyperexcitability of the intact contralesional cortex during the early stage post-lesion reveal the normally masked ipsilateral connections from the intact contralesional cortex (Netz et al., 1997; Liepert et al., 2000; Shimizu et al., 2002).

SCI-induced plasticity at the cortical level results from the loss of afferents or efferents, depriving the cortical area connected to these lost inputs. Immediately unresponsive after lesion of their afferents or efferents spinal pathways, the denervated cortical area tends to become invaded by the unaffected adjacent cortex (*e.g.* Schmidlin et al., 2004). Thus the adjacent body part representations for which inputs remain intact are being extended. As a general course, such cortical plastic changes are similarly observed for both the motor cortex, as described for M1 (Raineteau and Schwab, 2001), and the somatosensory cortex (for reviews see Buonomano and Merzenich, 1998; Kaas, 1991; Kaas et al., 2008). When affecting the motor output, SCI does not appear to result in cell loss in the motor cortex, which could explain the ability of the deprived cortex to be invaded by the adjacent cortex. The vast majority of the axotomized corticospinal neurons do not degenerate after SCI but present shrinkage of their soma (Wannier et al., 2005; Beaud et al., 2008). Activity has been described to increase bilaterally in M1 during early stage post-lesion, then, to increase in the contralesional M1 and the ipsilesional PMv during later recovery stage (see for review Nishimura and Isa, 2012). Such changes in activity level have been suggested to be accompanied by structural changes in the cortical circuits. This has been observed through the increase of the expression of a protein related to neurite extension (GAP-43) in layer V pyramidal cells in the cortical areas exhibiting the increased activity: bilateral M1 and ipsilateral PMv (see for review Nishimura and Isa, 2012). Such observation has also been made in S1. As further plastic changes, SCI injury induces cortical map reorganization in M1,

PMv and PMd contralateral to the lesion (Schmidlin et al., 2004, 2005; for review see Nishimura and Isa, 2012). The cortical map reorganization of M1 occurring following SCI parallels the functional recovery. Unilateral SCI leads also to a great reduction of the ipsilesional M1 representation (Schmidlin et al., 2005).

Subcortical plasticity

As part of the motor system, the brainstem structures involved in the motor control of voluntary movements are able to support plastic changes. Largely studied in case of SCI, it is usually admitted that the brainstem is subjected to post-lesion plasticity and is involved in the functional recovery. Extensively studied for the somatosensory system following lesion of the dorsal column and other sources of afferents loss, thalamic and brainstem relays are highly reorganized post-lesion (for reviews see Kaas et al., 1999; Kaas, 2004). The dorsal column nuclei (DCN; brainstem relays) are furthermore considered as the substrate of the observed reorganization in the somatosensory cortical area 3b (Kambi et al., 2014). Following lesion of the descending motor tracts in the spinal cord, the brainstem motor nuclei can be affected and reorganized. There is currently growing interest for the lesion-induced plasticity and the role in the functional recovery of both the red nucleus and the reticular formation brainstem structures.

Recent interest has emerged for the reorganization that may occur in the brainstem in case of cortical or spinal cord injury. Observed in stroke patients, the red nucleus exhibits an increase of neuronal activity in the 3 months assessed following cortical injury (Yeo and Jang, 2010; Ruber et al., 2012; Takenobu et al., 2014). This observed increase of neuronal activity in the ipsilesional red nucleus has been correlated to the functional recovery (Ruber et al., 2012). Thus, the red nucleus, as a part of the motor system, may participate to the functional recovery following cortical injury. Map reorganization has also been observed in the red nucleus following SCI resulting in the loss of the pre-lesion preference for the control of extensor muscles in favor to the quite equivalent control of extensor and flexor muscles post-lesion (Belhaj-Saïf and Cheney et al., 2000). Moreover the map reorganization, rearrangement of synaptic connections occurs following inputs loss in the red nucleus. This synaptic plasticity results in the sprouting of the corticorubral terminals and the formation of new synapses formations, as well as in the sprouting of GABA synapses (for review see Raineteau and Schwab, 2001).

Evidences have also revealed changes of the motor outputs of the pontomedullary reticular formation (PMRF) following cortical injury, exhibiting a role of reticulospinal tract in the functional recovery, particularly in reaching movements (Herbert et al., 2015). This PMRF plasticity was observed in the particular case of large cortical injury, for which neither ipsilesional nor contralesional reorganizations were observed. In the case of SCI, currently strong evidences support the role of the ipsilateral descending pathways in the functional recovery. Linking the role of the ipsilateral/contralesional cortex in the functional recovery, as discussed above, movements can be evoked with stimulation at the cortical level through the CST. However, similar stimulation highlights the brainstem site as origin for such ipsilateral control post-lesion and furthermore point out the reticular formation (Edgley et al., 1990). Bilateral responses of such stimulation involve the reticulospinal tract and, thus, suggest that the ipsilateral control by the contralesional intact cortex occurs through the corticobulbar pathways, such as the corticoreticulospinal tract (for review see Jankowska and Edgley, 2006). The ipsilateral pathways through the corticoreticulospinal tract appears to play a significant role in the functional recovery post-lesion (Davidson and Buford, 2006; Brus-Ramer et al., 2007, Pettersson et al., 2007). The possibility for the brainstem to be a site of origin for ipsilateral control post-lesion is considered in the chapter 3 of the present thesis.

Injury of the CNS and the following functional recovery involve plasticity in the spinal cord. The suggested role of the ipsilateral motor structures in the functional recovery following motor system lesion, including the CST and/or the corticoreticulospinal tract, requires the reconnection to the deprived motoneurons. These reconnections in the spinal cord are suggested to occur directly or not, involving possible reconnections through the propriospinal tract (Baker et al., 2015). There are evidences that new intraspinal circuits are formed spontaneously following SCI. It was demonstrated that injured axons sprouted in the cervical gray matter to contact propriospinal neurons bridging in turn the injured site to contact the lower motoneurons (Bareyre et al., 2004; Pierrot-deseilligny, 2002; Pettersson et al., 2007; Filli and Schwab, 2015).

Following CNS lesion, axons reestablish connection with motoneurons during the post-lesion functional recovery, considered to possibly result from the axonal sprouting or re-growth. Axonal regeneration differs from axonal sprouting as the first is the re-growth of sectioned axons whereas the second is the growth of collateral branches from spared fibers. The spontaneous capacity of the lesioned axons to regenerate in the adult central nervous system is very limited, almost inexistent, and does not lead to functional recovery. Compared

to the high regenerative capacity of lesioned peripheral axons, the limited axonal regeneration in the lesioned CNS is currently attributed to the non-permissive axonal environment of the lesioned site, in spite of the presence of regenerative responses (Schwab and Bartholdi, 1996; Hagg and Oudega; 2006). On the other hand, lesioned axons in the CNS have the intrinsic spontaneous capacity to sprout. Following cortical injury, collaterals sprouting at the spinal cord level from spared descending fibers on ipsi- and contralateral and from damaged fibers invade the denervated spinal cord in parallel to functional recovery (*e.g.* Zhang et al., 2010; Raineteau and Schwab, 2001; Hagg and Oudega; 2006). In the post-lesion functional recovery, participation of the CST appears to be important from M1 while the participation of CST from S1 appears to decline (Darian-Smith et al., 2013). An increase of the CST linkage from SMA to the contralateral side of the denervated spinal cord clearly exhibits a post-lesion participation of CST from the ipsilesional SMA (McNeal et al., 2010). At the spinal cord level, injury induces further plastic changes. Following dorsal column lesion, intense astrocytic activation but no synaptogenesis have been observed (Vessal et al., 2007).

Aberrant plasticity

Lesion-induced plasticity is extensively described to support functional recovery. However, lesion-induced plasticity can also give rise to aberrant and deleterious results. Aberrant sprouting results also from the injury-induced plasticity in the spinal cord leading to pain and dysreflexia. The main deleterious effect resulting from plasticity is the phantom limb phenomenon, resulting from limb amputation. This phenomenon is behaviorally expressed by the sensation of feeling from the amputated limb, either persistent or in response to somatosensory stimulation of a spared body part. Anatomically, the cortical plasticity challenged by deprivation of the amputated limb inputs results in the extension of the neighboring body part representations over this deprived area(s) (for reviews see Ebner et al., 1997; Kaas et al., 1999). Aberrant plasticity can also affect the motor aspect. Schieber and colleagues (2009) have observed that different movements and EMG patterns in the remaining proximal muscles can be evoked by stimulation of the M1 regions previously representing the phantom hand.

1.5. Principal therapies and treatments promoting recovery

Spontaneous recovery that occurs following CNS injury remains limited and the motor performances, albeit improved, never return back to the pre-lesion level. Currently, neither therapies nor treatments are available to fully recover from SCI or cortical injury. Numerous approaches are considered, exhibiting substantial improvement of the behavioral performances and abilities. This field of therapies and treatments is vast and various approaches are considered (for reviews see Horner and Gage, 2000; Thuret et al., 2006). Several functional/behavioral therapies have shown benefic effects, improving the impaired function post-lesion. Contrarily, several approaches for treatments exhibit more or less benefic effects on the post-lesion deficits, however not leading to full regeneration and not currently used as treatment.

1.5.1. Functional therapies

Activity-dependent plasticity property of the CNS has major implications for rehabilitative therapies. As described above for the CNS plasticity property in intact subject, cortical functions are permanently subjected to alteration and reorganization resulting of experiments, such as training, behavioral manipulations and external manipulations. Several functional therapies have been developed taking advantages of this plasticity, thus based on training, external manipulation and behavioral learning and rehabilitation (Thuret et al., 2006). These rehabilitative functional therapies challenge the normal plasticity mechanisms in the post-lesion context, thus stimulating and promoting the plastic changes induced by lesion.

Rehabilitative training following injury in M1 or in the spinal cord induces an improvement of functional recovery of the affected manual dexterity (for review see Higo, 2014). Training promotes the natural tendency of the brain to undergo plastic changes and learn novel behavior through existing cortical circuits, in this case a behavior lost after lesion. Depending on the time course of the post-lesion events and the functional recovery, specific time window appears to be more sensitive and efficient for rehabilitative training. Rehabilitative training in early times following SCI exhibits positive influence on the subsequent functional recovery (Yang et al., 2003; Sugiyama et al., 2013; Higo, 2014). Rehabilitative training in early or in later stages post-injury affects differently the perilesional cortical map organization (Barbay. et al., 2006). Early training appears to preserve at long-term higher degree of the spared part of the lesioned area among the perilesional cortical map organization (Nudo et al., 1996b; Nishibe et al., 2014). Occurring at long-term, such loss

prevention thus takes place after the behavioral improvement. Furthermore, rehabilitative training of the more impaired body part following cortical injury results in reduced body part representation over the intact hemisphere (Barbay et al., 2013). Such training-induced plasticity has been linked with the post-lesion decrease of the lesion-induced hyperexcitability of the intact contralesional hemisphere. While early post-injury training improves functional recovery and delays training result in a lack of this improvement, a too early behavioral rehabilitation training can results in contra-productive deleterious effects on functional recovery. This has been revealed through the increase of damage tissues following stroke (Risedal et al., 1999). Thus, a short delay in days before initiating rehabilitative training can present a benefit. Effectively, an increase of the plastic changes promoting functional recovery has been shown in rats subjected to SCI (Krajacic et al., 2009).

Therapies focusing on the hyperexcitability of the intact contralesional hemisphere present benefic outcomes on functional recovery. The family of rehabilitative therapies termed Constraint-Induced Movement Therapy (CIMT) is successfully used in a large variety of injuries affecting the voluntary motor control (Taub et al., 1999). CIMT is based on the learned nonuse of the affected limb and consists to the immobilization of the unaffected limb (Taub et al., 1999; Kunkel et al., 1999). The immediate paralysis of the affected limb following injury can finally result in habituation to the nonuse although the possibility of its use recovers. CIMT results in strong improvement of the functional recovery in association with long-lasting cortical plasticity. The cortical representation of the affected body part finally increases in size whereas the unaffected body part one decreases (Liepert et al., 1998). The improvements which can be achieved with CIMT starts both early and late, even very later, after the injury and after the functional recovery plateaued and are observed to result in long-lasting improvements (Kunkel et al., 1999; Wolf et al., 2006). The long-lasting improvement of the functional recovery with CIMT is associated with long-term brain plasticity (Liepert et al., 1998, 2000). Potentially, such activity-dependent plastic changes can be underlined by the LTP, which can thus support the observed associated increase of the cortical excitability. The interhemispheric inhibition can also sustain such plasticity. Thereby, immobilization of the unaffected limb leads to the decrease of the intact hemisphere activity resulting in a disinhibition of the affected region. Bilateral movement therapy based on CIMT, which involves interlimb coordination, is linked with behavioral recovery and cortical plasticity and has thus a promising potential as behavioral rehabilitation therapy (Cauraugh and Summers, 2005). Such behavioral movement therapy results in cortical plastic changes that are revealed using fMRI. Such analysis has shown an increase of the activity in the

sensorimotor cortical areas, including the contralateral secondary somatosensory cortex and contralateral PMd (Johansen-Berg et al., 2002b). These changes of cortical activities through delimited cortical areas are correlated with functional recovery improvement.

Another set of rehabilitative therapies targets the modified cortical activity following injury of the motor system. Using the transcranial Direct Current Stimulation (tDCS) or repetitive Transcranial Magnetic Stimulation (rTMS), the cortical activity can be artificially modulated, increased or inhibited depending on the protocol used (Nitsche and Paulus, 2000; Ziemann et al., 2008). Improved functional recovery has been reported with specific protocol of stimulation of the lesioned cortex as well as with specific ones for the unaffected cortex (Ziemann et al., 2008; for review see Dancause et al., 2015). Stimulation of the lesioned cortex increases its excitability, lasting for more or less long term. Inhibition of the unaffected cortex is currently of strong interest to improve functional recovery. This results of the observation that hyperexcitability of the intact contralesional hemisphere can prevent activity to occur in the lesioned cortex following injury. Specific protocol of stimulation resulting in the inhibition of the unaffected cortex thus decreases the hyperexcitability of the intact contralesional hemisphere and disinhibits the lesioned cortical activity from the remote spared cortex, thus released from the transcallosal inhibition. However, some contradictory data have been reported, with negative effects of such stimulations that inhibit the contralateral intact hemisphere (for review see Dancause et al., 2015). Such negative effects appear to be linked with the degree of impairment. Beneficial effects of such rehabilitative therapy have been observed in weak to mildly impaired patients, the worsened effects have been reported in patient moderately to severely impaired (Bradnam et al., 2012).

1.5.2. Treatments

There is currently no curative treatment available for the CNS lesions. Finding a curative treatment represents from long time a major interest. Different strategies are considered to promote recovery after CNS injury targeting different aspects of the lesion events. The main strategies can be classified depending upon the aspect targeted (for review see Horner and Gage, 2000): (1) therapies targeting the immune response, to decrease the deleterious aspects and increase the benefic effects (Kadhim et al., 2008); (2) manipulation of the intracellular signaling to disrupt the apoptosis and cell death processes. While the clear benefit of these strategies is to give rise to a broad generalized response, the *in vivo* applications appear not realistic, depending on the large variety of different responses and the application timing; (3) the insertion of bridging and artificial substrates in the lesion site to

overpass and to allow the axonal re-growth to reconnect the sectioned part is a promising strategy, although this strategy needs invasive surgery; (4) the cellular therapy presents currently great interest. Different cells types are currently tested to observe their ability to integrate and reshape the spared circuit, replacing the lost neurons and thus the lost functions (Eftekharpour et al., 2008). Promising results have been observed on the ability of these cells to survive and being integrated in circuit, as well as on their potential role in the functional recovery, although many obstacles remain for such treatment (*e.g.* Eftekharpour et al., 2008; Kaeser et al., 2010; Guo et al., 2012); (5) promising current therapies target the lesion site environment to make the environment permissive to axonal re-growth, removing the growth inhibition such as the inhibition played by the myelin with Nogo-A and the other played by the glial scar with the CSPGs; (6) large interest concerns the promotion of the axonal re-growth delivering neurotrophic factor, such as BDNF.

The two latter therapy strategies present promising interest as CNS lesion therapy. The two strategies are addressed in the present work and thus further introduce.

1.5.2.1. Prevention of the post-lesion inhibitory environment: role of Nogo-A

Following injury, environment of the lesion site become inhibitory for the lesioned axons, blocking their further re-growth. A major inhibitory source of regeneration after motor system injury is due to inhibitory signaling pathways. Three major myelin inhibitor molecules are known to be largely implicated in the myelin inhibitory pathway activation, preventing regeneration post-injuries (Nash et al., 2009; Rosochowicz et al., 2015): Nogo-A (Caroni and Schwab, 1988; GrandPre et al., 2000; Chen et al., 2000), OMpg (oligodendrocyte-myelin glycoprotein) (Wang et al., 2002) and MAG (myelin-associated glycoprotein) (McKerracher et al., 1994; Mukhopadhyay et al., 1994; Domeniconi et al., 2002). These three proteins have been shown to bind a common receptor, NgR1 (Nogo-66 receptor), known to play a primary role of inhibition, activating cascade leading to growth cone collapse and inhibition of axonal growth (Fournier et al., 2001; GrandPre et al., 2002; McGee and Strittmatter, 2003; Nash at al., 2009; Cafferty et al., 2010). Integration of the signal elicited by NgR1 requires association with co-receptors, NgR1 lacking trans-membrane domain. Three additional co-receptors are currently known to form complex with the NgR1 receptor: the $p75^{NTR}$, LINGO-1 and TROY/TAJ. The growth inhibition is induced by the formation of heterotrimer with two of these co-receptor and NgR1 (Schwab et al., 2006). The $p75^{NTR}$ receptor is distinctly involves autonomously in the apoptosis pathways (for review see Roux and Barker, 2002). The study of the Nogo protein expression has revealed the existence of several isoform not all restricted

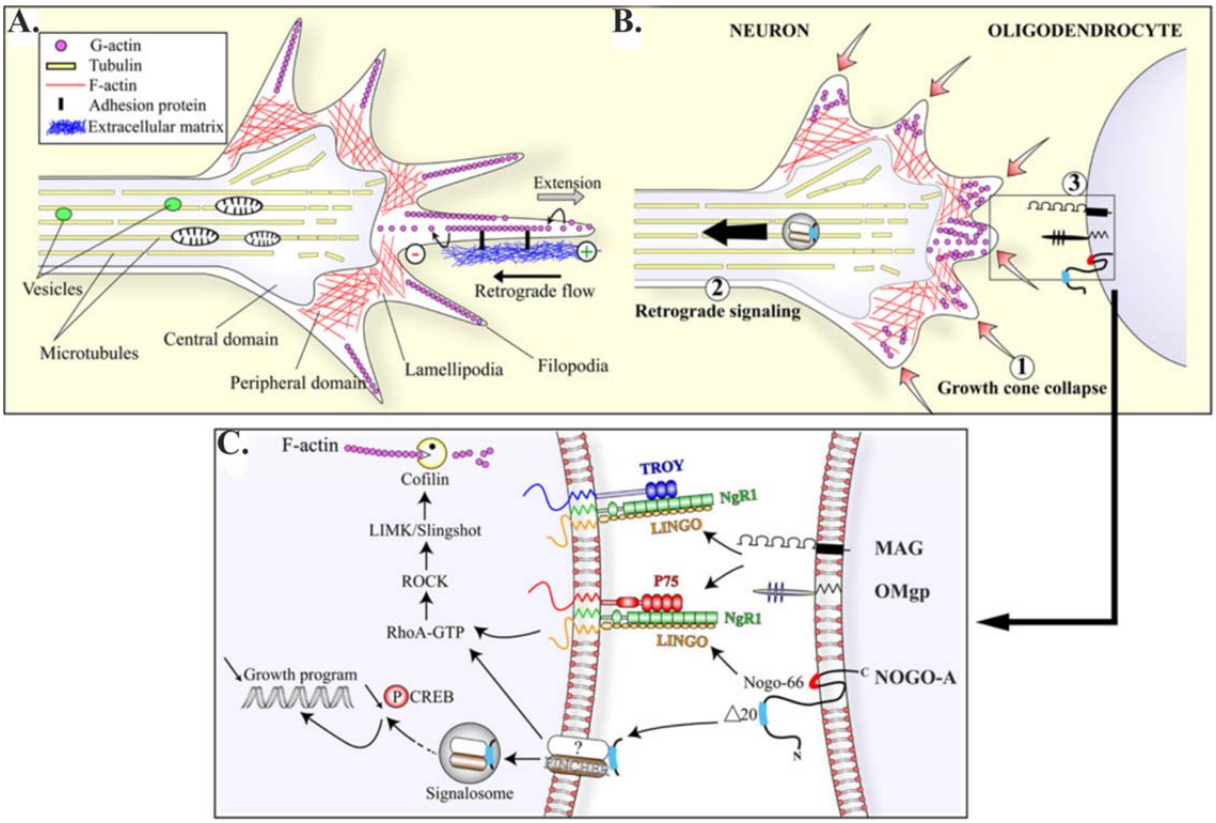

Figure 18: Illustration of the molecular mechanisms of the Nogo-A-mediated axonal growth inhibition (reproduced from Nudo et al., 1996).

to the CNS. Among the three main isoforms, whereas the two variants Nogo-B and -C are mostly observed outside the CNS, the Nogo-A is mainly present in the CNS, localized in the white matter in the myelin sheath membrane (Chen et al., 2000). Regulation at different steps of the Nogo-A transmission pathways (Fig. 18) is widely studied and associated with improvement of spontaneous recovery following motor injuries (Schwab, 2004; Filbin et al., 2003; Schwab and Strittmatter, 2014): (1) in vivo genetic inactivation of myelin inhibitor protein, Nogo-A, OMpg and MAG, improved recovery although their synergic (Cafferty et al., 2010), complementary or independent (Lee et al., 2010) roles are currently source of debate (Schnell and Schwab, 1990, 1993), (2) blockade of the activators binding on NgR, (3) blockade of NgR in an inactive state, (4) blockade of intracellular cascade at the kinase transducer level (Liu and Snider, 2001), decreasing of RhoA (Lehmann et al., 1999; Deng et al., 2013) or increasing the level of cAMP modulation involved in the signaling pathway (Cai et al., 1999; Neumann et al., 2002; Pearse et al., 2004). Intervention at one step of the cascade resulting from the NgR1 activation to block the growth cone collapse signal is shown to improve functional recovery and is associated with plastic changes comprising neural plasticity, sprouting and axonal regeneration (for reviews see Emerick and Kartje, 2004;

Schwab et al., 2006). Antibody blocking the axonal re-growth inhibitory myelin protein Nogo-A is a promising treatment making the environment permissive for lesioned axons re-growth and/or sprouting (GrandPre et al., 2000; Buchli and Schwab, 2005; Zorner and Schwab, 2010; for reviews see Pernet and Schwab, 2012; Wang et al., 2012; Schwab and Strittmatter, 2014). Antibody blocking Nogo-A has been correlated with an improvement of corticospinal axonal sprouting around spinal cord lesion site and with spontaneous behavioral recovery following spinal and cortical motor injuries, during a fine manual dexterity task in non-human primate (Fouad et al., 2004; Freund et al., 2006, 2007, 2009; Bashir et al., 2011; Hoogewoud et al., 2013) and in rodent (Schnell and Schwab, 1993; Thallmair et al., 1998; Papadopoulos et al., 2002; Li and Strittmatter, 2003; Lee et al., 2004). Such treatment with an antibody blocking the protein Nogo-A appears to be sensitive to the time at which the treatment is administered. Three days delayed in the initiation of such treatment increases the functional recovery (Wang et al., 2006) whereas 1 week delay did not lead to modify the effects (Li and Strittmatter, 2003).

1.5.2.2. Promotion of axonal re-growth: role of BDNF

Neuronal growth factor infusion is considered as a promising treatment, enhancing the axonal re-growth ability. Brain-Derived Neurotrophic Factor (BDNF) is one of the most studied neurotrophic factor, in the vast neurotrophin family. BDNF is considered as a high potential molecule for the treatment of numerous neurological diseases, particularly the spinal cord and cortical injury (for reviews see Lu and Tuszynski, 2008; Nagahara and Tuszynski, 2011). Described as a new factor supporting the survival and outgrowth of fibers, BDNF was the second neurotrophin discovered, after the Nerve Growth Factor (NGF), purified from the pig brain (Barde et al., 1982). Since, other neurotrophins with distinct profiles of trophic effects have been described forming a wide family of neurotrophic factors.

BDNF signaling pathways (Fig. 19; Kelamangalath and Smith, 2013) are involved in the inhibition of the growth cone collapse and the enhanced outgrowth. BDNF binds tyrosine kinases receptors family, the tropomyosin-related kinase (Trk). Three main isoforms are known to bind different neurotrophins, BDNF binding the TrkB isoform. TrkB is the high affinity receptor, but BDNF bind also the low affinity receptor $p75^{NTR}$ of the Tumor Necrosis Factor Receptor family (TNFα) (for reviews see Roux and Barker, 2002; Binder and Scharfman, 2004, Weishaupt et al., 2012; Kelamangalath and Smith, 2013). The $p75^{NTR}$ receptor is involved in two categories of signaling pathways: the survival and growth promotion pathways as co-receptor of TrkB receptor and in the apoptosis pathways

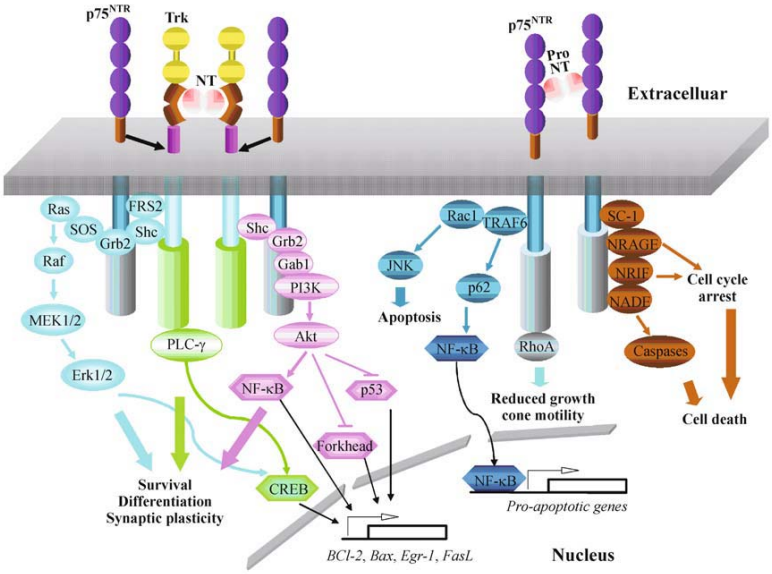

Figure 19: Illustration of the synaptic plasticity, axonal growth and pro-survival signaling pathways mediated through the tropomyosin-related kinase of the BDNF (TrkB) and of the pro-apoptotic and cell death pathways mediated through the $p75^{NTR}$ receptor (Modified from Kelamangalath and Smith, 2013)

autonomously (Bamji et al., 1998; Wang et al., 2000; Yeiser et al., 2004). BDNF is a major actor in axon guidance during development, a regulator of neuronal survival in adult CNS (for review see Huang and Reichardt, 2001) and has been involved in numerous neurological diseases. Well known for its beneficial role in the recovery following peripheral nerve injury (for reviews see Lu and Tuszynski, 2008; Nagahara and Tuszynski, 2011; Weishaupt et al., 2012), BDNF is highly involved in case of CNS lesion (for reviews see Lu and Tuszynski, 2008; Nagahara and Tuszynski, 2011). Early following spinal cord injury, an up-regulation of neurotrophins such as BDNF was observed (for review see Bareyre and Schwab, 2003). BDNF improves recovery post-lesion playing an anti-inflammatory role (Jiang et al., 2010). Although involved in a wide range of other processes (for review see Binder and Scharfman, 2004), BDNF is highly involved in the promotion of axonal growth and survival on different type of neurons (for review see Binder and Scharfman, 2004). BDNF exhibits a promoting role in the survival of axotomized axons, regeneration of injured fibers, plasticity, myelination and functional recovery (Sasaki et al., 2009; for review Weishaupt et al., 2012). The promotion of the re-growth and survival of axotomized axons is observed both for the ascending somatosensory axons and the different descending motor axons and can be observed both at the cortical level and at the spinal cord level, promoting the CST connections on descending interneurons in SCI (*e.g.* Bregman et al., 1997; Oudega and Hagg, 1999; Vavrek et al., 2006; Song et al., 2008; Hollis et al., 2009; Weishaupt et al., 2012). The beneficial role of BDNF in axonal re-growth and retrograde atrophy prevention remains a subject of debate for motor and somatosensory pathways, as it has also been involved in

deleterious effects, such as pain and hyperreflexia induction (for review see: Weishaupt et al., 2012).

The beneficial role of BDNF appears to be sensitive to the administration protocol. A dose-dependent relationship emerges for the BDNF action, with a dose response curve showing maximal effects for intermediate doses then decreasing for minimal and maximal doses (Mamounas et al., 2000). Furthermore, optimal BDNF action appears to respect a certain time window. Delaying the treatment with BDNF for 2 to 4 weeks in spite to its acute initiation exhibits highly improved beneficial effects on the supraspinal regeneration and the functional recovery (Mamounas et al., 2000; Coumans et al., 2001).

1.5.3. Combined therapy

Successes of all the rehabilitation therapies currently used and studied remain limited. Current opinion emphasizes that optimal regeneration may well require the application of combined therapies (Lu and Tuszynski, 2008). Still not optimal, different combinations have shown additional benefits on post-lesion recovery, associating several molecules or molecule with training (Shumsky et al., 2003; Zhou and Shine, 2003; Brock et al., 2010; Weishaupt et al., 2013; Wahl et al., 2014). However the difficulties of each therapy combined are not only added but additional difficulties can be linked to their association. Different optimal time periods and advantages for sequential treatment with a sequential protocol for anti-Nogo-A antibody treatment and training therapies have been observed (Wahl et al., 2014). Thus, variable results were observed for the different possibilities tested, some without benefit, as one can abolish the benefit of the other (Schnell et al., 1994; Novikova et al., 2000). Such strategies represent promising approaches requiring further investigations. This beneficial potential for combined therapies is raised in the present work addressing this question for the combination of the anti-Nogo-A antibody with the BDNF treatments in case of hemi-section of the spinal cord in macaque monkeys.

1.6. Experimental context and aims

The present thesis takes part of extensive studies in the macaque monkeys aiming to assess: (1) how the motor system lesion located at the spinal cord or at the cortical level affects behavioral, anatomical and electrophysiological parameters; (2) how a treatment with

an antibody directed against Nogo-A could promote recovery; (3) how a combination of the previous treatment with a neurotrophin, BDNF, could give rise to higher level of recovery.

The present thesis aims to provide anatomical, behavioral and electrophysiological evidences on the understanding of the motor system lesions and the following recovery, spontaneous or promoted by treatment. The present work addresses three general aims focused on the motor control of voluntary movement, more precisely the precision grip:

(1) The present work aims to provide further evidences to assess to what extent lesion in the motor system induces reorganization in the connected structures. The present work aims to detect plastic changes from the vicinity in the perilesional cortex, the contralesional cortex up to the brainstem and the somatosensory system at the brainstem level. In the present work, I investigate their participation in the post-lesion recovery.

(2) The second aim addresses the effects of motor system lesion and the following functional recovery distinguishing different components of the precision grip movement. In this study, I aim to address the possibility to observe differences of functional recovery and cortical M1 participation through an extensive behavioral study. This study aims to assess the possibility to distinguish deficit of different movement characteristics or phases observed following M1 lesion with an extensive behavioral study. The aim is to bring new evidences for the debated potential role of the contralesional cortex following M1 lesion.

(3) The present work addresses the possibility to improve the functional recovery assessing the beneficial potential of post-lesion treatments. The third aim intends to provide further evidences of the potential beneficial effects of the treatment blocking the Nogo-A following lesion of the motor system. Secondly, the present work addresses the possibility of higher degree of recovery combining the previous treatment with the neurotrophin BDNF treatment.

The different aims will be addressed through four chapters: (1) In the first chapter, I will provide electrophysiological data of the perilesional cortex reorganization following lesion of the M1 hand area. Behavioral data will be provided during the post-lesion time course. Such investigations allow testing the potential beneficial effects on these data of a treatment with the Nogo-A antibody. (2) In the second chapter of the present work, I will assess the role of the contralesional cortex secondary lesion following a primary lesion of the M1 hand area. This study will provide an extensive behavioral assessment of different parameters of the precision grip movements and their impairments following a primary lesion

of M1 hand area and a secondary consecutive lesion of the intact contralesional M1. (3) In the third chapter, I will focus on the electrophysiological properties of the descending pathways following spinal cord hemisection located at the C7/C8 level. This chapter will allow to localize the cortical or subcortical level of the motor command initiation using electrical cortical stimulation. Such investigations allow to test the potential beneficial effects on these data of a treatment combining the Nogo-A antibody with the neurotrophin BDNF. This study will further provide behavioral and anatomical data following such lesion and experimental treatment. (4) In the fourth chapter, I will assess the possibility for the somatosensory pathway to reorganize following lesion of the M1 hand area and spinal cord hemisection located at the C7/C8 level. This study will provide anatomical information concerning the primary somatosensory axon terminals fields reaching the first brainstem relay, the dorsal column nuclei, and concerning the dorsal column pathways integrity. Such investigations allow testing the potential beneficial effects on these data of a treatment with the Nogo-A antibody and another combining the Nogo-A antibody with the neurotrophin BDNF.

2. Experimental results

2.1. Chapter 1:

Long-term motor cortical map changes following unilateral lesion of the hand representation in the motor cortex in macaque monkeys showing functional recovery of hand functions

Alexander F. Wyss[a,1], Adjia Hamadjida[a,d,1], Julie Savidan[a,1], Yu Liu[a,e], Shahid Bashir[a,f], Anis Mir[b], Martin E. Schwab[c], Eric M. Rouiller[a,2] and Abderaouf Belhaj-Saïf[a,2]

a Faculty of Sciences and Fribourg Centre for Cognition, Department of Medicine, University of Fribourg, Chemin du Musée, Fribourg, Switzerland

b Novartis Pharma AG, Basel, Switzerland

c Brain Research Institute, University of Zürich and Department of Health Sciences and Technology, ETH Z¨ Zürich, Switzerland

d Université de Montréal, Département de Physiologie, Chemin de la Tour, Montréal QC, Canada

e Univ. Tennessee HSC, Memphis, TN, USA

f Faculty of Medicine, Department of Physiology, Autism Research and Treatment Center, King Saud University, Riyadh, Saudi Arabia and Berenson-Allen Center for Noninvasive Brain Stimulation, Department of Neurology, Beth Israel Deaconess Medical Center, Harvard Medical School, Boston, MA, USA

1 Equal first authorship.

2 Equal senior authorship.

Restorative Neurology and Neuroscience 31 (2013) 733–760
DOI 10.3233/RNN-130344
IOS Press

Long-term motor cortical map changes following unilateral lesion of the hand representation in the motor cortex in macaque monkeys showing functional recovery of hand functions

Alexander F. Wyss[a,1], Adjia Hamadjida[a,d,1], Julie Savidan[a,1], Yu Liu[a,e], Shahid Bashir[a,f], Anis Mir[b], Martin E. Schwab[c], Eric M. Rouiller[a,*,2] and Abderaouf Belhaj-Saif[a,2]

[a]*Faculty of Sciences and Fribourg Centre for Cognition, Department of Medicine, University of Fribourg, Chemin du Musée, Fribourg, Switzerland*

[b]*Novartis Pharma AG, Basel, Switzerland*

[c]*Brain Research Institute, University of Zürich and Department of Health Sciences and Technology, ETH Zürich, Switzerland*

[d]*Université de Montréal, Département de Physiologie, Chemin de la Tour, Montréal QC, Canada*

[e]*Univ. Tennessee HSC, Memphis, TN, USA*

[f]*Faculty of Medicine, Department of Physiology, Autism Research and Treatment Center, King Saud University, Riyadh, Saudi Arabia and Berenson-Allen Center for Noninvasive Brain Stimulation, Department of Neurology, Beth Israel Deaconess Medical Center, Harvard Medical School, Boston, MA, USA*

Abstract.

Purpose: How are motor maps modified within and in the immediate vicinity of a damaged zone in the motor cortex of non-human primates?

Methods: In eight adult macaque monkeys subjected to a restricted chemical lesion of the hand area in the primary motor cortex (M1), motor maps were established using intracortical micro-stimulation (ICMS) techniques. The monkeys were subdivided into five animals without treatment, whereas three monkeys received an anti-Nogo-A antibody treatment.

Results: Following permanent M1 injury, the lesion territory became largely non micro-excitable several months post-lesion, in spite of some recovery of hand function. Few sites within the lesion territory remained excitable, though irrespective to the degree of functional recovery. Around the lesion in M1, there was no reallocation of proximal shoulder/arm territories into distal hand functions. However, ICMS delivered at supra-threshold intensities in these proximal territories elicited digit movements. Post-lesion ICMS thresholds to elicit movements of forelimb muscle territories increased, independently from the degree of functional recovery. Further behavioural evidence for an enhancement of functional recovery promoted by the anti-Nogo-A antibody treatment is provided.

Conclusion: The degree of functional recovery is not related to a reorganization of motor maps within, and in the vicinity of, a M1 lesion.

Keywords: Primates, intracortical microstimulation, somatotopy, neuroplasticity

[1]Equal first authorship.

[2]Equal senior authorship.

*Corresponding author: Prof. Eric M. Rouiller, Department of Medicine, University of Fribourg, Chemin du Musée 5, CH-1700 Fribourg, Switzerland. Tel.: +41 26 300 86 09; Fax: +41 26 300 96 75; E-mail: Eric.Rouiller@unifr.ch.

1. Introduction

A lesion of the adult motor cortex results in a long-lasting hemi-paresis of the corresponding (opposite) body territory, although some spontaneous and incomplete functional recovery may occur during the weeks or months following the cortical damage (see e.g. Dancause and Nudo, 2011 for review). Knowledge of the mechanisms underlying this limited spontaneous recovery is crucial in order to develop strategies to enhance functional restitution from cortical damage, using rehabilitative training protocols and/or various treatments (pharmacological, cell therapy, brain stimulation, etc). Before clinical application can be done safely and efficiently, mechanisms of functional restitution should be elucidated in detail using animal models. In this context, the model of the non-human primate is especially valuable as the general organization of the motor system controlling voluntary movements in monkeys is similar to that of humans (Courtine et al., 2007; Lemon and Griffiths 2005; Lemon, 2008). In the past, several studies conducted in non-human primates have investigated the consequences (deficits) of a lesion of the motor cortex on the ability to perform voluntary movements, as well as to what extent and how some spontaneous recovery may contribute to the restitution of some motor control (e.g. Ogden and Franz, 1917; Glees and Cole, 1950; Travis, 1955; Brinkman and Kuypers, 1973; Passingham et al., 1983; Friel and Nudo, 1998; Rouiller, et al., 1998; Liu and Rouiller, 1999; Frost et al., 2003; Marshall et al., 2003; Plautz et al., 2003; Roitberg et al., 2003; Dancause et al., 2005, 2006; Pizzimenti et al., 2007; Eisner-Janowicz et al., 2008; Murata et al., 2008; Darling et al., 2009, 2010, 2011; Bihel et al., 2010; McNeal et al., 2010; Kaeser et al., 2010, 2011; Bashir et al., 2012; Hamadjida et al., 2012). The usually incomplete spontaneous recovery taking place after a unilateral lesion affecting the primary motor cortex (M1) is based, at least in part, on a vicarious phenomenon in which (ipsilesional) non-primary motor cortical areas (premotor cortex (PM), Supplementary motor area (SMA), or even the somatosensory cortex) may take over part of the lost function (Sasaki and Gemba, 1984; Widener and Cheney, 1997; Liu and Rouiller, 1999; Frost et al., 2003; Dancause et al., 2005, 2006; Eisner-Janowicz et al., 2008; McNeal et al., 2010). The incomplete functional recovery of manual dexterity in cases where the lesion of M1 affects the hand representation may include the emergence of compensatory movement patterns, favored by rehabilitative training (e.g. Friel and Nudo, 1998; Murata et al., 2008), or in combination with peri-infarct electrical stimulation (Plautz et al., 2003).

One may hypothesize that the more extensive (or severe) the lesion in M1, the more likely is the involvement of a non-primary motor cortical area in the incomplete functional recovery. If the lesion is however restricted to a part of M1, there is evidence that preserved territories in M1 may be re-organized to take over part of the lost motor function, if post-lesion training/practice takes place or in case of neonatal lesion (Glees and Cole, 1950; Nudo and Milliken, 1996; Nudo et al., 1996; Rouiller et al., 1998; Plautz et al., 2003). The re-organization of such peri-lesion territory in M1 consists in changes of somatotopic representations, as assessed by intracortical microstimulation (ICMS) by comparing pre-lesion and post-lesion motor maps. The goal of the present study was to investigate, in a relatively large group of eight adult macaque monkeys subjected to a restricted chemical (excitotoxic) lesion of the hand M1 representation, how the motor maps are modified within as well as at the vicinity of the damaged zone using ICMS performed pre-lesion and repeated post-lesion, after the incomplete functional recovery has reached a plateau. In other words, it is hypothesized that, as a result of ibotenic acid infusion in the hand area in M1, the lesioned territory remains non-responsive to ICMS post-lesion, in spite of an incomplete functional recovery. A further hypothesis is that the extent of functional recovery is related to the degree of motor map rearrangement in the cortical territories immediately adjacent to the lesion. Finally, the pool of eight monkeys subjected to a unilateral lesion of the motor cortex was subdivided into a subgroup of five (control) animals without treatment to improve functional recovery, and a subgroup of three monkeys which received an anti-Nogo-A antibody treatment (see Gonzenbach and Schwab, 2008; Schwab, 2010 for review on this therapy), known to enhance functional recovery after motor cortex lesion in the rat (Papadopoulos et al., 2002; Emerick et al., 2003; Emerick and Kartje, 2004; Seymour et al., 2005; Markus et al., 2005; Tsai et al., 2007, 2011; Cheatwood et al., 2008; Gillani et al., 2010). An assessment of the possible benefit of the anti-Nogo-A antibody treatment on functional recovery was conducted here from the eight monkeys, in parallel to the analysis of the electrophysiological data.

2. Methods

2.1. General survey of the experiments

The data were collected from 8 monkeys (*macaca fascicularis*, 3.5–6.5 kg, 4–6 years old, 1 female and 7 male), all trained to perform 3 different behavioral tasks aimed at assessing manual hand dexterity (Schmidlin et al., 2011; Kaeser et al., 2011, 2013; Hamadjida et al., 2012): (i) the modified Brinkman board task; (ii) the rotative Brinkman board task; (iii) the Brinkman box task (see Schmidlin et al., 2011 for a detailed description and for visualization of the 3 manual dexterity tasks). Once the monkeys attained a stable behavioral performance for several weeks (thus reaching a pre-lesion plateau), a chronic stainless steel chamber was implanted above the left hemisphere, to have access principally to the primary motor cortex (M1) and the dorsal and ventral premotor cortical areas (PMd and PMv, respectively). The hand area of M1 was defined based on a first series (pre-lesion) of daily ICMS sessions for a period of about 2 months, during which the behavioral training was pursued, though to a lesser extent. After completion of the pre-lesion ICMS map, behavioral training was more extensively repeated in order to confirm the pre-lesion plateau of manual dexterity obtained before the ICMS phase. Targeting the ICMS sites where a movement of the hand was elicited at low threshold, ibotenic acid was infused at multiple sites (Table 1) to generate a permanent lesion aimed unilaterally at the hand representation, as previously reported (Liu and Rouiller, 1999; Kaeser et al., 2010, 2011; Bashir et al., 2012; Hamadjida et al., 2012). The behavioral assessment was conducted daily over several months to quantify the deficits resulting from the lesion as well as the time course and extent of functional recovery during several months post-lesion (see Kaeser et al., 2010, 2011; Bashir et al., 2012; Hamadjida et al., 2012). After reaching a post-lesion plateau of behavioral recovery, stable over a few weeks, a second (post-lesion) series of daily ICMS session was performed, with the aim to investigate how the initial hand representation was modified by both the lesion and the functional recovery of manual dexterity. The second series of daily ICMS sessions also lasted approximately 2 months, as the same sites were re-explored. The aim of the present study was to specifically compare the pre-lesion and the post-lesion ICMS maps.

Surgical procedures and animal care, previously described in detail (Kaeser et al., 2010, 2011; Bashir et al., 2012; Hamadjida et al., 2012), were conducted in accordance to the Guide for the Care and Use of Laboratory Animals (ISBN 0-309-05377-3; 1996). The experimental protocol was approved first by the local (cantonal) ethical committee (surveying animal experimentation and evaluating research proposals). Finally, the experiments were authorized by the cantonal (Fribourg) and federal (Swiss) veterinary officers. The present experiments were covered by the following authorizations: FR 24/95/1; FR 44/92/3; FR 157/01, FR 157/03, FR 157/04, FR 156/04, FR 156/06, FR 157e/06; FR 185-08.

2.2. Manual dexterity tests (behavioral assessment)

The eight monkeys were trained to perform behavioral tasks aimed at quantifying manual dexterity (see above). In the present report, behavioral data derived from the modified Brinkman board task are reported. The task, modified from the original test (Brinkman and Kyupers, 1973; Brinkman, 1984), was designed to specifically assess manual dexterity in monkeys (see Schmidlin et al., 2011 for detail). The monkey, sat in a primate chair, is placed in front of a board comprising of 50 slots, 25 oriented vertically and 25 horizontally, each filled with a food pellet. Using either the left hand or the right hand, the monkey grasped pellets using the precision grip, by opposing the tip of the index finger to the tip of the thumb. The methods of analysis of the behavioral data have been presented in a recent report (Schmidlin et al., 2011). In the present study, motor performance was assessed by the score, given by the number of pellets retrieved during the first 30 seconds of the test, from either the vertical or the horizontal slots. A total score was calculated, corresponding to the sum of the scores obtained for the 2 slots orientations.

2.3. Surgical procedures

All surgical procedures were conducted under deep anesthesia. Before all implant surgeries, the monkeys were sedated with an intramuscular (i.m.) injection of ketamine (Ketalar®; Parke-Davis, 5 mg/kg) and atropine was injected to reduce bronchial secretion (0.05 mg/kg, i.m.). Monkeys were then deeply anesthetized with an intravenous (i.v.) perfusion of 1% propofol (Fresenius®) mixed with a 5% glucose saline

solution (1 volume propofol and 2 volumes of glucosaline, delivered at a dose of 0.1 mg/kg/min). To prevent brain edema, Dexamethasone (Decadon®) was injected i.m. (0.05 ml/kg diluted 1 : 1 in saline). Concomitantly, a preventive pain killer (Carprofen) was administered i.m. (Rimadyl®; 50 mg/ml, 4 mg/kg). To further reduce possible activation of pain receptors during the surgery itself, ketamine was added to the i.v. perfusion solution (0.0625 mg/kg/min), as previously reported (Freund et al., 2007). The surgery was carried out under continuous monitoring of the following parameters: heart rate, respiration rate, expired CO_2, arterial O_2 saturation and body temperature. Before surgery, all monkeys received a subcutaneous injection of the antibiotic Albipen® (Ampicillin 10%, 30 mg/kg). Immediately after surgery and offset of anesthesia, the monkey was continuously supervised by the experimenters until it was sufficiently awake and started to eat and drink. During the week following the surgery, additional doses of Carprofen were given daily (Rymadil® pills mixed with food, 4 mg/kg). Antibiotic (ampiciline as above) was administered on alternate days for the first week after surgery. All surgeries were performed in a facility under sterile conditions and approved by the cantonal veterinary office.

2.4. Cortical chronic chamber implant

After reaching a stable behavioral performance (prelesion plateau), a square or a rectangular stainless steel chamber was stereotaxically implanted above the forelimb area of M1 on the left hemisphere (except in Mk-JU which was implanted above the right hemisphere). The chamber was centered at stereotaxic coordinates 15 mm anterior and 15 mm lateral, and at an angle of 30° with respect to the mid-sagittal plane, allowing perpendicular electrode penetrations with respect to the cortical surface. Six to ten self-taped titanium screws were used to anchor the chamber to the skull. Moreover, for better stability, two flat wings soldered to the chamber, one rostral and one caudal, were also anchored to the skull by titanium screws. The edge of the chronic chamber next to the skull, as well as the titanium screws were covered with dental acrylic or orthopedic cement (Palacos®). Over the mid-occipital and frontal regions of the skull, two stainless steel cylinders were anchored with 3-4 titanium screws and then cemented as described above for the chronic chamber. These cylinders allowed head restraining during the cleaning of the chronic chamber and, most importantly, during the ICMS sessions conducted while the monkey was awake. Nevertheless, a partly flexible head restrain attached to the cylinders allowed limited movement of the head. To prevent infection, the chronic chamber was cleaned daily with Betadine and an antibiotic ointment (Morrhulan).

2.5. Intracortical microstimulation (ICMS) procedures

During the initial phase of behavioral training, the monkeys were progressively habituated to be passively manipulated, allowing the experimenter to generate passive movement of the forelimb and hindlimb. The goal of this habituation was to offer the possibility to the experimenter to modify the posture of the limbs during the subsequent ICMS sessions, for better assessment (visual and by palpation) of the overt motor response elicited by the electrical ICMS and searching for the threshold. Electrophysiological ICMS procedures (see Rouiller et al., 1998; Liu and Rouiller, 1999; Schmidlin et al., 2004, 2005) were performed twice in each monkey, first before the cortical lesion in order to guide the lesion procedure by mapping the M1 hand representation and, second, several months after the lesion when the monkeys reached a stable post-lesion manual performance (Table 1).

For ICMS, we used glass- or mylar-insulated platinum-iridium electrodes with typical impedances between 0.1 to 1.0 MΩ (Frederick Haer & Co., Bowdoinham, ME). The monkey sat in the primate chair, as described previously (Liu and Rouiller, 1999). The head was restrained and the electrode advancing system (Narishige group, Japan, Model MO-95) was attached to the chronic chamber. Electrode penetrations were performed systematically in and around the hand area of M1, distributed at a 1 mm grid interval, along the rostro-caudal and medio-lateral axes (Fig. 1A). The electrode was manually advanced (usually 1 mm step in depth), starting from 2 mm below the dura surface, along a maximal distance of 10–12 mm for penetrations targeting the rostral bank of the central sulcus, as recently illustrated (Kaeser et al., 2010).

The ICMS consisted of 12 electric pulses, delivered in a train of 33 ms duration, at a rate of 330 Hz. The effect of ICMS was assessed by visual inspection and/or palpation of muscle contraction at which a movement was elicited. The minimal current (ICMS threshold) producing the motor response was determined at each ICMS site along the electrode

Table 1
List of monkeys subjected to permanent primary motor cortex lesion and included in the present study with identification code

	Mk-CE	Mk-JU	Mk-GE	Mk-RO	Mk-BI	Mk-VA	Mk-SL	Mk-MO
Gender	Male	Male	Female	Male	Male	Male	Male	Male
Treatment	None	None	None	None	None	Anti-Nogo-A antibody	Anti-Nogo-A antibody	Anti-Nogo-A antibody
Age at time of lesion (rounded 0.5 year)	4.5	5	5	4	5	5.5	5.5	5.5
Weight at time of lesion	3.8	3.6	2.8	3.2	5	4.9	4.6	5.6
Volume of ibotenic acid injected (μL)	40	40	13	18	29.7	15.5	18	20
Number of ICMS sites injected with ibotenic acid	21	21	13	12	29	11	12	20
Time interval (months) between lesion and post-lesion ICMS mapping	11	10	3.25	5	7.3	10.5	16.5	3.2
Estimates of “unfolded hand area pre-lesion” (in mm^2)	**37**	**33**	**25**	**56**	**55**	**40**	**45**	**34**
Total volume of lesion (in mm^3) Gray matter (motor cortex + post-central gyrus)	**112.8**	**63.01**	**48.7**	**14**	**20.13**	**20**	**78.2**	**41.8**
Volume of lesion in post-central gyrus (in mm^3)	10.1	0	7.6	0	0	5.8	1.8	0
Lesion spread sub-cortically to the white matter (in mm^3)	86.5	28.9	0	0	0	0	130.6	0
Degree of functional recovery from M1 lesion (expressed in % of post-lesion total score at plateau with respect to pre-lesion total score in the modified Brinkman board task: all slots)	**42%**	**39%**	**38%**	**98%**	**74%**	**87%**	**73%**	**76%**
Degree of functional recovery from M1 lesion (expressed in % of post-lesion horizontal score at plateau with respect to pre-lesion horizontal score in the modified Brinkman board task: horizontal slots)	**9%**	**29%**	**11%**	**90%**	**36%**	**91%**	**77%**	**60%**
Degree of functional recovery from M1 lesion (expressed in % of post-lesion vertical score at plateau with respect to pre-lesion vertical score in the modified Brinkman board task: vertical slots)	**59%**	**46%**	**57%**	**100%**	**94%**	**87%**	**77%**	**84%**

Monkeys Mk-CE and Mk-JU were part of a pilot study (Liu and Rouiller, 1999), with the initial aim to generate fairly large lesions. In subsequent monkeys (Mk-GE and MK-VA), the volume of ibotenic acid was reduced to generate a lesion more focused to the M1 hand area. In the monkeys included later over the 8 years of the study (Mk-RO, Mk-BI, Mk-MO and Mk-SL), ibotenic acid was injected under propofol anaesthesia (as required by new ethical guidelines), and no longer in the awake state. The volume of ibotenic acid was thus slightly increased, as propofol is known to reduce the excitotoxicity of ibotenic acid (Snyder et al., 2007).

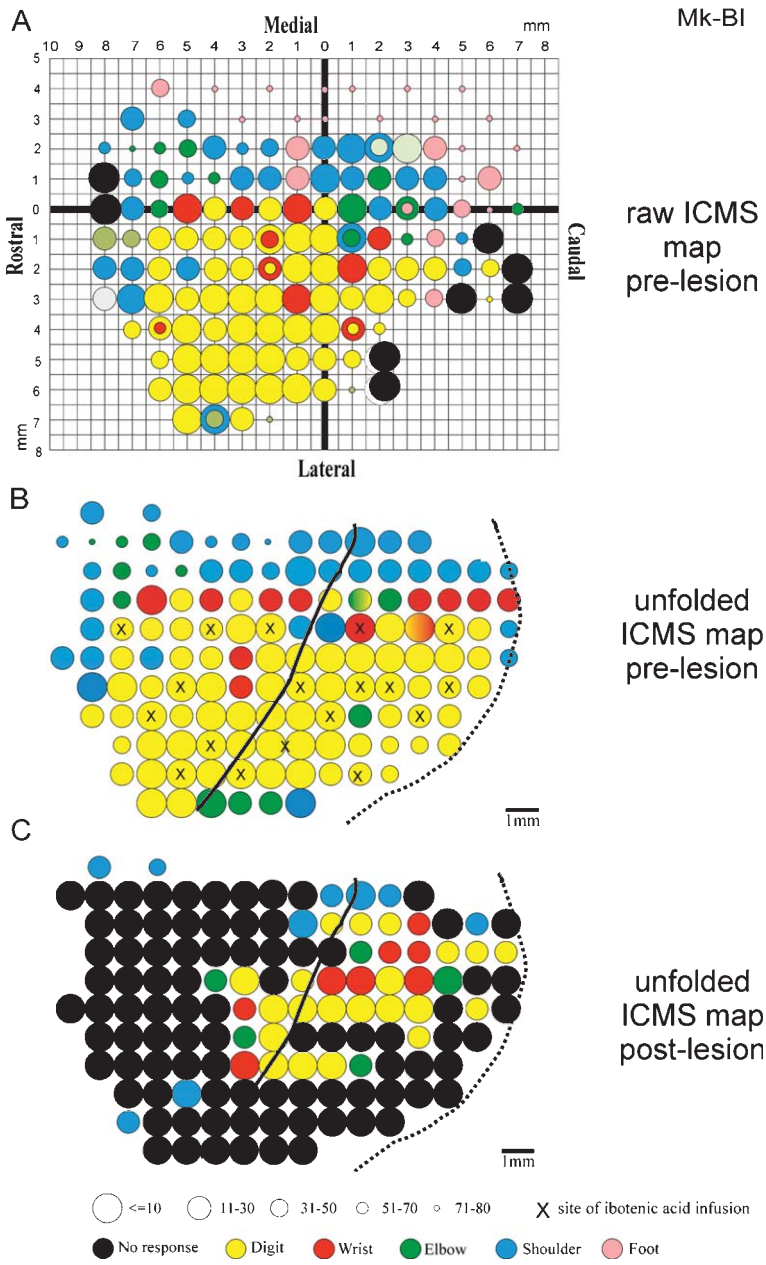

Fig. 1. Example of ICMS maps established in the untreated monkey Mk-BI, in the initial (raw) format pre-lesion (panel A) and after unfolding the central sulcus, pre-lesion (panel B) and post-lesion (panel C). In panel A, each circle corresponds to the location on the cortical surface of an electrode penetration. Still in panel A, the movement elicited by ICMS at the lowest threshold along each electrode penetration is represented by the color code shown on the bottom (e.g. wrist, finger, etc; at few sites, a circle represented with 2 colors indicate an effect at the same threshold for two body territories). The same ICMS sites as in panel A appear in panel B and C, plus some additional sites along the rostral bank of the central sulcus, as explained in the methods. Same color code in panels B and C as in panel A. In all panels, the set of circles on the bottom of the figure indicates the threshold (in microamps) at which the corresponding body movement was still observable at the lowest intensity. The five graded circle sizes (encountered in the ICMS maps) correspond to different threshold ranges, as indicated on the right of the circles. In each ICMS map, five graded circle sizes have been used to distinguish the excitability of each ICMS site. In panels B and C, the solid oblique line represents the approximate position of the central sulcus as it appears on the surface of the cerebral cortex, whereas the oblique dashed line represents the fundus of the central sulcus.

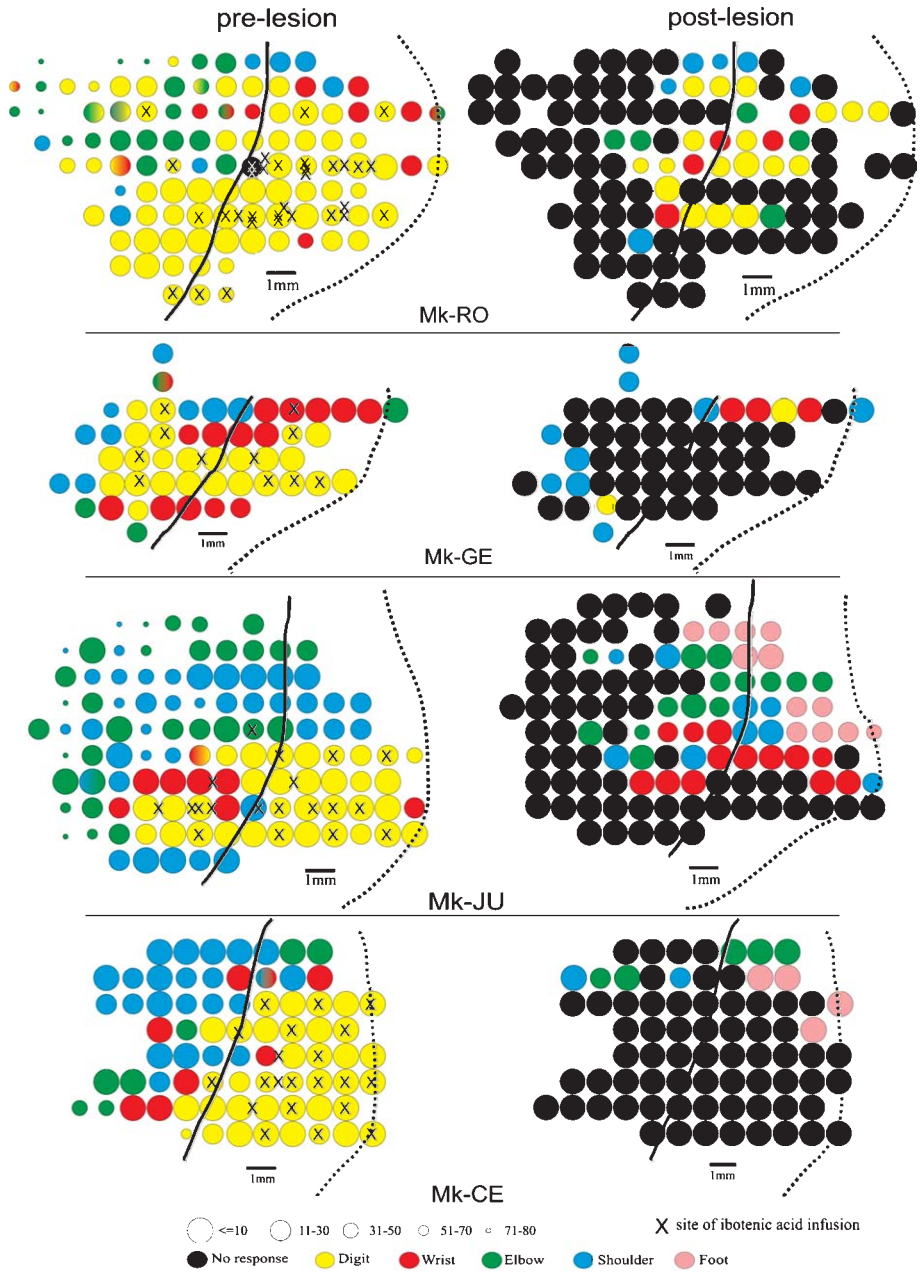

Fig. 2. Unfolded ICMS maps established pre-lesion (left column) and post-lesion (right column) in the untreated monkeys MK-RO, Mk-GE, Mk-JU and Mk-CE. same conventions as in Fig. 1. In Mk-JU, the ICMS map has been mirrored horizontally so that it appears as derived from the left hemisphere for better comparison with the other monkeys, although the mapping was conducted originally on the right hemisphere (see Fig. 4A: Mk-JU).

penetration. The intensity of stimulation ranged from 80 to 1 microamp. The intensity of 80 microamps was mostly applied at the beginning of the electrode penetration (close to surface) and was decreased until threshold. At the next ICMS site (1 mm deeper), the initial intensity of stimulation was set slightly above (10 microamps) the threshold intensity of the previous stimulation site. If this intensity did not elicit any

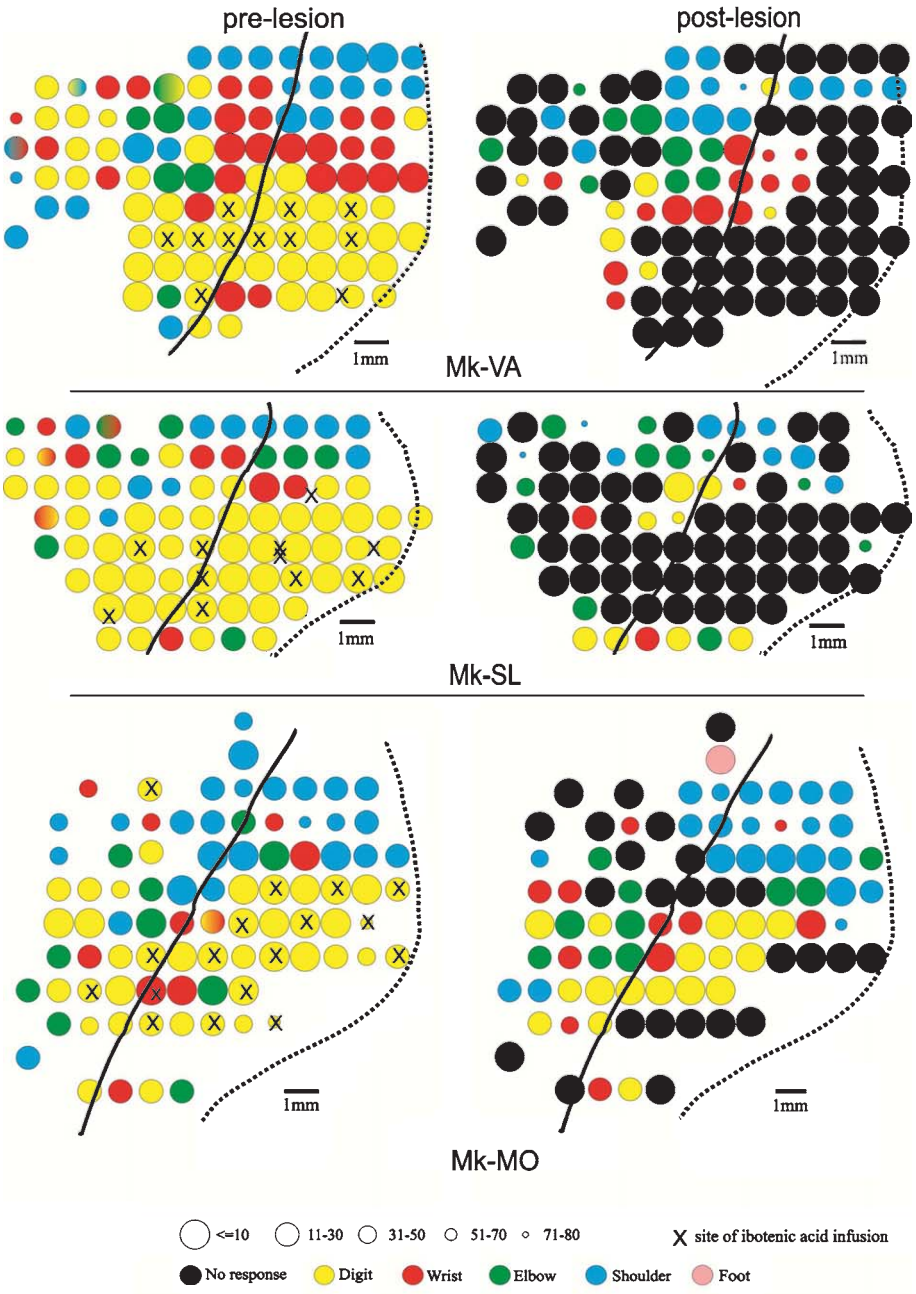

Fig. 3. Unfolded ICMS maps established pre-lesion (left column) and post-lesion (right column) in the three anti-Nogo-A antibody treated monkeys Mk-VA, Mk-SL and Mk-MO. Same conventions as in Fig. 1.

movement, then it was progressively increased until threshold, but not above 80 microamps (in the absence of response at 80 microamps, the site was considered as non-responsive). On the other hand, if the slightly increased intensity produced an effect, then it was decreased until threshold. During the entire stimulation period at each ICMS site, one experimenter held the monkey's forelimb and passively moved it to different postures to determine the effect of the ICMS on the different joints (fingers, wrist, elbow, shoulder, etc).

2.6. Cortical lesion and anti-Nogo-A antibody pump implant

In each monkey, after completion of the ICMS map and precise delineation of the hand representation in M1, as well as some behavioral retraining, a permanent lesion of M1 was performed unilaterally, targeted to the hand area. The cortical lesion was produced by infusion of ibotenic acid (Sigma) at multiple sites (Table 1), where movements of the fingers were obtained at low threshold in response to ICMS. The precise procedure of ibotenic acid infusion was described earlier (Liu and Rouiller, 1999; Kaeser et al., 2010; Hamadjida et al., 2012). In a separate and recent study, the time-course of the neurotoxic effect of ibotenic acid infusion in the cerebral cortex of a monkey was assessed based on cerebral blood flow and MRI measurements (Peuser et al., 2011). A volume of 1 μl to 1.5 μl of ibotenic acid solution (10 μg/μl phosphate buffer saline) was injected at each selected ICMS site, via a 10 μl Hamilton syringe replacing the electrode at the corresponding penetration site. The total volume of infusion was adapted to the extent and shape of the hand representation in M1 previously determined by ICMS. Ibotenic acid is expected to diffuse approximately 1.5 mm around the center of injection site (by analogy with diffusion of muscimol; see Martin, 1991). The distance between adjacent infusion sites thus ranged between 1.5 to 3 mm, in order to cover most of the hand representation. In the initial monkeys (Table 1: Mk-CE and Mk-JU), the infusion of ibotenic acid took place when the animal was awake and sat quietly in the primate chair. A few minutes after infusion of ibotenic acid, a progressive motor deficit of the contralateral hand appeared, reflected by a flaccid paralysis of the hand. In subsequent monkeys (Table 1), ibotenic acid was injected under anaesthesia.

On the day of the lesion, the monkeys subjected to a lesion of M1 were separated into two groups (Table 1). One group of five monkeys did not receive any treatment (control monkeys) whereas the second group of three monkeys was treated with the anti-Nogo-A antibody 11C7 (Oertle et al., 2003). The treated monkeys were implanted in the neck region (in a subcutaneous pouch), under deep anaesthesia, with two osmotic pumps (Alzet®, model 2ML2, 5 μl/h), containing the anti-Nogo-A antibody 11C7 at a concentration of 3 mg/ml. One osmotic pump was used to infuse the antibody intrathecally in the spinal cord at cervical level, as previously reported in our studies on spinal cord injury (Freund et al., 2006, 2007, 2009). The second osmotic pump was used to deliver the anti-Nogo-A antibody at cortical level, close to the lesion territory. The catheter of this second osmotic pump was tunnelled under the skin to the head of the monkey. Through a small opening in the skull, the tip of catheter was push under the dura in close proximity to the motor cortex. Once the catheters from both osmotic pumps were in place, the muscles and skin were sutured. The osmotic pumps delivered the antibody treatment during 4 weeks and then they were removed under deep anaesthesia. The untreated monkeys were not implanted with osmotic pumps.

2.7. Processing of ICMS data: Unfolding the motor cortex maps

ICMS data were represented in two different types of cortical maps: a standard (raw) ICMS map (see Liu and Rouiller, 1999; Kaeser et al., 2010: Supplemental Fig. 1 panel A) and an unfolded ICMS map (see Park et al., 2001, 2004; Kaeser et al., 2010: supplemental Fig. 1 panel C). The standard ICMS map consisted in projecting the lowest ICMS threshold obtained along an individual electrode track on the surface of the motor cortex, at the location of electrode penetration. The resulting ICMS map forms a grid with intervals of 1 mm × 1 mm and allows ICMS positioning on the brain surface (Fig. 1A). The limitation of this method is that electrode tracks running in the rostral bank of the central sulcus in parallel to the cortical layers is represented only by a single point on the surface, although the electrode may have stimulated layer V neurons at low threshold at several adjacent sites (see Kaeser et al., 2010: Supplemental Fig. 1). In contrast, the unfolded map represents all sites, including numerous ones in the rostral bank of the central sulcus, where the lowest thresholds were obtained by ICMS, presumably at the location of abundant pyramidal cells in layer V. This is in line with tracing data showing a high density of corticomotoneuronal cells in the rostral bank of the central sulcus (He et al., 1993, 1995; Rathelot and Strick, 2006). As a consequence, the multiple ICMS sites in layer V encountered along an individual electrode track in the rostral bank of the central sulcus appear in the unfolded ICMS map (see Kaeser et al., 2010: Supplemental Fig. 1). In summary, a two-dimensional rendering of cortical layer V in the rostral bank of the central sulcus required flattening and unfolding of its curvature. To this aim, all electrode tracks were first grouped

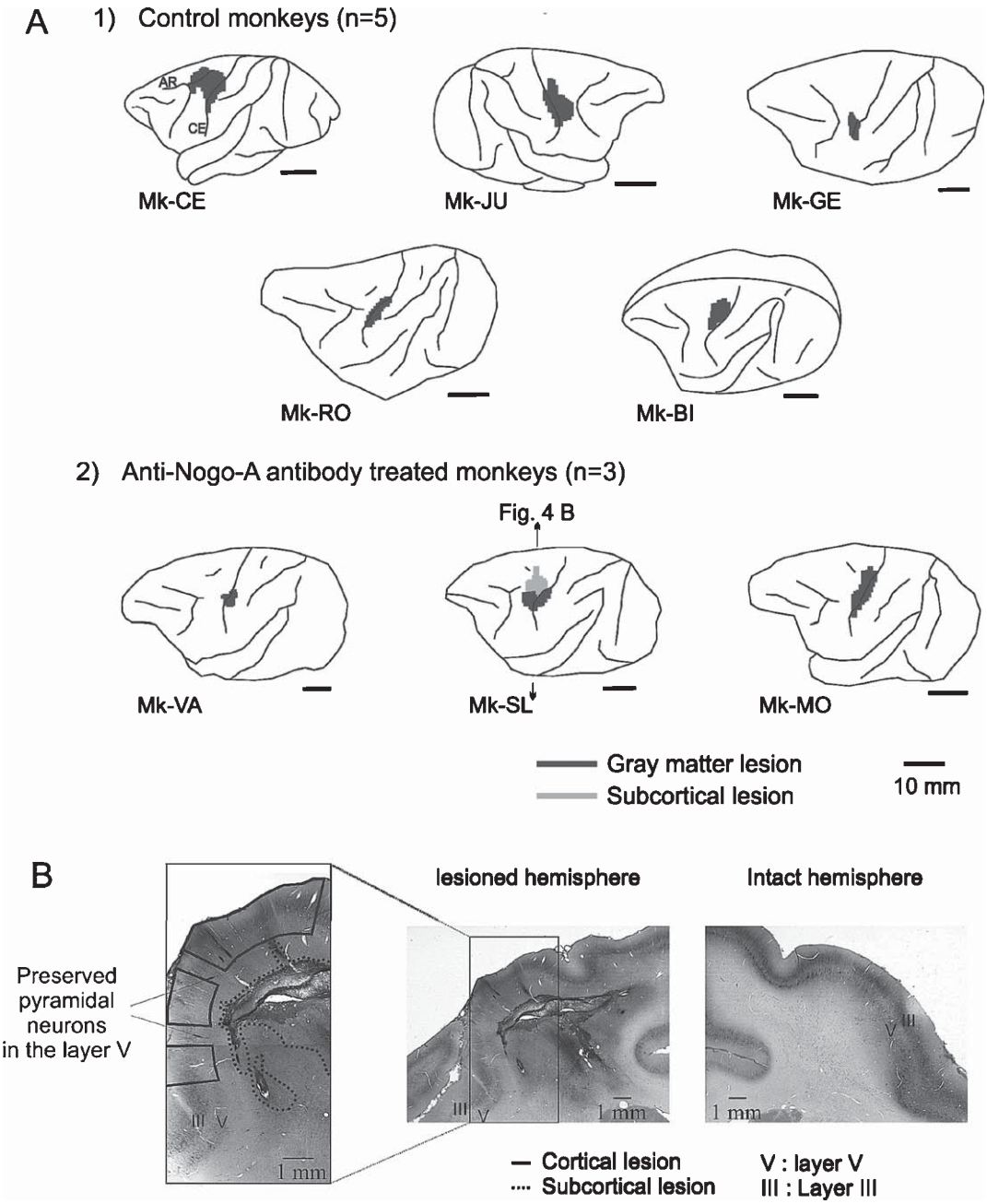

Fig. 4. Panel A: Lateral views, for control (1) and anti-Nogo-A antibody treated (2) monkeys, on the surface of the corresponding hemisphere of the lesion extent in the gray matter area (black area) and in subcortical area (gray area) for one monkey in the motor cortex, as seen in transparency of the cortical surface (same data as shown previously for some monkeys in Kaeser et al., 2010, 2011; Bashir et al., 2012; Hamadjida et al., 2012). The surface representation of the lesion does not reflect directly the actual volume of the gray matter territory impacted by the infusion of ibotenic acid (see for that Table 1 and Figs. 9 and 10). Panel B: View of SMI-32 staining in Mk-SL, showing the 2 hemispheres on a frontal histological section of the brain, at low magnification (middle and right pictures). In the intact hemisphere, the layer V containing the corticospinal neurons is continuous in the motor cortex all along its medio-lateral extent. In contrast, in the lesioned hemisphere, as shown on the left at higher magnification, three territories exhibit an interruption of the layer V, corresponding to cortical zones affected by the ibotenic acid injections (each delineated with a solid line). Note also the presence of a subcortical lesion outlined with a dashed contour, and corresponding to the gray zone displayed in panel A (2), for Mk-SL.

according to their medio-lateral coordinate. Within each group, the tracks were then ordered according to their rostro-caudal coordinate. On the basis of electrophysiological data and observations, a parasagittal diagram was constructed to represent the cortex that was explored and stimulated. The white matter was identified by a sharp increase of the ICMS effective intensity or even a loss of effect of ICMS on the forelimb joints. The reconstruction of the position of the precentral sulcus was based on the successive ICMS sites that produced effects at the lowest threshold, and the sensory cortex was identified by the absence of forelimb movement or by a significant increase of the ICMS effective intensity, mostly in the fundus of the central sulcus. For each electrode track, sites corresponding to cortical layer V were identified using a combination of electrode depths, and the lowest threshold ICMS intensity site. Electrode penetrations on the convexity of the precentral gyrus traversed cortical layers perpendicularly and, in such cases, it was relatively easy to identify the ICMS site closest to layer V, corresponding to the lowest threshold. For electrode penetrations running along the rostral bank of the central sulcus, roughly parallel to the cortical layers, it was more difficult to identify layer V sites. In such cases, output effects from sites at the same depth from different electrode tracks along the rostro-caudal axis were compared. This analysis yielded a series of reconstructed parasagittal cortical sections oriented along the rostro-caudal axis of the chronic chamber in the plane of the electrode tracks. The first ICMS site of the identified convexity of the rostral bank of the central sulcus was used as the axis for rotating and unfolding the layer V (see Kaeser et al., 2010: Supplemental Fig. 1).

2.8. Histological processing

As previously reported (Kaeser et al., 2010), at the end of the experiments (after completion of pharmacological investigations and tracer injections: see Hamadjida et al., 2012 and Hoogewoud et al., 2013), the monkeys were euthanized with an overdose of pentobarbital sodium (90 mg/kg body weight; i.p.). Trans-cardiac perfusion with 0.9% saline (500 ml) was followed by a solution of fixative (4,000 ml of 4% phosphate-buffered paraformaldehyde) and solutions of sucrose (10, 20, 30% in paraformaldehyde). The brains were soaked in a 30% solution of sucrose (in phosphate buffer) for cryo-protection for a few days. Frontal sections (50 μm thick) of the brain were cut using a cryostat and collected in five series. One series of sections was Nissl stained with cresyl violet, whereas a second series was processed to visualize the marker SMI-32, as previously described (Beaud et al. 2008; Liu et al., 2002; Wannier et al., 2005). The Nissl and SMI-32 consecutive series of sections were used to reconstruct the position and extent of the permanent lesion in the cerebral cortex. The SMI-32 stained sections displayed the pyramidal neurons in layers III and V (Fig. 4B). Finally, the lesion was transposed onto a lateral view of the cortical surface of the lesioned hemisphere (Fig. 4A). Using a specific tool of the Neurolucida software (based on the Cavalieri method; see e.g., Pizzimenti et al., 2007), the volume of the cortical lesion (in mm^3) affecting the cortical gray matter was calculated by extrapolation from the reconstructions of the lesion on consecutive histological sections of the brain taken at 0.25 mm interval (Table 1).

3. Results

3.1. Monkeys involved in the present study

The present data were collected from eight monkeys, already included in recent reports from this laboratory, related to the performance of the ipsilesional hand after M1 lesion (Kaeser et al., 2010; Bashir et al., 2012), or used as control ($n = 5$) in a preliminary approach to establish a cell therapy based on implantation of autologous adult progenitor cells (Kaeser et al., 2011), or aimed at investigating the changes of callosal connectivity in relation to the M1 lesion and the anti-Nogo-A antibody treatment (Hamadjida et al., 2012). Some of these animals were also used to pharmacologically investigate the role played by the ipsilesional premotor cortex (PM) in functional recovery (Hoogewoud et al., 2013). In all of these studies, the ID codes used for the monkeys are the same and therefore they can be easily identified in each individual report. In the present study, the eight monkeys subjected to M1 lesion were specifically analyzed to address the issue of motor map changes using ICMS (Table 1), representing the new contribution of the current report.

The permanent lesion in the motor cortex, resulting from ibotenic acid injections, were illustrated with corresponding views in SMI-32 and Nissl staining histological material in previous reports (Kaeser et al., 2010; Peuser et al., 2011). Another example is shown here in Fig. 4B (SMI-32 staining), derived from Mk-

SL. The lesion territories are characterized by an interruption of the layer V, which contains when intact the pyramidal neurons stained with SMI-32, corresponding to the corticospinal neurons. In between the three lesion areas, there are two zones in which the layer V still contains SMI-32 positive neurons, thus corresponding to small territories spared by the lesion.

3.2. Pre-lesion motor maps

In all monkeys, before the lesion of M1, ICMS experiments were conducted to delineate the hand representation in M1, defined as the cortical sites where ICMS elicited movements of the digits of the contralateral hand at the lowest threshold. After approximately 1–2 months of daily ICMS sessions, a raw cortical motor map was obtained (Fig. 1A; as illustrated in Mk-BI), showing the position on the cortical surface of the electrode penetrations. The hand area on the cortical surface corresponds to the sites of electrode penetrations along which the ICMS effect observed at the lowest threshold was a movement of digits of the contralateral hand (yellow circles in Fig. 1A). As expected, ICMS delivered at more medial and/or rostral electrode penetrations elicited at lowest threshold movement of more proximal body territories (wrist, elbow, shoulder) and/or face muscles or foot (Fig. 1A). To avoid damage of the cerebral cortex as might be induced by too many electrode penetrations, the ICMS was mostly focused on the hand representation in M1, without extensive mapping of either the adjacent motor cortical areas (PM, SMA) or of the other body territories in M1 (e.g. face, trunk, leg, etc).

A first analysis of these raw data aimed at obtaining a more comprehensive representation of the motor map focused on the hand representation by unfolding the central sulcus (mostly the rostral bank of the central sulcus, as explained in the methods: Fig. 1B). In the rostral bank of the central sulcus (where the hand representation is mostly located), the electrode penetrations are roughly parallel to the cortical layers. Consecutive ICMS sites eliciting digit movements at low threshold are encountered along the same electrode penetration (presumably following layer V), thus corresponding to an enlargement of the hand area (yellow circles) in the caudal direction (Fig. 1B in the same Mk-BI), as compared to the raw motor map (Fig. 1A). Similarly unfolded pre-lesion motor maps have been established for the other seven monkeys (left column in Figs. 2 and 3). In the unfolded map pre-lesion, only the ICMS responsive sites were considered. These data show that the extent of the hand area, as delineated by ICMS, is quite variable across monkeys (see Table 1: estimates of "unfolded" hand area). As expected for M1, most ICMS sites elicit corresponding body movements at low intensity (below 10 microamps).

The "x" symbols in the pre-lesion unfolded motor maps represent the ICMS sites selected for infusion of ibotenic acid to generate a permanent chemical lesion of the hand representation in M1. The reconstruction of the lesion, as seen on a lateral view of the cerebral cortex, is represented in Fig. 4A for each of the eight monkeys included in the present study. The volume of the lesion territory has been assessed (Table 1), from histological sections treated for the marker SMI-32, as previously reported in detail (Kaeser et al., 2010; Bashir et al., 2012; Hamadjida et al., 2012).

Starting a couple of days after the lesion, the behavioral sessions were pursued, as before lesion, to assess manual dexterity. As a result of unilateral ibotenic acid infusion in the hand area in M1, the contralateral hand was paralyzed, corresponding to a score of zero in all manual tests (see Liu and Rouiller, 1999; Kaeser et al., 2010, 2011; Schmidlin et al., 2011; Bashir et al., 2012; see Fig. 8A for the 3 treated monkeys). During the following weeks, there was a progressive recovery of manual dexterity, reaching a post-lesion plateau of manual performance. In most cases, the extent of functional recovery is incomplete (Table 1). After the post-lesion plateau of manual performance has been established for several weeks or months, a second series of ICMS sessions took place to determine the post-lesion motor map in the cortical area in and around the lesion. The time interval between the lesion of the motor cortex (ibotenic acid infusion) and the onset of the second ICMS mapping is indicated in Table 1 for each monkey.

3.3. Post-lesion motor maps

Post-lesion, the very same ICMS sites as in the unfolded pre-lesion map were re-visited, when the monkeys reached a post-lesion plateau. The unfolded ICMS maps established post-lesion (panel C in Fig. 1 and right columns in Figs. 2 and 3) appear very different from the pre-lesion unfolded ICMS maps. As expected for a permanent lesion induced by ibotenic acid infusion, a majority of territories became non-responsive to ICMS (black circles in Fig. 1C, right column in Figs. 2 and 3), in spite of high intensity

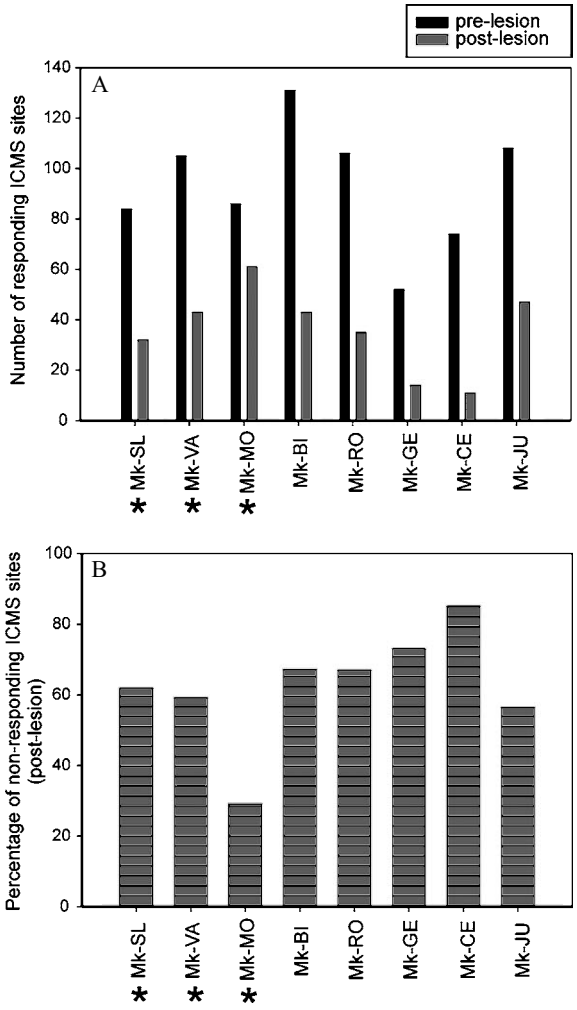

Fig. 5. A: Comparison pre- versus post-lesion for each monkey of the number of ICMS responsive sites (effect on joints elicited at an intensity lower than 80 microamps). B: Derived from panel A, the bar graphs show for each monkey the percentage of ICMS sites which became non-responsive as a result of the lesion in the motor cortex. In the two panels, the three monkeys on the left (asterisks) were subjected to anti-Nogo-A antibody treatment whereas the five monkeys on the right were control (untreated).

stimulation (up to 80 microamps). In one monkey (Mk-CE; Fig. 2), none of the pre-lesion sites where ICMS elicited digit movements were preserved by the lesion: the entire previous hand area was replaced post-lesion by a non micro-excitable territory (except at 2 sites, replaced by an effect on foot muscles). In Mk-JU, in the post-lesion ICMS map, there was a replacement of hand sites either by a non micro-excitable territory or by more proximal body territories, such as wrist, shoulder or even foot (Fig. 2). In all other monkeys (Figs. 1–3), a large proportion of ICMS sites belonging to the hand area pre-lesion became non-responsive post-lesion. However, in these monkeys (Mk-GE, Mk-VA, Mk-SL, Mk-RO, Mk-BI, Mk-MO, in increasing order), there were ICMS sites still eliciting digit movements at the lowest threshold along the corresponding electrode track. In parallel, in these monkeys, some other ICMS sites eliciting digit movements pre-lesion were replaced by more proximal muscle territories (Figs. 1–3). Overall, out of eight monkeys, the change of ICMS map post-lesion of the motor cortex was quite variable from one animal to the next. With extremely rare exceptions (one site in Mk-VA, one site in Mk-GE) none of the ICMS sites located pre-lesion clearly outside the hand area (e.g. proximal territory) was changed post-lesion into an ICMS site eliciting digit move-

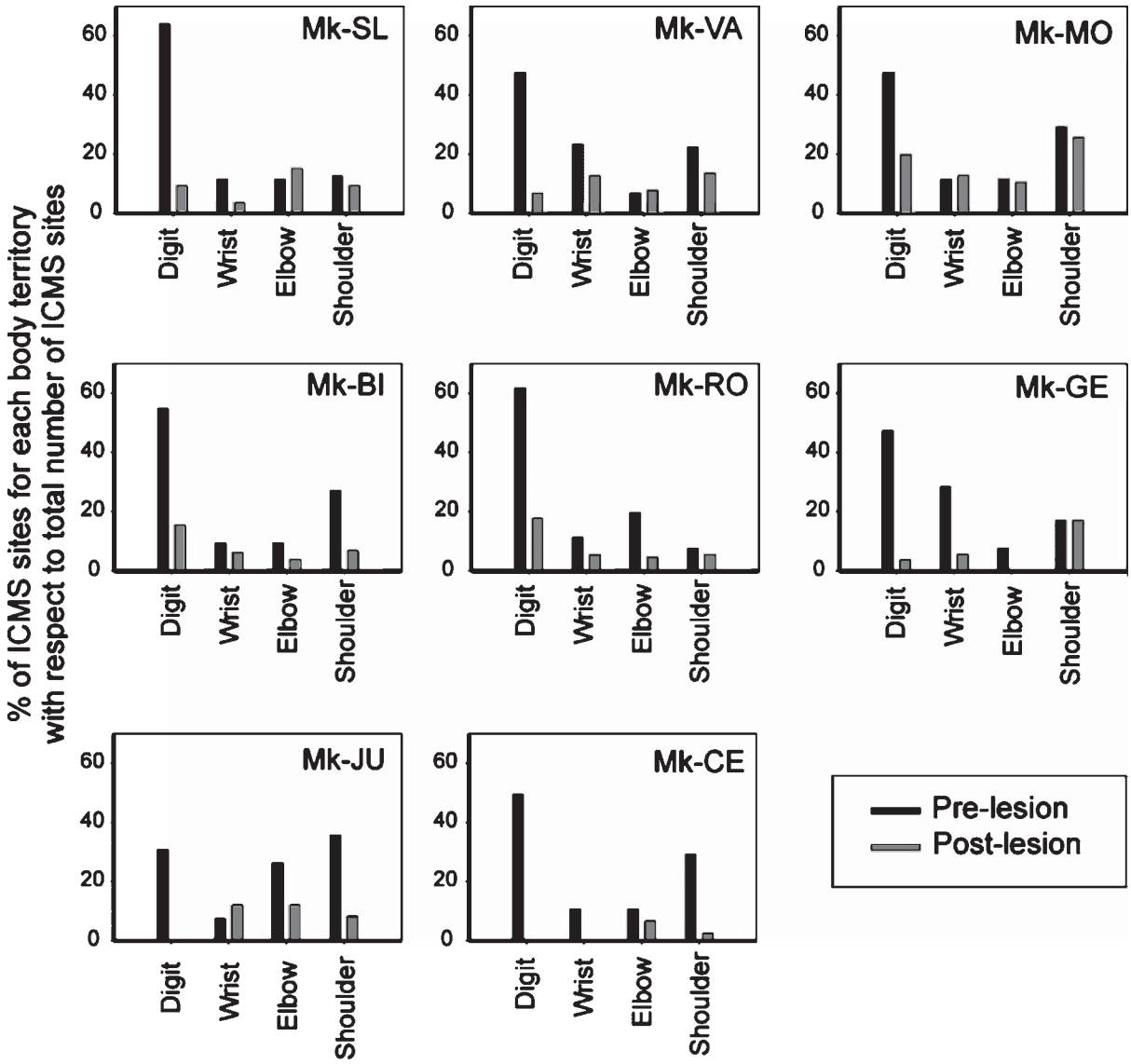

Fig. 6. For each monkey, the histograms show the distribution of the ICMS sites in M1 with respect to the body territory (forelimb), at which the current at threshold elicited a movement before the lesion of M1 (black bars). In each graph, the sum of the four black bars is 100%. The grey bars show the distribution of the same ICMS sites post-lesion, showing that a large proportion of ICMS sites became non-responsive (only the responsive ICMS sites post-lesion have been distributed; their sum is thus clearly smaller).

ments. On the other hand, when digit ICMS sites were present post-lesion, it was in general at a site that was already devoted to the hand area pre-lesion (Figs. 1–3).

3.4. Comparison of ICMS data pre-lesion versus post-lesion

The number of sites where ICMS was applied pre-lesion was quite variable from one monkey to the next and this is not a meaningful parameter. In contrast, as the very same ICMS sites were re-visited post-lesion, comparing this initial number to the number of still responding sites post-lesion provides a valuable assessment of ICMS map changes (Fig. 5). In all monkeys, there was a substantial decrease of responding ICMS sites post-lesion (Fig. 5A), though to a quite variable extent across animals, better seen when plotting the percent of non-responding ICMS sites post-lesion with

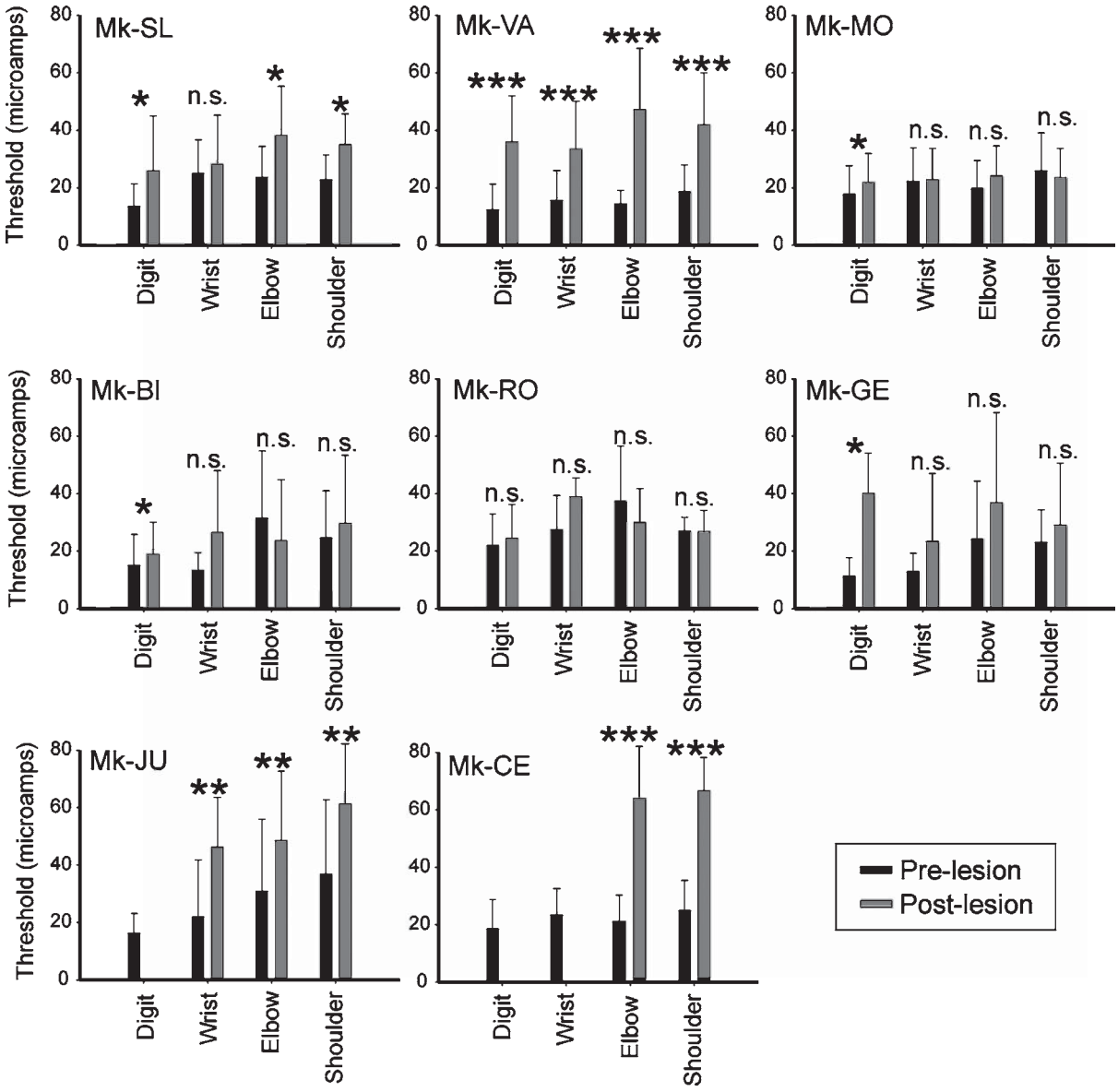

Fig. 7. For each monkey, the histograms show the distribution of the ICMS threshold values at which the effect was observed, pre-lesion (black bars) and post-lesion (grey bars). For each body territory (forelimb), the bars indicate the mean threshold and the standard deviation (SD). Note a general increase of threshold post-lesion as compared to pre-lesion. The number of ICMS sites considered post-lesion is much smaller than pre-lesion, as the majority of ICMS sites became non-responsive post-lesion (see Figs. 1–3; 5–6). The distributions of thresholds were compared pre- versus post-lesion in each monkey and for each territory (e.g. digit, wrist, etc), using the Mann and Whitney test: n.s. (not statistically significant) is for $p > 0.05$; * $p < 0.05$; ** $p < 0.01$; *** $p < 0.001$.

respect to the total number of responding sites pre-lesion (Fig. 5B). The percentage of non-responding ICMS sites ranged from 29% to 85%, in line with the relatively high number of black circles in Figs. 1–3. In Fig. 6, for each monkey, the bar graphs in black show the pre-lesion percent distribution of ICMS sites with respect to the corresponding body territories activated: as expected, as the goal of the ICMS sessions was to delineate the hand representation, the majority of ICMS sites elicited digit movements at threshold. The gray bar graphs in Fig. 6 show the same percent distribution but post-lesion, for the sites which still elicited

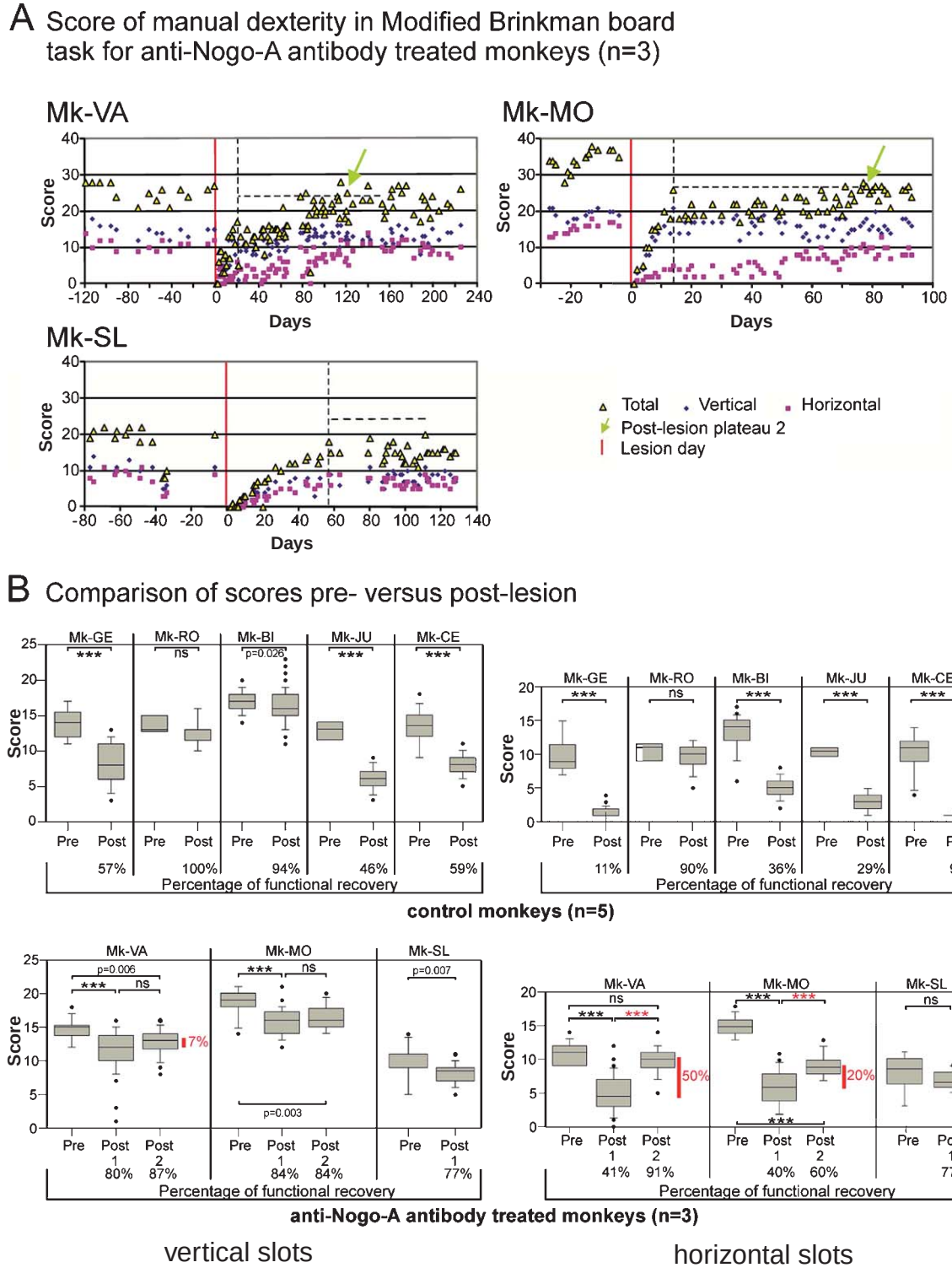
A Score of manual dexterity in Modified Brinkman board task for anti-Nogo-A antibody treated monkeys (n=3)
Mk-VA
Mk-MO
Mk-SL
Score
Days
Total
Vertical
Horizontal
Post-lesion plateau 2
Lesion day
B Comparison of scores pre- versus post-lesion
Mk-GE
Mk-RO
Mk-BI
Mk-JU
Mk-CE
Pre
Post
57%
100%
94%
46%
59%
11%
90%
36%
29%
9%
Percentage of functional recovery
control monkeys (n=5)
Mk-VA
Mk-MO
Mk-SL
p=0.006
p=0.003
p=0.007
7%
50%
20%
80%
87%
84%
84%
77%
41%
91%
40%
60%
77%
anti-Nogo-A antibody treated monkeys (n=3)
vertical slots
horizontal slots

a motor response. The percent of digit sites decreased dramatically or even totally disappeared (Mk-JU and Mk-CE). For nearly all other territories, there was also a decrease of responding sites, but generally to a lesser extent than for the digits. This observation suggests that the infusion of ibotenic acid in the hand representation also exerted a detrimental effect at some distance, either by diffusion of the neurotoxic drug and/or indirectly by affecting local networks.

Due to the motor cortex lesion, one would expect that the ICMS sites still present after the lesion in the ICMS map elicit movements at a higher threshold than pre-lesion. This prediction has been largely confirmed by the present experiments, as illustrated in Fig. 7. The increase of ICMS threshold was statistically significant for all body territories in monkeys Mk-VA, Mk-JU, Mk-CE and, except for the wrist, in Mk-SL. In three other monkeys (Mk-MO, Mk-BI and Mk-GE), the increase of threshold was statistically significant only for the digits. Finally, in the monkey with the smallest lesion (Mk-RO), there was no statistically significant increase of threshold post- versus pre-lesion. In only three cases (Mk-BI, Mk-RO and Mk-MO), the threshold was lower post-lesion than pre-lesion for the elbow territory in the first two monkeys and in the shoulder territory for the latter, but in all three cases the difference was not statistically significant. When present, the extent of the threshold increase post- versus pre-lesion was again quite variable from one monkey to the next (Fig. 7).

3.5. Behavioral data

Based on the modified Brinkman board task, manual dexterity was assessed by the number of pellets (score) retrieved during the first 30 seconds (Schmidlin et al., 2011) on each daily behavioral session. In contrast to our recent report (Kaeser et al., 2011) focused on the total number of pellets retrieved (total score), the score data were analyzed here separately for the vertical slots and the horizontal slots. Plots of the behavioral performance of the three anti-Nogo-A antibody treated monkeys are shown in Fig. 8 (panel A). Before the lesion, after an initial training phase (not shown), the monkeys reached a generally stable manual performance, reflected by a pre-lesion plateau of score. Immediately after the lesion, as expected, the manual dexterity of the contralesional hand dropped to zero. After the lesion, a progressive functional recovery took place during several weeks, to reach a post-lesion plateau. The beginning of the post-lesion plateau (vertical dashed line in panel A of Fig. 8), was determined based on criteria as defined in Kaeser et al. (2011). In two out of the three anti-Nogo-A antibody treated monkeys (Mk-MO and Mk-VA), there was a rebound of score, with a subsequent (significant) increase in the number of pellets retrieved, initiated on the day pointed out by the green arrow (see Kaeser et al. 2011, for criteria to define the onset of the rebound). The same, original plots of score, showing the deficit immediately after the lesion and the subsequent (spontaneous) functional recovery in the five control monkeys, have been published in recent reports (Kaeser et al., 2010, 2011; Bashir et al., 2012). These plots showed that, in the five control monkeys, there was no such rebound of score post-lesion, as observed in Mk-VA and Mk-MO (panel A in Fig. 8). The ratio of the post-lesion plateau score (median value) to the pre-lesion plateau score (median value) defines the percentage of functional recovery, computed for each monkey separately for vertical and

Fig. 8. **A:** Behavioral data for the three monkeys subjected to anti-Nogo-A antibody treatment, showing the manual dexterity performance (score) in the modified Brinkman board task, as a function of time corresponding to daily sessions pre-lesion (negative days) and post-lesion (positive days). The vertical red line represents the day of M1 lesion. Note the dramatic drop of manual dexterity immediately after the lesion of M1. The score (number of pellets retrieved in 30 seconds) is given for the vertical slots (blue diamonds), the horizontal slots (red squares), whereas the yellow triangles are for the total score (sum of vertical and horizontal slots). As described earlier (Kaeser et al., 2010), the vertical dashed line points to the onset of a first post-lesion plateau, most likely reflecting the "spontaneous" functional recovery level. The horizontal dashed line shows an upper limit of score given by the median value at first plateau plus twice the difference between the median value and the highest value at plateau. In two monkeys (Mk-VA and Mk-MO), the score reached this upper limit (green arrow) later during the post-lesion phase, interpreted as a second plateau or rebound of functional recovery, possibly reflecting the effect of the anti-Nogo-A antibody treatment. The same plots were presented earlier for the five control monkeys (Kaeser et al., 2011) and showed that none of the control monkeys exhibited such a rebound of functional recovery. **B:** Comparison in the form of box and whiskers plots of pre-lesion ("Pre") and post-lesion (Post 1) scores in the five control monkeys (top panels) and in the three anti-Nogo-A antibody treated monkeys, separately for the vertical slots (left) and the horizontal slots (right). In the two monkeys with a rebound of functional recovery, the middle box is for the first post-lesion plateau (Post 1) and the rightmost box is for the second post-lesion plateau (Post 2). The percent values in red are for the enhancement of functional recovery obtained by reaching the second plateau as compared to the first post-lesion plateau. In the Mann-Whitney test, comparison between pre-lesion and post-lesion median values (first or second plateaux), *** $p < 0.001$, whereas "n.s." is for not significant ($p > 0.05$).

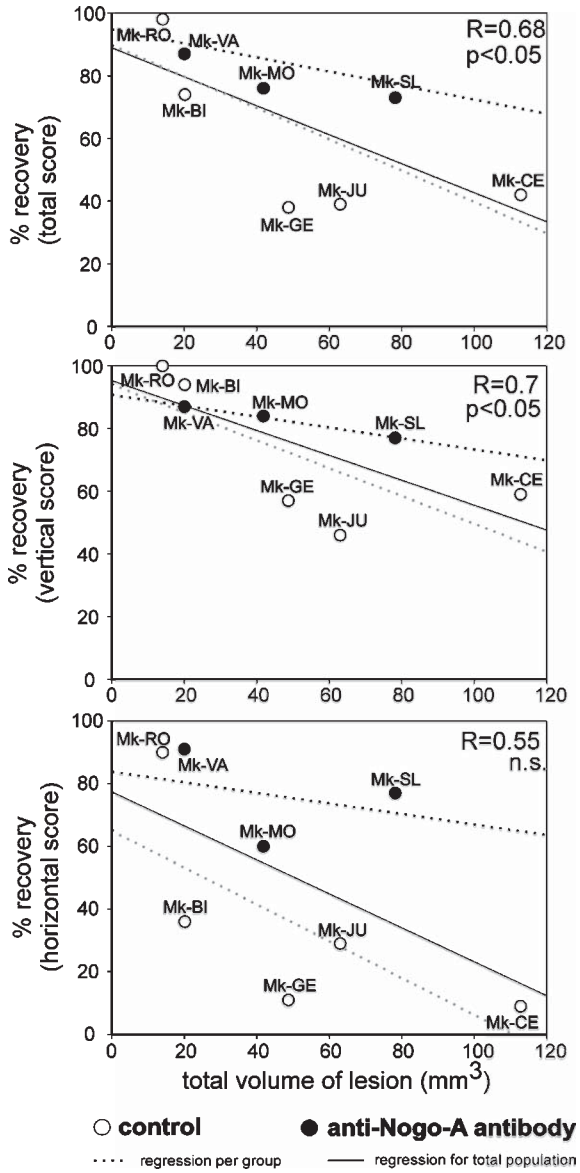

Fig. 9. Scatter plots of functional recovery (in percent) as a function of the volume of the lesion in the motor cortex (in mm^3), for the total score (top panel), the vertical slots (middle panel) and the horizontal slots (bottom panel). Control monkeys are represented by empty symbols whereas filled circles are for the anti-Nogo-A antibody treated monkeys. The regression line was calculated for all data points, reflecting the general trend towards a decrease of functional recovery for increasing lesion sizes, as expected. Coefficients of correlation are given in the upper right corner of each plot, with the corresponding *p* value. Regression lines for each group are indicated by dashed lines.

horizontal slots, as illustrated in the form of box and whisker plots in Fig. 8 (panel B; see also Table 1). In the five control monkeys, the degree of functional recovery ranged between 46% and 100% for the vertical slots and between 9% and 90% for the horizontal slots. Taking into account the final second plateau post-lesion in Mk-VA and Mk-MO, the degree of functional recovery among the three anti-Nogo-A antibody treated monkeys ranged between 77 and 87% for the vertical slots and between 60 and 91% for the horizontal slots.

In order to illustrate the benefit provided by the second post-lesion plateau, reflecting a rebound of functional recovery as observed in the anti-Nogo-A

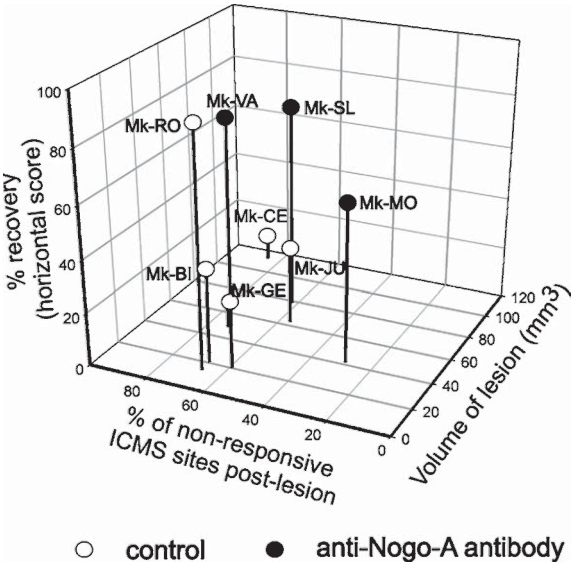

Fig. 10. 3D scatter plot showing the relationship between the degree of functional recovery (in %), the volume of the lesion (in mm^3) and the percent of non-responsive ICMS sites.

antibody treated monkeys Mk-VA and Mk-MO, video sequences are shown at the following URL address: http://www.unifr.ch/neuro/rouiller/FRJS/index.html.

In a control monkey (Mk-BI), three video sequences illustrate the manual dexterity of the monkey before lesion, in the acute phase (immediately post-lesion) and finally at the level of the unique post-lesion plateau (see also Fig. 8B). Immediately post-lesion, Mk-BI lost the ability to retrieve pellets with the contralesional (right) hand and therefore cheated by trying to use the left hand. At the level of the post-lesion plateau, Mk-BI recovered the manual dexterity to some extent, but mainly for the vertical slots which were preferentially aimed for, with fairly good success before aiming for the horizontal slots with much more difficulty and error occurrences (pellet pushed to neighbouring slots). As expressed by the score (number of pellets retrieved during the first 30 seconds of the test), the degree of functional recovery was more prominent for the vertical slots (94%) than for the horizontal slots (36%; see Fig. 8B). In contrast, in the anti-Nogo-A antibody treated monkey Mk-VA, functional recovery occurred into two phases (first and second post-lesion plateau; see Fig. 8A and B), with a comparable percentage of functional recovery for the vertical (87%) and the horizontal (91%) slots. The video sequences for Mk-VA also show the dramatic loss of manual dexterity immediately post-lesion, as compared to pre-lesion. In that case, in the acute phase, Mk-VA also tried to cheat by using the left hand, instead of the contralesional (right) hand. The two video sequences taken at post-lesion plateaux illustrate qualitatively the manual performance at the first (video sequence 3) and second post-lesion (video sequence 4) plateau, respectively. At post-lesion plateau 2, the same monkey Mk-VA was obviously more dextrous than at post-lesion plateau 1. At the latter (video sequence 3), Mk-VA focused on the vertical slots first, at a relatively slow pace, before aiming at the horizontal slots with great difficulty and several errors. At the second plateau (video sequence 4), Mk-VA aimed for both vertical and horizontal slots from the onset of the test, at a much higher pace for both slot orientations. Whilst Mk-VA completed the modified Brinkman board at the second plateau (all 50 slots emptied), for comparison, at first plateau, after the same amount of time, this monkey only emptied 28 out of 50 slots. Moreover, at the second post-lesion plateau (video sequence 4), Mk-VA scanned the Brinkman board more systematically than at the level of the first post-lesion plateau (video sequence 3). This comparison of video sequences 3 and 4 for Mk-VA thus emphasizes the substantial benefit provided by the rebound of functional recovery up to the second plateau, as observed for the 2 anti-Nogo-A antibody treated monkeys Mk-VA and Mk-MO.

The variability of the degree of functional recovery within the two subgroups of monkeys is related, at least in a large part, to the size of the cortical lesion. For this reason, the degree of functional recovery in percent was plotted as a function of the volume of the cortical lesion (Fig. 9). As expected, considering all eight monkeys, there was a general trend towards a decrease of functional recovery as a result of increasing lesion size (see regression lines in Fig. 9). First of all, the control monkey Mk-RO with the smallest lesion exhibited an excellent spontaneous functional recovery. Looking at the vertical slots data (middle panel in Fig. 9), the distribution of functional recovery for the control monkeys was fairly comparable to that obtained for the anti-Nogo-A antibody treated monkeys. In sharp contrast, the functional recovery was distributed in a clearly more disparate way when considering the horizontal slots (bottom panel in Fig. 9). As grasping from the horizontal slots is more challenging than from the vertical slots (see Freund et al., 2009; Schmidlin et al., 2011), the deficit in control monkeys is more prominent whereas, in the anti-Nogo-A antibody treated monkeys, the treatment resulted, irrespective of the lesion volume, in a substantial restitution of this sophisticated manual ability (combination of precision grip and arm pronation or supination movement needed for grasping from the horizontal slots). In more detail, the anti-Nogo-A antibody treated monkey Mk-VA with a larger lesion recovers the ability to grasp from the horizontal slots a bit more than the control monkey Mk-RO which displays a smaller lesion (bottom panel in Fig. 9). The two anti-Nogo-A antibody treated monkeys Mk-MO and Mk-SL recovered clearly better than the other control monkeys (bottom panel in Fig. 9). As expected, the plot based on the total score (sum of vertical and horizontal slots; top panel in Fig. 9) yields an intermediate figure between the two slot orientations taken separately. The difference between the two groups of monkeys with respect to functional recovery is reflected by their respective regression lines (Fig. 9), again with a more prominent difference observed for the horizontal slots than for the vertical ones.

To address the question of whether the functional recovery may also be correlated to the change of motor maps in M1 (in and around the lesion territory), the three parameters percent of functional recovery for horizontal slots, volume of lesion and the percentage of non-responsive ICMS sites post-lesion were plotted in 3D form (Fig. 10). It appears that the two subgroups of monkeys, differing to some extent with respect to the percentage of functional recovery (except the control monkey Mk-RO with the smallest lesion), superimpose to a large extent as far as the percentage of non-responsive ICMS sites is concerned. In other words, the number of ICMS sites in M1 still eliciting forelimb movements is a poor predictor of the functional recovery for the horizontal slots, which is a more sensitive parameter than the vertical slots. There is also overlap between the two subgroups of monkeys with respect to the volume of the cortical lesion.

4. Discussion

The results of the present study can be summarized as follows: 1) after permanent chemical lesion of the hand area in M1 in the adult macaque monkey, the lesion territory becomes mostly non micro-excitable several months post-lesion, in spite of some functional recovery (spontaneous or promoted by anti-Nogo-A antibody treatment); 2) some sites within the lesion territory remain excitable, but independent of the degree of functional recovery; 3) around the lesion in M1, there was no evidence for a reallocation of proximal territories to distal functions to replace, at least in part, the original hand representation affected by the lesion; 4) compared to pre-lesion, there was a post-lesion increase of thresholds at which ICMS elicited movements of the forelimb muscle territories, but again unrelated to the degree of functional recovery; 5) there is preliminary evidence for an enhancement of functional recovery promoted by the anti-Nogo-A antibody treatment, as reflected by the retrieval score for the horizontal slots in the modified Brinkman board task, extending to the non-human primates results previously obtained in rodents (Papadopoulos et al., 2002; Emerick et al., 2003; Emerick and Kartje, 2004; Seymour et al., 2005; Markus et al., 2005; Tsai et al., 2007, 2011; Cheatwood et al., 2008; Gillani et al., 2010).

Although the lesioned hand territory in M1 became, as expected, mostly non-responsive to ICMS, there were some sites where ICMS applied post-lesion elicited movements of the contralateral forelimb (Figs. 1–3). Do they correspond to preserved cortical sites, spared by an insufficient spread of ibotenic acid? This is most likely not the case, as the responsive sites post-lesion do not correspond to zones where the spots selected for infusion of ibotenic acid were more distant from each other than in zones which became completely non-responsive (see e.g. Mk-RO

and Mk-MO). In other words, a deficit of spread of ibotenic acid cannot systematically explain the persistence of micro-excitable sites post-lesion in the cortical area delineated pre-lesion as hand representation. Nevertheless, one cannot totally exclude that few small cortical territories were preserved, as illustrated for Mk-SL in Fig. 4B. Such preserved islands of intact cortex were however rarely observed, as in most monkeys the lesion formed a continuous territory (see Kaeser et al., 2010). Ibotenic acid infusion does not generate a cavity in the cerebral cortex (Peuser et al., 2011), in contrast to a surgical lesion, suggesting that during the period of recovery post-lesion, a few corticospinal neurons or indirect connections to the spinal cord were formed by unknown mechanisms.

In the present study, during the weeks post-lesion there was no sustained rehabilitative training protocol imposed on the monkeys (e.g. constraint induced-therapy), that would complement their daily test sessions. As a consequence, the daily manual dexterity tests correspond to an intermediate motor practice regime. Under these conditions of moderate rehabilitative training, we did not observe any dramatic change of motor maps at the periphery of the lesion in our adult monkeys (e.g. proximal arm/shoulder territory converted into digit sites). Such absence of reappearance of movements previously represented in the lesion zone is reminiscent of the results of Nudo and Milliken (1996), in absence of post-infarct intensive training in adult squirrel monkeys. This situation contrasts with a lesion of M1 performed neonatally in infant monkeys, in which the functional recovery at adult stage was associated with a re-arrangement of the somatotopic representation, with the emergence of a hand territory at a location normally occupied by proximal territories (Rouiller, et al., 1998). There is also a contrast with the data in adult squirrel monkeys obtained by Nudo et al. (1996), who observed a reappearance of hand representations around the lesion in former elbow and shoulder territories, but this change was triggered by a sustained rehabilitative training protocol, not conducted to such an extent in the present study. The present data thus confirm the notion that intensive training is necessary to trigger substantial cortical map reorganization, representing most likely a substrate for an enhanced functional recovery (see Dancause and Nudo for a recent review, 2011). The absence in the present study of cortical map reorganization around the lesion and related to the functional recovery is consistent with previous observations on two control monkeys subjected to M1 lesion, in which the territory immediately adjacent to the lesion is little, if at all, involved in the recovery, in contrast to the ipsilesional premotor cortex which played a significant role (Liu and Rouiller, 1999). As outlined above, a contribution of the perilesional territory in M1 may appear in the case of a very small lesion of the hand area (Glees and Cole, 1952) or when the lesion is followed by intense rehabilitative therapy (Nudo et al., 1996; Dancause and Nudo, 2011). On the contrary, restricted use of a forelimb leads to a reduction of the corresponding digit representation (Milliken et al., 2013).

An important consideration is the time interval between the cortical lesion and the time point at which the post-lesion ICMS mapping was repeated. In the present study, this time interval was quite variable across monkeys (Table 1) and, in most cases, clearly longer than in the studies conducted on squirrel monkeys by Nudo and collaborators (Nudo and Milliken, 1996; Nudo et al., 1996). Especially in the squirrel monkeys subjected to intensive rehabilitative training (Nudo et al., 1996), the ICMS mapping was repeated early post-lesion (about 5 weeks post infarct), close to the functional recovery itself (see their Fig. 1). In the present study, as one of our goal was to assess motor performance post-lesion in the long-term (a strategy which has permitted the observation of a second plateau in Mk-VA and Mk-MO in Fig. 8; see also Keaser et al., 2011 for other monkeys), the time interval was clearly longer. As a consequence, one may not exclude the possibility that motor maps may change when comparing for instance time points such as 1–2 months post-lesion and 5–15 months post-lesion. Indeed, it may be that peri-lesion territories (in the present case wrist, elbow, shoulder), when stimulated, exhibit effects on the digits at low threshold mainly during the restricted time window of the functional recovery itself (before reaching the post-lesion plateau), which are possibly maintained during the first weeks at plateau. Such "early" effects may be explained by rapid unmasking of existent connections to the most distal muscles from proximal territories, mostly silent before the lesion, as proposed by Dancause and Nudo (2011). As the post-lesion mapping conducted in the present study took place later, such early effects may have been less evident.

To explain the absence of re-appearance of hand representation at the immediate periphery of the lesion in the present study (Figs. 1–3), in regions formerly occupied by more proximal territories, it is important

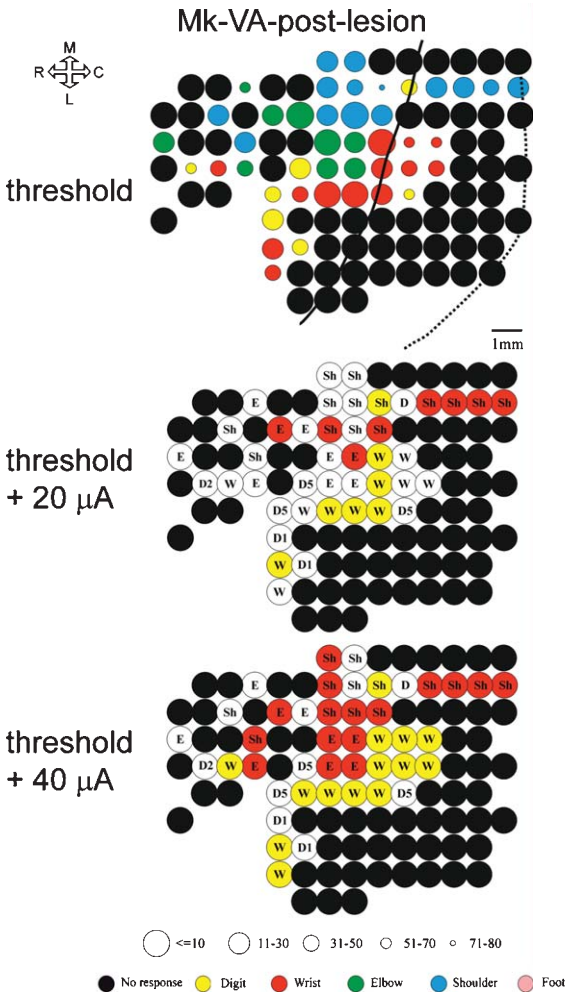

Fig. 11. Modification of unfolded ICMS maps post-lesion for Mk-VA as a function of the current intensity delivered at each stimulation site. The top panel is a repetition of the ICMS map obtained post-lesion at threshold (same as in Fig. 3, top right ICMS map; same conventions as in Fig. 1). In the middle panel, the ICMS map shows some "new" territories activated at 20 microamps above threshold: they are ICMS sites eliciting effect on digit and wrist muscles, depicted in yellow and red, respectively. The muscles activated at threshold at the same sites are indicated in the center of the red or yellow circles by the codes W = wrist, E = elbow and SH = shoulder. The ICMS map in bottom panel shows the effects elicited on digit and wrist muscles at 40 microamps above threshold. In the middle and bottom panels, the white circles are for sites with activation of the same body territories as observed at threshold; the colored circles are for sites at which an additional body territory (more distal) was activated, in addition to the one obtained at threshold (indicated by the letter in the center of the circle). The new territories in red are for additional wrist effects and in yellow are for additional digit effects. Note, as current increased, an increasing recruitment of more distal territories (digits and wrist), in addition to more proximal territories found at threshold for the same site of stimulation.

to remember the strict criterion applied here to establish the ICMS map (Figs. 1–3). The data represent at each stimulation site only the effect elicited by the lowest efficient current (threshold) and not influences on other territories which may occur at somewhat higher currents. In our post-lesion mapping experiments, we indeed also found, at peri-lesion sites representing proximal territories at threshold, ICMS effects on the digits, but at higher current intensities. In other words, these peri-lesion territories addressing digit motoneurons at higher current intensities (but not visible in the ICMS maps established at threshold) may well be the anatomical support for the restored manual dexterity (wrist and digit movements). The recruitment of additional distal territories post-lesion at current intensities above threshold is illustrated for Mk-VA in Fig. 11. At

both 20 and 40 microamps above threshold, there is evidence of additional effects on digits at sites where more proximal body territories are represented at threshold (wrist, elbow, shoulder), as well as of additional wrist effects at sites representing elbow and shoulder territories at threshold. The same phenomenon as depicted in Fig. 11 for Mk-VA was observed in the other monkeys, irrespective of the anti-Nogo-A antibody treatment. In other words, the anti-Nogo-A antibody treatment did not enhance the appearance of ICMS effects from M1 on digit muscles at current intensities above threshold. Indirectly, this observation suggests that the treatment does not appear to promote restoration of CS projections originating from the lesion territory in M1 or from its immediate surroundings. One may then hypothesize that the anti-Nogo-A antibody treatment may rather enhance compensatory sprouting of efferents or afferents to non-primary motor cortical areas, as observed for the callosal inputs to the ipsilesional PM (Hamadjida et al., 2012).

Based on the retrieval score for the horizontal slots in the modified Brinkman board task, the present study provides further evidence for an enhancement of functional recovery promoted by anti-Nogo-A antibody treatment (Fig. 9, bottom panel). Besides the trend for a better functional recovery in anti-Nogo-A antibody treated monkeys, from the qualitative point of view, two (Mk-MO, Mk-VA) of the three anti-Nogo-A antibody treated monkeys exhibited a rebound in the post-lesion plateau, representing an additional gain of functional recovery whose extent is indicated by the red brackets in Fig. 8B (see also Supplementary video material). The third anti-Nogo-A antibody treated monkey (Mk-SL) did not show such a rebound, but the functional recovery was surprisingly high in spite of a large lesion. The rebound in the post-lesion plateau (Mk-VA and Mk-MO in Fig. 8) is similar to the rebound observed in two monkeys which were transplanted with autologous adult progenitor cells (Kaeser et al., 2011). Interestingly, in sharp contrast, out of five control monkeys subjected to M1 lesion but without any treatment (neither anti-Nogo-A antibody nor progenitor cells transplantation) none exhibited a rebound of functional recovery in the post-lesion plateau (Kaeser et al., 2011). Both treatments (in 4 out 5 monkeys) thus provide a secondary enhancement of functional recovery, in addition to the level presumably reached by spontaneous recovery. As far as the effect of the anti-Nogo-A antibody treatment is concerned, the present behavioral data based on three treated monkeys compared to five control monkeys need to be extended to a larger population of monkeys subjected to a lesion of M1. Nevertheless, the evidence for a beneficial effect of anti-Nogo-A antibody treatment on functional recovery from motor cortex lesion reported here, based on the modified Brinkman board task, is in line with preliminary evidence based on another, complementary manual dexterity test, the Brinkman box (Hamadjida et al., 2012).

From the behavioral point of view, the present study emphasizes the pertinence of horizontal slots in the modified Brinkman board task. It is clearly more challenging than grasping from the vertical slots and it thus represents a more sensitive test, better suited to reflect a benefit of a therapy in our animal model, based on a compromise between a large enough lesion to detect a deficit sufficiently prominent to be compensated better after a treatment and a lesion not too large to avoid a poor condition for the monkeys due to an ethically unacceptable handicap. The sequence of movements to retrieve the pellets from the vertical slots is less difficult than for the pellets in the horizontal slots (see also Freund et al., 2009). For the vertical slots, the monkey performs the precision grip to grasp the pellet, without adjustment of the wrist posture. For the horizontal slots, the monkey has to perform a half pronation or supination of the wrist, followed by the precision grip and a flexion of the wrist. The behavioral data show that the lesioned monkeys have serious difficulty to execute this flexion. Thereby, the initial retrieval score of the two orientations is different and so is the functional recovery after the lesion of M1.

Following lesion of M1 and in the absence of treatment, there is evidence based on reversible inactivation experiments, that "spontaneous" functional recovery depends, at least in part, on the ipsilesional premotor cortex, spared by the injury (Liu and Rouiller, 1999; Hoogewoud et al., 2013). A possible anatomical support for such a vicarious contribution of PM after M1 lesion is the enhancement of the projection of PM to the post-central gyrus (Dancause et al., 2005). Along the same line, there is also anatomical and functional evidence that, after a lesion including M1 and the lateral PM, the ipsilesional SMA contributes to the incomplete functional recovery (McNeal et al., 2010; see also Eisner-Janowicz et al., 2008). In the present study, it is likely that the functional recovery observed in the five control monkeys subjected to M1 lesion results from a substitution to some extent of M1 by non-primary motor cortical areas, especially the ipsilesional PM.

Furthermore, the present ICMS data largely exclude a prominent role played by more proximal territories in M1 spared by the lesion, in line with reversible inactivation experiments conducted in two of the five control monkeys (Liu and Rouiller, 1999). The mechanisms of the vicarious contribution of PM and/or SMA may include sprouting of the corticospinal projections originating from these non-primary areas, as demonstrated for SMA after lesion of M1 and the lateral PM (McNeal et al., 2010). Through its projection to cervical and thoracic segments of the spinal cord (Rouiller et al., 1996; Dum and Strick, 1991), SMA is in position to take over some direct influence of M1 on hand motoneurons, though to a limited extent as its influence on distal motoneurons in the normal function is clearly less prominent than corticospinal inputs arising from M1 (Maier et al., 2002; Boudrias et al., 2006, 2010a). For PM, its corticospinal projection exerts effects on distal motoneurons, but they are also clearly lower than those originating from M1 (Boudrias et al., 2010b), reflecting mainly an indirect linkage with the motoneurons. In particular, PMv was shown to exert an influence mostly via its cortico-cortical projection to M1 (Cerri et al., 2003; Shimazu et al., 2004; Schmidlin et al., 2008; Prabhu et al., 2009), although some descending influence via intraspinal circuits in the spinal cord cannot be excluded (Sasaki et al., 2004; Takei and Seki, 2010; Alstermark et al., 2011; Kinoshita et al., 2012). Contributions of non-primary motor cortical areas to the functional recovery after lesion of M1, irrespective of whether they are direct or indirect, can be interpreted as an unmasking of pre-existing, but mostly silent, projections and/or axonal sprouting forming new connections (see Dancause and Nudo, 2011 for a recent review). It is likely that the anti-Nogo-A antibody treatment may have enhanced some axonal sprouting, especially involving the ipsilesional PM, as observed for the callosal projections from the intact hemisphere terminating in the ipsilesional PM (Hamadjida et al., 2012). Whether other connections of PM (or of other cortical areas, for instance SMA), such as their corticospinal, corticorubral and corticobulbar projections have also been promoted by the anti-Nogo-A antibody treatment remains an open question at present. As the anti-Nogo-A antibody was delivered not only around the lesion at cortical level, but also at cervical level, an enhancement of re-organization of intrapsinal circuits may also have promoted functional recovery (Bareyre et al., 2004).

The current pre-lesion ICMS maps shown in Figs. 1–3 for *macaca fascicularis* are fully consistent with previously published representations of the output map of M1 in macaque monkeys (*macaca mulata*), using the same unfolding procedure of the rostral bank of the central sulcus (Park et al., 2001, 2004): the extent of the distal (digits) representation is highly comparable, as well as the surrounding of the digits' area by more proximal territories (wrist, elbow, shoulder) medially, rostrally and also laterally, but to a much smaller extent (e.g. Mk-BI and Mk-JU for instance). However, laterally to the digits' area, most ICMS sites elicit movements of face muscles (Park et al., 2001, 2004; present study: not shown). Moreover, the pre-lesion ICMS maps in Figs. 1–3 confirm the presence of some overlap of the external rim of the digits' area with more proximal territories, as reported by Park et al. (2001, 2004). The pre-lesion raw ICMS maps established in the present study (as shown in Fig. 1 for Mk-BI) are also consistent with previously published ICMS data for intact macaque monkeys, but without unfolding procedure (e.g. Kwan et al., 1978; Sessle and Wiesendanger, 1982; Humphrey, 1986; Lemon, 1988; Aizawa et al., 1990).

In conclusion, the present study shows that the re-arrangement of motor maps in and around the lesioned territory in M1 is variable across monkeys, but without obvious relationship to the degree of functional recovery of manual dexterity. This conclusion holds for experimental conditions in which there was no intensive rehabilitative training during the weeks post-lesion. The situation is likely to be different in cases of more intensive rehabilitative training (see Nudo and Milliken, 1996; Nudo et al., 1996; Friel et al., 2000). Nevertheless, in the absence of such training, there is evidence that some functional restitution of manual dexterity after lesion of the hand representation in M1 in the adult macaque depends to a large extent on the vicarious role played by non primary motor areas (PM, SMA: see Liu and Rouiller, 1999; Eisner-Janowicz et al., 2008; Mc Neal et al., 2010). A significant rehabilitative therapy protocol needs to be implemented in order to favor the re-arrangement of the motor map in the immediate vicinity of the lesion (and perhaps also enhance the contribution of non-primary motor areas), although care should be taken to adopt the most adequate timing of such interventions. In addition, therapies such as neutralization of nerve growth inhibitors (present study; Hamadjida et al., 2012) or cell therapy (Kaeser et al., 2011) may further boost the capacity of functional restitution, although a larger number of monkeys is needed

to better decipher the precise mechanisms of such enhancements.

Acknowledgments

The authors wish to thank the technical assistance of Véronique Moret, Christine Roulin, Françoise Tinguely, Christiane Marti (histology), Alexandra Meszaros (lesion reconstruction), Eric Schmidlin, Jocelyne Bloch, Jean-François Brunet, Mélanie Kaeser (for contributing to some experiments), Josef Corpataux, Laurent Bossy (animal care taking), André Gaillard (mechanics), Bernard Aebischer (electronics), Laurent Monney (informatics). We thank Dr. Jennifer Miles-Chan for editing the manuscript.

Grant sponsors: Swiss National Science Foundation, Grants No. 31-61857.00, 310000-110005, 31003A-132465 (EMR), and 3100-063633, 31003A122527 (MES), the National Centre of Competence in Research (NCCR) on "Neural plasticity and repair"; Novartis Foundation; The Christopher Reeves Foundation (Springfield, NJ, USA); The Swiss Primate Competence Centre for Research (SPCCR: http://www.unifr.ch/neuro/rouiller/SPCCR/welcome.html).

Conflict of interest

The anti-Nogo-A antibody was provided by Novartis Pharma AG.

Supplementary video material

Manual dexterity performance is illustrated in the form of video sequences at different time points (pre-lesion, post-lesion immediately after the lesion, at post-lesion plateau) for the control Mk-BI and the anti-Nogo-A antibody treated Mk-VA (see text in the results section). The video sequences are accessible at: http://www.unifr.ch/neuro/rouiller/FRJS/index.html

References

[1] Aizawa, H., Mushiake, H., Inase, M., & Tanji, J. (1990). An output zone of the monkey primary motor cortex specialized for bilateral hand movement. *Exp Brain Res*, *82*, 219-221.

[2] Alstermark, B., Pettersson, L.G., Nishimura, Y., Yoshino-Saito, K., Tsuboi, F., Takahashi, M., & Isa, T. (2011). Motor command for precision grip in the macaque monkey can be mediated by spinal interneurons. *J Neurophysiol*, *106*, 122-126.

[3] Bareyre, F.M., Kerschensteiner, M., Raineteau, O., Mettenleiter, T.C., Weinmann, O., & Schwab, M.E. (2004). The injured spinal cord spontaneously forms a new intraspinal circuit in adult rats. *Nat Neurosci*, *7*, 269-277.

[4] Bashir, S., Kaeser, M., Wyss, A., Hamadjida, A., Liu, Y., Bloch, J., Brunet, J.F., Belhaj-Saif, A., & Rouiller, E.M. (2012). Short-term effects of unilateral lesion of the primary motor cortex (M1) on ipsilesional hand dexterity in adult macaque monkeys. *Brain Struct Funct*, *217*, 63-79.

[5] Beaud, M.L., Schmidlin, E., Wannier, T., Freund, P., Bloch, J., Mir, A., Schwab, M.E., & Rouiller, E.M. (2008). Anti-Nogo-A antibody treatment does not prevent cell body shrinkage in the motor cortex in adult monkeys subjected to unilateral cervical cord lesion. *BMC Neurosci*, *9*, 5.

[6] Bihel, E., Pro-Sistiaga, P., Letourneur, A., Toutain, J., Saulnier, R., Insausti, R., Bernaudin, M., Roussel, S., & Touzani, O. (2010). Permanent or transient chronic ischemic stroke in the non-human primate: Behavioral, neuroimaging, histological, and immunohistochemical investigations. *J Cereb Blood Flow Metab*, *30*, 273-285.

[7] Boudrias, M.H., Belhaj-Saif, A., Park, M.C., & Cheney, P.D. (2006). Contrasting properties of motor output from the supplementary motor area and primary motor cortex in rhesus macaques. *Cereb Cortex*, *16*, 632-638.

[8] Boudrias, M.H., Lee, S.P., Svojanovsky, S., & Cheney, P.D. (2010a). Forelimb muscle representations and output properties of motor areas in the mesial wall of rhesus macaques. *Cereb Cortex*, *20*, 704-719.

[9] Boudrias, M.H., McPherson, R.L., Frost, S.B., & Cheney, P.D. (2010b). Output properties and organization of the forelimb representation of motor areas on the lateral aspect of the hemisphere in rhesus macaques. *Cereb Cortex*, *20*, 169-186.

[10] Brinkman, C. (1984). Supplementary motor area of the monkey's cerebral cortex: Short- and long-term deficits after unilateral ablation and the effects of subsequent callosal section. *J Neurosci*, *4*, 918-929.

[11] Brinkman, J., & Kuypers, H.G.J.M. (1973). Cerebral control of contralateral and ipsilateral arm, hand and finger movements in the split-brain rhesus monkey. *Brain*, *96*, 653-674.

[12] Cerri, G., Shimazu, H., Maier, M.A., & Lemon, R.N. (2003). Facilitation from ventral premotor cortex of primary motor cortex outputs to macaque hand muscles. *J Neurophysiol*, *90*, 832-842.

[13] Cheatwood, J.L., Emerick, A.J., Schwab, M.E., & Kartje, G.L. (2008). Nogo-A expression after focal ischemic stroke in the adult rat. *Stroke*, *39*, 2091-2098.

[14] Courtine, G., Bunge, M.B., Fawcett, J.W., Grossman, R.G., Kaas, J.H., Lemon, R., Maier, I., Martin, J., Nudo, R.J., Ramon-Cueto, A., Rouiller, E.M., Schnell, L., Wannier, T., Schwab, M.E., & Edgerton, V.R. (2007). Can experiments in nonhuman primates expedite the translation of treatments for spinal cord injury in humans? *Nat Med*, *13*, 561-566.

[15] Dancause, N., Barbay, S., Frost, S.B., Plautz, E.J., Chen, D.F., Zoubina, E.V., Stowe, A.M., & Nudo, R.J. (2005). Extensive cortical rewiring after brain injury. *J Neurosci*, *25*, 10167-10179.

[16] Dancause, N., Barbay, S., Frost, S.B., Zoubina, E.V., Plautz, E.J., Mahnken, J.D., & Nudo, R.J. (2006). Effects of small ischemic lesions in the primary motor cortex on neu-

rophysiological organization in ventral premotor cortex. *J Neurophysiol*, *96*, 3506-3511.
[17] Dancause, N., & Nudo, R.J. (2011). Shaping plasticity to enhance recovery after injury. *Prog Brain Res*, *192*, 273-295.
[18] Darling, W.G., Pizzimenti, M.A., Rotella, D.L., Peterson, C.R., Hynes, S.M., Ge, J., Solon, K., McNeal, D.W., Stilwell-Morecraft, K.S., & Morecraft, R.J. (2009). Volumetric effects of motor cortex injury on recovery of dexterous movements. *Exp Neurol*, *220*, 90-108.
[19] Darling, W.G., Pizzimenti, M.A., Rotella, D.L., Hynes, S.M., Ge, J., Stilwell-Morecraft, K.S., Vanadurongvan, T., McNeal, D.W., Solon-Cline, K.M., & Morecraft, R.J. (2010). Minimal forced use without constraint stimulates spontaneous use of the impaired upper extremity following motor cortex injury. *Exp Brain Res*, *202*, 529-542.
[20] Darling, W.G., Pizzimenti, M.A., Hynes, S.M., Rotella, D.L., Headley, G., Ge, J., Stilwell-Morecraft, K.S., McNeal, D.W., Solon-Cline, K.M., & Morecraft, R.J. (2011). Volumetric effects of motor cortex injury on recovery of ipsilesional dexterous movements. *Exp Neurol*, *231*, 56-71.
[21] Dum, R.P., & Strick, P.L. (1991). The origin of corticospinal projections from the premotor areas in the frontal lobe. *J Neurosci*, *11*, 667-689.
[22] Eisner-Janowicz, I., Barbay, S., Hoover, E., Stowe, A.M., Frost, S.B., Plautz, E.J., & Nudo, R.J. (2008). Early and late changes in the distal forelimb representation of the supplementary motor area after injury to frontal motor areas in the squirrel monkey. *J Neurophysiol*, *100*, 1498-1512.
[23] Emerick, A.J., Neafsey, E.J., Schwab, M.E., & Kartje, G.L. (2003). Functional reorganization of the motor cortex in adult rats after cortical lesion and treatment with monoclonal antibody IN-1. *J Neurosci*, *23*, 4826-4830.
[24] Emerick, A.J., & Kartje, G.L. (2004). Behavioral recovery and anatomical plasticity in adult rats after cortical lesion and treatment with monoclonal antibody IN-1. Behav. *Brain Res*, *152*, 315-325.
[25] Freund, P., Schmidlin, E., Wannier, T., Bloch, J., Mir, A., Schwab, M.E., & Rouiller, E.M. (2006). Nogo-A-specific antibody treatment enhances sprouting and functional recovery after cervical lesion in adult primates. *Nature Med*, *12*, 790-792.
[26] Freund, P., Wannier, T., Schmidlin, E., Bloch, J., Mir, A., Schwab, M.E., & Rouiller, E.M. (2007). Anti-Nogo-A antibody treatment enhances sprouting of corticospinal axons rostral to a unilateral cervical spinal cord lesion in adult macaque monkey. *J Comp Neurol*, *502*, 644-659.
[27] Freund, P., Schmidlin, E., Wannier, T., Bloch, J., Mir, A., Schwab, M.E., & Rouiller, E.M. (2009). Anti-Nogo-A antibody treatment promotes recovery of manual dexterity after unilateral cervical lesion in adult primates–re-examination and extension of behavioral data. *Eur J Neurosci*, *29*, 983-996.
[28] Friel, K.M., & Nudo, R.J. (1998). Recovery of motor function after focal cortical injury in primates: Compensatory movement patterns used during rehabilitative training. *Somatosens Mot Res*, *15*, 173-189.
[29] Friel, K.M., Heddings, A.A., & Nudo, R.J. (2000). Effects of postlesion experience on behavioral recovery and neurophysiologic reorganization after cortical injury in primates. *Neurorehabil Neural Repair*, *14*, 187-198.
[30] Frost, S.B., Barbay, S., Friel, K.M., Plautz, E.J., & Nudo, R.J. (2003). Reorganization of remote cortical regions after ischemic brain injury: A potential substrate for stroke recovery. *J Neurophysiol*, *89*, 3205-3214.
[31] Gillani, R.L., Tsai, S.Y., Wallace, D.G., O'Brien, T.E., Arhebamen, E., Tole, M., Schwab, M.E., & Kartje, G.L. (2010). Cognitive recovery in the aged rat after stroke and anti-Nogo-A immunotherapy. *Behav Brain Res*, *208*, 415-424.
[32] Glees, P., & Cole, J. (1950). Recovery of skilled motor function after small repeated lesions of motor cortex in macaque. *J Neurophysiol*, *13*, 137-148.
[33] Gonzenbach, R.R., & Schwab, M.E. (2008). Disinhibition of neurite growth to repair the injured adult CNS: Focusing on Nogo. *Cell Mol Life Sci*, *65*, 161-176.
[34] Hamadjida, A., Wyss, A.F., Mir, A., Schwab, M.E., Belhaj-Saif, A., & Rouiller, E.M. (2012). Influence of anti-Nogo-A antibody treatment on the reorganization of callosal connectivity of the premotor cortical areas following unilateral lesion of primary motor cortex (M1) in adult macaque monkeys. *Exp Brain Res*, *223*, 321-340.
[35] He, S.Q., Dum, R.P., & Strick, P.L. (1993). Topographic organization of corticospinal projections from the frontal lobe: Motor areas on the lateral surface of the hemisphere. *J Neurosci*, *13*, 952-980.
[36] He, S.Q., Dum, R.P., & Strick, P.L. (1995). Topographic organization of corticospinal projections from the frontal lobe: Motor areas on the medial surface of the hemisphere. *J Neurosci*, *15*, 3284-3306.
[37] Hoogewoud, F., Hamadjida, A., Wyss, A.F., Mir, A., Schwab, M.E., Belhaj-Saif, A., & Rouiller, E.M. (2013). Comparison of functional recovery of manual dexterity after unilateral spinal cord lesion or motor cortex lesion in adult macaque monkeys. *Front Neurol*, *4*, 101.
[38] Humphrey, D.R. (1986). Representation of movements and muscles within the primate precentral. *Fed Proc*, *45*, 2687-2699.
[39] Kaeser, M., Wyss, A.F., Bashir, S., Hamadjida, A., Liu, Y., Bloch, J., Brunet, J.F., Belhaj-Saif, A., & Rouiller, E.M. (2010). Effects of Unilateral Motor Cortex Lesion on Ipsilesional Hand's Reach and Grasp Performance in Monkeys: Relationship With Recovery in the Contralesional Hand. *J Neurophysiol*, *103*, 1630-1645.
[40] Kaeser, M., Brunet, J.F., Wyss, A., Belhaj-Saif, A., Liu, Y., Hamadjida, A., Rouiller, E.M., & Bloch, J. (2011). Autologous adult cortical cell transplantation enhances functional recovery following unilateral lesion of motor cortex in primates: A pilot study. *Neurosurgery*, *68*, 1405-1417.
[41] Kaeser, M., Wannier, T., Brunet, J.F., Wyss, A., Bloch, J., & Rouiller, E.M. (2013). Representation of motor habit in a sequence of repetitive reach and grasp movements performed by macaque monkeys: Evidence for a contribution of the dorsolateral prefrontal cortex. *Cortex*, *49*, 1404-1419.
[42] Kinoshita, M., Matsui, R., Kato, S., Hasegawa, T., Kasahara, H., Isa, K., Watakabe, A., Yamamori, T., Nishimura, Y., Alstermark, B., Watanabe, D., Kobayashi, K., & Isa, T. (2012). Genetic dissection of the circuit for hand dexterity in primates. *Nature*, *487*, 235-238.
[43] Kwan, H.C., MacKay, W.A., Murphy, J.T., & Wong, Y.C. (1978). Spatial organization of precentral cortex in awake primates. II. Motor outputs. *J Neurophysiol*, *41*, 1120-1131.
[44] Lemon, R. (1988). The output map of the primate motor cortex. *Trends Neurosci*, *11*, 501-506.
[45] Lemon, R.N., & Griffiths, J. (2005). Comparing the function of the corticospinal system in different species: Organiza-

tional differences for motor specialization? *Muscle Nerve*, *32*, 261-279.

[46] Lemon, R.N. (2008). Descending pathways in motor control. *Annu Rev Neurosci*, *31*, 195-218.

[47] Liu, J., Morel, A., Wannier, T., & Rouiller, E.M. (2002). Origins of callosal projections to the supplementary motor area (SMA): A direct comparison between pre-SMA and SMA-proper in macaque monkeys. *J Comp Neurol*, *443*, 71-85.

[48] Liu, Y., & Rouiller, E.M. (1999). Mechanisms of recovery of dexterity following unilateral lesion of the sensorimotor cortex in adult monkeys. *Exp Brain Res*, *128*, 149-159.

[49] Maier, M.A., Armand, J., Kirkwood, P.A., Yang, H.W., Davis, J.N., & Lemon, R.N. (2002). Differences in the corticospinal projection from primary motor cortex and supplementary motor area to macaque upper limb motoneurons: An anatomical and electrophysiological study. Cereb. *Cortex*, *12*, 281-296.

[50] Markus, T.M., Tsai, S.Y., Bollnow, M.R., Farrer, R.G., O'Brien, T.E., Kindler-Baumann, D.R., Rausch, M., Rudin, M., Wiessner, C., Mir, A.K., Schwab, M.E., & Kartje, G.L. (2005). Recovery and brain reorganization after stroke in adult and aged rats. *Ann Neurol*, *58*, 950-953.

[51] Marshall, J.W., Ridley, R.M., Baker, H.F., Hall, L.D., Carpenter, T.A., & Wood, N.I. (2003). Serial MRI, functional recovery, and long-term infarct maturation in a non-human primate model of stroke. *Brain Res Bull*, *61*, 577-585.

[52] Martin, J.H. (1991). Autoradiographic estimation of the extent of reversible inactivation produced by microinjection of lidocaine and muscimol in the rat. *Neurosci Lett*, *127*, 160-164.

[53] McNeal, D.W., Darling, W.G., Ge, J., Stilwell-Morecraft, K.S., Solon, K.M., Hynes, S.M., Pizzimenti, M.A., Rotella, D.L., Vanadurongvan, T., & Morecraft, R.J. (2010). Selective long-term reorganization of the corticospinal projection from the supplementary motor cortex following recovery from lateral motor cortex injury. *J Comp Neurol*, *518*, 586-621.

[54] Milliken, G.W., Plautz, E.J., & Nudo, R.J. (2013). Distal forelimb representations in primary motor cortex are redistributed after forelimb restriction: A longitudinal study in adult squirrel monkeys. *J Neurophysiol*, *109*, 1268-1282.

[55] Murata, Y., Higo, N., Oishi, T., Yamashita, A., Matsuda, K., Hayashi, M., & Yamane, S. (2008). Effects of motor training on the recovery of manual dexterity after primary motor cortex lesion in macaque monkeys. *J Neurophysiol*, *99*, 773-786.

[56] Nudo, R.J., Wise, B.M., SiFuentes, F., & Milliken, G.W. (1996). Neural substrates for the effects of rehabilitative training on motor recovery after ischemic infarct. *Science*, *272*, 1791-1794.

[57] Nudo, R.J., & Milliken, G.W. (1996). Reorganization of movement representations in primary motor cortex following focal ischemic infarcts in adult squirrel monkeys. *J Neurophysiol*, *75*, 2144-2149.

[58] Oertle, T., Van der Haar, M.E., Bandtlow, C.E., Robeva, A., Burfeind, P., Buss, A., Huber, A.B., Simonen, M., Schnell, L., Brösamle, C., Kaupmann, K., Vallon, R., & Schwab, M.E. (2003). Nogo-A inhibits neurite outgrowth and cell spreading with three discrete regions. *J Neurosci*, *23*, 5393-5406.

[59] Ogden, R., & Franz, S.I. (1917). On cerebral motor control: The recovery from experimentally produced hemiplegia. *Psychobiology*, *1*, 33-49.

[60] Papadopoulos, C.M., Tsai, S.Y., Alsbiei, T., O'Brien, T.E., Schwab, M.E., & Kartje, G.L. (2002). Functional recovery and neuroanatomical plasticity following middle cerebral artery occlusion and IN-1 antibody treatment in the adult rat. *Ann Neurol*, *51*, 433-441.

[61] Park, M.C., Belhaj-Saif, A., Gordon, M., & Cheney, P.D. (2001). Consistent features in the forelimb representation of primary motor cortex in rhesus macaques. *J Neurosci*, *21*, 2784-2792.

[62] Park, M.C., Belhaj-Saif, A., & Cheney, P.D. (2004). Properties of primary motor cortex output to forelimb muscles in rhesus macaques. *J Neurophysiol*, *92*, 2968-2984.

[63] Passingham, R.E., Perry, V.H., & Wilkinson, F. (1983). The long-term effects of removal of sensorimotor cortex in infant and adult rhesus monkeys. *Brain*, *106*(Pt 3), 675-705.

[64] Peuser, J., Belhaj-Saif, A., Hamadjida, A., Schmidlin, E., Gindrat, A.D., Volker, A.C., Zakharov, P., Hoogewoud, H.M., Rouiller, E.M., & Scheffold, F. (2011). Follow-up of cortical activity and structure after lesion with laser speckle imaging and magnetic resonance imaging in nonhuman primates. *J Biomed Opt*, *16*, 096011.

[65] Pizzimenti, M.A., Darling, W.G., Rotella, D.L., McNeal, D.W., Herrick, J.L., Ge, J., Stilwell-Morecraft, K.S., & Morecraft, R.J. (2007). Measurement of reaching kinematics and prehensile dexterity in nonhuman primates. *J Neurophysiol*, *98*, 1015-1029.

[66] Plautz, E.J., Barbay, S., Frost, S.B., Friel, K.M., Dancause, N., Zoubina, E.V., Stowe, A.M., Quaney, B.M., & Nudo, R.J. (2003). Post-infarct cortical plasticity and behavioral recovery using concurrent cortical stimulation and rehabilitative training: A feasibility study in primates. *Neurol Res*, *25*, 801-810.

[67] Prabhu, G., Shimazu, H., Cerri, G., Brochier, T., Spinks, R.L., Maier, M.A., & Lemon, R.N. (2009). Modulation of primary motor cortex outputs from ventral premotor cortex during visually guided grasp in the macaque monkey. *J Physiol*, *587*, 1057-1069.

[68] Rathelot, J.A., & Strick, P.L. (2006). Muscle representation in the macaque motor cortex: An anatomical perspective. *Proc Natl Acad Sci U. S. A*, *103*, 8257-8262.

[69] Roitberg, B., Khan, N., Tuccar, E., Kompoliti, K., Chu, Y., Alperin, N., Kordower, J.H., & Emborg, M.E. (2003). Chronic ischemic stroke model in cynomolgus monkeys: Behavioral, neuroimaging and anatomical study. *Neurol Res*, *25*, 68-78.

[70] Rouiller, E.M., Moret, V., Tanné, J., & Boussaoud, D. (1996). Evidence for direct connections between the hand region of the supplementary motor area and cervical motoneurons in the macaque monkey. *Eur J Neurosci*, *8*, 1055-1059.

[71] Rouiller, E.M., Yu, X.H., Moret, V., Tempini, A., Wiesendanger, M., & Liang, F. (1998). Dexterity in adult monkeys following early lesion of the motor cortical hand area: The role of cortex adjacent to the lesion. *Eur J Neurosci*, *10*, 729-740.

[72] Sasaki, K., & Gemba, H. (1984). Compensatory motor function of the somatosensory cortex for dysfunction of the motor cortex following cerebellar hemispherectomy in the monkey. *Exp Brain Res*, *56*, 532-538.

[73] Sasaki, S., Isa, T., Pettersson, L.G., Alstermark, B., Naito, K., Yoshimura, K., Seki, K., & Ohki, Y. (2004). Dexterous finger movements in primate without monosynaptic corticomotoneuronal excitation. *J Neurophysiol*, *92*, 3142-3147.

[74] Schmidlin, E., Wannier, T., Bloch, J., & Rouiller, E.M. (2004). Progressive plastic changes in the hand representation of the primary motor cortex parallel incomplete recovery from a unilateral section of the corticospinal tract at cervical level in monkeys. *Brain Research*, *1017*, 172-183.

[75] Schmidlin, E., Wannier, T., Bloch, J., Belhaj-Saif, A., Wyss, A., & Rouiller, E.M. (2005). Reduction of the hand representation in the ipsilateral primary motor cortex following unilateral section of the corticospinal tract at cervical level in monkeys. *BMC Neuroscience*, *6*, 56.

[76] Schmidlin, E., Brochier, T., Maier, M.A., Kirkwood, P.A., & Lemon, R.N. (2008). Pronounced reduction of digit motor responses evoked from macaque ventral premotor cortex after reversible inactivation of the primary motor cortex hand area. *J Neurosci*, *28*, 5772-5783.

[77] Schmidlin, E., Kaeser, M., Gindrat, A.D., Savidan, J., Chatagny, P., Badoud, S., Hamadjida, A., Beaud, M.L., Wannier, T., Belhaj-Saif, A., & Rouiller, E.M. (2011). Behavioral assessment of manual dexterity in non-human primates. *J Vis Exp*, 3258.

[78] Schwab, M.E. (2010). Functions of Nogo proteins and their receptors in the nervous system. *Nat Rev Neurosci*, *11*, 799-811.

[79] Sessle, B.J., & Wiesendanger, M. (1982). Structural and functional definition of the motor cortex in the monkey (macaca fascicularis). *J Physiol (London)*, *323*, 245-265.

[80] Seymour, A.B., Andrews, E.M., Tsai, S.Y., Markus, T.M., Bollnow, M.R., Brenneman, M.M., O'Brien, T.E., Castro, A.J., Schwab, M.E., & Kartje, G.L. (2005). Delayed treatment with monoclonal antibody IN-1 1 week after stroke results in recovery of function and corticorubral plasticity in adult rats. J Cereb. *Blood Flow Metab*, *25*, 1366-1375.

[81] Shimazu, H., Maier, M.A., Cerri, G., Kirkwood, P.A., & Lemon, R.N. (2004). Macaque ventral premotor cortex exerts powerful facilitation of motor cortex outputs to upper limb motoneurons. *J Neurosci*, *24*, 1200-1211.

[82] Snyder, G.L., Galdi, S., Hendrick, J.P., & Hemmings, H.C. Jr (2007). General anesthetics selectively modulate glutamatergic and dopaminergic signaling via site-specific phosphorylation *in vivo*. *Neuropharmacology*, *53*, 619-630.

[83] Takei, T., & Seki, K. (2010). Spinal interneurons facilitate coactivation of hand muscles during a precision grip task in monkeys. *J Neurosci*, *30*, 17041-17050.

[84] Travis, A.M. (1955). Neurological deficiencies after ablation of the precentral motor area in Macaca mulatta. *Brain*, *78*, 155-173.

[85] Tsai, S.Y., Markus, T.M., Andrews, E.M., Cheatwood, J.L., Emerick, A.J., Mir, A.K., Schwab, M.E., & Kartje, G.L. (2007). Intrathecal treatment with anti-Nogo-A antibody improves functional recovery in adult rats after stroke. *Exp Brain Res*, *182*, 261-266.

[86] Tsai, S.Y., Papadopoulos, C.M., Schwab, M.E., & Kartje, G.L. (2011). Delayed anti-nogo-a therapy improves function after chronic stroke in adult rats. *Stroke*, *42*, 186-190.

[87] Wannier, T., Schmidlin, E., Bloch, J., & Rouiller, E.M. (2005). A unilateral section of the corticospinal tract at cervical level in primate does not lead to measurable cell loss in motor cortex. *J Neurotrauma*, *22*, 703-717.

[88] Widener, G.L., & Cheney, P.D. (1997). Effects on muscle activity from microstimuli applied to somatosensory and motor cortex during voluntary movement in the monkey. *J Neurophysiol*, *77*, 2446-2465.

2.2. Chapter 2:

Primary motor cortex role in case of sequential bilateral lesion on fine manual dexterity in the macaque monkey: a case study

Savidan J., Kaeser M., Gindrat A.D., Belhaj-Saïf A., Schmidlin E., Rouiller E.M.

Faculty of Sciences and Fribourg Centre for Cognition, Department of Medicine, University of Fribourg, Chemin du Musée, Fribourg, Switzerland

Abstract

This case report describes how a unilateral M1 lesion restricted to the hand area affects different aspects of the manual dexterity and the role played by the intact contralesional homologous M1 hand area in the functional recovery. An adult monkey was trained to perform two manual motor tasks: (*i*) the "modified Brinkman board" task to assess separately simple precision grip from complex precision grip, the latter comprising wrist deviation and pro-supination; (*ii*) the "modified Klüver board" task to assess movements ranging from power grip to precision grip and distinguishing the phase of grasping from the preshaping phase. The monkey was subjected to two consecutive unilateral M1 lesions targeting the hand area on each hemisphere. The second lesion occurred after the functional recovery from the primary lesion. The manual dexterity of the contralesional hand following each lesion was similarly affected, with deleterious effects increasingly pronounced from the power grip, to precision grip and then to the more complex precision grip. However, the secondary lesion presented a different profile of recovery with longer periods of paralysis although followed by better functional recovery, as compared to the primary lesion. Also affected similarly following each lesion, the manual dexterity performances of the ipsilesional hand were transiently disturbed for the complex precision grip only, to be finally slightly improved after recovery. The hand preshaping was impaired in the contralesional hand after both lesions, but remained impaired on the long-term only following the primary lesion. The related reaching times were only weakly affected, but exhibited an interesting bilaterally delayed following the primary lesion, then, bilaterally fairly restored following the secondary contralateral lesion. Regarding the primary lesion of the left M1, the intact contralesional M1, though not involved in the long-term functional recovery, was suggested to be involved in the early phase of the recovery. The observed ipsilesional improvement of functional recovery following each lesion can be suggested to result of the training induced by the contralesional hand immobility during the early phase post-lesion. This case report emphasized the suggested ipsilateral and/or bilateral role of M1, however not crucially, in the control of the complex manual dexterity as well as the importance of bilateral balance between M1 homologous counterparts activity in the cortical circuit controlling hand preshaping.

Introduction

Stroke affecting the primary motor cortex (M1) hand area has been reported to induce a wide range of deficits on different aspects of reach and grasp movements, depending on the size and location of the injury, similarly reported in case of transient inactivation (Rizzolatti and Luppino, 2001; Shelton and Reding, 2001; Olivier et al., 2007; Brown and Teskey, 2014). In monkeys, alterations of hand movements have been reported after unilateral transient inactivation or lesion of M1 followed by the occurrence of compensatory strategies, affecting motor parameters such as force (Brochier et al., 1999), trajectory (Cirstea et Levin, 2000), precision grip per se (Brochier et al., 1999, Liu and Rouiller, 1999, Murata et al., 2008, Kaeser et al., 2010; Wyss et al., 2013), flexion-extension (Schieber and Poliakov, 1998) and wrist movement (Hoffman and Strick, 1995). Depending on the size and location of the injury, spontaneous recovery occurs to a variable extent though incomplete. The precise mechanisms and anatomical basis for motor recovery remain unclear (for review: Nudo, 2006; Nudo and Barbay, 2014). In particular, the role of the intact M1 cortex of the contralesional hemisphere remains controversial. Nevertheless, the intact M1 cortex on the contralesional hemisphere exhibits high level of activity after lesion or stroke (Gonzalez et al., 2004; Babiloni et al., 1999), although the role of this increased activity in spontaneous recovery remains a matter of debate, and appears to be restricted to the early phases (Salmelin et al., 1995; Netz et al., 1997; Rehme et al., 2010). For instance contradictory results, though in different species, reported that the spontaneous functional recovery following M1 lesion was not affected by transient inactivation of the intact M1 cortex on the contralesional hemisphere in monkeys (Liu and Rouiller, 1999) but abolished recovery following large stroke in rats (Biernaskie et al., 2005). Nevertheless, the notion that the intact M1 provides full and direct support for the spontaneous functional recovery occurring after stroke appears to be inaccurate, albeit there is evidence supporting the role of the intact M1 in collaboration with non-primary areas (Jaillard et al., 2005; for review Dancause, 2006; Dancause et al., 2015). Furthermore, the intact M1 may be involved during certain phases of the functional recovery (*e.g.* acute phase) and not in others (*e.g.* plateau phase). It has been suggested that bilateral control exerted by M1 depends on the task complexity and the size of the cortical lesion (Biernaskie et al., 2005; Shibasaki et al., 1993; Salmelin et al., 1995; Chen, et al., 1996). Thus, depending on the motor task assessed, the role of the intact M1 in functional recovery may be either enhanced or masked. Two motor tasks have been extensively used to assess different aspects of hand grasp movements in a non-human primate model: (*i*) the modified

Brinkman board task testing the precision grip in different hand position (*e.g.* Liu and Rouiller, 1999; Schmidlin et al., 2004, 2005; Freund et al., 2006, 2009; Kaeser et al., 2007, 2010, 2011, 2013, 2014; Bashir et al., 2012; Wyss et al., 2013); (*ii*) the modified Klüver board task to assess various types of grip, ranging from power grip to precision grip (*e.g.* Nudo et al., 1992; Xerri et al., 1998; Murata et al., 2008; Sugiyama et al., 2013; Milliken et al., 2013; Qi et al., 2013).

The present case report in a non-human primate aimed at investigating the role of the contralesional intact M1 in case of sequential lesion of M1 on both hemispheres (one after the other), by following the time course of the subsequent functional recovery observed consecutively to each M1 lesion. For this purpose, the two complementary manual motor tests, namely the modified Brinkman board task and the modified Klüver board task, were used in parallel to assess manual dexterity, representing tasks of various complexities (*e.g.* type of grip, different posture). More specifically, we tested the hypotheses that: 1) after unilateral M1 lesion restricted to the hand area, several aspects of the fine manual dexterity are differently affected; 2) after unilateral M1 lesion restricted to the hand area, a secondary permanent lesion of the intact M1 does not preclude the functional recovery of the hand affected by the primary lesion; 3) after a subsequent secondary lesion of the contralesional M1 restricted to the homologous hand area, several aspects of fine manual dexterity are differently affected over a different functional recovery time course pattern than following the primary homologous M1 lesion.

Methods

Some methods used in the present study were similar to those described in previous reports from our laboratory but were repeated here for the sake of completeness. The relevant reports are cited in the corresponding sections of the following paragraphs.

General survey of the experiment

The present study was conducted on one adult male monkey (*Macaca fascicularis*; 9 Kg), aged from 10 years at the time of the sacrifice (Mk-DG). All experiments were carried out in accordance to the Guide for Care and Use of Laboratory Animals (ISBN 0-309-05377-3; 1996) and approved by local veterinary authorities, including the ethical assessment by the local (cantonal) Survey Committee on Animal Experimentation and a final acceptance delivered by the Federal Veterinary Office (BVET, Bern, Switzerland). The monkey was

purchased from a certified supplier (Harlan Buckshire, USA; monkey bred in China, followed by quarantine in the European Harlan Center, Milano, Italy).

To summarize the time course of the present case report (Fig. 1), the animal was first trained to perform two behavioral tasks: the "modified Brinkman board" and the "modified Klüver board" tasks. When stable performances were achieved in the two tasks, a first chronic chamber was implanted over the M1 hand area on the left hemisphere. Once the monkey recovered from the surgery, the behavioral tasks assessment was pursued. In parallel, daily ICMS (IntraCortical MicroStimulation) sessions were performed twice a week (alternatively with the behavioral tasks), to map the targeted hand area in the left M1. Once the ICMS protocol was completed, a focal lesion was performed by infusion of ibotenic acid in the identified hand area of the left M1. The functional recovery was assessed based on the two behavioral tasks, and during this period the chamber was removed. Four months after the first lesion of M1, a second chronic chamber was implanted, following the same implantation protocol, over the contralesional M1 hand area on the right hemisphere. Following the same protocol, once the monkey recovered from the surgery, the behavioral assessment was pursued alternatively with ICMS sessions performed twice a week to map the targeted hand area in the right M1. Afterwards, 5 months after the first lesion of the left M1 hand area, a solution of muscimol (GABA inhibitor), accidentally over-concentrated, was infused in the targeted hand area of the right M1, inducing a permanent lesion. The functional recovery from this secondary contralateral M1 lesion was assessed based on the same two behavioral tasks, though during a shorter period, two months less as compared to the first lesion.

Behavioral tasks

Two motor tasks well-known for fine precision grip assessment were used in parallel to precisely describe different parameters of the precision grip movement: the "modified Brinkman board" task and the "modified Klüver board" task (Fig. 2). Modifications of the motor performances in the two tasks performed by the monkey all along this experiment have defined separate time windows for analysis (Fig. 1). Firstly, after training, the monkey reached a period of stable performance: the pre-lesion plateau (PreL). Following the two lesions, the acute periods (AcP1 and AcP2), during which the monkey was not able to perform the task, were differentiated from the periods of recovery (RecP1 and RecP2) during which the various motor parameters exhibited improvement, to finally reach the post-lesion plateau periods (PlP1 and PlP2). A plateau was quantitatively defined as a period of maximal

and stable performance during several consecutive daily sessions (see *e.g.* Kaeser et al., 2010, 2011).

Modified Brinkman board task

As already described in detail in a previous report (Schmidlin et al., 2011), the modified Brinkman board task has extensively been used in our laboratory to assess normal precision grip in monkeys and humans (Chatagny et al., 2013; Kaeser et al., 2014) and its alterations following lesion at spinal cord (SCI) or at cortical (MCI) levels (SCI: Schmidlin et al., 2004, 2005; Beaud et al., 2008, 2012; Freund et al., 2006, 2007, 2009; Wannier-Morino et al., 2008 - MCI: Liu and Rouiller, 1999; Kaeser et al., 2010, 2011, 2013; Bashir et al., 2012; Wyss et al., 2013; Hoogewoud et al., 2013).

The modified Brinkman board task was performed 5 days a week, except alternatively with the ICMS days during the mapping periods and daily during the critical acute and recovery periods. The monkey had to freely retrieve banana flavored pellets in 25 vertical slots and 25 horizontal slots randomly distributed on the board (Fig. 2**A**). The monkey had to complete the modified Brinkman board four times per day, twice per hand, separately and alternatively for the left and the right hand first. Each session was recorded using three cameras positioned on the top and laterally, on the right and on the left, for offline analyses. The manual dexterity performance was quantitatively assessed with the two following parameters: the **score,** representing the number of pellets successfully grasped during the first 30 seconds (Fig. 2**B**), and the **contact time** (**CT**), representing the time of contact between the pellet and the monkey's fingers preceding a successful grasping (Fig. 2**C**). For each hand, from the two completed boards per day, only the data for the board with the higher total score was taken into consideration for further analyses to reduce the impact of possible external disturbances on performances. Scores were represented on two graphs (Fig. 2**B**), to visualize the time course of the effects and the recovery following the M1 lesions affecting the left hand then the right hand, separately for the vertical slots, the horizontal slots and the total representing the sum of vertical and horizontal scores. The CT was established for the first five horizontal slots and the first five vertical slots from the daily completed boards with the highest total score for each hand. From these analyses, percentages of functional recovery and of performance for score and CT were calculated. These computations were completed separately for the vertical and the horizontal slots, as the movement synergies to retrieve pellets from horizontal slots involved more complex movements of pro-supination and wrist deviations. Functional recovery was calculated for the contralesional hands respectively to the

primary or secondary lesion as the ratio in percentage between the performance at the pre-lesion plateau and the performance at the related post-lesion plateau (score: PlP/PreL; CT: PreL/PlP). Moreover, percentages of performance were calculated for the ipsilesional hands respectively to the primary or secondary lesion as the ratio between the performance at the pre-lesion plateau and the performance at the concerned post-lesion periods (score: AcP/PreL, ReP/PreL, PlP/PreL; CT: PreL/AcP, PreL/ReP, PreL/PlP). For comparisons of the scores and of the CT, statistical analyses were performed using one way ANOVA and the multiple comparisons Holm-Sidak method for post-hoc analyses.

Modified Klüver board task

The modified Klüver board task was performed every two days, 5 days a week, except 2 days a week alternatively with the ICMS days during the mapping periods and every two days, 7 days a week, during the critical acute and recovery periods. The monkey has to retrieve pellets from four wells of different diameters (15 mm, 21 mm, 30 mm and 40 mm of diameter, all 20 mm deep), filled automatically after a random delay (0.5, 1, 1.5 or 2 seconds) upon pressing on a lever (Fig. 2**D**). The monkey performed 50 trials per diameter, starting with the 15 mm up to the 40 mm diameter, separately and alternatively with the left or the right hand first. For automatic recordings of behavioral time parameters, the setup was designed with sensors located at three sites (Fig. 2**E**): on the lever to detect pressure and release, a series of sensors at the well entry and a series of sensors at the bottom of the well. Based on these detectors, two different phases of the task were analyzed: the **reaching** phase from the time point the monkey released the lever to the moment a finger entered in the well and the **grasping** phase during which the fingers were in the well to pick the pellet (Fig. 2**E)**. Signals from sensors were digitized and processed with CED 1401 interface using Spike 2 software (Cambridge Electronic Design, Cambridge, UK). The corresponding on/off signals were analyzed offline with Matlab R2012b (Mathworks Inc., Natick, MA, USA) to determine reaching and grasping times for each trial. Trials considered as errors, removed of the offline analysis, were defined as: pellets fallen or not picked at all, more than one pellet in the well and when the monkey was disturbed by external distracting events. In addition to these general criteria, specifically for the reaching analyses, trials in which the lever was released before the pellet arrival in the well were rejected and those in which reaching time values were higher than 500 ms were also rejected, considered as affected by external interferences. In cases for which several attempts were needed to correctly grasp pellets, all the grasping time values were added in a unique trial value. Similarly as for the modified Brinkman board,

functional recovery was calculated for the contralesional hands respectively to the primary or secondary lesion as the ratio in percentage between the performance at the pre-lesion plateau and the performance at the related post-lesion plateau (score: PlP/PreL; CT: PreL/PlP). Moreover, percentages of performance were calculated for the ipsilesional hands respectively to the primary or secondary lesion as the ratio between the performance at the pre-lesion plateau and the performance at the concerned post-lesion periods (score: AcP/PreL, ReP/PreL, PlP/PreL; CT: PreL/AcP, PreL/ReP, PreL/PlP).

Alongside the automatic recordings of the time values, strategies used during the reaching and grasping phases of the task were assessed (Fig. 2**F**). Strategies were analyzed offline on videos recorded using three fixed cameras (50 frames per seconds). The preshaping strategy during the reaching phase was assessed on the 5 first compelling trials of 3 to 10 sessions in each period of the lesion time windows. This strategy was assessed by measuring the distance between the tip of the thumb (D1) and the tip of the index (D2) on a lateral plane. Whatever the number of fingers (D2/D3/D4/D5) involved for the grasping, D2 was invariably used to perform the grip in order to pick pellets in the well. Although the distances between D1 and D2 were measured at each video frame, the space comprised between the lever and the well entry was divided in 3 different areas to gather all distances measured in each of these areas: the initiating area just after the monkey release the lever and initiate the movement, the transfer area where the monkey reached and prepared prehension to the target and the well entry area where the monkey prepared the entrance of finger(s) into the well (Fig. 2**F**). These areas were delineated for predefined distances between the D2 fingertip and the well entry point localized at the bottom most of the internal border of the well (D2-well border). Parallel systematic recording of this D2-well border distances has allowed to automatically gather the associated D1-D2 distances in each areas. Distances were measured using professional technical motions analysis software for videos (Dartfish ®; http://www.dartfish.com). The strategy during the grasping phase was assessed on the 25-30 first trials of 2 to 6 sessions in each period of lesion time windows. This grasping strategy was defined as the number of finger used to grasp the pellet and the associated number of flexion of the finger(s) to pick out the pellet of the well. The monkey used only four different finger configurations for grasping: D2 or D2+D3 or D2+D3+D4 or D2+D3+D4+D5 (Fig. 2**F**). The number of fingers was determined as the number of fingers inside the well at the time of the pellet grasping. Successful and failed trials were identified for each finger configurations and expressed in percentages. The number of flexions per retrieval was considered only for the successful trials and the total was normalized by the number of trials performed with the

corresponding successful configuration. Strategies were not analyzed for the contralesional hand, respective to the primary or secondary lesion, during periods of instable and increasing performance, such as AcP and ReP, but only for the respective primary and secondary ipsilesional hand during these time windows. However, merely for sake of illustration, the fingertips distances for the reaching strategy have been analyzed and represented during the ReP periods for the respective primary and secondary contralesioned hand, but not compared with the other period values taking into account the high variability observed during these periods. Statistical analyses were performed using non-parametric ANOVA and Dunn's test for post-hoc analysis.

Surgery

Anesthesia for surgical procedures was described in detail in a previous report from this laboratory (Lanz et al., 2013). Abbreviations for injections route were the following: i.v. for intravenous, i.m. for intramuscular and s.c. for subcutaneous. To summarize, sedation was induced with a mixture of ketamine (Ketanarkon®; 10 mg/kg; i.m.), benzodiazepine (Midazolam; 0.1 mg/kg; i.m.) and methadone (0.2 mg/kg; i.m.). Following sedation induction, the monkey was injected with: Atropine to reduce bronchial secretion (0.05 mg/kg, i.m.), Carprofen as a preventive pain killer (Rimadyl®; 50 mg/ml; 4 mg/kg; i.m.), Dexamethasone (Decadron®; 0.3 mg/kg diluted 1:1 in saline; i.m.) to prevent brain oedema and the antibiotic Synulox® (Amoxicillin-Clavulanic Acid; 8.75 mg/kg; s.c.) to prevent further infections. Deep anesthesia was maintained with the combination of an intravenous perfusion of propofol (diisopropylphenol; 1.2-3.6 mg/kg/h diluted 1:2 in Ringer) and an anesthetic gas (Sevoflurane; 2.5%; 0.5 to 1 L/min) mixed with a 50%/50% mixture of O_2 and air delivered via a tracheal cannula. During the entire surgery, the animal was continuously perfused with Ringer-lactate (5 ml/kg/h; i.v.). Additionally to the long term acting pain killer injected in prevention at the sedation step, supplementary pain killers were administered during the potentially painful steps of the surgery in order to prevent traumatic pain: the intubation step was treated with local anesthetics (drop of 0.5 ml in the larynx), the zones of incision (skin, muscles) was also treated with local anesthetics (lidocaine 1%; 8 ml at most s.c.) and potentially painful steps (*e.g.* craniotomy) was treated with a flow of opioid (Fentanyl; 0.1 µg/kg/min; i.v.). Pain and infections following surgery were prevented by postoperative treatment with Carprofen and antibiotic Synulox® during the two following weeks. All surgeries were performed in a facility under sterile conditions and approved by the (Swiss) cantonal veterinary office. During the entire surgical procedure, physiological parameters

were continuously monitored (*e.g.* body temperature, O_2 saturation, heart rate, respiration rate, exhaled CO_2) allowing adjustment of the flow of anesthetic agents (gas and propofol perfusion flows) to maintain normal physiological parameters.

Head chamber implants

Head chamber implants were designed as described in a previous report (Schmidlin et al., 2008) in order to access to the M1 hand area (Fig. 3). The two successive chambers were identical and implanted following the same protocol, firstly on the left and secondly on the right hemisphere (Fig. 3**A**). The chambers were designed to place and fix two grids (11 mm x 11 mm x 3 mm) inside, all made of Tecapeek (Fig. 3**A and B**). The two grids (11 mm x 11 mm x 3 mm) were perforated (8 mm x 8 mm) each mm for electrode and cannula penetrations (Fig. 3**B**). Under deep anesthesia, the head of the monkey was fixed in a stereotaxic headholder in order to position the chamber from the stereotaxic interaural (zero) reference, based on atlas coordinates and adjusted from MRI images. The two grids of the first chamber on the left hemisphere were centered above M1, the first positioned at 15 mm lateral and 15 mm anterior and the second positioned at 20 mm lateral and 20 mm anterior. The two grids of the second chamber on the right hemisphere were centered above M1 hand area, the first positioned at 17 mm lateral and 17 mm anterior and the second positioned at 22 mm lateral and 24 mm anterior. A skull window of the internal chamber dimensions (25 mm length and 12 mm width) was opened over the corresponding coordinates. The chamber was adjusted on the window's borders with 30° of inclination with respect to the brain curvature and was cemented (dental acrylic) along with four to six selftaped titanium screws anchored on the adjacent skull. The two grids were positioned epidurally and fixed on the internal border of the chamber allowing guidance of electrodes and cannula perpendicularly to the cortical surface (Fig. 3**B**).

Motor cortex lesions

Non extensive mapping of the hand area in M1 was performed, before each of the left and of the right M1 lesions. The mappings were achieved using the IntraCortical MicroStimulations (ICMS) method in order to localize the extent of the digits representation for the subsequently lesioned hand area on the precentral surface and in the wall of the central sulcus of the M1 cortex. ICMS were performed twice a week under light sedation and muscular activity was controlled visually or by manual palpation. The monkey was sedated with a mixture of ketamine and medetomidine (Ketasol® 4 mg/kg; Dorbene® 0.04 mg/kg; co-

injected i.m.), then lying down in a lateral decubitus position to control sedation and muscles contractions. Before starting the ICMS session, the medetomidine, a muscular relaxant, was partially reversed by injection of atipamezol (Alzane® 0.05 mg/kg), a medetomidine antagonist. Light anesthesia was maintained by injection of 0.05 ml of ketamine each 4 min till the end of the session. At this step, the rest of atipamezol was injected to complete the medetomidine reversion (Alzane® 0.2 mg/kg minus the first injection of 0.05 mg/kg) and the monkey was monitored up to recovery from the anesthesia. Tungsten microelectrodes with typical impedances between 0.1 to 1.0 MΩ (Frederick Haer & Co., Bowdoinham, ME) were used for ICMS. Electrodes were manually inserted and advanced at the selected grid locations, generally by steps of 1 mm depths, approximately starting at 2 mm of the pial surface up to 8 mm deep at most, when targeting the rostral bank of the central sulcus (Kaeser et al., 2010). ICMS consisted of 6 biphasic pulses (0.5 ms duration) delivered in trains of 30 ms long at a sweep rate of 0.5 Hz. The body part movements elicited, depth and intensity threshold of each ICMS site were collected. The two M1 lesions were chemically induced by drugs injection with a 10 µl Hamilton microsyringe connected to a cannula, targeting the digits representation of the hand area. The cannula was manually inserted and advanced through the grid holes selected from the ICMS sites eliciting digits movements at low ICMS intensities, characteristic of fast conducting and low threshold corticomotoneuronal M1 neurons (Wyss et al., 2013) (Fig. 3**C**). The primary permanent lesion of the left M1 cortex was achieved by infusions of the excitotoxic ibotenic acid 95% (Sigma #I-2765, 10 µg/µl in phosphate buffer saline) at a volume of 1 µl at each of 24 sites (Fig. 3**C**). Initially aimed to be reversible and more restricted, the secondary lesion of the right M1 cortex was achieved with microinjections of the reversible GABA agonist muscimol (Sigma #M-1523, 5 µg/µl in saline buffer), at a volume of 1 µl at each of 7 sites (Fig. 3**C**). It turned out that the concentration of muscimol was accidentally too high, leading to long lasting deficits. In order to cover the maximal surface of the digits representation among the hand area, adjacent sites of injection were spaced by 1 to 3 mm, in line with the diffusion of the substance established at 1.5 mm for muscimol (Martin et al., 1991), thus per analogy adapted to the ibotenic acid injections as well.

After reaching the plateau of behavioral performances following the primary lesion of the left M1 hand area, exactly 17 weeks and 3 days after the primary lesion, a second MRI was performed similarly to the first MRI performed during the pre-lesion period, in order to localize the lesion and its extent. The MRI acquisitions were performed under anesthesia,

induced with a mixture of ketamine (Ketasol® 10 mg/kg; i.m.) and benzodiazepine (Midazolam; 0.1 mg/kg; i.m.), then maintained with a flow of a mixture of propofol (diisopropylphenol 1%; 1.2-3.6 mg/kg/h diluted 1:1 in Ringer; i.v.) and ketamine (Ketasol® 3.75 mg/kg/h; i.v.). The head of Mk-DG was fixed in a stereotaxic headholder and the monkey was placed in ventral position for MRI acquisitions. The volume of the lesion was calculated on a parasagittal T2 Flair Cube 3D acquisition of the full head (TE = 140.1; TR = 6000; 800 µm slice thickness) acquired on a Discovery MR750 3.0T scanner (GE Medical System; Cantonal Hospital of Fribourg-Swizerland). The volume was estimated with the Cavalieri method using areas of region of interest surrounding the lesioned area and measured with Osirix software (http://www.osirix-viewer.com). Furthermore, the effects of the primary lesion of the left M1 hand area on the somatosensory cortical activity were assessed based on electrical stimulation to the right median nerve (contralateral to the M1 lesion). To this aim, somatosensory evoked potentials (SSEPs) were recorded from the scalp under sevoflurane anesthesia before and after the lesion, as previously described (Gindrat et al, 2014). Briefly, 33 electrodes regularly distributed over the whole scalp were used to collect SSEPs in response to electrical stimulation (square wave pulse, 400 µs duration, 0.5 Hz repetition rate, intensity just above the visible motor threshold) delivered to the right median nerve at the wrist. Data were processed with Cartool and SSEPs were obtained from the average of 150 stimulations.

Histology

At the end of the experiments, the monkey was deeply anaesthetized with ketamine and received a lethal dose of sodium pentobarbital (60mg/kg; i.v.) before a transcardiac perfusion with paraformaldehyde (4%) in 0.1 M of phosphate buffer (pH = 7.6) in order to fixate tissue, followed by solutions of increasing concentrations of sucrose (10, 20 and 30%; for detail see *e.g.* Wannier et al. 2005; Beaud et al., 2008). Brain was extracted and immerged into a solution of sucrose (30% in phosphate buffer, pH = 7.6). For anatomical reconstruction of the motor cortical lesion, the brain was sectioned in 50 µm thick coronal sections. Out of five series of sections, one series was Nissl stained with cresyl violet and a second series was labelled with the SMI-32 marker as already described in details in previous reports (Beaud et al., 2008, 2012; Wyss et al., 2013). The SMI-32 labelled consecutive sections were observed under light microscope using Neurolucida software to draw contours of the cortical lesion site (Wyss et al., 2013) and the Nissl ones for the contours of the subcortical lesion. Using

Neurolucida software, the volumes of the cortical lesions were calculated (in mm^3) based on the Cavalieri method (*e.g.* Pizzimenti et al., 2007).

Results

Behavioral assessment of the effects of the lesions

Behavioral recovery time windows

The different motor parameters, derived from the two behavioral tasks, were differently affected by the primary lesion as compared to the secondary lesion. This was firstly observed by the time duration of total paralysis (AcP), from the lesion until the day of the first attempt. Secondly, the duration of recovery (ReP) per se was assessed, going from the first attempt to the post-lesion plateau (Fig. 4). Generally, the monkey started to recover earlier after the primary lesion than after the secondary lesion. Contrarily, the recovery period was shorter after the secondary lesion, but only for the parameters assessing the grasping throughout the two tasks. Following the primary lesion of the left M1 hand area, the less challenging grips recovered earlier than the more challenging ones. The monkey recovered gradually, starting by the power grip in the large size wells (30 and 40 mm) of the modified Klüver board task, then the precision grip in the small size wells (15 and 21 mm) of the modified Klüver board task and the vertical slots of the modified Brinkman board task, and finally the complex movement of precision grip in a pro-supination position required for the horizontal slots of the modified Brinkman board task. Similar effects were observed resulting from the secondary lesion of the right M1 hand area, but not for the horizontal slots of the modified Brinkman board task, showing short and not highly delayed period of recovery. The recovery period for the reaching phase was shorter than for the grasping phase following the primary lesion but not following the secondary lesion. Interestingly, following the primary lesion, the duration of the recovery period covered quite variable time windows depending on the motor parameters, while starting earliest for the large well size (40 mm) of the modified Klüver board task.

Modified Brinkman board task

The time course of the score for each hand in the modified Brinkman board task shows the respective effects of the primary and the secondary M1 lesions (Fig. 2**B**). Scores reflected a stable performance of the contralateral hands before each M1 lesion, after which the score

dropped dramatically to zero before starting to recover during a phase of increasing performances up to a maximum of stable performance post-lesion (plateau). Further subtle and transient variations potentially hidden by the intersessions variability have been investigated for the scores, as well as for the contact times (CT), by plotting the data for each time windows (Fig. 5).

The primary and the secondary M1 lesions have significantly decreased the scores and increased the CT of the contralesional hand during the post-lesion plateau periods (PlP) (Fig. 5). After the primary lesion of the left M1 hand area, these two parameters were especially strongly affected for the right hand (Fig. 5**A**), impacting predominantly on the performance in the horizontal slots, with percentages of recovery at PlP1 of 45% for the score and 39% for the CT, whereas the percentage of recovery was 69% for the score and 47% for the CT in the vertical slots. Following the secondary lesion of the right M1 hand area, the left hand (Fig. 5**B**) was affected to a lesser extent than the right hand following the primary lesion, though significant, except for the CT in the vertical slots, with percentage of recovery at PlP2 comprised between 86% and 89% for all combined parameters, without differences between the orientation slots.

Effects were also observed on the ipsilesional hand. Following the primary lesion of the left M1 hand area, the ipsilesional left hand (Fig. 5**B**) was transiently affected during the AcP1 for the horizontal slots, especially the CT with percentage of performance significantly decreased by 50%, while the vertical slots were not affected, if not improved, but not to a statistically significant extent. As the vertical slots during the AcP1, all criteria were not affected, if not transiently improved during the ReP1 with percentages of performance ranging from 97% up to 118%, though still not statistically significant. At PlP1, the parameters of the ipsilesional left hand (Fig. 5**B**) were equivalent to the PreL level, if not slightly improved with percentages of performance ranging from 99% up to 110%. Following the secondary right M1 hand area lesion, the percentages of performance of the ipsilesional right hand (Fig. 5**A**) were transiently and slightly affected during the AcP2 in the horizontal slots, falling from 45% to 37% for the score and from 39% to 33% for the CT. The parameters for the vertical slots were not affected, if not improved for the CT with a percentage of recovery of 47% increased to a percentage of performance of 52%. At PlP2, the parameters of the ipsilesional right hand were improved as compared to the PlP1, even significantly for the score of total slots, representing an increase of 17%. This improvement at the PlP2 was observed together with an enhancement of the CTs, thus comparable to the ones in the PreL period.

Modified Klüver board task: Grasping phase

The two lesions significantly increased the time and modified the strategy to retrieve pellets from the four sizes of well for the contralesional hand during the post-lesion plateau periods (PlP) (Fig. 6). Times to grasp pellets in wells were strongly affected for the right hand (Fig. 6**A**) by the primary lesion of the left M1 hand area with percentages of recovery ranging from 43% for the 40 mm diameter, increasing with the smaller diameter size up to 61% for the 15 mm diameter at the PlP1. In a different way, times to grasp pellets in wells were affected to a lesser extent for the left hand (Fig. 6**B**) lesioned by the secondary lesion of the right M1 hand area with percentages of recovery ranging from 60% for the 15 mm diameter size, increasing with diameter size up to 87% for the 40 mm diameter at the PlP2. Interestingly, the two lesions have affected to a similar extent the times to grasp pellets in the smaller diameter well (15 mm). The differences were observed for the larger diameter wells, more affected after the primary lesion than following the secondary lesion compared to the 15 mm diameter. This probably reflected the differences observed for the corresponding strategies used to grasp pellets with each hand and their post-lesion modifications (Figs. 6**C** and **D**). The smaller diameter well, 15 mm, did not lead to other possibility than using the index finger, D2 configuration, to pick pellets in the well, thus post-lesion modifications for the contralesional hand were expressed by an increase of error for the right hand at PlP1 and of the number of flexions per retrieval in the left hand at PlP2. However, analyses for the larger diameters have shown different fingers configurations. PreL, the precision grip was preferably used to grasp with the right hand even in the larger diameters, using uniquely D2 configuration for the 21 mm and D2 or D2-3 configuration for the 30 mm well, while for the larger 40 mm diameter well, allowing 4 fingers penetration, the finger configurations used were a mix between D2-3 and D2-3-4. This favored use of more precision grip PreL switched post-lesion to the use of less precision grip configurations. Effectively, there was an increased use of the D2-3 in the 21 mm well, only the D2-3 in the 30 mm well and almost only the D2-3-4 for the 40 mm well. In contrast, different strategies were used to grasp with the left hand, not using the precision grip as frequently when not obliged, only for the 21 mm diameter well in combination with the D2-3 configuration of fingers, and using the four fingers configuration even in the 30 mm diameter well, normally not allowing penetration of four fingers. Post-lesion, the favored configurations switched in favor of fingers configurations in between the D2-3 and D2-3-4. For the configurations just occasionally used PreL, the number of flexions per retrieval was reduced post-lesion due to the increase of the frequency of use

while the favored configurations PreL, if still used post-lesion, occurred together with a high increase of the associated number of flexions per retrieval.

Effects were also observed on the ipsilesional hand. Following the primary lesion of the left M1 hand area, post-lesion performances at PlP1 for the left hand (Fig. 6**B**) were slightly but significantly decreased for the smallest diameter well (15 mm), with a percentage of performance of 91%, but improved for all the other diameter wells, with percentages of performance over 100%. The associated finger configurations and number of flexions per retrieval were not modified. Before recovery after the primary lesion, during the AcP1 and the ReP1, the ipsilesional left hand showed already the observations made at PlP1. Following the secondary right M1 hand area lesion, performances of the ipsilesional right hand were improved post-lesion at PlP2. This was reflected by the significant decrease of the time to grasp pellets for all well diameters, with percentages of performance increased from 52% for the 40 mm diameter well up to 75% for the 21 mm one. The associated strategies did not show any modification, excepted a slight tendency to increase the use of less precise grip, as observed for the 30 mm diameter well. Respectively to the secondary lesion, the ipsilesional right hand, which did not show any modification of the time performances at AcP2 compared to PlP1, was transiently altered during the ReP2 for the 2 smallest diameters, 15 and 21 mm. For the 2 largest diameters, the percentages of performance were slightly increased at each step up to the PlP2 level. The transient increase observed at ReP2 for the 21 mm diameter was paralleled with an increase of the percentage of use of the 2 fingers (D2-3) configuration in spite of the D2 one.

Generally, the numbers of flexions per retrieval were weakly and not constantly affected over the different well diameters, nevertheless tended to vary similarly with the time of grasping, but to a lesser extent.

Modified Klüver board task: Reaching phase

The reaching phase of the movement was also affected, but to a lesser extent following the two lesions. The primary lesion of the left M1 hand area significantly increased the time to reach the well at all well diameters after the lever was released (Fig. 7**A**-**B**). Slight increase of the reaching times were observed bilaterally with percentages of recovery across diameters comprised between 87% and 89% for the right contralesional hand (Fig. 7**A**) and comprised between 91% and 96% for the left ipsilesional hand (Fig. 7**B**) at the PlP1 period. Correspondingly, the right contralesional hand was hyperextended implying the loss of preshaping following the lesion. Distances between index and thumb tips were large until the

well border, where the monkey used its contact to approach the thumb from the index to further grasp the pellet, however never as closed as in PreL (Fig. 7**C-D**). The increase, to a lesser extent, of the reaching times observed for the ipsilesional left hand was not associated with modification of the preshaping, expressed by index and thumb tips distances similar to PreL in each zone at the PlP1. Then, considering the secondary lesion of the right M1 hand area, interesting reverse effects have been observed, the reaching time needed to reach the well tending to be restored at the pre-lesion performances, for all the diameters after the lever was released for both hands (Fig. 7**A-B**). All diameter wells were reached with time-intervals showing no significant differences at PlP2 as compared to PreL, except for the 15 mm diameter well for which times were improved as compared to the PlP1, but still increased as compared to the PreL. The corresponding percentages of performance calculated for the ipsilesional right hand values were improved, slightly from 91% for the 15 mm diameter increasingly higher up to 96% and 97% for the largest diameters (Fig. 7**A**). For the contralesional left hand, the reaching times were largely improved for all diameters with percentages of recovery comprised between 98% up to 107% across diameters (Fig. 7**B**). These decreases of the reaching time values contrasted with a delay of the preshaping forming for the contralesional left hand, with index and thumb tips distances larger in the initiating area, those in the two other areas remained comparable to the PreL (Fig. 7**C-D**). This tendency was reduced with diameter sizes increase. The ipsilesional right hand exhibited a modification of the preshaping strategy, in parallel to a decrease of the reaching times (Fig. 7**C**). This was characterized by an enclosure of the index and thumb tips in the initiating area followed by a reopening during the transfer finally enclosed at the well entry, as in the initiating area. This modification was more pronounced with an increase of the diameter wells. However the distances never recovered to the PreL values.

During the periods of instable performances following the primary lesion of the left M1 hand area, AcP1 and ReP1, reaching time values for the ipsilesional left hand were regularly increased, except for the smallest 15 mm diameter for which the reaching time values decreased transiently during the ReP1 period (Fig. 7**B**). Following the secondary lesion of the right M1 hand area, the reaching time values for the ipsilesional right hand transiently decreased during the AcP2 before being decreased at PlP2, except for the power grip in the largest diameter well (40 mm) (Fig. 7**A**). These reaching time values modifications paralleled the distances between the index and thumb tips, decreasing together with reaching times and reversely (Fig. 7**C-D**). Fingertips distances were represented during the ReP periods for the lesioned hand to illustrate the strong hyperextension observed following the lesion on both

sides, but the high variability observed in these periods has to be taken into account, thus preventing comparison with the others periods' values.

Assessment of the lesions: anatomy, EEG and MRI

Anatomical characterization and effects on the somatosensory cortical activity of the primary lesion were assessed before the secondary lesion during the stable period of the post-lesion plateau PlP1. Using MRI, the primary lesion was localized on the left M1 hand area and the volume was estimated at 21 mm^3 barely 4 months following the primary lesion.

The effects on the somatosensory cortical activity of the primary M1 lesion were investigated using topographical analyses of surface SomatoSensory Evoked Potentials (SSEPs) (Fig. 8**B-H**). Briefly, the K-means clustering of pre- and post-lesion SSEPs around the largest peak of Global Field Potential (GFP) resulted in 3 voltage maps (Fig. 8**F-G**), then fitted back to the individual recordings, which did not show significant modification of the topography of the somatosensory cortical activity. However, statistical analyses, summarized in Figure 8**H**, reflect modifications of the network activity, based on changes of latencies and duration parameters, following the primary lesion of the M1 hand area.

Post-mortem histological processing performed to reconstruct the two lesions showed volumes and locations of the lesions early (2 months post-lesion) after the recovery from the secondary lesion (Fig. 9). The primary lesion, at the time of the secondary lesion plateau, extended on the different cortical layers down to the subcortical white matter (Fig. 9**A**). The primary cortical lesion measured 32.2 mm^3 in the gray matter and 1.9 mm^3 subcortically in the white matter just contiguous to the gray matter lesion (Fig. 9**B**). The secondary lesion showed a different anatomical characteristic, affecting widely the subcortical white matter but the gray matter tissue was not directly damaged, presenting a loss of the typical six layered cortical organization with a deficit of the layer V neurons but not of the layer III neurons, remaining mostly intact (Fig. 9**A**). The loss of the layer V neurons represented a gray matter lesion volume of 37.5 mm^3, suggested to result from the white matter damage representing a white matter lesion volume of 3.4 mm^3 (Fig. 9**B**). These anatomical reconstructions showed the exact location of the primary lesion in the left M1 hand area and the wider extent of the secondary lesion from the right M1 hand area up to the leg M1 area.

Discussion

This case report presents the effects on manual dexterity of two sequential permanent lesions targeting consecutively each M1 hand area, one on each hemisphere. To summarize, it has been observed that: 1) as expected, the primary cortical lesion of the left M1 hand area dramatically and irreversibly impaired the grasping ability of the contralesional right hand, increasingly pronounced from the power grip, to precision grip and then to the more complex precision grip when associated to pro-supination movements and wrist deviations; 2) the primary M1 lesion, transiently impairing only the most complex grasping, tended then to improve the ipsilesional left hand manual dexterity, but to a limited extent; 3) as expected, the secondary cortical lesion of the right M1 hand area impaired the grasping ability of the contralesional left hand, however less predominantly than after the primary lesion; nevertheless a similar increasing deficit from the power grip to the precision grip was observed, though not extended to the complex precision grip; 4) the secondary M1 lesion has only transiently impaired the ipsilesional right hand, affecting firstly the complex grip in the acute period and secondly the precision grip during the recovery period, while all performances were improved after recovery; 5) the hand preshaping was impaired for the contralesional hand, but it remained highly impaired on the long-term only following the primary lesion. The associated reaching times of both hands were weakly affected following the primary cortical lesion of the left M1 hand area and recovered following the secondary lesion of the right M1 hand area; 6) EEG assessments represent preliminary data showing reorganization of the electrophysiological network activity of the somatosensory cortex following an unilateral M1 lesion.

Originality of the study

This study, although limited to a case report, presents two original aspects newly reported, at least to our knowledge. First of all, this is an original case of the same macaque monkey performing in parallel the two main manual tasks currently used in the literature, namely the modified Klüver board task and the modified Brinkman board task. This allows, to some extent, an original comparison of these two tasks. The “modified Brinkman board” task highlighted the important distinction between simple and complex precision grip. The complex precision grip presents a higher vulnerability, more susceptible to be affected following M1 lesion, impaired even when the simple precision grip was not affected. Such distinction cannot be observed with the “modified Klüver board” task. Complementarily, the “modified Klüver board” task highlighted large impairments of the power grip. Above all, it

allowed to observe, when the monkey was free to use or not the precision grip, clear modifications of grip strategies, which well compensated impairments of precision grip. Thus, the switched use of more power grip explains the shorter time needed to grasp. Although the monkey apparently used correctly the precision grip after recovery, it appeared that the forced use of the precision grip allowed the monkey to perform it with the help of the apparatus in our conditions, whereas in free conditions it clearly favored the power grip. This reflects the switch of the grasping strategy after M1 lesion. Not observed with the "modified Brinkman board" task, lesions differently affected the different phases of the movement, not necessarily implying that impairment of the preshaping is correlated to the grasp impairment. Assessed distinctly with these two complementary tasks, our observations suggest that multiple aspects of the grip movement interact and contribute to compensate the grip impairment as a whole.

Secondly, the monkey Mk-DG is a nearly unique case of consecutive bilateral permanent M1 lesion in the hand area in one hemisphere and later on the other hemisphere, the secondary lesion occurring with enough delay to allow recovery from the primary lesion (at plateau). This allowed the study of the contralateral intact M1 role for long term recovery, as well as its role for recovery following the secondary M1 lesion in case of impaired contralateral M1.

Muscimol-induced lesion

The reliability of the secondary lesion achieved with muscimol is questionable. Muscimol is largely used in the literature for reversible inactivation of cortical activity, thus the mechanisms underlying the lesion have to be clarified. It cannot be excluded that the lesion may be due in part to the muscimol toxicity itself, but may also result from mechanical compression due to large volume of liquid injected at the same location. Effectively, the histological staining emphasized the subcortical location of the secondary lesion in the white matter, the gray matter assumed to be not directly damaged but consecutively affected by the axonal lesion in the white matter with the loss of the layer V neurons. However the secondary lesion was induced with only 7 sites of infusion each of 1 µL as compared to the 24 sites of 1 µL each injected with ibotenic acid. This low volume does not support the above mechanical explanation, which can be discorded. Another explanation involves the prospective toxicity of the muscimol. Muscimol, as GABAa agonist, generates chloride ion (Cl^-) flux entry in the cell. Thus, the possibility that a highly concentrated solution of muscimol could modify for long-term the ionic flux leaving the GABAa channel in an open state causing ionic imbalance responsible of cell death is a subject of debate. The role of inhibitory neurotransmitter in

neuronal death through lethal entry of Cl^- has been suggested by some authors (Chen et al., 1998). A later study has related muscimol induction of neuronal death through GABAa auto-receptor (Honegger et al., 1998). Some authors have reported excitotoxic neuronal death through GABAa receptor, as the excitatory capacity expressed during development, which decreases the chloride gradient across the neuronal plasma membrane in case of long stimulation of the receptor (Xu et al., 2000). In view of these two possibilities, further investigations have to be conducted to further investigate the excitotoxic properties of muscimol at high concentration, but the mechanical explanation does not appear as the most convincing one in our experimental conditions.

Behavioral results

Before discussion of the results implications, some behavioral results deserve further comments. Although the aim of this study was not to compare the efficiency of these two behavioral tasks, a discrepancy has been noted between the two mostly comparable contact times of the vertical slots in the modified Brinkman board task and the grasping times of the smallest diameter in the modified Klüver board task. Multiple explanations can be proposed, but two of them may have equal or cumulative impact. The first explanation proposes that the high number of trials performed with the modified Klüver board task has increased the probability of the statistical significance of subtle modifications. The second explanation follows the reported increase of the negative effects with the increase well depth on the recovery of the precision grip following injury (Fukushima et al., 2007), related to the deeper wells of the modified Klüver board as compared to the well depth of the modified Brinkman board.

The two consecutive lesions massively and permanently impaired the grasping of the corresponding contralesional hand. The primary lesion affecting the contralesional right hand induced an increase of the impairment with diameter size increase while starting to recover earlier, probably reflecting the strategy modification from the precision grip preferential use pre-lesion in favor to the power grip preferential use post-lesion. The secondary lesion did not show a similar effect, inducing the expected increase of the impairment with diameter decrease. These impairments were associated with an unspecific strategy in between, resulting in the use of less precision grip for small diameter but the preferential use of power grip for the large diameter was slowly reduced due to the observed hyperextension, which negatively affected the entry of the fingers into the wells.

Interestingly, in spite of comparable volume of lesions, the behavioral data showed a better functional recovery following the secondary lesion than following the primary lesion, possibly explained by the different locations of the two lesions. The primary lesion affected all the layers of the gray matter while the secondary lesion affected mostly the layer V, generally sparing the layer III, thus preserving some corticocortical projections originating from superficial cortical layer of M1 to premotor areas (PMv and PMd), to the supplementary motor area (SMA) and to the cingulate motor areas (CMA) (Leichnetz, 1986; Dum and Strick, 2005). This is of major interest considering the proposed role of the secondary motor areas for the functional recovery following M1 lesion, especially the role of the premotor cortex (Liu and Rouiller, 1999; Hoogwoud et al.; 2013) probably related to the high interconnection between M1, PMv and PMd (Dum and Strick, 2005). Thus, the spared layer III partially preserved the highly interconnected circuit between M1, PMv and PMd and to result in better functional recovery following M1 lesion, as compared to cortical lesion affecting all cortical layers.

Role of the intact M1 in the spontaneous functional recovery

In accordance with a previous report on rat (Shanina et al., 2006), the secondary M1 permanent lesion did not abolish the functional recovery occurring after the primary M1 permanent lesion, indicating that, after a unilateral M1 lesion limited to the hand area, the intact hemisphere did not play a crucial role in the long-term functional recovery of the contralesional hand. This observation is consistent with a previous report of an absence of effect of a reversible secondary lesion of the intact M1 on the recovery from a unilateral M1 permanent lesion on the contralesional affected hand (Liu and Rouiller, 1999). The present confirmation of the absence of a role played by the intact M1 based on permanent (long-lasting) lesion is of importance as the previous observation was derived from reversible inactivation (Liu and Rouiller, 1999) using a low dose of muscimol, which may not have fully inactivated the intact M1 and which did not allow to observe effects of long term inactivation of intact M1. In both studies (Liu and Rouiller, 1999; present study), the possibility that a contribution of the intact M1 in the functional recovery after unilateral M1 lesion was not observed may be due to the moderate size of the primary cortical lesion, leaving thus open the possibility that a larger lesion would possibly involve the intact M1, as suggested in previous reports (Biernaskie et al., 2005; Liu and Rouiller, 1999).

Role of the ipsilateral M1 in complex movements

Our results suggest an ipsilateral and/or a bilateral role of the M1 hand cortical area in the control of voluntary movements. In line with a previous report from our laboratory (Bashir et al., 2012), the present study shows that the lesion of the M1 hand area may have a limited transient deleterious effect on the ipsilesional hand. These effects were limited to the finest precision grip and to complex precision grip synergies. Not differing than following the primary lesion, effects of the secondary lesion on the ipsilesional hand were observed as well on the precision grip transiently after the lesion. These data are consistent with the notion that bilateral M1 activation was present in the case of complex finger movements (Shibasaki et al., 1993; Salmelin et al., 1995; Chen et al., 1996; Ehrsson et al., 2000). Moreover, deficits of wrist movement ipsilateral to a stroke were reported in hemiparetic subjects (Yarosh et al., 2004). Therefore, the present results sustain the role, though not crucial, of an ipsilateral and/or a bilateral M1 implication for complex movements, thus affected by a unilateral lesion, however rapidly compensated and recovered.

Role of M1 in the early and late periods of recovery

Nevertheless the lack of evidence for an important role of the intact M1 in the observed functional recovery, the secondary lesion was followed by longer periods of total impairment than following the primary lesion (Fig. 4: time windows from day 0 to left extremity of the arrow as the acute post-lesion period). However, this longer period of total impairment before recovery, suggesting a strong impairment, is paradoxically followed by shorter periods of recovery and better percentages of recovery than following the primary lesion, suggesting rather a weaker impairment. These effects raised the question of the intact M1 role during the early period of recovery following M1 injury, specifically for complex fine manual dexterity. A recent review (Dancause et al., 2015) listed reports emphasizing the beneficial effects of contralesional cortex inhibition on the functional recovery following unilateral stroke when applied rapidly and for prolonged duration, effects lost for delayed and/or for shorter duration of the contralesional cortex inhibition. These considerations may not concern the effects of the secondary M1 lesion on the primary affected hand functional recovery in the present study, the secondary M1 lesion taking place long time after the primary M1 lesion. However, the secondary M1 lesion occurred whereas deficit resulting of the primary lesion were still present, thus the functional recovery following the secondary affected hand was concerned by the suggested benefic effects of the contralesional cortex inhibitions. These results relate to a previous report providing evidence that the normally masked ipsilateral connections of the intact contralesional cortex were revealed by a unilateral

M1 cortical lesion in human (Netz et al., 1997). The different time courses of recovery observed following the two M1 lesions could be related to the absence of these connections, in the present study, at the time of the secondary M1 lesion. Furthermore, an increase of the contralesional cortex activity was reported at an early stage following unilateral motor cortex lesion then followed by an extension of the increased cortical activity to non-primary areas (Rehme et al., 2010). Altogether, these data are in agreement with the suggested role played by the contralesional M1 in the early stage of the recovery, before occurrence of subsequent plasticity. Consequently, the primary lesioned cortex was no longer able to support the early stage of the recovery following the secondary lesion of the intact hemisphere, explaining the observed delayed onset of the recovery of higher motor functions, before being taken over at a later stage, by non-primary motor areas.

The interhemispheric disinhibition may have supported a role of the intact contralesional M1 in the present case of impact on the intact contralesional M1 following unilateral M1 lesion. The role of the interhemispheric disinhibition has been suggested to explain the observed improvement of the ipsilesional hand following the lesion (Manganotti et al., 2008). Using transcranial magnetic stimulation, the unaffected hemisphere has been reported to be disinhibited during early period following unilateral stroke, as suggested by the loss of the interhemispheric connection originated from the lesioned hemisphere (Shimizu et al., 2002). However, an fMRI study has described that the increase of the fMRI activity observed early following stroke in the unaffected hemisphere decreased in relation to behavioral recovery in stroke patient (Ward et al., 2003). Thus, the interhemispheric disinhibition did not appear to support a role of M1 in these unaffected hand improvements at long term and appeared thus more susceptible to play a role in the early period following the cortical lesion.

In the present case report, the improvement of each ipsilesional hand performances at plateau may be explained by the described effects of training. Less pronounced following the primary M1 lesion, the motor performances of the ipsilesional hand respective to the primary M1 lesion exhibited improvements. The effects of training on behavioral performances were described in healthy subjects exhibiting improvement of motor performances resulting of movement practices, which is admitted to be underlined by cortical plasticity (Nudo et al., 1996, 2001; Buonomano and Merzenich, 1998; Karni et al., 1998). More pronounced following the secondary M1 lesion, the ipsilesional hand motor performances impaired by the primary M1 lesion, albeit a transient impairment of the precision grip, exhibited improvement of the grasping performances at the plateau period for the precision grip and from the acute

period for the power grip. However the monkey did not receive behavioral training except the daily behavioral tasks, the immobility of one hand made the animal dependent of the remaining hand, increasing its daily use. The beneficial effects of behavioral training have been reported in monkeys subjected to motor cortical lesion (Murata et al., 2008), exhibiting an improvement and a refinement of grasping and preshaping strategies for monkeys intensively trained after lesion. The enforced use of the primary lesioned hand, due to the immobility of the second hand resulting of the secondary lesion of the intact M1, can act as a supplementary training in the daily life of the monkey. Concerning the firstly lesioned hand, its enforced use consequently to the paralysis of the secondary lesioned hand could be considered as a late training after injury, however shown to be not as beneficial as an early training for behavioral recovery after spinal cord injury (Sugiyama et al., 2013). Controversially, despite the reported detrimental effects of a too early behavioral rehabilitation training (i.e. increasing the damage tissue following stroke (Risedal et al., 1999)), a lack of beneficial effects of a late training has been reported, as compared to the promoting effects of an earlier training procedure (*e.g.* Yang et al., 2003; Sugiyama et al., 2013). The present case Mk-DG cannot be considered as a late training only. Effectively, and because it was observed for the two lesions, the immobility of one hand following injury may be assimilated to some extent as to a constrain-induced motor therapy (CIMT), known as rehabilitation greatly improving behavioral recovery in non-human primates, as well as in humans (see Taub et al., 1999 for review of the original studies). CIMT is effective even when started 3 to 9 months after stroke (Wolf et al., 2006). The present data does not clarify the mechanism supporting the functional recovery, but are in agreement with a role of the affected hand immobility as a consequent training to explain the moderate but significant improvement of the manual dexterity of the primary lesioned hand at long-term.

Further studies are needed to elucidate the mechanisms sustaining the functional recovery, probably not implying a direct role of intact contralateral M1, but rather a role of the adjacent cortical representations, as it was observed a cortical expansion of the motor output area size of the affected muscles over adjacent cortical representations of the damaged hemisphere (Liepert et al., 1998).

Role of M1 in the reaching phase

Our results suggest a bilateral effect of the M1 hand area lesion on the reaching times, subtle but statistically significant, bilaterally impaired following the primary lesion and bilaterally improved directly following the secondary lesion.

The anterior intraparietal cortex (AIP) and ventral premotor areas F5, highly interconnected together and with M1 (Leichnetz, 1986; Tokuno and Tanji, 1993; Luppino and Rizzolatti, 2000; Tanné-Gariépy et al., 2002; Dum and Strick, 2005; Stepniewska et al., 2006; Dancause et al., 2006), have been reported to sustain the hand preshaping in reach and grasp tasks, impaired following their respective inactivation (Gallese et al., 1994; Fogassi et al., 2001). Our results, suggesting a bilateral effect of the primary M1 lesion, and in line with M1-F5 strong interconnections, are consistent with the reported bilateral impairment of the preshaping following F5 transient inactivation (Fogassi et al., 2001). Interestingly, the secondary M1 lesion did not affect the preshaping as much as the primary M1 lesion did, but furthermore tended to revert the effects of the primary lesion on the secondary affected hand (left) and improved the primary affected hand (right). This observation suggests that the primary unilateral lesion of M1 hand area caused an imbalance among the cortical circuit controlling the correct preshaping and was in a way rectified by the secondary lesion of the homologous contralateral M1 hand area. The reaching time modifications were more or less explained by the preshaping strategy modifications because they were only linked to the primary lesioned hand after the secondary lesion. Thus, the reaching time modifications were not necessarily the result of the preshaping strategy modifications and further investigations have to be conducted to answer this question.

Conclusion

In this original case report of two subsequent M1 permanent lesions, giving some insight on the role of M1 in the planning and execution of normal movements and in the functional recovery from permanent lesion of the M1 hand area, the results can be summarized as follows: 1) after unilateral lesion of the M1 hand area, the hypothesis that the intact contralateral M1 does not play a major role in the long-term functional recovery was verified; 2) the intact contralateral M1 may however still be involved in the early phase of the functional recovery; 3) a bilateral, but not crucial, role of M1 in the execution of complex manual dexterity tasks was observed; 4) the importance of bilateral activity balance between M1 homologous counterparts in the cortical circuit controlling the preshaping is suggested; 5) the role of behavioral training, resulting of the lesioned hand immobility on the ipsilesional hand performances, specifically for the functional performances improvement of the primary affected hand following the secondary lesion of the intact contralateral M1 counterpart.

References

Babiloni, C., Carducci, F., Pizzella, V., Indovina, I., Romani, G. L., Rossini, P. M. & Babiloni, F. (1999). Bilateral neuromagnetic activation of human primary sensorimotor cortex in preparation and execution of unilateral voluntary finger movements. *Brain research,* 827, 234-236.

Bashir, S., Kaeser, M., Wyss, A., Hamadjida, A., Liu, Y., Bloch, J., Brunet, J. F., Belhaj-Saif, A. & Rouiller, E. M. (2012). Short-term effects of unilateral lesion of the primary motor cortex (M1) on ipsilesional hand dexterity in adult macaque monkeys. *Brain Structure and Function,* 217, 63-79.

Beaud, M. L., Schmidlin, E., Wannier, T., Freund, P., Bloch, J., Mir, A., Schwab, M. E. & Rouiller, E. M. (2008). Anti-Nogo-A antibody treatment does not prevent cell body shrinkage in the motor cortex in adult monkeys subjected to unilateral cervical cord lesion. *BMC.Neurosci.,* 9, 5.

Beaud, M. L., Rouiller, E. M., Bloch, J., Mir, A., Schwab, M. E., Wannier, T. & Schmidlin, E. (2012). Invasion of lesion territory by regenerating fibers after spinal cord injury in adult macaque monkeys. *Neuroscience,* 227, 271-282.

Biernaskie, J., Szymanska, A., Windle, V. & Corbett, D. (2005). Bi–hemispheric contribution to functional motor recovery of the affected forelimb following focal ischemic brain injury in rats. *European Journal of Neuroscience,* 21, 989-999.

Brochier, T., Boudreau, M. J., Pare, M. & Smith, A. M. (1999). The effects of muscimol inactivation of small regions of motor and somatosensory cortex on independent finger movements and force control in the precision grip. *Exp.Brain Res.,* 128, 31-40.

Brown, A. R. & Teskey, G. C. (2014). Motor cortex is functionally organized as a set of spatially distinct representations for complex movements. *Journal of Neuroscience,* 34, 13574-13585.

Buonomano, D. V. & Merzenich, M. M. (1998). Cortical plasticity: from synapses to maps. *Annu.Rev.Neurosci.,* 21, 149-186.

Chatagny, P., Badoud, S., Kaeser, M., Gindrat, A. D., Savidan, J., Fregosi, M., Moret, V., Roulin, C., Schmidlin, E. & Rouiller, E. M. (2013). Distinction between hand dominance and hand preference in primates: a behavioral investigation of manual dexterity in nonhuman primates (macaques) and human subjects. *Brain Behav.,* 3, 575-595.

Chen, R., Gerloff, C., Hallett, M. & Cohen, L. G. (1997). Involvement of the ipsilateral motor cortex in finger movements of different complexities. *Annals of neurology,* 41, 247-254.

Cirstea, M. C. & Levin, M. F. (2000). Compensatory strategies for reaching in stroke. *Brain,* 123 (Pt 5), 940-953.

Dancause, N. (2006). Vicarious function of remote cortex following stroke: recent evidence from human and animal studies. *Neuroscientist.,* 12, 489-499.

Dancause, N., Touvykine, B. & Mansoori, B. K. (2015). Inhibition of the contralesional hemisphere after stroke: reviewing a few of the building blocks with a focus on animal models. *Prog.Brain Res.,* 218, 361-387.

Dum, R. P. & Strick, P. L. (2005). Frontal lobe inputs to the digit representations of the motor areas on the lateral surface of the hemisphere. *Journal of Neuroscience,* 25, 1375-1386.

Ehrsson, H. H., Fagergren, A., Jonsson, T., Westling, G., Johansson, R. S. & Forssberg, H. (2000). Cortical activity in precision- versus power-grip tasks: an fMRI study. *Journal of Neurophysiology,* 83, 528-536.

Fogassi, L., Gallese, V., Buccino, G., Craighero, L., Fadiga, L. & Rizzolatti, G. (2001). Cortical mechanism for the visual guidance of hand grasping movements in the monkey: A reversible inactivation study. *Brain,* 124, 571-586.

Freund, P., Schmidlin, E., Wannier, T., Bloch, J., Mir, A., Schwab, M. E. & Rouiller, E. M. (2006). Nogo-A-specific antibody treatment enhances sprouting and functional recovery after cervical lesion in adult primates. *Nature Medicine,* 12, 790-792.

Freund, P., Wannier, T., Schmidlin, E., Bloch, J., Mir, A., Schwab, M. E. & Rouiller, E. M. (2007). Anti-Nogo-A antibody treatment enhances sprouting of corticospinal axons rostral to a unilateral cervical spinal cord lesion in adult macaque monkey. *J Comp Neurol,* 502, 644-659.

Freund, P., Schmidlin, E., Wannier, T., Bloch, J., Mir, A., Schwab, M. E. & Rouiller, E. M. (2009). Anti-Nogo-A antibody treatment promotes recovery of manual dexterity after unilateral cervical lesion in adult primates--re-examination and extension of behavioral data. *Eur.J.Neurosci.*, 29, 983-996.

Fukushima, J., Kasahara, S., Asaka, T., Saito, H. & Yamanaka, M. (2007). Behavioral findings during recovery after experimental stroke in monkeys-Assessment with modified hand performance test. *Journal of Physical Therapy Science*, 19, 33-40.

Gallese, V., Murata, A., Kaseda, M., Niki, N. & Sakata, H. (1994). Deficit of hand preshaping after muscimol injection in monkey parietal cortex. *Neuroreport,* 5, 1525-1529.

Gindrat, A. D., Quairiaux, C., Britz, J., Brunet, D., Lanz, F., Michel, C. M. & Rouiller, E. M. (2014). Whole-scalp EEG mapping of somatosensory evoked potentials in macaque monkeys. *Brain Struct.Funct.*.

Gonzalez, C. L. R., Gharbawie, O. A., Williams, P. T., Kleim, J. A., Kolb, B. & Whishaw, I. Q. (2004). Evidence for bilateral control of skilled movements: ipsilateral skilled forelimb reaching deficits and functional recovery in rats follow motor cortex and lateral frontal cortex lesions. *European Journal of Neuroscience,* 20, 3442-3452.

Hoffman, D. S. & Strick, P. L. (1995). Effects of a primary motor cortex lesion on step-tracking movements of the wrist. *Journal of Neurophysiology,* 73, 891-895.

Honegger, P., Pardo, B. & Monnet-Tschudi, F. (1998). Muscimol-induced death of GABAergic neurons in rat brain aggregating cell cultures. *Brain Res.Dev.Brain Res.,* 105, 219-225.

Hoogewoud, F., Hamadjida, A., Wyss, A. F., Mir, A., Schwab, M. E., Belhaj-Saif, A. & Rouiller, E. M. (2013). Comparison of functional recovery of manual dexterity after unilateral spinal cord lesion or motor cortex lesion in adult macaque monkeys. *Front Neurol.,* 4, 101.

Jaillard, A., Martin, C. D., Garambois, K., Lebas, J. F. & Hommel, M. (2005). Vicarious function within the human primary motor cortex? A longitudinal fMRI stroke study. *Brain,* 128, 1122-1138.

Kaeser, M., Wannier, T., Wyss, A. F., Belhaj-Sa+»f, A., Bloch, J., Brunet, J. F., Debatisse, D., Pralong, E. & Rouiller, E. M. (2007). Cortical plasticity assessed by somatosensory evoked potentials (SEPs) parallels functional recovery of manual dexterity after lesion of primary motor cortex (M1) in monkeys, poster presented at the Swiss Society for Neuroscience meeting. *2006 et au Swiss Society for Neuroscience meeting, Bern* .

Kaeser, M., Wyss, A. F., Bashir, S., Hamadjida, A., Liu, Y., Bloch, J., Brunet, J. F., Belhaj-Saif, A. & Rouiller, E. M. (2010). Effects of Unilateral Motor Cortex Lesion on

Ipsilesional Hand's Reach and Grasp Performance in Monkeys: Relationship With Recovery in the Contralesional Hand. *Journal of Neurophysiology*, 103, 1630-1645.

Kaeser, M., Brunet, J. F., Wyss, A., Belhaj-Saif, A., Liu, Y., Hamadjida, A., Rouiller, E. M. & Bloch, J. (2011). Autologous adult cortical cell transplantation enhances functional recovery following unilateral lesion of motor cortex in primates: a pilot study. *Neurosurgery*, 68, 1405-1417.

Kaeser, M., Wannier, T., Brunet, J. F., Wyss, A., Bloch, J. & Rouiller, E. M. (2013). Representation of motor habit in a sequence of repetitive reach and grasp movements performed by macaque monkeys: evidence for a contribution of the dorsolateral prefrontal cortex. *Cortex*, 49, 1404-1419.

Kaeser, M., Chatagny, P., Gindrat, A. D., Savidan, J., Badoud, S., Fregosi, M., Moret, V., Roulin, C., Schmidlin, E. & Rouiller, E. (2014). Variability of manual dexterity performance in non-human primates (). *International Journal of Comparative Psychology*, 27.

Karni, A., Meyer, G., Rey-Hipolito, C., Jezzard, P., Adams, M. M., Turner, R. & Ungerleider, L. G. (1998). The acquisition of skilled motor performance: fast and slow experience-driven changes in primary motor cortex. *Proc.Natl.Acad.Sci.U.S.A*, 95, 861-868.

Lanz, F., Lanz, X., Scherly, A., Moret, V., Gaillard, A., Gruner, P., Hoogewoud, H. M., Belhaj-Saif, A., Loquet, G. & Rouiller, E. M. (2013). Refined methodology for implantation of a head fixation device and chronic recording chambers in non-human primates. *J.Neurosci.Methods*, 219, 262-270.

Leichnetz, G. R. (1986). Afferent and efferent connections of the dorsolateral precentral gyrus (area 4, hand/arm region) in the macaque monkey, with comparisons to area 8. *J.Comp Neurol.*, 254, 460-492.

Liepert, J., Miltner, W. H., Bauder, H., Sommer, M., Dettmers, C., Taub, E. & Weiller, C. (1998). Motor cortex plasticity during constraint-induced movement therapy in stroke patients. *Neurosci.Lett.*, 250, 5-8.

Liu, Y. & Rouiller, E. M. (1999). Mechanisms of recovery of dexterity following unilateral lesion of the sensorimotor cortex in adult monkeys 1. *Exp.Brain Res.*, 128, 149-159.

Manganotti, P., Acler, M., Zanette, G. P., Smania, N. & Fiaschi, A. (2008). Motor cortical disinhibition during early and late recovery after stroke. *Neurorehabil.Neural Repair*, 22, 396-403.

Martin, J. H. (1991). Autoradiographic estimation of the extent of reversible inactivation produced by microinjection of lidocaine and muscimol in the rat. *Neurosci.Lett.*, 127, 160-164.

Milliken, G. W., Plautz, E. J. & Nudo, R. J. (2013). Distal forelimb representations in primary motor cortex are redistributed after forelimb restriction: a longitudinal study in adult squirrel monkeys. *Journal of Neurophysiology*, 109, 1268-1282.

Murata, Y., Higo, N., Oishi, T., Yamashita, A., Matsuda, K., Hayashi, M. & Yamane, S. (2008). Effects of motor training on the recovery of manual dexterity after primary motor cortex lesion in macaque monkeys. *Journal of Neurophysiology*, 99, 773-786.

Netz, J., Lammers, T. & H+Âmberg, V. (1997). Reorganization of motor output in the non-affected hemisphere after stroke. *Brain*, 120, 1579-1586.

Nudo, R. J., Jenkins, W. M., Merzenich, M. M., Prejean, T. & Grenda, R. (1992). Neurophysiological correlates of hand preference in primary motor cortex of adult squirrel monkeys. *Journal of Neuroscience*, 12, 2918-2947.

Nudo, R. J., Milliken, G. W., Jenkins, W. M. & Merzenich, M. M. (1996). Use-dependent alterations of movement representations in primary motor cortex of adult squirrel monkeys. *Journal of Neuroscience*, 16, 785-807.

Nudo, R. J., Plautz, E. J. & Frost, S. B. (2001). Role of adaptive plasticity in recovery of function after damage to motor cortex. *Muscle Nerve*, 24, 1000-1019.

Nudo, R. J. (2006). Mechanisms for recovery of motor function following cortical damage. *Current Opinion in Neurobiology*, 16, 638-644.

Nudo, R. J. & Barbay, S. (2014). The Mechanisms and Neurophysiology of Recovery FromStroke. *Stroke Recovery and Rehabilitation*.

Olivier, E., Davare, M., Andres, M. & Fadiga, L. (2007). Precision grasping in humans: from motor control to cognition. *Current Opinion in Neurobiology*, 17, 644-648.

Pizzimenti, M. A., Darling, W. G., Rotella, D. L., McNeal, D. W., Herrick, J. L., Ge, J., Stilwell-Morecraft, K. S. & Morecraft, R. J. (2007). Measurement of reaching kinematics and prehensile dexterity in nonhuman primates. *Journal of Neurophysiology*, 98, 1015-1029.

Qi, H. X., Chen, L. M. & Kaas, J. H. (2011). Reorganization of somatosensory cortical areas 3b and 1 after unilateral section of dorsal columns of the spinal cord in squirrel monkeys. *Journal of Neuroscience*, 31, 13662-13675.

Rehme, A. K., Fink, G. R., Von Cramon, D. Y. & Grefkes, C. (2010). The role of the contralesional motor cortex for motor recovery in the early days after stroke assessed with longitudinal FMRI. *Cerebral cortex*, bhq140.

Risedal, A., Zeng, J. & Johansson, B. B. (1999). Early training may exacerbate brain damage after focal brain ischemia in the rat. *J.Cereb.Blood Flow Metab*, 19, 997-1003.

Rizzolatti, G. & Luppino, G. (2001). The cortical motor system. *Neuron*, 31, 889-901.

Salmelin, R., Forss, N., Knuutila, J. & Hari, R. (1995). Bilateral activation of the human somatomotor cortex by distal hand movements. *Electroencephalography and clinical neurophysiology*, 95, 444-452.

Schieber, M. H. & Poliakov, A. V. (1998). Partial inactivation of the primary motor cortex hand area: effects on individuated finger movements. *Journal of Neuroscience*, 18, 9038-9054.

Schmidlin, E., Wannier, T., Bloch, J. & Rouiller, E. M. (2004). Progressive plastic changes in the hand representation of the primary motor cortex parallel incomplete recovery from a unilateral section of the corticospinal tract at cervical level in monkeys. *Brain Res.*, 1017, 172-183.

Schmidlin, E., Wannier, T., Bloch, J., Belhaj-Saif, A., Wyss, A. F. & Rouiller, E. M. (2005). Reduction of the hand representation in the ipsilateral primary motor cortex following unilateral section of the corticospinal tract at cervical level in monkeys. *BMC.Neurosci.*, 6, 56.

Schmidlin, E., Brochier, T., Maier, M. A., Kirkwood, P. A. & Lemon, R. N. (2008). Pronounced reduction of digit motor responses evoked from macaque ventral premotor cortex after reversible inactivation of the primary motor cortex hand area. *Journal of Neuroscience*, 28, 5772-5783.

Schmidlin, E., Kaeser, M., Gindrat, A. D., Savidan, J., Chatagny, P., Badoud, S., Hamadjida, A., Beaud, M. L., Wannier, T., Belhaj-Saif, A. & Rouiller, E. M. (2011). Behavioral assessment of manual dexterity in non-human primates. *J.Vis.Exp.*.

Shanina, E. V., Schallert, T., Witte, O. W. & Redecker, C. (2006). Behavioral recovery from unilateral photothrombotic infarcts of the forelimb sensorimotor cortex in rats: role of the contralateral cortex. *Neuroscience*, 139, 1495-1506.

Shelton, F. N. & Reding, M. J. (2001). Effect of lesion location on upper limb motor recovery after stroke. *Stroke*, 32, 107-112.

Shibasaki, H., Sadato, N., Lyshkow, H., Yonekura, Y., Honda, M., Nagamine, T., Suwazono, S., Magata, Y., Ikeda, A., Miyazaki, M. & . (1993). Both primary motor cortex and

supplementary motor area play an important role in complex finger movement. *Brain,* 116 (Pt 6), 1387-1398.

Shimizu, T., Hosaki, A., Hino, T., Sato, M., Komori, T., Hirai, S. & Rossini, P. M. (2002). Motor cortical disinhibition in the unaffected hemisphere after unilateral cortical stroke. *Brain,* 125, 1896-1907.

Sugiyama, Y., Higo, N., Yoshino-Saito, K., Murata, Y., Nishimura, Y., Oishi, T. & Isa, T. (2013). Effects of early versus late rehabilitative training on manual dexterity after corticospinal tract lesion in macaque monkeys. *Journal of Neurophysiology,* 109, 2853-2865.

Taub, E., Uswatte, G. & Pidikiti, R. (1999). Constraint-Induced Movement Therapy: a new family of techniques with broad application to physical rehabilitation--a clinical review. *J.Rehabil.Res.Dev.,* 36, 237-251.

Wannier-Morino, P., Schmidlin, E., Freund, P., Belhaj-Saif, A., Bloch, J., Mir, A., Schwab, M. E., Rouiller, E. M. & Wannier, T. (2008). Fate of rubrospinal neurons after unilateral section of the cervical spinal cord in adult macaque monkeys: effects of an antibody treatment neutralizing Nogo-A. *Brain Res.,* 1217, 96-109.

Wannier, T., Schmidlin, E., Bloch, J. & Rouiller, E. M. (2005). A unilateral section of the corticospinal tract at cervical level in primate does not lead to measurable cell loss in motor cortex. *J.Neurotrauma,* 22, 703-717.

Ward, N. S., Brown, M. M., Thompson, A. J. & Frackowiak, R. S. (2003). Neural correlates of motor recovery after stroke: a longitudinal fMRI study. *Brain,* 126, 2476-2496.

Wolf, S. L., Winstein, C. J., Miller, J. P., Taub, E., Uswatte, G., Morris, D., Giuliani, C., Light, K. E. & Nichols-Larsen, D. (2006). Effect of constraint-induced movement therapy on upper extremity function 3 to 9 months after stroke: the EXCITE randomized clinical trial. *JAMA,* 296, 2095-2104.

Wyss, A. F., Hamadjida, A., Savidan, J., Liu, Y., Bashir, S., Mir, A., Schwab, M. E., Rouiller, E. M. & Belhaj-Saif, A. (2013). Long-term motor cortical map changes following unilateral lesion of the hand representation in the motor cortex in macaque monkeys showing functional recovery of hand functions. *Restor.Neurol.Neurosci.,* 31, 733-760.

Xerri, C., Merzenich, M. M., Peterson, B. E. & Jenkins, W. (1998). Plasticity of primary somatosensory cortex paralleling sensorimotor skill recovery from stroke in adult monkeys. *Journal of Neurophysiology,* 79, 2119-2148.

Xu, W., Cormier, R., Fu, T., Covey, D. F., Isenberg, K. E., Zorumski, C. F. & Mennerick, S. (2000). Slow death of postnatal hippocampal neurons by GABA(A) receptor overactivation. *Journal of Neuroscience,* 20, 3147-3156.

Yang, Y. R., Wang, R. Y. & Wang, P. S. (2003). Early and late treadmill training after focal brain ischemia in rats. *Neurosci.Lett.,* 339, 91-94.

Yarosh, C. A., Hoffman, D. S. & Strick, P. L. (2004). Deficits in movements of the wrist ipsilateral to a stroke in hemiparetic subjects. *Journal of Neurophysiology,* 92, 3276-3285.

Figures

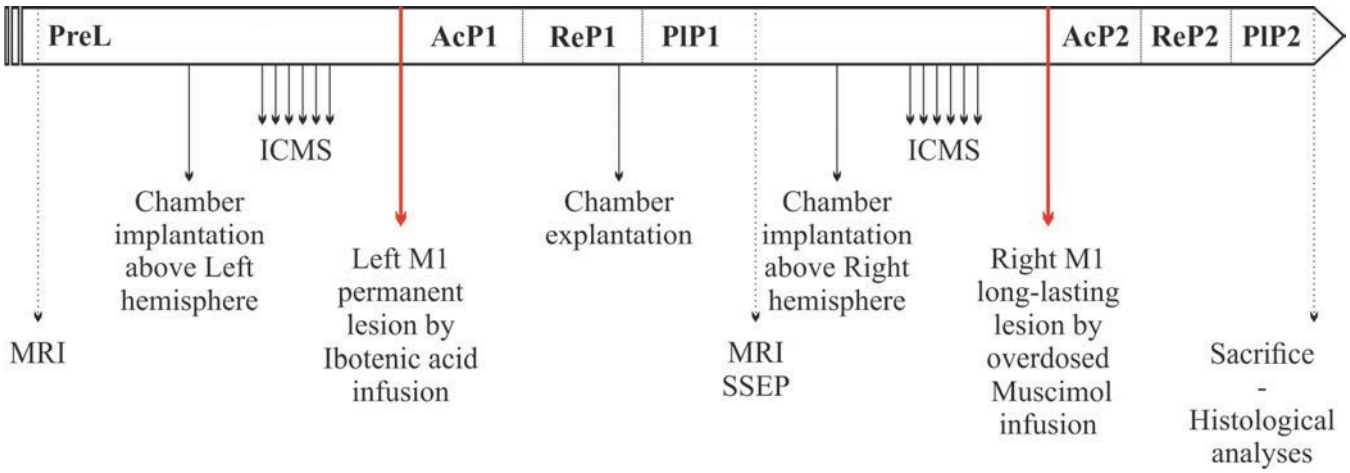

Figure 1: General survey

Schematic representation of the experimental protocol in Mk-DG. The different periods represent the different time-intervals of the functional recovery based on performances of the affected hand for each behavioral task: **PreL** for the **Pre-L**esion **P**eriod, **AcP1** for the **Ac**ute **P**eriod during which the lesioned hand was completely unable to perform the task following the primary lesion in the left M1 hand area, **ReP**1 for the subsequent **P**eriod of **Re**covery, **PlP**1 when the animal reached a stable recovered performance, referred to as **Pl**ateau **P**eriod. The AcP2, ReP2 and PlP2 characterize equivalent periods following the secondary lesion in the right M1 hand area.

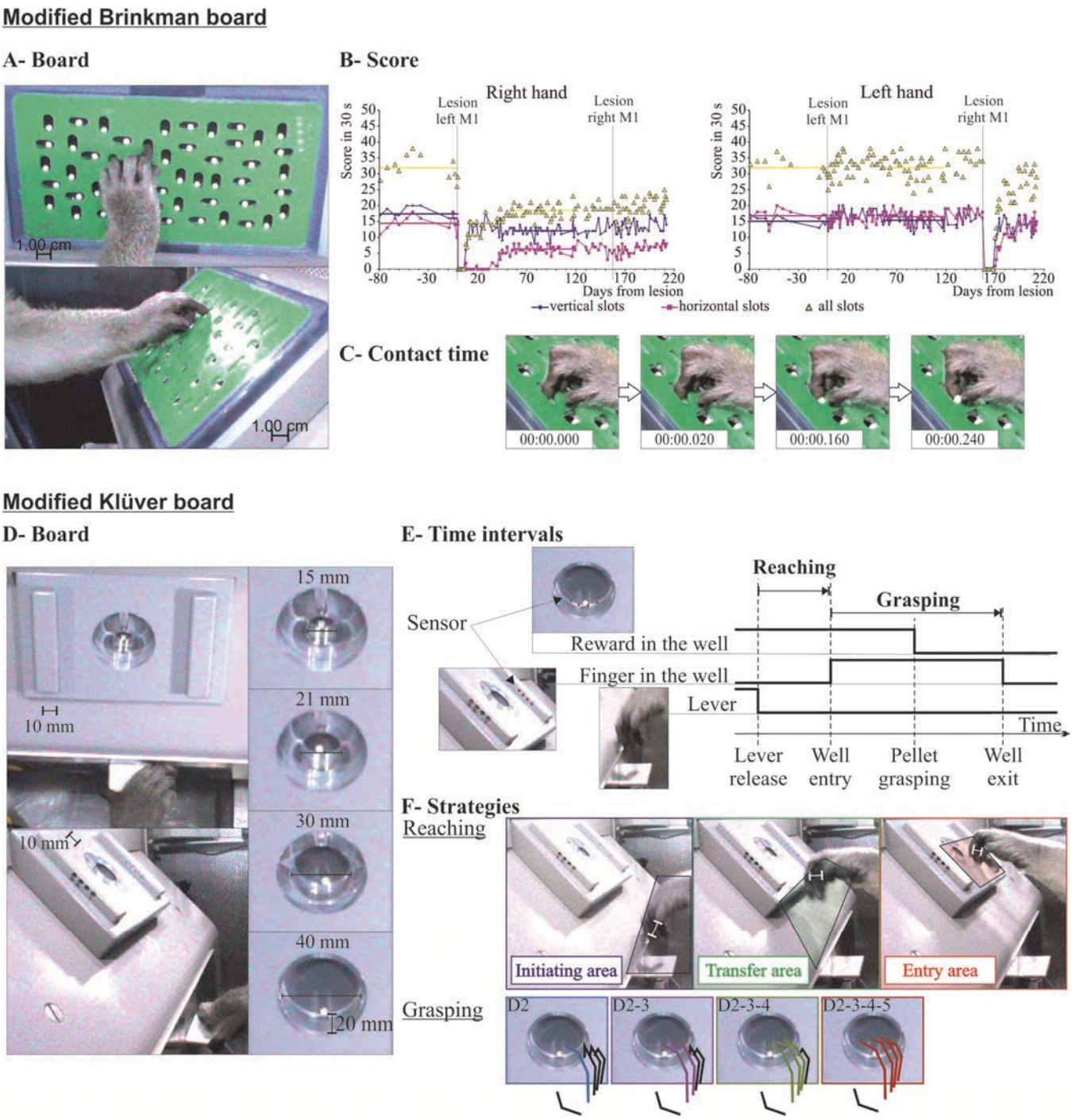

Figure 2: Behavioral methods

Illustrations of the setups and the parameters assessed in the two behavioral tasks. The "modified Brinkman board" task: **A**- top and lateral (right) view of the board containing 25 vertical and 25 horizontal slots randomly distributed and placed in front of the monkey. The parameters assessing the precision grip performances are the score and the contact time (CT): **B**- two graphs showing detailed results reflected by scores along the time course of the experiment, separately for the left hand and the

right hand, for the vertical slots (blue diamonds), the horizontal slots (purple squares) and the total score (vertical + horizontal slots; yellow triangles); **C**- the contact time, corresponding to the time-interval between the finger entry and the pellet is retrieved out of the well, as illustrated for an individual trial (time frames indicated in ms). The "modified Klüver board" task: **D**- top and lateral (left) view of the board containing four circular wells of different diameter, 15 mm, 21 mm, 30 mm and 40 mm, all 20 mm deep, placed in front of the monkey; the parameters assessing the grip performances are: **E**- the time-intervals calculated from the on/off waveforms, digitized and processed with CED 1401 interface using Spike 2 software from signals generated by three series of sensors in the bottom of the wells, at the entry of the wells and on the lever. The 2 phases of the movement determined by the sensors are: the **Reaching** phase, from the lever release to the finger's entry in the well, and the **Grasping** phase, from the finger's entry in the well to the fingers' exit out of the well; **F**- the strategies for the reaching and the grasping phases of the movement. The time course of the preshaping movement illustrates the strategy during the reaching phase at three time points, showing the delimitation of the three spatial areas (transparent zones) considered for analyses of the distance between the tip of the index and the tip of the thumb (white line): the initiating area (blue), the transfer area (green) and the entry area (red). The four Grasping strategies are schematized for the 40 mm diameter well. The broken lines represent the 5 fingers, in color for the used finger(s) in the corresponding configuration and in black for the unused finger(s) flexed on the border of the well. The color code is: D2 (blue) or D2-3 (purple) or D2-3-4 (green) or D2-3-4-5 (red).

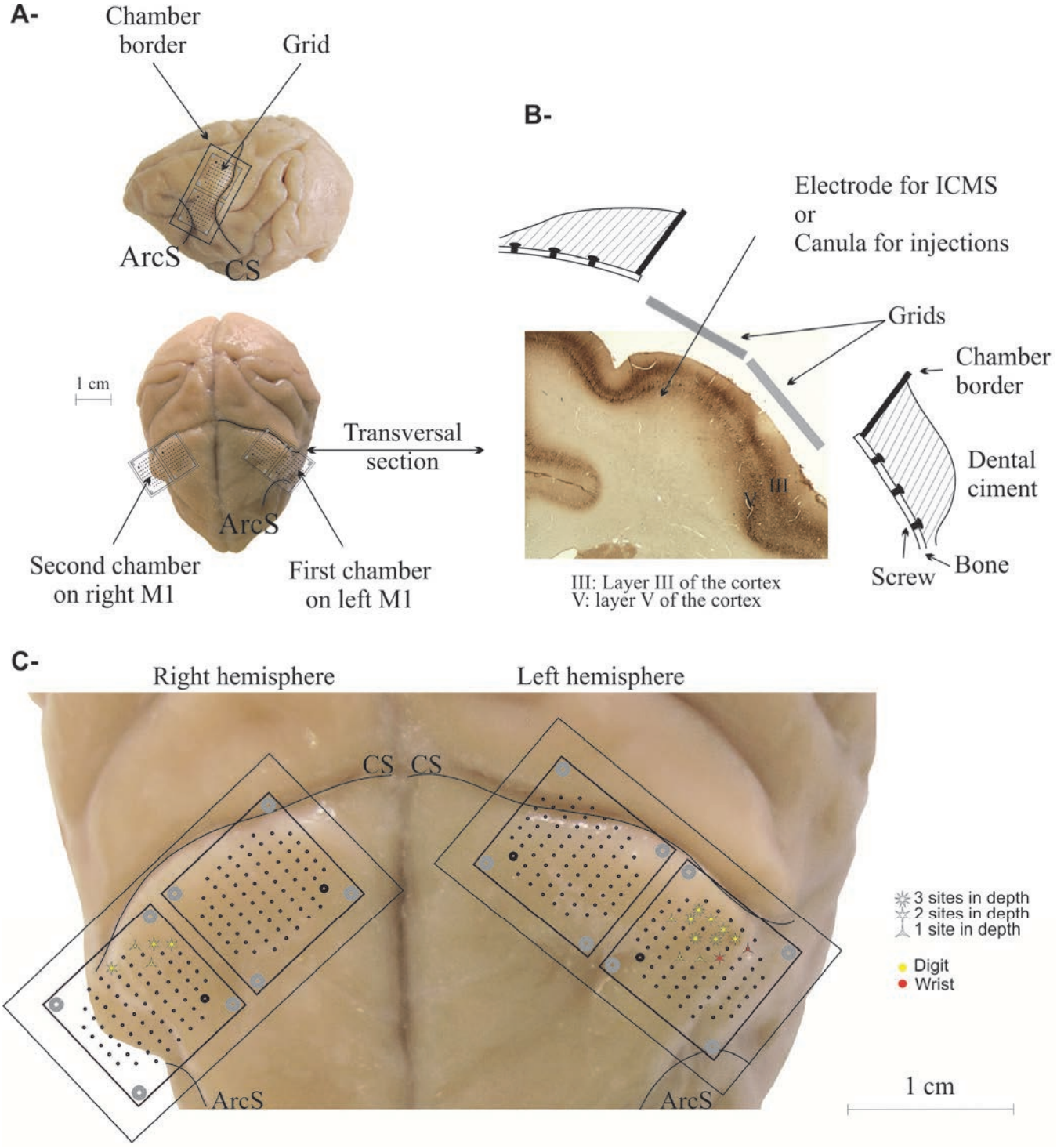

Figure 3: Head chronic chamber implants and M1 lesions

Localization of the head chamber implants over the M1 hand area of Mk-DG. **A-** Lateral view of the left hemisphere and top view of the brain showing the approximate locations of the grids inserted in the two head chamber implants over the right and left hemispheres. **B-** Schematic view of the head chamber implant over a frontal histological section of an unlesioned brain at low magnification,

stained for SMI-32. The schematic representation shows the perpendicular penetration of the electrode for ICMS and of the cannula for drug injection in the hole of the epidural grids. **C**- Enlarged view of the M1 area on both hemispheres showing the approximate representation and location of the two chamber implants. The sites of injection of ibotenic acid on the left M1 and muscimol on the right M1 are indicated with stars, as indicated in the inset on the right. The color code indicates the body part movements elicited during the ICMS sessions (yellow for the fingers and red for the wrist). CS: Central Sulcus, ArcS: Acruate Sulcus.

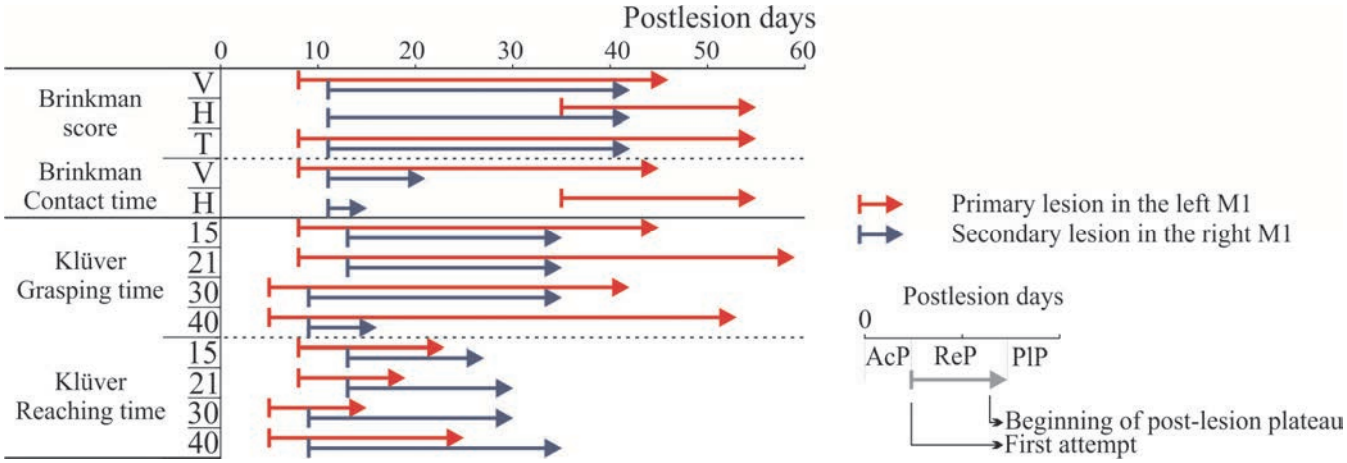

Figure 4: consecutive time-intervals post-lesions for the two behavioral tasks

Recovery time-intervals (days) for the respective contralateral hand following the primary lesion of the left M1 hand area (red arrows) and the secondary lesion of the right M1 hand area (blue arrows). The length of the arrow is a representation of the recovery phase (ReP) durations from the first day post-lesion of compelling attempt to the first day of the plateau for the modified Brinkman board task parameters (score and contact time) and for the modified Klüver board task time parameters (grasping and reaching phases). The time-interval between the day of the lesion (day 0) and the left extremity of the arrow is the period during which the subject was totally unable to perform the task (acute phase: AcP). The plateau phase (PlP) start from the head of the arrow. V: vertical slots; H: horizontal slots; T: vertical and horizontal slots mixed; 15, 21, 30 and 40 for the four well diameter sizes.

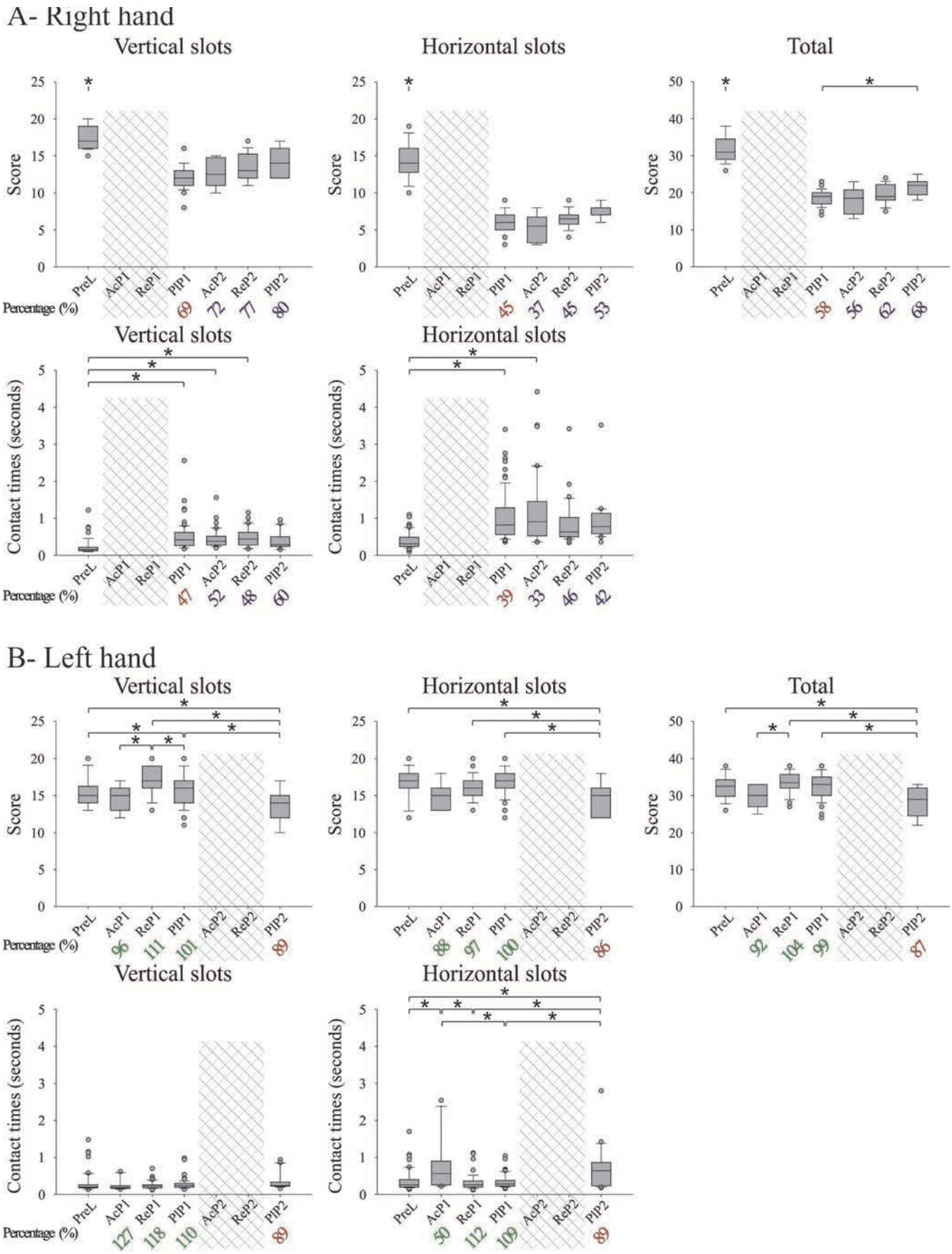
A- Right hand
Vertical slots
Horizontal slots
Total
Score
Contact times (seconds)
PreL
AcP1
RePl
PIP1
AcP2
ReP2
PIP2
Percentage (%)
69 72 77 80
45 37 45 53
58 56 62 68
47 52 48 60
39 33 46 42
B- Left hand
96 111 101 89
88 97 100 86
92 104 99 87
127 118 110 89
50 112 109 89

Figure 5.: "Modified Brinkman board task": comparisons of the effects of the primary and secondary lesions

Scores and contact times (CT) for the right hand (**A**) and for the left hand (**B**), for each time-intervals of the defined perilesional periods (see Fig. 1), except for the contralesional hand during the periods of total inactivation (AcP) and progressive recovery (ReP) indicated by a rectangle grid zone. On the box plots, the median and all outlier values are as habitually represented. Below the box plots, the percentages of functional recovery with respect to PreL values are indicated in red for the affected hand. The percentages of performances are represented in blue for the right unaffected hand and in green for the left unaffected hand aligned with the corresponding time periods. * for statistically significant differences ($p<0.05$); when positioned only above a single box, it means that this set of values is statistically significantly different from all the other sets of values of the graph.

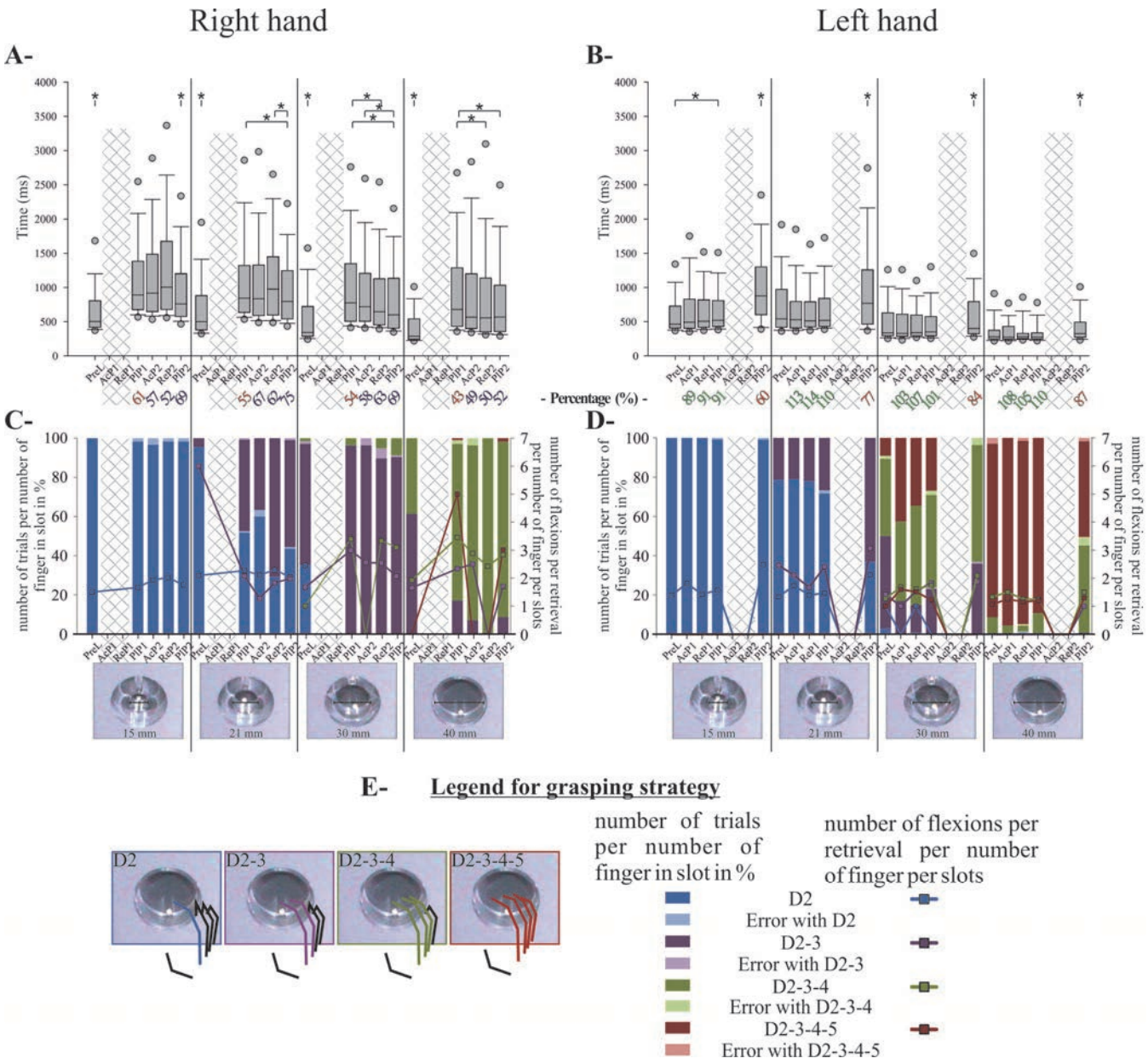

Figure 6.: "Modified Klüver board task": comparisons of the effects of the primary and secondary lesions during the grasping phase

Grasping time values (**A** and **B**) and strategies (**C** and **D**), for the right hand (**A** and **C**) and the left hand (**B** and **D**). Grasping times are represented by box plots (A and B) with the median, the 5^{th}/95^{th} percentiles and the outlier values. This unusual boxplot representation permits to hide extreme values and to increase visibility of the results. Below the box plots, the percentages of recovery (red) and the percentages of performance (blue for the right hand and green for the left hand) in line with each of the time-intervals of the defined perilesional periods. * for statistically significant differences ($p<0.05$); when positioned only above a single box, it means that this set of values is statistically significantly different from all the other sets of values of the graph.

The grasping strategies (**C** and **D**) are represented in the form of bar graphs by the number of trials performed with each finger configurations, either successful (dark color) or failed (light color), in % on the left Y axis, whereas straight lines represent the number of flexions per retrieval per finger configurations on the right Y axis. **E**- Legend of the color code used for the finger configuration for the two parameters assessed in panels **C** and **D**. Results are represented for each of the perilesions time-intervals (see Fig. 1), except for the periods of total inactivation (AcP) and progressive recovery (ReP) indicated by a shaded rectangle. All data were represented separately for each well diameter.

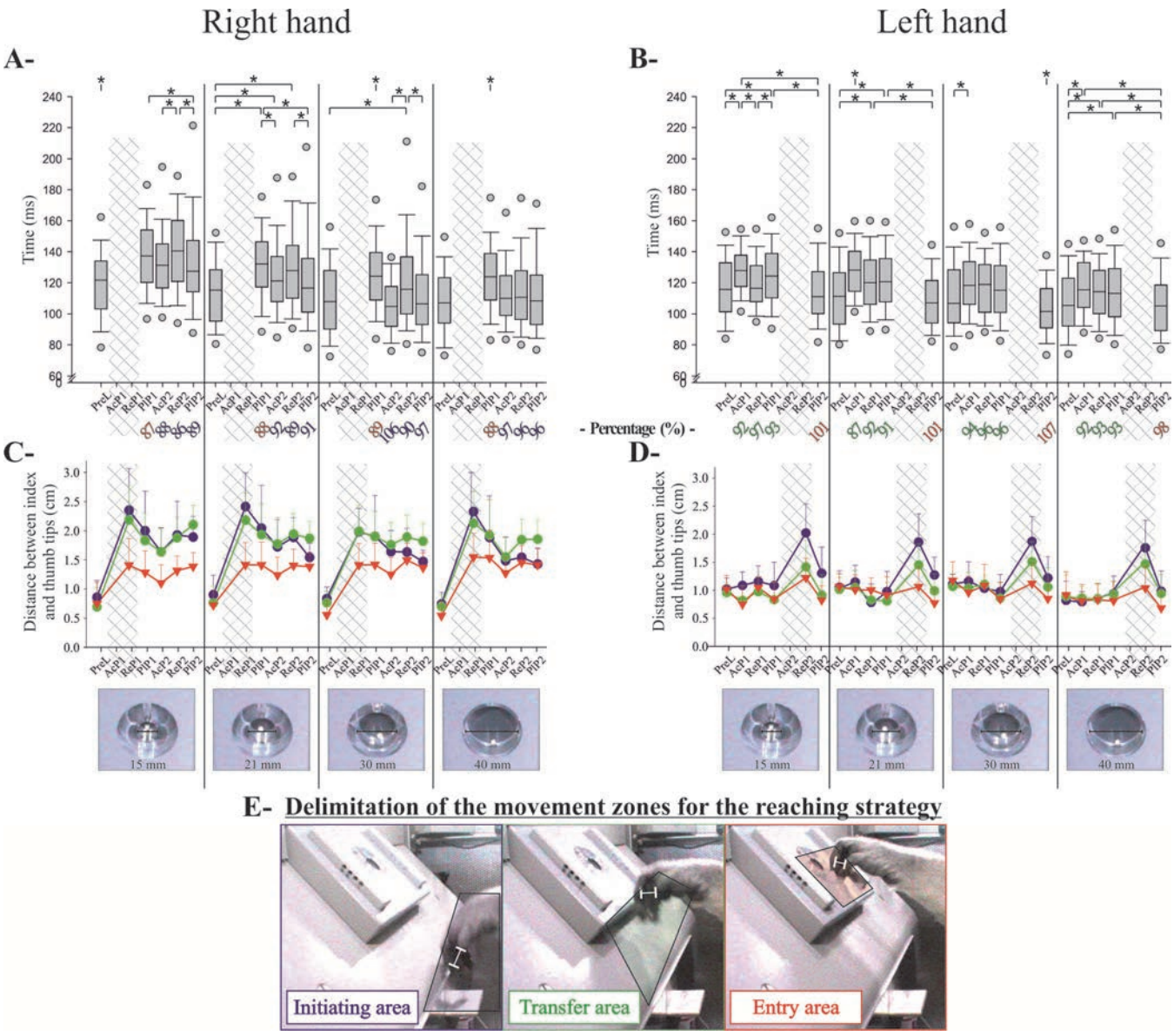

Figure 7.: "Modified Klüver board task": comparisons of the effects of the primary and secondary lesions during the reaching phase

Reaching time values (**A** and **B**) and strategies (**C** and **D**), for the right hand (**A** and **C**) and the left hand (**B** and **D**). Results are represented for each time-intervals of the defined perilesional periods (see Fig. 1), except for the periods of total inactivation (AcP) and progressive recovery (ReP) indicated by a rectangle grid zone. All data were represented separately for each well diameter, 15 mm, 21 mm, 30 mm and 40 mm. Times represented by box plots (**A** and **B**) with the median and the 5^{th}/95^{th} percentiles and the outlier values. This unusual boxplot representation permits to hide extreme values and to increase visibility of the results. Below the box plots, the percentages of recovery (red) and the percentages of performance (blue for the right hand and green for the left hand) in line with each of the time-intervals of the defined perilesional periods. * for statistically significant differences ($p<0.05$);

when positioned only above a single box, it means that this sets of values is statistically significantly different from all the other set of values of the graph.

The strategy is represented on the multiple straight lines graphs (**C** and **D**) showing means and standard deviations of the distances between index and thumb tips collected in the three zones of interest: initiating (blue), transfer (green) and entry (red) area as illustrated in panel **E**.

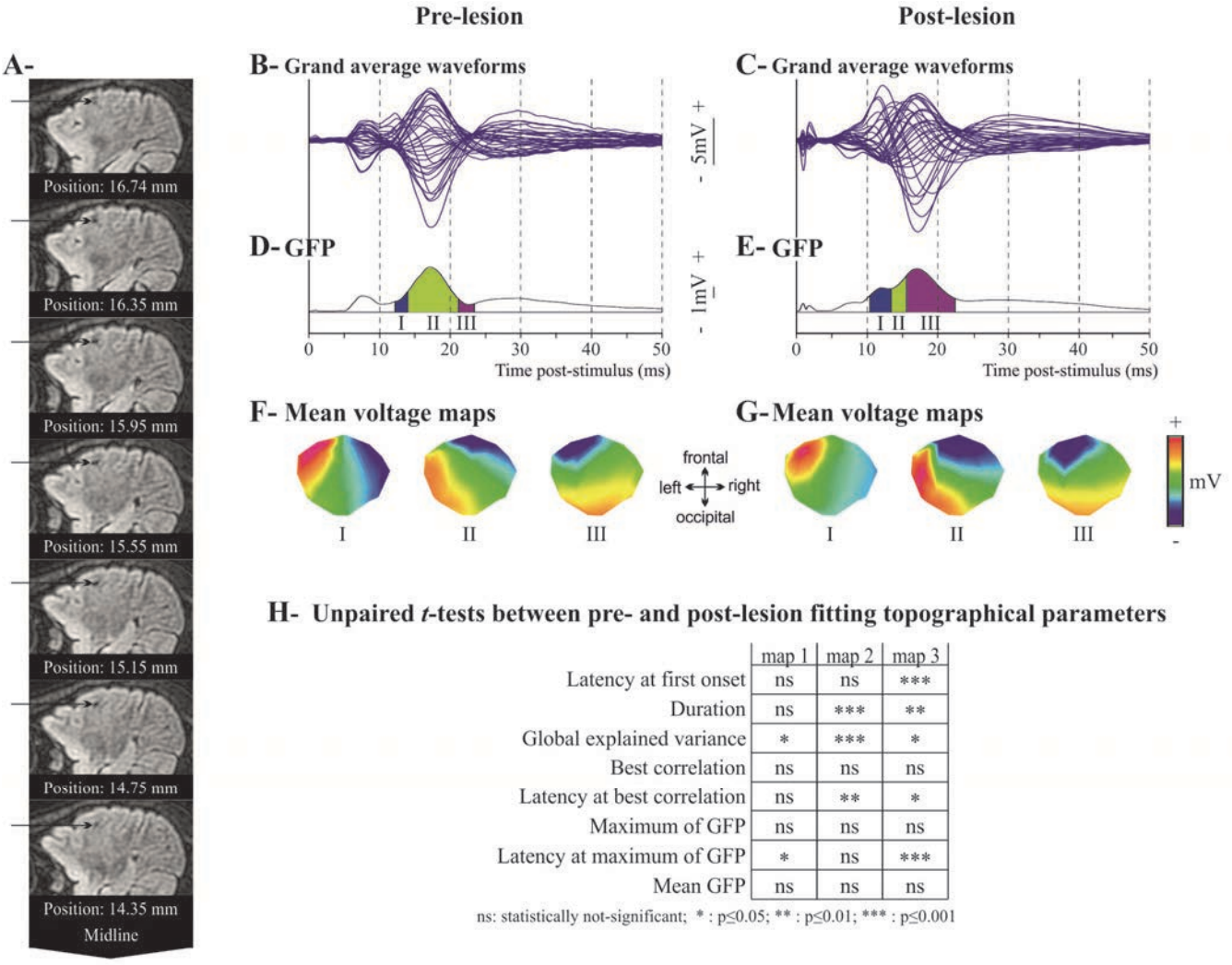

H- Unpaired *t*-tests between pre- and post-lesion fitting topographical parameters

	map 1	map 2	map 3
Latency at first onset	ns	ns	***
Duration	ns	***	**
Global explained variance	*	***	*
Best correlation	ns	ns	ns
Latency at best correlation	ns	**	*
Maximum of GFP	ns	ns	ns
Latency at maximum of GFP	*	ns	***
Mean GFP	ns	ns	ns

ns: statistically not-significant; * : p≤0.05; ** : p≤0.01; *** : p≤0.001

Figure 8.: MRI and SSEPs modification following the primary lesion of the left M1 hand area

A- MRI acquisition of the brain of Mk-DG at different parasagittal positions spaced by 400 µm from the midline, showing the primary lesion on the left M1 (arrow). **B**- Overlapped SSEP waveforms at all 32 electrodes after right median nerve stimulations before the lesion, computed against the average reference, during the first 50 ms following the stimulation. **D**- Global field power (GFP) waveform and temporal extent of the SSEPs component maps obtained by cluster analysis. **F**- Color-scaled mean voltage maps obtained for each cluster shown in **D**. The color scaling was adapted for each map (positive voltage: red, negative voltage: blue). **C**, **E** and **G** Same as **B**, **D** and **F** but for post-lesion SSEP data. **H**- Two-tailed unpaired t-tests, performed on the fitting results, compare 8 topographical parameters for each component map before and after the primary lesion: latency at first onset, duration, global explained variance, best spatial correlation (SC), latency at best SC, maximum of GFP, latency at maximum of GFP and mean GFP.

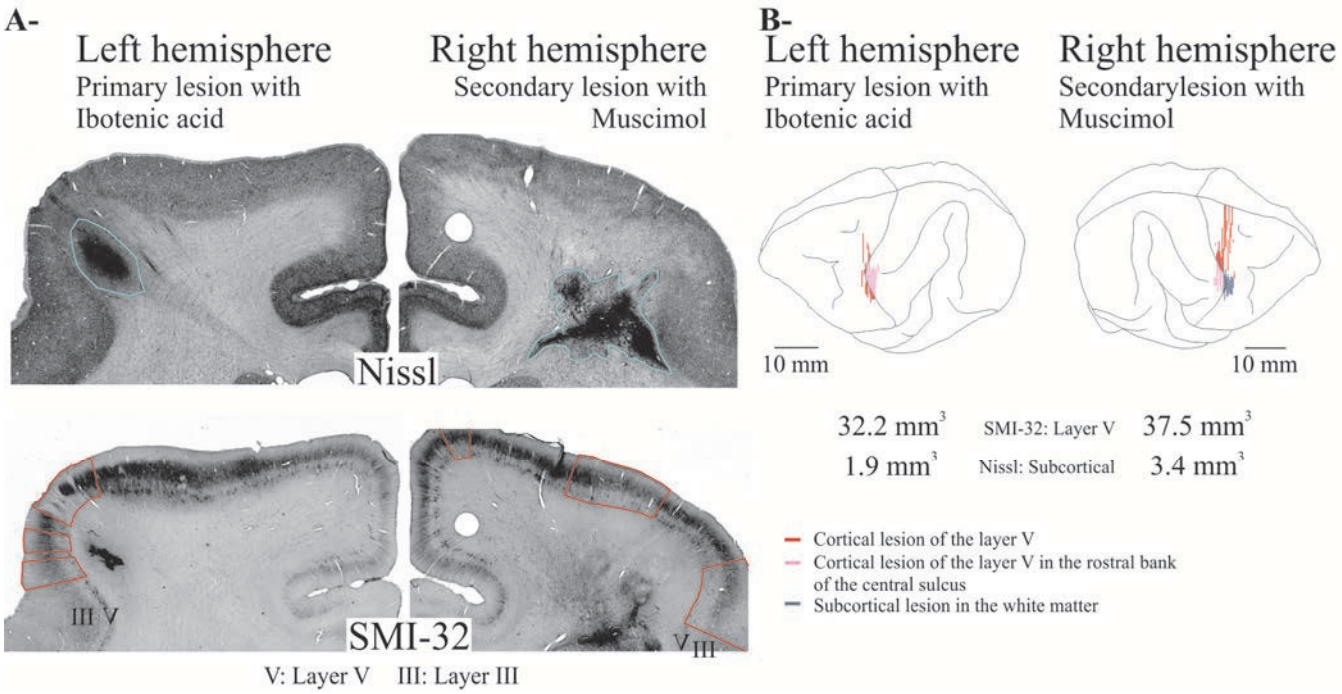

Figure 9.: Anatomical representation of the lesions

A- Nissl and SMI-32 staining of frontal histological sections of the two hemispheres of Mk-DG at low magnification. Nissl staining was used to delimit the subcortical lesion, delineated in blue, and SMI-32 staining to delimit the cortical lesion characterized by the missing layer V, delineated in red. **B-** Lesion reconstructions on the corresponding left and right hemispheres (lack of layer V) on the surface (red area) and localized in the rostral bank of the central sulcus (light red area) and subcortically (gray area). The subcortical lesion in the left hemisphere does not appear on this reconstruction, due to its overlap with the cortical lesion. This surface representation does not fully reflect the volume of the lesion given under the brain representation.

2.3. Chapter 3:

Electrophysiological assessment of functional recovery after hemisection of the spinal cord in adult macaque monkeys treated with anti-Nogo-A antibody and BDNF.

Savidan J., Beaud M.-L., Bloch J., Wannier T, Belhaj-Saïf A., Rouiller E.M.

Faculty of Sciences and Fribourg Centre for Cognition, Department of Medicine, University of Fribourg, Chemin du Musée, Fribourg, Switzerland

Abstract

The present report aimed to assess the electrophysiological and behavioral time course following spinal cord injury to evaluate the potential beneficial effects of a combination of treatment associating a blocker of the myelin inhibitory protein Nogo-A with the neurotrophin BDNF in macaque monkeys. The behavioral time course was assessed with the fine manual dexterity "modified Brinkman board" task in parallel with the electrophysiological properties assessed using Transcranial Electrical Stimulation (TES) to observe the modification of the motor evoked potential (MEP) in the intrinsic hand muscles (IHM) and the flexor hallucis brevis (FHB). This combined treatment did not exhibit improvement of the fine manual dexterity performances but was correlated with higher volumes of lesion. Electrophysiological results exhibited different profiles, but it can be noticed an increased propension to elicit MEP from subcortical structures, particularly for the monkeys receiving the combined treatment. Clear electrophysiological results showed that the ability to enhance MEP in FHB muscles disappear in the monkeys receiving the combined treatment. This study strongly suggested that our protocol of treatment combination leads to deleterious outcomes observed in parallel on the behavioral and electrophysiological outcomes but also finally on the anatomical characteristics of the lesion.

Abbreviations list

Mk-A	monkey of the group treated with anti-Nogo-A antibody
Mk-AB	monkey of the group with the combined treatment anti-Nogo-A antibody and BDNF
Mk-C	monkey of the group untreated with control antibody
CT	contact time
MEP	Motor Evoked Potential
TES	Transcranial Electrical Stimulation
EMG	Electromyographic
M1	primary motor cortex
FDI	first dorsal interosseus
APB	abductor pollicis brevis
FHB	flexor halluciss brevis
SD	standard deviation
IOM	intraoperative monitoring
SMA	supplementary motor
PreL	pre-lesion
PostL	post-lesion

Introduction

While some molecules and therapies are known to improve spontaneous functional recovery, there is no curative treatment available for lesion of the central nervous system. Lesions of the adult motor system give rise to only limited spontaneous recovery. A major source preventing functional recovery results from the inhibition of regeneration after motor system injury due to myelin inhibitory signaling pathways. One of these pathways is activated by the myelin inhibitor proteins Nogo-A binding the receptor NgR1, common to several myelin inhibitor proteins. This pathway is primarily involved in the inhibition of the activating cascade leading to growth cone collapse and inhibition of axonal growth post-injury (Caroni et al, 1988; GrandPre et al., 2000; Chen et al., 2000; Fournier et al., 2001; GrandPre et al., 2002; Nash at al., 2009). Thus, following motor system injury, a treatment with an antibody blocking the myelin protein Nogo-A is a promising treatment possibility, making the environment permissive for lesioned axons re-growth and/or sprouting (GrandPre et al., 2000; Buchli and Schwab, 2005; Zorner and Schwab, 2010; for review: Pernet and Schwab, 2012; Wang et al., 2012; Schwab and Strittmatter, 2014). Following both spinal and cortical motor injuries, an increase of corticospinal axonal sprouting around lesion site has been reported in association with spontaneous behavioral recovery, in a fine manual dexterity task in non-human primate (Fouad et al., 2004; Freund et al., 2006, 2007, 2009; Bashir et al., 2012; Hoogewoud et al., 2013) and in rodent (Schnell and Schwab, 1993; Thallmair et al., 1998; Papadopoulos et al., 2002; Li and Strittmatter, 2003; Lee et al., 2004). However, there is currently not a unique molecule preventing degeneration and damage of motor pathways, or allowing regeneration. Consequently, the concept emerged that regeneration could be further improved using combined therapies (Lu and Tuszynski, 2008). Thus, to achieve higher degrees of functional recovery, the present study intended to increase the beneficial potential of the anti-Nogo-A antibody treatment by stimulating in parallel the axonal growth with neurotrophic factors treatment. Brain-Derived Neurotrophic Factor (BDNF) is one of the most studied neurotrophic factors and is considered as a high potential molecule for the treatment of spinal cord injury. BDNF has been shown to promote axonal growth and survival on different type of neurons (for reviews see Binder and Scharfman, 2004; Lu and Tuszynski, 2008; Nagahara and Tuszynski, 2011).

Depending on their size and localization, motor system injuries alter or abolish widely and variably the different pathways involved in the correct planning and execution of voluntary movements control. To assess effects of motor system injury and effects of

treatment on the recovery, a wide range of techniques can be used. Since a long time, stimulation of the cortex was widely used in research and clinics to document the motor pathways and the different motor areas. Since the first stimulation of the cerebral cortex in intact human subject by Merten and Morton (1980), different variants of stimulation and recording of the motor and sensory central pathways and cortical areas have been developed and are currently used during surgery, as well as in research, to assess anatomical and electrophysiological characteristics and changes. Transcranial Electrical Stimulation (TES), firstly introduced as an Intra Operating Monitoring (IOM) during surgery by Boyd and his colleagues (1986), remains one of the most valuable IOM techniques. TES is routinely used to document changes in conduction time of motor tracts in neurological diseases and during surgery potentially damaging for the integrity of the motor pathways' conduction (Deletis and Sala, 2001a; Kim et al., 2012; Clark et al., 2013; for review see Deletis and Sala, 2008). In research, TES has been widely used to study motor cortical areas and pathways in human and non-human primates (*e.g.* Burke et al., 1990, 1993; Boyd et al., 1986; Calancie et al., 1987, 1998, 2001; Day et al., 1989; Edgley et al., 1990, 1997). TES allows a non-invasive and safe monitoring of function in spinal motor pathways, referred to as motor evoked potential (MEP) monitoring. MEPs reflect the function of the corticospinal (CS) tract and are compatible with real-time electromyography (EMG) monitoring.

In the present report, access was given to monkeys subjected to hemi-cervical cord lesion at C7/C8 level, followed by a combination of anti-Nogo-A antibody and BDNF treatments (Beaud, 2011). These monkeys were used here to test the application of TES in order to assess the transmission of electric signal from the brain to hindlimb and forelimb muscles on the lesioned and unlesioned sides. We aimed to assess, as well, if these electrophysiological data would parallel the behavioral observations and thus reflect the functional recovery. In case of positive correlation, TES may represent an additional readout of functional recovery and thus provide a basis to elucidate some mechanisms involved in the reorganization of descending motor pathways following hemi-cord lesion in our studies on potential effects of experimental spinal cord injuries treatments.

Methods

Subjects

The present study was conducted on six adult monkeys (*Macaca fascicularis*) (males, 3.0 to 5.3 Kg), aged from 3 to 5 years at the time of the cervical cord lesion (Table 1). Some

anatomical and functional recovery data derived from these monkeys were previously published (Beaud et al., 2012).

All experiments were carried out in accordance to the Guide for Care and Use of Laboratory Animals (ISBN 0-309-05377-3; 1996) and approved by local veterinary authorities, including the ethical assessment by the local (cantonal) Survey Committee on Animal Experimentation and a final acceptance delivered by the Federal Veterinary Office (BVET, Bern, Switzerland). The monkeys were obtained either from our own colony in our animal facility (before 2010) or were purchased from two certified suppliers (BioPrim, 31450 Baziège; France or Harlan Buckshire; Italy).

The original study (Beaud, 2011) was designed to assess the beneficial effects following hemi-cervical cord lesion at C7/C8 of a treatment consisting in a combination of two distinct molecules: the antibody against a myelin inhibitory protein Nogo-A and the growth factor BDNF, in order to improve the previously reported beneficial effects of this anti-Nogo-A antibody (Freund et al., 2006, 2007, 2009). The six monkeys were subjected to a unilateral spinal cord section at the cervical level C7/C8. These monkeys were distributed in two groups depending on whether they received a treatment: the first group of monkeys, referred to as “Mk-AB”, received the combined treatment (BDNF with anti-Nogo-A antibody) and the second group, referred to as “Mk-C”, received a control antibody. As listed in Table 1, the mentions “Mk-AB” or “Mk-C” were followed by the abbreviations of the monkey’s name to identify the six animals included in the study: Mk-CGa, Mk-CBo, Mk-ABB, Mk-ABMa, Mk-ABMx, and Mk-ABR. At the time of the investigations, the experimenters were blind of the presence or absence of treatment.

Additional data derived from other monkeys of previously published work were included, in order to correlate functional recovery with lesion volume. Separate data from these additional monkeys were published in studies which aimed to analyze the effects of anti-Nogo-A antibody treatment and the effects of anti-Nogo-A antibody combined with BDNF treatment. In these studies, authors have analyzed the effects of these treatments on the ability of CS axons to regenerate, on the functional recovery and on the size of CS neurons as well as the trajectory of fibers in the lesion site after hemi-cervical cord lesion at C7/C8 (Beaud et al., 2008, 2012; Freund et al., 2006, 2007, 2009; Wannier-Morino et al., 2008). Monkeys treated with anti-Nogo-A antibody were referred as the “Mk-A” group.

The various groups of monkeys with the different types of treatment were listed in Table 1 for the present study, the additional monkeys were already listed in previously

published reports (Beaud et al., 2008, 2012; Freund et al., 2006, 2007, 2009; Wannier-Morino et al., 2008).

Surgical procedures

All surgical procedures were described in detail in previous reports from this laboratory (Schmidlin et al., 2004, 2005, 2011; Wannier et al., 2005; Freund et al., 2006, 2007, 2009; Wyss et al., 2013). Abbreviations for injections route were the following: i.v. for intravenous, i.m. for intramuscular and s.c. for subcutaneous. To summarize, surgical procedures were conducted under deep anesthesia. Sedation was induced with an injection of ketamine (Ketalar®; Parke-Davis; 5 mg/kg; i.m.) and deep anesthesia was maintained with propofol (Fresenius®; 1%; i.v.) mixed with a 5% glucose saline solution (1 volume propofol and 2 volumes of gluco-saline, delivered at a dose of 0.1 mg/kg/min; i.v.). Ketamine was added to the i.v. perfusion solution (0.0625 mg/minute/kg) to further reduce pain during surgery. Following sedation induction, Atropine was injected to reduce bronchial secretion (0.05 mg/kg, i.m.), a preventive pain killer (Carprofen) was administered (Rimadyl®; 50mg/ml; dose: 4 mg/kg; i.m.), Dexamethasone was injected to prevent brain oedema (Decadron®; 0.05 ml/kg diluted 1:1 in saline; i.m.) and antibiotic Albipen® was injected to prevent further infections (Ampiciline 10%; 30 mg/kg; s.c.). Pain and infections following surgery were prevented by postoperative treatment with Carprofen and Ampiciline during the following week. All surgeries were performed in a facility under sterile conditions and approved by the (Swiss) cantonal veterinary office.

Cervical cord lesion

Hemilaminectomy procedure to produce a selective hemi-cervical cord lesion were described in detail in previous reports (Schmidlin et al., 2004, 2005; Wannier et al., 2005; Freund et al., 2006, 2007, 2009). Briefly, animals were placed in ventral decubitus position and the spinal processes from C2 to Th1 were exposed. Segments C6, C7 and Th1 were dissected and a complete C6 laminectomy and an upper C7 hemilaminectomy were then performed. The dorsal root entry zone at the C7/C8 border, covered by the 6th cervical vertebra, was then identified, providing an anatomical landmark for placing a surgical blade (No. 11; Paragon®), used to perform an incomplete hemisection of the cervical cord which completely cut the dorsolateral funiculus. The surgical blade was inserted 4 mm in depth perpendicularly to the spinal cord, and the section was prolonged laterally to completely cut the dorsolateral funiculus. The lesion was located at C7/C8 level, caudal with respect to the

main pool of biceps motoneurons but rostral to the pools of triceps, forearm, and hand muscle motoneurons (Jenny and Inukai et al., 1983). The muscles and the skin were sutured. After the spinal lesion, animals were kept alone in a separate cage for 2-5 days before replacing them in their own groups, in order to insure their physical conditions and better recovery from surgery.

Treatment

As previously reported (for anti-Nogo-A antibody treatment: Schmidlin et al., 2005; Freund et al., 2006, 2007, 2009; Beaud et al., 2008 - for combined treatment with anti-Nogo-A antibody and BDNF: Beaud et al., 2012; Beaud, 2011), the tested treatment was initiated at the time of the lesion and was administered with an osmotic minipump connected to a catheter inserted intrathecally in the vicinity of the cervical lesion site. Two animals have received a control antibody (Mk-CBo and MK-CGa), corresponding to a purified IgG of a mouse mAb (monoclonal antibody) directed against wheat auxin (AMS Biotechnology, Oxon, United Kingdom). The four others animals (Mk-ABB, Mk-ABMa, Mk-ABMx and Mk-ABR) were implanted with one pump delivering a monoclonal anti-Nogo-A antibody (14.8 mg in 4 weeks), which was raised by immunization with the whole Nogo-A-specific region of the human Nogo-A sequence, and with a second pump delivering the neurotrophic factor BDNF (1.4 mg in 4 weeks). The pumps were removed after 4 weeks. The characterization of the anti-Nogo-A antibody was performed as described in detail by Freund and collaborators (2007). The purified antibody hNogo-A mAB was found to be completely stable and shown to be distributed with the flow of cerebrospinal fluid over most of the spinal cord and brain within 7 days of infusion and penetrated deeply into the parenchyma (Weinmann et al., 2006). The antibody hNogo-A mAB was internalized together with endogenous Nogo-A protein into endosomal and lysosomal structures, leading to down-regulation of Nogo-A (Weinmann et al., 2006). The concentrations chosen for the anti-Nogo-A antibody treatment (3-10 mg/ml) were high in relation to the high-subnanomolar affinities of the antibody for Nogo-A. Therefore, differences in efficacy were not expected at these concentrations.

Behavioral investigations

The procedures of behavioral tests and analyses were published in detail by Schmidlin and colleagues (2011) and described in detail for five of these monkeys by Beaud and collaborators (2012). Behavioral investigations were not conducted in the monkey Mk-ABR.

Effects of lesion and treatment on fine manual dexterity were studied based on the "modified Brinkman board" task. The modified Brinkman board contains 50 slots, 25 oriented vertically and 25 horizontally, randomly distributed, where small banana-flavored pellets were disposed. Monkeys were regularly trained during weeks to retrieve food pellets from vertical and horizontal slots on the modified Brinkman board using their precision grip, between the tip of the thumb and the tip of the index. Monkeys had to retrieve pellets with one hand at the time, the first hand used in a given daily session alternatively changed each day. The manual dexterity performance was quantitatively assessed based on the **score** (number of pellets successfully grasped during the first 30 seconds) and the **contact time** (**CT** = time of contact between the pellet and the monkey's fingers preceding a successful grasping). The contact time (CT) was established for the first five horizontal slots and the first five vertical slots.

From these analyses, percentage of functional recovery for score and CT were calculated. These computations were completed separately for the vertical and the horizontal slots, because the sequences to retrieve pellets from horizontal slots involved more complex movements of wrist deviation and prosupination. Functional recovery was calculated in percentage between performances at the pre-lesion plateau and at the post-lesion plateau. Plateau was defined as a period of maximum, stable performance during several consecutive daily sessions (see *e.g.* Kaeser et al., 2010, 2011).

Anatomical reconstruction

At the end of the experiments, monkeys were deeply anaesthetized with ketamine and received a lethal dose of sodium pentobarbital (90mg/kg) before a transcardiac perfusion with paraformaldehyde (4%) in 0.1 M of phosphate buffer (pH=7.6) in order to fixate tissue, followed by solutions of increasing sucrose concentration (10, 20 and 30 %; see *e.g.* Wannier et al. 2005; Beaud et al., 2008 for detail). Brain and spinal cord were extracted and immerged into a sucrose solution (30% in phosphate buffer, pH=7.6). Spinal cord was sectioned in 30 µm-thick parasagittal sections at the level of the lesion (C3-T4). One of these series was stained with SMI-32 for anatomical reconstruction of the lesion. Method for SMI-32 staining was already described by Beaud and collaborators (2008, 2012), as well as the anatomical reconstruction of the lesion (Schmidlin et al., 2004; Wannier et al., 2005; Beaud et al., 2008; Freund et al., 2009). Briefly, sections were incubated with an anti-SMI-32 (IgG, Sigma, dilution 1:3000) with normal horse serum (2%) overnight at 4°C and were pre-amplified with avidin-biotin complex (Vectastein Elite Kits, Vector) before revelation with 3,3'-

diaminobenzidine tetrahydrochloride (0.05%). To summarize anatomical reconstruction procedure, borders of the lesion site and contours of the different parts of the spinal cord were drawn on longitudinal spinal cord sections stained with SMI-32, using neurolucida software. Drawings were aligned, allowing us to reconstruct the location and the extent of the lesion in the spinal cord, on a transverse view and to calculate the volume of the lesion in mm^3. Anatomical investigations were not conducted in the monkey Mk-ABR.

Transcranial Electrical Stimulation (TES)

Motor Evoked Potential (MEP) recordings evoked by TES have been initiated between one and three months before the cervical hemi-cord lesion and were pursued three months after the lesion. Experiments were conducted one session per week, or more if there was an impossibility or inability to capture EMG (Electromyographic) signal, starting after 2 or 3 weeks post-lesion. TES were carried out under anesthesia (a mixture of ketamine and medetomidine). A first injection was administered to start the experiment and, if necessary, a second, and last, injection was delivered during the test to complete the data acquisition. The monkeys were placed in ventral decubitus inside a Faraday cage.

TES were delivered using a stimulator (model 185; Digitimer Ltd., Welwyn Garden City, UK), applying tension in Volts (37 to 45 Hz), currently used and validated as IOM for the spinal cord assessment (*e.g.* Calancie et al., 1998; Fulkerson et al., 2011; Nuwer et al., 2013) and in research (*e.g.* Tsutsui et al., 2003; or the former corresponding model 180: Edgley et al., 1990, 1997). Stimulating electrodes were inserted under the scalp of the monkey over the targeted primary motor cortex (M1) and other part of the cortex (Fig. 1**A**). M1 was stimulated between negative electrode polarity, the reference one, and positive electrode polarity, the stimulating one. Based on the international 10-20 system, the reference electrode was placed on the front of the scalp at the Fz position and the stimulating one was placed alternatively over one of four following positions: right M1 at C3 position, left M1 at C4 position, median M1 at Cz position and caudal at Pz position. These four positions were selected in order to stimulate respectively the right and left hand area representation in M1, the foot area representation in M1 along the longitudinal cerebral fissure and largely the corticospinal tract at subcortical level (Fig. 1**A**).

EMGs were recorded with a custom software program (Neural Average - Ave2.5; University of Washington, Seattle, WA), used for data acquisition and averaging, on a PC computer via a CED 1401 acquisition interface and using pairs of multi-stranded stainless steel wires inserted directly in the muscles. EMG signals were amplified and filtered

(bandwidth 100-300 Hz to 5 KHz) by A-M Systems amplifiers, (Model 1700, A-M Systems Inc.). EMGs were recorded bilaterally at the same time from two intrinsic hand muscles (IHM): the first dorsal interosseous (FDI) and the abductor pollicis brevis (APB); and from an intrinsic foot muscle: the flexor hallucis brevis (FHB). Correct position of multi-stranded stainless steel wires was tested before each daily session by recording antidromic volley, stimulating median nerve for the hand muscles and tibial nerve for the foot muscles.

Experiments were conducted in two steps. Firstly, the EMG thresholds with the corresponding latency were determined. TES consisted of a single pulse (50 µs duration) starting at 50 volts up to 500 volts, by steps of 10 volts. Secondly, TES consisted of a single pulse (50 µs duration) repeated 20 to 30 times at fixed voltages (100 volts (100) and 250 volts (250)) and a double pulse (50 µs duration ; ISI=2 ms) at fixed voltages (50 volts (50dbl) and 100 volts (100dbl)). The EMGs recording window duration extended from 20 ms (milliseconds) before the cortical stimulation to 55 ms after the cortical stimulation. At least 0.8 sec separated two stimulations in the threshold and repeated stimulation procedures.

This protocol was slightly different for two subjects (MK-ABMx and MK-ABR), stimulated on contralateral (right) M1 hand area only and EMGs recorded exclusively in the IHM on the lesioned side (left). In these two subjects, only thresholds and their corresponding latencies data were collected, and no repetitive stimulations were undertaken.

TES analyses

EMG signals were rectified and averaged using the custom software program Neural Average and post-hoc analyses were performed by a double blind experimenter. To be validated as a compelling response, EMG had to grow up to 2 standard deviations (SD) as compared to the baseline. The baseline was determined during a pre-stimulation period of 20 ms of muscles' activity.

For all subjects, thresholds and the corresponding latencies and latencies of averaged repeated stimulations of the investigated muscles have been collected. Latencies were measured between the stimulus onset and the time point where EMG grew up to the 2 SDs (Fig. 1**B**). Threshold was defined as the minimum tension of stimulation, in volt, required to induce the first compelling EMG activity in muscles independently of the site of stimulation. Because threshold and latencies of APB and FDI were not significantly different (confer to ***Results***, paragraph **Cranial site of stimulation**), all the results were combined in a unique IHM pool of results. In the same way, the latencies and thresholds for the different sites of stimulation did not significantly differ between them, as well as latencies for repeated

stimulation. Under these conditions threshold for each acquisition session was selected between the four sites to collect the lowest voltage applied to elicit the first compelling MEPs. For repeated stimulation results, all latencies from the four sites for both the IHM and the FHB were averaged. Then, because data were in the majority not normally distributed, they were represented in box plot, pooled in three different periods of time referred to the lesion day, as delimited by behavioral readout (a pre-lesion, recovery and plateau period). This was not available for two monkeys (Mk-ABR and Mk-ABMx), as the stimulated protocol was conducted only over the contralateral M1 hand area (see above).

During the first series of acquisitions to determine threshold, tension was delivered starting at 50 volts up to 500 volts by step of 10 volts. Latencies were collected at each step for each IHM muscles at the four sites of stimulation in order to observe modifications of the latencies due to stimulation tension increase. Increase of stimulation tension after EMG threshold was reached exhibited decrease of latencies, reaching, not-systematically, a first plateau, then latencies may jumped suddenly to a second and then a third plateau. First value of plateau was determined as the first point of a series of equal latencies while stimulation voltages increased (Fig. 7**A**). We have assessed these four parameters during the pre-lesion period and the two post-lesion periods: the recovery period per se and the plateau period, such as previously for data acquired with the repeated stimulation protocol. Because the distributions of the majority of the data were not normally distributed, we used non-parametric statistical Kruskal-Wallis test and Dunn's method for post-hoc analyses.

For MEPs analyses, all latencies shorter than 5 ms were rejected, considered as artefactual. Effectively, considering conduction speed of electrical signal along axons (velocity comprised between 24 to 95 m/s, median value of 60 m/s for monkey (Edgley et al., 1997)) and delays for synaptic transmission (0.25 ms of delay at neuromuscular synaptic junction (Katz and Miledi, 1964) and 0.1 ms at least for synaptic delay of the corticospinal pathway (Canedo and Lamas, 1992), signals with less than 5ms latency were likely to be linked more to an artifact than to an early response. Taking into account the fastest fibers, 5 ms correspond to an excitation location situated at approximately 40 cm from the recorded muscle. The brainstem of a monkey (around 5 kg weight), is approximately distant from 30 cm to the distal hand muscles. Although anesthesia is known to increase synaptic delay, the increase was however limited to 0.75 ms under deep anesthesia (Brooks and Eccles, 1947).

Results

Anatomical data and Behavior

Monkeys involved in the present MEP study

Anatomical reconstruction showed the extent of the lesion on an horizontal plane, on the left side for Mk-ABMx monkey and on the right side of the spinal cord for the 4 other monkeys (Fig.2**A**). The summary table in figure 2**C** lists the volumes of the cervical hemi-cord lesion, ranging from 2.36 to 9.81 mm^3, with an hemi-section extent ranging from 73% to 95%. In all four monkeys, the dorsolateral funiculus was completely transected.

Results derived from the behavioral investigations (Fig. 2**B**) showed the great ability of the monkeys to retrieve small pellets during the fine manual dexterity task "modified Brinkman board" before the cervical cord lesion, as reflected by the pre-lesion plateau of score data. The effect of the cervical cord lesion was illustrated by the dramatic drop of score observed during the daily sessions immediately following the lesion, corresponding to an inability of monkey to perform this manual task. Then, there was a progressive functional recovery of manual dexterity, leading finally to a second (post-lesion) plateau, after the dash line on the graph. The degree of functional recovery was listed in the table of figure 2**C** for five monkeys. The functional recovery was higher in the control antibody treated group than in the combined treated group for both the contact time and the score (Fig. 2**C**). Percentages of score recovery were higher or equal in the control antibody treated group of monkeys for the vertical slots than for the horizontal slots. In the combined treated group, score was higher in one monkey for the vertical slots (Mk-ABMa), whereas it was higher for the horizontal slots in another monkey (Mk-ABB). Mk-ABMx exhibited a longer recovery period and a lower functional recovery than all the other monkeys, with no difference depending on slots orientation for scores, but exhibiting a lower functional recovery for horizontal slots point out by shorter contact time. Functional recoveries calculated for the contact time were higher for the control antibody treated group than for the combined treated group. Furthermore, in the two groups, percentages of functional recovery were higher for the contact times derived from the horizontal slots than from the vertical slots.

Additional monkeys derived from previously published work

In order to integrate the present experiment into the largest context of previous studies assessing the effects of treatments to promote spontaneous functional recovery, we included a

larger cohort of already published monkeys (Schmidlin et al., 2004, 2005; Freund et al., 2006, 2009; Beaud et al., 2008, 2012) to evaluate the link between the behavioral data and the size of cervical hemi-cord lesions (Fig. 3). These additional monkeys were included in studies analyzing the effect of treatments with anti-Nogo-A antibody alone (Mk-A) and of the combined treatment with anti-Nogo-A antibody and BDNF (Mk-AB) as compared to supplementary control antibody treated monkeys (Mk-C) following spinal cord hemi-section in monkeys.

Functional recovery was represented as function of the lesion volume in the larger cohort of monkeys. Figure 3**A** represents the functional recovery as function of the lesion volume for score (vertical (Fig.3**A**1) and horizontal slots (Fig.3**A**2) separately) and contact time (vertical (Fig.3**A**3) and horizontal (Fig.3**A**4) slots separately). Monkeys of Mk-A group were brought together and showed higher percentages of functional recovery than monkeys of the control antibody treated group for comparable lesion volumes. Monkeys of the Mk-AB group showed lower percentages of recovery as both those of the Mk-A and Mk-C group.

However, a striking observation was that monkeys of the Mk-AB group showed clearly higher volumes of lesion, statistically significant compared to the two other group ($F_{2,14}$=7.593; p=0.007; Fig. 3**B**). Post-hoc statistical analyses did not show difference between Mk-C and Mk-A group, and showed significant increase for the Mk-AB group as compared to the two others.

Cranial site of stimulation

Table 2 shows statistical analyses comparing thresholds and latencies recorded after the stimulation of the four different sites on the scalp. The four sites of stimulation have been compared, in a first step, for the thresholds and the corresponding latencies and, in a second step, for the latencies of the repeated stimulation at the four scalp sites. These comparisons were done for each monkey, for each group of muscles, for pre- and post-lesion periods and for each voltage of stimulation in case of repeated stimulation. Only three statistical significant differences were observed: 1)- firstly, significant differences were observed for MK-CGa at 100dbl and 250 volts of stimulation for the left IHM between the sites of stimulation but the differences were weakly significant (respectively H=9.661,df=3,p=0.034 and H=8.023, df=3, p=0.046). Furthermore, analyzing separately the two IHM, APB and FDI did not show significant differences (data not shown). 2)- secondly, significant difference was found for MK-CGa for the threshold in the left IHM in the post-lesion period. This significance is however weak (H=8.177, df=3, p=0.042) and the corresponding latencies were

not significantly different between the stimulation sites. We may explain these three cases by the small size of the samples. To conclude, this statistical analysis thus did not show major differences for MEPs thresholds and corresponding latencies and for MEPs latencies induced by repeated stimulations between the four cranial stimulation sites. As consequence, EMGs were considered as not affected by the stimulation site on the cortex in our experimental conditions. Latencies and thresholds recorded after stimulation at the four different sites of stimulation on the scalp were thus pooled for further analyses.

MEP threshold

Figure 4 shows MEPs thresholds and corresponding latencies for IHM and FHB muscles. Constantly, MEPs of IHM muscles were of shorter latencies than those of FHB muscles. A brief overview shows high variability of thresholds and corresponding latencies of MEPs over daily experimental sessions before the lesion (Fig. 4), especially in Mk-CGa, Mk-CBo and Mk-ABMa.

Results showed that one monkey exhibited a clear effect on thresholds and corresponding latencies following hemi-cord injury. In the acute period after injury, Mk-ABR (Fig. 4**B**2) thresholds exhibited a dramatic increase in stimulated voltages surprisingly correlated with very short latencies. Then thresholds voltages tended to decrease remaining however higher than pre-lesion, for latencies becoming longer. Globally, the cervical hemi-cord injury induced an increase of thresholds voltages. The results obtained for the monkey Mk-ABMx (Fig. 4**B**2) exhibited both certain difficulties to evoked MEPs in IHM during the first 55 days following the hemi-cord injury and a tendency for thresholds voltages increase associated with a slight increase in the corresponding latencies. After this period we observed a tendency of threshold and corresponding latencies to decrease. After lesion, the other monkeys did not exhibit massive and systematic modifications of MEPs thresholds and corresponding latencies, observed with post-lesion EMGs recordings for IHM evoked with TES in both the “Mk-C” and the “Mk-AB” group as compared to the pre-lesion period (Fig. 4).

Similarly, FHB MEPs recordings did not exhibit systematic and massive changes of the thresholds and corresponding latencies related to the lesion in the control antibody treated group (Fig.4**A**). As massive and persistent modification following hemi-cord lesion, the complete loss of MEPs signal in FHB muscle evoked by TES on the ipsilesional side was observed (Fig. 4**B**).

MEP threshold on the lesion day

MEPs recordings were conducted during the surgery aiming at producing the cervical lesion yielded direct effects of lesion on the electrophysiological properties of the sectioned CST (Fig.5). In line with others authors (Sloan, 2002), MEPs recordings on the lesion day showed great disparities in EMG signal quality due to deeper anesthesia with propofol as compared to a mixture of ketamin-domitor used to anesthetized monkeys on normal recording days. Such recordings on the lesion day were available for 2 monkeys only, one in each group. We observed two major features. First we observed that MEPs in HIM was still elicited after lesion on the lesioned right side and was not dramatically affected in both a control antibody treated monkey and a combined treated monkey. Secondly, concerning the FHB muscle, MEPs were still elicited after lesion for all muscles on both sides in the control antibody treated monkey (Mk-CGa), while the disappearance of MEPs in FHB muscles on both sides was already observed for the combined treated monkey (Mk-ABMa), immediately after the lesion.

MEP latencies induced by repeated TES

Latencies of MEPs induced by repeated TES (Fig. 6) have been assessed in four monkeys (Mk-ABB, Mk-ABMa, Mk-CBo and MK-CGa), with application, at fixed tension, of single pulse stimulation (named 100 for tension at 100 volts and 250 for tension at 250 volts) or of double pulse stimulation aiming to facilitate occurrence of MEPs (named 50dbl for double pulse at 50 volts tension and 100dbl for double pulse at 100 volts tension).

In line with thresholds data, the dramatic and systematic modification observed following hemi-cord injury was the total loss of FHB muscles' MEPs in subjects of the Mk-"AB" group, even with the double pulse stimulation improving MEPs' occurrences (data not shown). Otherwise, we did not observe dramatic and systematic modifications of latencies due to the hemi-cord lesion at all the different voltages of stimulation for the MEPs latencies of IHM muscles of the two groups as well as for MEPs latencies of FHB muscles of the Mk-"C" group.

In an effort to reveal electrophysiological modifications due to hemi-cord injury possibly hidden by the high intersession variability, it was intended to pool pre-lesion and post-lesion data for IHM, increasing data number aiming to increase power of the comparison to exhibit subtle effects. However, pooling all the post-lesion data would have brought bias due to the acute post-lesion period, during which cortical and spinal plasticity took place.

Considering this aspect, post-lesion data were separated in two groups based on the behavioral time course of the functional recovery (Fig. 1): the recovery period (RP) and the post-lesion plateau period (PP).

This data set representation of MEPs latencies induced by repetitive TES showed some common patterns of modification after hemi-cord injury. For the four monkeys, it has been observed a decrease of latencies for the lowest tension of stimulation on the unlesioned side during the RP. In a specific case, double pulse facilitation protocol applied on Mk-CBo during the RP prevents MEPs occurrence in IHM during this RP. During the PP, MEPs latencies on the unlesioned side for the Mk-C group tended to be similar to the pre-lesion period (Mk-CBo) or even longer (Mk-CGa), whereas for the Mk-AB group tended to be similar to the pre-lesion period (Mk-ABMa) or even shorter (Mk-ABB) as during the RP. These changes were similarly observed for all the tension assessed, already from the lowest stimulation tension applied 50dbl. Results for the lesioned side recording MEPs showed that for three of four subjects (Mk-CGa, Mk.CBo and MkABB) there were an increase of the latencies at the lowest stimulation applied, 50dbl, during the RP compare to the pre-lesion period. The other subject, Mk-ABMa, exhibited a small decrease in MEPs latencies evoked at 50dbl pulses as compared to the pre-lesion period, already presents during the RP as at the PP. This subject also exhibited MEPs latencies decrease for repeated stimulation at 250 volts during the RP, otherwise, did not exhibit other marked modification of MEPs latencies at the other stimulation voltages. In Mk-ABB, MEPs latencies had a slight tendency to be increase at the lower stimulation voltages, 50dbl and 100 volts, during the RP and to become shorter for the highest stimulation voltage, as compared to the pre-lesion period and the PP. Inversely, during the PP, MEPs latencies were shorter than during the pre-lesion period for higher stimulation voltages. In the Mk-C group, MEPs latencies were shorter than during the pre-lesion period, directly during the RP in Mk-CGa, but for 100 volts repeated stimulation during the RP and already for the 50dbl pulse stimulation during the PP, and, for Mk-CBo, during the RP at 100 volts repeated TES and during the PP at 100dbl repeated TES.

MEP latency jump

To determine threshold, TES were applied systematically starting at 50 volts up to 500 volts by 10 volts step. For each 10 volts steps of stimulation, latencies were collected for each site of stimulation and each IHM muscles (Fig. 7**A**). This protocol allowed the observation of typical patterns of latency changes by increasing stimulation voltage. In all monkeys, it has been observed a decrease of MEPs latencies associated with the increase of stimulation

voltages up to a first plateau (PI) of latencies, thus followed, less systematically, by a sudden jump to shorter latencies, to a second plateau (PII) and, seldom, the presence of a second sudden jump reaching a third plateau of shorter latencies (PIII) (Fig. 7**A**). This was interpreted by some authors as the ability of recruitment of corticospinal fibers from the threshold to PI of latencies corresponding to a maximal cortical recruitment and the ability of TES to stimulate deeper brain structures with higher stimulation voltages, respectively the brainstem and the pyramids (Edgley et al., 1990; Burke et al., 1990; Rothwell et al., 1994). Similarly to thresholds and repetitive stimulations, we have pooled data from each site and both IHM muscles together. As for the modification of MEPs latencies induced by repeated TES stimulation, subtle modification of MEPs threshold due to the cervical hemi-cord lesion could be masked by the high intersession variability. Thus, with the same criteria as for MEPs latencies induced by repeated stimulations, voltages and corresponding latencies for threshold, first (PI), second (PII) and third (PIII) plateau were pooled in three time periods as regard to the lesion day: pre-lesion period (PreL), recovery period (RP) and plateau period (PP). These data were represented in box plots (Fig. 7) for IHM MEPs latencies induced by repeated TES at the four fixed voltages for the unlesioned and the lesioned side of each monkey.

In the control antibody treated group (Fig. 7**B**1) different modification profiles were observed. Mk-CGa exhibited an increase of MEPs latencies of the four parameters assessed during the PP correlated with an increase of the voltage needed to reach PI, PII and PIII on the unlesioned side. On the lesioned side results showed that voltages needed to reach threshold, PI and PII were higher and associated with a decreased of the corresponding MEPs latencies during the RP as compares to the pre-lesion period. During the PP, voltages applied to reach thresholds and PI were comparable to the pre-lesion period, however corresponding MEPs latencies were as decreased as during the RP. Furthermore, we observed that, on the lesioned side, PII and PIII tend to disappear during the RP, a tendency accentuate during the PP. Concerning Mk-CBo, results showed a decrease of MEPs latencies on the unlesioned side already during the RP. On the lesioned side results showed that voltages needed to reach threshold, PI, PII, PIII were lower post-lesion and no correlated with an increase of corresponding latencies. Unlike Mk-CGa, results for Mk-CBo showed occurrence of PIII during the post-lesion period, even on the unlesioned side during the PP.

The combined treated group (Fig. 7**B**2) comprised 3 monkeys exhibiting comparable profiles (Mk-ABMa, Mk-ABB and Mk-ABMx) and a fourth one (Mk-ABR) with a different profile. On the unlesioned side data were available only for two monkeys Mk-ABMa and Mk-

ABB. For these two monkeys, results showed a tendency of the threshold latencies to transiently decrease only during the RP, correlated only with a decreased of the voltages needed to reach PI. Results on the unlesioned side at the PP for Mk-ABB were comparable to the pre-lesion period, however, for Mk-ABMa results showed that voltages needed to reach PI and PII increased and corresponding latencies were comparable to the pre-lesion period results. Results for the lesioned side, concerning the group of three comparable monkeys, showed a decreased of MEPs latencies of PI during the PP, correlated for Mk-ABMa and Mk-ABMx with higher voltages needed to reach PI. At threshold, MEPs recorded in Mk-ABB and Mk-ABMx IHM had a tendency to become transiently higher during the RP. Results showed that PIII were not reached excepted in the pre-lesion period for Mk-ABR. Otherwise, for MkABB on the unlesioned side and Mk-ABMx on the lesioned side, MEPs reached the PII post-lesion.

The fourth monkey, Mk-ABR, showed a different profile of modification. However its RP and PP was estimated based on electrophysiological data, as behavioral testing was not conducted for this monkey. Nevertheless electrophysiological data exhibited an interesting profile with a substantial modification of threshold and corresponding latencies comparing period from J0 to J13 with period after J21, which can correspond to some RP time of other monkeys. We observed a dramatic increase of the threshold appearance which correlated with a pronounced decrease of the corresponding latencies during the RP. These data corresponded to the PI data and neither PII nor PIII were observed. This was followed by a return to the pre-lesion voltage of stimulation needed to achieve threshold, associated with higher latencies at the PP, in parallel with reappearance of PII, the PIII was still not reached. These results possibly reflect a restoration of a cortical site of stimulation with a lower number and/or affected fibers and/or modified pathway reflecting the increased in latencies at PI.

Statistical data were not described in detail because they had to be considered with caution due to the low number of data in some cases.

Discussion

The main results of this study are as follows: 1) combined treatment did not improve functional recovery contrasting to the improvement observed for the anti-nogo-A antibody treatment as compared to the control antibody treatment. Monkeys of the combined treated group had higher volumes of lesion as both the control and the anti-nogo-A antibody treated groups; 2) hemi-cord lesion abolished FHB MEPs in the combined treated group and not in

the control antibody treated group and did not modified dramatically IHM MEPs in both groups, except in two monkeys with opposite patterns of modification; 3) repeated TES at fixed voltages exhibited a decrease of MEPs latencies in IHM on the unlesioned side as on the lesioned side excepted for the lower stimulation voltages for which MEPs latencies increase during the RP; 4) MEPs latencies for IHM muscles decreased with increasing stimulation voltages from threshold to a first plateau and then jumped to lower latencies; 5) tendency of latencies to be shorter post-lesion on the unlesioned side; 6) MEPs latencies for IHM in the combined treated group transitory increased at threshold during the recovery period, were shorter during the plateau period at PI and jump were more frequently observed following injury.

In this discussion, we first consider causes of variability due to the protocol. Secondly we focus on the pathways possibly involved in the electrophysiological activity observed in the present work in muscles following injury, preserved but modified. Finally we discuss about the observed lack of effect and even the deleterious effect of the combined treatment used in the present work.

Electrophysiological aspect of the lesion

To firstly focus on electrophysiological aspects of the present study, the high variability of MEPs results may be due to various aspects of the experimental design. This was not explained by poor placement of the recording electrodes in the targeted muscles, because nerve stimulation before each TES session showed EMG activity (Data not shown). Considering the validity of the stimulation protocol used in the present study (refer to ***Methods*** section **TES analyses**), we did not observe any difference between the four cortical sites of stimulation on both threshold and latencies of MEPs. We suggest that stimulations at the four cortical sites activated axons widely in the cortex and, deeply along axons to the brainstem.

The variability of stimulation sites along axonal pathways may be due to different parameters of anesthesia. Various protocols of anesthesia can induce variability in the occurrence of MEPs induced by TES. It has been shown that, depending of the drugs used (Sloan and Rogers, 2009a, 2009b; Di Lazzaro et al., 2003), the depth of anesthesia and body temperature are all parameters that can affect MEPs and their properties, such as latencies and amplitudes, in human subjects, cats and pigs (Browning et al., 1992; Meylaerts et al., 1999; Sloan, 2002). The use of Ketamine is in adequacy with MEPs method during Intra Operative Monitoring (IOM), because it does not modify EMGs responses evoked by TES and even

decreases the stimulation threshold (Di Lazzaro et al., 2003; Sloan, 2002). In another way, Ketamine increases the duration of the silent period in respect to two stimulations (Di Lazzaro et al., 2003). Because Ketamine was given in a single injection, thus neurons were not constantly depressed over time depending of the time curve of action and, considering the silent period, neurons were not similarly affected by the preceding stimulation. As a consequence, anesthesia during IOM needs to be more constant, using either a perfusion or volatile anesthetics (Sloan, 2002). Despite these considerations on the different aspect of the procedure affecting occurrence of MEPs, it has been shown that occurrence of MEPs were more affected in FHB muscles than in IHM (Kim et al., 2012). In correlation with this result, we also observed, for MEPs thresholds results, higher generation rate of MEPs induced by TES in IHM than in FHB muscles.

TES is known to activate directly neurons at the cell body level at the initial segment or at the internode along the axon (Patton and Amassian, 1954). Moreover, according to the present results, several authors have shown different jumps in latencies, and correlated these observations to deeper anatomical structure stimulation sites, from the brain to the brainstem. Rothwell and collaborators (1994) have shown that MEPs induced by TES exhibited a jump to shorter latencies with increasing stimulation voltages, corresponding to a jump of the stimulation site to the cerebral peduncle. Edgley and collaborators (1990) have shown that TES over the motor cortex could activate fibers deeply within the cranium, at the pyramidal decussation in anesthetized monkeys. In another study, Burke and collaborators (1990) reported identical observations in human subjects. These authors showed that TES site jumped from an initial presumed cortical level to distances (calculated assuming conduction velocity of 60-65 ms^{-1}) corresponding to the internal capsule, the cerebral peduncle and pyramidal decussation. Because our protocol did not consist of chronic implants, stimulating and recording electrodes were re-positioned for each daily session, implying that stimulation and recording sites were not strictly reproducible. For that reason, these different possible stimulation sites along the corticospinal pathway may explain only a part of the variability observed across sessions for thresholds and latencies of MEPs.

The use of MEPs recording induced by TES in a non-chronic procedure can be subject of debate, however this choice was in line with the aim to reduce invasiveness of the procedure and to reduce the high risk of infection associated with chronic EMG implant, as the risk for implant to be degraded over time.

Despite the variability observed, MEPs post-lesion was recorded with massive modifications of thresholds and corresponding latencies as compared to pre-lesion only for

IHM in one monkey of the combined treated group. The second massive and persistent modification observed was the disappearance of MEPs in FHB in monkeys of the combined treated group. Otherwise, in the others subjects, independent of the group and already observed from the lesion day recording session, no massive and systematic modifications have been observed. The following interpretations could be proposed. Firstly, the hemi-cord lesion was incomplete, therefore some axons of the corticospinal tract were spared. We cannot exclude the possibility that our lesion spared some CS axon in the targeted dorsolateral funiculus. However, in an horizontal plane, anatomical reconstruction of the lesion extent showed, in most cases, the completeness of the lesion regarding the dorsolateral funiculus responsible of the fine manual dexterity. Secondly, the lesion targeted at C7/C8, if slightly misplaced, may be too low along the cervical enlargement and thus spared relevant fibers. It has been shown that spinal cord motoneurons are organized in column along the gray matter and, for forelimb muscles, different columns extent from Th1 to C7 and even higher (Jenny and Inukai, 1983). Motoneurons controlling APB, for example, extend all along the Th1 and C8 segment, up to C7. A lesion at C7/C8 level may have spared some of the upper hand motoneurons, enough to induce normal MEPs in APB. However, this interpretation does not explain that although MEPs for IHM are not abolished, FHB were still present in monkeys of the control antibody group. A third explanation could involve the activation of ipsilateral CST, and contralateral CST decussating at the spinal level, from primary and secondary motor areas and of non-pyramidal pathways. It has been shown that following cortical injury, cortical zones adjacent to the lesion could play role in the functional recovery and, the larger the lesion the more remote are the areas possibly supporting the recovery (Liu and Rouiller, 1999). Moreover, in a previous paper from our laboratory, it has been shown that re-growth of the axotomized CS axons in the scar tissue is unsuccessful, thus not able to support the observed functional recovery (Freund et al., 2007). Results of the present study revealed subtle modifications. Data pooled over the different time windows of the functional recovery exhibited a decrease of MEPs latencies on the unlesioned IHM possibly reflecting the loss of interhemispheric inhibition due to the loss of transcallosal projection originating from the affected hemisphere of origin of the lesioned CS fibers. Existence of callosal projections between M1, but most of all with the non-primary motor areas, appeared to be developed for hand representations (Rouiller et al., 1994) and their inhibitory effects were revealed through electrophysiological assessments in human (*e.g.* Di Lazzaro et al., 1999). On another hand, the ability of TES to stimulate at deeper subcortical location was supported by the observations of first plateau latencies decrease and of the increase of following jump

occurrence in latencies with lower voltages of stimulation on the lesioned side. This facilitation to stimulate at deeper subcortical location following hemi-cord lesion is well illustrated for one monkey (Mk-ABR): (*i*) really short latencies were observed for thresholds during the recovery post-lesion period associated to higher stimulation voltages required to reach it, matching to the latencies of the first plateau reached, (*ii*) the loss of following jumps in latencies, thus already reach at the threshold. Differently, this facilitation to stimulate deeper structures appeared earlier but only for one monkey treated with the control antibody while it appeared mostly at the plateau period for monkeys treated with the combined antibody (except the apart Mk-ABR monkey). However, threshold pooled data have exhibited tendency for latencies to be longer transiently following hemi-cord lesion reflecting cortical site of stimulation impaired by lesion, and then, the ability to be easily initiated at deeper subcortical level after recovery. Correlating with these results, TES could deeply stimulate CST and probably directly the brainstem and the cerebral peduncle (Edgley et al., 1990; Burke et al., 1990; Rothwell et al., 1994). Thus, TES could activate others descending motor pathways controlling muscles activity on both sides of the body. These pathways have slower axonal conduction velocities and comprise more relays, which could explain the fact that our latency jumps were larger than reported by other authors recording directly at axonal level and not from muscles (Edgley et al., 1990; Burke et al., 1990; Rothwell et al., 1994). This could explain the fact that stimulations still induced EMGs activity even on the lesioned side for the foot muscles in the control antibody group while, at C7/C8 level, CST for the hindlimb are sectioned as revealed by the completeness of the dorsolateral funiculus section observed on an horizontal plan on the anatomical reconstructions of the lesion. Importance and role of the ipsilateral pathway in recovery is subjected to debate, contradictory studies showing both evidence and lack of evidence in favor of such role. Anatomical study on intact monkeys at the lumbar level showed that CST tract decussates widely in the dorsolateral pathway (87.9%), however a low proportion decussate in the ventral pathway (0.3%) and the rest (11%) descending in the ipsilateral pathway, in the dorsolateral location (10.1%) and in the ventral location (1%) (Lacroix et al., 2004; Rosenzweig et al., 2010). On intact monkeys, an anatomical study has shown that ipsilateral projections to the spinal cord at the cervical level originates mainly from M1 and supplementary motor area (SMA) (Dum and Strick., 1996) and an electrophysiological study has shown that ipsilateral facilitator projection originates mainly from SMA and also from M1 (Montgomery et al., 2013). However, ipsilateral SMA projections could not be the support of the functional recovery. Effectively, anatomical tracing studies firstly showed enhanced CS projections from SMA on the contralateral

motoneuron location in the grey matter of the spinal cord and not on the ipsilateral following M1 and lateral premotor cortical injury (McNeal et al., 2010). Secondly, transient inactivation of SMA in intact monkeys affected contralateral but not ipsilateral precision grip (Kermadi et al., 1997; Rouiller et al., 1997). Ipsilateral CST axons could be susceptible to have the same anatomical characteristics than the crossed dorsolateral CST axons in term of diameter and myelin layers (Brosalme and Schwab, 2000), thus being able to support the rapid conduction velocity required for the fine manual dexterity. It appeared from some studies that electrical activity of ipsilateral pathways is inhibited in normal condition but is unmasked in lesioned condition, revealing electrical activity in rats and human (Turton et al., 1996; Brus-Ramer at al., 2007; Netz et al., 2007). To support this ipsilateral role in the recovery some authors have shown massive increase of ipsilateral ICMS movements from the intact cortex following cortical injury in anti-Nogo-A antibody treated rats (Emerick et al., 2003) however not associated with an improvement of digit dexterity recovery (Emerick and Kartje, 2004). A recent study showed a lack of evidence for ipsilateral pathways to control EMGs activity of distal hindlimb muscles in healthy adult primate (Stereopoulos et al., 2011). Whereas, following injury, other studies suggest that ipsilateral pathways may contribute to the functional recovery. The disinhibition of the ipsilateral pathway could be due to the loss of the inhibitory transcallosal connectivity at the cortico-cortical level, but also at lower level (Gerolff et al., 1998). Anatomical study has shown sprouting of the ventral ipsilateral CST tract in rat following injury, not attributable to other pathways because bilateral injury of the pyramid was not followed by functional recovery (Weidner et al., 2001). After pyramidal tract lesion in rats, an increase of synaptic connections and total length of ipsilateral axons in the spinal cord were shown, correlated with a higher rate of nerve activity recorded following ipsilateral electrical stimulation of the pyramids (Brus-Ramer et al., 2007). A previous study has shown that a cervical lesion in C7/C8 in monkeys caused a substantial decrease in the ipsilesional M1 hand representation (Schmidlin et al., 2005), suggested to reflect the loss of projections in the ipsilateral pathways. It has been shown that ipsilateral pathways play a modest, but significant, role on the ipsilateral manual dexterity recovery after cortical injury of contralateral M1 in monkeys (Bashir et al., 2012). In human, a TMS study (Netz et al., 1997) has shown that ipsilateral pathways are not excitable in normal subject but are widely excitable in stroke subjects. However, the role of ipsilateral pathways in the recovery is still controversial. Recently, Zaaimi and collaborators (2012) showed a lack of evidence for the role of ipsilateral CST pathways in the functional recovery. Following pyramidal injury, they did not show responses of the hand/forearm motoneurons as a result of the intact pyramid

stimulation. Their results could be explained by the size of the lesion which included the middle part of the second pyramid, possibly containing the ipsilateral CST pathway for hand and forearm. The CST tract originating from M1 and controlling hindlimb muscles tend to become more medial descending through the cerebral peduncle (Morecraft et al., 2007). Amongst others pathways considered to be involved in the functional recovery, some authors have proposed that the reticulospinal tract is the most susceptible to play a role in the recovery after injury, possibly through direct connections (Pettersson et al., 2007; Davidson et al., 2007; Brus-Ramer et al., 2007; Riddle et al., 2009; Stereopoulos et al., 2011) or through propriospinal circuits in the spinal cord (Bareyre et al., 2004). In favor of a role of the ipsilateral tract in the recovery, Brus-Ramer and collaborators (2007) have shown the activation of the reticulospinal tract by electrical stimulation. They have shown that following pyramidal injury, stimulation in the deep radial nerve at threshold produced bilateral non-pyramidal responses attributable to reticulospinal stimulation with shorter latencies than contralateral responses. These results were in accordance with another study conducted by Davidson and Buford (2006) and showing a bilateral motor output from the pontomedullary reticular formation. Our results correlate with a possible activation of the ipsilateral ventral CST pathways and/or reticulospinal pathway after injury with minor modifications of the thresholds and the latencies. Effectively, a recent study on the effects of the combined treatment and the anti-Nogo-A antibody treatment has shown that fibers which grew in the scar were morphologically comparable to motoneurons' axons or to axons of other pathways and not to CS axons (Beaud et al., 2012). It possibly reflects a limit of our protocol of stimulation which was not enough focused with an electrode on the motor cortex and the reference on the frontal cortex. Stimulations have probably activated too widely the cortex and sub-cortical areas, including the brainstem.

Effects of the treatment

The most striking result of this study was the loss of MEPs in the FHB muscles following injury in the combined treated group. In this group, it has been observed a total disappearance in all the lower limb muscles EMGs activity recorded (data not shown). It could reveal not only a lack of effect but also a deleterious effect of the combined treatment. Anti-Nogo-A antibody treatment can induce, in rats and non-human primates, a great improvement of the functional recovery following spinal cord and cortical injury (for review see Pernet and Schwab, 2012). However, beneficial effects of a treatment with BDNF are controversial. In a review, Binder and Scharfman (2004) described BDNF, its role and

signaling pathways, evoking its potential non beneficial effects in contradiction with its neuroprotective role. The differential expression of receptors of Nogo and BDNF molecules can allow us to propose different hypotheses explaining the lack of effect of our combined treatment with BDNF and anti-Nogo-A antibody, in our experimental conditions.

Different isoforms and various expressions of the high affinity BDNF receptor, TrkB, depending on the tissue and the location of expression, modify the effects of this molecule. There is evidence for expression of different isoforms of TrkB receptors depending on the splicing of the protein (Klein et al., 1990; Middlemas et al., 1991). The full-length isoform of TrkB has been described as a trans-membrane protein with a catalytic intracellular domain implicated in the activation of a cascade involved in survival processes (for review Roux and Baker, 2002). Two truncated isoforms of TrkB receptor have been described (Klein et al., 1990) as trans-membrane protein without catalytic C-terminal cytoplasmic domain. Roles of these truncated isoforms are not well described but, in the absence of catalytic domain, a possible role in the internalization of the full-length isoform to regulate the neurotrophin activity by inhibition was suggested by some authors (Middlemas et al., 1991; Eide et al., 1996). The catalytic full-length isoforms of TrkB receptor is expressed on cells' membrane and is implicated in activation of catalytic cascade involved in survival process. It has been shown that, after SCI, expression of the three isoforms of high affinity receptor of neurotrophin, Trk-A, -B, -C, were not modified, except in the epicenter of the lesion where they were totally absent. It results in an increase of the expression of the truncated form of the TrkB receptor in non-neuronal cells in the region surrounding the border of the lesion site (King et al., 2000) and in glial scar after SCI (Frisen et al., 1993). Furthermore, the truncated form of TrkB receptor appeared to act as an inhibitory modulator on neurotrophin responsiveness when one of the different isoform is expressed and forms an heterodimer with the full-length form (Eide et al., 1996). Cells sequester the nonfunctional heterodimers and block BDNF signaling. Isoforms and expression sites of TrkB receptors modify the BDNF effects considering firstly the site of injection and secondly the type of nerve fibers considered. Firstly, it has been observed that the high affinity receptor of BDNF, TrkB, was detectable only on corticospinal neuronal soma and apical dendrites but not on their axon (Lu et al., 2001). Consequently, this point out a correlation between the presence of TrkB receptor on the soma of CS neuron and the neuronal death prevention as well as between absence of TrkB receptor in the corticospinal axons and the inability to promote corticospinal axonal growth for injection of BDNF at the spinal level. In view of these considerations, BDNF injection should be done at the somatic level (for CS neurons at cortical level). Other studies

showed beneficial effect of BDNF on CST axonal sprouting when it was applied at somatic level of the neurons (Vavrek et al., 2006; Zhou and Shine, 2003). This suggests that BDNF infusion site represent an important parameter considering that BDNF is no really susceptible to diffuse in the CNS. This results from the high amount of TrKB receptor and to the presence of an increasing proportion of the truncated form of TrKB receptor expression after lesion (King et al., 2000). Secondly, numerous studies showed an improvement of axonal growth of non-pyramidal tracts, such as the rubrospinal tract, reticulospinal tract, vestibulospinal tract and coeruleus tract (Xu et al., 1995; Bregman et al., 1997; Menei et al., 1998; Liu et al., 1999; Lu et al., 2001; Jin et al., 2002). When Lu and collaborators (Lu et al., 2001) showed a differential effect of BDNF depending on the presence of its receptor TrkB, they also showed that unlike CST other fibers expressed the TrkB receptor. Consequently, BDNF promotes growth of coeruleus axons, local motor (α motoN), and sensory axons but not CST axons. Interestingly, a recent study showed that CST expressed TrkB receptor (Brock et al., 2010). However, they did not differentiate the truncated and the full-length isoforms for the immunolabeling detection of TrkB receptor and, moreover, they shown, as previously, a differential capacity to regenerate: CS axons did not grow into the lesion site, in contrast to raphespinal and cerulospinal axons. Preservation and growth promotion of these pathways, for which nucleus are localized in brainstem, correlates with jump of latencies of PI for combined treated group post-lesion reflecting stimulation at deep anatomical level.

It has been shown that BDNF has differential effects: injected at the cortical level, BDNF has a protective and neurotrophic effect on CS neurons and, injected at the spinal cord level, BDNF has neurotrophic effect on fibers of non-pyramidal origin (Lu et al., 2001) (raphespinal, cerulospinal, reticulospinal, vestibulospinal), promoting their growth and sprouting.

Are there others parameters which could influence the effects of BDNF, such as dose used and time of injection? It has been shown that intrathecal infusion of BDNF at a dose up to 1.5 mg per day for a period of 46 to 63 days in adult sheep did not induce behavioral abnormality, whereas aversive behavioral effects start for doses higher than 2 mg per day (Dittrich et al., 1996). The dose used in our experiment did not appear to be toxic. Kwon and collaborators (2004) showed a lack of BDNF effects on rubrospinal tract recovery independently of the different doses tested. Considering the CST and the TrkB receptor expression, it does not seem that lower dose could have beneficial effects. An optimal time window for BDNF administration appears to present an optimization of the survival effects of BDNF. It has been observed an improvement of motor function recovery and an increase of

axonal growth below the lesion site in rat following spinal cord lesion when the treatment with BDNF was delayed by 2 to 4 weeks post-injury (Coumans et al., 2001). These authors considered serotoninergic and noradrenergic pathways but also the corticospinal pathway. Starting treatment after 4 weeks appeared to be beneficial for survival (Novikova et al., 2000). However, starting treatment 2 month after C3 axotomy showed a lack of effect on rubrospinal tract recovery, even with different doses, when BDNF was applied at the lesion site (Kwon et al., 2004). This was in correlation with the disappearance of the full-length isoform of the TrkB receptor on rubrospinal axons at the lesion site. After 7 days following spinal cord injury, the expression of TrkB receptor on the axotomized rubrospinal axons starts to decrease (Kobayashi et al., 1997). Infusion of BDNF prevents this decrease, indicating that axons could stay responsive during some time, but not after two months due to the loss of TrkB receptors (Kwon et al., 2004). On the other hand, expression of the truncated isoform in glial cells, except microglia, and Schwann cells increases after injury and decreases after 3 weeks (Frisen et al., 1993). These time windows appear to correspond to the time when full-length TrkB receptor is still expressed and the truncated isoform starts to decrease. Taking into consideration the time course of the TrkB different isoforms expression following injury and expression site of these receptors may greatly improve and modify treatment of spinal cord injury with BDNF.

Our results point out not only a lack of effect, but also deleterious effects of this combined BDNF and anti-Nogo-A antibody treatment. Prior to discuss about probable deleterious effect, we have to keep into consideration that the present study assessing effects of combined treatment was the following step of the previous study originally designed to assess effects of anti-Nogo-A antibody treatment on hemi-cord lesion. Thus, because monkeys treated with anti-Nogo-A antibody had exhibited functional recovery close to the pre-lesion level during the previous study and because the aim to assess the effects of a combined treatment was to further improve functional recovery, hemi-cord lesion was done with the intention to extend injury on an horizontal plane. However, experimental protocol implied that a monkey in treated group was tested in parallel with a monkey of the control treated group to guaranty double blind procedure. Then monkeys in the control treatment group had the same lesional procedure, and therefore this could not explain the considerable difference observed for functional recovery and lesion volume between, at least, the control treated group and the combined treated group.

A change in the $p75^{NTR}$ receptor expression following spinal cord injury may be linked with a deleterious effect as the result of the higher volumes of lesion observed and an increase

of the MEPs produced by stimulation at deep anatomical structure for the combined treated group. In spinal cord, neurotrophins involved in the transmission of cellular survival and axonal growth, have been shown to bind the high affinity receptors of the family of the tropomyosin receptor kinase (Trk) and the low affinity receptors of the family of the Tumor Necrosis Factor Receptor (TNFα) (for review Roux and Baker, 2002). In the spinal cord, BDNF links high affinity receptor Trk-B and low affinity receptor p75. Trk-B is a member of the tropomyosin receptor kinase family, with Trk-A binds by NGF and Trk-C binds by NT-3, and is involved in the transmission of cellular survival and growth. $p75^{NTR}$ is a member of the TNFα. In normal conditions, fixation of BDNF on its receptor in spinal cord is increased by the interaction between Trk-B and $p75^{NTR}$ to activate beneficial signalization pathways (Bibel et al., 1999). However, $p75^{NTR}$ is known to have a dual effect (Roux and Barker, 2002). When $p75^{NTR}$ is co-activated with Trk-B receptor, there is activation of the cell survival pathway. Inversely, $p75^{NTR}$ can be linked alone by one of the neurotrophin (*e.g.* NGF, BDNF, NT-3) thus activating a proapoptotic pathway (Wang et al., 2000; Roux and Barker, 2002; Yeiser et al., 2004). King and collaborators (2000) has shown that after spinal cord injury, there was no modification of the expression of Trk-A, -B (full-length) and -C. However, Lu and collaborators (Lu et al., 2001) have shown that monkeys with BDNF-secreting cells graft showed greater $p75^{NTR}$ density on axons and cells in the lesion site. Moreover, King and collaborators (2000) have observed that the normal increase of the $p75^{NTR}$ receptor expression following lesion in the Schwann cells in the lesion site was highly amplified by a BDNF treatment.

$p75^{NTR}$ is also known to be a co-receptor of Nogo-66 Receptor (NgR1) (for review Schwab et al., 2006). NgR1 binds 3 molecules with high affinity: Nogo, MAG and OMpg, involved in the signaling pathway to block axonal growth. In the same manner, as for neurotrophin, Nogo has to form an hetero-multimeric receptor complex with NgR1, and/or with two co-receptors, as $p75^{NTR}$, TROY/TAJ and Lingo-1, to activate cascade of axonal growth blocking (Mingorance et al., 2004). We can suppose that following spinal cord injury, injection of an antibody against Nogo molecule liberates NgR1, hence $p75^{NTR}$. The normal increase of $p75^{NTR}$ receptor expression following injury is highly amplified by the BDNF infusion. Thus injection of high dose of BDNF, even with its normal labeling on receptor Trk-B in its full-length and its elevated truncated isoform, allows fixation of sur-numeral BDNF with $p75^{NTR}$ receptor activating the proapoptotic pathway, thus, increasing the lesion size. This could explain our results showing: higher volumes of lesion and lower percentage of functional recovery; electrophysiological preservation of the IHM in both groups of monkeys,

but a loss of connectivity with the lower limb muscles after lesion in the combined treated group; tendency for the TES to stimulate subcortical structures in the combined treated group.

Conclusion

To conclude, following C7/C8 hemi-cord lesion, we suspected tendency for TES to elicit IHM MEPs at deeper subcortical level, through ipsilateral pathway and/or resulting of a decrease of interhemispheric inhibition on the unlesioned side from the lesioned side. The loss of lower limb muscle MEPs induced by TES in the combined treated monkeys can be linked with a deleterious effect of the combined BDNF and anti-Nogo-A antibody treatment inducing an increase of the lesion size, preventing the functional recovery observed for the anti-Nogo-A antibody treatment alone and increasing the ability of TES to stimulate at deeper subcortical location. This increase in lesion size could affect the ipsilateral pathways possibly implicated in the recovery following injury.

References

Bareyre, F. M., Kerschensteiner, M., Raineteau, O., Mettenleiter, T. C., Weinmann, O. & Schwab, M. E. (2004). The injured spinal cord spontaneously forms a new intraspinal circuit in adult rats. *Nat.Neurosci.,* 7, 269-277.

Bashir, S., Kaeser, M., Wyss, A., Hamadjida, A., Liu, Y., Bloch, J., Brunet, J. F., Belhaj-Saif, A. & Rouiller, E. M. (2012). Short-term effects of unilateral lesion of the primary motor cortex (M1) on ipsilesional hand dexterity in adult macaque monkeys. *Brain Struct.Funct.,* 217, 63-79.

Beaud, M. L., Schmidlin, E., Wannier, T., Freund, P., Bloch, J., Mir, A., Schwab, M. E. & Rouiller, E. M. (2008). Anti-Nogo-A antibody treatment does not prevent cell body shrinkage in the motor cortex in adult monkeys subjected to unilateral cervical cord lesion. *BMC.Neurosci.,* 9, 5.

Beaud, M. L. (2011). Anatomical organisation and functional recovery in spinal injured non-human primates treated with either an antibody against Nogo-A or a combination of this antibody with brain-derived neurotrophic factor (BDNF). Thesis, University of Fribourg.

Beaud, M. L., Rouiller, E. M., Bloch, J., Mir, A., Schwab, M. E., Wannier, T. & Schmidlin, E. (2012). Invasion of lesion territory by regenerating fibers after spinal cord injury in adult macaque monkeys. *Neuroscience,* 227C, 271-282.

Bibel, M., Hoppe, E. & Barde, Y. A. (1999). Biochemical and functional interactions between the neurotrophin receptors trk and p75NTR. *EMBO J.,* 18, 616-622.

Binder, D. K. & Scharfman, H. E. (2004). Brain-derived neurotrophic factor. *Growth Factors,* 22, 123-131.

Boyd, S. G., Rothwell, J. C., Cowan, J. M., Webb, P. J., Morley, T., Asselman, P. & Marsden, C. D. (1986). A method of monitoring function in corticospinal pathways during scoliosis surgery with a note on motor conduction velocities. *J.Neurol.Neurosurg.Psychiatry,* 49, 251-257.

Bregman, B. S., McAtee, M., Dai, H. N. & Kuhn, P. L. (1997). Neurotrophic factors increase axonal growth after spinal cord injury and transplantation in the adult rat. *Exp.Neurol.,* 148, 475-494.

Brock, J. H., Rosenzweig, E. S., Blesch, A., Moseanko, R., Havton, L. A., Edgerton, V. R. & Tuszynski, M. H. (2010). Local and remote growth factor effects after primate spinal cord injury. *Journal of Neuroscience,* 30, 9728-9737.

Brooks, C. M. & Eccles, J. C. (1947). A study of the effects of anaesthesia and asphyxia on the monosynaptic pathway through the spinal cord. *J.Neurophysiol.,* 10, 349-360.

Brosamle, C. & Schwab, M. E. (2000). Ipsilateral, ventral corticospinal tract of the adult rat: ultrastructure, myelination and synaptic connections. *J.Neurocytol.,* 29, 499-507.

Browning, J. L., Heizer, M. L. & Baskin, D. S. (1992). Variations in corticomotor and somatosensory evoked potentials: effects of temperature, halothane anesthesia, and arterial partial pressure of CO2. *Anesth.Analg.,* 74, 643-648.

Brus-Ramer, M., Carmel, J. B., Chakrabarty, S. & Martin, J. H. (2007). Electrical stimulation of spared corticospinal axons augments connections with ipsilateral spinal motor circuits after injury. *Journal of Neuroscience,* 27, 13793-13801.

Buchli, A. D. & Schwab, M. E. (2005). Inhibition of Nogo: a key strategy to increase regeneration, plasticity and functional recovery of the lesioned central nervous system. *Ann.Med.,* 37, 556-567.

Burke, D., Hicks, R. G. & Stephen, J. P. (1990). Corticospinal volleys evoked by anodal and cathodal stimulation of the human motor cortex. *J.Physiol,* 425, 283-299.

Burke, D., Hicks, R., Gandevia, S. C., Stephen, J., Woodforth, I. & Crawford, M. (1993). Direct comparison of corticospinal volleys in human subjects to transcranial magnetic and electrical stimulation. *J.Physiol,* 470, 383-393.

Calancie, B., Nordin, M., Wallin, U. & Hagbarth, K. E. (1987). Motor-unit responses in human wrist flexor and extensor muscles to transcranial cortical stimuli. *J.Neurophysiol.*, 58, 1168-1185.

Calancie, B., Harris, W., Broton, J. G., Alexeeva, N. & Green, B. A. (1998). "Threshold-level" multipulse transcranial electrical stimulation of motor cortex for intraoperative monitoring of spinal motor tracts: description of method and comparison to somatosensory evoked potential monitoring. *J.Neurosurg.,* 88, 457-470.

Canedo, A. & Lamas, J. A. (1993). Pyramidal and corticospinal synaptic effects over reticulospinal neurones in the cat. *J.Physiol,* 463, 475-489.

Caroni, P., Savio, T. & Schwab, M. E. (1988). Central nervous system regeneration: oligodendrocytes and myelin as non-permissive substrates for neurite growth. *Prog.Brain Res.*, 78, 363-370.

Chen, M. S., Huber, A. B., Van der Haar, M. E., Franck, M., Schnell, L., Spillmann, A. A., Christ, F. & Schwab, M. E. (2000). Nogo-A is a myelin-associated neurite outgrowth inhibitor and an antigen for monoclonal antibody IN-1. *Nature,* 403, 434-438.

Clark, A. J., Ziewacz, J. E., Safaee, M., Lau, D., Lyon, R., Chou, D., Weinstein, P. R., Ames, C. P., Clark, J. P., III & Mummaneni, P. V. (2013). Intraoperative neuromonitoring with MEPs and prediction of postoperative neurological deficits in patients undergoing surgery for cervical and cervicothoracic myelopathy. *Neurosurg.Focus.*, 35, E7.

Coumans, J. V., Lin, T. T., Dai, H. N., MacArthur, L., McAtee, M., Nash, C. & Bregman, B. S. (2001). Axonal regeneration and functional recovery after complete spinal cord transection in rats by delayed treatment with transplants and neurotrophins. *Journal of Neuroscience,* 21, 9334-9344.

Davidson, A. G. & Buford, J. A. (2006). Bilateral actions of the reticulospinal tract on arm and shoulder muscles in the monkey: stimulus triggered averaging. *Experimental Brain Research,* 173, 25-39.

Davidson, A. G., Schieber, M. H. & Buford, J. A. (2007). Bilateral spike-triggered average effects in arm and shoulder muscles from the monkey pontomedullary reticular formation. *Journal of Neuroscience,* 27, 8053-8058.

Day, B. L., Dressler, D., Maertens de, N. A., Marsden, C. D., Nakashima, K., Rothwell, J. C. & Thompson, P. D. (1989). Electric and magnetic stimulation of human motor cortex: surface EMG and single motor unit responses. *J.Physiol,* 412, 449-473.

Deletis, V. & Sala, F. (2008). Intraoperative neurophysiological monitoring of the spinal cord during spinal cord and spine surgery: a review focus on the corticospinal tracts. *Clin.Neurophysiol.*, 119, 248-264.

Di, L., V, Oliviero, A., Profice, P., Insola, A., Mazzone, P., Tonali, P. & Rothwell, J. C. (1999). Direct demonstration of interhemispheric inhibition of the human motor cortex produced by transcranial magnetic stimulation. *Experimental Brain Research,* 124, 520-524.

Di, L., V, Oliviero, A., Profice, P., Pennisi, M. A., Pilato, F., Zito, G., Dileone, M., Nicoletti, R., Pasqualetti, P. & Tonali, P. A. (2003). Ketamine increases human motor cortex excitability to transcranial magnetic stimulation. *J.Physiol,* 547, 485-496.

Dittrich, F., Ochs, G., Grosse-Wilde, A., Berweiler, U., Yan, Q., Miller, J. A., Toyka, K. V. & Sendtner, M. (1996). Pharmacokinetics of intrathecally applied BDNF and effects on spinal motoneurons. *Exp.Neurol.*, 141, 225-239.

Dum, R. P. & Strick, P. L. (1996). Spinal cord terminations of the medial wall motor areas in macaque monkeys. *Journal of Neuroscience,* 16, 6513-6525.

Edgley, S. A., Eyre, J. A., Lemon, R. N. & Miller, S. (1990). Excitation of the corticospinal tract by electromagnetic and electrical stimulation of the scalp in the macaque monkey. *J.Physiol,* 425, 301-320.

Edgley, S. A., Eyre, J. A., Lemon, R. N. & Miller, S. (1997). Comparison of activation of corticospinal neurons and spinal motor neurons by magnetic and electrical transcranial stimulation in the lumbosacral cord of the anaesthetized monkey. *Brain,* 120 (Pt 5), 839-853.

Eide, F. F., Vining, E. R., Eide, B. L., Zang, K., Wang, X. Y. & Reichardt, L. F. (1996). Naturally occurring truncated trkB receptors have dominant inhibitory effects on brain-derived neurotrophic factor signaling. *Journal of Neuroscience,* 16, 3123-3129.

Emerick, A. J., Neafsey, E. J., Schwab, M. E. & Kartje, G. L. (2003). Functional reorganization of the motor cortex in adult rats after cortical lesion and treatment with monoclonal antibody IN-1. *Journal of Neuroscience,* 23, 4826-4830.

Emerick, A. J. & Kartje, G. L. (2004). Behavioral recovery and anatomical plasticity in adult rats after cortical lesion and treatment with monoclonal antibody IN-1. *Behavioural Brain Research,* 152, 315-325.

Fouad, K., Klusman, I. & Schwab, M. E. (2004). Regenerating corticospinal fibers in the Marmoset (*Callitrix jacchus*) after spinal cord lesion and treatment with the anti-Nogo-A antibody IN-1. *European Journal of Neuroscience,* 20, 2479-2482.

Fournier, A. E., GrandPré, T. & Strittmatter, S. M. (2001). Identification of a receptor mediating Nogo-66 inhibition of axonal regeneration. *Nature.,* 409, 341-346.

Freund, P., Schmidlin, E., Wannier, T., Bloch, J., Mir, A., Schwab, M. E. & Rouiller, E. M. (2006). Nogo-A-specific antibody treatment enhances sprouting and functional recovery after cervical lesion in adult primates. *Nature Medicine,* 12, 790-792.

Freund, P., Wannier, T., Schmidlin, E., Bloch, J., Mir, A., Schwab, M. E. & Rouiller, E. M. (2007). Anti-Nogo-A antibody treatment enhances sprouting of corticospinal axons rostral to a unilateral cervical spinal cord lesion in adult macaque monkey. *J Comp Neurol,* 502, 644-659.

Freund, P., Schmidlin, E., Wannier, T., Bloch, J., Mir, A., Schwab, M. E. & Rouiller, E. M. (2009). Anti-Nogo-A antibody treatment promotes recovery of manual dexterity after unilateral cervical lesion in adult primates--re-examination and extension of behavioral data. *European Journal of Neuroscience,* 29, 983-996.

Frisen, J., Verge, V. M., Fried, K., Risling, M., Persson, H., Trotter, J., Hokfelt, T. & Lindholm, D. (1993). Characterization of glial trkB receptors: differential response to injury in the central and peripheral nervous systems. *Proc.Natl.Acad.Sci.U.S.A,* 90, 4971-4975.

Fulkerson, D. H., Satyan, K. B., Wilder, L. M., Riviello, J. J., Stayer, S. A., Whitehead, W. E., Curry, D. J., Dauser, R. C., Luerssen, T. G. & Jea, A. (2011). Intraoperative monitoring of motor evoked potentials in very young children. *J.Neurosurg.Pediatr.,* 7, 331-337.

Gerloff, C., Cohen, L. G., Floeter, M. K., Chen, R., Corwell, B. & Hallett, M. (1998). Inhibitory influence of the ipsilateral motor cortex on responses to stimulation of the human cortex and pyramidal tract. *J.Physiol,* 510 (Pt 1), 249-259.

GrandPre, T., Li, S. & Strittmatter, S. M. (2002). Nogo-66 receptor antagonist peptide promotes axonal regeneration. *Nature,* 417, 547-551.

GrandPré, T., Nakamura, F., Vartanian, T. & Strittmatter, S. M. (2000). Identification of the NOGO inhibitor of axon regeneration as a reticulon protein. *Nature,* 403, 439-444.

Hoogewoud, F., Hamadjida, A., Wyss, A. F., Mir, A., Schwab, M. E., Belhaj-Saif, A. & Rouiller, E. M. (2013). Comparison of functional recovery of manual dexterity after

unilateral spinal cord lesion or motor cortex lesion in adult macaque monkeys. *Front Neurol.*, 4, 101.

Jenny, A. B. & Inukai, J. (1983). Principles of motor organization of the monkey cervical spinal cord. *Journal of Neuroscience*, 3, 567-575.

Jin, Y., Fischer, I., Tessler, A. & Houle, J. D. (2002). Transplants of fibroblasts genetically modified to express BDNF promote axonal regeneration from supraspinal neurons following chronic spinal cord injury. *Exp.Neurol.*, 177, 265-275.

Katz, B. & Miledi, R. (1965). The measurement of synaptic delay, and the time course of acetylcholine release at the neuromuscular junction. *Proc.R.Soc.Lond B Biol.Sci.*, 161, 483-495.

Kermadi, I., Liu, Y., Tempini, A. & Rouiller, E. M. (1997). Effects of reversible inactivation of the supplementary motor area (SMA) on unimanual grasp and bimanual pull and grasp performance in monkeys. *Somatosens.Mot.Res.*, 14, 268-280.

Kim, S. M., Yang, H., Park, S. B., Han, S. G., Park, K. W., Yoon, S. H., Hyun, S. J., Kim, H. J., Park, K. S. & Lee, K. W. (2012). Pattern-specific changes and discordant prognostic values of individual leg-muscle motor evoked potentials during spinal surgery. *Clin.Neurophysiol.*, 123, 1465-1470.

King, V. R., Bradbury, E. J., McMahon, S. B. & Priestley, J. V. (2000). Changes in truncated trkB and p75 receptor expression in the rat spinal cord following spinal cord hemisection and spinal cord hemisection plus neurotrophin treatment. *Exp.Neurol.*, 165, 327-341.

Klein, R., Conway, D., Parada, L. F. & Barbacid, M. (1990). The trkB tyrosine protein kinase gene codes for a second neurogenic receptor that lacks the catalytic kinase domain. *Cell*, 61, 647-656.

Kobayashi, N. R., Fan, D. P., Giehl, K. M., Bedard, A. M., Wiegand, S. J. & Tetzlaff, W. (1997). BDNF and NT-4/5 prevent atrophy of rat rubrospinal neurons after cervical axotomy, stimulate GAP-43 and Talpha1-tubulin mRNA expression, and promote axonal regeneration. *Journal of Neuroscience*, 17, 9583-9595.

Kwon, B. K., Liu, J., Oschipok, L., Teh, J., Liu, Z. W. & Tetzlaff, W. (2004). Rubrospinal neurons fail to respond to brain-derived neurotrophic factor applied to the spinal cord injury site 2 months after cervical axotomy. *Exp.Neurol.*, 189, 45-57.

Lacroix, S., Havton, L. A., McKay, H., Yang, H., Brant, A., Roberts, J. & Tuszynski, M. H. (2004). Bilateral corticospinal projections arise from each motor cortex in the macaque monkey: A quantitative study. *Journal of Comparative Neurology*, 473, 147-161.

Lee, J. K., Kim, J. E., Sivula, M. & Strittmatter, S. M. (2004). Nogo receptor antagonism promotes stroke recovery by enhancing axonal plasticity. *Journal of Neuroscience*, 24, 6209-6217.

Li, S. & Strittmatter, S. M. (2003). Delayed systemic Nogo-66 receptor antagonist promotes recovery from spinal cord injury. *Journal of Neuroscience*, 23, 4219-4227.

Liu, Y. & Rouiller, E. M. (1999). Mechanisms of recovery of dexterity following unilateral lesion of the sensorimotor cortex in adult monkeys. *Experimental Brain Research*, 128, 149-159.

Liu, Y., Kim, D., Himes, B. T., Chow, S. Y., Schallert, T., Murray, M., Tessler, A. & Fischer, I. (1999). Transplants of fibroblasts genetically modified to express BDNF promote regeneration of adult rat rubrospinal axons and recovery of forelimb function. *Journal of Neuroscience*, 19, 4370-4387.

Lu, P., Blesch, A. & Tuszynski, M. H. (2001). Neurotrophism without neurotropism: BDNF promotes survival but not growth of lesioned corticospinal neurons 1. *J.Comp Neurol.*, 436, 456-470.

Lu, P. & Tuszynski, M. H. (2008). Growth factors and combinatorial therapies for CNS regeneration. *Exp.Neurol.*, 209, 313-320.

McNeal, D. W., Darling, W. G., Ge, J., Stilwell-Morecraft, K. S., Solon, K. M., Hynes, S. M., Pizzimenti, M. A., Rotella, D. L., Vanadurongvan, T. & Morecraft, R. J. (2010). Selective long-term reorganization of the corticospinal projection from the supplementary motor cortex following recovery from lateral motor cortex injury. *J.Comp Neurol*, 518, 586-621.

Menei, P., Montero-Menei, C., Whittemore, S. R., Bunge, R. P. & Bunge, M. B. (1998). Schwann cells genetically modified to secrete human BDNF promote enhanced axonal regrowth across transected adult rat spinal cord. *European Journal of Neuroscience*, 10, 607-621.

Merton, P. A. & Morton, H. B. (1980). Electrical-stimulation of human motor and visual-cortex through the scalp. *Journal of Physiology* 305, 9-10.

Meylaerts, S. A., De, H. P., Kalkman, C. J., Lips, J., De Mol, B. A. & Jacobs, M. J. (1999). The influence of regional spinal cord hypothermia on transcranial myogenic motor-evoked potential monitoring and the efficacy of spinal cord ischemia detection. *J.Thorac.Cardiovasc.Surg.*, 118, 1038-1045.

Middlemas, D. S., Lindberg, R. A. & Hunter, T. (1991). trkB, a neural receptor protein-tyrosine kinase: evidence for a full-length and two truncated receptors. *Mol.Cell Biol.*, 11, 143-153.

Mingorance, A., Seriano, E. & del Rio, J. A. (2004). Nogo, myelin and axonal regeneration. *Contributions to Science*, 2, 499-512.

Montgomery, L. R., Herbert, W. J. & Buford, J. A. (2013). Recruitment of ipsilateral and contralateral upper limb muscles following stimulation of the cortical motor areas in the monkey. *Experimental Brain Research*, 230, 153-164.

Morecraft, R. J., McNeal, D. W., Stilwell-Morecraft, K. S., Dvanajscak, Z., Ge, J. & Schneider, P. (2007). Localization of arm representation in the cerebral peduncle of the non-human primate. *J.Comp Neurol.*, 504, 149-167.

Nagahara, A. H. & Tuszynski, M. H. (2011). Potential therapeutic uses of BDNF in neurological and psychiatric disorders. *Nat.Rev.Drug Discov.*, 10, 209-219.

Nash, M., Pribiag, H., Fournier, A. E. & Jacobson, C. (2009). Central nervous system regeneration inhibitors and their intracellular substrates. *Mol.Neurobiol.*, 40, 224-235.

Netz, J., Lammers, T. & Homberg, V. (1997). Reorganization of motor output in the non-affected hemisphere after stroke. *Brain*, 120 (Pt 9), 1579-1586.

Novikova, L. N., Novikov, L. N. & Kellerth, J. O. (2000). Survival effects of BDNF and NT-3 on axotomized rubrospinal neurons depend on the temporal pattern of neurotrophin administration. *European Journal of Neuroscience*, 12, 776-780.

Nuwer, M. R., Emerson, R. G., Galloway, G., Legatt, A. D., Lopez, J., Minahan, R., Yamada, T., Goodin, D. S., Armon, C., Chaudhry, V., Gronseth, G. S. & Harden, C. L. (2012). Evidence-based guideline update: intraoperative spinal monitoring with somatosensory and transcranial electrical motor evoked potentials: report of the Therapeutics and Technology Assessment Subcommittee of the American Academy of Neurology and the American Clinical Neurophysiology Society. *Neurology*, 78, 585-589.

Papadopoulos, C. M., Tsai, S. Y., Alsbiei, T., O'Brien, T. E., Schwab, M. E. & Kartje, G. L. (2002). Functional recovery and neuroanatomical plasticity following middle cerebral artery occlusion and IN-1 antibody treatment in the adult rat. *Annals of Neurology*, 51, 433-441.

Patton, H. D. & Amassian, V. E. (1954). Single and multiple-unit analysis of cortical stage of pyramidal tract activation. *J.Neurophysiol.*, 17, 345-363.

Pernet, V. & Schwab, M. E. (2012). The role of Nogo-A in axonal plasticity, regrowth and repair. *Cell and Tissue Research,* 349, 97-104.

Pettersson, L. G., Alstermark, B., Blagovechtchenski, E., Isa, T. & Sasaski, S. (2007). Skilled digit movements in feline and primate--recovery after selective spinal cord lesions. *Acta Physiol (Oxf),* 189, 141-154.

Riddle, C. N., Edgley, S. A. & Baker, S. N. (2009). Direct and indirect connections with upper limb motoneurons from the primate reticulospinal tract. *Journal of Neuroscience,* 29, 4993-4999.

Rosenzweig, E. S., Courtine, G., Jindrich, D. L., Brock, J. H., Ferguson, A. R., Strand, S. C., Nout, Y. S., Roy, R. R., Miller, D. M., Beattie, M. S., Havton, L. A., Bresnahan, J. C., Edgerton, V. R. & Tuszynski, M. H. (2010). Extensive spontaneous plasticity of corticospinal projections after primate spinal cord injury. *Nat.Neurosci.,* 13, 1505-1510.

Rothwell, J., Burke, D., Hicks, R., Stephen, J., Woodforth, I. & Crawford, M. (1994). Transcranial electrical stimulation of the motor cortex in man: further evidence for the site of activation. *J.Physiol,* 481 (Pt 1), 243-250.

Rouiller, E. M., Babalian, A., Kazennikov, O., Moret, V., Yu, X. H. & Wiesendanger, M. (1994). Transcallosal connections of the distal forelimb representations of the primary and supplementary motor cortical areas in macaque monkeys. *Experimental Brain Research,* 102, 227-243.

Rouiller, E. M., Yu, X.-H. & Tampini, A. (1997). Effect of Inactivation of the Hand Representation of the Primary and Supplementary Motor Cortical Areas on Precision Grip Performance in Monkeys. In M. G. e. Hepp-Reymond M-C (Ed) *Perspectives of Motor Behavior and Its Neural Basis* (pp. 33-43). Basel: Karger.

Roux, P. P. & Barker, P. A. (2002). Neurotrophin signaling through the p75 neurotrophin receptor. *Prog.Neurobiol.,* 67, 203-233.

Schmidlin, E., Wannier, T., Bloch, J. & Rouiller, E. M. (2004). Progressive plastic changes in the hand representation of the primary motor cortex parallel incomplete recovery from a unilateral section of the corticospinal tract at cervical level in monkeys. *Brain Res.,* 1017, 172-183.

Schmidlin, E., Wannier, T., Bloch, J., Belhaj-Saif, A., Wyss, A. F. & Rouiller, E. M. (2005). Reduction of the hand representation in the ipsilateral primary motor cortex following unilateral section of the corticospinal tract at cervical level in monkeys. *BMC.Neurosci.,* 6, 56.

Schmidlin, E., Kaeser, M., Gindrat, A. D., Savidan, J., Chatagny, P., Badoud, S., Hamadjida, A., Beaud, M. L., Wannier, T., Belhaj-Saif, A. & Rouiller, E. M. (2011). Behavioral assessment of manual dexterity in non-human primates. *J.Vis.Exp.*.

Schnell, L. & Schwab, M. E. (1993). Sprouting and regeneration of lesioned corticospinal tract fibres in the adult rat spinal cord. *European Journal of Neuroscience,* 5, 1156-1171.

Schwab, J. M., Tuli, S. K. & Failli, V. (2006). The Nogo receptor complex: confining molecules to molecular mechanisms. *Trends Mol.Med.,* 12, 293-297.

Schwab, M. E. & Strittmatter, S. M. (2014). Nogo limits neural plasticity and recovery from injury. *Curr.Opin.Neurobiol.,* 27, 53-60.

Sloan, T. (2002). Anesthesia and Motor Evoked-Potentials Monitoring. In V Deletisand J Shills (eds) (Ed) *Neurophysiology in Neurosurgery* (pp. 451-464). San Diego: Academic Press.

Sloan, T. & Rogers, J. (2009). Dose and timing effect of etomidate on motor evoked potentials elicited by transcranial electric or magnetic stimulation in the monkey and baboon. *J.Clin.Monit.Comput.,* 23, 253-261.

Sloan, T. & Rogers, J. (2009). Differential effect of halothane on motor evoked potentials elicited by transcranial electric or magnetic stimulation in the monkey. *J.Clin.Monit.Comput.,* 23, 163-168.

Soteropoulos, D. S., Edgley, S. A. & Baker, S. N. (2011). Lack of evidence for direct corticospinal contributions to control of the ipsilateral forelimb in monkey. *Journal of Neuroscience,* 31, 11208-11219.

Thallmair, M., Metz, G. A. S., Z'Graggen, W. J., Raineteau, O., Kartje, G. L. & Schwab, M. E. (1998). Neurite growth inhibitors restrict plasticity and functional recovery following corticospinal tract lesions. *Nature Neurosci.,* 1, 124-131.

Tsutsui, S., Tamaki, T., Yamada, H., Iwasaki, H. & Takami, M. (2003). Relationships between the changes in compound muscle action potentials and selective injuries to the spinal cord and spinal nerve roots. *Clin.Neurophysiol.,* 114, 1431-1436.

Turton, A., Wroe, S., Trepte, N., Fraser, C. & Lemon, R. N. (1996). Contralateral and ipsilateral EMC responses to transcranial magnetic stimulation during recovery of arm and hand function after stroke. *Electroencephalogr.Clin.Neurophysiol.Electromyogr.Motor Control,* 101, 316-328.

Vavrek, R., Girgis, J., Tetzlaff, W., Hiebert, G. W. & Fouad, K. (2006). BDNF promotes connections of corticospinal neurons onto spared descending interneurons in spinal cord injured rats. *Brain,* 129, 1534-1545.

Wang, S., Bray, P., McCaffrey, T., March, K., Hempstead, B. L. & Kraemer, R. (2000). p75(NTR) mediates neurotrophin-induced apoptosis of vascular smooth muscle cells. *Am.J.Pathol.,* 157, 1247-1258.

Wang, T., Xiong, J. Q., Ren, X. B. & Sun, W. (2012). The role of Nogo-A in neuroregeneration: A review. *Brain Res Bull.,* 87, 499-503.

Wannier-Morino, P., Schmidlin, E., Freund, P., Belhaj-Saif, A., Bloch, J., Mir, A., Schwab, M. E., Rouiller, E. M. & Wannier, T. (2008). Fate of rubrospinal neurons after unilateral section of the cervical spinal cord in adult macaque monkeys: effects of an antibody treatment neutralizing Nogo-A. *Brain Res.,* 1217, 96-109.

Wannier, T., Schmidlin, E., Bloch, J. & Rouiller, E. M. (2005). A unilateral section of the corticospinal tract at cervical level in primate does not lead to measurable cell loss in motor cortex. *Journal of Neurotrauma,* 22, 703-717.

Weidner, N., Ner, A., Salimi, N. & Tuszynski, M. H. (2001). Spontaneous corticospinal axonal plasticity and functional recovery after adult central nervous system injury. Proc.Natl.Acad.Sci.U.S.A, 98, 3513-3518.

Weinmann, O., Schnell, L., Ghosh, A., Montani, L., Wiessner, C., Wannier, T., Rouiller, E., Mir, A. & Schwab, M. E. (2006). Intrathecally infused antibodies against Nogo-A penetrate the CNS and downregulate the endogenous neurite growth inhibitor Nogo-A. *Mol.Cell Neurosci.,* 32, 161-173.

Wyss, A. F., Hamadjida, A., Savidan, J., Liu, Y., Bashir, S., Mir, A., Schwab, M. E., Rouiller, E. M. & Belhaj-Saif, A. (2013). Long-term motor cortical map changes following unilateral lesion of the hand representation in the motor cortex in macaque monkeys showing functional recovery of hand functions. *Restor.Neurol.Neurosci.,* 31, 733-760.

Xu, X. M., Guenard, V., Kleitman, N., Aebischer, P. & Bunge, M. B. (1995). A combination of BDNF and NT-3 promotes supraspinal axonal regeneration into Schwann cell grafts in adult rat thoracic spinal cord. *Exp.Neurol.,* 134, 261-272.

Yeiser, E. C., Rutkoski, N. J., Naito, A., Inoue, J. & Carter, B. D. (2004). Neurotrophin signaling through the p75 receptor is deficient in traf6-/- mice. *Journal of Neuroscience,* 24, 10521-10529.

Zaaimi, B., Edgley, S. A., Soteropoulos, D. S. & Baker, S. N. (2012). Changes in descending motor pathway connectivity after corticospinal tract lesion in macaque monkey. *Brain,* 135, 2277-2289.

Zhou, L. & Shine, H. D. (2003). Neurotrophic factors expressed in both cortex and spinal cord induce axonal plasticity after spinal cord injury. *J.Neurosci.Res.,* 74, 221-226.

Zorner, B. & Schwab, M. E. (2010). Anti-Nogo on the go: from animal models to a clinical trial. *Ann.N.Y.Acad.Sci.,* 1198 Suppl 1, E22-E34.

Figures

Name	Sex	Species	Weight	Hemi-spinal lesion side	Treatment	Concentration	Volume of pumps (ml)	Pump removal (days after implantation)	Survival time with respect to lesion day (J0)
Mk-CGa	male	fascicularis	3	right	Control antiboby	7mg/ml	2	J+29	J+156
Mk-CBo	male	fascicularis	3.5	right	Control antiboby	7mg/ml	2	J+27	J+192
Mk-ABB	male	fascicularis	5.3	right	BDNF & hNogo-A	18 mg/ml 0.7 mg/ml	2	J+27	J+167
Mk-ABMa	male	fascicularis	3.4	right	BDNF & hNogo-A	18 mg/ml 0.7 mg/ml	2	J+29	J+148
Mk-ABMx	male	fascicularis	5	left	BDNF & hNogo-A	18 mg/ml 0.7 mg/ml	2	J+31	J+258
Mk-ABR	male	fascicularis	4	left	BDNF & hNogo-A	18 mg/ml 0.7 mg/ml	2	J+31	J+125

Table 1.: Summary of animals.

Recapitulative table, presenting the characteristics of each monkey and their treatments. Mk-C corresponds to the control antibody treated group and Mk-AB to the combined treated group (anti-Nogo-A and BDNF treatment), highlight in grey. J+ correspond to the number of days from the lesion day (J_0).

A-

		PreL				PostL			
		FHB		IHM		FHB		IHM	
		Left muscles	Right muscles	Left muscles	Right muscles	Left muscles	Right muscles	Left muscles	Right muscles
MK-CGa	Threshold	H=5.256, df=3, P=0.154	H=1.827, df=3, P=0.609	H=5.620, df=3, P=0.132	H=3.868, df=3, P=0.276	H=5.326, df=3, P=0.149	H=3.115, df=3, P=0.374	**H=8.177, df=3, P=0.042**	H=1.442, df=3, P=0.696
	Latencies	H=1.104, df=3, P=0.776	H=1.133, df=3, P=0.769	H=4.285, df=3, P=0.232	H=1.670, df=3, P=0.644	H=2.220, df=3, P=0.528	H=2.173, df=3, P=0.537	H=1.399, df=3, P=0.706	H=2.097, df=3, P=0.553
MK-CBo	Threshold	H=3.789, df=3, $P_{(exact)}$=0.400	H=2.777, df=3, P=0.427	H=3.093, df=3, P=0.378	H=4.964, df=3, $P_{(exact)}$=0.124	NA	H=1.741, df=3, P=0.628	H=3.037, df=3, P=0.386	H=5.542, df=3, P=0.136
	Latencies	H=3.200, df=3, P=0.700	H=7.472, df=3, P=0.058	H=1.866, df=3, P=0.601	H=0.321, df=3, $P_{(exact)}$=0.971	NA	H=232, df=3, P=0.972	H=0.479, df=3, P=0.924	H=1.371, df=3, P=0.712
MK-ABB	Threshold	H=3.090, df=3, P=0.378	H=3.457, df=3, P=0.326	H=2.370, df=3, P=0.499	H=6.249, df=3, P=0.100	H=2.005, df=3, P=0.571	NA	H=7.200, df=3, P=0.066	H=3.015, df=3, P=0.389
	Latencies	H=1.476, df=3, P=0.688	H=2.268, df=3, P=519	H=0.379, df=3, P=0.945	H=1.837, df=3, P=0.607	H=0.928, df=3, P=0.819	NA	H=2.048, df=3, P=0.563	H=2.142, df=3, P=0.544
MK-ABMa	Threshold	H=2.034, df=3, P=0.565	H=3.377, df=3, P=0.337	H=0.843, df=3, P=0.843	H=1.693, df=3, P=0.638	H=1.514, df=3, P=0.679	NA	H=0.529, df=3, P=0.913	H=3.091, df=3, P=0.378
	Latencies	H=0.739, df=3, P=0.864	H=2.410, df=3, P=0.492	H=1.706, df=3, P=0.636	H=0.395, df=3, P=0.941	H=0.939, df=3, P=0.816	NA	H=0.645, df=3, P=0.886	H=0.550, df=3, P=0.908

B-

		PreL				PostL			
		FHB		IHM		FHB		IHM	
		Left muscles	Right muscles	Left muscles	Right muscles	Left muscles	Right muscles	Left muscles	Right muscles
MK-CGa	50dbl	NA	NA	H=4.648, df=3, P=0.199	NA	NA	NA	H=1.570, df=3, P=0.666	H=0.661, df=3, P=0.882
	100	H=1.392, df=3, $P_{(exact)}$=0.771	H=2.226, df=3, $P_{(exact)}$=0.604	H=2.643, df=3, P=0.450	H=0.410, df=3, $P_{(exact)}$=0.961	H=3.956, df=3, P=0.266	H=3.127, df=3, $P_{(exact)}$=0.488	H=2.900, df=3, P=0.407	H=3.011, df=3, P=0.390
	100dbl	H=2.146, df=3, P=0.543	H=2.231, df=3, P=0.526	**H=8.661, df=3, P=0.034**	H=0.51, df=3, P=0.919	H=4.887, df=3, P=0.180	H=3.051, df=3, $P_{(exact)}$=0.453	H=0.841, df=3, P=0.840	H=0.147, df=3, P=0.986
	250	H=3.830, df=3, P=0.280	H=4.238, df=3, P=0.237	**H=8.023, df=3, P=0.046**	H=6.090, df=3, P=0.107	H=2.972, df=3, P=0.396	H=3.826, df=3, P=0.281	H=1.942, df=3, P=0.585	H=0.395, df=3, P=0.941
MK-CBo	50dbl	NA	NA	H=3.053, df=3, P=0.284	NA	NA	NA	H=1.598, df=3, P=0.660	H=2.667, df=3, P=0.446
	100	H=3.789, df=3, $P_{(exact)}$=0.400	NA	H=3.085, df=3, P=0.379	H=1.450, df=3, P=0.694	NA	H=0.178, df=3, $P_{(exact)}$=0.992	H=2.744, df=3, P=0.433	H=2.801, df=3, P=0.423
	100dbl	H=3.800, df=3, P=0.400	H=3.956, df=3, $P_{(exact)}$=0.309	H=0.663, df=3, P=0.882	H=2.210, df=3, P=0.530	NA	H=0.901, df=3, $P_{(exact)}$=0.853	H=0.0427, df=3, P=0.998	H=1.144, df=3, P=0.766
	250	H=3.200, df=3, $P_{(exact)}$=0.700	H=0.980, df=3, $P_{(exact)}$=0.844	H=0.746, df=3, P=0.862	H=4.592, df=3, P=0.204	NA	H=1.750, df=3, P=0.626	H=4.584, df=3, P=0.205	H=0.850, df=3, P=0.837
MK-ABB	50dbl	NA	NA	H=2.524, df=3, $P_{(exact)}$=0.800	H=1.750, df=3, $P_{(exact)}$=0.857	H=4.500, df=3, $P_{(exact)}$=0.217	NA	H=2.198, df=3, P=0.532	H=2.874, df=3, $P_{(exact)}$=0.492
	100	H=0.169, df=3, $P_{(exact)}$=0.981	H=1.673, df=3, P=0.643	H=2.711, df=3, P=0.438	H=2.518, df=3, P=0.472	H=1.623, df=3, P=0.654	NA	H=1.551, df=3, P=0.671	H=0.968, df=3, P=0.809
	100dbl	H=1.344, df=3, P=0.719	H=1.000, df=3, P=0.801	H=2.308, df=3, P=0.511	H=1.928, df=3, P=0.587	H=1.144, df=3, P=0.766	NA	H=0.348, df=3, P=0.951	H=0.520, df=3, P=0.914
	250	H=1.435, df=3, P=0.697	H=0.828, df=3, P=0.828	H=1.903, df=3, P=0.593	H=0.132, df=3, P=0.988	H=1.888, df=3, P=0.596	NA	H=0.967, df=3, P=0.809	H=0.729, df=3, P=0.866
MK-ABMa	50dbl	NA	H=1.787, df=3, P=0.618	H=0.926, df=3, P=0.819	H=0.289, df=3, P=0.962	NA	NA	H=4.104, df=3, P=0.250	H=2.714, df=3, P=0.438
	100	H=0.75, df=3, P=0.861	H=1.431, df=3, P=0.698	H=3.466, df=3, P=0.325	H=1.878, df=3, P=0.598	H=3.800, df=3, $P_{(exact)}$=0.400	NA	H=2.783, df=3, P=0.426	H=0.673, df=3, P=0.879
	100dbl	H=0.0325, df=3, P=0.998	H=6.470, df=3, P=0.091	H=4.514, df=3, P=0.211	H=3.224, df=3, P=0.358	H=0.800, df=3, $P_{(exact)}$=1.000	NA	H=0.562, df=3, P=0.905	H=3.457, df=3, P=0.326
	250	H=0.305, df=3, P=0.959	H=1.546, df=3, P=0.976	H=1.394, df=3, P=0.707	H=1.241, df=3, P=0.743	H=3.962, df=3, P=0.266	NA	H=0.300, df=3, P=0.960	H=4.621, df=3, P=0.202

Table 2.: Statistical analyses comparing different sites of stimulation.

Statistical comparison with the non-parametric Kruskal-Wallis test between the 4 sites of stimulation for each monkey, for each voltage of stimulation, for each muscle, for each side, for pre- and post-lesion periods (PreL and PostL respectively). Comparison for the threshold protocol between latencies and threshold (**A**) and between latencies for repeated stimulation protocol (**B**). "NA" is when there were not enough data or not data at all for statistical analyses. Highlight point out statistically significant differences.

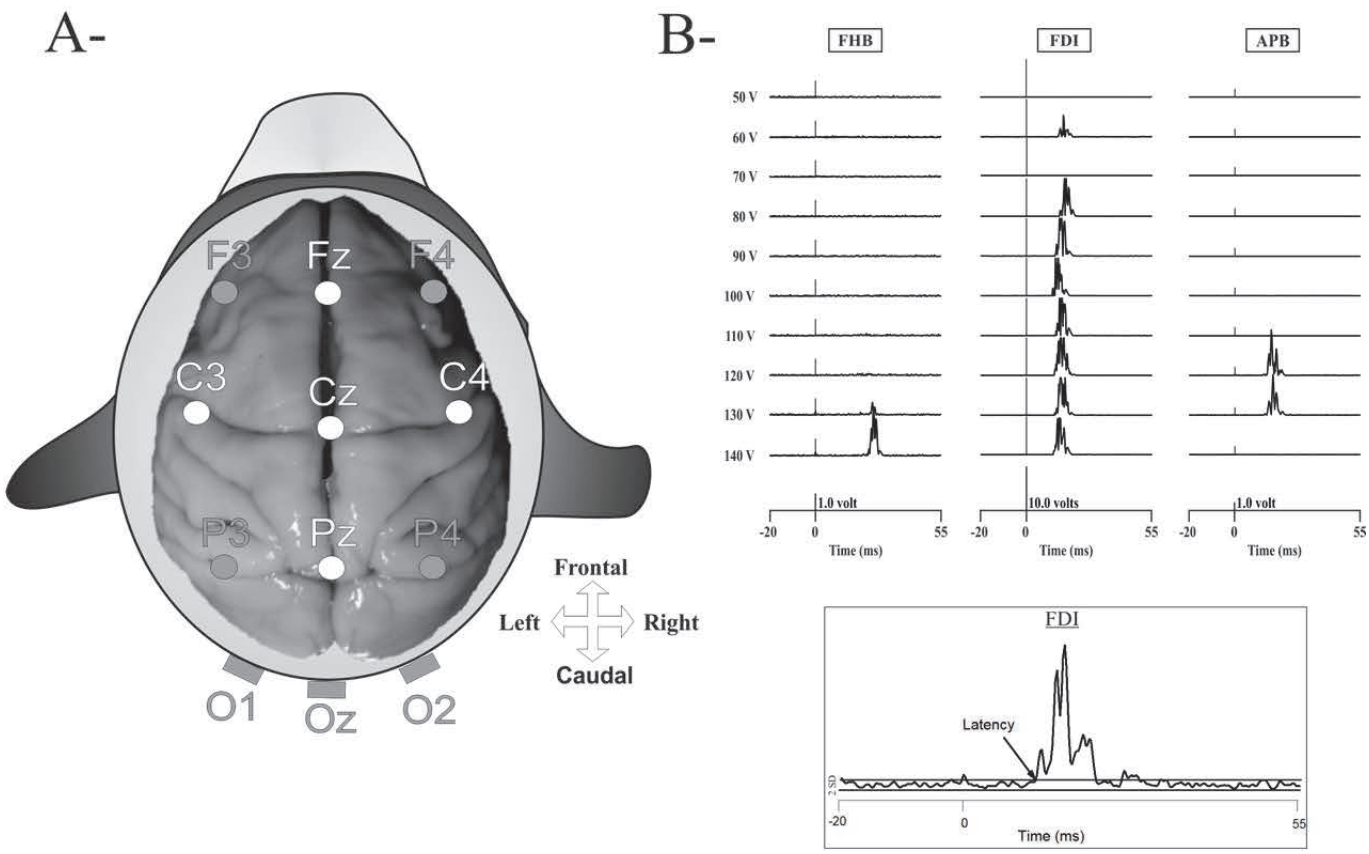

Fig. 1: Method

Topographical localization of electrode (white circle) on the scalp of monkey based on the international 10-20 system adapted for monkey scalp (white and grey circle) (**A**). Example of MEPs recorded in the three muscles for threshold determination protocol, for stimulations starting at 50 Volts up to 140 Volts (**B**). On bottom, criteria for determination of latency, for FDI muscle example. Horizontal lines correspond to ± 2SDs (Standard Deviations). Time 0 correspond to the stimulus trigger.

A-

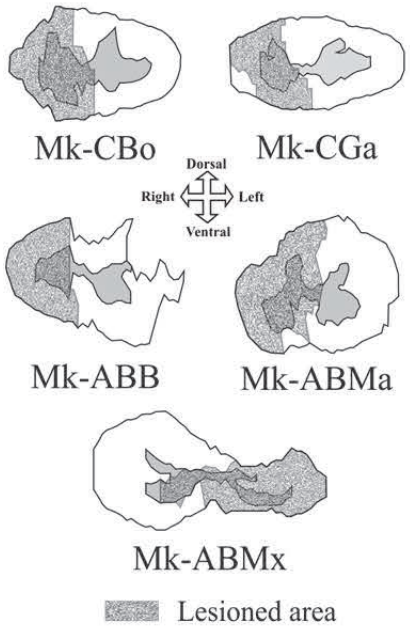

B-

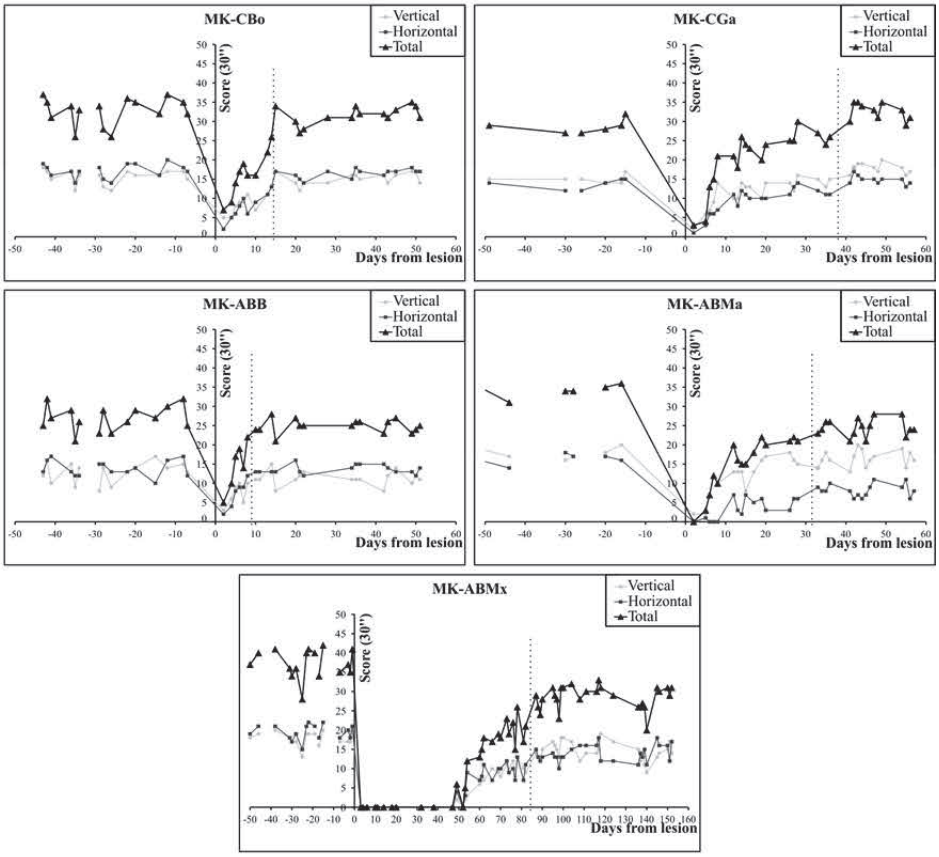

C-

	Anatomy			Behavior-Functional recovery(%)			
name	**Hemisection extent (%)**	**Volume of lesion (mm3)**	**Completeness of dlf section**	**Score (vert)**	**Score (horiz)**	**Contact time (vert)**	**Contact time (horiz)**
Mk-CGa	**73**	**3.76**	Yes	**100**	**100**	**75**	**100**
Mk-CBo	**93**	**4.11**	Yes	**100**	**97**	**94**	**100**
Mk-ABB	**83**	**2.36**	Yes	**84**	**100**	**57**	**72**
Mk-ABMa	**94**	**9.81**	Yes	**89**	**43**	**50**	**59**
Mk-ABMx	**95**	**9.55**	Yes	**78**	**71**	**72**	**53**

Fig. 2: Anatomy and behavior

Anatomical representation of the lesion size and extent on transverse spinal cord section at the C7/C8 lesion level (**A**). Behavioral data exhibiting the ability of monkey to perform fine manual dexterity during the "modified Brinkman board" task (**B**). Graphs represent the number of pellets retrieved in 30 second (scores) for each session before and after the lesion for the lesioned hand. Dash line delimits the two post-lesion periods: before correspond to the recovery period (RP) and after represent the plateau period (PP). Summary table for anatomical and behavioral parameters in relation to the lesion (**C**).

A-

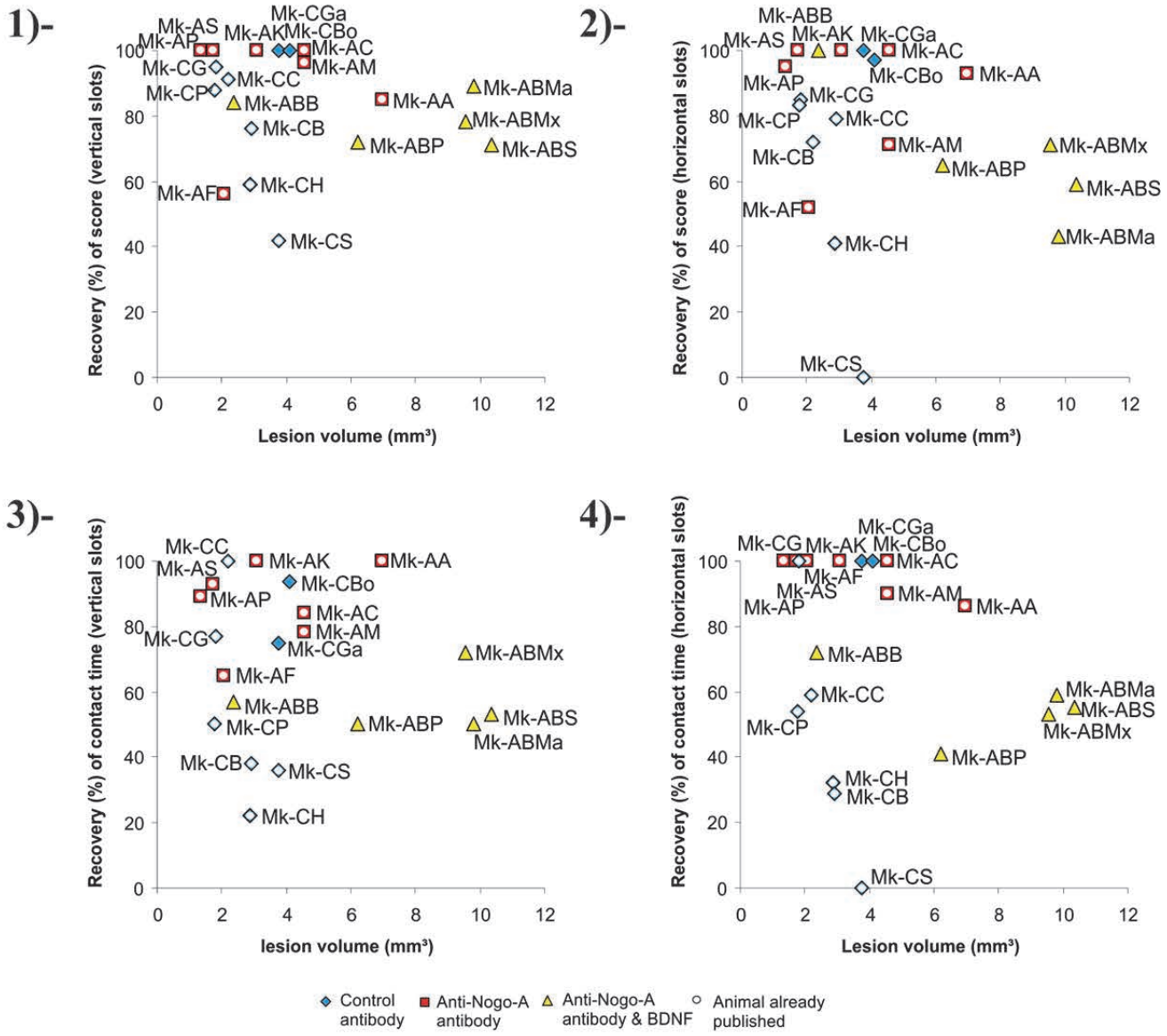
1)-
Recovery (%) of score (vertical slots)
Lesion volume (mm³)
Mk-CGa
Mk-AS
Mk-AK
Mk-CBo
Mk-AP
Mk-AC
Mk-AM
Mk-CG
Mk-CC
Mk-CP
Mk-ABMa
Mk-ABB
Mk-AA
Mk-ABMx
Mk-CB
Mk-ABP
Mk-ABS
Mk-AF
Mk-CH
Mk-CS
2)-
Recovery (%) of score (horizontal slots)
Lesion volume (mm³)
Mk-ABB
Mk-AS
Mk-AK
Mk-CGa
Mk-AC
Mk-AP
Mk-CBo
Mk-AA
Mk-CG
Mk-CP
Mk-CC
Mk-CB
Mk-AM
Mk-ABMx
Mk-ABP
Mk-ABS
Mk-AF
Mk-ABMa
Mk-CH
Mk-CS
3)-
Recovery (%) of contact time (vertical slots)
lesion volume (mm³)
Mk-CC
Mk-AS
Mk-AK
Mk-AA
Mk-CBo
Mk-AP
Mk-AC
Mk-AM
Mk-CG
Mk-CGa
Mk-ABMx
Mk-AF
Mk-ABB
Mk-CP
Mk-ABP
Mk-ABS
Mk-ABMa
Mk-CB
Mk-CS
Mk-CH
4)-
Recovery (%) of contact time (horizontal slots)
Lesion volume (mm³)
Mk-CGa
Mk-CG
Mk-AK
Mk-CBo
Mk-AC
Mk-AF
Mk-AS
Mk-AM
Mk-AP
Mk-AA
Mk-ABB
Mk-CC
Mk-ABMa
Mk-ABS
Mk-CP
Mk-ABMx
Mk-ABP
Mk-CH
Mk-CB
Mk-CS
Control antibody
Anti-Nogo-A antibody
Anti-Nogo-A antibody & BDNF
Animal already published

B-

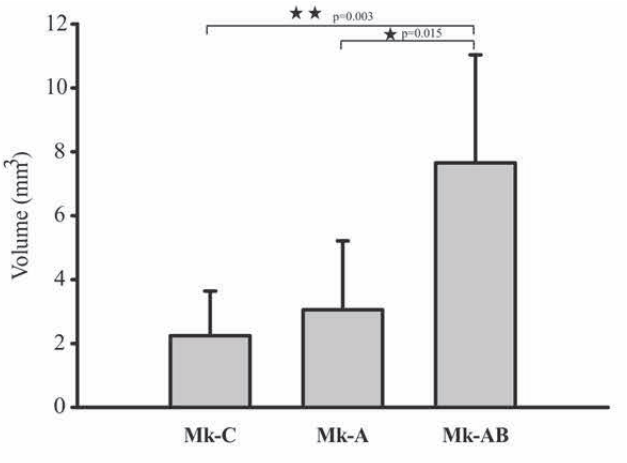
★★ p=0.003
★ p=0.015
Volume (mm³)
Mk-C
Mk-A
Mk-AB

Fig. 3: Supplementary, already published, behavioral and anatomical data

Supplementary behavioral and volumes of lesion data including previously published monkeys. Comparison of functional recovery as function to the lesion volume (reproduced from Beaud, 2011) for (**A**): **1)-** score of vertical slots, **2)-** score of horizontal slots, **3)-** contact time of vertical slots, and **4)-** contact time of horizontal slots. ANOVA and Fisher post-hoc tests were used for statistical comparison of lesion volumes between groups (**B**).

A-

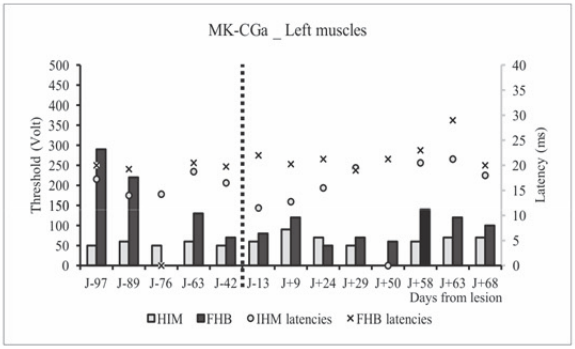
MK-CGa _ Left muscles
Threshold (Volt)
Latency (ms)
J-97 J-89 J-76 J-63 J-42 J-13 J+9 J+24 J+29 J+50 J+58 J+63 J+68
Days from lesion
HIM FHB IHM latencies FHB latencies

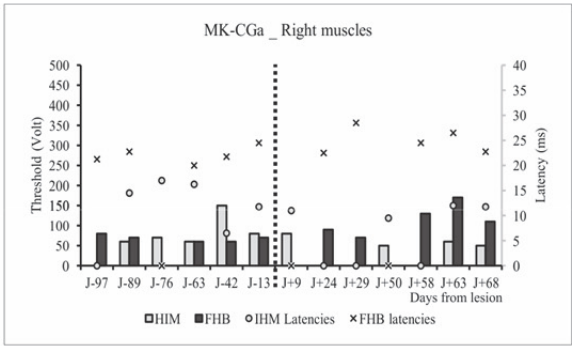
MK-CGa _ Right muscles
Threshold (Volt)
Latency (ms)
J-97 J-89 J-76 J-63 J-42 J-13 J+9 J+24 J+29 J+50 J+58 J+63 J+68
Days from lesion
HIM FHB IHM Latencies FHB latencies

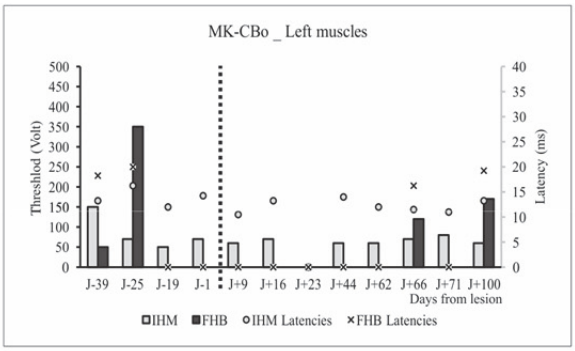
MK-CBo _ Left muscles
Threshlod (Volt)
Latency (ms)
J-39 J-25 J-19 J-1 J+9 J+16 J+23 J+44 J+62 J+66 J+71 J+100
Days from lesion
IHM FHB IHM Latencies FHB Latencies

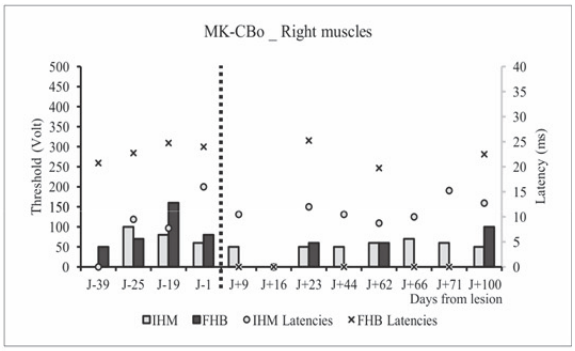
MK-CBo _ Right muscles
Threshold (Volt)
Latency (ms)
J-39 J-25 J-19 J-1 J+9 J+16 J+23 J+44 J+62 J+66 J+71 J+100
Days from lesion
IHM FHB IHM Latencies FHB Latencies

B- 1)-

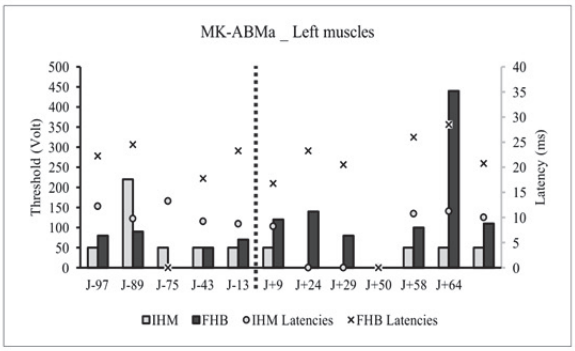
MK-ABMa _ Left muscles
Threshold (Volt)
Latency (ms)
J-97 J-89 J-75 J-43 J-13 J+9 J+24 J+29 J+50 J+58 J+64
IHM FHB IHM Latencies FHB Latencies

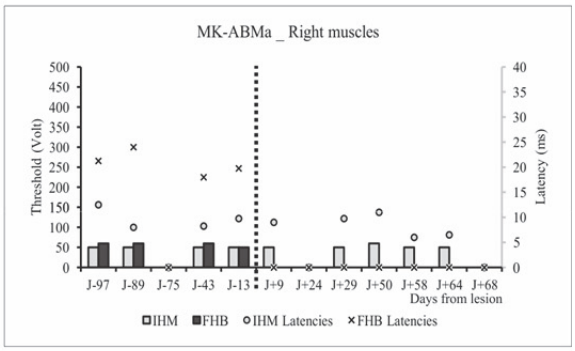
MK-ABMa _ Right muscles
Threshold (Volt)
Latency (ms)
J-97 J-89 J-75 J-43 J-13 J+9 J+24 J+29 J+50 J+58 J+64 J+68
Days from lesion
IHM FHB IHM Latencies FHB Latencies

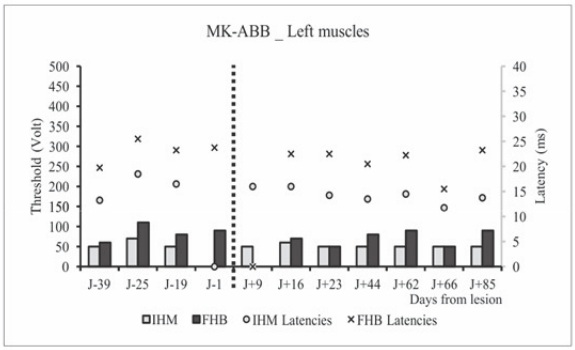
MK-ABB _ Left muscles
Threshold (Volt)
Latency (ms)
J-39 J-25 J-19 J-1 J+9 J+16 J+23 J+44 J+62 J+66 J+85
Days from lesion
IHM FHB IHM Latencies FHB Latencies

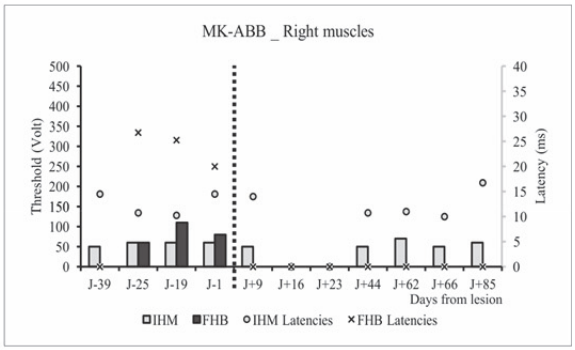
MK-ABB _ Right muscles
Threshold (Volt)
Latency (ms)
J-39 J-25 J-19 J-1 J+9 J+16 J+23 J+44 J+62 J+66 J+85
Days from lesion
IHM FHB IHM Latencies FHB Latencies

2)-

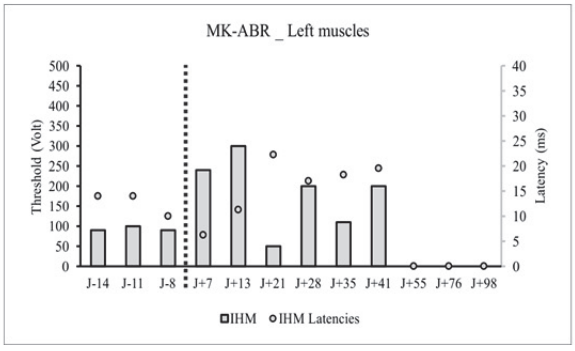
MK-ABR _ Left muscles
Threshold (Volt)
Latency (ms)
J-14 J-11 J-8 J+7 J+13 J+21 J+28 J+35 J+41 J+55 J+76 J+98
IHM IHM Latencies

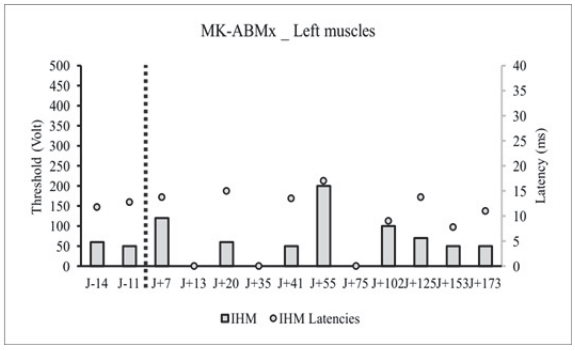
MK-ABMx _ Left muscles
Threshold (Volt)
Latency (ms)
J-14 J-11 J+7 J+13 J+20 J+35 J+41 J+55 J+75 J+102 J+125 J+153 J+173
IHM IHM Latencies

Fig. 4: MEPs thresholds

Thresholds in volts (histogram) and corresponding latencies in millisecond (circle and cross) of MEPs induced by TES, for IHM (Light grey bar graph and circle) and FHB (Dark grey bar graph and cross) left (Contralesional side) and right muscles (Ipsilesional side), for the control antibody group (**A**), for the combined treated group (**B1**) and for only IHM of the left muscles (Ipsilesioned side) of two monkeys of the combined treated group (**B2**). The dashed line represents the lesion day (J0).

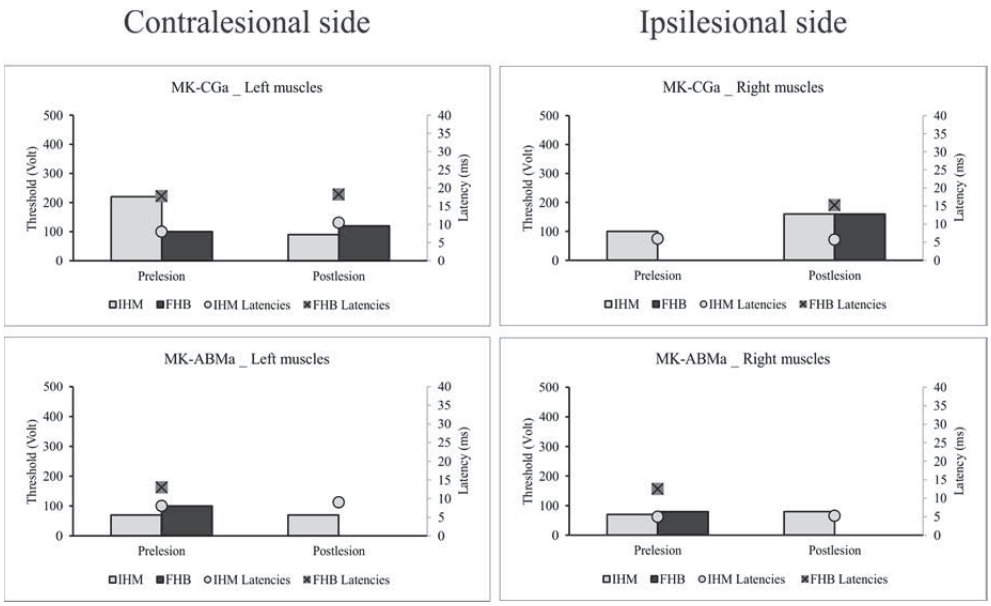

Fig. 5: MEPs threshold at the lesion day

Thresholds (volts) and corresponding latencies (ms) of MEPs recorded on the lesion day for two monkeys, one in the control antibody treated group (MK-CGa) and one in the Mk-AB group (Mk-ABMa). Recording were done before and after the hemi-cord lesion under deep anesthesia (propofol). Same conventions of representation as in Fig. 4 have been used.

A-

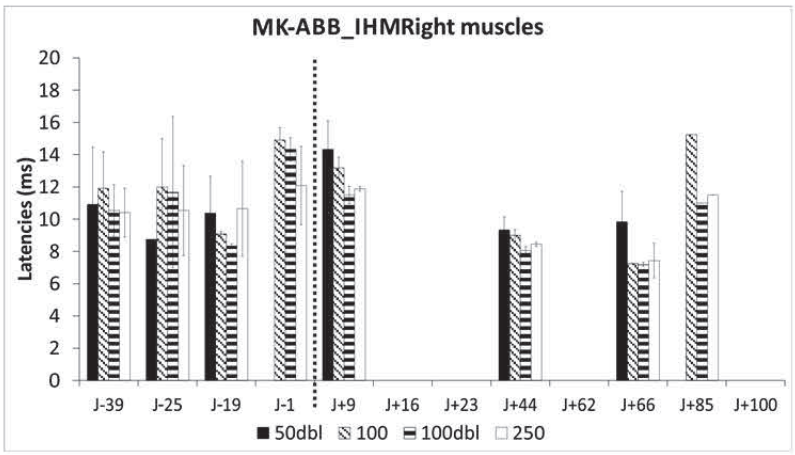
MK-ABB_IHMRight muscles
Latencies (ms)
20
18
16
14
12
10
8
6
4
2
0
J-39
J-25
J-19
J-1
J+9
J+16
J+23
J+44
J+62
J+66
J+85
J+100
50dbl
100
100dbl
250

B-

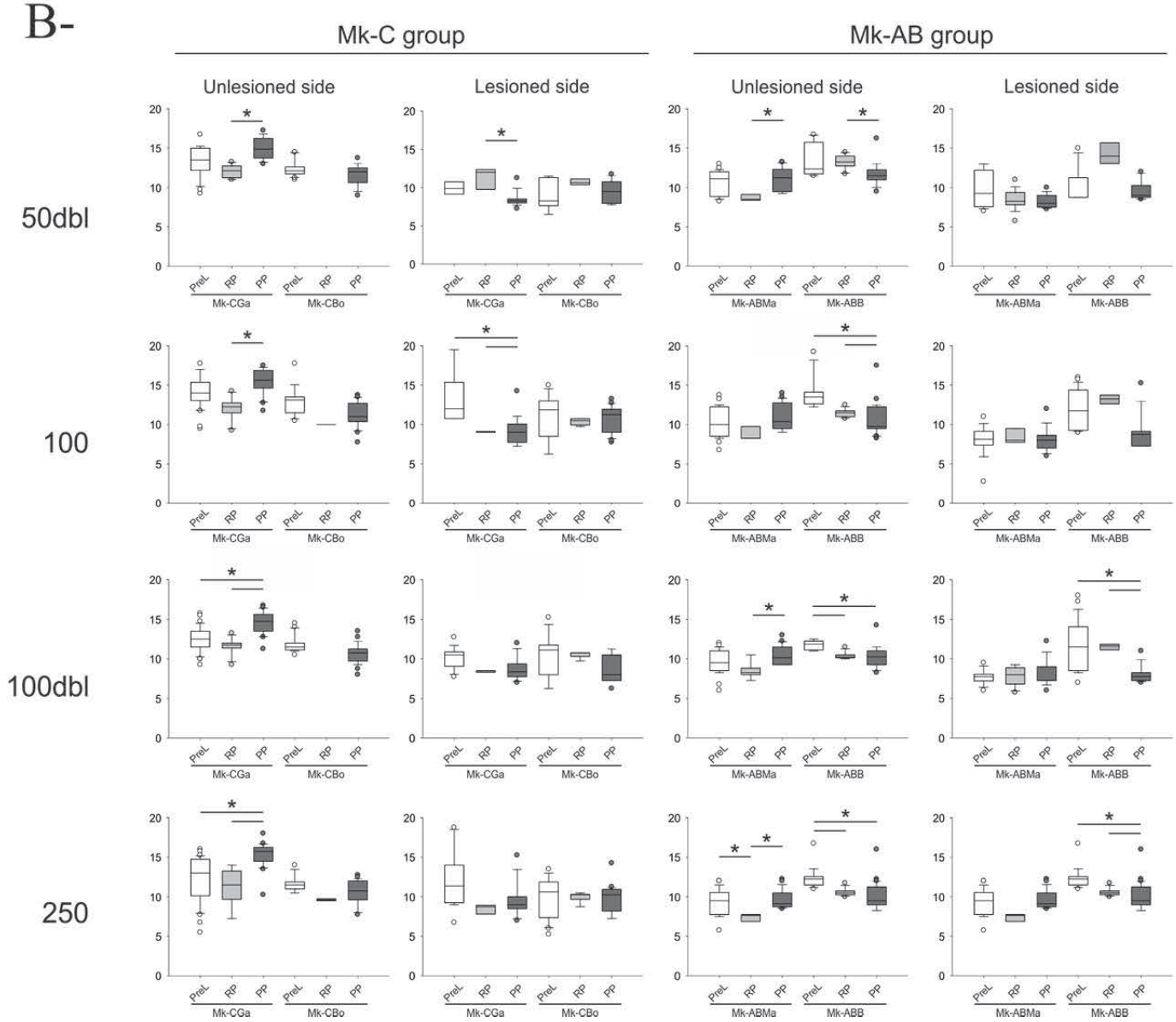
Mk-C group
Mk-AB group
Unlesioned side
Lesioned side
Unlesioned side
Lesioned side
50dbl
100
100dbl
250
PreL
RP
PP
Mk-CGa
Mk-CBo
Mk-ABMa
Mk-ABB

Fig. 6: MEP latencies induced by repeated stimulation

MEPs latencies induced by repeated stimulation with simple pulses at 100 volts (**100**) and 250 volts (**250**), or with double pulses (ISI = 2 ms) at 50 volts (**50dbl**) and 100 volts (**100dbl**). Bar graph represents an example of the time course since the lesion day (**A**) of an average of all the stimulation sites with standard deviation of MEPs latencies for all the stimulation voltages in Mk-ABB right IHM of the lesioned side. Box plots represent MEPs latencies (ms) of the IHM acquired with the repeated stimulation protocol (**B**), for each voltage of stimulation applied, for each side of each monkey, pooled in the three time periods defined with the behavioral time course: pre-lesion period (PreL, white box plots), recovery period (RP, light grey box plots) and plateau period (PP, dark grey box plots). (*) is for significant difference ($p<0.05$) with Dunn's method used in case of significant differences for Kruskal-Wallis test.

A-

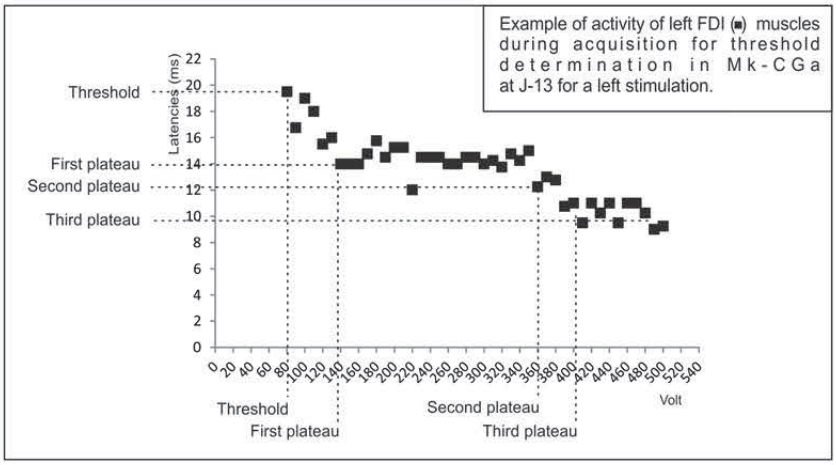
Example of activity of left FDI (■) muscles during acquisition for threshold determination in Mk-CGa at J-13 for a left stimulation.
Latencies (ms)
Threshold
First plateau
Second plateau
Third plateau
Volt

B- 1)-

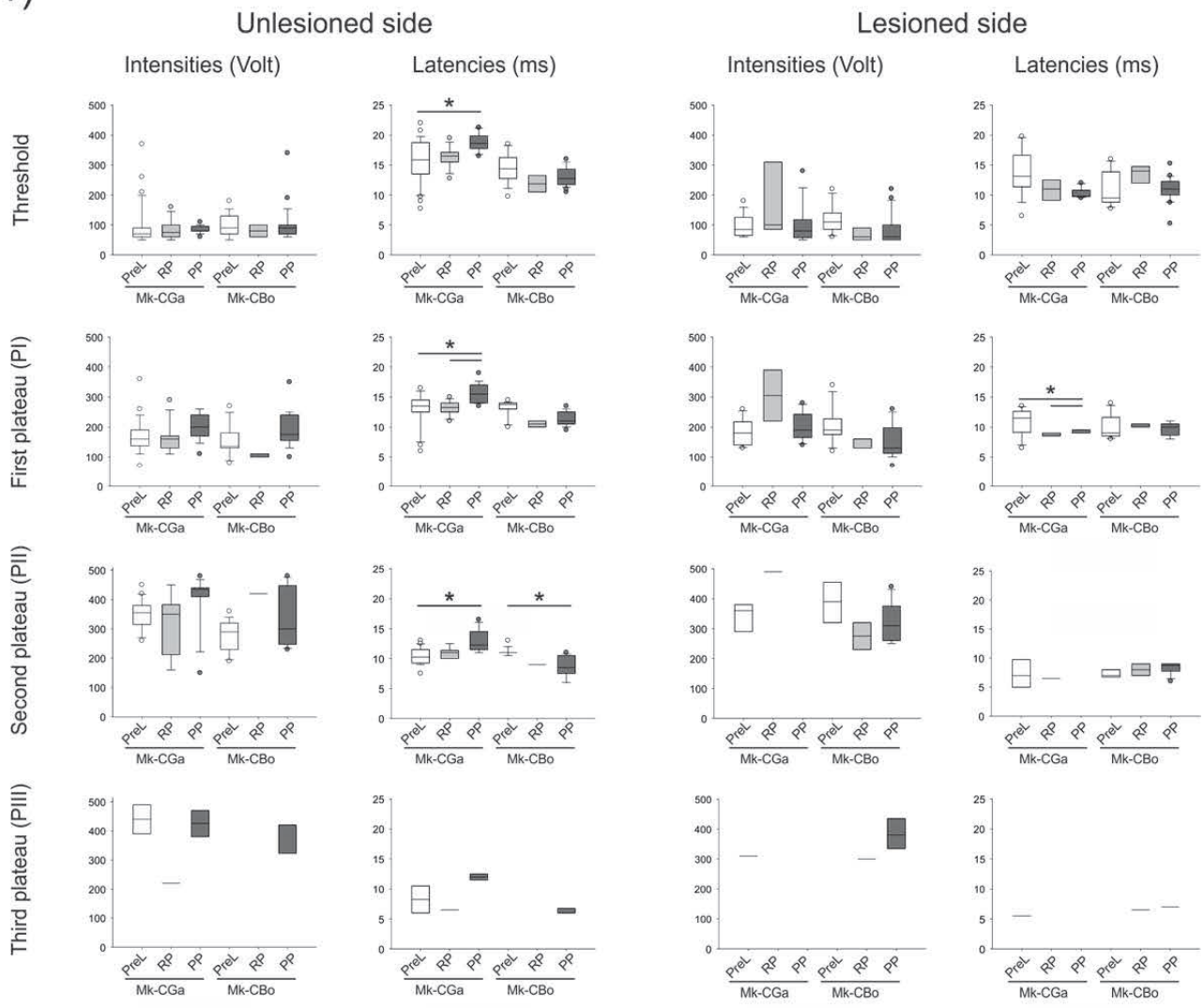
Unlesioned side
Lesioned side
Intensities (Volt)
Latencies (ms)
Threshold
First plateau (PI)
Second plateau (PII)
Third plateau (PIII)
PreL
RP
PP
Mk-CGa
Mk-CBo

B- 2)-

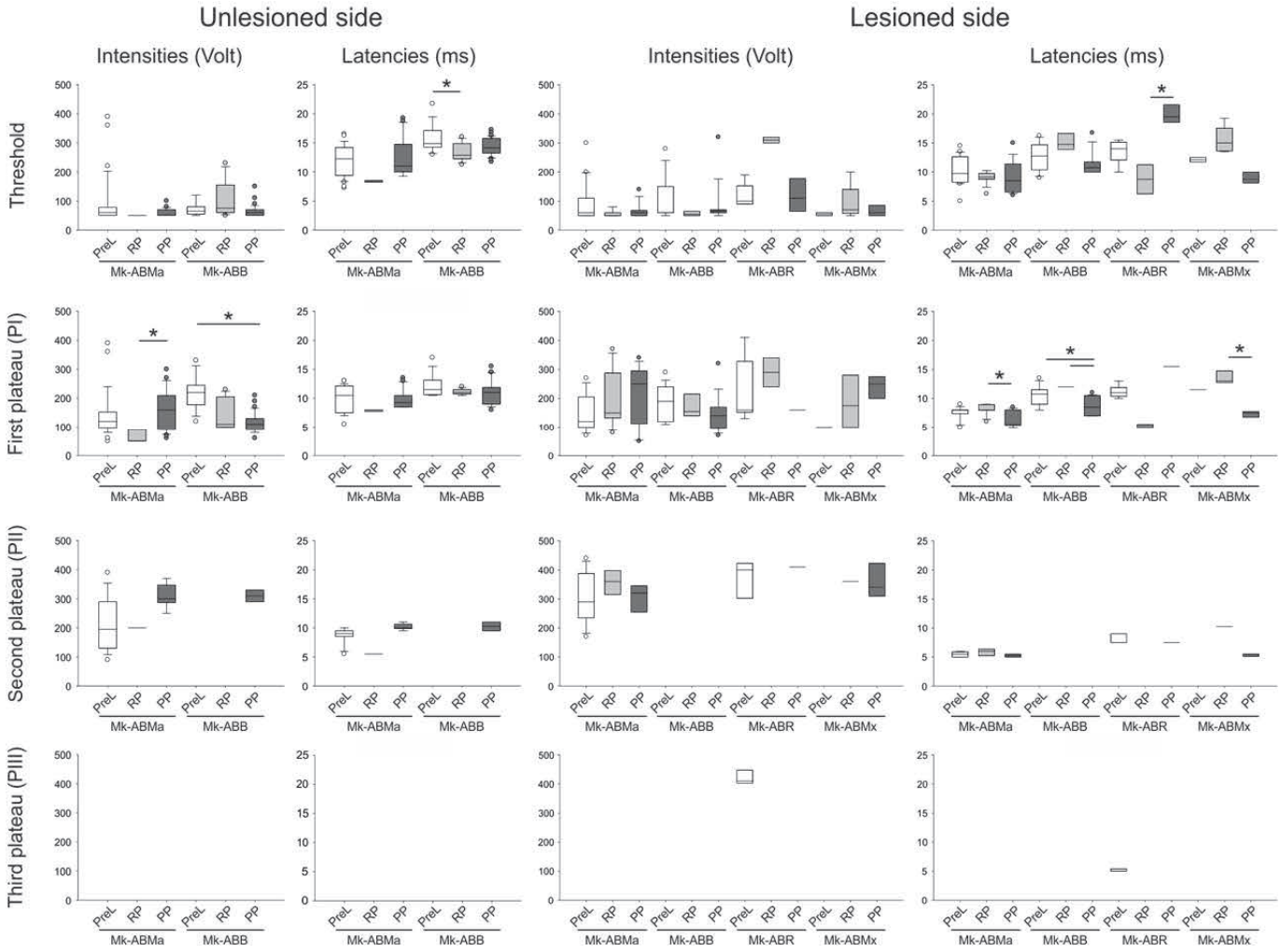

Fig. 7: Jump

Box plots represent latencies (ms) and tensions (volt) of stimulation for threshold, first, second and third plateau collected during the pre-lesion (PreL, white box plots), the recovery period (RP, light grey box plots) and the plateau period (PP, dark grey box plots) based on behavioral time course from the lesion day. An example of the latencies (**A**), referred to the stimulation voltage step, shows the latencies course for caudal stimulation site of Mk-ABMa in a pre-lesion session at each 10 volts step of stimulation from 50 up to 500 volts. Data were collected for each stimulation sites of each IHM and pooled for non-parametric comparisons using median values (**B**) for control antibody treated group (**B1**) and combined treated group (**B2**). (*) is for significant difference ($p<0.05$) with Dunn's post-hoc method for significant differences with Kruskal-Wallis test.

2.4. Chapter 4:

Subcortical reorganization in the dorsal column nuclei following motor system lesions and effect of an anti-Nogo-A antibody treatment alone and combined with BDNF

Savidan J., Beaud M.L., Wannier T., Rouiller E.M.

Faculty of Sciences and Fribourg Centre for Cognition, Department of Medicine, University of Fribourg, Chemin du Musée, Fribourg, Switzerland

Abstract

The somatosensory and the motor system are highly interconnected, both involved in common function for the control of voluntary movement. Reorganization following lesion occurs at more and less remote central structures. Thus the present reports assessed the possibility that reorganization occurs in the dorsal column nuclei (DCN) following lesion of the motor system, at the spinal (SCI) or cortical (M1) level in macaque monkeys. The second aspect of the study concerns the possibility that a treatment with an anti-Nogo-A antibody following MCI or a combination of treatment with anti-Nogo-A antibody and BDNF can prevent such reorganization. Direct section of the primary sensory axon induced a decrease of their terminals reaching the gracile nucleus and none of both treatment lead to prevent this decrease, the combined treatment was even associated with more sever damages. Lesions of the motor system tended to increase the size of primary sensory axon terminals reaching the cuneate nucleus. In case of MCI these increases were suggested to be prevented by an anti-Nogo-A antibody treatment whereas a combination of the previous treatment with BDNF in case of SCI did not prevent such increase but exhibited a more pronounced increase of the area of primary sensory axon terminals reaching the cuneate nucleus for similar length as compared to untreated and lesioned monkeys. This study suggests that the great reorganization occurring directly as a result of lesion of the primary sensory axon terminals reaching the DCN is not prevented with an anti-Nogo-A antibody treatment and the deficit is even exacerbated with the combination of treatment. This study also suggests that subtle reorganization of remote structures such as DCN occurs indirectly resulting of lesion of the motor system prevented with an anti-Nogo-A antibody treatment.

Introduction

Cortical injury induces deficit of the function controlled by the lesioned cortical area, lesion of the hand area in the primary motor cortex (M1) causing deficit of motor hand behaviors. However, cortical functions were shown to not be strictly segregated but rather more intermingled across multiple cortical areas. For instance, a motor role has been identified for the somatosensory cortex whereas a sensory role is played by the motor cortex (Matyas et al., 2010; Hatsopoulos and Suminski, 2011). Such widely distributed roles are consistent with anatomical studies demonstrating not only the presence of sensory inputs to the motor cortex and the presence of motor inputs to the somatosensory cortex (*e.g.* Asanuma, 1981; Künzle, 1978; Stepniewska et al., 1993), but also the presence of projections from the somatosensory cortex onto motoneurons in the spinal cord (Rathelot and Strick, 2006). The primary somatosensory cortex has been shown to be involved in the execution of precision grip between the thumb and the index finger of macaque monkeys in a task involving force adjustment (Wannier et al., 1991), while its inactivation produced an alteration of precision grip movements (Brochier et al., 1999). Motor deficits of the fine manual dexterity resulting from somatosensory pathways injury were reported to be irrespective of the anatomical level of the lesion, from dorsal roots crush (*e.g.* Darian-Smith and Ciferri, 2005; Darian-Smith, 2007) to dorsal column lesion (*e.g.* Song et al., 2008; Kaas et al., 2008; Qi et al., 2011, 2013) and to primary somatosensory cortex injury (*e.g.* Xerri et al., 1998; Coq and Xerri, 1999). In contrast, fewer studies reported the effects of motor system lesion on the somatosensory system. However, a study showed that the secondary premotor cortex present increased projections to the primary somatosensory cortex (Dancause et al., 2005). Another study suggested such effects showing that a monkey visually inspected their hand in order to detect the presence of a reward following M1 lesion targeting the distal forelimb area (Nudo et al., 2000). Anatomical reorganizations of the somatosensory pathways resulting from motor system injury remain to be investigated.

Irrespective of the structures studied to assess the effects of central nervous system injury, a recurrent purpose in research remains to promote the subsequent functional recovery. Numerous studies have investigated molecular approaches to promote axonal regrowth and/or sprouting, using different strategies. Basically, two approaches can promote axonal regeneration and regrowth, first, by making the environment permissive to axonal growth and, second, by increasing the level of neurotrophic molecules promoting intrinsic axonal growth.

Firstly, based on the characterization of the highly inhibitory property of the Nogo-A protein in spinal cord myelin sheath (Caroni and Schwab, 1988), numerous studies showed the beneficial potentials to block this molecule and its signaling pathways to promote functional recovery and neural repair in case of various central nervous system pathologies, especially following spinal cord injury or stroke (GrandPre et al., 2000; Buchli and Schwab, 2005; Zorner and Schwab, 2010; Wang et al., 2012; for review: Pernet and Schwab, 2012; Schwab and Strittmatter, 2014). Treatment with an antibody against Nogo-A promotes functional recovery from spinal cord or motor cortex injuries, enhancing sprouting of corticospinal and other pathways and promoting reorganization of territories close and distant to the lesion site in rodent (Schnell and Schwab, 1993; Thallmair et al., 1998; Papadopoulos et al., 2002; Li and Strittmatter, 2003; Lee et al., 2004) and in non-human primate (Fouad et al., 2004; Freund et al., 2006, 2007, 2009; Wyss et al., 2013; Hoogewoud et al., 2013). This anti-Nogo-A antibody treatment has also induced remote effects, such as allowing regeneration of lesioned pyramidal projections in the sensory dorsal column nuclei (DCN) in the brainstem after pyramidotomy in rodent (Thallmair et al., 1998).

Secondly, subsequent to the purification of "a new factor supporting the survival and outgrowth of fibers" in the pig brain (Barde et al., 1982), BDNF (Brain Derived Neuortrophic Factor), a member of the Neurotrophins family, has been identified as a major actor in axon guidance during development, and as regulator of neuronal survival in adult central nervous system (for review see Huang and Reichardt, 2001). While the beneficial role played by BNDF in peripheral nerve injury recovery was largely recognized (for review see Lu and Tuszynski, 2008; Nagahara and Tuszynski, 2011; Weishaupt et al., 2012), its beneficial role in axonal regrowth and retrograde atrophy prevention remains a subject of debate for motor and sensory pathways (for review see Weishaupt et al., 2012). The interest in BDNF as a potential therapy for axonal regrowth following injury derives from the expression of its receptors TrkB and p75 by sensory neuron (Kaplan and Miller, 2000; Numakawa et al., 2010) and from the observed up-regulation of neurotrophins such as BDNF following spinal cord injury (for review see Bareyre and Schwab, 2003). Optimal regeneration may well require the application of combined therapies involving several molecules (Lu and Tuszynski, 2008).

The present study aimed to firstly test the hypothesis that a C7/C8 spinal cord hemi-section directly impacts on the nucleus gracilis by decreasing the number of its incoming primary sensory axon terminals ispilesional. In this context, the possibility that a treatment combining an antibody against Nogo-A and BDNF may prevent this decrease was tested. The second hypothesis was that a C7/C8 spinal cord hemi-section does not directly affect the

primary sensory axons terminating in the cuneate nucleus. If verified, one may still investigate whether a treatment combining an antibody against Nogo-A and BDNF can influence these unlesioned axon terminals reaching the cuneate nucleus. This question remains pertinent in this model as the neutralization of Nogo-A has been suggested to induce a growth response in the intact adult CNS (for review see Schwab, 2004) and improve regeneration of lesioned CST projections to the DCN (Thallmair et al., 1998). The third main hypothesis of the present study aimed at testing a possible effect of motor cortical hand area injury on the primary sensory axon terminals reaching the cuneate nucleus. Such an effect may take place via the corticocuneate projections, themselves affected by the motor cortex lesion. Although the corticocuneate projections originate predominantly from the somatosensory cortex, a contingent was identified as originating from the motor areas 4 and 6 (Bentivoglio and Rustioni, 1986; Kuypers and Tuerk, 1964; Cheema et al., 1985; Martinez et al., 1995). In link with this hypothesis, the present study aimed at assessing whether an anti-Nogo-A antibody treatment may induce plasticity of the cuneate nucleus afferent projections, indirectly affected by the cortical injury.

Methods

Some methods used in the present study are similar to those described in previous reports from this laboratory and, therefore, repeated here for the sake of completeness. The relevant reports are cited accordingly.

Animals

The present study was conducted on ten adult monkeys (*Macaca fascicularis*) (8 males and 2 females, 3.0 to 5.6 Kg), aged from 4 to 6 years at the time of the sacrifice. All experiments were carried out in accordance to the Guide for Care and Use of Laboratory Animals (ISBN 0-309-05377-3; 1996) and approved by local veterinary authorities, including the ethical assessment by the local (cantonal) Survey Committee on Animal Experimentation. A final acceptance was delivered by the cantonal federal Veterinary Offices. The monkeys were obtained either from our own colony in our animal facility (before 2010) or were purchased from two certified suppliers (BioPrim, 31450 Baziège; France or Harlan Buckshire; Italy).

Monkeys included in the present study were originally enrolled in two main projects. Data derived from the monkeys Mk-AB-B, Mk-AB-S, Mk-AB-P and Mk-C-Bo, subjected to hemi-cervical cord section, were already published in previous reports aiming to analyze the beneficial effects of anti-Nogo-A antibody treatment and its putative improvement with a combined BDNF treatment. In these studies, the authors analyzed the effects of these treatments after spinal cord injury on the ability of corticospinal (CS) axons to regenerate, on the functional recovery and on the size of CS neurons as well as the trajectory of fibers in and around the lesion site (Beaud et al., 2008, 2012; Freund et al., 2006, 2007, 2009; Wannier-Morino et al., 2008). Data derived from the monkeys Mk-A-SL, Mk-A-MO, Mk-C-BI and Mk-C-RO, subjected to a primary motor cortex injury targeting the hand representation, were already published in previous reports that analyzed the effects of anti-Nogo-A antibody treatment on the lesioned M1 hand area reorganization and the perilesional cortex (Wyss et al., 2013), on the callosal connectivity of the premotor cortex (Hamadjida et al., 2012) and on the "unaffected" hand behavioral ability (Kaeser et al., 2010; Bashir et al., 2012).

Surgery

All surgical procedures were described in detail in previous reports from this laboratory (Schmidlin et al., 2004, 2005, 2011; Wannier et al., 2005; Freund et al., 2006, 2007, 2009; Wyss et al., 2013). Abbreviations for injections route were as follows: i.v. for intravenous, i.m. for intramuscular and s.c. for subcutaneous. To summarize, surgical procedures were conducted under deep anesthesia. Sedation was induced with an injection of ketamine (Ketalar®; Parke-Davis, 5 mg/kg; i.m.) and deep anesthesia was maintained with perfusion of 1% propofol (Fresenius®) mixed with a 5% glucose saline solution (1 volume propofol and 2 volumes of gluco-saline, delivered at a dose of 0.1 mg/kg/min; i.v.). Ketamine was added to the perfusion solution (0.0625 mg/minute/kg; i.v.) to further reduce pain during surgery. Following sedation induction, medication consisted of: Atropine to reduce bronchial secretion (0.05 mg/kg; i.m.), Carprofen as a preventive pain killer (Rimadyl®; 50mg/ml; dose: 4 mg/kg; i.m.), Dexamethasone (Decadron®; 0.05 ml/kg diluted 1:1 in saline; i.m.) to prevent brain edema and Ampiciline as antibiotic (Albipen®; 10%; 30 mg/kg; s.c.) to prevent infections. Pain and infections following surgery were prevented by postoperative treatment with Carprofen and Ampiciline during the following week. All surgeries were performed in a facility under sterile conditions and approved by the (Swiss) cantonal veterinary office.

Motor system lesion

Spinal cord injury (SCI)

Hemilaminectomy procedure to perform a selective hemi-cervical cord lesion was described in detail in previous reports (Schmidlin et al., 2004, 2005; Wannier et al., 2005; Freund et al., 2006, 2007, 2009). Briefly, animals were placed in ventral decubitus position and the spinal processes from C2 to Th1 were exposed. Segments C6, C7 and Th1 were dissected and a complete C6 laminectomy and an upper C7 hemilaminectomy were then performed. The dorsal root entry zone at the C7/C8 border, covered by the 6th cervical vertebra, was then identified, providing an anatomical landmark for placing a surgical blade (No. 11; Paragon®), used to perform hemisection of the cervical cord which completely cut the dorsolateral funiculus. The surgical blade was inserted 4 mm in depth perpendicularly to the spinal cord and the section was prolonged laterally to completely cut the dorsolateral funiculus. The lesion was located at C7/C8 level, caudal with respect to the main pool of biceps motoneurons but rostral to the pools of triceps, forearm and hand muscle motoneurons (Jenny and Inukai et al., 1983). The muscles and the skin were sutured. After the spinal lesion, the animals were kept alone in a separate cage for 2-5 days before replacing them in their own groups, in order to ensure their physical conditions and better recovery from surgery.

Primary motor cortex injury (MCI) of hand representation

Cortical lesion required access to M1 with a chronic chamber implant to map the hand representation, allowing targeted lesion of M1 hand area by microinfusion of excitotoxic neurotoxin. Procedures were described in detail in previous reports (Liu and Rouiller, 1999; Kaeser et al., 2010). Briefly, a stainless steel chamber was surgically implanted under anesthesia over the M1 forelimb area. The chamber was centered at the stereotaxic coordinates 15 mm anterior and 15 mm lateral, and at an angle of 30 degrees with respect to the mid-sagittal plane, allowing perpendicular electrode penetrations with respect to the cortical surface. The chamber was soldered with two flat wings anchored to the skull by titanium screws. The edge of the chronic chamber next to the skull and six to ten selftape titanium screws anchored in the skull were covered with dental acrylic or orthopedic cement (Palacos®). More recently, a new technic was developed to avoid the use of cement (Lanz et al., 2013). Over the mid-occipital and frontal regions of the skull, two stainless steel cylinders were anchored with 3-4 titanium screws and then cemented as described above for the chronic chamber. These cylinders allowed head restraining during the cleaning of the chronic chamber

and, most importantly, during the ICMS sessions conducted in awake monkeys. Nevertheless, a partly flexible head restrain attached to the cylinders allowed limited movement of the head. To prevent infection, the chronic chamber was cleaned daily with Betadine and an antibiotic ointment (Morrhulan). The hand area in M1 was delimited using intracortical microstimulation (ICMS) in awake and head restrained monkeys. Glass- or mylar-insulated platinum-iridium electrodes with typical impedances between 0.1 to 1.0 MΩ (Frederick Haer & Co., Bowdoinham, ME) and electrode advancing system (Narishige group, Japan, Model MO-95) directly attached to the chronic chamber were used. Electrodes were manually advanced in and around the hand area of M1, systematically at a 1 mm grid interval along the caudo-rostral and medio-lateral axes (Wyss et al., 2013) and starting from 2 mm below the dura surface, along a maximal distance of 10–12 mm (by 1 mm step in depth). The ICMS consisted of 12 electric pulses, delivered in a train of 33 ms duration, at a rate of 330 Hz and intensity ranging from 3 to 80 microamps. The effects of ICMS were assessed by visual inspection and/or palpation of muscle contractions and minimal intensities and locations were reported on cortical maps (Wyss et al., 2013; Kaeser et al., 2010). Lesion of M1 was induced by ibotenic acid (Sigma; 10 µg/µl in phosphate buffer) infusion at cortical ICMS sites eliciting fingers movements at low intensity of stimulation. Using a Hamilton microsyringe, a volume of 1 µL to 1.5 µL of ibotenic acid solution was injected at each site (for more details see Liu and Rouiller, 1999). The total volume and numbers of ICMS sites infused with ibotenic acid are listed in Table 1.

Treatment

Concerning monkeys subjected to spinal cord injury (SCI), as previously reported (for anti-Nogo-A antibody treatment: Schmidlin et al., 2005; Freund et al., 2006, 2007, 2009; Beaud et al., 2008; for combined treatment with anti-Nogo-A antibody and BDNF: Beaud et al., 2012; Beaud, 2011), the tested treatment was initiated at the time of the lesion and was administered with osmotic minipumps connected to a catheter inserted intrathecally in the vicinity of the cervical lesion site. One animal has received a control antibody (Mk-C-Bo), a purified IgG of a mouse mAb (monoclonal antibody) directed against wheat auxin (AMS Biotechnology, Oxon, United Kingdom; 14.8 mg over 4 weeks). The three treated animals (Mk-AB-B, Mk-AB-S and Mk-AB-P) were implanted with one minipump delivering a monoclonal anti-Nogo-A antibody (14.8 mg in 4 weeks), which was raised by immunization with the whole Nogo-A-specific region of the human Nogo-A sequence, and with a second

minipump delivering the neurotrophic factor BDNF (1.4 mg in 4 weeks). The minipumps were removed after 4 weeks.

Concerning monkeys subjected to motor cortex injury (MCI), as previously reported (Bashir et al., 2012; Hamadjida et al., 2012; Wyss et al., 2013), the tested treatment was initiated at the time of the lesion and was administered with two osmotic minipumps (Alzet®, model 2ML2, 5 µl/h). The two treated animals (Mk-A-SL and Mk-A-MO) were implanted with minipumps delivering a monoclonal anti-Nogo-A antibody, 11C7, (3 mg/ml). The two minipumps were implanted in the neck region. The first minipump was connected to a catheter inserted intrathecally at C7-C8 cervical spinal cord level (as described for spinal cord injury minipump implant). The second catheter was tunneled under the skin up to the head and the tip pushed under the dura through a small opening in the skull in close proximity to the motor cortex in order to infuse the lesion territory vicinity. The minipumps were removed after 4 weeks. The two control animals did not receive any treatment (Mk-C-BI and MK-C-RO) and thus were not implanted with minipumps.

Two monoclonal antibodies were used in this study: the mAB hNogo-A, recognizing a defined Nogo-A region of the human Nogo-A sequence, and the 11C7, directed against a rat Nogo-A sequence of 18 amino acids (aa623-640) and building a strong inhibitory region of the Nogo-A protein. On Western blots, both anti-Nogo-A antibodies can identify in a monospecific manner the primate-Nogo-A protein (Oertle et al., 2003; Weinmann et al., 2006). The characterization of the anti-Nogo-A antibody hNogo-A mAB was performed as described in detail by Freund and collaborators (2007). The antibodies used as treatment are listed in Table 1.

Tracer injection

Cholera toxin B subunit (CB: 0.5%, Sigma-C9903) has been used as transganglionic tracer to selectively label ascending sensory fibers and their terminal fields in the dorsal column nuclei in the brainstem (Fig. 1). CB was injected under anesthesia (a mixture of ketamine and medetomidine), in subcutaneous route, with a Hamilton microsyringe, in the first and the second phalanges of the first (thumb/first toe) and second (index/second toe) fingers of the 4 limbs (Fig. 1). A total of 160 µl of CB at 0.5% in distilled water was injected, distributed in 10 µl in 3 injection sites per phalanges, except for two subjects. The first subject, Mk-AB-B, received a total of 170 µl of CB at 0.5%, distributed in 15 µl in 3 injections in the distal phalange of each first finger of the 4 limbs and 10 µl in 3 injections in the other phalanges. The second subject, Mk-A-SL, received a total of 120 µl of CB at 0.5%,

distributed in 7.5 µl in the two distal phalanges of each first finger of the 4 limbs. At least a period of one week (more detail in Table 1) of CB transport was observed before sacrifice.

Histology

Anatomical reconstruction

At the end of the experiments, monkeys were deeply anaesthetized with ketamine and received a lethal dose of sodium pentobarbital (90 mg/kg; i.p.) before a transcardiac perfusion with paraformaldehyde (4%) in 0.1 M of phosphate buffer (pH=7.6) in order to fixate tissue, followed by solutions of increasing concentration of sucrose (10, 20 and 30 %; see *e.g.* Wannier et al. 2005; Beaud et al., 2008 for detail). Brain, brainstem and spinal cord were extracted and immerged into a sucrose solution (30% in phosphate buffer, pH=7.6). For anatomical reconstruction of spinal cord lesion (Fig. 2), the spinal cord was sectioned in 30 µm-thick parasagital sections at the level of the lesion (C3-T4). One of these series was stained with SMI-32 for anatomical reconstruction of the lesion. Method for SMI-32 staining was already described in previous reports (Beaud et al., 2008, 2012) as well as the anatomical reconstruction of the lesion (Schmidlin et al., 2004; Wannier et al., 2005; Beaud et al., 2008; Freund et al., 2009). Briefly, sections were incubated with an anti-SMI-32 antibody (IgG, Sigma, dilution 1:3000) with normal horse serum (2%) overnight at 4°C and were pre-amplified with avidin-biotin complex (Vectastein Elite Kits, Vector) before revelation with 3,3'-diaminobenzidine tetrahydrochloride (0.05%). To summarize the anatomical reconstruction procedure, borders of the lesion sites and contours of the different part of the spinal cord were drawn on longitudinal spinal cord sections stained for SMI-32, using neurolucida software. Drawings were aligned to allow the reconstruction showing the location and the extent of the lesion in the spinal cord on a transverse view and to calculate the volume of the lesion in mm^3. For anatomical reconstruction of motor cortical lesion (Fig. 2), the brain was sectioned in 50 µm-thick coronal sections. Out of five series of sections, one series was stained for anatomical reconstruction of lesion with the SMI-32 marker (as described above for spinal cord sections). Under light microscope and using neurolucida software, consecutive sections labeled for SMI-32 marker were used to draw borders and contours of the lesion site defined as the cortical areas where pyramidal neurons in layers III and V are missing (Wyss et al., 2013). Using Neurolucida software, volumes of cortical lesions affecting the cortical gray matter were calculated (in mm^3) by extrapolation based on the Cavalieri method (Pizzimenti et al., 2007).

CB immunohistochemical staining

The brainstem was sectioned in 3 or 5 series of 50 µm-thick transversal sections. The method described in the report of Rouiller and collaborators (1994) was used to reveal the transganglionic tracer CB. Briefly, sections were rinsed in a solution of Tris buffered saline (TBS-T, 0.05M, pH 8.6) with Triton X100 at 0.5% before overnight incubation at 4°C with primary antibody against CB (Goat anti-choleragenoid; List Biological Laboratories-Product numero: 703; 1:10000). Sections were rinsed with TBS-T and incubated with a secondary antibody Rb-anti-goat IgG (Sigma, 1:40) diluted in TBS-T for 90 min at room temperature. An amplification step was performed with the peroxidase anti-peroxidase (PAP) method by incubation with goat PAP (Nordic, 1:400) diluted in TBS-T for 90 min. Immunohistostaining was revealed with a 0.05% Diaminobenzidine (DAB) solution in Tris-HCL (0.05M, pH 7.6) buffer in two steps: a first preincubation step of 15-30 min and a second step of 30 min incubation with addition of 0.01% H_2O_2.

Myelin histochemical staining

Spinal cord block of the cervical level C3 was sectioned in 50 µm-thick transversal sections. Myelin was revealed using the histochemical gold-chloride protocol described by Schmued (1990). Briefly, free floating sections were incubated in a 0.2% solution of gold-chloride (Gold (III) chloride hydrate, Sigma) dissolved in phosphate buffer (0.02M, pH 7.4) and 0.6% sodium chloride. Sections were incubated variable times (ranging from 30 min to 132 min) depending of the staining rate, monitored under light microscope. Staining rate to reach optimal staining was variably affected by tissue quality due to multiple parameters, such as perfusion, duration and quality of sections storages. Once optimal staining was reached, sections were rinsed in a normal saline solution at 0.9% NaCl in distillated water and blocked in a 5% solution of sodium thiosulfate for 5 min. Finally, sections were mounted on slides, dehydrated and covered.

Histological analysis

Images were captured using Neurolucida software (MicroBrightField, Williston, VT, USA) from light microscope (Olympus) at 12.5X magnification (Fig. 1). For each monkey, images of all slices were captured at once and under the same light conditions. Images were analyzed using NIH ImageJ software (Dr. Wayne Rasband, National Institutes of Health, Bethesda, MD) (Fig. 1). CB and myelin staining were analyzed in grayscale intensity by

processing images in 8 bits gray type. Regions of interest (ROI) were drawn, surrounding the observed staining in the DCN in brainstem on both sides of each section with CB staining. Both cuneate and gracile nuclei were analyzed in monkeys subjected to SCI, as well as in intact monkeys. Only the cuneate nucleus was analyzed in monkeys subjected to MCI given that the injury was restrained to the hand motor area targeted electrophysiologically in awake monkeys. For myelin staining at C3 level of the spinal cord, ROIs were drawn to delimit the anatomical contours of the dorsal sensory fasciculi cuneatus and gracilis based on the online spinal cord atlas of Tokuno and collaborators (2011) and on our own observations. For CB and myelin, staining was measured in number of pixels in the delimited ROIs. A threshold was determined for each monkey to select pixels with gray value corresponding to the CB staining and to the myelin staining. Concerning the CB staining, as for pictures acquisition under microscope, all parameters were kept constant for the staining measurement all along the brainstem sections in the same subject. For each monkey, CB staining was compared between the two sides of each section as paired values with the non-parametric Wilcoxon test. Concerning myelin staining, each stained area was divided by the total area of the corresponding ROI to normalize area of myelin per fasciculus in order to overcome bias induced by differential tissue shrinkage and mounting manipulations, the staining measurement depending directly to the size of these areas.

Results

CB labeled sensory terminal fields in dorsal column nuclei (DCN), influence of levels of lesion and treatments

Primary sensory axon terminal projections originating from the two distal phalanges of the first and second fingers of the 4 limbs were assessed in the DCN by measuring CB labeling areas in brainstem along the caudo-rostral axis (Fig. 1A). The areas of CB labeled axonal terminal fields in the gracilis (Fig. 3) and cuneate (Fig. 4 and 5) nuclei were compared between the two sides of the brainstem in intact monkeys, monkeys subjected to spinal cord hemisection (SCI) (Fig. 4) and monkeys subjected to cortical M1 hand area lesion (MCI) (Fig. 5), distinguishing untreated and treated monkeys in the two lesioned monkey groups.

Gracile nucleus, effects of hemi-cervical cord injury

As the afferents from the hindlimb are relayed to the gracile nucleus and considering an hemi-section at C7/C8 including part if not the entire dorsal funiculus, one expects a substantial decrease of CB labeled axonal terminal fields on the ipsilesional side as compared to the contralesional side in SCI monkeys, but not in intact monkeys (Fig. 1**A**). In the present study, a further goal was to test the hypothesis that a treatment with anti-Nogo-A antibody combined with BDNF can impact on the lesioned sensory pathways in monkeys subjected to SCI.

Microphotographs taken from Mk-AB-B brainstem show CB labeled axonal terminal fields in the areas surrounded with a black contour, corresponding to the gracile nucleus at the medial most and dorsal most location along the caudo-rostral axis of the brainstem on a transversal axis (Fig. 3**A**). In all monkeys, a sparse CB labeling was observed in the caudal half of the gracile nucleus, which then increased to reach a zone of dense axonal terminal fields in the rostral third part of the gracile nucleus (Fig. 3), well illustrated on the bar graphs (Fig. 3**B**, **C** and **D**). The length values of the caudo-rostral extent of the CB labeled axonal terminal fields in the gracile nucleus ranged from 5 mm to 6.25 mm (Fig. 3). Compared to intact monkeys (Fig. 3**B**), the animals subjected to SCI exhibited a dramatically lower areas of CB labeling on the lesioned side, as shown in figure 3**C** and **D**. This reduced CB labeling was however localized at the same rostral location as in intact monkeys. Three monkeys subjected to SCI (Mk-AB-B, Mk-AB-S, Mk-C-Bo), independently of the treatment group, exhibited statistically significant lower area of CB labeled terminal fields on the lesioned side than on the intact side all along the gracile nucleus. Regarding the treatment groups, the observed decrease of the CB labeled terminal fields areas on the lesioned side on each section along the caudo-rostral axis was however less statistically significant in the untreated monkey (Fig. 3**C**; Mk-C-Bo, $p=0.03$), compared to the monkeys subjected to the combined treatment (Fig. 3**D**; Mk-AB-B, $p=0.005$, and Mk-AB-S, $p<0.001$). One of the monkeys which received the combined treatment, Mk-AB-P, exhibited a total absence of CB labeling in the gracile nucleus on both sides. A possible interpretation may be a failure of the CB staining in this animal. However, this bilateral deficit of CB staining appeared to be rather the outcome of a bilateral section of the fasciculus gracilis, as supported by the myelin staining results described below [**Myelin labelling normalized areas in the dorsal column funiculi correlated with the effects of treatments**].

Cuneate nucleus, effects of motor system injury at two different levels: hemi-spinal cord and primary motor cortex hand area injury

The cuneate nucleus (Fig. 4**A** and 5**B**) is located lateral to the gracile nucleus, the CB labeled terminal fields appearing to cover a somewhat longer caudo-rosral extent than in the gracile nucleus and to be larger at each section level. These anatomical observations were confirmed on the bar graphs, representing the area of CB labeled axonal terminal fields on both sides of each histological section in two intact (Fig. 4**B** and 5**B**), 4 SCI (Fig. 4**C** and **D**) and 4 MCI (Fig. 5**C** and **D**) monkeys. The extents of CB labeled terminal fields along the caudo-rostral axis of the cuneate nucleus were longer than those observed for the gracile nucleus terminal fields (Fig. 3), with values ranging from 5.85 mm to 9 mm (Mk-C-RO was ignored due to the most caudal brainstem sections missing). As for the gracile nucleus, a sparse distribution of CB labeling was observed in the caudal half of the cuneate nucleus, becoming denser and larger in the rostral half (Figs. 4 and 5).

Effects of SCI at C7/C8 level on CB labeled axonal terminal fields in the cuneate nucleus

The cuneate nucleus receives afferent information from the forelimb which enter the spinal cord at higher rostro-caudal levels than the intended hemi-section at C7/C8. As a result, one did not expect a direct impact of the SCI on the CB labelling in the cuneate nucleus, in contrast to what was observed above in the gracile nucleus (Fig. 1**A**). In the present study, a further goal was to test the hypothesis that a treatment combining anti-Nogo-A antibody with BDNF may impact on the unsectioned cuneate sensory pathway in monkeys subjected to SCI.

CB labelling in the cuneate nucleus did not show dramatic imbalance between both sides in the SCI monkey Mk-AB-B, as shown in figure 4**A** (zone delineated with black contour). The effects of SCI on the CB labeled sensory terminal fields in the cuneate nucleus (Fig. 4**C**) were compared between the lesioned and the unlesioned sides, in the intact monkeys (Fig. 4**B**) and in the lesioned monkeys receiving the combined treatment (Fig. 4**D**). Unlike the strong differences observed in the gracile nucleus (Fig. 3), comparisons as paired values between the lesioned and the unlesioned sides in the untreated monkey Mk-C-Bo subjected to SCI (Fig. 4**C**) did not reveal a significant decrease of CB labeling, similarly to the intact monkeys (Fig. 4**B**). Differences in CB labeling areas between the unlesioned and the lesioned sides were observed in one injured monkey receiving the treatment, Mk-AB-P (Fig. 4**D**), indicating lessened CB labeled terminal fields in the cuneate nucleus arising from

the first two hand fingers on the lesioned side. However, the decrease was not massive, in line with the moderate statistical significance (Mk-AB-P, p=0.03).

Topographically, the distribution of the CB labeled terminal fields in the cuneate nucleus appeared to be different in the monkeys subjected to SCI (Fig. 4**C** and **D**). Two main zones of abundant CB labeled terminal fields were observed, localized one after the other in the rostral part of the cuneate nucleus, in contrast to the single one present in the intact monkeys (Fig. 4**B**). Regarding the caudo-rostral extent of the CB labeled terminal fields, only one treated monkey (Fig. 4**D**), Mk-AB-P, did not show this increase of extent along the caudo-rostral axis observed in the other monkeys subjected to SCI (Fig. 4**C** and **D**). Furthermore, the apparent tendency that the total quantity of CB labeled terminal fields in the rostral main area of the cuneate nucleus could be higher for the group of SCI monkeys, untreated and treated (Fig. 4**C** and **D**) as compared to the intact monkeys (Fig. 4**B**) is examined below [*Comparison of the area size and length of CB labeled axonal terminal fields in the cuneate nucleus* between groups].

Effects of MCI on CB labeled axonal terminal fields in the cuneate nucleus

On the contrary to SCI, MCI is not expected to exert a direct impact on the primary sensory afferents in the cuneate (or gracile) nucleus, as MCI does not directly affect these projections (Fig. 1**B**). One can hypothesize that the distribution of the CB labeling in the cuneate nucleus should be comparable on each side, as in intact monkeys. However, due to the presence, albeit weak, of corticocuneate projections arising from the motor areas (Bentivoglio and Rustioni, 1986; Kuypers and Tuerk, 1964; Cheema et al., 1985; Martinez et al., 1995), the previous hypothesis may prove to be inaccurate and one may alternatively hypothesize that the distribution of the CB labeling in the cuneate nucleus may be affected following MCI, due to a lack of corticocuneate inputs. Not only suggested to result in a growth response in intact adult CNS (for review: Schwab, 2004), it has been observed that anti-Nogo-A antibody treatment following MCI enhanced the callosal inputs to the adjacent ipsilesional premotor cortex (Hamadjida et al., 2012), an area involved in the functional recovery (Liu and Rouiller, 1999; Hoogwoud et al., 2013). In the present study, a further goal was to test the hypothesis that a treatment with anti-Nogo-A antibody can impact on sensory pathways in monkeys subjected to MCI, by analyzing the primary afferents terminal fields into the cuneate nucleus.

The effects of MCI on the bilateral CB labeled sensory terminal fields in the cuneate nucleus of the untreated monkeys (Fig. 5**C**) were compared with those in intact monkeys (Fig.

5**B**) and in anti-Nogo-A antibody treated monkeys (Fig. 5**D**). Comparably to the intact monkeys (Fig. 5**B**), and as for the monkeys subjected to SCI (Fig. 4**C** and **D**), comparisons between the lesioned and the unlesioned sides as paired values did not exhibit massive and significant side imbalance of CB labeling receptive fields in the cuneate nucleus in the untreated monkeys subjected to MCI (Fig. 5**C**). Differences in CB labeling areas between the unlesioned and the lesioned sides appeared for the MCI monkeys subjected to the treatment (Fig. 5**D**). These significant differences indicate lessened CB labeled terminal fields in the cuneate nucleus from the two first hand fingers on the unlesioned side for the two monkeys of the MCI treated group (Mk-A-MO: p=0.003 and Mk-A-SL: p=0.04; Fig. 5**D**). However, this side imbalance appears to be not massive (Fig. 5**A**) although statistically significant, as for the SCI treated monkeys discussed above (Fig. 4**D**).

Topographically, the distribution of the CB labeled terminal fields in the cuneate nucleus appeared to be different in the monkeys subjected to MCI, as it was observed for those subjected to SCI (Fig. 4**C** and **D**). Similarly to the untreated (Fig. 4**C**) and treated (Fig. 4**D**) groups of SCI monkeys, two main zones of abundant CB labeled terminal fields were observed, localized one after the other in the rostral part of the cuneate nucleus, in the untreated group of MCI monkeys (Fig. 5 **C**), in contrast to the single one present in the intact monkeys (Fig. 5**B**). However, this distribution differed from the single main zone of abundant CB labeled terminal fields observed in the monkeys of the MCI treated group (Fig. 5**D**), similar to what was observed in the intact monkeys (Fig. 5**B**). Regarding the caudo-rostral extent of the CB labeled terminal fields, as for the SCI monkey Mk-AB-P, only one monkey of the treated MCI group (Fig. 5**D**), Mk-A-MO, did not show this increase of extent along the caudo-rostral axis observed for the other monkeys subjected to MCI (Fig. 5**C** and **D**) (observation not available for Mk-C-RO in the untreated MCI group due to missing most caudal sections of the brainstem; Fig. 5**C**).

Furthermore, the total quantity of CB labeled terminal fields in the rostral main area of the cuneate nucleus compared to the monkeys of the intact group (Fig. 5**B**) appeared to be higher, as observed in the group of SCI monkeys (Fig. 4**C** and **D**), only for one of the untreated MCI monkey Mk-C-BI (Fig. 5**C**), whereas it appeared to be not different for the three remaining monkeys of the MCI group, Mk-C-RO, Mk-A-MO and Mk-A-SL (Fig. 5**C** and **D**). These apparent differences are examined in the following paragraph.

Comparison of the area size and length of CB labeled axonal terminal fields in the cuneate nucleus between groups

To observe an eventual increase of the length of the CB labeled terminal fields, comparisons were done between the total quantities of CB labeled terminal fields and the corresponding lengths in the cuneate nucleus. These comparisons were restricted to the rostral main area of CB labeling. The concerned zone of main CB labeled terminal fields area in rostral location starts at the first slice of high increase of CB labeling and finishes with the last slice of high labeling before the rostral end of CB labeling (Fig. 6**A**). To mention, statistical comparison between lesioned and unlesioned side, with the non-parametric Wilcoxon test for paired values, restricted to this rostral main area of CB labeling did not reveal any statistical differences (data not shown) contradictorily to the previous comparisons along the total area of CB labeling (Fig. 3, 4, 5).

A rapid overview showed a consistent increase of the size of CB labeled terminal fields areas (Y axis; in pixels) with the corresponding lengths increase (Fig. 6**B**). Generally, the lesioned and treated monkeys, irrespectively to the lesion type, appeared to shift on the left as compared to the untreated SCI and MCI and the intact monkeys all gathered on an inferior line values. This reflects larger area sizes for comparable lengths of the main CB labeled axonal terminal fields in the cuneate nucleus. However, different profiles were observed. As previously described, except for rostrocaudal lengths of three monkeys (Mk-A-SL: 2100 µm, Mk-A-MO: 2700 µm and Mk-AB-P: 2500 µm), the main zone of CB labeled terminal fields tended to be more extended along the rostro-caudal axis (X axis) in monkeys subjected to motor system injuries (Mk-C-RO: 3150 µm, Mk-C-BI: 4250 µm, Mk-C-Bo: 3250 µm, Mk-AB-S: 3500 µm and Mk-AB-B: 3750 µm) as compared to those of the two intact monkeys (Mk-I-R12: 2500 µm and Mk-I-R13: 2500 µm). For the two intact monkeys, the CB labeled terminal fields areas among the shortest length was associated with the lowest size (Mk-I-R12: $1.42e^{+5}$ pixels and $1.72e^{+5}$ pixels; Mk-I-R13: $1.18e^{+5}$ pixels and $1.25e^{+5}$ pixels). The first profile concerns the three monkeys with similar length of the main area as compared to the intact monkeys. This profile concerns the two MCI treated monkeys. Still compared to the intact monkeys, these two MCI treated monkeys exhibited an amount of CB labeling moderately higher on both side for Mk-A-SL (unlesioned $1.7e^{+5}$ pixels and lesioned $1.78e^{+5}$ pixels), but for Mk-A-MO, higher only on the lesioned side ($1.42e^{+5}$ pixels) and similar on the unlesioned side ($1.95e^{+5}$ pixels). The third monkey with similar length of the main area as compared to the intact monkeys was of the SCI treated group, Mk-AB-P, and

exhibited an associated amount of CB labeled terminal fields strongly higher on the unlesioned side ($2.39e^{+5}$ pixels) than on the lesioned side ($1.43e^{+5}$ pixels) closer as for intact monkeys. The second profile concerns the two other monkeys of the SCI treated group, Mk-AB-S and Mk-AB-B, with higher sizes and lengths of main CB labeled terminal field areas than those of intact monkeys. These SCI treated monkeys showed the same higher size on the unlesioned side (Mk-AB-S: $3.13e^{+5}$ pixels and Mk-AB-B: $3.34e^{+5}$ pixels) than on the lesioned side (Mk-AB-S: $2.98e^{+5}$ pixels and Mk-AB-B: $2.98e^{+5}$ pixels). To generalize, Mk-AB-P, only on the unlesioned side, Mk-AB-S; Mk-AB-B and Mk-A-SL presented higher area size of the main sensorial CB projections in the cuneate nucleus for similar lengths than both untreated lesioned and intact monkeys groups. The third profile concerns the lesioned and untreated monkeys. The untreated monkeys subjected to MCI (Mk-C-RO and Mk-C-BI) exhibited higher lengths and sizes of this main area as compared to the intact monkeys. For the first untreated monkey, Mk-C-RO, size of CB labeled terminal fields area was higher on the lesioned side ($2.15e^{+5}$ pixels) than on the unlesioned side ($1.78e^{+5}$ pixels) and for the second one, Mk-C-BI, higher on the unlesioned side ($3.53e^{+5}$ pixels) than on the lesioned side ($3.01e^{+5}$ pixels). The untreated monkey subjected to SCI, Mk-C-Bo, exhibited higher size and length of main CB labeled terminal fields area than those of intact monkeys. Areas size for Mk-C-Bo was not higher on the lesioned side ($2.15e^{+5}$ pixels) compared to the unlesioned side ($1.88e^{+5}$ pixels) than the differences observed for the intact monkeys. Generally the lesioned and untreated monkeys groups presented lower area size of the main sensorial CB projections for similar lengths in the cuneate nucleus than lesioned and treated monkeys groups.

Relationship between the normalized area of myelin labelling in the dorsal column funiculi and CB labeled terminal fields in SCI monkeys

In further analyses conducted in SCI monkeys, myelin labelling was assessed on transverse sections at C3 level. The areas of myelin labelling in the dorsal column pathways of the spinal cord was measured, and used as a proxy of the integrity of the sensory ascending pathways. This set of analyses compared the relation between the amount of CB labeled terminal fields in the DCN and the integrity of the corresponding ascending pathways (Fig. 7).

Deficits of myelin labelling appeared clearly on the hemi-spinal cord injured side, by a decrease up to a total lack of staining on transversal cervical spinal cord sections stained for myelin (Fig. 7**A**). The fasciculi cuneatus and gracilis were delineated on both sides with systematic anatomical landmarks (see methods for detail) delineating the ROIs. On the dorsal part, a deficit of myelin was observed variably in the delineated ROI for the fasciculus gracilis

(not all shown), depending on the extent of lesion in the dorsal funiculus at C7/C8 level. For majority, a deficit of myelin labelling was observed in the medial border of the delineated ROI of the fasciculus cuneatus, as shown in the two monkeys depicted in figure 7**A**. As addressed in the discussion, this region representing the only myelin loss in the Mk-C-Ga example represents the area of projections of the ascending pathways from the trunk. This links the spinal cord level of the trunk projections under the C7/C8 level of the lesion which not affects the most medially located projections from the lower limb neither the ones from the upper limb projecting above the lesion level.

The areas of myelin labelling were measured (in number of pixels) in each ROI and normalized by the total size of the corresponding ROI, thus corresponding to normalized areas in numbers of pixels. Significant statistical analyses with linear regression (Fig. 7**B**) showed high dependence between the myelin normalized areas in the fasciculus gracilis and the areas of CB labeled axonal terminals fields in the gracile nucleus (r^2=0.81; p<0.001). This correlation was not found between the cuneate nucleus and the corresponding pathways because not directly lesioned (data not shown).

Myelin labelling normalized areas in the dorsal column funiculi correlated with the effects of treatments

Overall, from our laboratory, a large pool of monkeys subjected to SCI is available from previous studies, untreated (control antibody) or treated either with anti-Nogo-A antibody or with the latter combined with BDNF (Beaud et al., 2008, 2012; Beaud, 2011; Freund et al., 2006, 2007, 2009; Wannier-Morino et al., 2008). Thus, the following results assessed the effects of these two treatments on the two dorsal column pathways integrity in SCI monkeys based on myelin normalized areas.

Bar graphs (Fig. 8 **A** and **B**) represent the normalized area of myelin staining on the unlesioned side and lesioned side in 19 monkeys distributed in four groups: intact (n=2), SCI untreated (n=5), SCI treated with anti-Nogo-A antibody (n=7) and SCI treated with the combination of anti-Nogo-A antibody with BDNF (n=5). As expected, the lesion at C7-C8 level produced clearly more deficits ipsilesionally in myelin labelling at C3 level in the funiculus gracilis (Fig. 8**B**) than in the funiculus cuneatus (Fig. 8**A**), although the inter-individual variability was substantial in both funiculi. As compared to the intact monkeys exhibiting no side differences, the majority of SCI monkeys showed a moderate deficit of myelin labelling in the cuneatus funiculus on the lesioned side, without clear difference between the treatment groups (control antibody; anti-Nogo-A antibody; anti-Nogo-A antibody

and BDNF). This deficit well represents the highly frequent deficit of myelin labelling observed in the medial border of the delineated ROI of the fasciculus cuneatus associated to the trunk projections (Fig. 7**A**). In the funiculus gracilis, two monkeys (Mk-A-A and Mk-AB-P) exhibited a nearly complete loss of myelin labelling bilaterally (Fig. 8**B**), an observation largely consistent with the SCI involving the dorsal columns on both sides, especially in Mk-A-A (Fig. 8**C**). A large deficit of ipsilesional myelin labelling only was found in Mk-A-M, Mk-AB-B; Mk-AB-Ma; Mk-AB-SL (Fig. 8**B**), fairly in line with the lesion characteristics (Fig. 8**C**). Surprisingly, the less prominent side imbalance of myelin labelling in the funiculus gracilis was found in the untreated group (Fig. 8**B**), with a less clear difference in terms of lesion location as compared to the other two groups of SCI monkeys. An individual assessment did not allow generalization concerning the treatments effects on the affected myelin normalized area of the dorsal column fasciculi due to the high inter-individual variability.

The means of the myelin normalized areas exhibited variable deficit of myelin on the hemi-spinal cord injury side for all SCI groups as compared to the intact monkey group (Fig. 9**A**). For the fasciculus cuneatus, the moderate deficit observed on the lesioned side, in the range values for the three SCI groups, was significant only for the Mk-AB- group ($p=0.006$). The two other groups, Mk-C- and Mk-A-, exhibited higher variability and were thus non-significant. For the fasciculus gracilis, the deficits observed were, as for previous CB staining results, more prominent than for the fasciculus cuneatus. For the three SCI groups, both sides presented deficits, and for both sides, deficits were increasingly higher from the Mk-C-, Mk-A- to Mk-AB- group. The highest deficit of myelin normalized area between the two sides was observed for the Mk-AB- group. However these large effects on myelin normalized area, the differences observed between the three SCI groups were not significant due to the high variability. The total of normalized myelin areas for dorsal column fasciculi also showed effects of hemi-spinal cord injury on both sides for the three SCI groups, with nevertheless higher deficits on the lesioned side, only significant for the Mk-AB group ($p=0.021$). Effects observed were less pronounced for the Mk-C- group and for the Mk-A- group.

Because deficit of the dorsal column fasciculi could be directly due to the lesion size, the total normalized myelin area in the dorsal column fasciculi was correlated with the volume of lesion for each subject (Fig. 9**B**). In this scatter plot, the total of normalized myelin area represents the sum of both fasciculi of both sides. The results firstly showed the association of lowest volumes of lesion of the Mk-C- group with weak deficit of the total normalized myelin area in the dorsal column fasciculi. Secondly, the lesion volumes of the

Mk-A- group were more variable, exhibiting constant decrease of the normalized myelin areas in the dorsal column fasciculi associated with the increase of the lesion volumes. Lastly, the Mk-AB- group, exhibiting higher volumes of lesion for the majority of subjects, showed lower normalized myelin areas in the dorsal column fasciculi for the lowest volumes of lesion, however not increased in association with lesion volumes. Indeed, values of myelin normalized areas in the dorsal column fasciculi for the three subjects with the highest lesion volumes of the Mk-AB- group were of the same order than subjects with lowest lesion volumes.

Discussion

The main results of this study can be summarized as follow: 1) hemi-cervical cord lesion at the C7/C8 level gave rise to a direct massive deficit of primary somatosensory projections in the gracile nucleus originating from the first two toes. This deficit was not prevented by the combined BDNF and anti-Nogo-A antibody treatment and was even suggested to be aggravated; 2) lesion of the motor system at C7/C8 cervical cord level (below forelimb projections) or in M1 hand area, gave rise only to modest modifications of primary somatosensory projections in the cuneate nucleus originating from the two first hand fingers. Results suggested that these modifications were affected the treatments. The area and/or rostro-caudal length of CB sensory terminal fields increased specifically on the unlesioned side in the monkeys subjected to SCI and treated with the combination of BDNF and the anti-Nogo-A antibody as compared to the monkeys of the control treated group. In contrast, in the monkeys subjected to MCI and treated only with the anti-Nogo-A antibody, CB sensory terminal fields area was specifically increased on both sides and this increase was not associated with an increase of the rostro-caudal extent as compared to the monkeys of the control treated group; 3) there was a high dependency between the normalized myelin area in the dorsal column fasciculus and the CB labeled terminal fields amount in the DCN in case of direct lesion of the dorsal column fasciculus; 4) however the low lesion volumes for the untreated monkeys group did not allow comparison, the deficit of normalized myelin areas exhibited similar ranges than those of the untreated monkeys group for equivalent lesion volumes. Proportional higher deficits were observed in relation with the lesion volumes increased in the anti-Nogo-A antibody treated SCI monkeys. In contrast, the only one monkey of the combined treated SCI group with comparable lesion volume exhibited higher deficits of myelin normalized area. However and differently than for the anti-Nogo-A antibody treated

SCI monkeys, although presenting higher volumes of lesion, the majority of combined treated SCI monkeys did not exhibit increasing deficit in relation to the increased lesion volumes.

Prior to discuss the implications of these results, the validity of the CB tracing methodology deserves further debate. It must be kept in mind that the diffusion of the CB tracer under the skin at the injection sites may be variable across fingers and monkeys. However, in accordance with already published studies, CB staining originating from the two first hand fingers has been shown to project to the ventromedial zone of the cuneate nucleus, as seen on transverse brainstem sections for D1, and in a lateral ventral position for D2. These locations for D1 and D2 CB terminal fields are consistent with a previous report for the *Macaca fascicularis* by Strata and colleagues (2003). In the same way, the localization of CB labeled terminal fields in the ventromedial part of the gracile nucleus for T1 and T2 injections sites match up with the anatomical description reported for the *Macaca fascicularis* by Qi and Kaas (2006).

Sensory pathways reorganization following motor system injury

This study gave some thoughts about reorganizations of the sensory pathway following injury. Firstly, and in accordance with previous results for the gracile nucleus and fasciculus, lesion of the sensory dorsal column pathway gave rise to a dramatic decrease of CB terminal fields in the corresponding nucleus (*e.g.* Glendinning et al., 1992; Darian-Smith, 2004; Qi et al., 2011). The gracile nucleus, in the present study, exhibited a pronounced loss of CB labeled terminal fields in monkeys subjected to cervical cord hemi-section linking the myelin loss in the dorsal column gracilis funiculus. Secondly, the present study assessed the integrity of the cuneate sensory pathway at the spinal cord and brainstem level after injury targeting the upper limb motor system. The two levels of lesion in the motor system indirectly affect the sensory system of the upper limb: the M1 hand area and at the spinal cord level below the dermal sensory projection level for the hand and above the motoneuron column controlling the intrinsic hand muscles.

To extrapolate the non-decrease of the CB labeled terminal fields in the cuneate nucleus observed following lesion of the motor system, the indirect effects of such lesions did not appear to result in transneuronal atrophy subsequently to the atrophy and loss of M1 hand area electrophysiological activity. Effectively, a first transneuronal atrophy expressed by a progressive loss of neuron in the DCN over time after deafferentiation was shown to be followed by a secondary transneuronal atrophy of the connected ventral posterieur lateral thalamic nuclei thus potentially by a tertiary transneuronal atrophy of S1 (Woods et al., 2000).

Studies showing atrophy and shrinkage of sensory areas and nuclei assessed these effects following sensory pathway injury at different levels from nerve crush to cortical injury (*e.g.* Darian-Smith and Cifferri, 2006; Song et al., 2008; Kaas et al., 2008; Qi et al., 2011, 2013; Jain et al., 1997, 2008; Kambi et al., 2011; Xerri et al., 1998; Coq and Xerri, 1999). However the present results not only demonstrated a lack of atrophy or a decrease of the primary sensory terminal fields in the cuneate nucleus, but furthermore demonstrated an increase of the main terminal field areas in this first brainstem relay of this pathway. Different studies assessing different aspects of lesions reported the ability of the cortical areas receiving projections of the lesioned zone to enlarge in spite of the frequently observed volume decreased and invasion of the deprived areas by the projections of the surrounding ones. An electrophysiological and anatomical study of the somatosensory reorganization in monkey with irreversible hand immobility has shown an increase of the digit area representation in the somatosensory cortex area 3b and 1 (Florence et al., 1998). This appears to not be a specificity of the somatosensory system in the review of Nudo (2006), suggesting that cortical areas with input and output projections from a lesioned zone was also subjected to reorganization/plasticity observing an enlargement of the premotor projection area, PMv, of the ipsilateral lesioned M1. Activity of the sensory pathways may be enhanced following motor pathway injury, at cortical or spinal cord levels, thus sensory areas could be enlarged due to the lesion. In the two types of motor system lesions, previous reports from our laboratory analyzing these monkeys showed, firstly, a cell body shrinkage in the M1 area of projections of the lesioned pathway in SCI monkeys (Beaud et al., 2008) and, secondly, the electrophysiological loss of activity in the M1 lesioned area (Wyss et al., 2013). The potential of adjacent and distant areas to enlarge after stroke could be the result of the GABAa receptor expression decrease within the cortex and thalamus in both hemispheres, as shown by Redecker and colleagues (2002). This explanation also correlates with studies showing the possibility to rapidly redistribute the function lost after stroke within the spared cortical hemisphere by activating already existing pathways. These studies reported a post-stroke enhancement of the cortical and subcortical excitability concerning the areas highly connected before stroke, the development of this connectivity allowed to sustain the recovery (Frost et al., 2003; Dancause, 2006; Eisner-Janowicz et al., 2008; Brown et al., 2009; Mohajerani et al., 2011). S1 has been presented as the second largest source of corticospinal tract axons after the precentral gyrus in a retrograde tracer injection study and a diffusion tensor imaging study (Galea and Darian-Smith, 1994; Seo and Jang, 2013). Thus a possible enlargement of S1 following the loss of M1 inputs correlates with a functional magnetic resonance imaging

study, showing that S1 was activated by movement of the recovered hand in two M1 stroke patients, while this effect was not observed for the unlesioned hand or for control subjects (Jang et al., 2005). The possibility of an enlargement of S1 following motor system injury leads to the possibility for the connected areas and nuclei to enlarge as a consequence of transneuronal interactions. Importance of the corticocuneate pathway made this nucleus a main source of afferences and efferences for S1 area (Bentivoglio and Rustioni, 1986; Aguilar et al., 2003; Soto et al., 2004; Kuypers and Tuerk, 1964; Cheema et al., 1985), thus potentially subjected to subsequent transneuronal reorganizations. Homogeneous mechanisms of plasticity governing the brainstem and cortex during reorganization and recovery from injury (Mowery et al., 2014) emphasize the possibility for the DCN cuneatus to reorganize as the cortical area 3b.

An explanation involving re-innervation of the deprived area of terminal fields by the surrounding spared D1 and D2 terminal fields in the cuneate nucleus was not retained. Even if the lesion at spinal cord level spared the dorsal sensory tracts for D1 and D2 but lesioned fibers for lower parts of the body as the arm and trunk (shown by the myelin staining loss in the dorsal column fasciculi) the CB labeled terminal fields were localized at the normal D1 and D2 locations of the somatotopic organization in the DCN and fasciculi (Qi and Kaas, 2006). Furthermore, these considerations did not concern the motor cortical lesion, not directly affecting the integrity of the dorsal column pathway.

Myelination of the ascending sensory fibers is a critical fiber feature in the signal transduction for conduction velocities required for their role in correct movement realization. Thus the myelin sheath integrity is an important characteristic, reflecting anatomical integrity of the nerve fibers. Although CB was injected in the two first fingers of the 4 limbs and while the myelin staining labelled indistinguishably fibers from all the body parts in the dorsal column, a significant correlation was found between these two parameters. However, the positive and significant correlation between the CB labeled terminal fields in the DCN and the myelin integrity in the dorsal column fasciculi have to be taken cautiously. It is important to note an inescapable discrepancy between origins of fibers stained with the CB, from the two first fingers of the 4 limbs, and origins of those stained with myelin, representing the whole pathway from all the body parts. A second discrepancy was observed in a previous study showing that CB labeled fibers observed to regrow through the lesion site and presenting electrophysiological activity exhibited some failure revealing myelin sheath disturbance. This was confirmed with immunostaining analyses showing that these regrowth CB axons were unmyelinated (Tan et al., 2007). In spite and in view of these data, a direct transection of the

fibers traced with CB showed a great co-variation of the CB labeled terminal fields in the nucleus with the loss of the myelination in the pathway. This was not the case for the cuneate pathway unlesioned for D1 and D2, the myelin loss observed in the dorsal column funiculus representing the loss of the more proximal and lower part of the body, such as the arm and trunk, projecting lower to the C7-C8 level of the spinal cord. This localization of the more proximal and lower part of the body as the arm and trunk along the medial wall of the funiculus correlates with the already published anatomy of spinal cord pathway localization (Takuno et al., 2011). Thus the myelination in the dorsal column pathway could be a great indicator of direct lesion effects on sensory pathways and its projections in the DCN.

Effect of treatments on the sensory pathway reorganization

CB

The striking effect of treatment with the anti-Nogo-A antibody concerns the comparable size of the main area of CB labeled terminal fields in the nucleus cuneatus between the two monkeys of the treated MCI group and the intact monkeys. The other monkey exhibiting this effect was in the SCI group treated with the combined treatment. As it has been observed an enhancement of the callosal projections in the adjacent ipsilesional premotor area (Hamadjida et al., 2012), the more distant cuneate nucleus could be subjected to plasticity following the M1 hand area lesion. The anti-Nogo-A antibody treatment can affect these remote structures, as was the closer premotor area proposed to sustain the functional recovery following M1 hand area lesion (Liu and Rouiller, 1999; Hoogwoud et al., 2013). These results suggest that blocking Nogo-A, which is known to improve the functional recovery through neural plasticity, sprouting and axonal regeneration (Schnell and Schwab, 1993; Thallmair et al., 1998; Papadopoulos et al., 2002; Li and Strittmatter, 2003; Lee et al., 2004; Fouad et al., 2004; Freund et al., 2006, 2007, 2009; Bashir et al., 2012; Hoogewoud et al., 2013; Wyss et al., 2013), promoted transneuronal reorganization resulting in the prevention of the increase of sizes/lengths of the CB labeled terminal fields following the motor system lesion, remaining close to pre-lesional sizes/lengths (similar to intact monkeys sizes range). This possibility is supported by the numerous corticocuneate projections originating from pyramidal neurons of the somatosensory and motor areas (Bentivoglio and Rustioni, 1986; Kuypers and Tuerk, 1964; Cheema et al., 1985; Martinez et al., 1995). These corticocuneate projections have been shown to influence intracuneate circuits in the DCN through inhibition and disinhibition (Lue et al., 1997, 2001; Aguilar et al., 2003; Soto et al.,

2004). The combined treatment did not lead to preservation or regeneration of the lesioned sensory projections in the DCN (see gracile nucleus results), these projections appeared even more affected compared to the untreated monkeys. As shown in previous reports from our laboratory (Beaud, 2011; Chapter 3 of the present thesis), combination of these two molecules at the spinal cord lesion level was not only non-benefic but could even be deleterious, activating the demonstrated proapoptotic pathway of the fibers (Wang et al., 2000). From the past decade, studies of the BDNF receptor $p75^{NTR}$ have highlighted its ability to activate signaling pathway implied in the cell death and apoptosis processes under certain conditions (Ibáñez and Simi, 2012). Our combination of the two molecules BDNF and antibody against Nogo-A at the spinal cord lesion level is thus suggested to reveal these conditions, not only non-benefic but even deleterious, promoting the proapoptotic pathway of the fibers by too high level of exogenous BDNF (Beaud, 2011; Chapter 3 of the present thesis). We cannot exclude the possibility to explain the higher lesion volumes as resulting from the increase of the depth scalpel penetration depending of the experimenter bias during the spinal cord lesion procedure. However, each time the experimental procedures were conducted in a monkey of the treated group, experimental procedures were conducted in parallel in a monkey of the control group, and were thus subjected to similar protocol conditions. Furthermore, the lesion volumes of the compared untreated monkey remained in similar range than two of the three combined treated SCI monkeys.

Myelin

According to a previous study, our results suggested that neurite growth inhibitor molecules are not implicated in the inhibition of the ascending sensory fibers regeneration (Oudega et al., 2000), although sensory axons express the NgR receptor for Nogo molecule (Hunt et al., 2002). The present results of the normalized myelin area analyses for monkeys of the SCI group receiving the combined treatment link a previous report pointing a lack of improvement of the growth promoting effects of nerve growth factor with an antibodies treatment blocking the Nogo pathway (Oudega et al., 2000). However, the present results do not provide indication on the possibility for axon to regrow but to remain not re-myelinated, as it was suggested by previous work showing that CB labeled fibers regrew through the lesion site with electrophysiological activity but without myelination (Tan et al., 2007). The present results suggest a lack of effect of Nogo-A blocking, alone and in combination with the neurotrophin factor BDNF, in the protection and/or the regrowth and/or sprouting of myelinated sensory pathway in the lesioned dorsal column location. The previous report

indicating the lack of myelination of regrown CB labeled fibers (Tan et al., 2007) and the present results contradict the previous study reporting the beneficial role of BDNF in the remyelination of regrown axon (McTigue et al., 1998).

As already discussed above, the non-beneficial and even detrimental effect of a treatment of SCI with a combination of BDNF and anti-Nogo-A antibody were observed through higher deficit in myelin normalized area in the dorsal column fasciculi. However, a dual effect can be evoked and the results could suggest that the combined treatment can nevertheless preserve the normalized area of myelin in the dorsal column fasciculi of further decrease in spite of the high increase of the SCI volume. Thus, this nevertheless showed beneficial effects, neuroprotection and/or regrowth and remyelination, for sensory ascending pathways.

References

Aguilar, J., Rivadulla, C., Soto, C. & Canedo, A. (2003). New corticocuneate cellular mechanisms underlying the modulation of cutaneous ascending transmission in anesthetized cats. *Journal of Neurophysiology,* 89, 3328-3339.

Asanuma, H. (1981). Functional role of sensory inputs to the motor cortex. *Prog.Neurobiol.,* 16, 241-262.

Barde, Y. A., Edgar, D. & Thoenen, H. (1982). Purification of a new neurotrophic factor from mammalian brain. *EMBO J.,* 1, 549-553.

Bareyre, F. M. & Schwab, M. E. (2003). Inflammation, degeneration and regeneration in the injured spinal cord: insights from DNA microarrays. *Trends in Neurosciences,* 26, 555-563.

Bashir, S., Kaeser, M., Wyss, A., Hamadjida, A., Liu, Y., Bloch, J., Brunet, J. F., Belhaj-Saif, A. & Rouiller, E. M. (2012). Short-term effects of unilateral lesion of the primary motor cortex (M1) on ipsilesional hand dexterity in adult macaque monkeys. *Brain Struct.Funct.,* 217, 63-79.

Beaud, M. L., Schmidlin, E., Wannier, T., Freund, P., Bloch, J., Mir, A., Schwab, M. E. & Rouiller, E. M. (2008). Anti-Nogo-A antibody treatment does not prevent cell body shrinkage in the motor cortex in adult monkeys subjected to unilateral cervical cord lesion. *BMC.Neurosci.,* 9, 5.

Beaud, M. L. (2011). Anatomical organisation and functional recovery in spinal injured non-human primates treated with either an antibody against Nogo-A or a combination of this antibody with brain-derived neurotrophic factor (BDNF). *Thesis, University of Fribourg*.

Beaud, M. L., Rouiller, E. M., Bloch, J., Mir, A., Schwab, M. E., Wannier, T. & Schmidlin, E. (2012). Invasion of lesion territory by regenerating fibers after spinal cord injury in adult macaque monkeys. *Neuroscience,* 227, 271-282.

Bentivoglio, M. & Rustioni, A. (1986). Corticospinal neurons with branching axons to the dorsal column nuclei in the monkey. *J Comp Neurol,* 253, 260-276.

Bentivoglio, M. & Rustioni, A. (1986). Corticospinal neurons with branching axons to the dorsal column nuclei in the monkey. *J.Comp Neurol.,* 253, 260-276.

Brochier, T., Boudreau, M. J., Pare, M. & Smith, A. M. (1999). The effects of muscimol inactivation of small regions of motor and somatosensory cortex on independent finger movements and force control in the precision grip. *Exp.Brain Res.,* 128, 31-40.

Brown, C. E., Aminoltejari, K., Erb, H., Winship, I. R. & Murphy, T. H. (2009). In vivo voltage-sensitive dye imaging in adult mice reveals that somatosensory maps lost to stroke are replaced over weeks by new structural and functional circuits with prolonged modes of activation within both the peri-infarct zone and distant sites. *Journal of Neuroscience,* 29, 1719-1734.

Buchli, A. D. & Schwab, M. E. (2005). Inhibition of Nogo: a key strategy to increase regeneration, plasticity and functional recovery of the lesioned central nervous system. *Ann.Med.,* 37, 556-567.

Cheema, S. S., Rustioni, A. & Whitsel, B. L. (1985). Sensorimotor cortical projections to the primate cuneate nucleus. *Journal of Comparative Neurology,* 240, 196-211.

Coq, J. O. & Xerri, C. (1999). Acute reorganization of the forepaw representation in the rat SI cortex after focal cortical injury: neuroprotective effects of piracetam treatment. *European Journal of Neuroscience,* 11, 2597-2608.

Dancause, N. (2006). Vicarious function of remote cortex following stroke: recent evidence from human and animal studies. *Neuroscientist.,* 12, 489-499.

Darian-Smith, C. (2004). Primary afferent terminal sprouting after a cervical dorsal rootlet section in the macaque monkey. *J.Comp Neurol.*, 470, 134-150.

Darian-Smith, C. & Ciferri, M. (2006). Cuneate nucleus reorganization following cervical dorsal rhizotomy in the macaque monkey: its role in the recovery of manual dexterity. *J.Comp Neurol.*, 498, 552-565.

Darian-Smith, C. (2007). Monkey models of recovery of voluntary hand movement after spinal cord and dorsal root injury. *ILAR.J.*, 48, 396-410.

Eisner-Janowicz, I., Barbay, S., Hoover, E., Stowe, A. M., Frost, S. B., Plautz, E. J. & Nudo, R. J. (2008). Early and late changes in the distal forelimb representation of the supplementary motor area after injury to frontal motor areas in the squirrel monkey. *Journal of Neurophysiology*, 100, 1498-1512.

Florence, S. L., Taub, H. B. & Kaas, J. H. (1998). Large-scale sprouting of cortical connections after peripheral injury in adult macaque monkeys. *Science*, 282, 1117-1121.

Fouad, K., Klusman, I. & Schwab, M. E. (2004). Regenerating corticospinal fibers in the Marmoset (*Callitrix jacchus*) after spinal cord lesion and treatment with the anti-Nogo-A antibody IN-1. *European Journal of Neuroscience*, 20, 2479-2482.

Freund, P., Schmidlin, E., Wannier, T., Bloch, J., Mir, A., Schwab, M. E. & Rouiller, E. M. (2006). Nogo-A-specific antibody treatment enhances sprouting and functional recovery after cervical lesion in adult primates. *Nature Medicine*, 12, 790-792.

Freund, P., Wannier, T., Schmidlin, E., Bloch, J., Mir, A., Schwab, M. E. & Rouiller, E. M. (2007). Anti-Nogo-A antibody treatment enhances sprouting of corticospinal axons rostral to a unilateral cervical spinal cord lesion in adult macaque monkey. *J Comp Neurol*, 502, 644-659.

Freund, P., Schmidlin, E., Wannier, T., Bloch, J., Mir, A., Schwab, M. E. & Rouiller, E. M. (2009). Anti-Nogo-A antibody treatment promotes recovery of manual dexterity after unilateral cervical lesion in adult primates--re-examination and extension of behavioral data. *European Journal of Neuroscience*, 29, 983-996.

Frost, S. B., Barbay, S., Friel, K. M., Plautz, E. J. & Nudo, R. J. (2003). Reorganization of remote cortical regions after ischemic brain injury: a potential substrate for stroke recovery. *Journal of Neurophysiology*, 89, 3205-3214.

Galea, M. P. & Darian-Smith, I. (1994). Multiple corticospinal neuron populations in the macaque monkey are specified by their unique cortical origins, spinal terminations, and connections. *Cereb.Cortex*, 4, 166-194.

Glendinning, D. S., Cooper, B. Y., Vierck, C. J., Jr. & Leonard, C. M. (1992). Altered precision grasping in stumptail macaques after fasciculus cuneatus lesions. *Somatosens.Mot.Res.*, 9, 61-73.

GrandPre, T., Nakamura, F., Vartanian, T. & Strittmatter, S. M. (2000). Identification of the Nogo inhibitor of axon regeneration as a Reticulon protein. *Nature*, 403, 439-444.

Hamadjida, A., Wyss, A. F., Mir, A., Schwab, M. E., Belhaj-Saif, A. & Rouiller, E. M. (2012). Influence of anti-Nogo-A antibody treatment on the reorganization of callosal connectivity of the premotor cortical areas following unilateral lesion of primary motor cortex (M1) in adult macaque monkeys. *Exp.Brain Res.*, 223, 321-340.

Hatsopoulos, N. G. & Suminski, A. J. (2011). Sensing with the motor cortex. *Neuron*, 72, 477-487.

Hoogewoud, F., Hamadjida, A., Wyss, A. F., Mir, A., Schwab, M. E., Belhaj-Saif, A. & Rouiller, E. M. (2013). Comparison of functional recovery of manual dexterity after unilateral spinal cord lesion or motor cortex lesion in adult macaque monkeys. *Front Neurol.*, 4, 101.

Huang, E. J. & Reichardt, L. F. (2001). Neurotrophins: roles in neuronal development and function. *Annu.Rev.Neurosci.*, 24, 677-736.

Hunt, D., Mason, M. R., Campbell, G., Coffin, R. & Anderson, P. N. (2002). Nogo receptor mRNA expression in intact and regenerating CNS neurons. *Mol.Cell Neurosci.*, 20, 537-552.

Ibanez, C. F. & Simi, A. (2012). p75 neurotrophin receptor signaling in nervous system injury and degeneration: paradox and opportunity. *Trends Neurosci.*, 35, 431-440.

Jain, N., Catania, K. C. & Kaas, J. H. (1997). Deactivation and reactivation of somatosensory cortex after dorsal spinal cord injury. *Nature*, 386, 495-498.

Jain, N., Qi, H. X., Collins, C. E. & Kaas, J. H. (2008). Large-scale reorganization in the somatosensory cortex and thalamus after sensory loss in macaque monkeys. *Journal of Neuroscience*, 28, 11042-11060.

Jang, S. H., Ahn, S. H., Yang, D. S., Lee, D. K., Kim, D. K. & Son, S. M. (2005). Cortical reorganization of hand motor function to primary sensory cortex in hemiparetic patients with a primary motor cortex infarct. *Arch.Phys.Med.Rehabil.*, 86, 1706-1708.

Jenny, A. B. & Inukai, J. (1983). Principles of motor organization of the monkey cervical spinal cord. *Journal of Neuroscience*, 3, 567-575.

Kaas, J. H., Qi, H. X., Burish, M. J., Gharbawie, O. A., Onifer, S. M. & Massey, J. M. (2008). Cortical and subcortical plasticity in the brains of humans, primates, and rats after damage to sensory afferents in the dorsal columns of the spinal cord. *Exp.Neurol.*, 209, 407-416.

Kaeser, M., Wyss, A. F., Bashir, S., Hamadjida, A., Liu, Y., Bloch, J., Brunet, J. F., Belhaj-Saif, A. & Rouiller, E. M. (2010). Effects of Unilateral Motor Cortex Lesion on Ipsilesional Hand's Reach and Grasp Performance in Monkeys: Relationship With Recovery in the Contralesional Hand. *Journal of Neurophysiology*, 103, 1630-1645.

Kambi, N., Tandon, S., Mohammed, H., Lazar, L. & Jain, N. (2011). Reorganization of the primary motor cortex of adult macaque monkeys after sensory loss resulting from partial spinal cord injuries. *Journal of Neuroscience*, 31, 3696-3707.

Kaplan, D. R. & Miller, F. D. (2000). Neurotrophin signal transduction in the nervous system. *Current Opinion in Neurobiology*, 10, 381-391.

Kunzle, H. (1978). Cortico-cortical efferents of primary motor and somatosensory regions of the cerebral cortex in macaca fascicularis. *Neurosci.*, 3, 25-39.

Kuypers, H. G. J. M. & Tuerk, J. D. (1964). The distribution of the cortical fibres within the nuclei cuneatus and gracilis in the cat. *J.Anat.(Lond.)*, 98, 143-162.

Lanz, F., Lanz, X., Scherly, A., Moret, V., Gaillard, A., Gruner, P., Hoogewoud, H. M., Belhaj-Saif, A., Loquet, G. & Rouiller, E. M. (2013). Refined methodology for implantation of a head fixation device and chronic recording chambers in non-human primates. *J.Neurosci.Methods*, 219, 262-270.

Lee, J. K., Kim, J. E., Sivula, M. & Strittmatter, S. M. (2004). Nogo receptor antagonism promotes stroke recovery by enhancing axonal plasticity. *Journal of Neuroscience*, 24, 6209-6217.

Li, S. & Strittmatter, S. M. (2003). Delayed systemic Nogo-66 receptor antagonist promotes recovery from spinal cord injury. *Journal of Neuroscience*, 23, 4219-4227.

Liu, Y. & Rouiller, E. M. (1999). Mechanisms of recovery of dexterity following unilateral lesion of the sensorimotor cortex in adult monkeys. *Exp.Brain Res.*, 128, 149-159.

Lu, P. & Tuszynski, M. H. (2008). Growth factors and combinatorial therapies for CNS regeneration. *Exp.Neurol.*, 209, 313-320.

Lue, J. H., Lai, S. M., Wang, T. J., Shieh, J. Y. & Wen, C. Y. (1997). Synaptic relationships between corticocuneate terminals and glycine-immunoreactive neurons in the rat cuneate nucleus. *Brain Res.*, 771, 167-171.

Lue, J. H., Chen, S. H., Shieh, J. Y. & Wen, C. Y. (2001). Afferent synaptic contacts on glycine-immunoreactive neurons in the rat cuneate nucleus. *Synapse,* 41, 139-149.

Martinez, L., Lamas, J. A. & Canedo, A. (1995). Pyramidal tract and corticospinal neurons with branching axons to the dorsal column nuclei of the cat. *Neuroscience,* 68, 195-206.

Matyas, F., Sreenivasan, V., Marbach, F., Wacongne, C., Barsy, B., Mateo, C., Aronoff, R. & Petersen, C. C. (2010). Motor control by sensory cortex. *Science,* 330, 1240-1243.

McTigue, D. M., Horner, P. J., Stokes, B. T. & Gage, F. H. (1998). Neurotrophin-3 and brain-derived neurotrophic factor induce oligodendrocyte proliferation and myelination of regenerating axons in the contused adult rat spinal cord. *Journal of Neuroscience,* 18, 5354-5365.

Mohajerani, M. H., Aminoltejari, K. & Murphy, T. H. (2011). Targeted mini-strokes produce changes in interhemispheric sensory signal processing that are indicative of disinhibition within minutes. *Proc.Natl.Acad.Sci.U.S.A,* 108, E183-E191.

Mowery, T. M., Kostylev, P. V. & Garraghty, P. E. (2014). AMPA and GABA(A/B) receptor subunit expression in the cuneate nucleus of adult squirrel monkeys during peripheral nerve regeneration. *Neurosci.Lett.,* 559, 141-146.

Nagahara, A. H. & Tuszynski, M. H. (2011). Potential therapeutic uses of BDNF in neurological and psychiatric disorders. *Nat.Rev.Drug Discov.,* 10, 209-219.

Nudo, R. J., Friel, K. M. & Delia, S. W. (2000). Role of sensory deficits in motor impairments after injury to primary motor cortex. *Neuropharmacology,* 39, 733-742.

Nudo, R. J. (2006). Mechanisms for recovery of motor function following cortical damage. *Current Opinion in Neurobiology,* 16, 638-644.

Numakawa, T., Suzuki, S., Kumamaru, E., Adachi, N., Richards, M. & Kunugi, H. (2010). BDNF function and intracellular signaling in neurons. *Histol.Histopathol.,* 25, 237-258.

Oertle, T., van der Haar, M. E., Bandtlow, C. E., Robeva, A., Burfeind, P., Buss, A., Huber, A. B., Simonen, M., Schnell, L., Brosamle, C., Kaupmann, K., Vallon, R. & Schwab, M. E. (2003). Nogo-A inhibits neurite outgrowth and cell spreading with three discrete regions. *Journal of Neuroscience,* 23, 5393-5406.

Oudega, M., Rosano, C., Sadi, D., Wood, P. M., Schwab, M. E. & Hagg, T. (2000). Neutralizing antibodies against neurite growth inhibitor NI-35/250 do not promote regeneration of sensory axons in the adult rat spinal cord. *Neuroscience,* 100, 873-883.

Papadopoulos, C. M., Tsai, S. Y., Alsbiei, T., O'Brien, T. E., Schwab, M. E. & Kartje, G. L. (2002). Functional recovery and neuroanatomical plasticity following middle cerebral artery occlusion and IN-1 antibody treatment in the adult rat. *Annals of Neurology,* 51, 433-441.

Pernet, V. & Schwab, M. E. (2012). The role of Nogo-A in axonal plasticity, regrowth and repair
1. *Cell Tissue Res.,* 349, 97-104.

Pizzimenti, M. A., Darling, W. G., Rotella, D. L., McNeal, D. W., Herrick, J. L., Ge, J., Stilwell-Morecraft, K. S. & Morecraft, R. J. (2007). Measurement of reaching kinematics and prehensile dexterity in nonhuman primates. *Journal of Neurophysiology,* 98, 1015-1029.

Qi, H. X. & Kaas, J. H. (2006). Organization of primary afferent projections to the gracile nucleus of the dorsal column system of primates. *J.Comp Neurol.,* 499, 183-217.

Qi, H. X., Chen, L. M. & Kaas, J. H. (2011). Reorganization of somatosensory cortical areas 3b and 1 after unilateral section of dorsal columns of the spinal cord in squirrel monkeys. *Journal of Neuroscience,* 31, 13662-13675.

Qi, H. X., Gharbawie, O. A., Wynne, K. W. & Kaas, J. H. (2013). Impairment and recovery of hand use after unilateral section of the dorsal columns of the spinal cord in squirrel monkeys. *Behav.Brain Res.,* 252, 363-376.

Rathelot, J. A. & Strick, P. L. (2006). Muscle representation in the macaque motor cortex: an anatomical perspective. *Proc.Natl.Acad.Sci.U.S.A,* 103, 8257-8262.

Redecker, C., Wang, W., Fritschy, J. M. & Witte, O. W. (2002). Widespread and long-lasting alterations in GABA(A)-receptor subtypes after focal cortical infarcts in rats: mediation by NMDA-dependent processes. *J.Cereb.Blood Flow Metab,* 22, 1463-1475.

Rouiller, E. M., Babalian, A., Kazennikov, O., Moret, V., Yu, X. H. & Wiesendanger, M. (1994). Transcallosal connections of the distal forelimb representations of the primary and supplementary motor cortical areas in macaque monkeys. *Exp.Brain Res.,* 102, 227-243.

Schmidlin, E., Wannier, T., Bloch, J. & Rouiller, E. M. (2004). Progressive plastic changes in the hand representation of the primary motor cortex parallel incomplete recovery from a unilateral section of the corticospinal tract at cervical level in monkeys. *Brain Res.,* 1017, 172-183.

Schmidlin, E., Wannier, T., Bloch, J., Belhaj-Saif, A., Wyss, A. F. & Rouiller, E. M. (2005). Reduction of the hand representation in the ipsilateral primary motor cortex following unilateral section of the corticospinal tract at cervical level in monkeys. *BMC.Neurosci.,* 6, 56.

Schmidlin, E., Kaeser, M., Gindrat, A. D., Savidan, J., Chatagny, P., Badoud, S., Hamadjida, A., Beaud, M. L., Wannier, T., Belhaj-Saif, A. & Rouiller, E. M. (2011). Behavioral assessment of manual dexterity in non-human primates. *J.Vis.Exp.*.

Schmued, L. C. (1990). A rapid, sensitive histochemical stain for myelin in frozen brain sections. *J.Histochem.Cytochem.,* 38, 717-720.

Schnell, L. & Schwab, M. E. (1993). Sprouting and regeneration of lesioned corticospinal tract fibres in the adult rat spinal cord. *European Journal of Neuroscience,* 5, 1156-1171.

Schwab, M. E. (2004). Nogo and axon regeneration. *Current Opinion in Neurobiology,* 14, 118-124.

Schwab, M. E. & Strittmatter, S. M. (2014). Nogo limits neural plasticity and recovery from injury. *Current Opinion in Neurobiology,* 27, 53-60.

Seo, J. P. & Jang, S. H. (2013). Different characteristics of the corticospinal tract according to the cerebral origin: DTI study. *AJNR Am.J.Neuroradiol.,* 34, 1359-1363.

Song, X. Y., Li, F., Zhang, F. H., Zhong, J. H. & Zhou, X. F. (2008). Peripherally-derived BDNF promotes regeneration of ascending sensory neurons after spinal cord injury. *PLoS.One.,* 3, e1707.

Soto, C., Aguilar, J., Martin-Cora, F., Rivadulla, C. & Canedo, A. (2004). Intracuneate mechanisms underlying primary afferent cutaneous processing in anaesthetized cats. *European Journal of Neuroscience,* 19, 3006-3016.

Stepniewska, I., Preuss, T. M. & Kaas, J. H. (1993). Architectonics, somatotopic organization, and ipsilateral cortical connections of the primary motor area (M1) of owl monkeys. *J.Comp Neurol.,* 330, 238-271.

Strata, F., Coq, J. O. & Kaas, J. H. (2003). The chemo- and somatotopic architecture of the Galago cuneate and gracile nuclei. *Neuroscience,* 116, 831-850.

Tan, A. M., Petruska, J. C., Mendell, L. M. & Levine, J. M. (2007). Sensory afferents regenerated into dorsal columns after spinal cord injury remain in a chronic pathophysiological state. *Exp.Neurol.,* 206, 257-268.

Thallmair, M., Metz, G. A. S., Z'Graggen, W. J., Raineteau, O., Kartje, G. L. & Schwab, M. E. (1998). Neurite growth inhibitors restrict plasticity and functional recovery following corticospinal tract lesions. *Nature Neurosci.,* 1, 124-131.

Tokuno, H., Tanaka, I., Senoo, A., Umitsu, Y., Akazawa, T., Nakamura, Y. & Watson, C. (2011). Internet-based atlas of the primate spinal cord. *Neurosci.Res.,* 70, 128-132.

Wang, T., Xiong, J. Q., Ren, X. B. & Sun, W. (2012). The role of Nogo-A in neuroregeneration: a review. *Brain Res.Bull.,* 87, 499-503.

Wannier-Morino, P., Schmidlin, E., Freund, P., Belhaj-Saif, A., Bloch, J., Mir, A., Schwab, M. E., Rouiller, E. M. & Wannier, T. (2008). Fate of rubrospinal neurons after unilateral section of the cervical spinal cord in adult macaque monkeys: effects of an antibody treatment neutralizing Nogo-A. *Brain Res.,* 1217, 96-109.

Wannier, T. M., Maier, M. A. & Hepp-Reymond, M. C. (1991). Contrasting properties of monkey somatosensory and motor cortex neurons activated during the control of force in precision grip. *Journal of Neurophysiology,* 65, 572-589.

Weinmann, O., Schnell, L., Ghosh, A., Montani, L., Wiessner, C., Wannier, T., Rouiller, E., Mir, A. & Schwab, M. E. (2006). Intrathecally infused antibodies against Nogo-A penetrate the CNS and downregulate the endogenous neurite growth inhibitor Nogo-A. *Mol.Cell Neurosci.,* 32, 161-173.

Weishaupt, N., Blesch, A. & Fouad, K. (2012). BDNF: the career of a multifaceted neurotrophin in spinal cord injury. *Exp.Neurol.,* 238, 254-264.

Woods, T. M., Cusick, C. G., Pons, T. P., Taub, E. & Jones, E. G. (2000). Progressive transneuronal changes in the brainstem and thalamus after long-term dorsal rhizotomies in adult macaque monkeys. *Journal of Neuroscience,* 20, 3884-3899.

Wyss, A. F., Hamadjida, A., Savidan, J., Liu, Y., Bashir, S., Mir, A., Schwab, M. E., Rouiller, E. M. & Belhaj-Saif, A. (2013). Long-term motor cortical map changes following unilateral lesion of the hand representation in the motor cortex in macaque monkeys showing functional recovery of hand functions. *Restor.Neurol.Neurosci.,* 31, 733-760.

Xerri, C., Merzenich, M. M., Peterson, B. E. & Jenkins, W. (1998). Plasticity of primary somatosensory cortex paralleling sensorimotor skill recovery from stroke in adult monkeys. *Journal of Neurophysiology,* 79, 2119-2148.

Zorner, B. & Schwab, M. E. (2010). Anti-Nogo on the go: from animal models to a clinical trial. *Ann.N.Y.Acad.Sci.,* 1198 Suppl 1, E22-E34.

	Intact monkeys		Spinal cord injured monkeys				Motor cortical injured monkeys			
	MkI-R12	MkI-R13	MkC-Bo	MkAB-B	MkAB-S	MkAB-P	MkC-Ro	MkC-Bi	MkA-Mo	MkA-Sl
General										
Sex	female	female	male	male	male	male	male	male	male	male
Species	fascicularis	fascicularis	fascicularis	fascicularis	fascicularis	fascicularis	fascicularis	fascicularis	fascicularis	fascicularis
Origin of monkeys	Own colony	Own colony	Bio Prim	Bio Prim	Buckshire US	Buckshire US	Bio Prim	Bio Prim	Bio Prim	Bio Prim
Weight	4	3	3.5	5.3	4.2	4.6	3.2	5	5.6	4.6
Age at the sacrifce (rounded 0.5 year)	6	4.5	4.5	6.5	4.5	5	5	6	6	6.5
Lesion										
Spinal										
Hemi-spinal lesion side	__	__	right	right	left	left	__	__	__	__
Survival time with respect to lesion day (J0)	__	__	J+192	J+167	J+173	J+180	__	__	__	__
Hemisection extent (%)	__	__	93	83	93	77	__	__	__	__
Volume of lesion (mm3)	__	__	4.11	2.36	10.37	6.2	__	__	__	__
Cortical										
Hemisphere lesion side	__	__	__	__	__	__	left	left	left	left
Survival time with respect to lesion day (J0)	__	__	__	__	__	__	J+286	J+301	J+195	J+271
Volume of ibotenic acid injected (µL) (Number of ICMS sites of injections)	__	__	__	__	__	__	18 (in 12 cortical fingers ICMS sites)	29.7 (in 29 cortical fingers ICMS sites)	20 (in 20 cortical fingers ICMS sites)	18 (in 12 cortical fingers ICMS sites)
Volume of lesion in post-central gyrus (mm3)	__	__	__	__	__	__	0	0	0	1.8
Total volume of lesion (in mm³) Gray matter (motor cortex + post-central gyrus)	__	__	__	__	__	__	14	20.13	41.8	78.2
Treatment										
Treatment	__	__	Control antiboby	BDNF & hNogo-A	BDNF & hNogo-A	BDNF & hNogo-A	Control antiboby	Control antiboby	11C7	11C7
Concentration	__	__	7mg/ml	18 mg/ml 0.7 mg/ml	18 mg/ml 0.7 mg/ml	18 mg/ml 0.7 mg/ml	7mg/ml	7mg/ml	3 mg/ml	3 mg/ml
Volume of pumps (ml) for deliberation	__	__	2	2	2	2	2	2	2	2
Tracer										
CB volume (µl) and concentration (%)	160 ; 0.5%	160 ; 0.5%	160 ; 0.5%	170 ; 0.5%	160 ; 0.5%	160 ; 0.5%	160 ; 0.5%	160 ; 0.5%	160 ; 0.5%	120 ; 0.5%
CB transport time (days)	14	14	8	7	12	12	7	12	6	14

Table 1: Summary of animals

Recapitulative table of detailed information for each monkey included in the present study. Mk-C- corresponds to the control antibody treated group, Mk-AB- to the combined treated group (anti-Nogo-A and BDNF treatment), Mk-A- to the anti-Nogo-A antibody treated group and Mk-I- to the intact group. (J+) corresponds to the number of days from the lesion day (J_0).

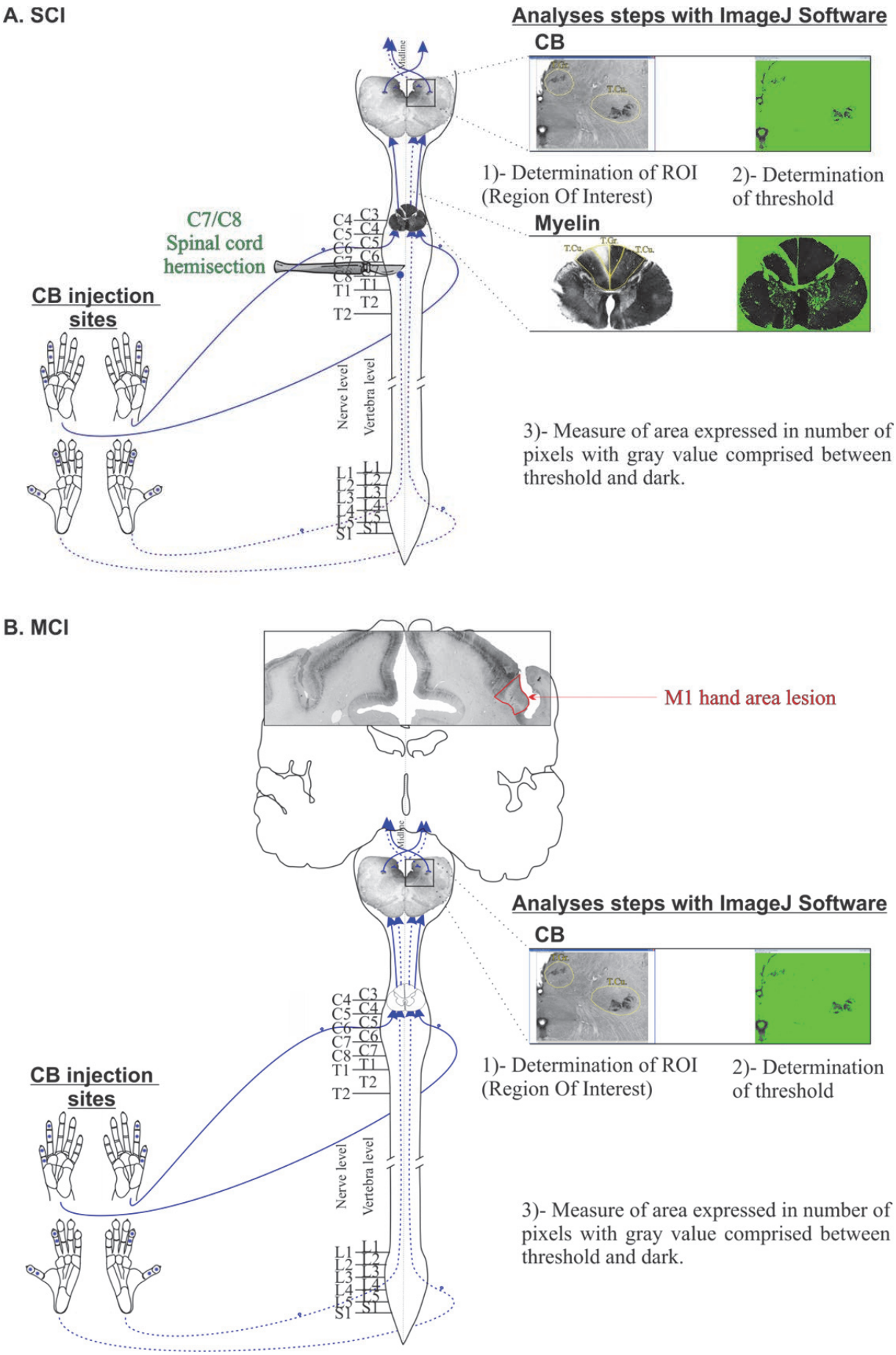
A. SCI
Analyses steps with ImageJ Software
CB
Myelin
1)- Determination of ROI
(Region Of Interest)
2)- Determination
of threshold
3)- Measure of area expressed in number of
pixels with gray value comprised between
threshold and dark.
C7/C8
Spinal cord
hemisection
CB injection
sites
Nerve level
Vertebra level
B. MCI
M1 hand area lesion
Analyses steps with ImageJ Software
CB
1)- Determination of ROI
(Region Of Interest)
2)- Determination
of threshold
3)- Measure of area expressed in number of
pixels with gray value comprised between
threshold and dark.
CB injection
sites
Nerve level
Vertebra level

Figure 1: Method for analyses of CB and myelin labelling

Schematic representations of the Cholera toxin B subunit (CB) method used to study the primary somatosensory afferents in the monkeys subjected to spinal cord injury (**A.** SCI) and the monkeys subjected to motor cortical injury (**B.** MCI).

From the left to the right, these schematic representations illustrate: the injection sites (blue dots) of Cholera toxin B subunit (CB) in the two first phalanges of the two first fingers of both forelimbs and hindlimbs; the routes of transganglionic transport (blue lines) to the DCN in the brainstem through the tractus cuneatus for the upper limbs (blue straight lines) and the tractus gracilis for the lower limbs (blue dotted lines); Neurolucida images captured under light microscope of transverse sections of brainstem, stained for CB, and cervical spinal cord at C3 level, stained for myelin. These sections illustrate the levels of the analyses of primary somatosensory projections in the DCN (CB labelling) and pathways (Myelin staining). The dorsal column fasciculi and the consecutive steps for images analyses using imageJ software are shown on the rightmost panels. Cu.N., cuneate nucleus; Gr.N., gracile nucleus; T.Cu., tractus cuneatus; T.Gr., tractus gracilis. The panels **A** and **B** also represent schematically the rationale of the present study (see introduction).

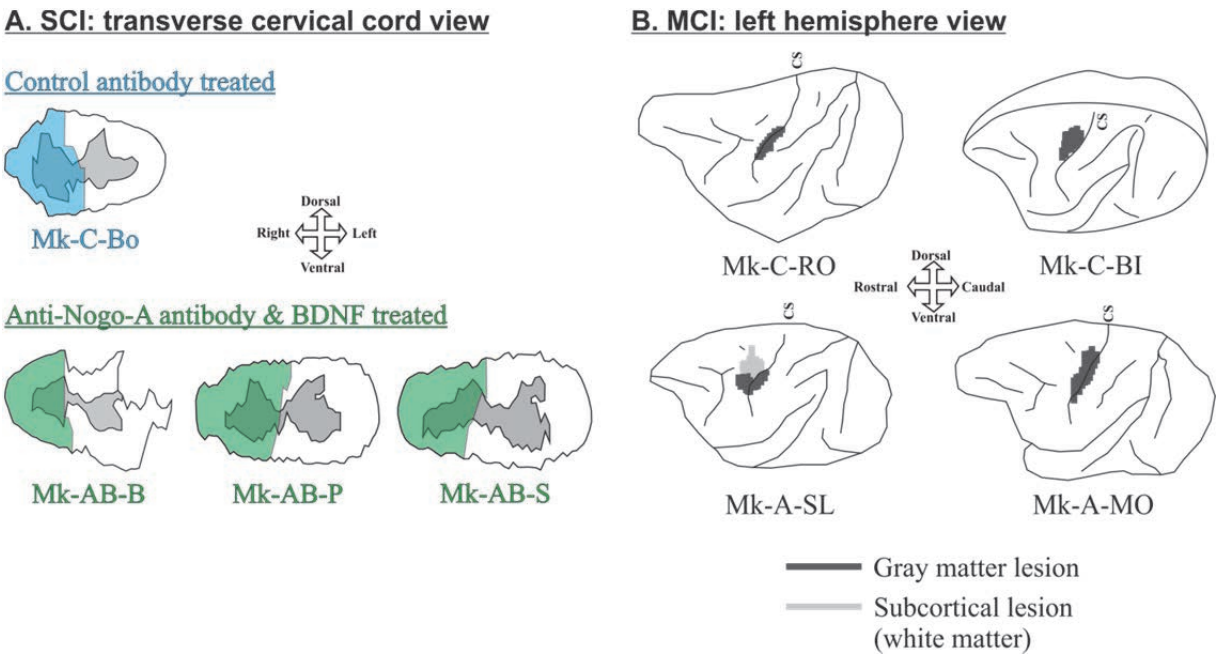

Figure 2: Representation of the spinal cord and motor cortical injury

Anatomical reconstructions for each monkeys injected with CB of the spinal cord injury (SCI) on a transverse section at C7/C8 level (**A.**) and the unilateral motor cortical injury (MCI) on a schematic lateral view of the brain (**B.**). CS, central sulcus. Color code differentiates SCI monkeys, either untreated (marked in blue) from those subjected to the combined anti-Nogo-A antibody and BDNF treatment (marked in green) groups. Same reconstructions as shown in previous reports (SCI: Beaud et al., 2008, 2012; Freund et al., 2006, 2007, 2009; Wannier-Morino et al., 2008 - MCI: Wyss et al., 2013; Hamadjida et al., 2012; Kaeser et al., 2010; Bashir et al., 2012).

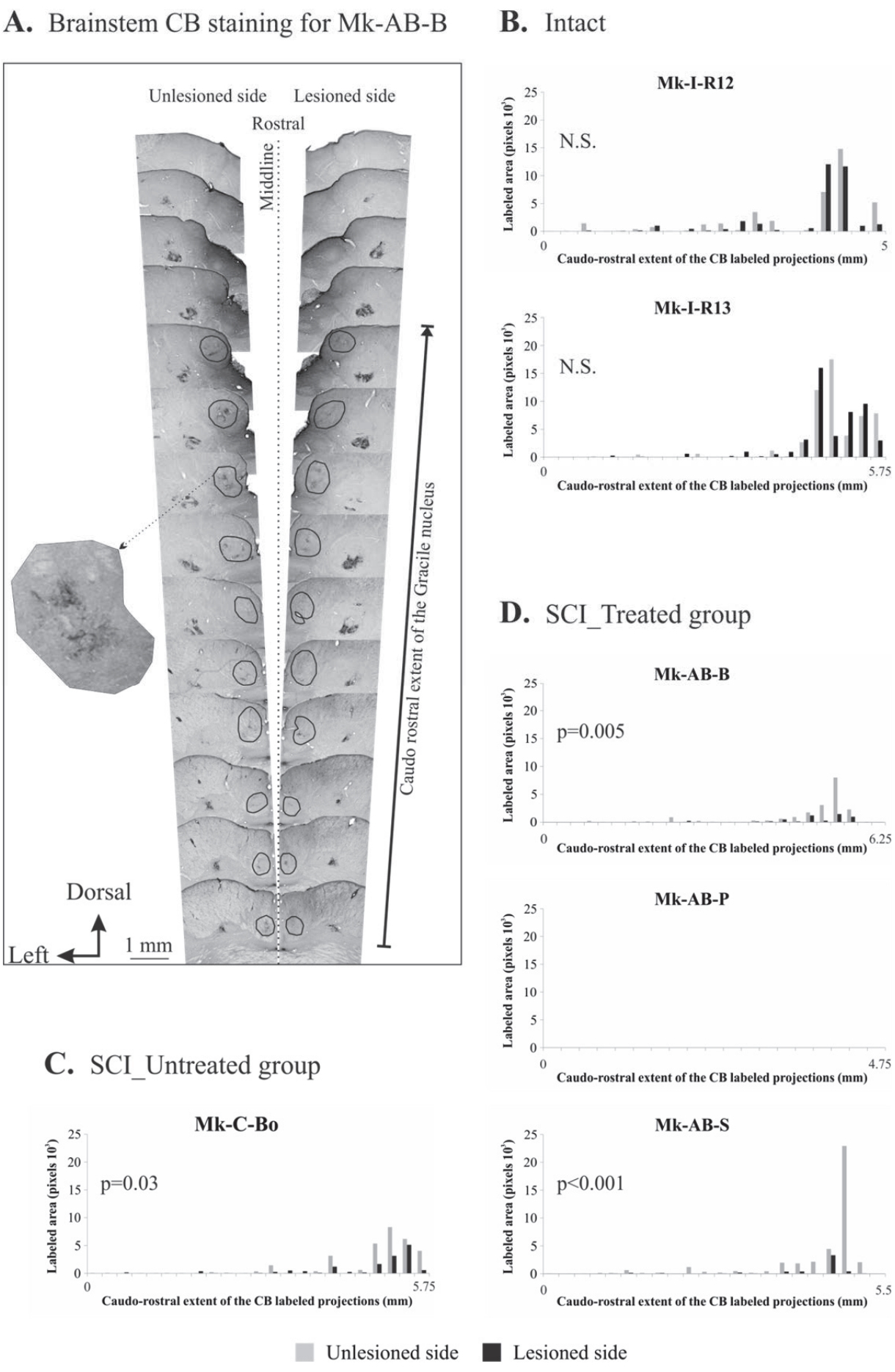
A. Brainstem CB staining for Mk-AB-B
Unlesioned side
Lesioned side
Rostral
Middline
Caudo rostral extent of the Gracile nucleus
Dorsal
Left
1 mm
B. Intact
Mk-I-R12
N.S.
Labeled area (pixels 10³)
Caudo-rostral extent of the CB labeled projections (mm)
Mk-I-R13
N.S.
D. SCI_Treated group
Mk-AB-B
p=0.005
Mk-AB-P
C. SCI_Untreated group
Mk-C-Bo
p=0.03
Mk-AB-S
p<0.001
Unlesioned side
Lesioned side

Figure 3: SCI-Gracile nucleus: CB labelling

Distribution of the CB labeled primary somatosensory axonal terminal fields in the gracile nucleus. An example of CB labeled terminal fields (surrounded with black contour) is shown in the gracile nucleus along the caudo-rostral extent in Mk-AB-B (**A.**). The bar graphs represent the CB labeled axonal terminal fields given by the number of pixels measured with imageJ software, along the caudo-rostral axis for each individual brainstem section, on the lesioned side in black and on the unlesioned side in gray. The CB labelling area results are indicated separately in 2 intact monkeys (**B.**), a monkey subjected to SCI without treatment (Control antibody; **C.**) and in 3 SCI monkeys treated with the combination of anti-Nogo-A antibody and BDNF (**D.**). A distance of 250 µm separates two consecutive sections along the caudo-rostral axis in all monkeys. Comparison of the lesioned side versus the unlesioned side with the non-parametric Wilcoxon test for paired values: N.S. is for statistically non-significant difference.

A. Brainstem CB staining for Mk-AB-B

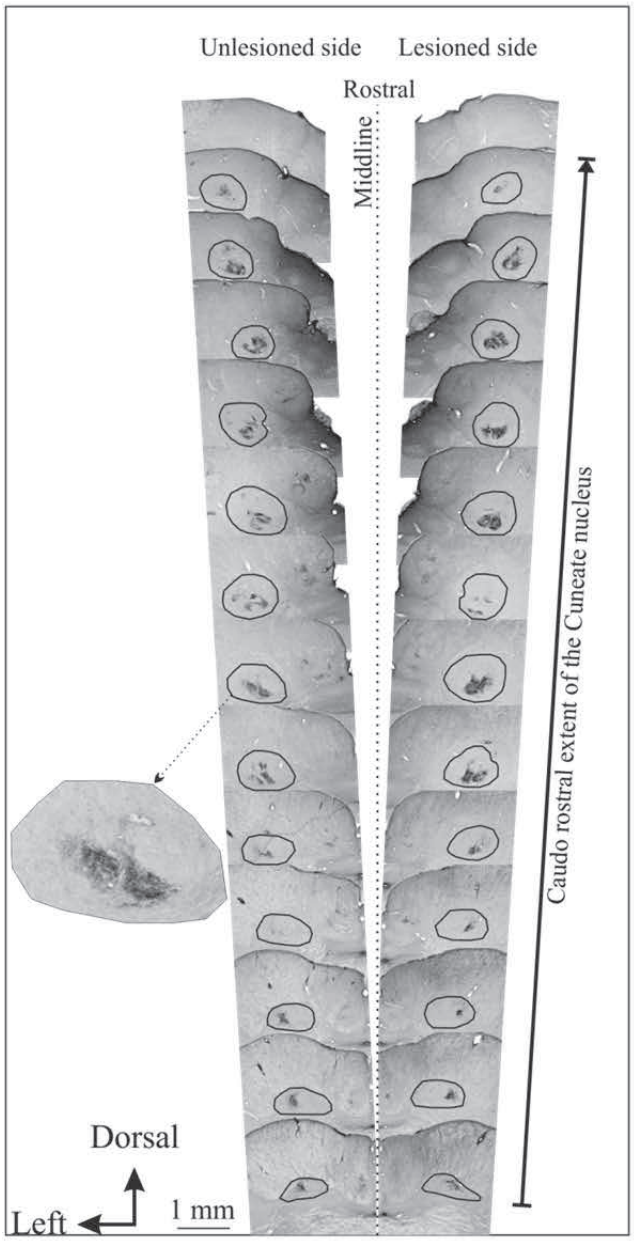

B. Intact

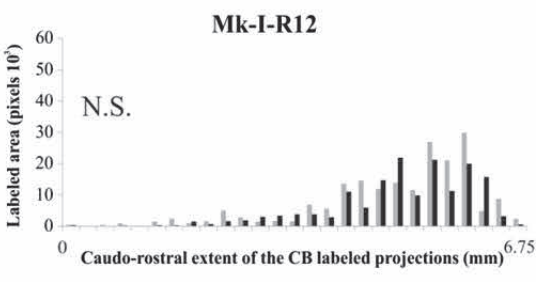

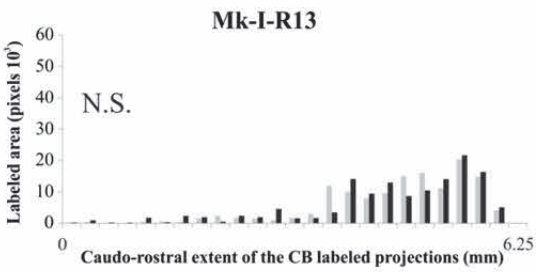

D. SCI_Treated group

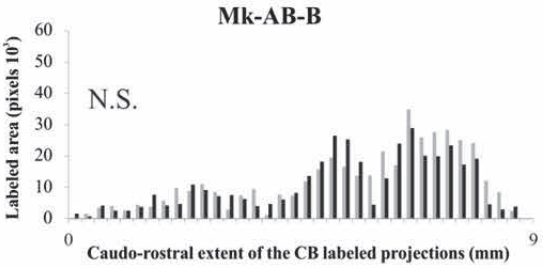

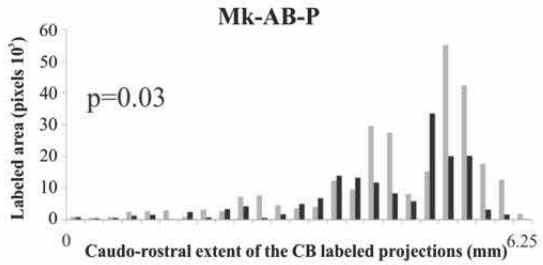

C. SCI_Untreated group

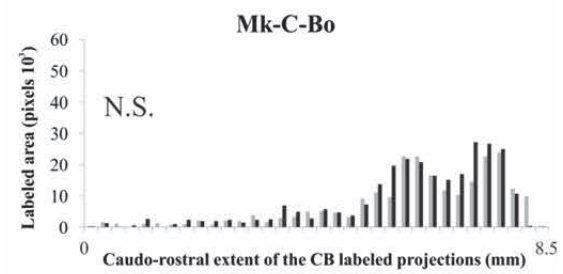

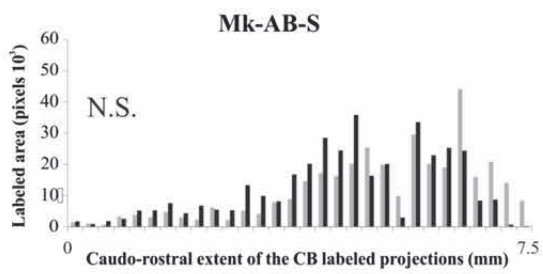

Unlesioned side Lesioned side

Figure 4: SCI-Cuneate nucleus: CB labelling

Same data as in figure 3 but for CB labelling in the cuneate nucleus, with similar monkeys. See legend of figure 3 for details.

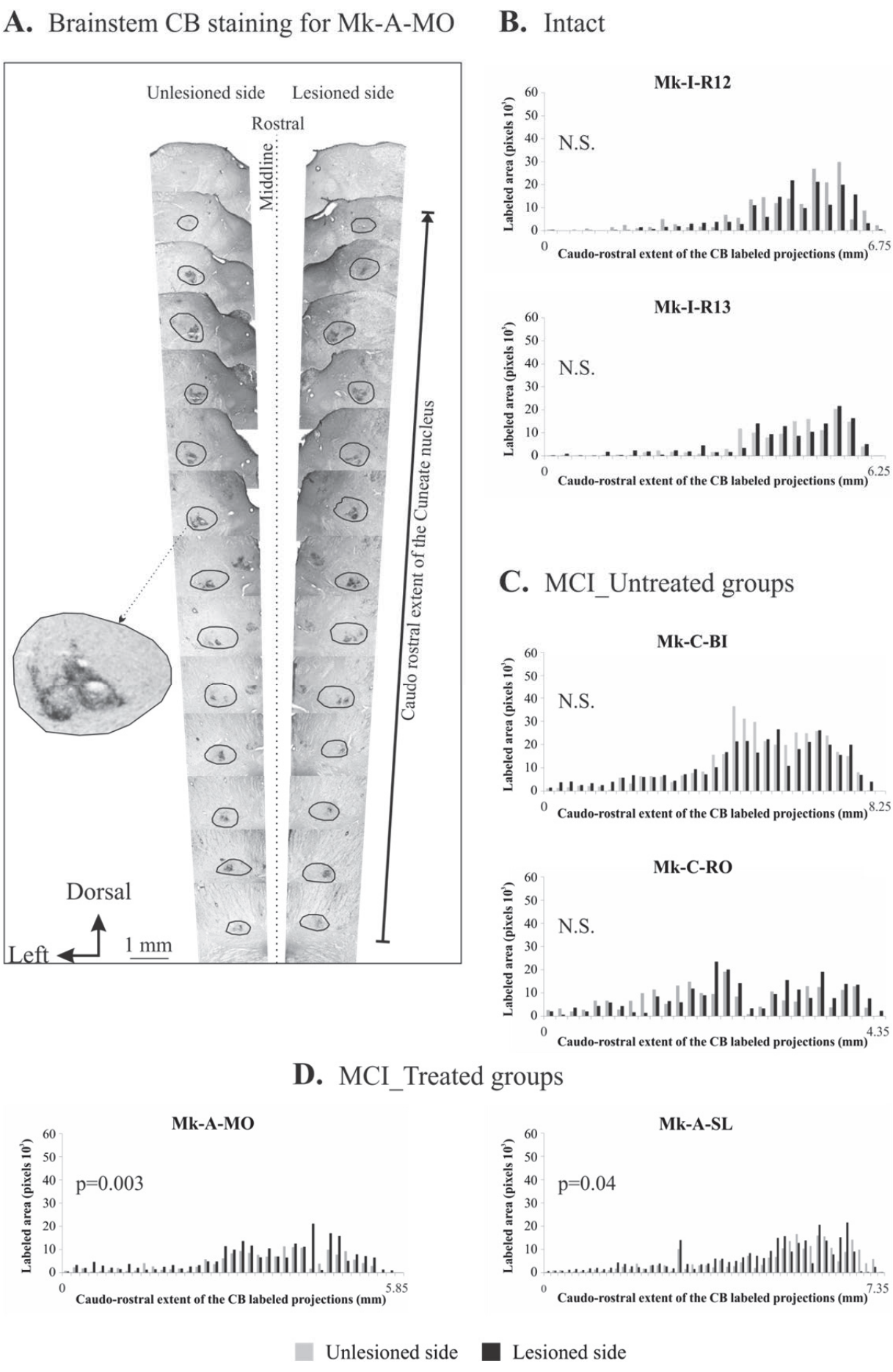
A. Brainstem CB staining for Mk-A-MO
Unlesioned side
Lesioned side
Rostral
Middline
Caudo rostral extent of the Cuneate nucleus
Dorsal
Left
1 mm
B. Intact
Mk-I-R12
N.S.
Labeled area (pixels 10²)
Caudo-rostral extent of the CB labeled projections (mm)
6.75
Mk-I-R13
N.S.
6.25
C. MCI_Untreated groups
Mk-C-BI
N.S.
8.25
Mk-C-RO
N.S.
4.35
D. MCI_Treated groups
Mk-A-MO
p=0.003
5.85
Mk-A-SL
p=0.04
7.35
Unlesioned side
Lesioned side

Figure 5: MCI-Cuneate nucleus: CB labelling

Same data as in figure in figure 4 (CB labelling in the cuneate nucleus), but for another groups of monkeys subjected to MCI. The CB labelling area results are indicated separately in 2 the same intact monkeys (**B.**) as in the figure 4, two monkeys subjected to MCI without treatment (Control antibody; **C.**) and in 2 MCI monkeys treated with the anti-Nogo-A antibody (**D.**). Distance of 250 µm separates each slice along the caudo-rostral axis for intact monkeys and Mk-C-BI but of 150 µm for the others monkeys subjected to MCI: Mk-A-SL, Mk-A-MO and Mk-C-RO. Convention are conserved from the figure 3.

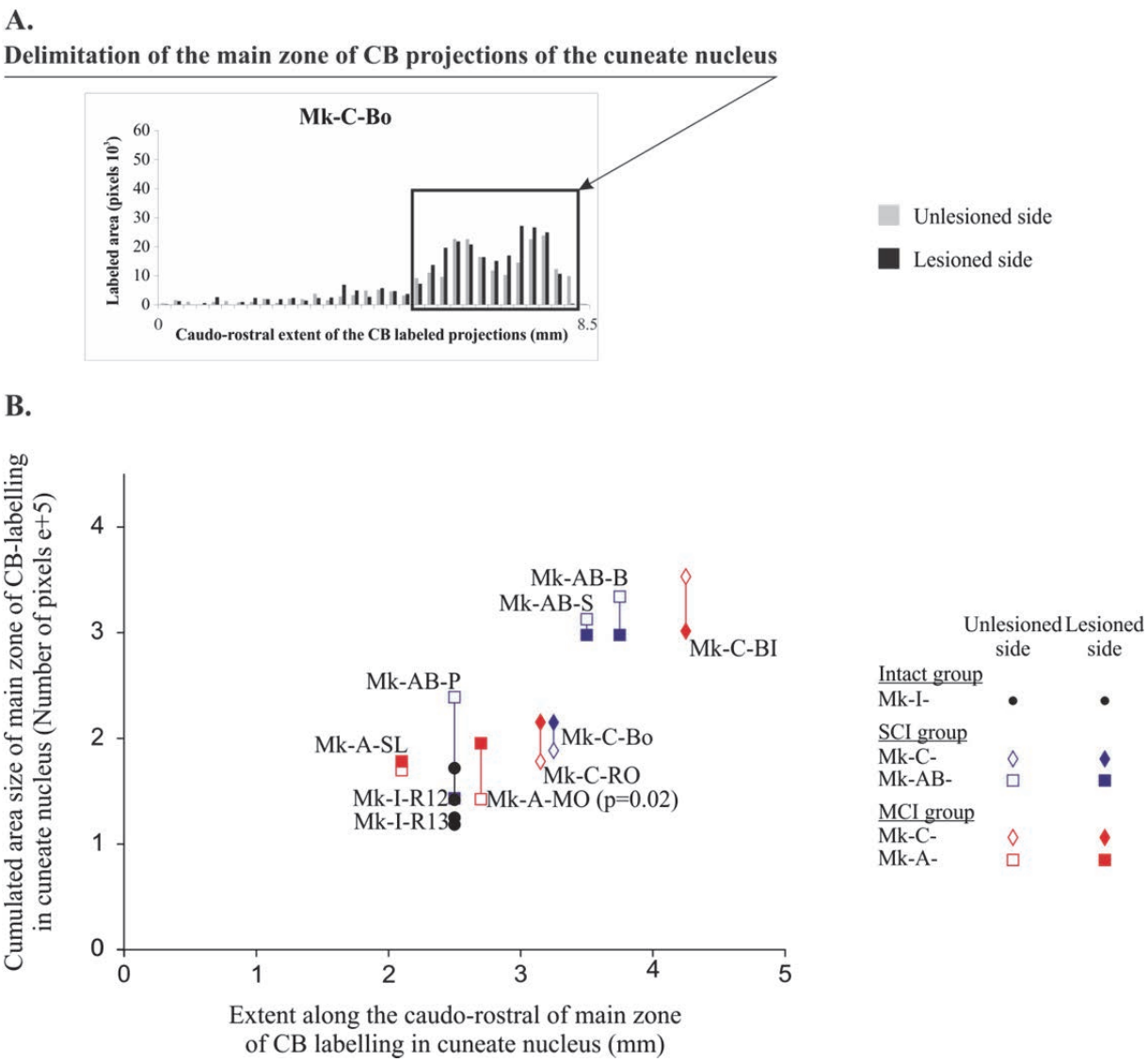

Figure 6: Summary of the area and the length of CB terminal field of the cuneate nucleus

(**A.**) Repetition of the distribution of CB labeled terminal fields in the cuneate nucleus in Mk-C-Bo to illustrate the location of the main rostral zone of labelling. (**B.**) Scatter plots represent size, in number of pixels on the Y axis, and the length, in mm on the X axis, of the main area of CB labeled terminal fields in the cuneate nucleus. Area size represents the sum of area of the slices as the reflect of the quantity of CB labeling in the main zone of CB labelling, and length represents the number of slice multiply by the thickness of each slice plus the distance between them. Area sizes and lengths are co-represented on the bidirectional scatter plots for the unlesioned (open symbol) and the lesioned (full symbol) side. Color code differentiate intact (in black), SCI (in blue) and MCI (in red), untreated (diamond) and treated (square) monkeys.

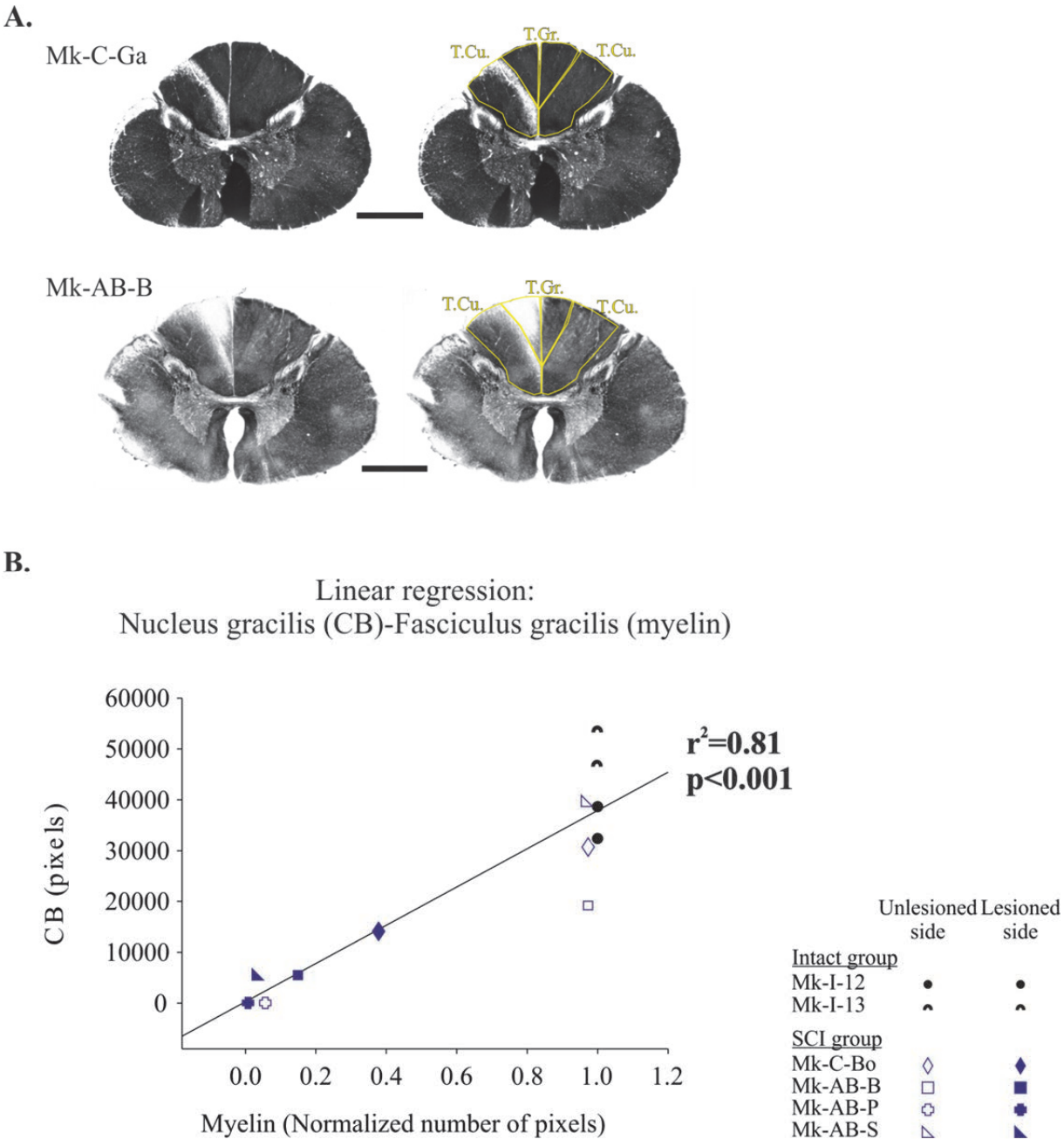

Figure 7: Dorsal column fasciculi and comparison with CB labeled terminal fields area in gracile nucleus

(**A.**) Examples of myelin staining with gold tri-chloride hydrate in Mk-C-Ga and Mk-AB-B on a transverse section at cervical level C3. Scale bar is 0.5 mm. On the rightmost repeated myelin sections, yellow contours surround the region of interest (ROI) for fasciculus cuneatus (Cu. T.) and fasciculus gracilis (Gr.T.). (**B.**) Linear regression between normalized area of myelin in the fasciculus gracilis (in normalized number of pixels) and the area of CB labeled terminal fields of the sensory ascending pathways of the dorsal column in the gracile

nucleus (in pixels). Data derived from the lesioned (full symbol) and unlesioned (open symbol) side of all subjects. Each monkey is represented with distinct symbols detailed in the legend on the right part of the graph, black for the intact and blue for the SCI monkeys. Statistical values (r^2 and p) derived from linear regression with all data.

A. Amount of myelinated fibres in fasciculus cuneatus

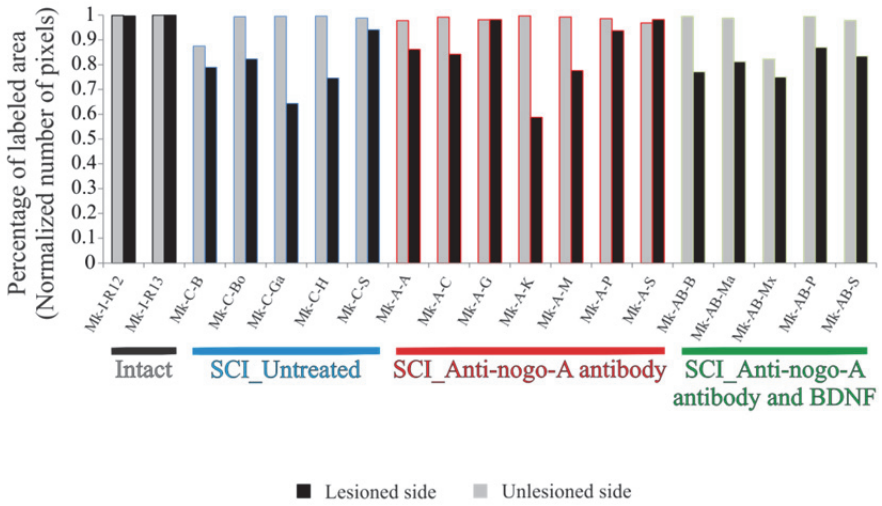

B. Amount of myelinated fibres in fasciculus gracilis

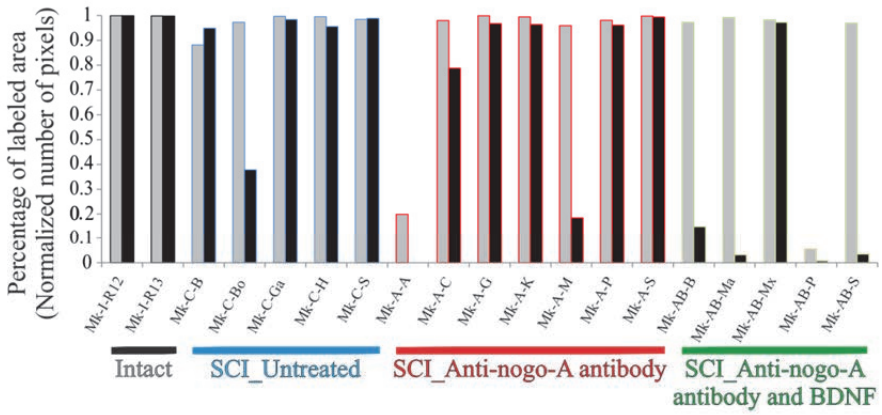

C. Additional anatomical reconstruction of the spinal cord lesion transverse view for the monkeys included in the myelin analyses

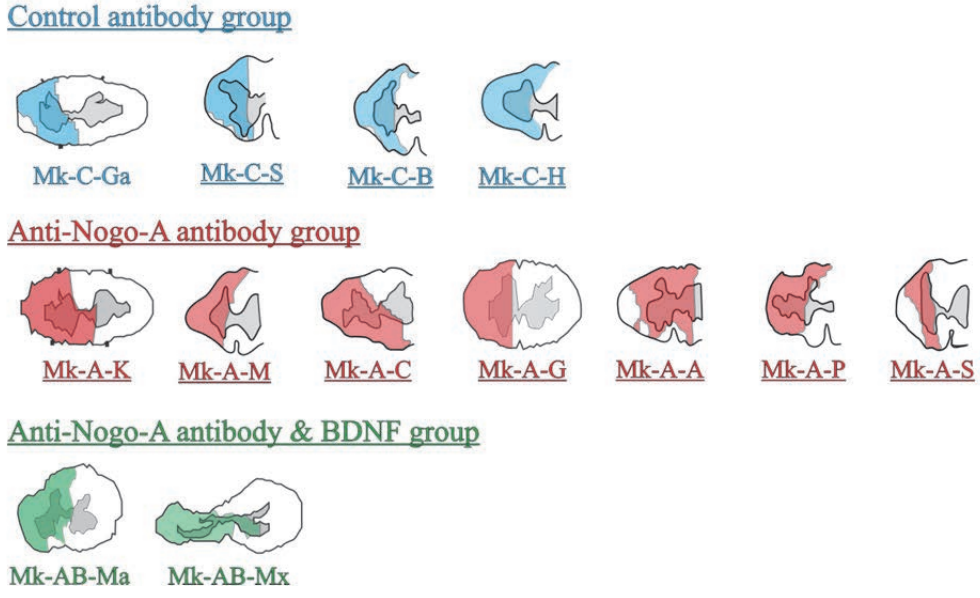

Figure 8: Myelin staining in dorsal column fasciculi: analyses including previously published SCI monkeys

Myelin normalized area (normalized number of pixels) in the dorsal column fasciculi, cuneatus (**A.**) and gracilis (**B.**). Anatomical reconstruction of the hemi-spinal cord lesion on transverse sections (**C.**) in previously published SCI monkeys. Monkeys of the three SCI groups are represented: the untreated (blue), the anti-Nogo-A antibody (red) and the combined anti-Nogo-A antibody and BDNF (green) group, compared to the intact group of monkey (black) bars in **A** and **B**. In the bar graphs, data are distinguished for the lesioned side (bar filled in black) and the unlesioned side (bar filled in gray). See figure 2 for anatomical lesion reconstructions of the monkeys injected with CB (Mk-C-Bo; Mk-AB-B; Mk-AB-P; Mk-AB-S).

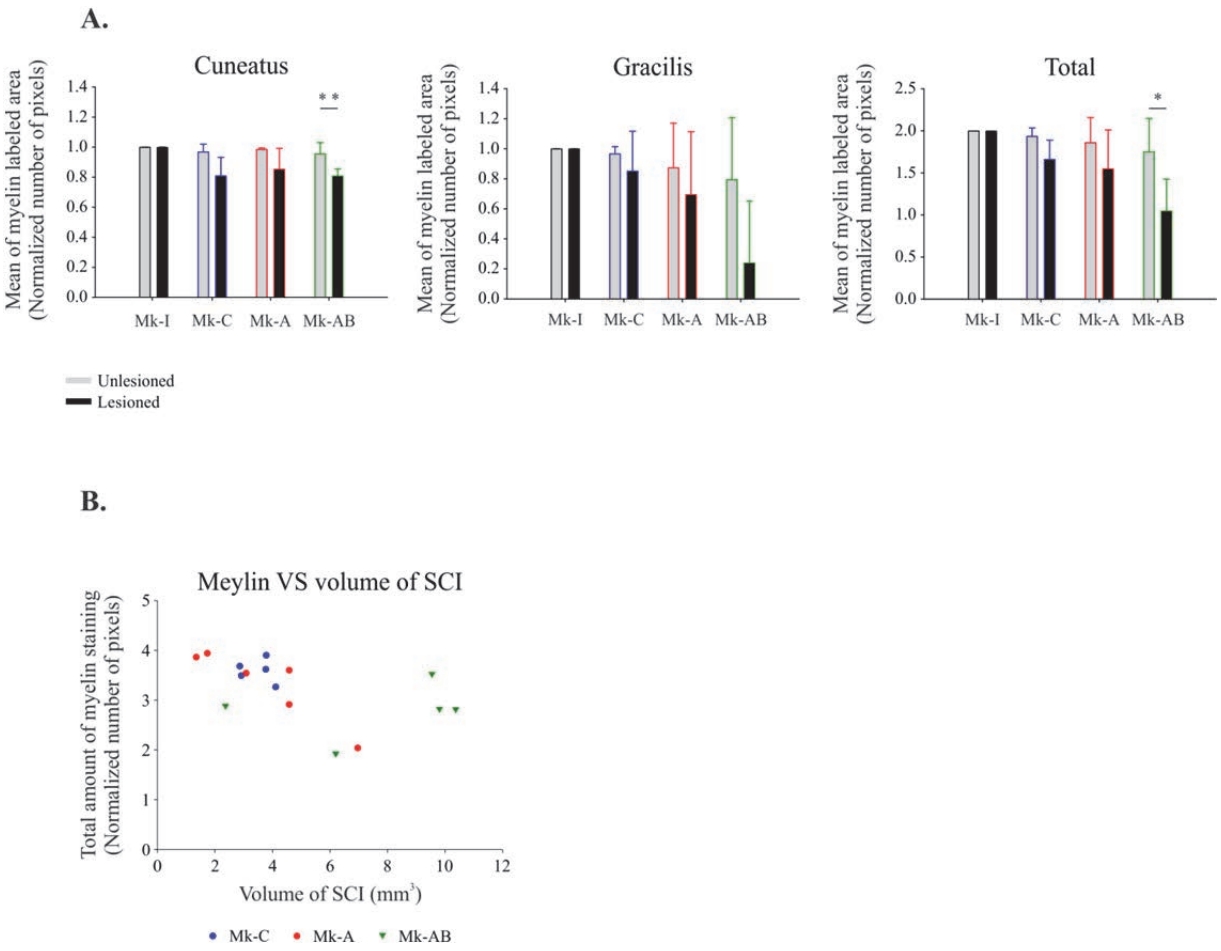

Figure 9: Summary, average and effects of treatment on myelin normalized area in the dorsal column fasciculus

(**A.**) Mean and standard deviation of the myelin normalized area (pixels normalized) for the cuneatus, the gracilis fasciculus and the total myelin normalized area (sum of the cuneatus and gracilis), for each monkey groups: intact (marked in black), untreated (marked in blue), anti-Nogo-A antibody (marked in red) and combined anti-Nogo-A antibody and BDNF (marked in green). Data are represented for the lesioned side (bar filled black) and unlesioned side (bar filled white). Statistical comparison of the lesioned and the unlesioned side used t-test. * is for $p<0.05$; ** is for $p<0.01$; the rest were not statistically significant. (**B.**) Scatter plot of the total normalized area of myelin of the dorsal column fasciculus correlated with the volume of the SCI for each of the monkeys, with the same color code as in (**A.**) for monkeys of the SCI group.

3. General discussion

The present work, addressing the effects of lesions of the motor system (*e.g.* motor cortex or spinal cord) and the possibility to promote the functional recovery, provides additional original experimental evidences on: (*i*) the extent of lesion-induced plastic changes occurring in the interconnected CNS structures also contributing to the motor control; (*ii*) the effects of M1 hand area lesion and on the extent and mechanisms of the subsequent functional recovery affecting the different parameters required to perform different configurations of manual dexterity, which thus emphasize the role of the intact contralesional M1; (*iii*) the possibility to further experimentally promote such post-lesion plasticity using treatments in order to improve the functional recovery.

Detailed discussions of the results, implications and perspectives have already been addressed in the four specific discussion chapters. The following general discussion focuses then on the main findings and on the common and general aspects reported across the different chapters. I first discuss the extent of the lesion-induced plasticity in the CNS, considering that reorganization can affect all the interconnected structures involved in the motor control, from adjacent to distant structures, as far as in the somatosensory brainstem nuclei. Then I discuss the necessity of extensive behavioral studies to address the participation of the different CNS structures in the post-lesion recovery. This aspect relates to the notion that the different structures of networks are differently involved in different aspects of voluntary movements. In the last paragraph, I discuss the interests of the anti-Nogo-A antibody treatment and of its combination with the neurotrophin BDNF treatment to improve the functional recovery following spinal cord or cortical injury affecting the motor control.

3.1. General summary of the results

The present experimental findings provide a first set of behavioral, electrophysiological and anatomical information on the extent of the plasticity occurring following lesion of the motor system, at cortical level or spinal cord level, and on the role of the different structures in the functional recovery post-lesion. My results showed: (1) a tendency for reorganization of the perilesional cortex following M1 hand area lesion, that was however not perceptible at first; (2) a certain degree of implication of the contralesional intact hemisphere in the functional recovery following cortical lesion of M1 hand area, affecting certain of the different parameters required to perform different configurations of manual

dexterity; (3) an increased participation and excitability of deep subcortical structures involved in the motor control following spinal cord hemisection at C7/C8 level; (4) a suggested plasticity of the somatosensory brainstem relay, the dorsal column nuclei (DCN), following motor system lesion at both cortical and spinal cord levels.

A second set of results provides evidences on the importance of an extensive behavioral assessment to describe the degree of participation of various structures to the functional recovery. This second set of results focused on the contralesional intact M1 following unilateral M1 hand area lesion. Albeit the contralesional M1 of the intact hemisphere is highly suggested to not participate to the functional recovery of the precision grip, my findings suggest a certain degree of participation. I report that the contralesional M1 of the intact hemisphere could be involved: (1) in the early stage post-lesion; (2) in chronic stages for complex movement requiring the associated use of wrist movements and finest precision grip in deep slots; (3) in the context of the necessity of a correct bilateral balance between M1 of the two hemispheres for the correct preshaping during a manual task using precision grip.

The third main finding of my thesis concerns the effects of different treatments on the functional recovery. My results provide preliminary evidences in favor of a promoting effect of the anti-Nogo-A antibody treatment on functional recovery following M1 hand area lesion. My findings also cautiously suggest that this treatment could prevent the reorganization of the somatosensory system observed in the DCN brainstem relay. Trying to promote the effects of the anti-Nogo-A antibody treatment, its combination with BDNF has been assessed in case of spinal cord hemisection at C7/C8 level. Such combination led not only to a lack of promoting effects but rather to a loss of the beneficial effects of anti-Nogo-A antibody treatment and even to deleterious effects. In the field of the functional recovery promotion, my thesis provides interesting additional findings supporting the notion of a promotion of the functional recovery consequently to a late immobilization of the healthy hand. This effect was observed consequently to a secondary lesion of the intact contralesional M1 resulting in the temporary non-use of the intact hand until the limited spontaneous functional recovery take place.

3.2. Functional implications

3.2.1. Extent of the lesion-induced plasticity in the CNS and potential role in post-lesion recovery

Considering that the motor system is composed of many interconnected areas and structures, a lesion of the motor system affects such network of interconnected structures and therefore all components of the network may be affected and subjected to further plastic changes post-lesion.

The plastic changes and behavioral findings described at the different levels related to functional implications are discussed below, separately for each anatomical level considered in my thesis, giving rise to common considerations. The present electrophysiological data indicate that the lesioned digit representation does not reemerge in the perilesional cortex in non-extensively trained monkeys, in accordance with Nudo and Milliken (1996). However, in spite of this lack of post-lesion reorganization of the perilesional cortex observed at first, modification of the electrophysiological parameters defining the reorganization (using supra-threshold cortical stimulations), has thus allowed to reveal the possibility for reorganization and participation in the post-lesion recovery. This could explain the discrepancy between the apparent lack of reorganization and the great propensity of plastic changes following lesion described in the general introduction of the present thesis. The suggested role of the perilesional cortex in the post-lesion recovery following M1 hand area lesion could result from reorganization observable at supra-threshold stimulations. Reorganization is also suggested to occur in the contralesional M1 in case of M1 hand area lesion, although not directly observed in the present work. The role of the contralesional M1 was highlighted in the present work by the behavioral performances alterations resulting from bilateral consecutives M1 hand area lesions. The contralesional M1 is suggested to participate in complex movement recovery and in preshaping at chronic stages, but is also suggested to be involved at early stage post-lesion in the functional recovery for grasping motor tasks. The role played by the contralesional cortex is further addressed in the following paragraph concerning the interest to distinguish the different aspects of movement in order to assess the functional recovery and the anatomical support for this functional recovery. However, post-lesion effects and roles during these different movement aspects logically refer to the pre-lesion role of the contralateral M1 (ipsilateral to the hand) in the complex movements and the preshaping, as described in the general introduction. According to other studies described in

the general introduction, brainstem structures are susceptible to plastic changes and to consequently participate to functional recovery as a part of the network. The present findings suggest an increase of the ability to stimulate the intrinsic hand muscles at the subcortical level, potentially at brainstem level. The potential role of the ipsilateral corticospinal tract and/or the reticulospinal tract is largely suggested to correlate with the present findings concerning the motor evoked potentials, as discussed in detail in the previous Chapter 3. The plastic changes following the spinal cord hemisection at C7/C8 are characterized by an increase of the subcortical structures excitability and/or a decrease of the amount of excitable fibers at the cortical level facilitating the jump to deeper structures for higher levels of cortical stimulations. These findings taken together with the previous findings from our laboratory emphasize the large extent of post-lesion plastic changes that occur following C7/C8 hemi-cord lesion, for instance in the form of axonal sprouting at spinal cord level (Freund et al., 2006, 2007, 2009), reorganization of the contralesional affected and ipsilesional unaffected M1 (Schmidlin et al., 2005), the modification of the pyramidal neuronal morphology in the contralesional affected M1 (Beaud et al., 2008) and in the magnocellular part of the red nucleus (Wannier et al., 2005). My findings suggest that plastic changes occur also in the somatosensory system following lesion restricted to motor system at both the cortical and the spinal cord levels. As observed in the present results at the brainstem relay level in the DCN, M1 hand area lesion and hemisection of the spinal cord at C7/C8 level are suggested to increase the caudo-rostral extent of the area of the primary sensory axon terminals reaching the first brainstem relay. However, the question remains whether such plastic changes contribute to functional recovery or result in deleterious aberrant plasticity. Thus, at a first approach, my findings emphasized that the perilesional cortex as well as the intact contralesional M1 do not support functional recovery following M1 hand area lesion. However, in a second approach, detailed plastic changes were observed in the perilesional cortex and the intact contralesional M1, possibly involved in specific aspects of the precision grip, when the behavior was extensively studied to observe distinctly particular movement attributes. Thus, plastic changes are suggested to occur in these cortical regions. Furthermore, plastic changes are believed to take place at the brainstem level in case of hemisection of the spinal cord at C7/C8. The present thesis emphasizes the increased participation of the brainstem in the movement occurrence following SCI at C7/C8 and highlights that motor system injury led to reorganization among the somatosensory system at the brainstem primary relay level. These findings support the large extent and even long distance effects of lesion-induced plasticity following motor system lesion affecting the relevant network of

interconnected structures. This plasticity does not necessarily mean that these structures directly support the observed functional recovery, but rather that they can participate directly or indirectly to the precision grip motor control in the post-lesion situation. These considerations also imply that the spared motor structures are involved in the functional recovery aspects to tentatively recover the lost functions but in the same range than those sustained pre-lesion.

The present work suggests that, post-lesion, the spared structures of the considered network are involved in the functional recovery. The plastic changes suggested in the present work are believed to occur even in structures apparently not directly affected, such as the primary sensory axon terminals in the first brainstem relay, the DCN. However, the existence of the corticocuneate and corticogracilis projections reported in the general introduction makes the DCN susceptible to plastic changes in case of motor system lesion affecting the corticospinal tract. This implies that the entire sensorimotor network could be affected and that the functional recovery may involve reorganization among the existing spared network to compensate the lost functions, thus reorganizing the pre-lesion existing connections, as recently suggested (for review Grefkes and Fink, 2011). Interestingly in our case, some of the monkeys subjected to M1 hand area lesion have been included in both studies of the present work showing plastic changes in the somatosensory brainstem DCN and in the perilesional cortex. In the same way, some of the monkeys subjected to hemisection of the spinal cord at C7/C8 have been included in both studies of the present work showing plastic changes in the somatosensory brainstem DCN and in brainstem motor structures. These evidences emphasize the multi-sites and long distant reorganization occurring following lesions of the motor system. The functional recovery appears to be rather sustained by a modified network organization than by another structure. With this consideration, it can be suggested that many interconnected cortical areas as well as subcortical structures participate in association to functional recovery. Not addressed in my thesis, the ipsilesional premotor cortex (PM) has often been proposed to be prominently involved in the functional recovery following unilateral M1 lesion. The view that a reorganized network based on pre-lesion existing interconnections is involved in the functional recovery is in line with the proposed prominent role of PMv in the functional recovery following unilateral M1 hand area lesion (Liu and Rouiller, 1999; Nudo et al., 2006; Hoogwoud et al.; 2013). The prominent role in the functional recovery allocated to PMv is consistent with its dense connections to M1 pre-lesion and thus its strong involvement in the network sustaining the fine manual dexterity movement

execution. Supporting this concept, the importance of PMv in the functional recovery has been suggested to occur through its projections onto the brainstem reticular formation (Borra E. et al., 2010). This study accords with the notions underlined by my results showing an increased participation of the subcortical structure to evoke voluntary movements and the structures advanced to participate to the functional recovery. Thus, many sites of reorganization can intervene to sustain the functional recovery, each within their range of functions: perilesional M1, PM, contralesional M1 and subcortical brainstem motor structures.

3.2.2. Distinction of different movement parameters and relative post-lesion participation, as assessed for the contralateral M1

CNS regions sustaining the functional recovery are suggested to depend on the lesion size. However, they can be differently involved depending on the movement attributes, the movement types and the task complexity, used to define the functional recovery. As mentioned above, assessment of the effects of the motor system lesion and the following functional recovery depends on the parameters used to define them. This topic will be discussed to highlight the consequence on the potential role of different CNS regions in the functional recovery which were at first instance apparently not involved. Because the lesion induced modification of the cortical and subcortical characteristics, anatomical organization and electrophysiological properties are different post-lesion. In this context, the pertinence to define recovery with the pre-lesion characteristics is questionable. My findings particularly highlight such issue, arguing that lesioned digit representation can reemerge among the perilesional cortex using increased cortical stimulation intensities in ICMS investigations. The present results showed differential effects of M1 hand area lesion on various types and parameters defining manual dexterity. This has been suggested to reflect different degrees of participation of M1 in the intact hemisphere. My results emphasize the multiple effects on different parameters of M1 hand area lesion (Murata et al., 2008; Fukushima et al., 2007). The probability to differently affect various parameters takes its importance with the present work revealing a role of M1 of the intact hemisphere in the functional recovery, thus participating to certain aspects of manual dexterity. The extent of functional recovery largely depends on the task used to evaluate the behavioral performance. Using two motor tasks assessing precision grip, different parameters were observed and, furthermore, variability in the degree of impairment and in the degree of recovery were observed. The role of the contralesional

intact M1 appeared for complex movements, defined in the present work to be precision grip associated with wrist adjustments and precision grip during the task presenting deep slots, requiring higher precision grip control (Fukushima et al., 2007). This observation was in accordance with studies showing an increase of the contralesional motor cortex activity following stroke for complex movements (Lotze et al., 2006). Generally used separately to assess the functional recovery, the consecutive effects of lesion and the role of CNS motor regions, these two tasks gave rise to complementary observations on the different parameters of the precision grip. Thus, the relative role of different CNS regions in the functional recovery has to be taken cautiously. The use of behavioral tasks restricting the observation to limited parameters can lead to misleading interpretations, as it is suggested for the contralesional intact M1 following M1 hand area lesion.

3.2.3. Treatments

My data provide additional evidences on the beneficial effects of the anti-Nogo-A antibody treatment following motor cortex lesion. Previous works from our laboratory reported improvement of the functional recovery in the model of spinal cord hemisection at C7/C8 in macaque monkeys using recurrently the modified Brinkman board task (Freund et al., 2006, 2007, 2009). My findings extend such functional recovery improvement to the case of M1 lesion restricted to hand area. My results provide evidence that the anti-Nogo-A antibody treatment does not prevent or restore the lesioned primary somatosensory terminal projections in the DCN, in line with a previous report (Oudega et al., 2000). However, my results indicate that the anti-Nogo-A antibody treatment could prevent reorganization of such primary somatosensory terminal projections in the DCN in case of lesion restricted to the motor system. Such results might parallel observations made in a previous report showing the regeneration of the corticospinal projections to these DCN in case of SCI (Thallmair M. et al., 1998). The treatment with the anti-Nogo-A antibody appears to promote axonal sprouting and regrowth differentially in the motor descending pathways but not in the ascending somatosensory pathways, although Nogo-A is a myelin-related protein present on both pathways.

In the context of the growing interest for combined therapies aiming to reach enhanced degrees of functional recovery, my work provides evidences for contrasting effects with the use of a combination of treatments with anti-Nogo-A antibody and BDNF. Combination of therapies is challenged by characteristics and limits of each therapy. However, my findings

suggest the existence of additional limits. Possible explanations for the observed lack of synergy between the two treatments and the even deleterious effects have been extensively detailed in the Chapter 3. To sum up, the dose, time window and injection site used in the present work were optimal to favor beneficial effects of the anti-Nogo-A antibody treatment. In contrast, administration protocol used for the BDNF treatment is highly variable in the literature. The appropriate protocol of BDNF administration remains to be defined, regarding the efficient period, dose and site of injection. As described in the Chapter 3 of my thesis, the optimal protocol of administration should be delayed by 2 to 4 weeks with a dose lower than 2 mg per days and a cortical/subcortical site of injection due to the presence of the BDNF receptor detected predominantly at the somatic level (Dittrich et al., 1996; Novikova et al., 2000; Coumans et al., 2001; Lu et al., 2001; Zhou and Shine, 2003; Vavrek et al., 2006). BDNF was administered with the anti-Nogo-A antibody at the lesion time and at the lesion site, thus, in our protocol, neither the time window nor the injection site were apparently optimal for the BDNF action. Furthermore, these two molecules present a certain probability of interaction among their respective pathways. These two molecules bind to a common receptor, the $p75^{NTR}$, involved in the survival and growth promotion pathways and in the apoptosis pathways, as described in the general introduction. Our protocol appeared to favor the competition between the two molecules and to stimulate the apoptosis pathways. As observed in a study combining the anti-Nogo-A antibody treatment with a training therapy (Wahl et al., 2014), it appears that each therapy procedure has to be individually respected to be combined. Thus, the difficulty to combine therapies could result in the difficulty of time application. In our context combining the anti-Nogo-A antibody treatment with BDNF, the first treatment must be initiated immediately after the lesion and the second must be delayed by 2 to 4 weeks. Both intrathecal treatments must be administered at different time points and sites of injection, thus requiring an invasive approach. However, considering the numerous strategies that have already been assessed, no optimal therapy appears to lead to full recovery following injury of the motor system. Thus, combination of therapies currently remains potentially powerful to further improve the functional recovery, but the optimal protocol of combination is still unknown and consequently needs to be more deeply investigated.

The present work provides further evidences on the possibility to promote functional recovery by observing the beneficial potential of functional therapy. Such functional therapies appear to be less invasive and, thus, more easily applicable at different times in combination with other therapies. Not used as a training therapy in our experiment, the late immobilization

by lesion of the intact hand increases the performances of the primary lesioned hand by its enforced use as observed in case of the Constrain Induce Movement Therapy (CIMT). However not directly assessed in the present work, several evidences however suggest an improvement of the functional recovery at late stage post-injury possibly attributable to such intact hand immobilization. My results highlight a rebound of the functional recovery after secondary lesion resulting in the immobilization of the primary intact hand. Such immobilization is well known to induce plasticity in intact subjects and in case of lesion of the motor system as described in the general introduction. Such rebound has already been observed in our laboratory in related studies assessing the potential beneficial effects of a treatment with adult autologous progenitor cells applied to the treated animals following a M1 hand area lesion in monkey (Kaeser et al., 2010).

3.3. Future directions

First of all, the experimental protocol has to be probably reconsidered. The functional recovery is experimentally assessed in animal models, such as the non-human primate in the present work, using repeated motor task over days which result in training. Such training is observable in our experimental protocol with the learning phase observed in previous report even in the modified Brinkman board task considered to be instinctive and relatively natural for the subject (Kaeser et al., 2014). Consecutively to training, the motor sequences of the behavioral motor task are assumed to be over-represented due to cortical plasticity (Karni et al., 1998). This implies that trained motor sequences are automatically subjected to better functional recovery than untrained sequences. This can be due to their enlarged and refined connectivity between the different cortical and subcortical regions for learned motor sequence consecutive to motor training. It is thus reasonable to suppose that the effects of overtraining can induce bias showing artificially prompted functional recovery for such specific sequence associated with lower functional recovery for general behavior. The possibility to assess natural and innate behavioral task of the daily life in animals will provide better comparison with human studies and, in this case, the functional recovery would concern rather the general voluntary behavior than specific motor sequences.

Regarding the present findings, future directions can be proposed aiming to assess the effects of the motor system lesion and the consecutive functional recovery as well as to find optimal therapy for complete functional recovery. Firstly, the motor control post-lesion should be addressed such as pre-lesion, considering the entire network. Thus, the post-lesion

motor control has to be considered resulting of a cooperative participation of different spared areas involved in the different aspects of the voluntary movements' motor control. To this aim, an extensive behavioral assessment is needed, which can distinguish different aspects of the voluntary movements, allowing to specifically observe the participation of different motor structures in the different voluntary movement features realization. Secondly, common agreement is needed on validated behavioral tasks to assess functional recovery. At least the development of a common evaluation scale, such as those existing for humans, should be generalized and adapted to animal models, this would be of great interest for easier comparison through the literature. Finally, concerning the possibility to promote the functional recovery, combined therapy remains a promising approach, but still risky. Indeed, protocols of administration of each therapy have to be individually respected. Furthermore, the potential of interaction between the pathways of each therapy has to be compared before combination in order to prevent possible and deleterious interactions which could lead to a lack of effector even to contra-productive effects.

Taking into account such important improvements would likely allow to develop better strategies to treat and help patients with brain or spinal cord injuries affecting motor control.

4. References

Adkins, D. L., Boychuk, J., Remple, M. S. & Kleim, J. A. (2006). Motor training induces experience-specific patterns of plasticity across motor cortex and spinal cord. *J.Appl.Physiol (1985.),* 101, 1776-1782.

Aguilar, J., Rivadulla, C., Soto, C. & Canedo, A. (2003). New corticocuneate cellular mechanisms underlying the modulation of cutaneous ascending transmission in anesthetized cats. *J.Neurophysiol.,* 89, 3328-3339.

Alstermark, B., Isa, T., Pettersson, L. G. & Sasaki, S. (2007). The C3-C4 propriospinal system in the cat and monkey: a spinal pre-motoneuronal centre for voluntary motor control. *Acta Physiol (Oxf),* 189, 123-140.

Andriessen, T. M., Horn, J., Franschman, G., van der Naalt, J., Haitsma, I., Jacobs, B., Steyerberg, E. W. & Vos, P. E. (2011). Epidemiology, severity classification, and outcome of moderate and severe traumatic brain injury: a prospective multicenter study. *J.Neurotrauma,* 28, 2019-2031.

Aou, S., Woody, C. D. & Birt, D. (1992). Increases in excitability of neurons of the motor cortex of cats after rapid acquisition of eye blink conditioning. *Journal of Neuroscience,* 12, 560-569.

Arundine, M. & Tymianski, M. (2004). Molecular mechanisms of glutamate-dependent neurodegeneration in ischemia and traumatic brain injury. *Cell Mol.Life Sci.,* 61, 657-668.

Asanuma, H. & Sakata, H. (1967). Functional organization of a cortical efferent system examined with focal depth stimulation in cats. *Journal of Neurophysiology,* 30, 35-54.

Asanuma, H. (1981). Functional role of sensory inputs to the motor cortex. *Prog.Neurobiol.,* 16, 241-262.

Ashe, J. & Georgopoulos, A. P. (1994). Movement parameters and neural activity in motor cortex and area 5. *Cereb.Cortex,* 4, 590-600.

Baker, S. N., Olivier, E. & Lemon, R. N. (1997). Coherent oscillations in monkey motor cortex and hand muscle EMG show task-dependent modulation. *J.Physiol.(Lond.),* 501, 225-241.

Baker, S. N., Zaaimi, B., Fisher, K. M., Edgley, S. A. & Soteropoulos, D. S. (2015). Pathways mediating functional recovery. *Prog.Brain Res.,* 218, 389-412.

Bamji, S. X., Majdan, M., Pozniak, C. D., Belliveau, D. J., Aloyz, R., Kohn, J., Causing, C. G. & Miller, F. D. (1998). The p75 neurotrophin receptor mediates neuronal apoptosis and is essential for naturally occurring sympathetic neuron death. *J.Cell Biol.,* 140, 911-923.

Barbas, H. & Garcia-Cabezas, M. A. (2015). Motor cortex layer 4: less is more. *Trends Neurosci.,* 38, 259-261.

Barbay, S., Plautz, E. J., Friel, K. M., Frost, S. B., Dancause, N., Stowe, A. M. & Nudo, R. J. (2006). Behavioral and neurophysiological effects of delayed training following a small ischemic infarct in primary motor cortex of squirrel monkeys. *Experimental Brain Research,* 169, 106-116.

Barbay, S., Guggenmos, D. J., Nishibe, M. & Nudo, R. J. (2013). Motor representations in the intact hemisphere of the rat are reduced after repetitive training of the impaired forelimb. *Neurorehabil.Neural Repair,* 27, 381-384.

Barde, Y. A., Edgar, D. & Thoenen, H. (1982). Purification of a new neurotrophic factor from mammalian brain. *EMBO J.*, 1, 549-553.

Bareyre, F. M. & Schwab, M. E. (2003). Inflammation, degeneration and regeneration in the injured spinal cord: insights from DNA microarrays. *Trends Neurosci.,* 26, 555-563.

Bareyre, F. M., Kerschensteiner, M., Raineteau, O., Mettenleiter, T. C., Weinmann, O. & Schwab, M. E. (2004). The injured spinal cord spontaneously forms a new intraspinal circuit in adult rats. *Nat.Neurosci.,* 7, 269-277.

Barker, A. T., Freeston, I. L., Jalinous, R. & Jarratt, J. A. (1987). Magnetic stimulation of the human brain and peripheral nervous system: an introduction and the results of an initial clinical evaluation. *Neurosurgery*, 20, 100-109.

Bashir, S., Kaeser, M., Wyss, A., Hamadjida, A., Liu, Y., Bloch, J., Brunet, J. F., Belhaj-Saif, A. & Rouiller, E. M. (2012). Short-term effects of unilateral lesion of the primary motor cortex (M1) on ipsilesional hand dexterity in adult macaque monkeys. *Brain Struct.Funct.,* 217, 63-79.

Beaud, M. L., Schmidlin, E., Wannier, T., Freund, P., Bloch, J., Mir, A., Schwab, M. E. & Rouiller, E. M. (2008). Anti-Nogo-A antibody treatment does not prevent cell body shrinkage in the motor cortex in adult monkeys subjected to unilateral cervical cord lesion. *BMC.Neurosci.,* 9, 5.

Belhaj-Saif, A., Karrer, J. H. & Cheney, P. D. (1998). Distribution and characteristics of poststimulus effects in proximal and distal forelimb muscles from red nucleus in the monkey. *J.Neurophysiol.,* 79, 1777-1789.

Belhaj-Saif, A. & Cheney, P. D. (2000). Plasticity in the distribution of the red nucleus output to forearm muscles after unilateral lesions of the pyramidal tract. *J.Neurophysiol.,* 83, 3147-3153.

Bentivoglio, M. & Rustioni, A. (1986). Corticospinal neurons with branching axons to the dorsal column nuclei in the monkey. *J.Comp Neurol.,* 253, 260-276.

Bernhard, C. G. & Bohm, E. (1954). Cortical representation and functional significance of the corticomotoneuronal system. *AMA.Arch.Neurol.Psychiatry,* 72, 473-502.

Biernaskie, J., Szymanska, A., Windle, V. & Corbett, D. (2005). Bi-hemispheric contribution to functional motor recovery of the affected forelimb following focal ischemic brain injury in rats. *Eur.J.Neurosci.,* 21, 989-999.

Binder, D. K. & Scharfman, H. E. (2004). Brain-derived neurotrophic factor. *Growth Factors,* 22, 123-131.

Borra, E., Belmalih, A., Gerbella, M., Rozzi, S. & Luppino, G. (2010). Projections of the hand field of the macaque ventral premotor area F5 to the brainstem and spinal cord. *J.Comp Neurol.,* 518, 2570-2591.

Bortoff, G. A. & Strick, P. L. (1993). Corticospinal terminations in two new-world primates: further evidence that corticomotoneuronal connections provide part of the neural substrate for manual dexterity. *Journal of Neuroscience,* 13, 5105-5118.

Boussaoud, D., Tanne-Gariepy, J., Wannier, T. & Rouiller, E. M. (2005). Callosal connections of dorsal versus ventral premotor areas in the macaque monkey: a multiple retrograde tracing study. *BMC Neurosci.,* 6, 67.

Bradnam, L. V., Stinear, C. M., Barber, P. A. & Byblow, W. D. (2012). Contralesional hemisphere control of the proximal paretic upper limb following stroke. *Cereb.Cortex,* 22, 2662-2671.

Bregman, B. S., McAtee, M., Dai, H. N. & Kuhn, P. L. (1997). Neurotrophic factors increase axonal growth after spinal cord injury and transplantation in the adult rat. *Exp.Neurol.,* 148, 475-494.

Brinkman, C. & Porter, R. (1979). Supplementary motor area in the monkey: activity of neurons during performance of a learned motor task. *J.Neurophysiol.,* 42, 681-709.

Brinkman, J. & Kuypers, H. G. (1973). Cerebral control of contralateral and ipsilateral arm, hand and finger movements in the split-brain rhesus monkey. *Brain,* 96, 653-674.

Brochier, T., Boudreau, M. J., Pare, M. & Smith, A. M. (1999). The effects of muscimol inactivation of small regions of motor and somatosensory cortex on independent finger movements and force control in the precision grip. *Experimental Brain Research,* 128, 31-40.

Brock, J. H., Rosenzweig, E. S., Blesch, A., Moseanko, R., Havton, L. A., Edgerton, V. R. & Tuszynski, M. H. (2010). Local and remote growth factor effects after primate spinal cord injury. *Journal of Neuroscience,* 30, 9728-9737.

Brodmann (2007). *Brodmann's: Localisation in the Cerebral Cortex*. Springer Science & Business Media.

Buchli, A. D. & Schwab, M. E. (2005). Inhibition of Nogo: a key strategy to increase regeneration, plasticity and functional recovery of the lesioned central nervous system. *Ann.Med.,* 37, 556-567.

Buford, J. A. & Davidson, A. G. (2004). Movement-related and preparatory activity in the reticulospinal system of the monkey. *Experimental Brain Research,* 159, 284-300.

Buonomano, D. V. & Merzenich, M. M. (1998). Cortical plasticity: from synapses to maps. *Annu.Rev.Neurosci.,* 21, 149-186.

Burke, D., Hicks, R. G. & Stephen, J. P. (1990). Corticospinal volleys evoked by anodal and cathodal stimulation of the human motor cortex
3. *J.Physiol,* 425, 283-299.

Burman, K., Darian-Smith, C. & Darian-Smith, I. (2000). Macaque red nucleus: origins of spinal and olivary projections and terminations of cortical inputs. *J.Comp Neurol.,* 423, 179-196.

Burton, H. (1986). Second somatosensory cortex and related areas. *Sensory-motor areas and aspects of cortical connectivity* (pp. 31-98). Springer.

Butefisch, C. M., Davis, B. C., Wise, S. P., Sawaki, L., Kopylev, L., Classen, J. & Cohen, L. G. (2000). Mechanisms of use-dependent plasticity in the human motor cortex. *Proc.Natl.Acad.Sci.U.S.A,* 97, 3661-3665.

Cafferty, W. B., Duffy, P., Huebner, E. & Strittmatter, S. M. (2010). MAG and OMgp synergize with Nogo-A to restrict axonal growth and neurological recovery after spinal cord trauma. *Journal of Neuroscience,* 30, 6825-6837.

Cai, D., Shen, Y., De, B. M., Tang, S. & Filbin, M. T. (1999). Prior exposure to neurotrophins blocks inhibition of axonal regeneration by MAG and myelin via a cAMP-dependent mechanism. *Neuron,* 22, 89-101.

Caminiti, R., Johnson, P. B., Burnod, Y., Galli, C. & Ferraina, S. (1990). Shift of preferred directions of premotor cortical cells with arm movements performed across the workspace. *Experimental Brain Research,* 83, 228-232.

Caminiti, R., Johnson, P. B., Galli, C., Ferraina, S. & Burnod, Y. (1991). Making arm movements within different parts of space: the premotor and motor cortical representation of a coordinate system for reaching to visual targets. *Journal of Neuroscience,* 11, 1182-1197.

Carmichael, S. T. & Chesselet, M. F. (2002). Synchronous neuronal activity is a signal for axonal sprouting after cortical lesions in the adult. *Journal of Neuroscience,* 22, 6062-6070.

Caroni, P. & Schwab, M. E. (1988). Antibody against myelin-associated inhibitor of neurite growth neutralizes nonpermissive substrate properties of CNS white matter. *Neuron,* 1, 85-96.

Castiello, U. (2005). The neuroscience of grasping. *Nat.Rev.Neurosci.,* 6, 726-736.

Cauraugh, J. H. & Summers, J. J. (2005). Neural plasticity and bilateral movements: A rehabilitation approach for chronic stroke. *Prog.Neurobiol.,* 75, 309-320.

Cheema, S., Fyffe, R., Light, A. & Rustioni, A. (1984). Arborizations of single corticofugal axons in the feline cuneate nucleus stained by iontophoretic injection of horseradish peroxidase. *Brain Res.,* 290, 158-164.

Cheema, S., Rustioni, A. & Whitsel, B. L. (1985). Sensorimotor cortical projections to the primate cuneate nucleus. *J.Comp Neurol.,* 240, 196-211.

Chen, M. S., Huber, A. B., van der Haar, M. E., Frank, M., Schnell, L., Spillmann, A. A., Christ, F. & Schwab, M. E. (2000). Nogo-A is a myelin-associated neurite outgrowth inhibitor and an antigen for monoclonal antibody IN-1. *Nature,* 403, 434-439.

Chen, R., Gerloff, C., Hallett, M. & Cohen, L. G. (1997). Involvement of the ipsilateral motor cortex in finger movements of different complexities. *Ann.Neurol.,* 41, 247-254.

Cheney, P. D. (1980). Response of rubromotoneuronal cells identified by spike-triggered averaging of EMG activity in awake monkeys. *Neurosci.Lett.,* 17, 137-142.

Cheney, P. D. & Fetz, E. E. (1985). Comparable patterns of muscle facilitation evoked by individual corticomotoneuronal (CM) cells and by single intracortical microstimuli in primates: evidence for functional groups of CM cells. *J.Neurophysiol.,* 53, 786-804.

Cheney, P. D., Mewes, K. & Widener, G. (1991). Effects on wrist and digit muscle activity from microstimuli applied at the sites of rubromotoneuronal cells in primates. *J.Neurophysiol.,* 66, 1978-1992.

Cheney, P. D., Hill-Karrer, J., Belhaj-Saif, A., McKiernan, B. J., Park, M. C. & Marcario, J. K. (2000). Cortical motor areas and their properties: implications for neuroprosthetics. *Prog.Brain Res.,* 128, 135-160.

Chouinard, P. A. & Paus, T. (2006). The primary motor and premotor areas of the human cerebral cortex. *Neuroscientist.,* 12, 143-152.

Cisek, P., Crammond, D. J. & Kalaska, J. F. (2003). Neural activity in primary motor and dorsal premotor cortex in reaching tasks with the contralateral versus ipsilateral arm. *J.Neurophysiol.,* 89, 922-942.

Cisek, P. & Kalaska, J. F. (2005). Neural correlates of reaching decisions in dorsal premotor cortex: specification of multiple direction choices and final selection of action. *Neuron,* 45, 801-814.

Coallier, E., Michelet, T. & Kalaska, J. F. (2015). Dorsal premotor cortex: neural correlates of reach target decisions based on a color-location matching rule and conflicting sensory evidence. *J.Neurophysiol.,* 113, 3543-3573.

Cooke, D. F., Taylor, C. S., Moore, T. & Graziano, M. S. (2003). Complex movements evoked by microstimulation of the ventral intraparietal area. *Proceedings of the National Academy of Sciences,* 100, 6163-6168.

Coons, A. H. (1971). The development of immunohistochemistry. *Ann.N.Y.Acad.Sci.,* 177, 5-9.

Coq, J. O. & Xerri, C. (1999). Acute reorganization of the forepaw representation in the rat SI cortex after focal cortical injury: neuroprotective effects of piracetam treatment. *Eur.J.Neurosci.,* 11, 2597-2608.

Coumans, J. V., Lin, T. T., Dai, H. N., MacArthur, L., McAtee, M., Nash, C. & Bregman, B. S. (2001). Axonal regeneration and functional recovery after complete spinal cord transection in rats by delayed treatment with transplants and neurotrophins. *Journal of Neuroscience,* 21, 9334-9344.

Courtine, G., Bunge, M. B., Fawcett, J. W., Grossman, R. G., Kaas, J. H., Lemon, R., Maier, I., Martin, J., Nudo, R. J., Ramon-Cueto, A., Rouiller, E. M., Schnell, L., Wannier, T., Schwab, M. E. & Edgerton, V. R. (2007). Can experiments in nonhuman primates expedite the translation of treatments for spinal cord injury in humans? *Nat.Med.,* 13, 561-566.

Crammond, D. J. & Kalaska, J. F. (2000). Prior information in motor and premotor cortex: activity during the delay period and effect on pre-movement activity. *J.Neurophysiol.,* 84, 986-1005.

Crosson, B., Ford, A., McGregor, K. M., Meinzer, M., Cheshkov, S., Li, X., Walker-Batson, D. & Briggs, R. W. (2010). Functional imaging and related techniques: an introduction for rehabilitation researchers. *J.Rehabil.Res.Dev.,* 47, vii-xxxiv.

Culberson, J. L. & Brushart, T. M. (1989). Somatotopy of digital nerve projections to the cuneate nucleus in the monkey. *Somatosens.Mot.Res.,* 6, 319-330.

Dancause, N., Barbay, S., Frost, S. B., Plautz, E. J., Chen, D., Zoubina, E. V., Stowe, A. M. & Nudo, R. J. (2005). Extensive cortical rewiring after brain injury. *Journal of Neuroscience,* 25, 10167-10179.

Dancause, N. (2006). Vicarious function of remote cortex following stroke: recent evidence from human and animal studies. *Neuroscientist.,* 12, 489-499.

Dancause, N., Barbay, S., Frost, S. B., Mahnken, J. D. & Nudo, R. J. (2007). Interhemispheric connections of the ventral premotor cortex in a new world primate. *J.Comp Neurol.,* 505, 701-715.

Dancause, N., Touvykine, B. & Mansoori, B. K. (2015). Inhibition of the contralesional hemisphere after stroke: reviewing a few of the building blocks with a focus on animal models. *Prog.Brain Res.,* 218, 361-387.

Daoudal, G. & Debanne, D. (2003). Long-term plasticity of intrinsic excitability: learning rules and mechanisms. *Learn.Mem.*, 10, 456-465.

Darian-Smith, C. & Ciferri, M. M. (2005). Loss and recovery of voluntary hand movements in the macaque following a cervical dorsal rhizotomy. *J.Comp Neurol.*, 491, 27-45.

Darian-Smith, C. (2007). Monkey models of recovery of voluntary hand movement after spinal cord and dorsal root injury. *ILAR.J.*, 48, 396-410.

Darian-Smith, C., Lilak, A. & Alarcon, C. (2013). Corticospinal sprouting occurs selectively following dorsal rhizotomy in the macaque monkey. *J.Comp Neurol.*, 521, 2359-2372.

Darling, W. G., Pizzimenti, M. A., Rotella, D. L., Peterson, C. R., Hynes, S. M., Ge, J., Solon, K., McNeal, D. W., Stilwell-Morecraft, K. S. & Morecraft, R. J. (2009). Volumetric effects of motor cortex injury on recovery of dexterous movements. *Exp.Neurol.*, 220, 90-108.

Davidson, A. G. & Buford, J. A. (2004). Motor outputs from the primate reticular formation to shoulder muscles as revealed by stimulus-triggered averaging. *Journal of Neurophysiology*, 92, 83-95.

Davidson, A. G. & Buford, J. A. (2006). Bilateral actions of the reticulospinal tract on arm and shoulder muscles in the monkey: stimulus triggered averaging
4. *Experimental Brain Research*, 173, 25-39.

Davidson, A. G., Schieber, M. H. & Buford, J. A. (2007). Bilateral spike-triggered average effects in arm and shoulder muscles from the monkey pontomedullary reticular formation
1. *Journal of Neuroscience*, 27, 8053-8058.

De Noordhout, A. M., Rapisarda, G., Bogacz, D., Gerard, P., De, P., V, Pennisi, G. & Delwaide, P. J. (1999). Corticomotoneuronal synaptic connections in normal man: an electrophysiological study. *Brain*, 122 (Pt 7), 1327-1340.

Debanne, D. (2009). Plasticity of neuronal excitability in vivo. *J.Physiol*, 587, 3057-3058.

Deng, Q., Cai, W., Li, S., Zhang, Y. & Su, B. (2013). Small Nogo-66-binding peptide promotes neurite outgrowth through RhoA inhibition after spinal cord injury. *Brain Res.Bull.*, 99, 140-144.

Devinsky, O., Morrell, M. J. & Vogt, B. A. (1995). Contributions of anterior cingulate cortex to behaviour. *Brain*, 118 (Pt 1), 279-306.

Dinse, H. R. & Merzenich, M. M. (2002). Adaptation of inputs in the somatosensory system. *Perceptual learning*, 19-42.

Dittrich, F., Ochs, G., Grosse-Wilde, A., Berweiler, U., Yan, Q., Miller, J. A., Toyka, K. V. & Sendtner, M. (1996). Pharmacokinetics of intrathecally applied BDNF and effects on spinal motoneurons. *Exp.Neurol.*, 141, 225-239.

Domeniconi, M., Cao, Z., Spencer, T., Sivasankaran, R., Wang, K., Nikulina, E., Kimura, N., Cai, H., Deng, K., Gao, Y., He, Z. & Filbin, M. (2002). Myelin-associated glycoprotein interacts with the Nogo66 receptor to inhibit neurite outgrowth. *Neuron*, 35, 283-290.

Doyle, K. P., Simon, R. P. & Stenzel-Poore, M. P. (2008). Mechanisms of ischemic brain damage. *Neuropharmacology*, 55, 310-318.

Dum, R. P. & Strick, P. L. (1991). The origin of corticospinal projections from the premotor areas in the frontal lobe. *Journal of Neuroscience,* 11, 667-689.

Dum, R. P. & Strick, P. L. (1996). Spinal cord terminations of the medial wall motor areas in macaque monkeys. *Journal of Neuroscience,* 16, 6513-6525.

Dum, R. P. & Strick, P. L. (2002). Motor areas in the frontal lobe of the primate. *Physiol Behav.,* 77, 677-682.

Dum, R. P. & Strick, P. L. (2005). Frontal lobe inputs to the digit representations of the motor areas on the lateral surface of the hemisphere. *Journal of Neuroscience,* 25, 1375-1386.

Duncan, P. W., Jorgensen, H. S. & Wade, D. T. (2000). Outcome measures in acute stroke trials: a systematic review and some recommendations to improve practice. *Stroke,* 31, 1429-1438.

Duncan, P. W., Lai, S. M. & Keighley, J. (2000). Defining post-stroke recovery: implications for design and interpretation of drug trials. *Neuropharmacology,* 39, 835-841.

Dykes, R. W. & Ruest, A. (1986). What makes a map in somatosensory cortex? *Sensory-motor areas and aspects of cortical connectivity* (pp. 1-29). Springer.

Ebner, F. F., Rema, V., Sachdev, R. & Symons, F. J. (1997). Activity-dependent plasticity in adult somatic sensory cortex. *Seminars in Neuroscience* 9[1], 47-58.

Edgerton, V. R., Tillakaratne, N. J., Bigbee, A. J., de Leon, R. D. & Roy, R. R. (2004). Plasticity of the spinal neural circuitry after injury. *Annu.Rev.Neurosci.,* 27, 145-167.

Edgley, S. A., Eyre, J. A., Lemon, R. N. & Miller, S. (1990). Excitation of the corticospinal tract by electromagnetic and electrical stimulation of the scalp in the macaque monkey. *J.Physiol,* 425, 301-320.

Eftekharpour, E., Karimi-Abdolrezaee, S. & Fehlings, M. G. (2008). Current status of experimental cell replacement approaches to spinal cord injury. *Neurosurg.Focus.,* 24, E19.

Ehrsson, H. H., Fagergren, A., Jonsson, T., Westling, G., Johansson, R. S. & Forssberg, H. (2000). Cortical activity in precision- versus power-grip tasks: an fMRI study. *J.Neurophysiol.,* 83, 528-536.

Eisner-Janowicz, I., Barbay, S., Hoover, E., Stowe, A. M., Frost, S. B., Plautz, E. J. & Nudo, R. J. (2008). Early and late changes in the distal forelimb representation of the supplementary motor area after injury to frontal motor areas in the squirrel monkey. *J.Neurophysiol.,* 100, 1498-1512.

Eisner-Janowicz, I., Barbay, S., Hoover, E., Stowe, A. M., Frost, S. B., Plautz, E. J. & Nudo, R. J. (2008). Early and late changes in the distal forelimb representation of the supplementary motor area after injury to frontal motor areas in the squirrel monkey. *J.Neurophysiol.,* 100, 1498-1512.

Elbert, T., Pantev, C., Wienbruch, C., Rockstroh, B. & Taub, E. (1995). Increased cortical representation of the fingers of the left hand in string players. *Science,* 270, 305-307.

Emerick, A. J. & Kartje, G. L. (2004). Behavioral recovery and anatomical plasticity in adult rats after cortical lesion and treatment with monoclonal antibody IN-1. *Behavioural Brain Research,* 152, 315-325.

Evarts, E. V. (1966). Pyramidal tract activity associated with a conditioned hand movement in the monkey. *J.Neurophysiol.*, 29, 1011-1027.

Evarts, E. V. (1968). Relation of pyramidal tract activity to force exerted during voluntary movement. *J.Neurophysiol.*, 31, 14-27.

Ferreri, F. & Rossini, P. M. (2013). TMS and TMS-EEG techniques in the study of the excitability, connectivity, and plasticity of the human motor cortex. *Rev.Neurosci.*, 24, 431-442.

Fetz, E. E., Cheney, P. D. & German, D. C. (1976). Corticomotoneuronal connections of precentral cells detected by postspike averages of EMG activity in behaving monkeys. *Brain Res.*, 114, 505-510.

Fetz, E. E. & Cheney, P. D. (1979). Muscle fields and response properties of primate corticomotoneuronal cells. *Prog.Brain Res.*, 50, 137-146.

Fetz, E. E. & Cheney, P. D. (1980). Postspike facilitation of forelimb muscle activity by primate corticomotoneuronal cells. *J.Neurophysiol.*, 44, 751-772.

Fetz, E. E. (1992). Are movement parameters recognizably coded in the activity of single neurons? *Behavioral and brain sciences*, 15, 679-690.

Filbin, M. T. (2003). Myelin-associated inhibitors of axonal regeneration in the adult mammalian CNS. *Nat.Rev.Neurosci.*, 4, 703-713.

Filli, L. & Schwab, M. E. (2015). Structural and functional reorganization of propriospinal connections promotes functional recovery after spinal cord injury. *Neural Regen.Res.*, 10, 509-513.

Firmin, L., Field, P., Maier, M. A., Kraskov, A., Kirkwood, P. A., Nakajima, K., Lemon, R. N. & Glickstein, M. (2014). Axon diameters and conduction velocities in the macaque pyramidal tract. *Journal of Neurophysiology*, 112, 1229-1240.

Fogassi, L., Gallese, V., Buccino, G., Craighero, L., Fadiga, L. & Rizzolatti, G. (2001). Cortical mechanism for the visual guidance of hand grasping movements in the monkey: A reversible inactivation study. *Brain*, 124, 571-586.

Fogassi, L. & Luppino, G. (2005). Motor functions of the parietal lobe. *Curr.Opin.Neurobiol.*, 15, 626-631.

Fournier, A. E., GrandPre, T. & Strittmatter, S. M. (2001). Identification of a receptor mediating Nogo-66 inhibition of axonal regeneration. *Nature*, 409, 341-346.

Friel, K. M., Barbay, S., Frost, S. B., Plautz, E. J., Hutchinson, D. M., Stowe, A. M., Dancause, N., Zoubina, E. V., Quaney, B. M. & Nudo, R. J. (2005). Dissociation of sensorimotor deficits after rostral versus caudal lesions in the primary motor cortex hand representation. *J.Neurophysiol.*, 94, 1312-1324.

Fritsch, G. & Hitzig, E. (2009). Electric excitability of the cerebrum (Uber die elektrische Erregbarkeit des Grosshirns). *Epilepsy Behav.*, 15, 123-130.

Frost, S. B., Barbay, S., Friel, K. M., Plautz, E. J. & Nudo, R. J. (2003). Reorganization of remote cortical regions after ischemic brain injury: a potential substrate for stroke recovery. *J.Neurophysiol.*, 89, 3205-3214.

Fu, Q. G., Flament, D., Coltz, J. D. & Ebner, T. J. (1995). Temporal encoding of movement kinematics in the discharge of primate primary motor and premotor neurons. *J.Neurophysiol.*, 73, 836-854.

Fukushima, J., Kasahara, S., Asaka, T., Saito, H. & Yamanaka, M. (2007). Behavioral findings during recovery after experimental stroke in monkeys-Assessment with modified hand performance test. *Journal of Physical Therapy Science*, 19, 33-40.

Fukushima, K. (1997). Corticovestibular interactions: anatomy, electrophysiology, and functional considerations. *Experimental Brain Research*, 117, 1-16.

Galea, M. P. & Darian-Smith, I. (1994). Multiple corticospinal neuron populations in the macaque monkey are specified by their unique cortical origins, spinal terminations, and connections. *Cereb.Cortex*, 4, 166-194.

Galea, M. P. & Darian-Smith, I. (1997). Manual dexterity and corticospinal connectivity following unilateral section of the cervical spinal cord in the macaque monkey. *J.Comp Neurol.*, 381, 307-319.

Gallese, V., Murata, A., Kaseda, M., Niki, N. & Sakata, H. (1994). Deficit of hand preshaping after muscimol injection in monkey parietal cortex. *Neuroreport*, 5, 1525-1529.

Garcia-Cabezas, M. A. & Barbas, H. (2014). Area 4 has layer IV in adult primates. *Eur.J.Neurosci.*, 39, 1824-1834.

Gentilucci, M., Fogassi, L., Luppino, G., Matelli, M., Camarda, R. & Rizzolatti, G. (1988). Functional organization of inferior area 6 in the macaque monkey. I. Somatotopy and the control of proximal movements. *Experimental Brain Research*, 71, 475-490.

Georgopoulos, A. P., Kalaska, J. F., Caminiti, R. & Massey, J. T. (1982). On the relations between the direction of two-dimensional arm movements and cell discharge in primate motor cortex. *Journal of Neuroscience*, 2, 1527-1537.

Ghosh, S. & Porter, R. (1988). Corticocortical synaptic influences on morphologically identified pyramidal neurones in the motor cortex of the monkey. *J.Physiol*, 400, 617-629.

Gindrat, A. D., Chytiris, M., Balerna, M., Rouiller, E. M. & Ghosh, A. (2015). Use-dependent cortical processing from fingertips in touchscreen phone users. *Curr.Biol.*, 25, 109-116.

Glees, P. & Cole, J. (1950). Recovery of skilled motor functions after small repeated lesions of motor cortex in macaque. *Journal of Neurophysiology*, 13, 137-148.

Gould, H. J., III, Cusick, C. G., Pons, T. P. & Kaas, J. H. (1986). The relationship of corpus callosum connections to electrical stimulation maps of motor, supplementary motor, and the frontal eye fields in owl monkeys. *J.Comp Neurol.*, 247, 297-325.

GrandPre, T., Nakamura, F., Vartanian, T. & Strittmatter, S. M. (2000). Identification of the Nogo inhibitor of axon regeneration as a Reticulon protein. *Nature*, 403, 439-444.

GrandPre, T., Li, S. & Strittmatter, S. M. (2002). Nogo-66 receptor antagonist peptide promotes axonal regeneration. *Nature*, 417, 547-551.

Graziano, M. (2006). The organization of behavioral repertoire in motor cortex. *Annu.Rev.Neurosci.*, 29, 105-134.

Greenough, W. T., Larson, J. R. & Withers, G. S. (1985). Effects of unilateral and bilateral training in a reaching task on dendritic branching of neurons in the rat motor-sensory forelimb cortex. *Behav.Neural Biol.*, 44, 301-314.

Grefkes, C. & Fink, G. R. (2005). The functional organization of the intraparietal sulcus in humans and monkeys. *J.Anat.*, 207, 3-17.

Guo, X., Bu, X., Li, Z., Yan, Z., Jiang, J. & Zhou, Z. (2012). Comparison of autologous bone marrow mononuclear cells transplantation and mobilization by granulocyte

colony-stimulating factor in experimental spinal injury. *Int.J.Neurosci.,* 122, 723-733.

Hagemann, G., Redecker, C., Neumann-Haefelin, T., Freund, H. J. & Witte, O. W. (1998). Increased long-term potentiation in the surround of experimentally induced focal cortical infarction. *Ann.Neurol.*, 44, 255-258.

Hagg, T. & Oudega, M. (2006). Degenerative and spontaneous regenerative processes after spinal cord injury. *J.Neurotrauma,* 23, 264-280.

Hamada, M., Murase, N., Hasan, A., Balaratnam, M. & Rothwell, J. C. (2013). The role of interneuron networks in driving human motor cortical plasticity. *Cereb.Cortex,* 23, 1593-1605.

Hamel-Paquet, C., Sergio, L. E. & Kalaska, J. F. (2006). Parietal area 5 activity does not reflect the differential time-course of motor output kinetics during arm-reaching and isometric-force tasks. *J.Neurophysiol.*, 95, 3353-3370.

He, S. Q., Dum, R. P. & Strick, P. L. (1993). Topographic organization of corticospinal projections from the frontal lobe: motor areas on the lateral surface of the hemisphere. *Journal of Neuroscience,* 13, 952-980.

He, S. Q., Dum, R. P. & Strick, P. L. (1995). Topographic organization of corticospinal projections from the frontal lobe: motor areas on the medial surface of the hemisphere. *Journal of Neuroscience,* 15, 3284-3306.

Hebb, D. (1949). *The Organization of Behaviour: A Neuropsychological Theory*. **New York, NY:** Wiley.

Hepp-Reymond, M.-C. (1988). Functional organization of motor cortex and its participation in voluntary movements. In H. D. Seklis & J. Erwin (Eds) *Comparative Primate Biology, Vol 4: Neurosciences* (pp. 501-624). New York: Alan R. Liss.

Hepp, R., Trouche, E. & Wiesendanger, M. (1974). Effects of unilateral and bilateral pyramidotomy on a conditioned rapid precision grip in monkeys (Macaca fascicularis). *Experimental Brain Research,* 21, 519-527.

Herbert, W. J., Powell, K. & Buford, J. A. (2015). Evidence for a role of the reticulospinal system in recovery of skilled reaching after cortical stroke: initial results from a model of ischemic cortical injury. *Experimental Brain Research*.

Hess, G. & Donoghue, J. P. (1994). Long-term potentiation of horizontal connections provides a mechanism to reorganize cortical motor maps. *J.Neurophysiol.,* 71, 2543-2547.

Hicks, T. P. & Dykes, R. W. (1983). Receptive field size for certain neurons in primary somatosensory cortex is determined by GABA-mediated intracortical inhibition. *Brain Res.*, 274, 160-164.

Higo, N. (2014). Effects of rehabilitative training on recovery of hand motor function: A review of animal studies. *Neuroscience research,* 78, 9-15.

Hocherman, S. & Wise, S. P. (1990). Trajectory-selective neuronal activity in the motor cortex of rhesus monkeys (Macaca mulatta). *Behav.Neurosci.*, 104, 495-499.

Hodgson, J. A., Roy, R. R., de, L. R., Dobkin, B. & Edgerton, V. R. (1994). Can the mammalian lumbar spinal cord learn a motor task? *Med.Sci.Sports Exerc.*, 26, 1491-1497.

Hodgson, J. A., Roy, R. R., de Leon, R., Dobkin, B. & Edgerton, V. R. (1994). Can the mammalian lumbar spinal cord learn a motor task? *Medicine & Science in Sports & Exercise*.

Hoff, E. C. (1932). Central nerve terminals in the mammalian spinal cord and their examination by experimental degeneration. *Proceedings of the Royal Society of London.Series B, Containing Papers of a Biological Character,* 175-188.

Hohlfeld, R., Kerschensteiner, M. & Meinl, E. (2007). Dual role of inflammation in CNS disease. *Neurology,* 68, S58-S63.

Hollis, E. R., Jamshidi, P., Low, K., Blesch, A. & Tuszynski, M. H. (2009). Induction of corticospinal regeneration by lentiviral trkB-induced Erk activation. *Proc.Natl.Acad.Sci.U.S.A,* 106, 7215-7220.

Holstege, G. (1987). Anatomical evidence for an ipsilateral rubrospinal pathway and for direct rubrospinal projections to motoneurons in the cat. *Neurosci.Lett.,* 74, 269-274.

Holstege, J. C. & Kuypers, H. G. (1987). Brainstem projections to spinal motoneurons: an update. *Neuroscience,* 23, 809-821.

Holstege, G., Blok, B. F. & Ralston, D. D. (1988). Anatomical evidence for red nucleus projections to motoneuronal cell groups in the spinal cord of the monkey. *Neurosci.Lett.,* 95, 97-101.

Hoogewoud, F., Hamadjida, A., Wyss, A. F., Mir, A., Schwab, M. E., Belhaj-Saif, A. & Rouiller, E. M. (2013). Comparison of functional recovery of manual dexterity after unilateral spinal cord lesion or motor cortex lesion in adult macaque monkeys. *Front Neurol.,* 4, 101.

Horner, P. J. & Gage, F. H. (2000). Regenerating the damaged central nervous system. *Nature,* 407, 963-970.

Huang, E. J. & Reichardt, L. F. (2001). Neurotrophins: roles in neuronal development and function. *Annu.Rev.Neurosci.,* 24, 677-736.

Hyvarinen, J. & Shelepin, Y. (1979). Distribution of visual and somatic functions in the parietal associative area 7 of the monkey. *Brain Res.,* 169, 561-564.

Iriki, A., Pavlides, C., Keller, A. & Asanuma, H. (1989). Long-term potentiation in the motor cortex. *Science,* 245, 1385-1387.

Iwamura, Y., Tanaka, M., Sakamoto, M. & Hikosaka, O. (1983). Functional subdivisions representing different finger regions in area 3 of the first somatosensory cortex of the conscious monkey. *Experimental Brain Research,* 51, 315-326.

Jang, S. H., Ahn, S. H., Yang, D. S., Lee, D. K., Kim, D. K. & Son, S. M. (2005). Cortical reorganization of hand motor function to primary sensory cortex in hemiparetic patients with a primary motor cortex infarct. *Arch.Phys.Med.Rehabil.,* 86, 1706-1708.

Jankowska, E. & Edgley, S. A. (2006). How can corticospinal tract neurons contribute to ipsilateral movements? A question with implications for recovery of motor functions. *Neuroscientist.,* 12, 67-79.

Jenkins, W. M., Merzenich, M. M., Ochs, M. T., Allard, T. & Guic-Robles, E. (1990). Functional reorganization of primary somatosensory cortex in adult owl monkeys after behaviorally controlled tactile stimulation. *Journal of Neurophysiology,* 63, 82-104.

Jenny, A. B. (1979). Commissural projections of the cortical hand motor area in monkeys. *J.Comp Neurol.*, 188, 137-145.

Jenny, A. B. & Inukai, J. (1983). Principles of motor organization of the monkey cervical spinal cord. *Journal of Neuroscience*, 3, 567-575.

Jiang, Y., Wei, N., Zhu, J., Lu, T., Chen, Z., Xu, G. & Liu, X. (2010). Effects of brain-derived neurotrophic factor on local inflammation in experimental stroke of rat. *Mediators.Inflamm.*, 2010, 372423.

Johansen-Berg, H., Rushworth, M. F., Bogdanovic, M. D., Kischka, U., Wimalaratna, S. & Matthews, P. M. (2002a). The role of ipsilateral premotor cortex in hand movement after stroke. *Proc.Natl.Acad.Sci.U.S.A*, 99, 14518-14523.

Johansen-Berg, H., Dawes, H., Guy, C., Smith, S. M., Wade, D. T. & Matthews, P. M. (2002b). Correlation between motor improvements and altered fMRI activity after rehabilitative therapy. *Brain*, 125, 2731-2742.

Jones, E. G. (1986). Connectivity of the primate sensory-motor cortex. *Sensory-motor areas and aspects of cortical connectivity* (pp. 113-183). Springer.

Kaas, J. H. (1983). What, if anything, is SI? Organization of first somatosensory area of cortex. *Physiol Rev.*, 63, 206-231.

Kaas, J. H. (1991). Plasticity of sensory and motor maps in adult mammals. *Annu.Rev.Neurosci.*, 14, 137-167.

Kaas, J. H., Florence, S. L. & Jain, N. (1999). Subcortical contributions to massive cortical reorganizations. *Neuron*, 22, 657-660.

Kaas, J. H. (2004). Somatosensory System. In G.Paxinos & J.K.Mai (Eds) *The Human Nervous System* (pp. 1059-1092). New York: Elsevier Academic Press.

Kaas, J. H., Qi, H. X., Burish, M. J., Gharbawie, O. A., Onifer, S. M. & Massey, J. M. (2008). Cortical and subcortical plasticity in the brains of humans, primates, and rats after damage to sensory afferents in the dorsal columns of the spinal cord. *Exp.Neurol.*, 209, 407-416.

Kaas, J. H., Gharbawie, O. A. & Stepniewska, I. (2011). The organization and evolution of dorsal stream multisensory motor pathways in primates. *Front Neuroanat.*, 5, 34.

Kably, B. & Drew, T. (1998). Corticoreticular pathways in the cat. I. Projection patterns and collaterization. *J.Neurophysiol.*, 80, 389-405.

Kaczmarek, L. & Chaudhuri, A. (1997). Sensory regulation of immediate-early gene expression in mammalian visual cortex: implications for functional mapping and neural plasticity. *Brain Res.Brain Res.Rev.*, 23, 237-256.

Kadhim, H. J., Duchateau, J. & Sebire, G. (2008). Cytokines and brain injury: invited review. *J.Intensive Care Med.*, 23, 236-249.

Kadhim, H. J., Duchateau, J. & Sebire, G. (2008). Cytokines and brain injury: invited review. *J.Intensive Care Med.*, 23, 236-249.

Kaeser, M., Wyss, A. F., Bashir, S., Hamadjida, A., Liu, Y., Bloch, J., Brunet, J. F., Belhaj-Saif, A. & Rouiller, E. M. (2010). Effects of Unilateral Motor Cortex Lesion on Ipsilesional Hand's Reach and Grasp Performance in Monkeys: Relationship With Recovery in the Contralesional Hand. *J.Neurophysiol.*, 103, 1630-1645.

Kaeser, M., Chatagny, P., Gindrat, A. D., Savidan, J., Badoud, S., Fregosi, M., Moret, V., Roulin, C., Schmidlin, E. & Rouiller, E. (2014). Variability of manual dexterity

performance in non-human primates (). *International Journal of Comparative Psychology*, 27.

Kakei, S., Hoffman, D. S. & Strick, P. L. (1999). Muscle and movement representations in the primary motor cortex. *Science*, 285, 2136-2139.

Kalaska, J. F. (1996). Parietal cortex area 5 and visuomotor behavior. *Canadian journal of physiology and pharmacology*, 74, 483-498.

Kambi, N., Halder, P., Rajan, R., Arora, V., Chand, P., Arora, M. & Jain, N. (2014). Large-scale reorganization of the somatosensory cortex following spinal cord injuries is due to brainstem plasticity. *Nat.Commun.*, 5, 3602.

Kandel, E. R., Schwartz, J. H. & Jessell, T. M. (2000). *Principles of neural science*. McGraw-Hill New York.

Karni, A., Meyer, G., Jezzard, P., Adams, M. M., Turner, R. & Ungerleider, L. G. (1995). Functional MRI evidence for adult motor cortex plasticity during motor skill learning. *Nature*, 377, 155-158.

Karni, A., Meyer, G., Rey-Hipolito, C., Jezzard, P., Adams, M. M., Turner, R. & Ungerleider, L. G. (1998). The acquisition of skilled motor performance: fast and slow experience-driven changes in primary motor cortex. *Proc.Natl.Acad.Sci.U.S.A*, 95, 861-868.

Keizer, K. & Kuypers, H. G. (1989). Distribution of corticospinal neurons with collaterals to the lower brain stem reticular formation in monkey (Macaca fascicularis). *Experimental Brain Research*, 74, 311-318.

Keizer, K. (1989). Collateralization of the pathways descending from the cerebral cortex to brain stem and spinal cord in cat and monkey.

Kelamangalath, L. & Smith, G. M. (2013). Neurotrophin treatment to promote regeneration after traumatic CNS injury. *Front Biol.(Beijing)*, 8, 486-495.

Kermadi, I., Liu, Y., Tempini, A. & Rouiller, E. M. (1997). Effects of reversible inactivation of the supplementary motor area (SMA) on unimanual grasp and bimanual pull and grasp performance in monkeys. *Somatosens.Mot.Res.*, 14, 268-280.

Kermadi, I., Liu, Y., Tempini, A., Calciati, E. & Rouiller, E. M. (1998). Neuronal activity in the primate supplementary motor area and the primary motor cortex in relation to spatio-temporal bimanual coordination. *Somatosens.Mot.Res.*, 15, 287-308.

Kermadi, I., Liu, Y. & Rouiller, E. M. (2000). Do bimanual motor actions involve the dorsal premotor (PMd), cingulate (CMA) and posterior parietal (PPC) cortices? Comparison with primary and supplementary motor cortical areas. *Somatosens.Mot.Res.*, 17, 255-271.

Kleim, J. A., Hogg, T. M., VandenBerg, P. M., Cooper, N. R., Bruneau, R. & Remple, M. (2004). Cortical synaptogenesis and motor map reorganization occur during late, but not early, phase of motor skill learning. *Journal of Neuroscience*, 24, 628-633.

Kleim, J. A., Chan, S., Pringle, E., Schallert, K., Procaccio, V., Jimenez, R. & Cramer, S. C. (2006). BDNF val66met polymorphism is associated with modified experience-dependent plasticity in human motor cortex. *Nat.Neurosci.*, 9, 735-737.

Klussmann, S. & Martin-Villalba, A. (2005). Molecular targets in spinal cord injury. *J.Mol.Med.(Berl)*, 83, 657-671.

Kneisley, L. W., Biber, M. P. & LaVail, J. H. (1978). A study of the origin of brain stem projections to monkey spinal cord using the retrograde transport method. *Exp.Neurol.*, 60, 116-139.

Kobayashi, M. & Pascual-Leone, A. (2003). Transcranial magnetic stimulation in neurology. *Lancet Neurol.*, 2, 145-156.

Krajacic, A., Ghosh, M., Puentes, R., Pearse, D. D. & Fouad, K. (2009). Advantages of delaying the onset of rehabilitative reaching training in rats with incomplete spinal cord injury. *Eur.J.Neurosci.*, 29, 641-651.

Krubitzer, L., Clarey, J., Tweedale, R., Elston, G. & Calford, M. (1995). A redefinition of somatosensory areas in the lateral sulcus of macaque monkeys. *Journal of Neuroscience*, 15, 3821-3839.

Kuchler, M., Fouad, K., Weinmann, O., Schwab, M. E. & Raineteau, O. (2002). Red nucleus projections to distinct motor neuron pools in the rat spinal cord. *J.Comp Neurol.*, 448, 349-359.

Kunkel, A., Kopp, B., Muller, G., Villringer, K., Villringer, A., Taub, E. & Flor, H. (1999). Constraint-induced movement therapy for motor recovery in chronic stroke patients. *Arch.Phys.Med.Rehabil.*, 80, 624-628.

Kurata, K. (1991). Corticocortical inputs to the dorsal and ventral aspects of the premotor cortex of macaque monkeys. *Neurosci.Res.*, 12, 263-280.

Kuypers, H. G. (1964). The descending pathways to the spinal cord, their anatomy and function. *Prog.Brain Res.*, 11, 178-202.

Kuypers, H. G. & Lawrence, D. G. (1967). Cortical projections to the red nucleus and the brain stem in the Rhesus monkey. *Brain Res.*, 4, 151-188.

Kuypers, H. G. J. M. & Tuerk, J. D. (1964). The distribution of cortical fibres within the nuclei cuneatus and gracilis in the cat. *Journal of anatomy*, 98, 143.

Kuypers, H. G. J. M. (1981). Anatomy of the descending pathways. *Comprehensive Physiology*.

Künzle, H. (1978). Cortico-cortical efferents of primary motor and somatosensory regions of the cerebral cortex in Macaca fascicularis. *Neuroscience*, 3, 25-39.

Lacroix, S., Havton, L. A., McKay, H., Yang, H., Brant, A., Roberts, J. & Tuszynski, M. H. (2004). Bilateral corticospinal projections arise from each motor cortex in the macaque monkey: a quantitative study. *J.Comp Neurol.*, 473, 147-161.

Lasek, R. J. (1967). Bidirectional transport of radioactively labelled axoplasmic components. *Nature*, 216, 1212-1214.

Laubach, M., Wessberg, J. & Nicolelis, M. A. (2000). Cortical ensemble activity increasingly predicts behaviour outcomes during learning of a motor task. *Nature*, 405, 567-571.

Lawrence, D. G. & Kuypers, H. G. (1968a). The functional organization of the motor system in the monkey. I. The effects of bilateral pyramidal lesions. *Brain*, 91, 1-14.

Lawrence, D. G. & Kuypers, H. G. (1968b). The functional organization of the motor system in the monkey. II. The effects of lesions of the descending brain-stem pathways. *Brain*, 91, 15-36.

Lawrence, D. G. & Hopkins, D. A. (1976). The development of motor control in the rhesus monkey: evidence concerning the role of corticomotoneuronal connections. *Brain*, 99, 235-254.

Lawrence, D. G., Porter, R. & Redman, S. J. (1985). Corticomotoneuronal synapses in the monkey: light microscopic localization upon motoneurons of intrinsic muscles of the hand. *J.Comp Neurol.,* 232, 499-510.

Lee, J. K., Geoffroy, C. G., Chan, A. F., Tolentino, K. E., Crawford, M. J., Leal, M. A., Kang, B. & Zheng, B. (2010). Assessing spinal axon regeneration and sprouting in Nogo-, MAG-, and OMgp-deficient mice. *Neuron,* 66, 663-670.

Lee, S., Ueno, M. & Yamashita, T. (2011). Axonal remodeling for motor recovery after traumatic brain injury requires downregulation of gamma-aminobutyric acid signaling. *Cell Death.Dis.,* 2, e133.

Lehmann, M., Fournier, A., Selles-Navarro, I., Dergham, P., Sebok, A., Leclerc, N., Tigyi, G. & McKerracher, L. (1999). Inactivation of Rho signaling pathway promotes CNS axon regeneration. *Journal of Neuroscience,* 19, 7537-7547.

Leichnetz, G. R. (1986). Afferent and efferent connections of the dorsolateral precentral gyrus (area 4, hand/arm region) in the macaque monkey, with comparisons to area 8. *J.Comp Neurol.,* 254, 460-492.

Leinonen, L., Hyvarinen, J., Nyman, G. & Linnankoski, I. (1979). I. Functional properties of neurons in lateral part of associative area 7 in awake monkeys. *Experimental Brain Research,* 34, 299-320.

Lemon, R. N., Mantel, G. W. & Muir, R. B. (1986). Corticospinal facilitation of hand muscles during voluntary movement in the conscious monkey. *J.Physiol,* 381, 497-527.

Lemon, R. N. (2008). Descending pathways in motor control. *Annu.Rev.Neurosci.,* 31, 195-218.

Liepert, J., Tegenthoff, M. & Malin, J. P. (1995). Changes of cortical motor area size during immobilization. *Electroencephalogr.Clin.Neurophysiol.,* 97, 382-386.

Liepert, J., Miltner, W. H., Bauder, H., Sommer, M., Dettmers, C., Taub, E. & Weiller, C. (1998). Motor cortex plasticity during constraint-induced movement therapy in stroke patients. *Neurosci.Lett.,* 250, 5-8.

Liepert, J., Hamzei, F. & Weiller, C. (2000). Motor cortex disinhibition of the unaffected hemisphere after acute stroke. *Muscle Nerve,* 23, 1761-1763.

Liu, C. N. & Chambers, W. W. (1964). An Experimental study of the corticoΓÇÉspinal system in the monkey (Macaca mulatta). The spinal pathways and preterminal distribution of degenerating fibers following discrete lesions of the preΓÇÉand postcentral gyri and bulbar pyramid. *Journal of comparative neurology,* 123, 257-283.

Liu, J., Morel, A., Wannier, T. & Rouiller, E. M. (2002). Origins of callosal projections to the supplementary motor area (SMA): a direct comparison between pre-SMA and SMA-proper in macaque monkeys. *J.Comp Neurol.,* 443, 71-85.

Liu, R. Y. & Snider, W. D. (2001). Different signaling pathways mediate regenerative versus developmental sensory axon growth. *Journal of Neuroscience,* 21, RC164.

Liu, Y. & Rouiller, E. M. (1999). Mechanisms of recovery of dexterity following unilateral lesion of the sensorimotor cortex in adult monkeys. *Experimental Brain Research,* 128, 149-159.

Lotze, M., Erb, M., Flor, H., Huelsmann, E., Godde, B. & Grodd, W. (2000). fMRI evaluation of somatotopic representation in human primary motor cortex. *Neuroimage.,* 11, 473-481.

Lotze, M., Markert, J., Sauseng, P., Hoppe, J., Plewnia, C. & Gerloff, C. (2006). The role of multiple contralesional motor areas for complex hand movements after internal capsular lesion. *Journal of Neuroscience,* 26, 6096-6102.

Lu, P., Blesch, A. & Tuszynski, M. H. (2001). Neurotrophism without neurotropism: BDNF promotes survival but not growth of lesioned corticospinal neurons. *J.Comp Neurol.,* 436, 456-470.

Lu, P. & Tuszynski, M. H. (2008). Growth factors and combinatorial therapies for CNS regeneration. *Exp.Neurol.,* 209, 313-320.

Lue, J. H., Lai, S. M., Wang, T. J., Shieh, J. Y. & Wen, C. Y. (1997). Synaptic relationships between corticocuneate terminals and glycine-immunoreactive neurons in the rat cuneate nucleus. *Brain Res.,* 771, 167-171.

Lue, J. H., Chen, S. H., Shieh, J. Y. & Wen, C. Y. (2001). Afferent synaptic contacts on glycine-immunoreactive neurons in the rat cuneate nucleus. *Synapse,* 41, 139-149.

Luke, L. M., Allred, R. P. & Jones, T. A. (2004). Unilateral ischemic sensorimotor cortical damage induces contralesional synaptogenesis and enhances skilled reaching with the ipsilateral forelimb in adult male rats. *Synapse,* 54, 187-199.

Luppino, G., Matelli, M., Camarda, R. & Rizzolatti, G. (1993). Corticocortical connections of area F3 (SMA-proper) and area F6 (pre-SMA) in the macaque monkey. *J.Comp Neurol.,* 338, 114-140.

Luppino, G., Murata, A., Govoni, P. & Matelli, M. (1999). Largely segregated parietofrontal connections linking rostral intraparietal cortex (areas AIP and VIP) and the ventral premotor cortex (areas F5 and F4). *Experimental Brain Research,* 128, 181-187.

Luppino, G. & Rizzolatti, G. (2000). The Organization of the Frontal Motor Cortex. *News Physiol Sci.,* 15, 219-224.

Luppino, G., Rozzi, S., Calzavara, R. & Matelli, M. (2003). Prefrontal and agranular cingulate projections to the dorsal premotor areas F2 and F7 in the macaque monkey. *Eur.J.Neurosci.,* 17, 559-578.

MacKay-Lyons, M. (2002). Central pattern generation of locomotion: a review of the evidence. *Phys.Ther.,* 82, 69-83.

Maier, M. A., Armand, J., Kirkwood, P. A., Yang, H. W., Davis, J. N. & Lemon, R. N. (2002). Differences in the corticospinal projection from primary motor cortex and supplementary motor area to macaque upper limb motoneurons: an anatomical and electrophysiological study. *Cereb.Cortex,* 12, 281-296.

Mamounas, L. A., Altar, C. A., Blue, M. E., Kaplan, D. R., Tessarollo, L. & Lyons, W. E. (2000). BDNF promotes the regenerative sprouting, but not survival, of injured serotonergic axons in the adult rat brain. *Journal of Neuroscience,* 20, 771-782.

Marconi, B., Genovesio, A., Giannetti, S., Molinari, M. & Caminiti, R. (2003). Callosal connections of dorso-lateral premotor cortex. *Eur.J.Neurosci.,* 18, 775-788.

Massion, J. (1967). The mammalian red nucleus. *Physiol Rev.,* 47, 383-436.

Matelli, M., Luppino, G. & Rizzolatti, G. (1985). Patterns of cytochrome oxidase activity in the frontal agranular cortex of the macaque monkey. *Behavioural Brain Research,* 18, 125-136.

Matelli, M., Luppino, G. & Rizzolatti, G. (1991). Architecture of superior and mesial area 6 and the adjacent cingulate cortex in the macaque monkey. *J.Comp Neurol.,* 311, 445-462.

Matsumura, M. & Kubota, K. (1979). Cortical projection to hand-arm motor area from post-arcuate area in macaque monkeys: a histological study of retrograde transport of horseradish peroxidase. *Neurosci.Lett.,* 11, 241-246.

Matsuzaka, Y., Aizawa, H. & Tanji, J. (1992). A motor area rostral to the supplementary motor area (presupplementary motor area) in the monkey: neuronal activity during a learned motor task. *J.Neurophysiol.,* 68, 653-662.

Matyas, F., Sreenivasan, V., Marbach, F., Wacongne, C., Barsy, B., Mateo, C., Aronoff, R. & Petersen, C. C. (2010). Motor control by sensory cortex. *Science,* 330, 1240-1243.

Maynard, F. M., Jr., Bracken, M. B., Creasey, G., Ditunno, J. F., Jr., Donovan, W. H., Ducker, T. B., Garber, S. L., Marino, R. J., Stover, S. L., Tator, C. H., Waters, R. L., Wilberger, J. E. & Young, W. (1997). International Standards for Neurological and Functional Classification of Spinal Cord Injury. American Spinal Injury Association. *Spinal Cord.,* 35, 266-274.

McGee, A. W. & Strittmatter, S. M. (2003). The Nogo-66 receptor: focusing myelin inhibition of axon regeneration. *Trends Neurosci.,* 26, 193-198.

McKerracher, L., David, S., Jackson, D. L., Kottis, V., Dunn, R. J. & Braun, P. E. (1994). Identification of myelin-associated glycoprotein as a major myelin-derived inhibitor of neurite growth. *Neuron,* 13, 805-811.

McKiernan, B. J., Marcario, J. K., Karrer, J. H. & Cheney, P. D. (1998). Corticomotoneuronal postspike effects in shoulder, elbow, wrist, digit, and intrinsic hand muscles during a reach and prehension task. *J.Neurophysiol.,* 80, 1961-1980.

McKinley, W., Santos, K., Meade, M. & Brooke, K. (2007). Incidence and outcomes of spinal cord injury clinical syndromes. *J.Spinal Cord.Med.,* 30, 215-224.

McNeal, D. W., Darling, W. G., Ge, J., Stilwell-Morecraft, K. S., Solon, K. M., Hynes, S. M., Pizzimenti, M. A., Rotella, D. L., Vanadurongvan, T. & Morecraft, R. J. (2010). Selective long-term reorganization of the corticospinal projection from the supplementary motor cortex following recovery from lateral motor cortex injury. *J.Comp Neurol.,* 518, 586-621.

Merton, P. A. & Morton, H. B. (1980). Electrical-stimulation of human motor and visual-cortex through the scalp. *Journal of Physiology* 305, 9-10.

Merzenich, M. M., Kaas, J. H., Wall, J., Nelson, R. J., Sur, M. & Felleman, D. (1983). Topographic reorganization of somatosensory cortical areas 3b and 1 in adult monkeys following restricted deafferentation. *Neuroscience,* 8, 33-55.

Mewes, K. & Cheney, P. D. (1991). Facilitation and suppression of wrist and digit muscles from single rubromotoneuronal cells in the awake monkey. *J.Neurophysiol.,* 66, 1965-1977.

Mitz, A. R. & Wise, S. P. (1987). The somatotopic organization of the supplementary motor area: intracortical microstimulation mapping. *Journal of Neuroscience,* 7, 1010-1021.

Mohajerani, M. H., Aminoltejari, K. & Murphy, T. H. (2011). Targeted mini-strokes produce changes in interhemispheric sensory signal processing that are indicative of disinhibition within minutes. *Proc.Natl.Acad.Sci.U.S.A,* 108, E183-E191.

Montgomery, L. R., Herbert, W. J. & Buford, J. A. (2013). Recruitment of ipsilateral and contralateral upper limb muscles following stimulation of the cortical motor areas in the monkey. *Experimental Brain Research,* 230, 153-164.

Morecraft, R. J. & Van Hoesen, G. W. (1992). Cingulate input to the primary and supplementary motor cortices in the rhesus monkey: evidence for somatotopy in areas 24c and 23c. *J.Comp Neurol.,* 322, 471-489.

Morecraft, R. J., Herrick, J. L., Stilwell-Morecraft, K. S., Louie, J. L., Schroeder, C. M., Ottenbacher, J. G. & Schoolfield, M. W. (2002). Localization of arm representation in the corona radiata and internal capsule in the non-human primate. *Brain,* 125, 176-198.

Morecraft, R. J., McNeal, D. W., Stilwell-Morecraft, K. S., Dvanajscak, Z., Ge, J. & Schneider, P. (2007). Localization of arm representation in the cerebral peduncle of the non-human primate. *J.Comp Neurol.,* 504, 149-167.

Morecraft, R. J., Ge, J., Stilwell-Morecraft, K. S., McNeal, D. W., Pizzimenti, M. A. & Darling, W. G. (2013). Terminal distribution of the corticospinal projection from the hand/arm region of the primary motor cortex to the cervical enlargement in rhesus monkey. *J.Comp Neurol.,* 521, 4205-4235.

Morel, A., Liu, J., Wannier, T., Jeanmonod, D. & Rouiller, E. M. (2005). Divergence and convergence of thalamocortical projections to premotor and supplementary motor cortex: a multiple tracing study in the macaque monkey. *Eur.J.Neurosci.,* 21, 1007-1029.

Mowery, T. M., Kostylev, P. V. & Garraghty, P. E. (2014). AMPA and GABA(A/B) receptor subunit expression in the cuneate nucleus of adult squirrel monkeys during peripheral nerve regeneration. *Neurosci.Lett.,* 559, 141-146.

Muakkassa, K. F. & Strick, P. L. (1979). Frontal lobe inputs to primate motor cortex: evidence for four somatotopically organized 'premotor' areas. *Brain Res.,* 177, 176-182.

Mukhopadhyay, G., Doherty, P., Walsh, F. S., Crocker, P. R. & Filbin, M. T. (1994). A novel role for myelin-associated glycoprotein as an inhibitor of axonal regeneration. *Neuron,* 13, 757-767.

Murata, Y., Higo, N., Oishi, T., Yamashita, A., Matsuda, K., Hayashi, M. & Yamane, S. (2008). Effects of motor training on the recovery of manual dexterity after primary motor cortex lesion in macaque monkeys. *J.Neurophysiol.,* 99, 773-786.

Murata, Y., Higo, N., Hayashi, T., Nishimura, Y., Sugiyama, Y., Oishi, T., Tsukada, H., Isa, T. & Onoe, H. (2015). Temporal plasticity involved in recovery from manual dexterity deficit after motor cortex lesion in macaque monkeys. *Journal of Neuroscience,* 35, 84-95.

Murphy, T. H. & Corbett, D. (2009). Plasticity during stroke recovery: from synapse to behaviour. *Nat.Rev.Neurosci.,* 10, 861-872.

Nachev, P., Kennard, C. & Husain, M. (2008). Functional role of the supplementary and pre-supplementary motor areas. *Nat.Rev.Neurosci.,* 9, 856-869.

Nagahara, A. H. & Tuszynski, M. H. (2011). Potential therapeutic uses of BDNF in neurological and psychiatric disorders. *Nat.Rev.Drug Discov.,* 10, 209-219.

Nash, M., Pribiag, H., Fournier, A. E. & Jacobson, C. (2009). Central nervous system regeneration inhibitors and their intracellular substrates. *Mol.Neurobiol.,* 40, 224-235.

Netz, J., Lammers, T. & Homberg, V. (1997). Reorganization of motor output in the non-affected hemisphere after stroke. *Brain,* 120 (Pt 9), 1579-1586.

Neumann, S., Bradke, F., Tessier-Lavigne, M. & Basbaum, A. I. (2002). Regeneration of sensory axons within the injured spinal cord induced by intraganglionic cAMP elevation. *Neuron,* 34, 885-893.

Nishibe, M., Urban, E. T., III, Barbay, S. & Nudo, R. J. (2015). Rehabilitative training promotes rapid motor recovery but delayed motor map reorganization in a rat cortical ischemic infarct model. *Neurorehabil.Neural Repair,* 29, 472-482.

Nishimura, Y. & Isa, T. (2012). Cortical and subcortical compensatory mechanisms after spinal cord injury in monkeys. *Exp.Neurol.,* 235, 152-161.

Nitsche, M. A. & Paulus, W. (2000). Excitability changes induced in the human motor cortex by weak transcranial direct current stimulation. *J.Physiol,* 527 Pt 3, 633-639.

Nitsche, M. A. & Paulus, W. (2000). Excitability changes induced in the human motor cortex by weak transcranial direct current stimulation. *J.Physiol,* 527 Pt 3, 633-639.

Noback, C. R., Strominger, N. L., Demarest, R. J. & Ruggiero, D. A. (2005). *The human nervous system: structure and function*. Springer Science & Business Media.

Novikova, L. N., Novikov, L. N. & Kellerth, J. O. (2000). Survival effects of BDNF and NT-3 on axotomized rubrospinal neurons depend on the temporal pattern of neurotrophin administration. *Eur.J.Neurosci.,* 12, 776-780.

Nudo, R. J., Jenkins, W. M., Merzenich, M. M., Prejean, T. & Grenda, R. (1992). Neurophysiological correlates of hand preference in primary motor cortex of adult squirrel monkeys. *Journal of Neuroscience,* 12, 2918-2947.

Nudo, R. J. & Milliken, G. W. (1996). Reorganization of movement representations in primary motor cortex following focal ischemic infarcts in adult squirrel monkeys. *J.Neurophysiol.,* 75, 2144-2149.

Nudo, R. J., Wise, B. M., SiFuentes, F. & Milliken, G. W. (1996). Neural substrates for the effects of rehabilitative training on motor recovery after ischemic infarct. *Science,* 272, 1791-1794.

Nudo, R. J., Friel, K. M. & Delia, S. W. (2000). Role of sensory deficits in motor impairments after injury to primary motor cortex. *Neuropharmacology,* 39, 733-742.

Nudo, R. J., Plautz, E. J. & Frost, S. B. (2001). Role of adaptive plasticity in recovery of function after damage to motor cortex. *Muscle Nerve,* 24, 1000-1019.

Nudo, R. J. (2006). Mechanisms for recovery of motor function following cortical damage. *Curr.Opin.Neurobiol.,* 16, 638-644.

Olivier, E., Davare, M., Andres, M. & Fadiga, L. (2007). Precision grasping in humans: from motor control to cognition. *Curr.Opin.Neurobiol.,* 17, 644-648.

Oudega, M. & Hagg, T. (1999). Neurotrophins promote regeneration of sensory axons in the adult rat spinal cord. *Brain Res.,* 818, 431-438.

Oudega, M., Rosano, C., Sadi, D., Wood, P. M., Schwab, M. E. & Hagg, T. (2000). Neutralizing antibodies against neurite growth inhibitor NI-35/250 do not promote regeneration of sensory axons in the adult rat spinal cord. *Neuroscience,* 100, 873-883.

Oujamaa, L., Relave, I., Froger, J., Mottet, D. & Pelissier, J. Y. (2009). Rehabilitation of arm function after stroke. Literature review. *Ann.Phys.Rehabil.Med.,* 52, 269-293.

Pandya, D. N. & Vignolo, L. A. (1969). Interhemispheric projections of the parietal lobe in the rhesus monkey. *Brain Res.,* 15, 49-65.

Park, M. C., Belhaj-Saïf, A., Gordon, M. & Cheney, P. D. (2001). Consistent features in the forelimb representation of primary motor cortex in rhesus macaques. *Journal of Neuroscience,* 21, 2784-2792.

Park, M. C., Belhaj-Saïf, A. & Cheney, P. D. (2004). Properties of primary motor cortex output to forelimb muscles in rhesus macaques. *Journal of Neurophysiology,* 92, 2968-2984.

Pascual-Leone, A. & Torres, F. (1993). Plasticity of the sensorimotor cortex representation of the reading finger in Braille readers. *Brain,* 116 (Pt 1), 39-52.

Paus, T. (2001). Primate anterior cingulate cortex: where motor control, drive and cognition interface. *Nat.Rev.Neurosci.,* 2, 417-424.

Pearse, D. D., Pereira, F. C., Marcillo, A. E., Bates, M. L., Berrocal, Y. A., Filbin, M. T. & Bunge, M. B. (2004). cAMP and Schwann cells promote axonal growth and functional recovery after spinal cord injury. *Nat.Med.,* 10, 610-616.

Penfield, W. & Rasmussen, T. (1950). The cerebral cortex of man; a clinical study of localization of function.

Pernet, V. & Schwab, M. E. (2012). The role of Nogo-A in axonal plasticity, regrowth and repair. *Cell Tissue Res.,* 349, 97-104.

Peterson, B. W. (1979). Reticulospinal projections to spinal motor nuclei. *Annu.Rev.Physiol,* 41, 127-140.

Pettersson, L. G., Alstermark, B., Blagovechtchenski, E., Isa, T. & Sasaski, S. (2007). Skilled digit movements in feline and primate--recovery after selective spinal cord lesions. *Acta Physiol (Oxf),* 189, 141-154.

Picard, N. & Strick, P. L. (1996). Motor areas of the medial wall: a review of their location and functional activation. *Cereb.Cortex,* 6, 342-353.

Pierrot-Deseilligny, E. (2002). Propriospinal transmission of part of the corticospinal excitation in humans. *Muscle Nerve,* 26, 155-172.

Porter, R. (1985). The corticomotoneuronal component of the pyramidal tract: corticomotoneuronal connections and functions in primates. *Brain Res.,* 357, 1-26.

Porter, R. & Lemon, R. (1993). *Corticospinal function and voluntary movement*. Oxford University Press, USA.

Preuss, T. M., Stepniewska, I. & Kaas, J. H. (1996). Movement representation in the dorsal and ventral premotor areas of owl monkeys: a microstimulation study. *J.Comp Neurol.,* 371, 649-676.

Purves, D., Augustine, G. J., Fitzpatrick, D., Katz, L. C., Lamantia, A. S., McNamara, J. O. & Williams, S. M. (2001). Neuroscience. 2nd. *Sunderland: Sinauer*.

Qi, H. X. & Kaas, J. H. (2006). Organization of primary afferent projections to the gracile nucleus of the dorsal column system of primates. *J.Comp Neurol.,* 499, 183-217.

Qi, H. X., Chen, L. M. & Kaas, J. H. (2011). Reorganization of somatosensory cortical areas 3b and 1 after unilateral section of dorsal columns of the spinal cord in squirrel monkeys. *Journal of Neuroscience,* 31, 13662-13675.

Qi, H. X., Gharbawie, O. A., Wynne, K. W. & Kaas, J. H. (2013). Impairment and recovery of hand use after unilateral section of the dorsal columns of the spinal cord in squirrel monkeys. *Behavioural Brain Research,* 252, 363-376.

Rack, P. (1987). Control of Human Voluntary Movement. *Journal of neurology, neurosurgery, and psychiatry,* 50, 1090.

Raineteau, O. & Schwab, M. E. (2001). Plasticity of motor systems after incomplete spinal cord injury. *Nat.Rev.Neurosci.,* 2, 263-273.

Rao, S. M., Binder, J. R., Hammeke, T. A., Bandettini, P. A., Bobholz, J. A., Frost, J. A., Myklebust, B. M., Jacobson, R. D. & Hyde, J. S. (1995). Somatotopic mapping of the human primary motor cortex with functional magnetic resonance imaging. *Neurology,* 45, 919-924.

Rathelot, J. A. & Strick, P. L. (2006). Muscle representation in the macaque motor cortex: an anatomical perspective. *Proc.Natl.Acad.Sci.U.S.A,* 103, 8257-8262.

Rathelot, J. A. & Strick, P. L. (2009). Subdivisions of primary motor cortex based on cortico-motoneuronal cells. *Proc.Natl.Acad.Sci.U.S.A,* 106, 918-923.

Redecker, C., Wang, W., Fritschy, J. M. & Witte, O. W. (2002). Widespread and long-lasting alterations in GABA(A)-receptor subtypes after focal cortical infarcts in rats: mediation by NMDA-dependent processes. *J.Cereb.Blood Flow Metab,* 22, 1463-1475.

Rehme, A. K., Fink, G. R., von Cramon, D. Y. & Grefkes, C. (2011). The role of the contralesional motor cortex for motor recovery in the early days after stroke assessed with longitudinal FMRI. *Cereb.Cortex,* 21, 756-768.

Rehme, A. K., Eickhoff, S. B., Wang, L. E., Fink, G. R. & Grefkes, C. (2011). Dynamic causal modeling of cortical activity from the acute to the chronic stage after stroke. *Neuroimage.,* 55, 1147-1158.

Remple, M. S., Bruneau, R. M., VandenBerg, P. M., Goertzen, C. & Kleim, J. A. (2001). Sensitivity of cortical movement representations to motor experience: evidence that skill learning but not strength training induces cortical reorganization. *Behavioural Brain Research,* 123, 133-141.

Rexed, B. (1954). A cytoarchitectonic atlas of the spinal cord in the cat. *J.Comp Neurol.,* 100, 297-379.

Riddle, C. N., Edgley, S. A. & Baker, S. N. (2009). Direct and indirect connections with upper limb motoneurons from the primate reticulospinal tract. *Journal of Neuroscience,* 29, 4993-4999.

Rioult-Pedotti, M. S., Friedman, D., Hess, G. & Donoghue, J. P. (1998). Strengthening of horizontal cortical connections following skill learning. *Nat.Neurosci.,* 1, 230-234.

Risedal, A., Zeng, J. & Johansson, B. B. (1999). Early training may exacerbate brain damage after focal brain ischemia in the rat. *J.Cereb.Blood Flow Metab,* 19, 997-1003.

Rizzolatti, G., Fogassi, L. & Gallese, V. (1997). Parietal cortex: from sight to action. *Curr.Opin.Neurobiol.,* 7, 562-567.

Rizzolatti, G., Luppino, G. & Matelli, M. (1998). The organization of the cortical motor system: new concepts. *Electroencephalogr.Clin.Neurophysiol.*, 106, 283-296.

Rizzolatti, G. & Luppino, G. (2001). The cortical motor system. *Neuron*, 31, 889-901.

Rosenzweig, E. S., Courtine, G., Jindrich, D. L., Brock, J. H., Ferguson, A. R., Strand, S. C., Nout, Y. S., Roy, R. R., Miller, D. M., Beattie, M. S., Havton, L. A., Bresnahan, J. C., Edgerton, V. R. & Tuszynski, M. H. (2010). Extensive spontaneous plasticity of corticospinal projections after primate spinal cord injury. *Nat.Neurosci.*, 13, 1505-1510.

Rosochowicz, T. W., Wrotek, S. & Kozak, W. (2015). Axonal regeneration inhibitors: emerging therapeutic options. *Acta Neurol.Belg.*.

Rouiller, E. M., Babalian, A., Kazennikov, O., Moret, V., Yu, X. H. & Wiesendanger, M. (1994). Transcallosal connections of the distal forelimb representations of the primary and supplementary motor cortical areas in macaque monkeys. *Experimental Brain Research*, 102, 227-243.

Rouiller, E. M., Moret, V., Tanne, J. & Boussaoud, D. (1996). Evidence for direct connections between the hand region of the supplementary motor area and cervical motoneurons in the macaque monkey. *Eur.J.Neurosci.*, 8, 1055-1059.

Rouiller, E. M., Yu, X.-H. & Tampini, A. (1997). Effect of Inactivation of the Hand Representation of the Primary and Supplementary Motor Cortical Areas on Precision Grip Performance in Monkeys. In M. G. e. Hepp-Reymond M-C (Ed) *Perspectives of Motor Behavior and Its Neural Basis* (pp. 33-43). Basel: Karger.

Rouiller, E. M., Tanne, J., Moret, V., Kermadi, I., Boussaoud, D. & Welker, E. (1998). Dual morphology and topography of the corticothalamic terminals originating from the primary, supplementary motor, and dorsal premotor cortical areas in macaque monkeys. *J.Comp Neurol.*, 396, 169-185.

Rouiller, E. M., Tanne, J., Moret, V. & Boussaoud, D. (1999). Origin of thalamic inputs to the primary, premotor, and supplementary motor cortical areas and to area 46 in macaque monkeys: a multiple retrograde tracing study. *J.Comp Neurol.*, 409, 131-152.

Rouiller, E. M. & Welker, E. (2000). A comparative analysis of the morphology of corticothalamic projections in mammals. *Brain Res.Bull.*, 53, 727-741.

Roux, P. P. & Barker, P. A. (2002). Neurotrophin signaling through the p75 neurotrophin receptor. *Prog.Neurobiol.*, 67, 203-233.

Rozzi, S., Ferrari, P. F., Bonini, L., Rizzolatti, G. & Fogassi, L. (2008). Functional organization of inferior parietal lobule convexity in the macaque monkey: electrophysiological characterization of motor, sensory and mirror responses and their correlation with cytoarchitectonic areas. *Eur.J.Neurosci.*, 28, 1569-1588.

Ruben, J., Schwiemann, J., Deuchert, M., Meyer, R., Krause, T., Curio, G., Villringer, K., Kurth, R. & Villringer, A. (2001). Somatotopic organization of human secondary somatosensory cortex. *Cereb.Cortex*, 11, 463-473.

Ruber, T., Schlaug, G. & Lindenberg, R. (2012). Compensatory role of the cortico-rubro-spinal tract in motor recovery after stroke. *Neurology*, 79, 515-522.

Sakata, H. & Taira, M. (1994). Parietal control of hand action. *Curr.Opin.Neurobiol.*, 4, 847-856.

Salmelin, R., Forss, N., Knuutila, J. & Hari, R. (1995). Bilateral activation of the human somatomotor cortex by distal hand movements. *Electroencephalogr.Clin.Neurophysiol.,* 95, 444-452.

Sanes, J. N. & Donoghue, J. P. (2000). Plasticity and primary motor cortex. *Annu.Rev.Neurosci.,* 23, 393-415.

Sasaki, M., Radtke, C., Tan, A. M., Zhao, P., Hamada, H., Houkin, K., Honmou, O. & Kocsis, J. D. (2009). BDNF-hypersecreting human mesenchymal stem cells promote functional recovery, axonal sprouting, and protection of corticospinal neurons after spinal cord injury. *Journal of Neuroscience,* 29, 14932-14941.

Schieber, M. H. & Poliakov, A. V. (1998). Partial inactivation of the primary motor cortex hand area: effects on individuated finger movements. *Journal of Neuroscience,* 18, 9038-9054.

Schieber, M. H. (2001). Constraints on somatotopic organization in the primary motor cortex. *J.Neurophysiol.,* 86, 2125-2143.

Schieber, M. H. (2007). Chapter 2 Comparative anatomy and physiology of the corticospinal system. *Handb.Clin.Neurol.,* 82, 15-37.

Schieber, M. H., Lang, C. E., Reilly, K. T., McNulty, P. & Sirigu, A. (2009). Selective activation of human finger muscles after stroke or amputation. *Adv.Exp.Med.Biol.,* 629, 559-575.

Schmidlin, E., Wannier, T., Bloch, J. & Rouiller, E. M. (2004). Progressive plastic changes in the hand representation of the primary motor cortex parallel incomplete recovery from a unilateral section of the corticospinal tract at cervical level in monkeys. *Brain Res.,* 1017, 172-183.

Schmidlin, E., Wannier, T., Bloch, J., Belhaj-Saif, A., Wyss, A. F. & Rouiller, E. M. (2005). Reduction of the hand representation in the ipsilateral primary motor cortex following unilateral section of the corticospinal tract at cervical level in monkeys. *BMC.Neurosci.,* 6, 56.

Schmidlin, E., Brochier, T., Maier, M. A., Kirkwood, P. A. & Lemon, R. N. (2008). Pronounced reduction of digit motor responses evoked from macaque ventral premotor cortex after reversible inactivation of the primary motor cortex hand area. *Journal of Neuroscience,* 28, 5772-5783.

Schnell, L. & Schwab, M. E. (1990). Axonal regeneration in the rat spinal cord produced by an antibody against myelin-associated neurite growth inhibitors. *Nature,* 343, 269-272.

Schnell, L. & Schwab, M. E. (1993). Sprouting and regeneration of lesioned corticospinal tract fibres in the adult rat spinal cord. *Eur.J.Neurosci.,* 5, 1156-1171.

Schnell, L., Schneider, R., Kolbeck, R., Barde, Y. A. & Schwab, M. E. (1994). Neurotrophin-3 enhances sprouting of corticospinal tract during development and after adult spinal cord lesion. *Nature,* 367, 170-173.

Schulz, R., Braass, H., Liuzzi, G., Hoerniss, V., Lechner, P., Gerloff, C. & Hummel, F. C. (2015). White matter integrity of premotor-motor connections is associated with motor output in chronic stroke patients. *Neuroimage.Clin.,* 7, 82-86.

Schwab, J. M., Tuli, S. K. & Failli, V. (2006). The Nogo receptor complex: confining molecules to molecular mechanisms. *Trends Mol.Med.,* 12, 293-297.

Schwab, M. E. & Bartholdi, D. (1996). Degeneration and regeneration of axons in the lesioned spinal cord. *Physiol Rev.*, 76, 319-370.
Schwab, M. E. (2004). Nogo and axon regeneration. *Curr.Opin.Neurobiol.*, 14, 118-124.
Schwab, M. E. & Strittmatter, S. M. (2014). Nogo limits neural plasticity and recovery from injury. *Curr.Opin.Neurobiol.*, 27, 53-60.
Sergio, L. E., Hamel-Paquet, C. & Kalaska, J. F. (2005). Motor cortex neural correlates of output kinematics and kinetics during isometric-force and arm-reaching tasks. *J.Neurophysiol.*, 94, 2353-2378.
Sessle, B. J. & Wiesendanger, M. (1982). Structural and functional definition of the motor cortex in the monkey (Macaca fascicularis). *J.Physiol*, 323, 245-265.
Shapovalov, A. I., Karamjan, O. A., Kurchavyi, G. G. & Repina, Z. A. (1971). Synaptic actions evoked from the red nucleus on the spinal alpha-motorneurons in the Rhesus monkey. *Brain Res.*, 32, 325-348.
Shapovalov, A. I. (1972). Extrapyramidal monosynaptic and disynaptic control of mammalian alpha-motoneurons. *Brain Res.*, 40, 105-115.
Shelton, F. N. & Reding, M. J. (2001). Effect of lesion location on upper limb motor recovery after stroke. *Stroke*, 32, 107-112.
Sherrington, C. S. (1910). Flexion-reflex of the limb, crossed extension-reflex, and reflex stepping and standing. *J.Physiol*, 40, 28-121.
Shibasaki, H., Sadato, N., Lyshkow, H., Yonekura, Y., Honda, M., Nagamine, T., Suwazono, S., Magata, Y., Ikeda, A. & Miyazaki, M. (1993). Both primary motor cortex and supplementary motor area play an important role in complex finger movement. *Brain*, 116, 1387-1398.
Shima, K. & Tanji, J. (1998). Role for cingulate motor area cells in voluntary movement selection based on reward. *Science*, 282, 1335-1338.
Shimizu, T., Hosaki, A., Hino, T., Sato, M., Komori, T., Hirai, S. & Rossini, P. M. (2002). Motor cortical disinhibition in the unaffected hemisphere after unilateral cortical stroke. *Brain*, 125, 1896-1907.
Shumsky, J. S., Tobias, C. A., Tumolo, M., Long, W. D., Giszter, S. F. & Murray, M. (2003). Delayed transplantation of fibroblasts genetically modified to secrete BDNF and NT-3 into a spinal cord injury site is associated with limited recovery of function. *Exp.Neurol.*, 184, 114-130.
Silver, J. & Miller, J. H. (2004). Regeneration beyond the glial scar. *Nature Reviews Neuroscience*, 5, 146-156.
Song, X. Y., Li, F., Zhang, F. H., Zhong, J. H. & Zhou, X. F. (2008). Peripherally-derived BDNF promotes regeneration of ascending sensory neurons after spinal cord injury. *PLoS.One.*, 3, e1707.
Soto, C., Aguilar, J., Martin-Cora, F., Rivadulla, C. & Canedo, A. (2004). Intracuneate mechanisms underlying primary afferent cutaneous processing in anaesthetized cats. *Eur.J.Neurosci.*, 19, 3006-3016.
Stefan, K., Kunesch, E., Cohen, L. G., Benecke, R. & Classen, J. (2000). Induction of plasticity in the human motor cortex by paired associative stimulation. *Brain*, 123 Pt 3, 572-584.

Stepniewska, I., Preuss, T. M. & Kaas, J. H. (1993). Architectonics, somatotopic organization, and ipsilateral cortical connections of the primary motor area (M1) of owl monkeys. *J.Comp Neurol.*, 330, 238-271.

Stepniewska, I., Preuss, T. M. & Kaas, J. H. (2006). Ipsilateral cortical connections of dorsal and ventral premotor areas in New World owl monkeys. *J.Comp Neurol.*, 495, 691-708.

Strata, F., Coq, J. O. & Kaas, J. H. (2003). The chemo- and somatotopic architecture of the Galago cuneate and gracile nuclei. *Neuroscience*, 116, 831-850.

Sugiyama, Y., Higo, N., Yoshino-Saito, K., Murata, Y., Nishimura, Y., Oishi, T. & Isa, T. (2013). Effects of early versus late rehabilitative training on manual dexterity after corticospinal tract lesion in macaque monkeys. *J.Neurophysiol.*, 109, 2853-2865.

Takenobu, Y., Hayashi, T., Moriwaki, H., Nagatsuka, K., Naritomi, H. & Fukuyama, H. (2014). Motor recovery and microstructural change in rubro-spinal tract in subcortical stroke. *Neuroimage.Clin.*, 4, 201-208.

Tanne-Gariepy, J., Rouiller, E. M. & Boussaoud, D. (2002). Parietal inputs to dorsal versus ventral premotor areas in the macaque monkey: evidence for largely segregated visuomotor pathways. *Experimental Brain Research*, 145, 91-103.

Taub, E., Uswatte, G. & Pidikiti, R. (1999). Constraint-Induced Movement Therapy: a new family of techniques with broad application to physical rehabilitation--a clinical review. *J.Rehabil.Res.Dev.*, 36, 237-251.

Teo, J. T., Terranova, C., Swayne, O., Greenwood, R. J. & Rothwell, J. C. (2009). Differing effects of intracortical circuits on plasticity. *Experimental Brain Research*, 193, 555-563.

Thallmair, M., Metz, G. A., Z'Graggen, W. J., Raineteau, O., Kartje, G. L. & Schwab, M. E. (1998). Neurite growth inhibitors restrict plasticity and functional recovery following corticospinal tract lesions. *Nat.Neurosci.*, 1, 124-131.

Thuret, S., Moon, L. D. & Gage, F. H. (2006). Therapeutic interventions after spinal cord injury. *Nat.Rev.Neurosci.*, 7, 628-643.

Tokuno, H. & Tanji, J. (1993). Input organization of distal and proximal forelimb areas in the monkey primary motor cortex: a retrograde double labeling study. *J.Comp Neurol.*, 333, 199-209.

Tokuno, H., Tanaka, I., Senoo, A., Umitsu, Y., Akazawa, T., Nakamura, Y. & Watson, C. (2011). Internet-based atlas of the primate spinal cord. *Neurosci.Res.*, 70, 128-132.

Touvykine, B., Mansoori, B. K., Jean-Charles, L., Deffeyes, J., Quessy, S. & Dancause, N. (2015). The Effect of Lesion Size on the Organization of the Ipsilesional and Contralesional Motor Cortex. *Neurorehabil.Neural Repair*.

Vavrek, R., Girgis, J., Tetzlaff, W., Hiebert, G. W. & Fouad, K. (2006). BDNF promotes connections of corticospinal neurons onto spared descending interneurons in spinal cord injured rats. *Brain*, 129, 1534-1545.

Vessal, M., Aycock, A., Garton, M. T., Ciferri, M. & Darian-Smith, C. (2007). Adult neurogenesis in primate and rodent spinal cord: comparing a cervical dorsal rhizotomy with a dorsal column transection. *Eur.J.Neurosci.*, 26, 2777-2794.

Wahl, A. S., Omlor, W., Rubio, J. C., Chen, J. L., Zheng, H., Schroter, A., Gullo, M., Weinmann, O., Kobayashi, K., Helmchen, F., Ommer, B. & Schwab, M. E.

(2014). Neuronal repair. Asynchronous therapy restores motor control by rewiring of the rat corticospinal tract after stroke. *Science,* 344, 1250-1255.

Wang, K. C., Koprivica, V., Kim, J. A., Sivasankaran, R., Guo, Y., Neve, R. L. & He, Z. (2002). Oligodendrocyte-myelin glycoprotein is a Nogo receptor ligand that inhibits neurite outgrowth. *Nature,* 417, 941-944.

Wang, S., Bray, P., McCaffrey, T., March, K., Hempstead, B. L. & Kraemer, R. (2000). p75(NTR) mediates neurotrophin-induced apoptosis of vascular smooth muscle cells. *Am.J.Pathol.,* 157, 1247-1258.

Wang, T., Xiong, J. Q., Ren, X. B. & Sun, W. (2012). The role of Nogo-A in neuroregeneration: a review. *Brain Res.Bull.,* 87, 499-503.

Wang, Y., Pillai, S., Wolpaw, J. R. & Chen, X. Y. (2006). Motor learning changes GABAergic terminals on spinal motoneurons in normal rats. *Eur.J.Neurosci.,* 23, 141-150.

Wannier, T., Schmidlin, E., Bloch, J. & Rouiller, E. M. (2005). A unilateral section of the corticospinal tract at cervical level in primate does not lead to measurable cell loss in motor cortex. *J.Neurotrauma,* 22, 703-717.

Weinrich, M. & Wise, S. P. (1982). The premotor cortex of the monkey. *Journal of Neuroscience,* 2, 1329-1345.

Weishaupt, N., Blesch, A. & Fouad, K. (2012). BDNF: the career of a multifaceted neurotrophin in spinal cord injury. *Exp.Neurol.,* 238, 254-264.

Weishaupt, N., Li, S., Di, P. A., Sipione, S. & Fouad, K. (2013). Synergistic effects of BDNF and rehabilitative training on recovery after cervical spinal cord injury. *Behavioural Brain Research,* 239, 31-42.

Werner, C. & Engelhard, K. (2007). Pathophysiology of traumatic brain injury. *Br.J.Anaesth.,* 99, 4-9.

Widener, G. L. & Cheney, P. D. (1997). Effects on muscle activity from microstimuli applied to somatosensory and motor cortex during voluntary movement in the monkey. *J.Neurophysiol.,* 77, 2446-2465.

Wilson, V. J. & Peterson, B. W. (1981). Vestibulospinal and reticulospinal systems. *Comprehensive Physiology*.

Withers, G. S. & Greenough, W. T. (1989). Reach training selectively alters dendritic branching in subpopulations of layer II-III pyramids in rat motor-somatosensory forelimb cortex. *Neuropsychologia,* 27, 61-69.

Wolf, S. L., Winstein, C. J., Miller, J. P., Taub, E., Uswatte, G., Morris, D., Giuliani, C., Light, K. E. & Nichols-Larsen, D. (2006). Effect of constraint-induced movement therapy on upper extremity function 3 to 9 months after stroke: the EXCITE randomized clinical trial. *JAMA,* 296, 2095-2104.

Wolpaw, J. R. & Tennissen, A. M. (2001). Activity-dependent spinal cord plasticity in health and disease. *Annu.Rev.Neurosci.,* 24, 807-843.

Wolpaw, J. R. (2007). Spinal cord plasticity in acquisition and maintenance of motor skills. *Acta Physiol (Oxf),* 189, 155-169.

Woolsey, C. N., Settlage, P. H., Meyer, D. R., Sencer, W., Pinto, H. T. & Travis, A. M. (1952). Patterns of localization in precentral and "supplementary" motor areas and their relation to the concept of a premotor area. *Res.Publ.Assoc.Res.Nerv.Ment.Dis.,* 30, 238-264.

Wu, C. W., Bichot, N. P. & Kaas, J. H. (2000). Converging evidence from microstimulation, architecture, and connections for multiple motor areas in the frontal and cingulate cortex of prosimian primates. *J.Comp Neurol.,* 423, 140-177.

Wyss, A. F., Hamadjida, A., Savidan, J., Liu, Y., Bashir, S., Mir, A., Schwab, M. E., Rouiller, E. M. & Belhaj-Saif, A. (2013). Long-term motor cortical map changes following unilateral lesion of the hand representation in the motor cortex in macaque monkeys showing functional recovery of hand functions. *Restor.Neurol.Neurosci.,* 31, 733-760.

Xerri, C., Coq, J. O., Merzenich, M. M. & Jenkins, W. M. (1996). Experience-induced plasticity of cutaneous maps in the primary somatosensory cortex of adult monkeys and rats. *J.Physiol Paris,* 90, 277-287.

Xerri, C., Merzenich, M. M., Peterson, B. E. & Jenkins, W. (1998). Plasticity of primary somatosensory cortex paralleling sensorimotor skill recovery from stroke in adult monkeys. *J.Neurophysiol.,* 79, 2119-2148.

Yang, Y. R., Wang, R. Y. & Wang, P. S.-G. (2003). Early and late treadmill training after focal brain ischemia in rats. *Neuroscience letters,* 339, 91-94.

Yeiser, E. C., Rutkoski, N. J., Naito, A., Inoue, J. & Carter, B. D. (2004). Neurotrophin signaling through the p75 receptor is deficient in traf6-/- mice. *Journal of Neuroscience,* 24, 10521-10529.

Yeo, S. S. & Jang, S. H. (2010). Changes in red nucleus after pyramidal tract injury in patients with cerebral infarct. *NeuroRehabilitation.,* 27, 373-377.

Z'Graggen, W. J., Conforto, A. B., Wiest, R., Remonda, L., Hess, C. W. & Kaelin-Lang, A. (2009). Mapping of direction and muscle representation in the human primary motor cortex controlling thumb movements. *J.Physiol,* 587, 1977-1987.

Zartl, M., Kapfer, T. & Muellbacher, W. (2014). Functional topography of cortical thumb movement representations in human primary motor cortex. *Brain Topogr.,* 27, 228-239.

Zarzecki, P. (1986). Functions of corticocortical neurons of somatosensory, motor, and parietal cortex. *Sensory-Motor Areas and Aspects of Cortical Connectivity* (pp. 185-215). Springer.

Zemmar, A., Weinmann, O., Kellner, Y., Yu, X., Vicente, R., Gullo, M., Kasper, H., Lussi, K., Ristic, Z., Luft, A. R., Rioult-Pedotti, M., Zuo, Y., Zagrebelsky, M. & Schwab, M. E. (2014). Neutralization of Nogo-A enhances synaptic plasticity in the rodent motor cortex and improves motor learning in vivo. *Journal of Neuroscience,* 34, 8685-8698.

Zhang, Y., Xiong, Y., Mahmood, A., Meng, Y., Liu, Z., Qu, C. & Chopp, M. (2010). Sprouting of corticospinal tract axons from the contralateral hemisphere into the denervated side of the spinal cord is associated with functional recovery in adult rat after traumatic brain injury and erythropoietin treatment. *Brain Res.,* 1353, 249-257.

Zhou, L. & Shine, H. D. (2003). Neurotrophic factors expressed in both cortex and spinal cord induce axonal plasticity after spinal cord injury. *J.Neurosci.Res.,* 74, 221-226.

Ziemann, U., Paulus, W., Nitsche, M. A., Pascual-Leone, A., Byblow, W. D., Berardelli, A., Siebner, H. R., Classen, J., Cohen, L. G. & Rothwell, J. C. (2008). Consensus: Motor cortex plasticity protocols. *Brain Stimul.,* 1, 164-182.

Zorner, B. & Schwab, M. E. (2010). Anti-Nogo on the go: from animal models to a clinical trial. *Ann.N.Y.Acad.Sci.*, 1198 Suppl 1, E22-E34.

Julie SAVIDAN

Route de la pisciculture, 13
1700 Fribourg - Suisse
Phone : + 41(0) 265343860
Email : savidan.julie@gmail.com

SKILLS

- Monkey motor behavioural tests: Modified Brinkman board test, Modified Klüver board test
- Monkey surgery participation: chronic EMG wireless implant, chronic head chamber implant
- Electrophysiological technics on macaque monkey model: transcranial electrical stimulation, transcranial magnetic stimulation, ICMS
- Immunohistochemistry
- Rat's surgery on venous system and intracerebral injection
- Rodent behavioural tests : conditioned place preference, Morris water maze, elevated plus maze, passive avoidance, y-maze, forced swimming test, open-field, rotarod
- Software competence: Spike2, Fiji, Matlab (basics)

EDUCATION

2009-Present — **Doctoral school BEFRI** - University of Fribourg-Bern
Neurosciences

2006-2007 — **Master of Science II** - University of Bordeaux II
Professional master in Neuropsychopharmacology and addictology

2005-2006 — **Master of Science I** - University of Bordeaux II
Neurosciences

2005 — **Licence Degree** - Scientific university of Nantes
Cellular biology and animal physiology

2001-2003 — **1st year of Medicine** - Medicine University of Nantes
Equivalence for 2nd year of DEUG in Life Science

PROFESSIONAL EXPERIENCE

2009-Present — **University of Fribourg,** laboratory of neurophysiology of action and hearing **–** Doctoral student in neurosciences
Study of spinal cord and cortical injury outcomes and treatments targeting the motor control in the macaque monkey model.

2008-05-15 / 2008-12-24 (7 months) — **Genfit, biotechnological society,** in vivo department – Research technician
Development of an animal model for Parkinson disease, behavioral test and immunochemistery.

2007 (6 months) — **General Pharmacology department,** CERB – Training period
Development of an animal model for testing addiction in rodent (conditioned place preference).

2006 (2 months) — **Signal and Cellular Interaction Laboratory,** UMR 5017 – Training period
Confocal Microscopy, RNA extraction, RT-PCR.

2004 (2 weeks) — **Immunology Laboratory, Nantes Hospital –** Training period
Study of stump cells injections in therapeutical traitment of parkinson disease.

Fellowship

2010 **FENS (Federation of European Neurosciences Societies) 2010**
SSN (Swiss Society for Neuroscience) travel fellowship

Publications

Kaeser, M., Chatagny, P., Gindrat, A. D., **Savidan, J.**, Badoud, S., Fregosi M., Moret V., Roulin C., Schmidlin# E. and Rouiller E.M.# **(2014)**. Variability of manual dexterity performance in non-human primates (). *International Journal of Comparative Psychology*, *27*(2).

Wyss, A. F.*, Hamadjida, A.*, **Savidan, J.***, Liu, Y., Bashir, S., Mir, A., Schwab, M. E., Rouiller, E. M. & Belhaj-Saif, A. **(2013).**Long-term motor cortical map changes following unilateral lesion of the hand representation in the motor cortex in macaque monkeys showing functional recovery of hand functions. *Restor Neurol Neurosci* **31**, 733-760.

Chatagny, P., Badoud, S., Kaeser, M., Gindrat, A. D., **Savidan**, J., Fregosi, M., Moret, V., Roulin, C., Schmidlin, E. & Rouiller, E. M. **(2013).**Distinction between hand dominance and hand preference in primates: a behavioral investigation of manual dexterity in nonhuman primates (macaques) and human subjects. *Brain Behav* **3**, 575-595.

Schmidlin, E., Kaeser, M., Gindrat, A. D., **Savidan, J.**, Chatagny, P., Badoud, S., Hamadjida, A., Beaud, M. L., Wannier, T., Belhaj-Saif, A. & Rouiller, E. M. **(2011).**Behavioral assessment of manual dexterity in non-human primates. *J Vis Exp*.

* Equal first authorship.

Equal senior authorship.

Oral presentation

2012 **Medicin seminar,** University of Fribourg
Reorganization of sensory afferences to dorsal column nuclei following spinal cord injury in monkey?

Award

2010 **Travel grant,** Swiss Society of Neurosciences
Fens Meeting in Amsterdam